MICRONUTRIENTS: THE BORDERLINE BETWEEN THEIR BENEFICIAL ROLE AND TOXICITY IN PLANTS

EDITED BY: Antonios Chrysargyris, Monica Höfte, Nikos Tzortzakis, Spyridon Alexandros Petropoulos and Francesco Di Gioia

PUBLISHED IN: Frontiers in Plant Science



frontiers Research Topics

Frontiers eBook Copyright Statement

The copyright in the text of individual articles in this eBook is the property of their respective authors or their respective institutions or funders. The copyright in graphics and images within each article may be subject to copyright of other parties. In both cases this is subject to a license granted to Frontiers.

The compilation of articles constituting this eBook is the property of Frontiers.

Each article within this eBook, and the eBook itself, are published under the most recent version of the Creative Commons CC-BY licence. The version current at the date of publication of this eBook is CC-BY 4.0. If the CC-BY licence is updated, the licence granted by Frontiers is automatically updated to the new version.

When exercising any right under the CC-BY licence, Frontiers must be attributed as the original publisher of the article or eBook, as applicable.

Authors have the responsibility of ensuring that any graphics or other materials which are the property of others may be included in the CC-BY licence, but this should be checked before relying on the CC-BY licence to reproduce those materials. Any copyright notices relating to those materials must be complied with.

Copyright and source acknowledgement notices may not be removed and must be displayed in any copy, derivative work or partial copy which includes the elements in question.

All copyright, and all rights therein, are protected by national and international copyright laws. The above represents a summary only. For further information please read Frontiers' Conditions for Website Use and Copyright Statement, and the applicable CC-BY licence.

ISSN 1664-8714
ISBN 978-2-88974-621-7
DOI 10.3389/978-2-88974-621-7

About Frontiers

Frontiers is more than just an open-access publisher of scholarly articles: it is a pioneering approach to the world of academia, radically improving the way scholarly research is managed. The grand vision of Frontiers is a world where all people have an equal opportunity to seek, share and generate knowledge. Frontiers provides immediate and permanent online open access to all its publications, but this alone is not enough to realize our grand goals.

Frontiers Journal Series

The Frontiers Journal Series is a multi-tier and interdisciplinary set of open-access, online journals, promising a paradigm shift from the current review, selection and dissemination processes in academic publishing. All Frontiers journals are driven by researchers for researchers; therefore, they constitute a service to the scholarly community. At the same time, the Frontiers Journal Series operates on a revolutionary invention, the tiered publishing system, initially addressing specific communities of scholars, and gradually climbing up to broader public understanding, thus serving the interests of the lay society, too.

Dedication to Quality

Each Frontiers article is a landmark of the highest quality, thanks to genuinely collaborative interactions between authors and review editors, who include some of the world's best academicians. Research must be certified by peers before entering a stream of knowledge that may eventually reach the public - and shape society; therefore, Frontiers only applies the most rigorous and unbiased reviews.
Frontiers revolutionizes research publishing by freely delivering the most outstanding research, evaluated with no bias from both the academic and social point of view. By applying the most advanced information technologies, Frontiers is catapulting scholarly publishing into a new generation.

What are Frontiers Research Topics?

Frontiers Research Topics are very popular trademarks of the Frontiers Journals Series: they are collections of at least ten articles, all centered on a particular subject. With their unique mix of varied contributions from Original Research to Review Articles, Frontiers Research Topics unify the most influential researchers, the latest key findings and historical advances in a hot research area! Find out more on how to host your own Frontiers Research Topic or contribute to one as an author by contacting the Frontiers Editorial Office: frontiersin.org/about/contact

MICRONUTRIENTS: THE BORDERLINE BETWEEN THEIR BENEFICIAL ROLE AND TOXICITY IN PLANTS

Topic Editors:
Antonios Chrysargyris, Cyprus University of Technology, Cyprus
Monica Höfte, Ghent University, Belgium
Nikos Tzortzakis, Cyprus University of Technology, Cyprus
Spyridon Alexandros Petropoulos, University of Thessaly, Greece
Francesco Di Gioia, The Pennsylvania State University (PSU), United States

Citation: Chrysargyris, A., Höfte, M., Tzortzakis, N., Petropoulos, S. A., Di Gioia, F., eds. (2022). Micronutrients: The Borderline Between Their Beneficial Role and Toxicity in Plants. Lausanne: Frontiers Media SA. doi: 10.3389/978-2-88974-621-7

Table of Contents

05 ***Editorial: Micronutrients: The Borderline Between Their Beneficial Role and Toxicity in Plants***
Antonios Chrysargyris, Monica Höfte, Nikos Tzortzakis, Spyridon A. Petropoulos and Francesco Di Gioia

08 ***Boron: More Than an Essential Element for Land Plants?***
Greice Leal Pereira, João Antonio Siqueira, Willian Batista-Silva, Flávio Barcellos Cardoso, Adriano Nunes-Nesi and Wagner L. Araújo

18 ***Evidences for a Nutritional Role of Iodine in Plants***
Claudia Kiferle, Marco Martinelli, Anna Maria Salzano, Silvia Gonzali, Sara Beltrami, Piero Antonio Salvadori, Katja Hora, Harmen Tjalling Holwerda, Andrea Scaloni and Pierdomenico Perata

36 ***Advances in Mineral Nutrition Transport and Signal Transduction in Rosaceae Fruit Quality and Postharvest Storage***
Qian Bai, Yuanyue Shen and Yun Huang

48 ***New Aspects of Uptake and Metabolism of Non-organic and Organic Iodine Compounds—The Role of Vanadium and Plant-Derived Thyroid Hormone Analogs in Lettuce***
Sylwester Smoleń, Małgorzata Czernicka, Iwona Kowalska, Kinga Kęska, Maria Halka, Dariusz Grzebelus, Marlena Grzanka, Łukasz Skoczylas, Joanna Pitala, Aneta Koronowicz and Peter Kováčik

74 ***Effectiveness of Foliar Biofortification of Carrot With Iodine and Selenium in a Field Condition***
Roksana Rakoczy-Lelek, Sylwester Smoleń, Marlena Grzanka, Krzysztof Ambroziak, Joanna Pitala, Łukasz Skoczylas, Marta Liszka-Skoczylas and Hubert Kardasz

90 ***Effect of the Boron Concentration in Irrigation Water on the Elemental Composition of Edible Parts of Tomato, Green Bean, Potato, and Cabbage Grown on Soils With Different Textures***
Márk Rékási, Péter Ragályi, Anna Füzy, Nikolett Uzinger, Péter Dobosy, Gyula Záray, Nóra Szűcs-Vásárhelyi, András Makó and Tünde Takács

103 ***Iron Deficiency Leads to Chlorosis Through Impacting Chlorophyll Synthesis and Nitrogen Metabolism in* Areca catechu *L.***
Jia Li, Xianmei Cao, Xiaocheng Jia, Liyun Liu, Haowei Cao, Weiquan Qin and Meng Li

120 ***Biofortification of Sodium Selenate Improves Dietary Mineral Contents and Antioxidant Capacity of Culinary Herb Microgreens***
Rachel G. Newman, Youyoun Moon, Carl E. Sams, Janet C. Tou and Nicole L. Waterland

129 ***Migration of Chlorine in Plant–Soil–Leaching System and Its Effects on the Yield and Fruit Quality of Sweet Orange***
Xiaodong Liu, Chengxiao Hu, Zongying Zhu, Muhammad Riaz, Xiaoman Liu, Zhihao Dong, Yu Liu, Songwei Wu, Zhenhua Tan and Qiling Tan

141 ***Variability in Physiological Traits Reveals Boron Toxicity Tolerance in Aegilops Species***
Mohd. Kamran Khan, Anamika Pandey, Mehmet Hamurcu, Zuhal Zeynep Avsaroglu, Merve Ozbek, Ayse Humeyra Omay, Fevzi Elbasan, Makbule Rumeysa Omay, Fatma Gokmen, Ali Topal and Sait Gezgin

156 ***Insights Into Manganese Solubilizing* Bacillus *spp. for Improving Plant Growth and Manganese Uptake in Maize***
Ayesha Ijaz, Muhammad Zahid Mumtaz, Xiukang Wang, Maqshoof Ahmad, Muhammad Saqib, Hira Maqbool, Ahmad Zaheer, Wenqiang Wang and Adnan Mustafa

174 ***Physiological and Morphological Responses of Hydroponically Grown Pear Rootstock Under Phosphorus Treatment***
Guodong Chen, Yang Li, Cong Jin, Jizhong Wang, Li Wang and Juyou Wu

188 ***Cobalt: An Essential Micronutrient for Plant Growth?***
Xiu Hu, Xiangying Wei, Jie Ling and Jianjun Chen

212 ***Characterization of Metal Tolerance Proteins and Functional Analysis of GmMTP8.1 Involved in Manganese Tolerance in Soybean***
Jifu Li, Rongshu Dong, Yidan Jia, Jie Huang, Xiaoyan Zou, Na An, Jianling Song and Zhijian Chen

228 ***Interaction Effects of Nitrogen Rates and Forms Combined With and Without Zinc Supply on Plant Growth and Nutrient Uptake in Maize Seedlings***
Yanfang Xue, Wei Yan, Yingbo Gao, Hui Zhang, Liping Jiang, Xin Qian, Zhenling Cui, Chunyan Zhang, Shutang Liu, Huimin Wang, Zongxin Li and Kaichang Liu

240 ***Bioactive Nutrient Fortified Fertilizer: A Novel Hybrid Approach for the Enrichment of Wheat Grains With Zinc***
Muhammad Asif Ali, Farrukh Naeem, Nadeem Tariq, Ijaz Ahmed and Asma Imran

frontiers in Plant Science

EDITORIAL
published: 11 February 2022
doi: 10.3389/fpls.2022.840624

Editorial: Micronutrients: The Borderline Between Their Beneficial Role and Toxicity in Plants

Antonios Chrysargyris[1], Monica Höfte[2]*, Nikos Tzortzakis[1]*, Spyridon A. Petropoulos[3]* and Francesco Di Gioia[4]**

[1] Department of Agricultural Sciences, Biotechnology and Food Science, Cyprus University of Technology, Limassol, Cyprus, [2] Department of Plants and Crops, Ghent University, Ghent, Belgium, [3] Department of Agriculture, Crop Production and Rural Environment, University of Thessaly, Magnissia, Greece, [4] Department of Plant Science, The Pennsylvania State University, University Park, PA, United States

Keywords: mineral nutrition, plant metabolism, human health, toxicity, deficiency

Editorial on the Research Topic

Micronutrients: The Borderline Between Their Beneficial Role and Toxicity in Plants

OPEN ACCESS

Edited and reviewed by:
Levent Ozturk,
Sabancı University, Turkey

****Correspondence:***
Antonios Chrysargyris
a.chrysargyris@cut.ac.cy
Monica Höfte
Monica.Hofte@ugent.be
Nikos Tzortzakis
nikolaos.tzortzakis@cut.ac.cy
Spyridon A. Petropoulos
spetropoulos@uth.gr
Francesco Di Gioia
fxd92@psu.edu

Specialty section:
This article was submitted to Plant Nutrition, a section of the journal Frontiers in Plant Science

Received: *21 December 2021*
Accepted: *17 January 2022*
Published: *11 February 2022*

Citation:
Chrysargyris A, Höfte M, Tzortzakis N, Petropoulos SA and Di Gioia F (2022) Editorial: Micronutrients: The Borderline Between Their Beneficial Role and Toxicity in Plants. Front. Plant Sci. 13:840624. doi: 10.3389/fpls.2022.840624

MICRONUTRIENTS: INTRODUCTION

Plant nutrition management in commercial crops through the application of macro and micronutrients is essential not only for achieving high yields but also for fulfilling market requirements for high quality end-products (Sarwar et al., 2010). Common nutrition practices focus on the application of macronutrients through synthetic fertilizers without considering micronutrients (Baldantoni et al., 2019). In addition, it is not uncommon the irrational use of excessive fertilizer rates which may result in soil and/or ground water contamination and phytotoxicity (Ayoub, 1999). Recent research focusing on crop micronutrient management revealed several mechanisms involved in micronutrients' uptake and translocation in plants, and their role in plant physiological processes (Thapa et al., 2021). Moreover, several reports suggest specific strategies that could help toward the optimization of micronutrients application management in modern crop production (Shukla et al., 2021).

Apart from their role in plant growth and development, micronutrients are also essential in plant tolerance against stressors and in plant innate immunity, by being involved in metabolic processes that control plant response and perception to stressors (Jan et al., 2022). However, despite the well-proven beneficial role of micronutrients, excessive applications of such nutrients may lead to plant toxicity, soil contamination and environmental problems, and detrimental health effects (Rehman et al., 2019). Moreover, considering that plant-derived micronutrients are essential for human health, another important aspect in crop nutrition is the biofortification of end-products with micronutrients that could help fighting against mineral deficiencies that plague a great part of world population (Di Gioia et al., 2019).

The present Research Topic gathers several studies that focus on the beneficial role of micronutrients in plant nutrition, while aiming at the same time to set the borderlines between excessive use and deficiencies in plant development.

MICRONUTRIENTS: THE BORDERLINE BETWEEN BENEFICIAL ROLES AND TOXICITY IN PLANTS

The review article of Bai et al. provides insights into the function, transport, and signal transduction of mineral nutrients associated with Rosaceae fruit quality, and

postharvest storage at physiological and molecular levels. The role of nitrogen (N), phosphorus (P) and iron (Fe) was pointed, affecting fruit quality, interaction with other minerals and increasing oxidative stress response and antioxidant enzymes activities. This knowledge will contribute to provide theoretical basis to improve fertilizer use efficiency and the sustainable development of the fruit industry. Crop micronutrients uptake is influenced by macronutrients levels. In this context, Chen et al. studied the effect of P in hydroponically grown pear seedlings, observing that higher P rates decreased *zinc (Zn)*, *copper (Cu)* and *manganese (Mn)* and enhanced *boron (B)* and to some extent *Fe* content. *Chlorine (Cl)* is another micronutrient essential for plant growth. Liu et al. investigated the importance of Cl-containing fertilizers on citrus production and reported increased yield, vitamin C, and improved flavor and juice yield of citrus via enhanced N and K content. Moreover, the application of Cl-containing fertilizer may limit the risk of excessive sulfur (S) in citrus production. *Zinc* biofortification and the importance of Zn in human health is reported by Ali et al., who evaluated the effects of a bioactive nutrient fortified fertilizer containing Zn on 15 wheat varieties. The study revealed that beneficial microbes coated on urea were an effective biofortification means for Zn, resulting in increased Zn uptake and wheat yield. Xue et al. reported that Zn accumulation in maize improved with increasing N rates. The nitrogen form also affected the accumulation of Zn, with NH_4^+ nutrition being effective in enhancing tolerance of maize seedlings to Zn-deficiency stress.

Another important micronutrient is Fe whose deficiency can cause chlorosis in many crops. Li, Cao et al. studied Fe deficiency in *Areca catechu* (L.) seedlings and reported chloroplast degeneration and reduced chlorophyll synthesis in chlorotic leaves. Iron-deficient plants showed a down-regulation of nitrate reductase and glutamate synthase gene expression but accumulated more organic acids and flavonoids. In the case of Fe excess, peroxidase-related genes were upregulated as a defense strategy against Fe toxicity.

Manganese is an essential micronutrient for plant growth as it is involved in the structure of photosynthetic proteins and enzymes. However, Mn deficiency might be observed in dry, calcareous and sandy soils, resulting in crop yield reduction. Ijaz et al. studied Mn solubilization and the ability of *Bacillus* spp. strains to solubilize Mn. The Mn-solubilizing bacterial strains were isolated from the maize rhizosphere and could be used as potential bioinoculants to promote plant growth under Mn deficiency. On the other hand, Mn in excess can be toxic to plants as reported by Li, Dong et al., who suggested that metal tolerance proteins (MTPs) may play a critical role in Mn tolerance in plants, including soybean (*Glycine max*). In the same study, it was demonstrated that GmMTP8.1, an endoplasmic reticulum-localized Mn transporter, contributes to confer Mn tolerance by stimulating export of Mn out of leaf cells and increasing sequestration of Mn into intracellular compartments.

Boron is another key micronutrient required for plant growth and development, but causing severe symptoms of phytotoxicity when applied in excess. Khan et al. investigated different B levels in 19 *Aegilops* accessions and one bread wheat cultivar. The impact of B toxicity stress affected growth parameters, with more pronounced effects on shoots rather than roots. In this study, it was also proposed that some of the studied *Aegilops* accessions could potentially be used for developing introgression lines or as pre-breeding material to genetically improve B toxicity-tolerance traits. In another study, Rékási et al. reported that in tomato, green bean, potato, and cabbage irrigated with water containing 0.1 or 0.5 mg/L of B and grown in different soil types, the accumulation of B in plant tissue was influenced by plant species and soil type. Moreover, irrigation with 0.1 mg/L B accelerated tomato fruit ripening and doubled chlorophyll content while 0.5 mg/L B negatively affected green beans nutritional value. Additionally, Pereira et al. reported that when B is absorbed by the roots, it is preferably distributed to developing tissues, such as meristems and reproductive organs. This highlights the potential role of B in mediating plant development programs, by promoting the transition from the vegetative to reproductive phase, as well as enabling land plants to complete their life cycle. Indeed, understanding the mechanisms behind the accepted (and potential) functions of B may help to elucidate how and to what extent B is an important element for plants.

Agronomic biofortification is a new approach used to enhance mineral content in plant tissue and as such may prevent nutritional deficiencies and chronic diseases in humans. Examining the biofortification of several herbs with *selenium (Se)*, Newman et al. found that biofortification not only increased Se levels, but also enhanced total phenols and antioxidant capacity, turning crops tested into functional food. Rakoczy-Lelek et al. also reported on the effectiveness of foliar biofortification of carrots with Se and *iodine (I)* and found that levels of Se and I translocated from leaves to the storage roots were within ranges considered safe for consumption. However, no synergistic or antagonistic interaction between Se and I was observed in terms of biofortification effectiveness in roots, suggesting the possibility to biofortify carrots with multiple minerals. Additional work on I uptake, translocation and metabolism in lettuce was performed by Smoleń et al. by testing different sources of I whether or not combined with vanadium (V) fertilization. The study revealed that several genes (i.e., *per64-like*, *samdmt*, *msams5*, and *cipk6*) played a functional role. It was proposed that the protein encoded by *cipk6* may function as a triiodothyronine (T3) or thyroxine (T4) receptor, mainly in lettuce roots. Additionally, the *per64-like*, rather than the *per12-like* gene, may encode a V-dependent haloperoxidase (vHPO), an enzyme that participates in I uptake. New evidence for the nutritional role of I in plants is reported by Kiferle et al. I specifically regulates the expression of genes involved in the plant defense response, suggesting that I may protect against both biotic and abiotic stress. Additionally, I is functionally involved in plant nutrition, as proteomic analysis of I-treated *Arabidopsis thaliana* plants revealed that iodinated proteins identified in the shoots were mainly associated with the chloroplast and were functionally involved in photosynthetic processes, whereas those in the roots mostly belonged and/or were related to the activities of various peroxidases.

Finally, Hu et al. highlighted and proposed *cobalt (Co)* as an essential micronutrient for plants, as it is essential for many lower plants, such as marine algal species, as well

as for higher plants of the *Fabaceae* or *Leguminosae* family. Co is a component of several plant metabolic enzymes and proteins, with possible roles in key metabolisms, such as plant nitrogen fixation.

MICRONUTRIENTS: CONCLUDING REMARKS AND FUTURE PERSPECTIVE

The present Research Topic provides important updates on the essential role mineral micronutrients play in plant growth and development and highlights the complex interplay of factors contributing to determine plant micronutrients availability, uptake, transport, and metabolism. Required in a narrow range of concentrations, micronutrients are a common cause of stress for plants when in deficiency or in excess. This Research Topic contributes to define micronutrients fertilization and management strategies that are critical to ensure optimal plant growth and achieve high crop yield and quality standards. Moreover, considering plants are an important dietary source of micronutrients essential for human health, this Research Topic also emphasizes the pressing need to address micronutrient deficiencies affecting a large portion of the global human population. As such, it contributes to advance the development of sustainable strategies for the biofortification of food crops. Among those, agronomic biofortification proposed as an effective strategy for enhancing the micronutrient profile of target crops, emerges in this Research Topic as a new area of research that advances our understanding of micronutrients metabolism in plants while contributing to address nutrition security issues. Finally, besides providing an update of the state of the art of micronutrient research, this Research Topic offers a perspective on future research needs and priorities. Emerging areas of research related to micronutrients include investigating (i) micronutrient roles and function in plant metabolism and their uptake and transport within the plant as a function of different genetic and environmental factors; (ii) novel fertilizer management strategies to address plant micronutrient deficiency or toxicity stress, (iii) the use of plant grafting and epigenetic technology to address micronutrients deficiency and/or toxicity stress; (iv) sustainable strategies for the development of functional food through agronomic biofortification techniques, including the use of biofertilizers, biostimulants, supplemental artificial lighting, and micronutrient nanoparticles.

AUTHOR CONTRIBUTIONS

All authors listed have made a substantial, direct, and intellectual contribution to the work and approved it for publication.

REFERENCES

Ayoub, A. T. (1999). Fertilizers and the environment. *Nutr. Cycl. Agroecosyst.* 55, 117–121. doi: 10.1023/A:1009808118692

Baldantoni, D., Saviello, G., and Alfani, A. (2019). Nutrients and non-essential elements in edible crops following long-term mineral and compost fertilization of a Mediterranean agricultural soil. *Environ. Sci. Pollut. Res.* 26, 35353–35364. doi: 10.1007/s11356-018-3353-8

Di Gioia, F., Petropoulos, S. A., Ozores-Hampton, M., Morgan, K., and Rosskopf, E. N. (2019). Zinc and iron agronomic biofortification of Brassicaceae microgreens. *Agronomy* 9, 110677. doi: 10.3390/agronomy9110677

Jan, A. U., Hadi, F., Ditta, A., Suleman, M., and Ullah, M. (2022). Zinc-induced anti-oxidative defense and osmotic adjustments to enhance drought stress tolerance in sunflower (*Helianthus annuus* L.). *Environ. Exp. Bot.* 193, 104682. doi: 10.1016/j.envexpbot.2021.104682

Rehman, M., Liu, L., Wang, Q., Saleem, M. H., Bashir, S., Ullah, S., et al. (2019). Copper environmental toxicology, recent advances, and future outlook: a review. *Environ. Sci. Pollut. Res.* 26, 18003–18016. doi: 10.1007/s11356-019-05073-6

Sarwar, N., Saifullah, Malhi, S. S., Zia, M. H., Naeem, A., Bibi, S., et al. (2010). Role of mineral nutrition in minimizing cadmium accumulation by plants. *J. Sci. Food Agric.* 90, 925–937. doi: 10.1002/jsfa.3916

Shukla, A. K., Behera, S. K., Tripathi, R., Prakash, C., Nayak, A. K., Kumar, P. S., et al. (2021). Evaluation of spatial spreading of phyto-available sulphur and micronutrients in cultivated coastal soils. *PLoS ONE* 16, 1–16. doi: 10.1371/journal.pone.0258166

Thapa, S., Bhandari, A., Ghimire, R., Xue, Q., and Kidwaro, F. (2021). Managing micronutrients for improving soil fertility, health, and soybean yield. *J. Sustain.* 11766, 1–15. doi: 10.3390/su132111766

Conflict of Interest: The authors declare that the research was conducted in the absence of any commercial or financial relationships that could be construed as a potential conflict of interest.

Publisher's Note: All claims expressed in this article are solely those of the authors and do not necessarily represent those of their affiliated organizations, or those of the publisher, the editors and the reviewers. Any product that may be evaluated in this article, or claim that may be made by its manufacturer, is not guaranteed or endorsed by the publisher.

Copyright © 2022 Chrysargyris, Höfte, Tzortzakis, Petropoulos and Di Gioia. This is an open-access article distributed under the terms of the Creative Commons Attribution License (CC BY). The use, distribution or reproduction in other forums is permitted, provided the original author(s) and the copyright owner(s) are credited and that the original publication in this journal is cited, in accordance with accepted academic practice. No use, distribution or reproduction is permitted which does not comply with these terms.

frontiers in Plant Science

REVIEW
published: 14 January 2021
doi: 10.3389/fpls.2020.610307

Boron: More Than an Essential Element for Land Plants?

*Greice Leal Pereira, João Antonio Siqueira, Willian Batista-Silva, Flávio Barcellos Cardoso, Adriano Nunes-Nesi and Wagner L. Araújo**

Departamento de Biologia Vegetal, Universidade Federal de Viçosa, Viçosa, Brazil

Although boron (B) is an element that has long been assumed to be an essential plant micronutrient, this assumption has been recently questioned. Cumulative evidence has demonstrated that the players associated with B uptake and translocation by plant roots include a sophisticated set of proteins used to cope with B levels in the soil solution. Here, we summarize compelling evidence supporting the essential role of B in mediating plant developmental programs. Overall, most plant species studied to date have exhibited specific B transporters with tight genetic coordination in response to B levels in the soil. These transporters can uptake B from the soil, which is a highly uncommon occurrence for toxic elements. Moreover, the current tools available to determine B levels cannot precisely determine B translocation dynamics. We posit that B plays a key role in plant metabolic activities. Its importance in the regulation of development of the root and shoot meristem is associated with plant developmental phase transitions, which are crucial processes in the completion of their life cycle. We provide further evidence that plants need to acquire sufficient amounts of B while protecting themselves from its toxic effects. Thus, the development of *in vitro* and *in vivo* approaches is required to accurately determine B levels, and subsequently, to define unambiguously the function of B in terrestrial plants.

Keywords: B deficiency, developmental programs, meristem regulations, metabolism, shoot growth, root growth

OPEN ACCESS

Edited by:
Spyridon Alexandros Petropoulos, University of Thessaly, Greece

Reviewed by:
Ibrahim Ilker Ozyigit, Marmara University, Turkey
Cuncang Jiang, Huazhong Agricultural University, China

****Correspondence:***
Wagner L. Araújo
wlaraujo@ufv.br

Specialty section:
This article was submitted to Plant Nutrition, a section of the journal Frontiers in Plant Science

Received: *25 September 2020*
Accepted: *18 December 2020*
Published: *14 January 2021*

Citation:
Pereira GL, Siqueira JA, Batista-Silva W, Cardoso FB, Nunes-Nesi A and Araújo WL (2021) Boron: More Than an Essential Element for Land Plants? Front. Plant Sci. 11:610307. doi: 10.3389/fpls.2020.610307

THE COMPLEXITY THAT LIES BEHIND THE ELEMENT BORON

Boron (B) was first described in the 1920s by a demonstration wherein *Vicia faba* L. (field bean) and other plants exhibited reduced root growth in the absence of B, but this could partially be rescued following the resupply of B (Warington, 1923). Later, it was suggested that B might play a pivotal role during the transition from aquatic to terrestrial environments, driving this evolutionary transition in plants (Lewis, 1980). Similarly, studies on the first vascular plant *Zosterophyllum shengfengense* suggested that B is primordial and originated in the root system in the terrestrial environment (Lewis, 1980).

In land plants, B plays important functions, including a structural role in cell walls, maintenance of plasma membrane functions, stimulation of reproductive tissues, and improvement of seed quality, and is influential in the biosynthesis of some metabolic compounds, such as antioxidants and polyphenols (Cakmak and Römheld, 1997; Marschner, 2012). Additionally, this element is involved in nucleic acid synthesis, phenolic metabolism, carbohydrate biosynthesis and translocation, pollen tube growth, and root elongation as well as it decrease indole-3-acetic acid (IAA) oxidase activity and, therefore, increased IAA content (Brown et al., 2002; Shireen et al., 2018; Landi et al., 2019). However, the molecular mechanisms underlying these functions remain largely unknown. Nevertheless, compelling evidence has demonstrated an elaborate system involved in both the uptake and transport of B in different plants (Miwa and Fujiwara, 2010). It was previously believed that the uptake process is exclusively passive and unregulated; however, it is now evident that plants detect the external and internal conditions of B, regulating and modulating the expression and/or accumulation of specific transporters in roots and shoots to maintain B homoeostasis in the plant (Miwa and Fujiwara, 2010).

Recently, from another perspective, B was assumed to be a rather toxic element, causing substantial damage to plant cells even at low levels (Reid et al., 2004; Landi et al., 2019). Moreover, B essentiality is questionable considering that the responses to its deficiency are largely caused by the toxicity of phenylpropanoids (Lewis, 2019). It is noteworthy that alleles mediating tolerance to high levels of B in the soil remain in the wheat elite cultivar genomes following the selection of wild breeds cultivated by the first farmers in the Mediterranean region (Pallotta et al., 2014). Remarkably, these tolerance alleles are widespread in elite wheat cultivars developed in countries with soils containing extremely low levels of B. Evidence of a genetic distribution correlated to B levels in soils from different geographic regions suggests the possibility of alternative roles in contrasting environments. Collectively, this implies that combining B tolerance alleles with the level of B in the soil is important for mediating plant developmental programs. Accordingly, B can induce molecular pathways, which correspond to a series of actions among molecules in a cell that can turn genes on and off, thereby regulating developmental phase transitions (**Figure 1**). These transitions are involved in the coordination of the transition of plants to the adult phase (Redondo-Nieto et al., 2012; Lu et al., 2014; Xu et al., 2016; Kobayashi et al., 2018; Sakamoto et al., 2018).

Over the last century, several independent and complementary studies have provided compelling evidence for the involvement of B and its significance for plant development and growth. Remarkably, this aspect was recently contested based on metabolic responses that might be confused with B deficiency responses. Here, we summarize the complex B relationships in the soil, as well as how these relationships might influence an elaborate system of transporters governing B uptake from the rhizosphere. We further discuss the preferential B distribution and remobilization among tissues and their functional implications. Furthermore, we revisit the functions of B in mediating single genetic mechanisms in meristem cells, which might contribute to explaining the essentiality of this element. Finally, we provide compelling evidence supporting the essentiality of B in mediating plant developmental programs. We further posit that the development of new tools to precisely determine B levels *in vivo* is necessary to unequivocally demonstrate the essentiality of B.

BORON DYNAMICS AND TRANSPORT INSIDE PLANTS

The patterns of B distribution in the rhizosphere and B behavior in the soil directly affect its availability to plants. The soil solution contains predominantly boric acid (H_3BO_3) and borate anion [$B(OH)_4^-$], in which the chemical equilibrium strongly depends on the soil pH (Klochko et al., 2006). Another variable that strongly influences the physicochemical properties of H_3BO_3 is the ionization constant (pK_a). Generally speaking, pK_a can be defined as the pH of a solution where the concentration of the undissociated species is equal to that of the ionized species, that is, [HA] = [A]. Thus, in solutions with pH lower than pK_a, there is a higher H_3BO_3 concentration. At higher pH, the form $B(OH)_4^-$ predominates. Because of its small ionization constant (pK_a 9.25), H_3BO_3 is the predominant form under conditions of pH below the pK_a (Tanaka and Fujiwara, 2008).

Following the mass flow phenomenon, B is directed to the roots where this nutrient might be taken up from the soil solution (Marschner, 2012). Both metabolic and non-metabolic processes predominantly regulate the B uptake mechanisms. The mechanism of passive diffusion through the plasma membrane is considered an exclusive process for B uptake by roots (Nable et al., 1990; Brown and Hu, 1994; Hu and Brown, 1997). However, field results revealed significant differences in both the concentration and total B content between different species and genotypes cultivated under identical conditions (Nable, 1988). This suggests that the differences in B uptake between species are possibly caused by differences in membrane permeability to boric acid/borate (Huang and Graham, 1990; Hu and Brown, 1997) and that the absorption of B through lipid bilayers occurs through a combination of passive transport (diffusion) and possibly transport mediated by channels (Dordas et al., 2000). Intriguingly, by combining genetic and biochemical approaches, the presence of B-specific transporters was demonstrated not only in roots but also in leaves and reproductive organs (Takano et al., 2008; Chatzissavvidis and Therios, 2011).

The activity of B transporters is tightly regulated in response to the levels of B in the soil solution, optimizing B uptake and use, and maintaining nutrient homoeostasis in different plant tissues (Takano et al., 2008; Yoshinari and Takano, 2017). Briefly, plants control the capture and transport of B through the rapid regulation of two different classes of B transporters, namely, the channels of the MAJOR INTRINSIC PROTEIN (MIP) family and the boric acid/borate transporters of the BOR family (Matthes et al., 2020). The Nodulin 26-like intrinsic protein (NIP) family contains the major B transporters, including the root transporters NIP5;1 (boric acid channel) and BOR1 (boric acid/borate exporter), which are assumed to be the proteins responsible for maintaining B homoeostasis (Takano et al., 2008).

NIP5;1 is located preferentially on the plasma membrane, with its polarity facing the soil side (Takano et al., 2006; Wang et al., 2017), whereas BOR1 is also located on the plasma membrane but with its polarity toward to stela, playing a key role in xylem loading (Wakuta et al., 2016; Yoshinari et al., 2019). According to the activities of these transporters, the directional and radial B transport from the soil solution into xylem is mediated under low soil levels of B (Sakamoto et al., 2011). From there, B is mobilized into the xylem and transported through the flow to the shoot (Matthes et al., 2020).

In contrast, under excess B, the transporter BOR4 is involved with B exclusion from cells and tissues, enhancing tolerance to B toxicity (Miwa et al., 2007; Yoshinari et al., 2019). Additionally, NIP6;1 corresponds to a channel that facilitates the permeability of boric acid across the plasma membrane and was recently considered completely impermeable to water (Tanaka et al., 2016). NIP6;1 transcript accumulation occurs in response to B deficiency. This transporter is predominantly expressed in the stem node regions, mainly in the phloem region (Tanaka et al., 2016). Thus, a sophisticated system for B uptake and translocation based on the families NIP and BOR is present in land plants, in which the expression of NIP5 isoforms is highly induced in both roots and shoots (Diehn et al., 2019; **Figure 1**).

In agreement with the differential activity of B transporters across distinct plant organs, it has been demonstrated that, with the aid of mathematical and computer science tools, the function of B transporters can be effectively predicted and experimentally validated in different species. For instance, by using the FORESTS database, a BOR1 homolog was found in *Eucalyptus* (Domingues et al., 2005), whereas the recent usage of 18 different plant genomes allowed the identification of 80 and 34 homologs of BOR1 and NIP5;1, respectively (Ozyigit et al., 2020). In addition, Kurt and Aydın (2020) identified and characterized five BOR1 transporters in potato (*Solanum tuberosum*) by using an *in silico* study. By performing an extensive co-expression network of each transporter, it was revealed that (i) there is a potential interaction between B transporters and genes involved in cell wall and (ii) a co-expression between StBOR1 transporters and plant immunity system (Kurt and Aydın, 2020). Thus, the identification of similar sequences for B transporters in different plants species reinforces the motion that those genes are most likely members of highly conserved gene families in plants that are expressed in different plant tissues/organs and involved in many biological processes (Yoshinari and Takano, 2017; Diehn et al., 2019). We posit that the combination of experimental research with

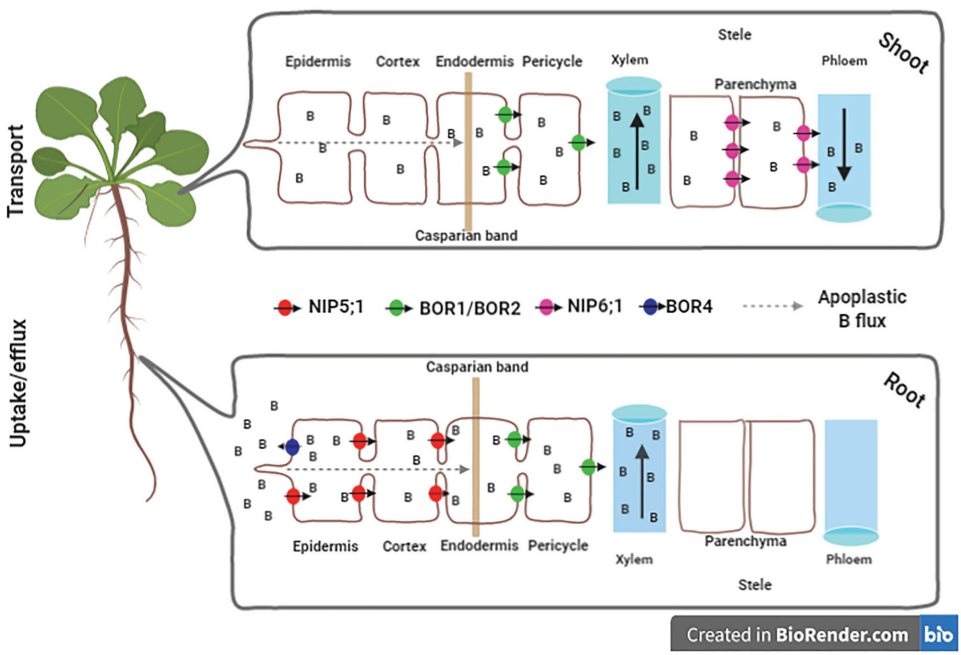


FIGURE 1 | Overview of homeostasis of the boron (B) levels in plant cell mediated by transports. In *Arabidopsis thaliana* roots, B homeostasis is mainly based on three transport mechanisms across the plasma membrane. The first is the simple diffusion of boric acid (H_3BO_3), without charge through the lipid bilayers. The second mechanism represents the facilitated diffusion mediated by channels of the aquaporin family, such as NIP5;1. The third refers to the B movement by specific transports (e.g., BOR 1, BOR2, and BOR4). The uptake channels NIP5;1 is expressed in the plasma membranes of root cap and epidermal cells with outside/soil-facing polarity (Takano et al., 2006; Wang et al., 2017). NIP5;1 mediates the efficient radial transport of B from the soil through the epidermis and cortex to the endoderm. The Casparian band developed in the endoderm limits the apoplastic flow of B to the stele. BOR1 and BOR2 are expressed at the endodermis in meristematic and maturation zones (Miwa et al., 2013; Reid, 2014; Yoshinari et al., 2019). BOR1 and BOR2 are polarly localized in the stele-side plasma membrane domain (Takano et al., 2010; Miwa et al., 2013). BOR4 located in the root epidermis aid in the efflux of B from the root to the soil solution (Miwa et al., 2007). In shoots, NIP6;1 is necessary for the transport of B from xylem to phloem in nodal regions, being located in the parenchyma of the stele (Tanaka et al., 2016). Figures were created using the software biorender (app.biorender.com).

theoretical and predictory approaches are fundamental to adequately understand the precise regulation and function of B transporters in both model and non-model plant species.

Using a mathematical modeling approach, it has been recently demonstrated that the precise regulation of the abundance of transporters ensures constant B concentration in the root cells (Matthes et al., 2020). Accordingly, transcripts encoding NIP members were also detected in floral tissues and showed expression patterns dependent on the developmental stage, which appeared to contribute to B distribution in the flowers of B-deficient plants (Diehn et al., 2019). In maize (*Zea mays*), double mutants for functional homologs of BOR1 (*RTE* and *RTE2*) were characterized by a slow developmental time of the shoot apical meristem (SAM), which displays reduced fertility and small ears (Chatterjee et al., 2014, 2017). It appears reasonable to assume that an elaborate genetic network allows land plants to cope with B levels *via* a tightly regulated response to this nutrient.

Since large amounts of gene expression data are currently available, it seems reasonable to anticipate that the growing power of bioinformatics coupled with computational resources will open new avenues to discover proteins involved in B transport. In fact, the combination of computational and imaging tools is becoming a recurrent feature in studies of complex and dynamic characteristics in plants (Tsaftaris et al., 2016). However, the fundamental challenge is to understand the mechanisms underlying changes in time and space of B transporters. By coupling mathematics and experimental approaches, a two-dimensional cross-sectional model of the *Arabidopsis thaliana* root meristem was developed taking into account spatial nuances of the location, polarity, and intensity of the B transporters (Shimotohno et al., 2015). However, the levels and activity of the transporter were static. Nonetheless, a rapid regulation of B transporters, through the dynamic regulation of these transporters, was further observed (Sotta et al., 2017). Furthermore, a mathematical model was generated by capturing the spatio-temporal distribution of B through root cross sections (Sotta et al., 2017). In summary, the mapping of the vast majority of B transporters was found along the roots although B transport can occur at different rates along the roots since certain transporters have distinct locations.

Significant progress has been recently obtained with the use of X-ray crystallography allowing the establishment of the structure-function relationship of proteins involved in the transport of B, that plays an important role in the perception of B levels in different tissues (Hrmova et al., 2020). Understanding the three-dimensional (3-D) structure of a transporter provides crucial insights into its function, identifying the main motifs or residues that may interact with potential substrates. Notwithstanding this fact, the results of this model are rather incomplete and thus the combination of multidisciplinary studies to fully elucidate the precise molecular mechanisms, structural dynamics, and regulation of B transporters is seemingly still required (Hrmova et al., 2020). Under a high supply of B, the BOR1 accumulated in the plasma membrane is rapidly ubiquitinated and transported to multivesicular bodies (endocytosis), and subsequently targeted for the vacuole for degradation (Takano et al., 2010; Wakuta et al., 2016; Yoshinari et al., 2018). Recently, Yoshinari et al. (2019) observed that AP2-dependent endocytosis maintains the polar localisation of BOR1 to support plant growth under low-B conditions, whereas the B-induced vacuolar sorting of BOR1 is mediated through an AP2-independent endocytic pathway. This response was assumed to be important for plant acclimatization to high B conditions (Tanaka and Fujiwara, 2008). Curiously, B-transporter genes specific to wheat roots (*Triticum turgidum* L. var. Durum) which modulate adaptation for B in the soil, exhibited allele origin and dispersion worldwide, which is important for the tolerance to distinct B levels (Pallotta et al., 2014).

Thus, these tolerance alleles display a large natural variability mediating B responses, which appears to have been remodeled following selective breeding of elite cultivars because of the contrasting environments during selection (Pallotta et al., 2014). Collectively, compelling evidence obtained during the last decades indicates intrinsic relationships between B transporters and plant development in general, which exhibit evolutionary patterns that drive plant breeding, highlighting the importance of this element, and consequently, in contrast with characteristics of a toxic element. Remarkably, there is virtually no current evidence of any plant that evolved specific morphoanatomical or genetic mechanisms to deal with toxic levels of B, rather there is only the regulation of B transporters.

BORON TRANSLOCATION AND DISTRIBUTION

Following B uptake by the roots, transpiration drives B translocation through xylem cells (Marschner, 2012). By analyzing B tolerance, beyond intrinsic regulation mediated by transporters in distinctly tolerant species, it was possible to verify that differential B tolerance is also attributed to the ability to restrict nutrient translocation from roots into shoots, allowing a high B accumulation in roots. Plants with this capacity have been indicated for phytoremediation in areas with high levels of B (Xin and Huang, 2017).

Boron can also be transported *via* the phloem, allowing its translocation between vegetative and reproductive tissues (Camacho-Cristóbal et al., 2008), although this is highly variable among species. The mobility is due in part to B complexation with polyols. Accordingly, in restricted mobility plants, B is relatively immobile in phloem; therefore, the most common deficiency symptom can be observed in young leaves and meristematic tissue, which is related to the death of the apical meristem (Will et al., 2011; Marschner, 2012). Additionally, in certain plant species, including apples, nectarines, *Arabidopsis*, and citruses, B can be transported in the phloem in quantities that are sufficient to meet plant requirements (Brown and Hu, 1996; Takano et al., 2001; Wu et al., 2019). The transport of B *via* phloem occurs by the formation of B-diol complexes, which are important for nutrient remobilization among tissues (Brown and Hu, 1996; Hu et al., 1997). B can easily bind to cis-hydroxyl groups of sugar alcohols (mannitol and sorbitol), allowing B to be transported through the phloem (Reid, 2014),

yet the translocated amount depends on the plant B status and the synthesis of photoassimilates (Du et al., 2020). It seems reasonable to suggest that the molecular aspects involved in both B translocation and remobilization are likely a critical knowledge barrier to B nutrition that must be further investigated to fully elucidate the essential nature of B for land plants.

The precise determination of B at the cellular level has not been achieved, given that the actual B measurements do not consider the dynamics of the element and the differential affinity of B for each B transporter. It has been suggested that the cytological content of B is the only B detection site, but detailed studies on B variation in other cell sites are lacking, such as in organelles. Therefore, it is clear that more detailed and high-resolution techniques are required and must consider the dynamics of this element in both space/time. Furthermore, its dynamics in living cells should be investigated. We posit that this may be achieved by the development of genetically encoded sensors or chemical sensors for H_3BO_3, similar to nanobiotechnology, which allows the development of intelligent plant sensors that communicate chemical signals and the physiological and nutritional state of plants (Giraldo et al., 2019). To this end, the conventional approach suggested is the measurement of B stable isotopes, namely ^{10}B and ^{11}B, allowing the analysis of B pools in plant tissues (Dannel et al., 2000). The recent application of ablation laser-ICP-MS (inductively coupled plasma mass spectrometry) allowed the development of a mathematical model that enabled the analysis of B distribution along roots of *A. thaliana* at an extremely high resolution (Shimotohno et al., 2015). To overcome the challenges of B detection in different plant tissues, the fluorinated-18 4-fluorophenylboronic acid radiotracer approach ([18F] FPBA) was recently used (Housh et al., 2020). The images obtained by autoradiography provided insightful information on the patterns of static B location in both root and shoot tissues (Housh et al., 2020), revealing different locations of B distribution. Briefly, both the root tip and the stretching zone are the ones that exhibited the most intense sign of the tracer with a region between the two devoid of any sign, showing a clear demand for B in these regions (Housh et al., 2020). Consequently, future studies using such tools are important to determine element distribution throughout the plant and behavior of specific tissue levels.

The revolution recently obtained by the development and characterization of genetically encoded biosensors for cytosolic H_3BO_3, based on the fluorescent proteins of the transporters NIP5; 1 and BOR1 (Fukuda et al., 2018), has contributed to the first visualization of B in living plant cells. The fluorescence intensity in roots and shoots of the transgenic plants was high under B-limiting conditions and gradually decreased with an increasing concentration of B (Fukuda et al., 2018), which confirms sensor functionality. Such biosensors allow not only the visualization of the distribution but also the dynamics of B at physiologically relevant levels in various tissue and cell types. As a result, these sensors can be used by a wider range of purposes, including determination of whether the phenotype studied is influenced by differences in the concentration of B, demonstrating the importance of B for plant growth and development. Therefore, it is clear that the revolution afforded by next-generation sequencing means that appropriate tools and resources are becoming available to fully unravel the function of B in different crops. Thus, it becomes necessary that tools such as *in situ* hybridizations (Thisse and Thisse, 2008), promoter-gene fusions (Van Dyk et al., 2001), metabolite sensors (Wang and Lei, 2018), single-cell sequencing (Hwang et al., 2018), and laser microdissection (Nelson et al., 2006) be collectively considered. We anticipate that this will open new avenues for understanding B dynamics and will ultimately allow increased plant yield by tailoring approaches to tap into more specific attributes of desired species.

BORON MEDIATING DEVELOPMENTAL TRANSITIONS IN BOTH SHOOTS AND ROOTS

The indirect concept of nutrient essentiality posits that, in the absence of determined plant nutrients, plants do not complete their life cycle (Arnon and Stout, 1939). In this context, developmental transitions are required for land plants to complete their life cycle, and these transitions are regulated through the proliferation and differentiation of cells. Recently, the organogenesis of both zebrafish (*Danio rerio*) and *A. thaliana* are B dependent, as revealed by alterations in N-glycosylation patterns that arrest cell fates during the development of both species (Reguera et al., 2019). Furthermore, by mimicking B depletion using phenylboronic acid (PBA), it was observed that *A. thaliana* wild type plants treated with PBA were similar to the rootless mutant *monopteros*, wherein PBA disrupts auxin transport dynamics during early embryo development (Matthes and Torres-Ruiz, 2016). Briefly, B depletion culminated with the development of irregular cotyledons, dramatic deformations of the vascular system, large vacuoles, and a reduced number of epidermal cells with the complete absence of root apical meristem (RAM; Matthes and Torres-Ruiz, 2016). Similarly, B transporters (e.g., BOR1 and NIP5;1) were used as reliable markers to study cell polarity axes during embryogenesis, whereas other genes failed to reveal the precise localisation of cell membranes resulting from asymmetric cell divisions in *Arabidopsis* embryos (Liao and Weijers, 2018). Indeed, BOR1 is an optimal gene marker for early embryo cells, whereas NIP5;1 provides more stable signals in late embryonic cells (Liao and Weijers, 2018; **Figure 2A**). Collectively, these results suggest an important role for B in mediating embryo development owing to B transporter localisation, which further indicates asymmetric cell division. Notably, highly specific induction of B transporters has been described for RAM and shoot apical meristem (SAM; Durbak et al., 2014; Sakamoto et al., 2019). Thus, it seems reasonable to suggest that B is most likely a direct regulator of cell division and differentiation, particularly at these specific sites, which is consistent with the fact that B is an essential micronutrient.

The preferential distribution of B in developing tissues of rice (*Oryza sativa*) is seemingly regulated in consonance with the expression of *NIP*, *OsNIP3;1* (Shao et al., 2018). Accordingly,

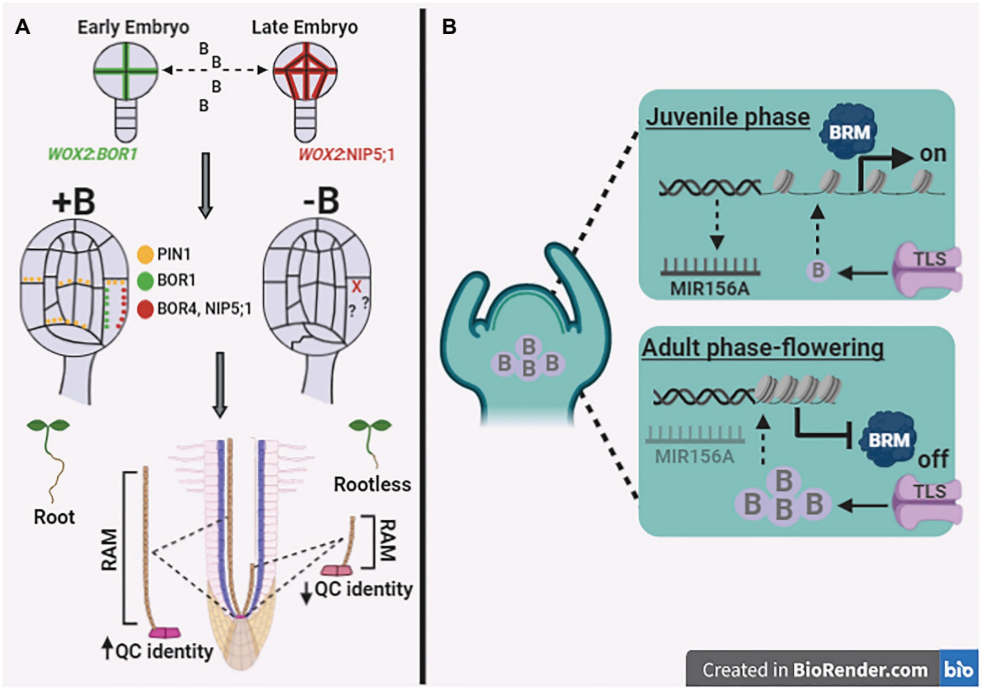


FIGURE 2 | Boron mediating crucial developmental processes in roots and shoots. **(A)** The asymmetric cell divisions at early embryos exhibit a remarkable pattern related to BOR1, whereas NIP5;1 are the better marker for these divisions on late embryogenesis, suggesting the B role in orientating embryo development. Curiously, the B deficiency induction on mature embryos alters not only BOR1 and NIP5;1 gene expression patterns but also disrupts auxin transport among the different cell-types impairing root apical meristem (RAM) formation, which result in a rootless *A. thaliana* plants. Furthermore, B deficiency on mature plants reduce length and identity of quiescent center (QC) at RAM, which altogether suggest that B display influence on overall root developmental stages. **(B)** Shoot apical meristem (SAM) exhibits the B transport differently regulated according with developmental phase, the TRUNCATED LEAF SYNDROME (TLS) transporter remobilize low B levels into SAM at juvenile phase. Apparently, the reduced levels of B enables the activity of Brahma (BRM) chromatin remodeler allowing the expression of miR156A, which arrest the flowering transition in juvenile tissues. The adult phase transition to flowering would be mediated by the increase on B levels at SAM, which would promote blocking of BRM activity, which represses miR156A expression releasing flowering induction. Dotted arrows indicate mechanisms not completely elucidated. Figures were created using the software biorender (app.biorender.com).

knockout plants for this gene exhibited reductions in B content in newly developed leaves coupled with improved B translocation to old leaves, suggesting that OsNIP3;1 plays a key role in the distribution of B in developing tissues (Shao et al., 2018). Furthermore, it has been demonstrated that B contributes to the maintenance of the identity of the root quiescent center (QC) and that B deficiency dramatically inhibits cell proliferation (Poza-Viejo et al., 2018). Cell division was strongly affected by B deficiency in the DNA replication phases in the RAM (Poza-Viejo et al., 2018). Furthermore, B deficiency reduced not only brassinolide accumulation but also RAM size and length of mature cells. Remarkably, these responses are dependent on the downregulation of brassinosteroid (BR) signaling genes, regardless of B transport and translocation (Zhang et al., 2019). Exogenous application of 24-epibrassinolide (eBL), a bioactive BR, rescued root growth inhibition under B deficiency, and application of the BR biosynthesis inhibitor, BRZ, aggravates root growth inhibition of wild type plants under B deficiency. Taken together, these results indicate that B deficiency downregulates BR signaling to inhibit root growth. B starvation positively regulates the expression of SHORT ROOT (SHR) and SCARECROW (SCR) genes, which can further induce the expression of miR 165 enabling *PHABULOSA* (PHB) to reduce the influence of cytokinins on root development (Lu et al., 2014). Under low B levels, NIP5;1 facilitates B influx into the roots, whereas protein activity is increased in the RAM following the transference of roots from low B levels to optimal B levels (Gómez-Soto et al., 2019). Together, these studies demonstrated that both meristem activity and fate are regulated in response to B levels, and collectively suggest that this micronutrient is of pivotal significance in mediating the developmental phase transitions of plants.

Mechanisms associated with root organogenesis are extremely sensitive to B deficiency, and they are likely regulated through B signaling (Abreu et al., 2014). By using mathematical modeling and further experimental validation, it was established that B flux does not display a continuous increase from root tips toward the mature zone (Shimotohno et al., 2015). Accordingly, B absorbed at the root tip is likely used only at this root site, whereas the mature root zones display higher importance to drive B transport for the shoot (Shimotohno et al., 2015). It is also important to mention that B acts by blocking the accumulation of aluminium (Al) in the apical root zone (Li et al., 2018), where Al might induce QC differentiation

and reduce cell division and root elongation. This is in agreement with the hypothesis that B plays a protective role in the RAM. Moreover, the reduced cell differentiation observed in *Medicago sativa* root nodules under B deprivation indicated that B plays specific functions in the initial phases of root organogenesis (Reguera et al., 2009). Additionally, B increases the degree of methyl esterification of pectin in the root apex, indicating higher plant resistance to Al toxicity because of increased cell wall plasticity (Riaz et al., 2018).

Genomic factors that induce cell differentiation and are involved in damage to DNA and DNA double-strand breaks (DSB) are triggered by high levels of B in plants (Hu et al., 2016). DSB induced under toxic B levels might be mitigated through the degradation of BRAHMA (BRM) protein, given that BRM binds to acetylated histone residues opening chromatin and causes to be DNA more exposed to B-related damage (Sakamoto et al., 2018). Additionally, BRM temporally regulates the expression of miR156, the master regulator of the transition from the juvenile to the adult phase, and as such, mutations in BRM accelerated the exit from the vegetative phase (Xu et al., 2016). B transport is critical for vegetative and reproductive maize development, where Tassel-Less1 (TLS1) protein facilitates meristematic B transport, which appears to be fundamental to meristem fate and inflorescence development (Durbak et al., 2014). Briefly, during the juvenile phase, there is an increased activity of BRM, allowing the expression of miR156A, which inhibits TLS and interrupts the flowering transition. On the other hand, the transition from the adult vegetative phase to flowering appears to be regulated by B transport, which reduces BRM activity and miR156A expression by releasing the flowering-TLS induction (**Figure 2B**).

Flowers are singular organs representing the last developmental phases; therefore, it is not surprising that efforts should be made to understand flower development and the roles B plays in this process, which is an exciting yet understudied field of plant biology. It has been demonstrated that NIP7;1, a facilitator of boric acid transport, is predominantly expressed in young flower anthers in a narrow developmental window (Routray et al., 2018). Accordingly, *nip7;1* mutants exhibit several defects in reproductive structures (Routray et al., 2018), indicating that proper control of B homoeostasis in both meristem and reproductive organs is critical for the biological success of vascular plants. Thus, this evidence suggests that obtaining and maintaining an optimal B level in flower-related tissues is often imperative for successful plant reproduction.

Because B has been described as an essential micronutrient (Warington, 1923), substantial advances in our understanding of B-related pathways have been achieved illustrating the role of B in plants. Nevertheless, Lewis (2019) argued against B essentiality for land plants by proposing an alternative point of view over the direct metabolic effect of B. Briefly, Lewis (2019) suggested that B is, and always has been, potentially toxic for plants and, perhaps more importantly, that this attribute must be fully avoided for normal growth, development, and reproduction. This assumption relies on the fact that not only B but also phenolics (compounds considered toxic for cellular metabolism) are interconnected. Thus, plants must have evolved the ability to mitigate adverse effects of both B and phenolics by chemical (such as organic complexes: *cis*-diols for B and lignins for phenolics) and physical (movement into vacuoles/apoplasts) sequestration (Lewis, 2019). Hence, B complexes formed in the cell wall are most likely a mechanism allowing detoxification of such compounds and cannot be presented as evidence of B essentiality. Here, we add further complications to this assumption given that our current knowledge concerning the micronutrient gradient and distribution among distinct organs and tissues is rather limited and requires significant advances in nutritional microscopic techniques (e.g., development of micronutrient specific sensors and nutritional living-microscopy). We posit here that the temporal control of micronutrient levels in different developmental phases could help to unequivocally describe the novel and specific roles of B. It is reasonable to assume that even minimal changes in the levels of B in specific organs (e.g., meristem, anthers, and flowers) have probably remained unnoticed in several studies; thus, this has led to the proposition that B is not an essential micronutrient. Although Lewis (2019) suggested that B is a toxic element with which plants have evolved to cope, we believe that the metabolic reprogramming suggested still must be unequivocally confirmed. One possible way is to use mutant plants in the biosynthetic pathways of the free neutralizing agents (e.g., polyphenols) suggested and investigate their response to different B levels, in conjunction with precise quantification methods. In this case, one must expect that such plants will display toxic effects at much higher B concentrations, without changing the levels of these compounds.

In contrast to the premise of Lewis (2020), we strongly argue that the gradually evolving function of B in the regulation of meristem fate discussed above highlights the potential role of this micronutrient at very low doses and during a very short development window. Therefore, we postulate that B essentiality should not be discussed only in the context of both the biomolecule constitution and from an unnoticed metabolic viewpoint, but also regarding its importance for specific cell types in RAM and SAM (**Figure 2**). It is reasonable to assume that B is likely able to induce cell proliferation and differentiation, triggering the proper development of vascular plants. Although our theoretical growth proposal is rather distinct from the theoretical metabolic mechanism postulated by Lewis (2020), we believe that this inference should be seriously considered when designing strategies to test B essentiality.

CONCLUSION AND FUTURE PERSPECTIVES

In recent years, the importance of B in plant growth and development has attracted much attention because its specific and complementary functions are not fully understood. However, significant advances have attested to the essentiality of this element for land plants. Nevertheless, Lewis (2019) purposely not only challenged the essentiality of B in the conventional sense but also speculated that it is toxic and as such cannot have a primary role. Although the biological speculation of

such a statement remained elusive, several exciting and testable research avenues were recently provided by Lewis (2019, 2020) and Matthes et al. (2020).

We further provide another alternative to unequivocally demonstrate the essentiality of B. Once B is absorbed by the roots, it is preferably distributed to developing tissues, such as meristems and reproductive organs. Although we cannot rule out the metabolic mechanism suggested previously (Lewis, 2019), this differential B distribution provides at least circumstantial evidence highlighting the potential role of B in mediating plant development programs, by promoting the transition from the vegetative to reproductive phase (**Figure 1**), as well as enabling land plants to complete their life cycle. To accurately understand the role of B and thus convincingly prove its essentiality, we argue the importance of developing new diagnostic tools that allow the detection of minimal changes in B levels in different tissues and specific cells. The discussion highlighted both in Lewis (2019) and here should attract research from different but complementary fields to investigate hypotheses and add analytical techniques to the "parts list" of B functions to test their application and relevance. Although the application of these techniques requires substantial financial investment, it is highly possible to bring returns in the form of improved mechanistic functions of B.

Neither Lewis (2019) nor we have provided experimental evidence to unequivocally demonstrate B essentiality (or not). However, it opens several research avenues that should be pursued. Lewis (2019) expertly presented a theoretical proposal for the metabolic mechanism by which B toxicity is not only overcome but also put to reasonably good purpose in particular circumstances. Future directions of research are also accurately presented with several independent hypotheses. We further add complexity to this exciting discussion here by focussing on the role played by B in the regulation and control of axillary meristem fate. Future research is required to fully elucidate the role of B in the cell division of the quiescent center, and several open questions remain: What is the crosstalk and how can it target endoreplication? Does this response change with different photoperiods? How are the B transporters regulated during the day? Which oscillator modulates B and mediates growth responses? By answering these questions, we will likely close gaps in our current understanding of how B works within land plants. Understanding the mechanisms behind the accepted (and challenged) functions of B may help to elucidate how and to what extent B is important, and ultimately contribute to an enhanced understanding of its biological function, with significant practical applications in agriculture.

AUTHOR CONTRIBUTIONS

GP and WA organized and wrote the manuscript. JS, WB-S, FC, and AN-N provided critical evaluation and edited the text. All authors contributed to the article and approved the submitted version.

FUNDING

This work was supported by funding from the National Council for Scientific and Technological Development (CNPq-Brazil grant no. 402511/2016-6) and the Foundation for Research Assistance of the Minas Gerais State (FAPEMIG-Brazil grant no. APQ-01171-17) to WA. Scholarships granted by the CNPq to GP and by the Agency for the Support and Evaluation of Graduate Education (CAPES-Brazil) to JS and WB-S, and research fellowships granted by CNPq to AN-N and WA are gratefully acknowledged.

ACKNOWLEDGMENTS

We wish to apologize to all colleagues whose work has not been mentioned due to space limitations.

REFERENCES

Abreu, I., Poza, L., Bonilla, I., and Bolaños, L. (2014). Boron deficiency results in early repression of a cytokinin receptor gene and abnormal cell differentiation in the apical root meristem of *Arabidopsis thaliana*. *Plant Physiol. Biochem.* 77, 117–121. doi: 10.1016/j.plaphy.2014.02.008

Arnon, D. I., and Stout, P. R. (1939). The essentiality of certain elements in minute quantity for plants with special reference to copper. *Plant Physiol.* 14, 371–375. doi: 10.1104/pp.14.2.371

Brown, P. H., Bellaloui, N., Wimmer, M. A., Bassil, E. S., Ruiz, J., Hu, H., et al. (2002). Boron in plant biology. *Plant Biol.* 4, 211–229. doi: 10.1055/s-2002-25740

Brown, P. H., and Hu, H. (1994). Boron uptake by sunflower, squash and cultured tobacco cells. *Physiol. Plant.* 91, 435–441. doi: 10.1111/j.1399-3054.1994.tb02971.x

Brown, P. H., and Hu, H. (1996). Phloem mobility of boronis species dependent: evidence for phloem mobility in sorbitol-rich species. *Ann. Bot.* 77, 497–505. doi: 10.1006/anbo.1996.0060

Cakmak, I., and Römheld, V. (1997). Boron deficiency-induced impairments of cellular functions in plants. *Plant Soil* 193, 71–83. doi: 10.1023/A:1004259808322

Camacho-Cristóbal, J. J., Rexach, J., and González-Fontes, A. (2008). Boron in plants: deficiency and toxicity. *J. Integr. Plant Biol.* 50, 1247–1255. doi: 10.1111/j.1744-7909.2008.00742.x

Chatterjee, M., Liu, Q., Menello, C., Galli, M., and Gallavotti, A. (2017). The combined action of duplicated boron transporters is required for maize growth in boron-deficient conditions. *Genetics* 206, 2041–2051. doi: 10.1534/genetics.116.198275

Chatterjee, M., Tabi, Z., Galli, M., Malcomber, S., Buck, A., Muszynski, M., et al. (2014). The boron efflux transporter ROTTEN EAR is required for maize inflorescence development and fertility. *Plant Cell* 26, 2962–2977. doi: 10.1105/tpc.114.125963

Chatzissavvidis, C., and Therios, I. (2011). "Boron in higher plants" in *Boron: Compounds, production and application*. ed. G. L. Perkins (New York: Nova Science Publishers Inc.), 147–176.

Dannel, F., Pfefffer, H., and Romheld, V. (2000). Characterization of root boron pools, boron uptake and boron translocation in sunflower using the stable isotopes ^{10}B and ^{11}B. *Funct. Plant Biol.* 27, 397–405. doi: 10.1071/PP99086

Diehn, T. A., Bienert, M. D., Pommerrening, B., Liu, Z., Bienert, M. D., Pommerrening, B., et al. (2019). Boron demanding tissues of *Brassica napus* express specific sets of functional Nodulin26-like Intrinsic Proteins and BOR1 transporters. *Plant J.* 100, 68–82. doi: 10.1111/tpj.14428

Domingues, D. S., Leite, S. M. M., Farro, A. P. C., Coscrato, V. E., Mori, E. S., Furtado, E. L., et al. (2005). Boron transport in Eucalyptus. 2. Identification in silico of a putative boron transporter for xylem loading in eucalypt. *Genet. Mol. Biol.* 28, 625–629. doi: 10.1590/S1415-47572005000400017

Dordas, C., Chrispeels, M. J., and Brown, P. H. (2000). Permeability and channelmediated transport of boric acid across membrane vesicles isolated from squash roots. *Plant Physiol.* 124, 1349–1362. doi: 10.1104/pp.124.3.1349

Du, W., Pan, Z. -Y., Hussain, S. B., Han, Z. -X., Peng, S. -A., and Liu, Y. -Z. (2020). Foliar supplied boron can be transported to roots as a boron-sucrose complex via phloem in citrus trees. *Front. Plant Sci.* 11:e250. doi: 10.3389/fpls.2020.00250

Durbak, A. R., Phillips, K. A., Pike, S., O'Neill, M. A., Mares, J., Gallavotti, A., et al. (2014). Transport of boron by the tassel-less1 aquaporin is critical for vegetative and reproductive development in maize. *Plant Cell* 26, 2978–2995. doi: 10.1105/tpc.114.125898

Fukuda, M., Wakuta, S., Kamiyo, J., Fujiwara, T., and Takano, J. (2018). Establishment of genetically encoded biosensors for cytosolic boric acid in plant cells. *Plant J.* 95, 763–774. doi: 10.1111/tpj.13985

Giraldo, J. P., Wu, H., Newkirk, G. M., and Kruss, S. (2019). Nanobiotechnology approaches for engineering smart plant sensors. *Nat. Nanotechnol.* 14, 541–553. doi: 10.1038/s41565-019-0470-6

Gómez-Soto, D., Galván, S., Rosales, E., Bienert, P., Abreu, I., Bonilla, I., et al. (2019). Insights into the role of phytohormones regulating pAtNIP5;1 activity and boron transport in *Arabidopsis thaliana*. *Plant Sci.* 287:110198. doi: 10.1016/j.plantsci.2019.110198

Housh, A. B., Matthes, M. S., Gerheart, A., Wilder, S. L., Kil, K.-E., Schueller, M., et al. (2020). Assessment of a 18F-phenylboronic acid radiotracer for imaging boron in maize. *Int. J. Mol. Sci.* 21:976. doi: 10.3390/ijms21030976

Hrmova, M., Gilliham, M., and Tyerman, S. D. (2020). Plant transporters involved in combating boron toxicity: beyond 3D structures. *Biochem. Soc. Trans.* 48, 1683–1696. doi: 10.1042/BST20200164

Hu, H., and Brown, P. H. (1997). Absorption of boron by plant roots. *Plant Soil* 193, 49–58. doi: 10.1023/A:1004255707413

Hu, Z., Cools, T., and De Veylder, L. (2016). Mechanisms used by plants to cope with DNA damage. *Annu. Rev. Plant Biol.* 67, 439–462. doi: 10.1146/annurev-arplant-043015-111902

Hu, H., Penn, S. G., Lebrilla, C. B., and Brown, P. H. (1997). Isolation and characterization of soluble boron complex in higher plants. The mechanism of phloem mobility of boron. *Plant Physiol.* 113, 649–655. doi: 10.1104/pp.113.2.649

Huang, C., and Graham, R. D. (1990). Resistance of wheat genotypes to boron toxicity is expressed at cellular level. *Plant Soil* 126, 295–300. doi: 10.1007/BF00012832

Hwang, B., Lee, J. H., and Bang, D. (2018). Single-cell RNA sequencing technologies and bioinformatics pipelines. *Exp. Mol. Med.* 50:e96. doi: 10.1038/s12276-018-0071-8

Klochko, K., Kaufman, A. J., Yao, W., Byrne, R. H., and Tossell, J. A. (2006). Experimental measurement of boron isotope fractionation in seawater. *Earth Planet. Sci. Lett.* 248, 261–270. doi: 10.1016/j.epsl.2006.05.034

Kobayashi, M., Miyamoto, M., Matoh, T., Kitajima, S., Hanano, S., Sumerta, I. N., et al. (2018). Mechanism underlying rapid responses to boron deprivation in *Arabidopsis* roots. *J. Plant Nutr. Soil Sci.* 64, 106–115. doi: 10.1080/00380768.2017.1416670

Kurt, F., and Aydın, A. (2020). An in-silico study: interaction of BOR1-type boron (B) transporters with a small group of functionally unidentified proteins under various stresses in potato (*Solanum tuberosum*). *Commagene J. Biol.* 4, 134–139. doi: 10.31594/commagene.798805

Landi, M., Margaritopoulou, T., Papadakis, I. E., and Araniti, F. (2019). Boron toxicity in higher plants: an uptade. *Planta* 250, 1011–1032. doi: 10.1007/s00425-019-03220-4

Lewis, D. H. (1980). Boron, lignification and the origin of vascular plants—a unified hypothesis. *New Phytol.* 84, 209–229. doi: 10.1111/j.1469-8137.1980.tb04423.x

Lewis, D. H. (2019). Boron the essential element for vascular plants that never was. *New Phytol.* 221, 1685–1690. doi: 10.1111/nph.15519

Lewis, D. H. (2020). The status of boron as an essential element for vascular plants. I. A response to González-Fontes (2019) 'Why boron is an essential element for vascular plants'. *New Phytol.* 226:1231. doi: 10.1111/nph.16030

Li, X., Li, Y., Mai, J., Tao, L., Qu, M., Liu, J., et al. (2018). Boron alleviates aluminum toxicity by promoting root alkalization in transition zone via polar auxin transport. *Plant Physiol.* 177, 1254–1266. doi: 10.1104/pp.18.00188

Liao, C. Y., and Weijers, D. (2018). A toolkit for studying cellular reorganization during early embryogenesis in *Arabidopsis thaliana*. *Plant J.* 93, 963–976. doi: 10.1111/tpj.13841

Lu, Y. B., Yang, L. T., Qi, Y. P., Li, Y., Li, Z., Chen, Y. B., et al. (2014). Identification of boron-deficiency-responsive microRNAs in *Citrus sinensis* roots by Illumina sequencing. *BMC Plant Biol.* 14:a123. doi: 10.1186/1471-2229-14-123

Marschner, P. (2012). *Marchner's mineral nutrition of higher plants. 3rd Edn.* San Diego: Academic Press.

Matthes, M. S., Robil, J. M., and McSteen, P. (2020). From element to development: the power of the essential micronutrient boron to shape morphological processes in plants. *J. Exp. Bot.* 71, 1681–1693. doi: 10.1093/jxb/eraa042

Matthes, M., and Torres-Ruiz, R. A. (2016). Boronic acid treatment phenocopies monopteros by affecting PIN1 membrane stability and polar auxin transport in *Arabidopsis thaliana* embryos. *Development* 143, 4053–4062. doi: 10.1242/dev.131375

Miwa, K., and Fujiwara, T. (2010). Boron transport in plants: co-ordinate regulation of transporters. *Ann. Bot.* 105, 1103–1108. doi: 10.1093/aob/mcq044

Miwa, K., Takano, J., Omori, H., Seki, M., Shinozaki, K., and Fujiwara, T. (2007). Plants tolerant of high boron levels. *Science* 318:1417. doi: 10.1126/science.1146634

Miwa, K., Wakuta, S., Takada, S., Ide, K., Takano, J., Naito, S., et al. (2013). Roles of BOR2, a boron exporter, in cross linking of Rhamnogalacturonan II and root elongation under boron limitation in Arabidopsis. *Plant Physiol.* 163, 1699–1709. doi: 10.1104/pp.113.225995

Nable, R. O. (1988). Effects of B toxicity among several barley wheat cultivars: a preliminary examination of the resistance mechanism. *Plant Soil* 112, 45–52.

Nable, R. O., Lance, R. C. M., and Cartwight, B. (1990). Uptake of boron and silicon by barley genotypes with differing susceptibilities to boron toxicity. *Ann. Bot.* 66, 83–90. doi: 10.1093/oxfordjournals.aob.a088003

Nelson, T., Tausta, S. L., Gandotra, N., and Liu, T. (2006). Laser microdissection of plant tissue: what you see is what you get. *Annu. Rev. Plant Biol.* 57, 181–201. doi: 10.1146/annurev.arplant.56.032604.144138

Ozyigit, I. I., Filiz, E., Saracoglu, I. A., and Karadeniz, S. (2020). Exploration of two major boron transport genes BOR1 and NIP5;1 in the genomes of different plants. *Biotechnol. Biotechnol. Equip.* 34, 455–468. doi: 10.1080/13102818.2020.1773311

Pallotta, M., Schnurbusch, T., Hayes, J., Hay, A., Baumann, U., Paull, J., et al. (2014). Molecular basis of adaptation to high soil boron in wheat landraces and elite cultivars. *Nature* 514, 88–91. doi: 10.1038/nature13538

Poza-Viejo, L., Abreu, I., González-García, M. P., Allauca, P., Bonilla, I., Bolaños, L., et al. (2018). Boron deficiency inhibits root growth by controlling meristem activity under cytokinin regulation. *Plant Sci.* 270, 176–189. doi: 10.1016/j.plantsci.2018.02.005

Redondo-Nieto, M., Maunoury, N., Mergaert, P., Kondorosi, E., Bonilla, I., and Bolaños, L. (2012). Boron and calcium induce major changes in gene expression during legume nodule organogenesis. Does boron have a role in signalling? *New Phytol.* 195, 14–19. doi: 10.1111/j.1469-8137.2012.04176.x

Reguera, M., Abreu, I., Sentís, C., Bonilla, I., and Bolaños, L. (2019). Altered plant organogenesis under boron deficiency is associated with changes in high-mannose N-glycan profile that also occur in animals. *J. Plant Physiol.* 243:153058. doi: 10.1016/j.jplph.2019.153058

Reguera, M., Espí, A., Bolaños, L., Bonilla, I., and Redondo-Nieto, M. (2009). Endoreduplication before cell differentiation fails in boron-deficient legume nodules. Is boron involved in signaling during cell cycle regulation? *New Phytol.* 183, 8–12. doi: 10.1111/j.1469-8137.2009.02869.x

Reid, R. (2014). Understanding the boron transport network in plants. *Plant Soil* 385, 1–13. doi: 10.1007/s11104-014-2149-y

Reid, R. J., Hayes, J. E., Post, A., Stangoulis, J. C. R., and Graham, R. D. (2004). A critical analysis of the causes of boron toxicity in plants. *Plant Cell Environ.* 27, 1405–1414. doi: 10.1111/j.1365-3040.2004.01243.x

Riaz, M., Yana, L., Wua, X., Hussainb, S., Aziza, O., Imrana, M., et al. (2018). Boron reduces aluminum-induced growth inhibition, oxidative damage and alterations in the cell wall components in the roots of trifoliate orange. *Ecotoxicol. Environ. Saf.* 153, 107–115. doi: 10.1016/j.ecoenv.2018.02.002

Routray, P., Li, T., Yamasaki, A., Yoshinari, A., Takano, J., Choi, W. G., et al. (2018). Nodulin Intrinsic Protein 7;1 is a tapetal boric acid channel involved in pollen cell wall formation. *Plant Physiol.* 178, 1269–1283. doi: 10.1104/pp.18.00604

Sakamoto, T., Sotta, N., Suzuki, T., Fujiwara, T., and Matsunaga, S. (2019). The 26S proteasome is required for the maintenance of root apical meristem by modulating auxin and cytokine responses under high-boron stress. *Front. Plant Sci.* 10:590. doi: 10.3389/fpls.2019.00590

Sakamoto, T., Tsujimoto, Y. T., Uraguchi, S., Yoshizumi, T., Matsunaga, S., Mastui, M., et al. (2011). Condensin II alleviates DNA damage and is essential for tolerance of boron overload stress in *Arabidopsis*. *Plant Cell* 23, 3533–3546. doi: 10.1105/tpc.111.086314

Sakamoto, T., Tsujimoto-Inui, Y., Sotta, N., Hirakawa, T., Matsunaga, T. M., Fukao, Y., et al. (2018). Proteasomal degradation of BRAHMA promotes boron tolerance in *Arabidopsis*. *Nat. Commun.* 9:5285. doi: 10.1038/s41467-018-07393-6

Shao, J. F., Yamaji, N., Liu, X. W., Yokosho, K., Shen, R. F., and Ma, J. F. (2018). Preferential distribution of boron to developing tissues is mediated by the intrinsic protein OsNIP3. *Plant Physiol.* 176, 1739–1750. doi: 10.1104/pp.17.01641

Shimotohno, A., Sotta, N., Sato, T., De Ruvo, M., Marée, A. F., Grieneisen, V. A., et al. (2015). Mathematical modeling and experimental validation of the spatial distribution of boron in the root of *Arabidopsis thaliana* identify high boron accumulation in the tip and predict a distinct root tip uptake function. *Plant Cell Physiol.* 56, 620–630. doi: 10.1093/pcp/pcv016

Shireen, F., Nawaz, M. A., Chen, C., Zhang, Q., Zheng, Z., Sohail, H., et al. (2018). Boron: functions and approaches to enhance its availability in plants for sustainable agriculture. *Int. J. Mol. Sci.* 19:1856. doi: 10.3390/ijms19071856

Sotta, N., Duncan, S., Tanaka, M., Sato, T., Marée, A. F., Fujiwara, T., et al. (2017). Rapid transporter regulation prevents substrate flow traffic jams in boron transport. *eLife* 6:e27038. doi: 10.7554/eLife.27038

Takano, J., Miwa, K., and Fujiwara, T. (2008). Boron transport mechanisms: collaboration of channels and transporters. *Trends Plant Sci.* 13, 451–457. doi: 10.1016/j.tplants.2008.05.007

Takano, J., Tanaka, M., Toyoda, A., Miwa, K., Kasai, K., Fuji, K., et al. (2010). Polar localization and degradation of *Arabidopsis* boron transporters through distinct trafficking pathways. *Proc. Natl. Acad. Sci. U. S. A.* 107, 5220–5225. doi: 10.1073/pnas.0910744107

Takano, J., Wada, M., Ludewig, U., Schaaf, G., von Wirén, N., and Fujiwara, T. (2006). The *Arabidopsis* major intrinsic protein NIP5;1 is essential for efficient boron uptake and plant development under boron limitation. *Plant Cell* 18, 1498–1509. doi: 10.1105/tpc.106.041640

Takano, J., Yamagami, M., Noguchi, K., Hayashi, H., and Fujiwara, T. (2001). Preferential translocation of boron to young leaves in *Arabidopsis thaliana* regulated by the *BOR1* gene. *Soil Sci. Plant Nutr.* 47, 345–357. doi: 10.1080/00380768.2001.
10408398

Tanaka, M., and Fujiwara, T. (2008). Physiological roles and transport mechanisms of boron: perspectives from plants. *Pflugers Arch.* 456, 671–677. doi: 10.1007/s00424-007-0370-8

Tanaka, M., Sotta, N., Yamazumi, Y., Yamashita, Y., Miwa, K., Murota, K., et al. (2016). The minimum open reading frame, AUG-Stop, induces boron-dependent ribosome stalling and mRNA degradation. *Plant Cell* 28, 2830–2849. doi: 10.1105/tpc.16.00481

Thisse, C., and Thisse, B. (2008). High-resolution *in situ* hybridization to whole-mount zebrafish embryos. *Nat. Protoc.* 3, 59–69. doi: 10.1038/nprot.2007.514

Tsaftaris, S. A., Minervini, M., and Scharr, H. (2016). Machine learning for plant phenotyping needs image processing. *Trends Plant Sci.* 21, 989–991. doi: 10.1016/j.tplants.2016.10.002

Van Dyk, T. K., Wei, Y., Hanafey, M. K., Dolan, M., Reeve, M. J., Rafalski, J. A., et al. (2001). A genomic approach to gene fusion technology. *Proc. Natl. Acad. Sci. U. S. A.* 98, 2555–2560. doi: 10.1073/pnas.041620498

Wakuta, S., Fujikawa, T., Naito, S., and Takano, J. (2016). Tolerance to excess-boron conditions acquired by stabilization of a BOR1 variant with weak polarity in *Arabidopsis*. *Front. Cell Dev. Biol.* 4:4. doi: 10.3389/fcell.2016.00004

Wang, Y. P., and Lei, Q. Y. (2018). Metabolite sensing and signaling in cell metabolism. *Signal Transduct. Target Ther.* 3:30. doi: 10.1038/s41392-018-0024-7

Wang, S., Yoshinari, A., Shimada, T., Hara-Nishimura, I., Mitani-Ueno, N., Feng Ma, J., et al. (2017). Polar localization of the NIP5;1 boric acid channel is maintained by endocytosis and facilitates boron transport in *Arabidopsis* roots. *Plant Cell* 29, 824–842. doi: 10.1105/tpc.16.00825

Warington, K. (1923). The effect of boric acid and borax on the broad bean and certain other plants. *Ann. Bot.* 37, 629–672.

Will, S., Eichert, T., Fernández, V., Möhring, J., Müller, T., and Römheld, V. (2011). Absorption and mobility of foliar-applied boron in soybean as affected by plant boron status and application as a polyol complex. *Plant Soil* 344, 283–293. doi: 10.1007/s11104-011-0746-6

Wu, X., Riaz, M., Yan, L., and Jiang, C. (2019). Distribution and mobility of foliar-applied boron (^{10}B) in citrange rootstock under different boron condition. *J. Plant Growth Regul.* 39, 575–582. doi: 10.1007/s00344-019-10001-6

Xin, J., and Huang, B. (2017). Comparison of boron uptake, translocation, and accumulation in reed, cattail, and vetiver: an extremely boron-tolerant plant, vetiver. *Plant Soil* 416, 17–25. doi: 10.1007/s11104-017-3186-0

Xu, Y., Guo, C., Zhou, B., Li, C., Wang, H., Zheng, B., et al. (2016). Regulation of vegetative phase change by SWI2/SNF2 chromatin remodeling ATPase BRAHMA. *Plant Physiol.* 172, 2416–2428. doi: 10.1104/pp.16.01588

Yoshinari, A., Hosokawa, T., Amano, T., Beier, M. P., Kunieda, T., Shimada, T., et al. (2019). Polar localization of the borate exporter BOR1 requires AP2-dependent endocytosis. *Plant Physiol.* 179, 1569–1580. doi: 10.1104/pp.18.01017

Yoshinari, A., and Takano, J. (2017). Insights into the mechanisms underlying boron homeostasis in plants. *Front. Plant Sci.* 8:1951. doi: 10.3389/fpls.2017.01951

Yoshinari, A., Korbei, B., and Takano, J. (2018). TOL proteins mediate vacuolar sorting of the borate transporter BOR1 in *Arabidopsis thaliana*. *Soil Sci. Plant Nutr.* 64, 598–605. doi: 10.1080/00380768.2018.1504322

Zhang, C., He, M., Wang, S., Chu, L., Wang, C., Yang, N., et al. (2019). Boron deficiency-induced root growth inhibition is mediated by brassinosteroid signalling regulation in *Arabidopsis*. bioRxiv [Preprint]. doi: 10.1101/2019.12.12.874222

Conflict of Interest: FC is an agronomist at U.S. Borax | Rio Tinto, a borate supplier company. U.S. Borax | Rio Tinto had no role in study design, data collection and analysis, decision to publish, or preparation of the manuscript described here.

The remaining authors declare that the research was conducted in the absence of any commercial or financial relationships that could be construed as a potential conflict of interest.

Copyright © 2021 Pereira, Siqueira, Batista-Silva, Cardoso, Nunes-Nesi and Araújo. This is an open-access article distributed under the terms of the Creative Commons Attribution License (CC BY). The use, distribution or reproduction in other forums is permitted, provided the original author(s) and the copyright owner(s) are credited and that the original publication in this journal is cited, in accordance with accepted academic practice. No use, distribution or reproduction is permitted which does not comply with these terms.

frontiers in Plant Science

ORIGINAL RESEARCH
published: 17 February 2021
doi: 10.3389/fpls.2021.616868

Evidences for a Nutritional Role of Iodine in Plants

Claudia Kiferle[1†], Marco Martinelli[1†], Anna Maria Salzano[2†], Silvia Gonzali[1], Sara Beltrami[1], Piero Antonio Salvadori[3], Katja Hora[4], Harmen Tjalling Holwerda[4], Andrea Scaloni[2] and Pierdomenico Perata[1*]*

[1] Plant Lab, Institute of Life Sciences, Scuola Superiore Sant'Anna, Pisa, Italy, [2] Proteomics and Mass Spectrometry Laboratory, Institute for the Animal Production System in the Mediterranean Environment (ISPAAM), National Research Council, Napoli, Italy, [3] Institute of Clinical Physiology, National Research Council, Pisa, Italy, [4] SQM International N.V., Antwerpen, Belgium

Little is known about the role of iodine in plant physiology. We evaluated the impact of low concentrations of iodine on the phenotype, transcriptome and proteome of *Arabidopsis thaliana*. Our experiments showed that removal of iodine from the nutrition solution compromises plant growth, and restoring it in micromolar concentrations is beneficial for biomass accumulation and leads to early flowering. In addition, iodine treatments specifically regulate the expression of several genes, mostly involved in the plant defence response, suggesting that iodine may protect against both biotic and abiotic stress. Finally, we demonstrated iodine organification in proteins. Our bioinformatic analysis of proteomic data revealed that iodinated proteins identified in the shoots are mainly associated with the chloroplast and are functionally involved in photosynthetic processes, whereas those in the roots mostly belong and/or are related to the action of various peroxidases. These results suggest the functional involvement of iodine in plant nutrition.

Keywords: iodine, Arabidopsis, plant growth, plant nutrition, plant phenotype, transcriptomics, proteomics

OPEN ACCESS

Edited by:
Antonios Chrysargyris, Cyprus University of Technology, Cyprus

Reviewed by:
Artem Kasianov, Russian Academy of Sciences, Russia
Iwona Ledwożyw-Smoleń, University of Agriculture in Krakow, Poland

***Correspondence:**
Claudia Kiferle
c.kiferle@santannapisa.it;
c.kiferle@sssup.it
Pierdomenico Perata
p.perata@santannapisa.it

† These authors have contributed equally to this work

Specialty section:
This article was submitted to Plant Nutrition, a section of the journal Frontiers in Plant Science

Received: *13 October 2020*
Accepted: *04 January 2021*
Published: *17 February 2021*

Citation:
Kiferle C, Martinelli M, Salzano AM, Gonzali S, Beltrami S, Salvadori PA, Hora K, Holwerda HT, Scaloni A and Perata P (2021) Evidences for a Nutritional Role of Iodine in Plants. Front. Plant Sci. 12:616868. doi: 10.3389/fpls.2021.616868

INTRODUCTION

Plants need macro- and micro-nutrients for their growth and development. Nutrients are chemical elements that are components of biological molecules and/or influence essential metabolic functions. The elements that to date are considered as plant nutrients are C, H, O, N, P, K (primary nutrients), Ca, Mg, S (secondary nutrients), and Fe, Zn, Cu, Mn, B, Cl, Mo, Co, and Ni (micro-nutrients) (Mengel and Kirkby, 2001).

Halogens are the least represented chemical group of plant micro-nutrients, chloride being the only micro-nutrient currently recognised in plant physiology, due to its regulatory action in proton-transfer reactions in the photosystem II (Brahmachari et al., 2018). Studying the effect of different concentrations and forms of iodine on the growth of several crops of agricultural importance, Borst Pauwels (1961) referred to iodine as a micro-nutrient for plant, and a similar conclusion was derived by Lehr et al. (1958) working on tomato.

A growing number of recent studies reporting the effect of iodine on plant growth have focused on the benefit of increasing iodine content in plants as a biofortificant in human and animal health (Medrano-Macías et al., 2016; Gonzali et al., 2017). Plant tissues generally increase their iodine content following its exogenous administration. However, the presence of iodine as a trace element/contaminant in the soil/nutrient solution/atmosphere cannot be avoided, thus preventing the effects related to the presence/absence of this element from being easily observed

(Fuge and Johnson, 1986; Ashworth, 2009). The functional role of iodine as a plant nutrient might therefore have been masked.

Plants can absorb iodine from roots or above ground structures (stomata and cuticular waxes) (Medrano-Macías et al., 2016; Gonzali et al., 2017), translocate it mainly through the xylematic route and volatilise it as methyl iodide (CH_3I) through the action of halide ion-methyltransferase (HMT) and halide/thiol methyltransferase (HTMT) enzymes (Medrano-Macías et al., 2016; Gonzali et al., 2017).

Little is known about the chemical forms of iodine inside plant tissues. Inorganic iodine, in particular iodide (I^-), however, seems to be predominant (Weng et al., 2008). Plants can also incorporate iodine into organic molecules, such as iodosalicylates, iodobenzoates (Smoleń et al., 2020), monoiodotyrosine (MIT), di-iodotyrosine (DIT) and triiodothyronine (T3) (Eales, 1997; Smoleń et al., 2020). Interestingly, MIT and DIT have a key role in the physiology of vertebrates, as they are precursors of the two thyroid hormones (THs) triiodothyronine (T3) and L-thyroxine (T_4) as part of the thyroglobulin protein (Zimmermann et al., 2008).

In plants, the presence of a thyroglobulin-like protein has never been reported, and the metabolic role of MIT, DIT and T3 molecules, if any, and their biosynthetic mechanism are still unknown. Nevertheless, protein iodination has been verified in several seaweed species (Hou et al., 2000; Romarís-Hortas et al., 2014), even if it has not yet been demonstrated in plants.

Iodine is likely involved in several physiological and biochemical processes (Medrano-Macías et al., 2016; Gonzali et al., 2017). The presence of low concentrations of iodine is often associated with beneficial effects on plant growth, production and stress resistance, whereas toxic effects are observed when applying iodine at high concentrations, especially in the I^- form, which is more phytotoxic than iodate (IO_3^-) (Voogt et al., 2010; Medrano-Macías et al., 2016; Gonzali et al., 2017; Incrocci et al., 2019). Thresholds for beneficial or toxic concentrations have been reported for all micro-nutrients (Welch and Shuman, 1995). Interestingly, the concentrations of iodine added to nutrient solutions that have been associated with positive effects for plants (ranging from approximately 10^2–10^4 nM) (Medrano-Macías et al., 2016; Gonzali et al., 2017) are comparable with those generally effective for other elements described as plant micro-nutrients (Sonneveld, 2002), suggesting that iodine may play a similar role in plant nutrition.

We explored the role of iodine as a nutrient for plants using various experimental approaches. Our results showed that iodine, when supplied at a well-defined concentration range, positively affected the phenotype of *Arabidopsis thaliana* plants, and altered the organism's transcriptome. Most importantly, protein iodination was observed for the first time. These results are strongly suggestive of the role of iodine as a plant nutrient.

MATERIALS AND METHODS

Plant Material and Cultivation System

Plants of *Arabidopsis thaliana*, ecotype Columbia 0, *Solanum lycopersicum* L., cv. Micro-Tom, *Lactuca sativa* L., var. crispa, *Triticum turgidum* L., var. durum, and *Zea mays* L., var. saccharata, were used in the experiments, as summarised in **Supplementary Figure S1**.

The cultivation protocol commonly applied in all the experiments is described as follows: seeds of the different species were sown on rockwool plugs and vernalised for 3 days. After this period, plants were hydroponically cultivated in a growth chamber (22°C day/18°C night with a 12 h photoperiod, a quantum irradiance of 100 μmol photons m^{-2} s^{-1} and a relative humidity close to 35%), in a floating system. A base nutrient solution, renewed once a week, was prepared minimising iodine contamination by dissolving in MilliQ water the following amounts of ultrapure salts: 1.25 mM KNO_3, 1.50 mM $Ca(NO_3)_2$, 0.75 mM $MgSO_4$, 0.50 mM KH_2PO_4, 50 μM KCl, 50 μM H_3BO_3, 10 μM $MnSO_4$, 2.0 μM $ZnSO_4$, 1.5 μM $CuSO_4$, 0.075 μM $(NH_4)_6Mo_7O_{24}$, and 72 μM Fe-EDTA. At preparation, the pH and the electrical conductivity (EC) values were 6.0 and 0.6 dS m^{-1}, respectively, whereas the iodine concentration in the nutrient solution was below the detection limit of 8 nM, as determined by ICP-MS analysis. The technical peculiarities of each experiment are described in the devoted sections.

Phenotypical Determinations

Two separate experiments were performed. In both experiments, Arabidopsis plants were initially fed with the base nutrient solution. After 15 days of growth, plants homogeneous in size and leaf number were selected, grouped, and fed with different concentration and/or type of halogen-containing salts added to the nutrient solution. Plants were distributed in nine separate hydroponic trays (three different trays/treatment), and a total number of 90 plants were cultivated for each experimental condition (30 plants/tray).

In the first experiment (exp. 1—phenotype), 0.20 or 10 μM KIO_3 was added to the nutrient solution. One month later, during the formation/elongation of the main inflorescence, half of the plants (15 plants/tray) was harvested and characterised according to the main morphological traits, such as rosette and inflorescence fresh weight (FW), dry weight (DW), dry matter content, rosette diameter, and inflorescence length. The remaining half was allowed to complete the growing cycle and was characterised in terms of flowering and seed production. Flowering, defined as the presence of the first open flower on the stem, was recorded at intervals of 3 days and expressed on a percentage basis. The percentage of bloomed plants/tray was calculated at each assessment date. Toward the final part of the plants' life cycle, a periodical harvesting of the produced/matured seeds was carried out until the complete plant desiccation. Seed production was determined in terms of total seed weight/tray (15 plants/tray), number of seeds/silique and number of siliques/plant.

In the second experiment (exp. 2—phenotype), plants were treated by adding either KI, NaI or KBr (0, 10, or 30 μM) to the nutrient solution. Fifteen days after the salt treatment, half of the plants was characterised in terms of plant FW, DW and dry matter content, while the other half was subsequently characterised in terms of flowering (recorded with intervals of 2 days), as described for experiment 1-phenothype.

Total RNA Extraction and Processing

Gene expression analysis was performed on 3-week-old Arabidopsis plants hydroponically grown on the base nutrient solution (control plants) or in the same medium to which 10 μM of KBr, NaI, or KI was added. Plant material was collected 48 h after the beginning of the treatment. Each sample consisted of a pool of rosettes or roots sampled from three different plants, which were immediately frozen in liquid nitrogen and stored at −80°C until further analysis.

Total RNA from rosettes was extracted as described by Perata et al. (1997), avoiding the use of aurintricarboxylic acid. RNA from roots was extracted using the Spectrum^{TM} Plant Total RNA Kit (Sigma-Aldrich). RNA was subsequently processed for microarray and qPCR analysis. The TURBO DNA-free kit (Thermo Fisher Scientific) was used to remove DNA contaminations and the iScript TM cDNA synthesis kit (Bio-Rad Laboratories) was used for RNA reverse-transcription.

Microarray Analysis

RNA from rosettes and roots was processed and hybridised to Affymetrix GeneChip Arabidopsis ATH1 Genome Arrays as described by Loreti et al. (2005). Normalisation was performed using Microarray Suite 5.0 (MAS5.0). Differentially expressed genes (DEGs) were selected based on the two following criteria: $\log_2$FC treated/control $\geq$ 2 and mas5-Detection $p \leq 0.05$. In addition, the absolute expression level $\geq$ 100 mas5-Signal was chosen to select only well-expressed genes. Rosette and root DEGs resulting from KI, NaI, and KBr treatments were processed and visualised in a Venn diagram. Only DEGs commonly regulated by KI- and NaI-treated plants and not responding to KBr treatments were considered specifically linked with the iodine treatment. This group of DEGs was then subjected to gene set enrichment using Gorilla[1] and analysed with Mapman[2], whereas the co-expression analysis was performed using Genevestigator[3].

Gene Expression Analysis (RT-qPCR)

Quantitative PCR (ABI Prism 7300 Sequence Detection System, Applied Biosystems) was performed using 30 ng cDNA and the iQ SYBR Green Supermix (Bio-Rad Laboratories). *UBIQUITIN10* (*At4g05320*) and *TIP4* (*At2g25810.1*) were used as reference genes. Relative expression levels were calculated using GeNorm[4]. The list of the primers and their sequences are reported in **Supplementary Table S1**. Four biological replicates were analysed, each consisting of a pool of rosettes or roots sampled from three different plants.

Feeding With Radioactive Iodine

Two separate experiments were performed by feeding radioactive iodine (^{125}I—NaI, PerkinElmer) to hydroponically grown *Arabidopsis thaliana* (exp. 1—radioactive) or tomato, lettuce, wheat and maize (exp. 2—radioactive) plants. Treatments were performed on 1-month-old plants. The solution of ^{125}I was prepared by dissolving 60 μl of the commercial radioactive ^{125}I product (2.4 mCi/100 μl—9.41 μM) in 250 ml of base nutrient solution. Plants were individually transferred into plastic tubes and treated with the hydroponic solution (with or without Na^{125}I). Sampling was performed after 48 h of incubation by collecting leaf and root material, which was immediately frozen in liquid nitrogen, and stored at −80°C until the analysis. Control, non-treated plants (no ^{125}I added during their growth) were used in both experiments.

Protein Extraction, Electrophoresis, and Gel Autoradiography

Leaf and root samples from ^{125}I-fed and control plants were ground to fine powder in liquid nitrogen. The protein extraction buffer (50 mM TrisHCl, pH 7.0, 1% w/v SDS, P9599 protease inhibitor cocktail, Sigma-Aldrich) was added to the powder. The resulting solution was vortexed vigorously, and then centrifuged (18,407 *g*, 30 min, 4°C). Radioactive iodine solution (10 μl; prepared as described above) was added to the control samples during the extraction process to check for the occurrence of false positive signals (technical artifacts), possibly due to unspecific binding of iodine with the protein extract.

Protein extracts were dissolved in a 5 × Laemmli buffer, treated at 95°C for 10 min, and a volume of 20 μl (corresponding, approximately, to 65 or 20 μg of proteins, in shoot and root samples, respectively) was loaded to Invitrogen NuPAGE gels (10% Bis-Tris Midi Gels, Thermo Fisher Scientific), together with a protein marker (Precision Plus Protein^{TM} Dual Color Standards, Bio-Rad). After electrophoresis, the gel was rinsed in MilliQ water, and the proteins were fixed (40:7:53 ethanol/glacial acetic acid/H_2O – 30 min) and then stained (EZ Blue Gel Staining reagent, Sigma-Aldrich – 30 min) on an orbital shaker. After rinsing, gels were exposed to a multipurpose phosphor storage screen (Cyclone Storage Phosphor System, PerkinElmer) in order to obtain a digital image of the radioactivity distribution. Radioactive signals were quantified after 72 h of gel exposure using a Cyclone Phosphor Imaging System (PerkinElmer). In order to prevent the occurrence of any radioactive emissions from the control samples, after each image acquisition, gels were re-exposed for 15 days, and the absence of ^{125}I labelled bands was verified in the newly acquired images.

Database Search for Iodinated Peptides in Protein Datasets From Proteomic Data Repositories

Mass spectrometry data were downloaded from the PRIDE (PRoteomics IDEntification database) archive[5] (Perez-Riverol et al., 2019). The PRIDE archive was searched to select *A. thaliana* datasets based on the analysis of specific plant organs, such as cauline, rosette and roots, and/or subcellular districts, such as chloroplasts and mitochondria. Datasets were excluded if enrichment/immunopurification strategies were used during protein purification. Finally, 21 experimental

[1] http://cbl-gorilla.cs.technion.ac.il

[2] http://mapman.gabipd.org/mapman

[3] https://genevestigator.com

[4] http://medgen.ugent.be/~jvdesomp/genorm

[5] https://www.ebi.ac.uk/pride/archive

sets of nano-LC-ESI-MS/MS raw data included in 14 PRIDE repositories (March 2020) were obtained and re-analyzed by database searching. Only raw files corresponding to the analysis of control/non-treated plants were downloaded and the experimental protocols and the search parameters for each different dataset were annotated. **Supplementary Table S2** lists the experimental sets, with details on the MS instrument, plant organ and/or subcellular compartment, sample preparation, and proteomic strategies adopted.

Raw files were searched separately using Proteome Discoverer 2.4 (Thermo Fisher Scientific, United States) with the Mascot v. 2.6 search engine (Matrix Science Ltd., United Kingdom) against the TAIR10 database[6] (71,567 sequences, accessed May 2017) and a database containing common laboratory contaminants on the MaxQuant website[7]. Workflows were built for each experimental dataset, considering the specific mass tolerance values used for the original search and reported on the PRIDE repository, or in the publication associated with the dataset.

For all the workflows, Cys carbamidomethylation was set as a fixed modification, while iodination at Tyr and His (Δm = +125.8966 Da), oxidation at Met, protein N-terminal acetylation, deamidation at Asp, and pyroglutamate formation at N-terminal Gln were selected as variable modifications. Isotopic labelling was also considered in the modification parameters when performed for protein quantification.

Trypsin was selected as the proteolytic enzyme and peptides were allowed to have a maximum of two missed cleavages. The minimum peptide length was set at six amino acids. The site probability threshold for peptide modification was set at 75. Only high confidence peptide identifications were retained by setting the target false discovery rate (FDR) for PSM at 0.01 and further filtered to keep only peptides ($P < 0.05$) with a Mascot Ion score > 30. In addition, the results of the identification analysis were processed by putting together the output of iodinated peptides from all the datasets and further applying a filter to keep only those identified with a Mascot Ion score > 50, in at least one dataset, to limit the identification to peptides with the best scoring matches and corresponding to high certainty. The presence of the MS/MS spectrum of the unmodified counterpart was verified for each iodinated peptide to further validate the identification.

Protein Bioinformatics

Proteins containing iodinated peptides were functionally annotated according to MapMan categories by using the Mercator pipeline[8]. Final outputs were integrated with data from the available literature. Protein interaction networks were obtained with STRING v. 11[9], which was also used to provide information on known gene ontology categories. Venn diagrams were depicted using a web tool at http://bioinformatics.psb.ugent.be/webtools/Venn. The Protein Abundance Database (PAXdb) was also queried to evaluate quantitative levels of modified *A. thaliana* proteins at https://pax-db.org.

Statistical Analysis

Data concerning phenotypical determinations and qPCR-based gene expression analysis were analysed by one-way ANOVA coupled with the LSD *post hoc* test, when they followed a normal distribution and there was homogeneity of variances. When one of these two prerequisites was violated, a Kruskal-Wallis test for non-parametric statistic was performed and the significance letters were graphically assigned using a box-and-whisker plot with a median notch. Significant differences between the means ($P < 0.05$) are indicated by different letters in the figures and tables.

RESULTS

Effects of Iodine on the Plant Phenotype

The effects of low amounts of KIO_3 (0.20 or 10 μM) on hydroponically grown Arabidopsis plants, compared to plants cultivated on a control nutrient solution, were evaluated in terms of plant morphology, biomass, and seed production (exp. 1-phenotype). No phytotoxicity symptoms were observed on plants and the most significant phenotypical effect was a delay of flowering in the control plants, compared to KIO_3 (either 0.20 or 10 μM) (**Figures 1A,B**). Twelve days after the opening of the first flower, plants treated with 0.20 or 10 μM KIO_3 were close to complete flowering, as 87 and 96% of the plants had bloomed, respectively, vs. 69% of the control plants (**Figure 1B**). Control plants took about 18 days to complete blooming.

Plant biomass, evaluated 1 month after the addition of KIO_3 to the nutrient solution, was significantly lower in control plants, both in FW and DW (**Figure 1C**). When compared to the control, the plant FW increased by approximately 7.7 and 13% with addition of 0.20 and 10 μM KIO_3 in the nutrient solution, respectively, whereas the DW increased by 13 and 22%, respectively. The effect on plant FW was mostly ascribable to the inflorescence, as no significant differences were evident in terms of the rosette FW values (**Supplementary Table S3**). The concentration of iodine in the nutrient solution had a marked effect on the inflorescence length, which was approximately 41 and 45% longer compared to the control in 0.20 and 10 μM KIO_3 treated plants, respectively (**Figure 1C**), and a comparable effect was seen on the inflorescence FW and DW (**Supplementary Table S3**). Additionally, the rosette diameter in the control was smaller, and the application of 0.20 or 10 μM KIO_3 increased it by approximately 5 and 9%, respectively (**Figure 1C**). The plant dry matter content positively correlated with the increased iodate concentrations (**Figure 1C**).

Seed production was determined in terms of total seed weight, seeds/silique and number of siliques/plant. The number of seeds contained in each silique was not affected by iodate treatments (**Supplementary Table S3**), whereas the number of siliques produced by each plant was lower in the control, compared to the addition of both 0.20 and 10 μM KIO_3 (**Figure 1C**). This influenced the total seed production, which, 1 month after the

[6] www.arabidopsis.org

[7] https://www.maxquant.org/maxquant/

[8] http://mapman.gabipd.org/web/guest/app/Mercator

[9] http://string-db.org

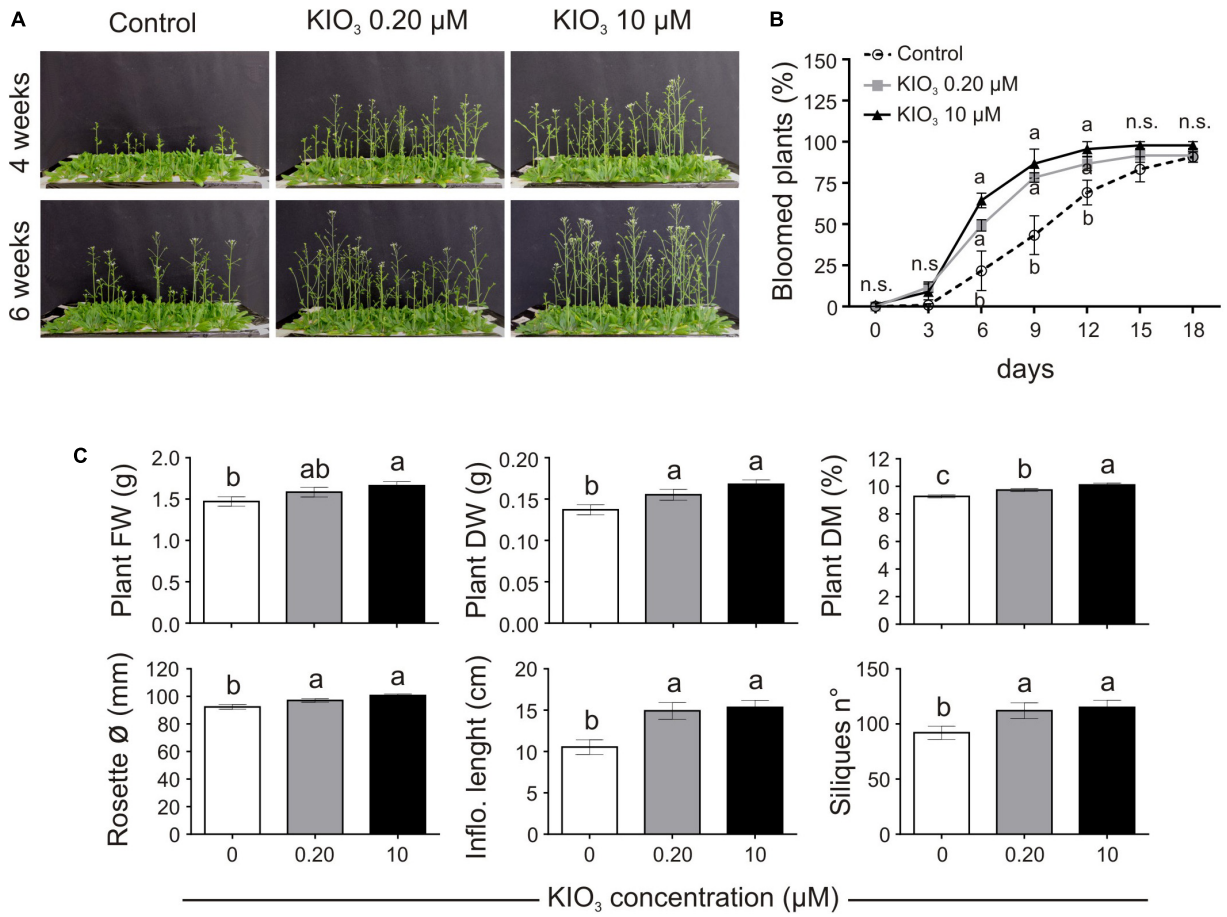


FIGURE 1 | Impact of iodine on plant growth and development (exp. 1-phenotype). **(A)** Lateral view of plants after 4 or 6 weeks from the onset of KIO_3 treatment. **(B)** Flowering time curve; the percentage of bloomed plants/tray was calculated every 3 days after the opening of the first flower (day 0). **(C)** Morphological data on plant FW, DW, dry matter content, rosette diameter, inflorescence length and number of produced siliques/plant, determined 1 month after the onset of KIO_3 treatments. Values indicated by different letters significantly differ from each other (according with one-way ANOVA, LSD *post hoc* test, $P \leq 0.05$). In particular, the statistical analysis of flowering **(B)** was performed by comparing the percentage of bloomed plants of each tray (considered as biological replicates) within each sampling point. When data followed a Normal distribution and there was homogeneity of variances, they were subjected to one-way ANOVA and values indicated by different letters significantly differ from each other (LSD *post hoc* test, $P \leq 0.05$). When one of this two prerequisite was violated, a Kruskal-Wallis test was performed. Error bars (±SE) are shown in graphs.

addition of KIO_3 to the nutrient solution, was much higher in plants treated with iodate (more than 50 and 35%, respectively, in 0.20 and 10 µM KIO_3 treated plants in comparison with the control) (**Supplementary Table S3**).

Adding exogenous iodine in the form of KIO_3 countered the delay in flowering of control plants (**Figures 1A,B**). This was confirmed in experiment 2 (exp. 2-phenotype), when iodine was added in the form of KI or NaI (**Figures 2A,B**). The possible effects of potassium or bromide, as an alternative halogen, were evaluated and then ruled out, as a similar behaviour was observed in plants treated with KI or NaI, but not with KBr (**Figures 2A,B**).

The application of 10 µM KI and NaI promoted flowering, without negatively impacting the plant biomass production (**Figure 2C**), whereas 30 µM KI or NaI reduced plant growth (**Figure 2C**), although the promoting effect of iodine on flowering was still present (**Figures 2A,B**). Four days after the opening of the first flower (day 0), more than 50% of KI- and NaI-treated plants had bloomed vs. 14% of the control plants and 10% and 14% of the 10 and 30 µM KBr-treated plants, respectively. Moreover, the floral transition was almost complete in 10 µM KI- and NaI-fed plants in the subsequent 6 days (10 days after day 0). Two and four more days were required for 30 µM KI- and NaI-fed plants, respectively (12 and 14 days after day 0), whereas the control and KBr-treated plants completed blooming in the subsequent 18 days (22 days after day 0) (**Figure 2A**).

Effects of Iodine on Gene Expression

The response of plants to iodine was analyzed at the transcriptomic level. To identify genes whose expression was specifically altered by iodine, Arabidopsis plants were treated by adding 10 µM of NaI, KI, or KBr to the nutrient solution, compared to the untreated control plants. The resulting RNAs were analyzed by hybridisation on ATH1 microarrays. To rule out the possible generic effects of halogens, we searched the

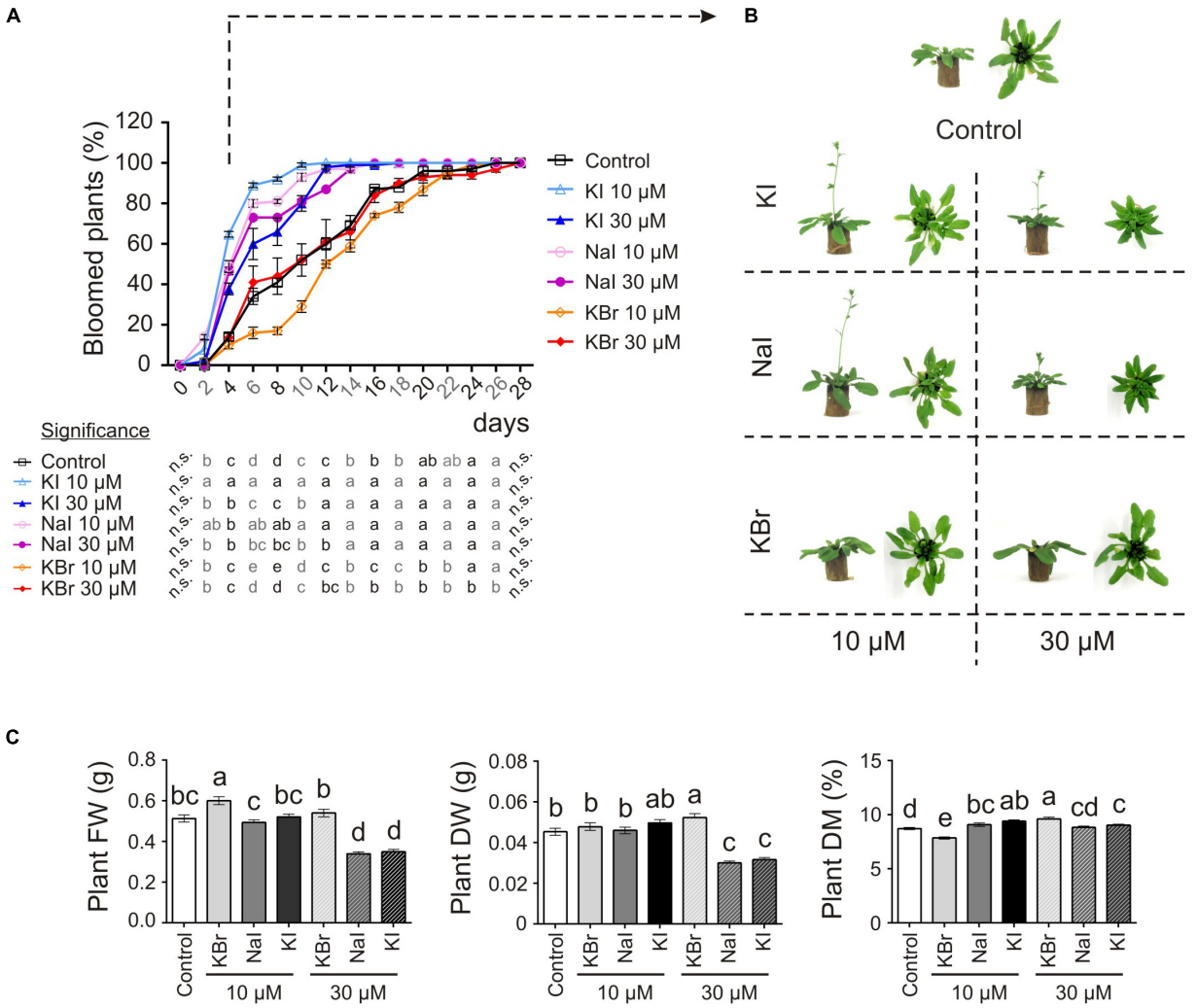


FIGURE 2 | Impact of iodine on plant growth and development (exp. 2-phenotype). **(A)** Flowering curve; the percentage of bloomed plants/tray was calculated every 2 days after the opening of the first flower (day 0). **(B)** Representative control, and KI-, NaI- or KBr-treated plants (10 and 30 µM) after 15 days from the onset of the treatments. Pictures were taken after 4 days from the opening of the first flower on the main stem. **(C)** Morphological data on plant FW, DW, dry matter content determined 15 days after the onset of the treatments. Values indicated by different letters significantly differ from each other (according with one-way ANOVA, LSD *post hoc* test, $P \leq 0.05$). In particular, the statistical analysis of flowering **(A)** was performed by comparing the percentage of bloomed plants of each tray (considered as biological replicates) within each sampling point. When data followed a Normal distribution and there was homogeneity of variances, they were subjected to one-way ANOVA and values indicated by different letters significantly differ from each other (LSD *post hoc* test, $P \leq 0.05$). When one of this two prerequisite was violated, a Kruskal-Wallis test was performed. Error bars (±SE) are shown in graphs.

microarray dataset for genes that responded to KI and NaI, but not to KBr. In addition, a comparison between KBr- and KI-treated plants enabled us to rule out the possible transcriptional regulation of genes exerted by potassium, as K^+ ion was common to both salts.

Data visualisation with a Venn diagram showed that several genes were specifically regulated by iodine, as up- or down-regulated genes in both NaI- and KI- but not in KBr-treated plants were 33 (51% of DEGs) and 15 (33% of DEGs) in the shoot (**Figure 3A**), and 398 (95% of DEGs) and 133 (79% of DEGs) in the root (**Figure 3B**), respectively. The similarity and specificity in the expression pattern of KI- and NaI-treated plants were confirmed by the heatmaps generated from the analysis of the shoot (**Figure 3C**) and root (**Figure 3D**) expression data.

To validate the microarray analysis, a subset of three I^--induced and three I^--repressed genes were analysed by qPCR, corroborating the specific regulation of iodine on their expression in both shoot (**Figure 3E**) and root (**Figure 3F**) samples.

The complete list of the KI and NaI commonly and not responding to KBr up- and down-regulated genes is reported in **Supplementary Tables S4, S5** (shoot tissue), and **Supplementary Tables S6, S7** (root tissue), respectively.

The polypeptides codified by the iodine-regulated genes did not show a preferential site of action in the cell, as their predicted localisations include cytoplasm, chloroplast,

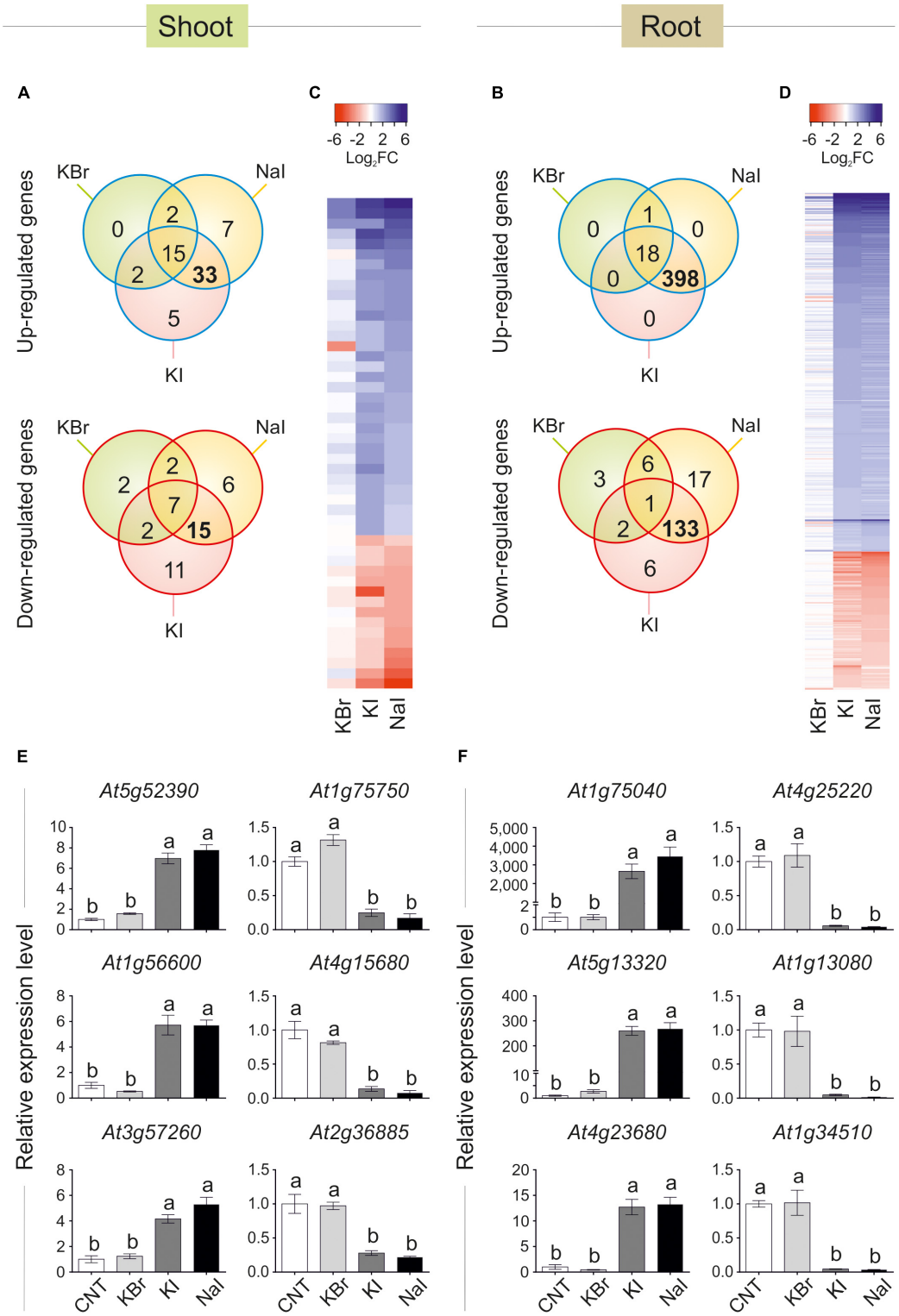


FIGURE 3 | Transcriptional regulation of gene expression induced by iodine. Venn diagram showing the number of genes differentially regulated in shoot **(A)** or root **(B)** tissues of KBr-, NaI-, and KI-treated plants (10 μM—48 h), when compared with the control. Heatmap showing the pattern of expression of the genes analysed in the shoot **(C)** or root **(D)** tissues in response to NaI, KI or KBr treatments, when compared with the control. qPCR validation of selected genes up- or down-regulated by iodine treatments (commonly regulated by NaI and KI, but not KBr) in shoot **(E)** or root **(F)** tissues. qPCR data are mean ± SE of four biological replicates, each composed of a pool of three different rosettes. Values indicated by different letters significantly differ from each other (according with one-way ANOVA, LSD *post hoc* test, $P \leq 0.05$).

cell wall, nucleus, mitochondrion, vacuole and apoplast (**Supplementary Tables S4–S7**).

The gene ontology (GO) analysis identified several functional categories regulated by iodine in the roots (**Figure 4**, **Supplementary Figure S2** and **Supplementary Tables S8, S9**), whereas no statistically significant GO terms were identified by analysing the DEG data on the shoots.

The most representative biological processes affected by iodine in the roots were related to the *response to stimulus* (GO:0050896), and the downstream categories associated with *response to abiotic* (GO:0009628) and *biotic stimulus* (GO:0009607) (**Figure 4** and **Supplementary Table S8**). The main molecular functions regulated by iodine in the roots were related to *antioxidant* (GO:0016209) and *oxidoreductase activity* (GO:0016491) and related child terms, in particular *peroxidase activity* (GO:0004601) and *oxidoreductase activity*, *acting on peroxide as acceptor* (GO:0016684) (**Supplementary Figure S2** and **Supplementary Table S9**).

DEGs analysis performed with MapMan highlighted an over-representation of several genes in root samples that were related to calcium regulation and protein modification/degradation (**Supplementary Figure S3A**), together with genes encoding for the large enzyme families including peroxidases, oxidases, glutathione S-transferases, and cytochrome P450 (**Supplementary Figure S3B**).

The relatively low number of genes regulated by iodine in the shoots prevented a gene ontology analysis from being performed. However, in terms of the most well characterised genes specifically regulated by iodine treatments in the shoot, the main pathways affected were directly or indirectly involved in biotic (approximately 48 or 40% of up- or down-regulates genes, respectively) or abiotic (approximately 45 or 33% of up- or down-regulates genes, respectively) stress response pathways (**Supplementary Tables S4, S5**). Several genes playing a role in the transition to flowering (*At4g19191* and *At1g75750*) and embryo and pollen development (i.e., *At1g21310*, *At3g54150*) are also worth mentioning.

The involvement of iodine in the defence response, highlighted by the previous analyses performed on root samples, was also suggested by querying all publicly available microarray datasets (see footnote) using the list of iodine-responsive genes of both shoot (**Supplementary Figure S4**) and root (**Supplementary Figure S5**) tissues. The majority of the up- or down-regulated genes were commonly modulated by the presence of fungal infection, salicylic acid (SA) or synthetic analogues of SA, such as benzothiadiazole (Kouzai et al., 2018).

Protein Iodination in Plants

Iodine can be found in plant tissues not only in a mineral form but also in organic compounds (Wang et al., 2014; Smoleń et al., 2020). To verify the possible *in vivo* incorporation of iodine into proteins, we carried out two different experiments by feeding hydroponically grown plants with ^{125}I and carrying out the autoradiography of the SDS-PAGE of the relative protein extracts to detect possible radio-labelled proteins. The experiments were performed first with Arabidopsis plants, and then with other species, namely maize, tomato, wheat and lettuce.

The experiment carried out with Arabidopsis plants revealed the presence of at least six radio-labelled bands at different molecular mass values in the protein extracts from shoot tissues (**Figure 5A**; exp. 1-radioactive) and eleven radio-labelled bands from root tissues (**Figure 5B**; exp. 1-radioactive), indicating the presence of proteins likely containing iodo-amino acids. Iodinated proteins were preferentially present in root tissues, as the abundance and intensity of ^{125}I-labelled bands were higher in the root than in the shoot extracts. No radioactive signals were observed in the shoot and root control samples (samples added with ^{125}I solution during protein extraction).

Several ^{125}I -labelled bands were also observed in the leaf extracts of tomato, wheat and lettuce samples, whereas no ^{125}I-containing bands were visible in the leaf protein extracts of maize (**Figure 5A**; exp. 2-radioactive). A clear radioactive signal was detected in several root proteins extracted from all the species analysed, including maize (**Figure 5B**; exp. 2-radioactive). Also in this case, the intensity of the radiolabelled bands was higher in root than in shoot extracts. A good degree of conservation of the molecular mass values of the putatively iodinated proteins was observed among the five plant species analysed (**Figure 5**).

Identification of Iodinated Proteins in *Arabidopsis thaliana*

The identification of the radiolabelled proteins described above was hampered by the presence of a radioactive isotope, which meant that our samples did not meet the safety rules for proteomic facilities. To maximise the probability of success in identifying targets of protein iodination, we then focused on the nano-LC-ESI-MS/MS raw data already acquired within the framework of experimental studies on different organs/subcellular districts of *Arabidopsis thaliana,* and released in the public repository PRoteomics IDEntification Database (PRIDE) Archive (Perez-Riverol et al., 2019).

The datasets considered for our analysis refer to many different experimental conditions in terms of plant growth, treatment, and cultivation regimen, as well as sample processing and fractionation performed before proteomic analysis. No experiments were explicitly related to iodination studies; the presence of iodine occurred accidentally, as a consequence of its natural presence in the cultivation environment (i.e., soil, air, irrigation water), or because it was conventionally present in the MS growing medium (Murashige and Skoog, 1962), which is widely used in studies based on *in vitro* plant tissue culture.

In proteins, iodination affects various amino acids, depending on the reaction conditions (Ramachandran, 1956), but generally following the reactivity order Tyr >> His $\geq$ Trp > Cys.

Mono-iodination at Tyr and His residues were thus considered in the searching parameters as variable modifications. The output of the database search, in terms of proteins iodinated at Tyr or His residues has been reported in **Supplementary Table S10**.

The iodinated peptides were identified in 16 out of the 21 datasets analysed. A total of 106 iodinated peptides, corresponding, respectively, to 42 and 40 protein accessions in

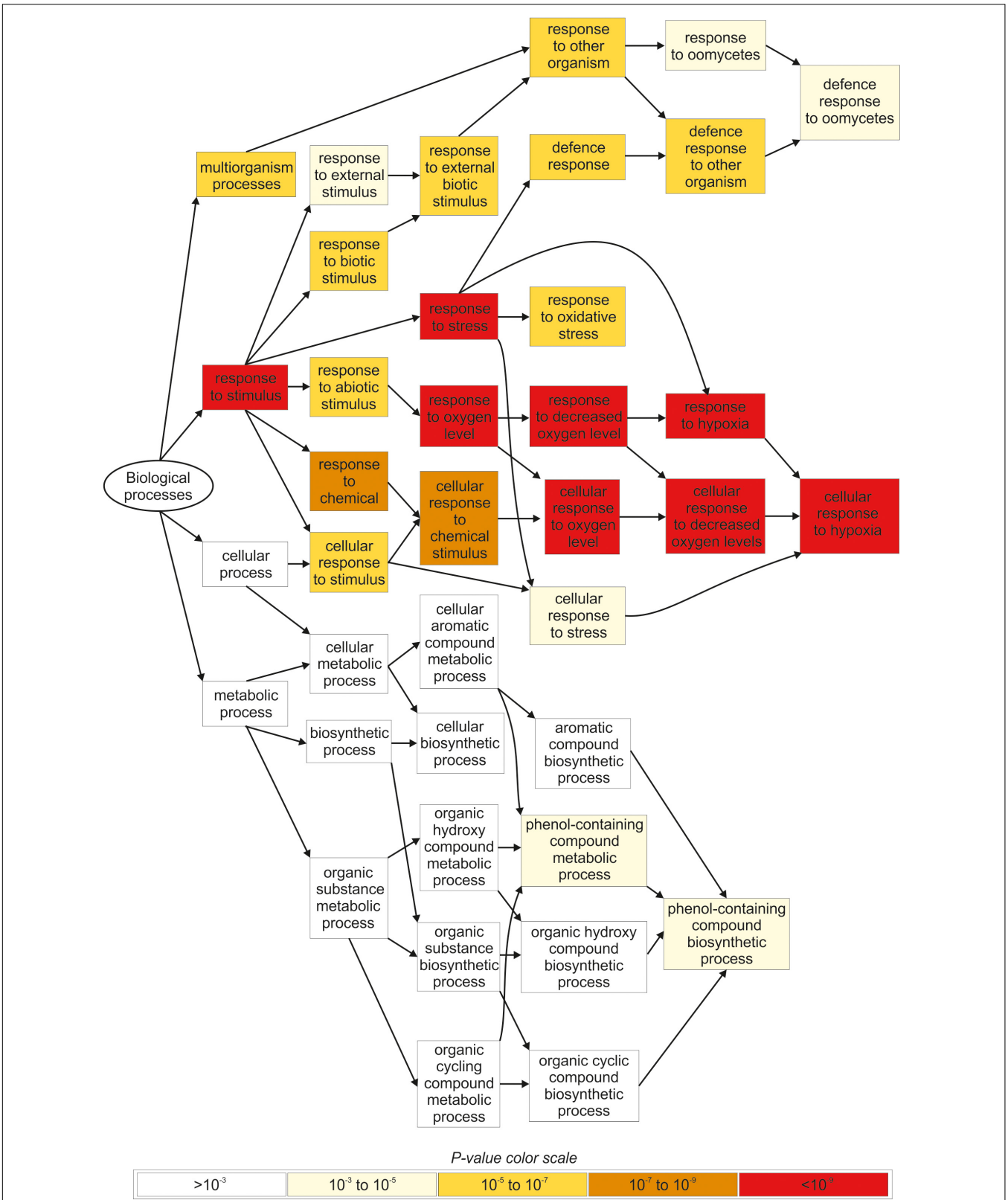


FIGURE 4 | Overview of the main biological processes affected by iodine based on the GO terms enrichment analysis carried out in root tissues. Only genes regulated in NaI- and KI-treated plants, and not in KBr-treated plants, when compared with the control, were analysed. The figure was extracted from GOrilla (http://cbl-gorilla.cs.technion.ac.il) and reproduced. In this analysis, DEGs with $\log_2FC \geq 2.5$ or $\log_2FC \leq -2.5$ were used.

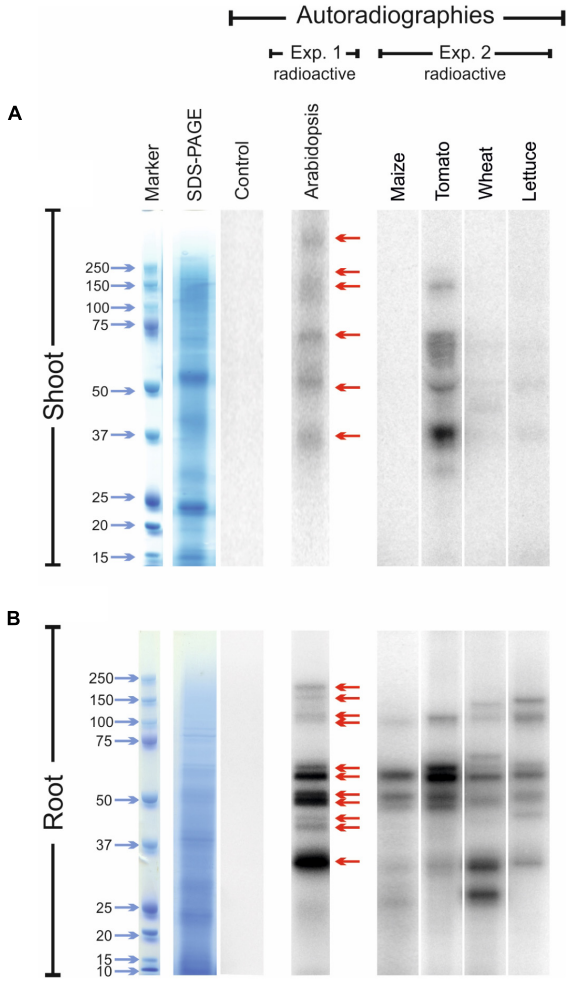


FIGURE 5 | Autoradiographies of the SDS-PAGE gels. Comparison between the position and relative intensities of ^{125}I radiolabelled bands of representative shoot **(A)** and root **(B)** protein extracts from ^{125}I treated Arabidopsis (exp. 1-radioactive), and maize, tomato, wheat and lettuce plants (exp. 2-radioactive). Sampling was performed after 48 h of ^{125}I incubation. In both the experiments, autoradiographies were acquired after 72 h of gel exposition to the multipurpose phosphor storage screen. Representative pictures of total stained protein extracts (SDS-PAGE) and of the autoradiographies of control samples after 15 days of exposition are also shown. Controls consisted in protein extracts obtained from plants untreated with ^{125}I during their growth, to which the radioactive solution containing ^{125}I was added during the extraction process.

the TAIR10 database of *A. thaliana* leaves (chloroplast, cauline, and rosette) (**Table 1**) and roots (**Table 2**), were identified. Iodinated sequences differently modified for deamidation, and/or protein N-terminal acetylation, and/or Met oxidation are reported as a unique iodinated peptide inventory.

Most of the modified peptides were found to be iodinated at Tyr residues, while His iodination was identified in only five peptides. Representative MS/MS spectra of Tyr-iodinated peptides are reported in **Figure 6A**.

To evaluate the entire output of iodinated peptides identified, iodinated sequences for chloroplasts, caulines, rosettes, and roots were processed and visualised in a Venn diagram (**Figure 6B**). This showed the presence of the common iodinated peptides for the chloroplast cauline and rosette subsets. The root subset was clearly distinct from the other three subsets that were all from the green parts of the plant.

Iodinated Proteins in *A. thaliana* Leaves

Iodinated peptides identified in 11 datasets of cauline, rosette, and leaf-isolated chloroplasts were assigned to 42 proteins (**Supplementary Table S10**). Most of the modified species were in the dataset of chloroplastic proteins (**Figure 6B**). STRING interaction analysis of the modified proteins revealed a single network of 40 iodinated proteins (PPI enrichment $p < 1.0e^{-16}$) (**Supplementary Figure S6A** and **Supplementary Table S11**). A total of 31 of the 40 proteins in this network were involved in *photosynthesis* (GO:0015979) (**Supplementary Table S12**), as also attested by their functional analysis, according to MapMan categories (**Supplementary Figure S6B** and **Supplementary Table S13**). Moreover, the main molecular functions in which iodinated proteins are involved were related to *chlorophyll binding* (GO:0016168), *protein domain specific binding* (GO:0019904), *tetrapyrrole binding* (GO:0046906), and *electron transfer activity* (GO:0009055) (**Supplementary Table S12**). In particular, ten proteins were identified in two or more datasets, thus resulting in the most representative targets of the iodination reaction. Some of these proteins were constituents of the photosystem II (PSII), i.e., proteins of the reaction centre (PsbA, PsbB), oxygen evolving centre (PsbO, PsbP) and light harvesting complex II (LHCB1B1), or part of the photosystem I (PSI) (PsaF, PETE2). Three proteins showed ribulose-1,5-bisphosphate carboxylase/oxygenase (RuBisCo) activity and were involved in the Calvin Cycle (RBCL, ORF110A, RBCS1A). These proteins were largely abundant in leaf tissues, especially the PSII component PsbB and RuBisCo large and small chains (RBCL, RBCS1A), according to the data reported in PAXdb.

Iodinated Proteins in *A. thaliana* Roots

Iodinated peptides identified in 5 datasets of roots were assigned to 40 proteins (**Supplementary Table S10**). The STRING interaction analysis recognised three networks containing 24 of the 40 iodinated proteins (**Supplementary Figure S7A** and **Supplementary Table S11**). The GO analysis for these proteins showed a significant over-representation of biological processes related to the *response to stress* (GO:0006950), *response to oxidative stress* (GO:0006979), *response to toxic substances* (GO:0009636), and *response to stimulus* (GO:0050896). For the molecular functions, the most enriched categories were *copper ion binding* (GO:0005507) and *peroxidase activity* (GO:0004601) (**Supplementary Table S14**).

The functional analysis of the iodinated proteins in roots, according to MapMan categories, highlighted a broad range of biological roles (**Supplementary Figure S7B** and **Supplementary Table S13**). In particular, among the iodinated proteins identified, 12 were found in two or more datasets. Five proteins belonged to the classical plant (class III) peroxidase subfamily (At4g30170, At1g05240, At2g37130, At3g01190, At5g17820). The alignment of the protein sequences of the peroxidases mentioned above

TABLE 1 | Iodinated peptides identified in *A. thaliana* leaves (chloroplast, cauline, and rosette) by database searching of mass spectrometric data retrieved from PRIDE repository.

Protein accession	Description	Iodinated sequence	Iodinated site	DATASET
ATCG00120.1	ATP synthase subunit alpha	EAYPGDVFYLHSR	[Y3]	ChlorBN
		SVYEPLQTGLIAIDSMIPIGR	[Y3]	ChlorBN
ATCG00480.1	ATP synthase subunit beta	GIYPAVDPLDSTSTMLQPR	[Y3]	ChlorBN
		GSITSIQAVYVPADDLTDPAPATTFAHLDATTVLSR	[Y10]	ChlorBN
		IVGEEHYETAQQVK	[Y7]	ChlorBN, Chlo3516
		VALVYGQMNEPPGAR	[Y5]	ChlorBN
		VGLTALTMAEYFR	[Y11]	ChlorBN
AT4G04640.1	ATPase, F1 complex, gamma subunit protein	GLGLEYTVISVGK	[Y6]	ChlorBN
AT1G29910.1	Chlorophyll A/B binding protein 3	YLGPFSGESPSYLTGEFPGDYGWDTAGLSADPETFAR	[Y1]*	ChlorBN
AT1G20340.1	Cupredoxin superfamily protein	NNAGYPHNVVFDEDEIPSGVDVAK	[H7]*	CAU, Ros
AT5G66190.1	Ferredoxin-NADP(+)-oxidoreductase 1	LVYTNDGGEIVK	[Y3]	ChlorBN
AT4G38970.1	Fructose-bisphosphate aldolase 2	ATPEQVAAYTLK	[Y9]	ChlorBN
AT5G42270.1	FtsH extracellular protease family	DYSMATADVVDAEVR	[Y2]	ChlorBN
AT3G09260.1	Glycosyl hydrolase superfamily protein	CSSYVNAK	[Y4]	ChlorBN
		GPALWDIYCR	[Y8]	ChlorBN
		FGLYYVDFK	[Y4]*	ChlorBN
AT4G10340.1	Light harvesting complex of photosystem II 5	SEIPEYLNGEVAGDYGYDPFGLGK	[Y15]*	ChlorBN
		TGALLLDGNTLNYFGK	[Y13]	ChlorBN
AT5G54270.1	Light-harvesting chlorophyll B-binding protein 3	YLGPFSVQTPSYLTGEFPGDYGWDTAGLSADPEAFAK	[Y21]*	ChlorBN
AT2G34430.1	Light-harvesting chlorophyll-protein complex II subunit B1	YLGPFSGEPPSYLTGEFPGDYGWDTAGLSADPETFAR	[Y12]*	ChlorBN, PXD010730, LFD
AT2G24940.1	Membrane-associated progesterone binding protein 2	SFYGSGGDYSMFAGK	[Y3]	Ros
AT4G22890.5	PGR5-LIKE A	FLEASMAYVSGNPILNDEEYDKLK	[Y20]	ChlorBN
ATCG00540.1	Photosynthetic electron transfer A	GGYEITIVDASNGR	[Y3]	ChlorBN
AT4G03280.1	Photosynthetic electron transfer C	GDPTYLVVENDK	[Y5]	ChlorBN
AT4G28750.1	Photosystem I reaction centre subunit IV/PsaE protein	VNYANISTNNYALDEVEEVAA	[Y3]	ChlorBN
AT2G20260.1	Photosystem I subunit E-2	VNYANISTNNYALDEVEEVK	[Y3]	ChlorBN
AT1G31330.1	Photosystem I subunit F	LYAPESAPALALNAQIEK	[Y2]	ChlorBN, Ros
AT1G52230.1	Photosystem I subunit H2	SVYFDLEDLGNTTGQWDVYGSDAPSPYNPLQSK	[Y19]	ChlorBN
ATCG00340.1	Photosystem I, PsaA/PsaB protein	TSYGFDVLLSSTSGPAFNAGR	[Y3]	ChlorBN
AT1G03600.1	Photosystem II family protein	DIYSALNAVSGHYVSFGPTAPIPAK	[Y3]	ChlorBN
AT1G06680.1	Photosystem II subunit P-1	SITDYGSPEEFLSQVNYLLGK	[Y5]*	ChlorBN, PXD010730
AT1G79040.1	Photosystem II subunit R	YGANVDGYSPIYNENEWSASGDVYK	[Y12]*	ChlorBN
AT2G05100.1	Photosystem II light harvesting complex gene 2.1	STPQSIWYGPDRPK	[Y8]	ChlorBN
		YLGPFSENTPSYLTGEYPGDYGWDTAGLSADPETFAK	[Y12]*	ChlorBN
AT2G20890.1	Photosystem II reaction centre PSB29 protein	AYIEALNEDPK	[Y2]	ChlorBN
AT2G30790.1	Photosystem II subunit P-2	SITDYGSPEQFLSQVNYLLGK	[Y5]*	ChlorBN
AT3G50820.1	Photosystem II subunit O-2	GGSTGYDNAVALPAGGR	[Y6]	ChlorBN, Chlo3516
AT4G05180.1	Photosystem II subunit Q-2	YYSETVSSLNNVLAK	[Y2]	ChlorBN
AT4G21280.1	Photosystem II subunit QA	LFDTIDNLDYAAK	[Y10]	ChlorBN
		YYAETVSALNEVLAK	[Y2]*	ChlorBN
ATCG00020.1	Photosystem II reaction centre protein A	ETTENESANEGYR	[Y12]	ChlorBN, TMAR
		FGQEEETYNIVAAHGYFGR	[Y8]	ChlorBN

(Continued)

TABLE 1 | Continued

Protein accession	Description	Iodinated sequence	Iodinated site	DATASET
ATCG00270.1	Photosystem II reaction centre protein D	AAEDPEFETFYTK	[Y11]	ChlorBN
ATCG00280.1	Photosystem II reaction centre protein C	DIQPWQERRSAEYMTHAPLGSLNSVGGVATEINAVNYVSPR	[H16]	LFD
		RSAEYMTHAPLGSLNSVGGVATEINAVNYVSPR	[H8]	CAU, Ros
		SAEYMTHAPLGSLNSVGGVATEINAVNYVSPR	[H7]*	ChlorBN, LFP
ATCG00680.1	Photosystem II reaction centre protein B	LAFYDYIGNNPAK	[Y4]*	ChlorBN, TMAR, CAU,Ros
		YQWDQGYFQQEIYR	[Y7]*	ChlorBN
AT5G07020.1	Proline-rich family protein	AVDYSGPSLSYYINK	[Y12]	ChlorBN
AT1G74470.1	Pyridine nucleotide-disulphide oxidoreductase	SIDAGDYDYAIAFQER	[Y7]	ChlorBN
ATMG00280.1	Ribulose bisphosphate carboxylase large chain, catalytic domain	GGLYFTKDDENVNSQPFMR	[Y4]	CLLF, LFD, LFP, LFPT
AT1G67090.1	Ribulose bisphosphate carboxylase small chain 1A	EYPNAFIR	[Y2]	ChlorBN, CAU, Ros
ATCG00490.1	Ribulose-bisphosphate carboxylases	GHYLNATAGTCEEMIKR	[Y3]*	ChlorBN, Chlo10545,CAU
		LTYYTPEYETKDTDILAAFR	[Y8]*	CAU, Ros
AT1G71500.1	Rieske (2Fe-2S) domain-containing protein	SPAEGAYSEGLLNAR	[Y7]	ChlorBN
AT2G39730.1	Rubisco activase	GLAYDTSDDQQDITR	[Y4]	ChlorBN
AT1G54780.1	Thylakoid lumen 18.3 kDa protein	ADAFEYADQVLEK	[Y6]	ChlorBN
		ETYVVDDAGVLSR	[Y3]	ChlorBN

Protein Accession and Description, sequence of iodinated peptide and iodination site have been reported. In the case of peptide sequences in which more than one iodinated residues were identified, the asterisk indicates the iodination site identified with the highest score. The datasets in which the iodinated peptides were identified have been indicated.

showed that iodinated residues in all peptides preferentially corresponded to conserved Tyr residues, while only two iodinated tyrosines were unrelated (**Supplementary Figure S8**).

The other iodinated proteins included: (i) copper amine oxidase (CUAOy2), a cell-wall oxidase showing primary amine oxidase activity; (ii) beta-galactosidase 5 (BGAL5), a glycoside hydrolase involved in the modification of cell wall polysaccharides; (iii) glycosyl hydrolases family 32 protein (ATBFRUCT1), acting as a cell wall invertase; (iv) Pole Ole1 allergen/extension domain (IPR006041)-containing proline-rich protein-like 1 (PRPL1-MOP10) and root hair specific 13 protein (RHS13), which are cell-wall components; (v) D-mannose binding lectin protein (MBL1); and (vi) glyceraldehyde-3-phosphate dehydrogenase C sub 1 (GAPC1), a key enzyme in glycolysis. According to PAXdb, some of the above-reported proteins are abundant in the roots.

DISCUSSION

Iodine Influences Plant Growth and Development and Can Modulate the Plant Transcriptome

Establishing whether iodine is important for a plant's life is complex, as it is always present in variable amounts in the soil, water, and atmosphere. Plants can take up iodine from the soil solution through the root system, but they also assimilate it from the air or absorb it through the leaves if dissolved in salt solutions or in rain. All these processes occur naturally (Fuge and Johnson, 1986; Ashworth, 2009), thus a plant cannot be grown in the complete absence of iodine.

To identify whether iodine can act as a micro-nutrient we supplied it to plants at very low concentrations (in the micromolar range). These concentrations are typical of many mineral elements that are beneficial or essential when taken up in low doses, and phytotoxic when in excess (Welch and Shuman, 1995). We observed a difference in plant growth between the control and iodine-treated plants. Where these could be perceived as positive effects of addition of a beneficial compound, these can also be interpreted as a negative effect of removal of iodine from the plant's nutrition. An increase in biomass and seed production, together with a very evident hastening of flowering, was observed by feeding plants with KIO_3 (**Figure 1** and **Supplementary Table S1**) or KI (**Figure 2**) at 0.2 and/or 10 μM. On addition of iodine, flowering was always early and appeared to be specific for iodine, since it was present in the KIO_3, KI and NaI treatments but completely absent in KBr (**Figures 1**, **2**). However, the positive effects of iodine on growth were lost at 30 μM. This suggests that a concentration of 30 μM applied as I^- may be above the toxicity threshold.

In the range of 1–10 μM iodine increases biomass in vegetables, e.g., spinach (Zhu et al., 2003), lettuce (Blasco et al., 2013), tomato (Lehr et al., 1958; Borst Pauwels, 1961), and strawberry (Li et al., 2016), or staple crops, e.g.,

TABLE 2 | Iodinated peptides identified in *A. thaliana* roots by database searching of mass spectrometric data retrieved from PRIDE repository.

Protein accession	Description	Iodinated sequence	Iodinated site	DATASET
AT5G09810.1	Actin 7	NYELPDGQVITIGAER	[Y2]	Root
AT1G28290.1	Arabinogalactan protein 31	NGYFLLLAPK	[Y3]	RT
AT5G08680.1	ATP synthase alpha/beta family protein	VGLTGLTVAEYFR	[Y11]	Root
AT1G45130.1	Beta-galactosidase 5	YDEDIATYGNR	[Y1]	RT, RTTP, RTUZ
AT2G43610.1	Chitinase family protein	YCSPSTTYPCQPGK	[Y1]	Root
AT3G43670.1	Copper amine oxidase family protein	GTAYENVEDLGEK	[Y4]	RT, RTUZ
AT1G78850.1	D-mannose binding lectin protein	TGDSSLVAYVK	[Y9]	Root, RT, RTTP
AT5G20080.1	FAD/NAD(P)-binding oxidoreductase	IFYTVDNPTK	[Y3]	Root
AT4G20830.1	FAD-binding Berberine family protein	DVDIGVNDHGANSYK	[Y14]	RTTP
AT5G44380.1	FAD-binding Berberine family protein	YGLAGDNVLDVK	[Y1]	RTUZ
AT5G50950.1	FUMARASE 2	IGYDNAAAVAK	[Y3]	Root
AT3G04120.1	Glyceraldehyde-3-phosphate dehydrogenase C sub1	LKGILGYTEDDVVSTDFVGDNR	[Y7]	RT, RTTP, RTUZ
AT4G16260.1	Glycosyl hydrolase superfamily protein	AFYTNLASR	[Y3]	Root
		LYDPNQAALNALR	[Y2]	Root
AT3G13790.1	Glycosyl hydrolases family 32 protein	HDYYTIGTYDR	[Y4]*	RT, RTUZ
AT3G19390.1	Granulin repeat cysteine protease family protein	VVTIDGYEDVPQNDEK	[Y7]	Root
AT3G12580.1	Heat shock protein 70	NALENYAYNMR	[Y6]	Root
		TTPSYVAFTDSER	[Y5]	Root
AT5G42020.1	Heat shock protein 70 (Hsp 70) family protein	NALETYVYNMK	[Y8]*	Root
AT3G16430.1	Jacalin-related lectin 31	VYVGQAQDGISAVK	[Y2]	Root
AT2G22170.1	Lipase/lipooxygenase, PLAT/LH2 family protein	VYDKYGDYIGIR	[Y8]*	Root
AT3G16460.1	Mannose-binding lectin superfamily protein	IYASYGGEGIQYVK	[Y5]*	Root
AT3G48890.1	Membrane-associated progesterone binding protein 3	MFYGPGGPYALFAGK	[Y3]	Root
AT4G19410.1	Pectinacetylesterase family protein	DITGGSYIQSYYSK	[Y7]	RT
AT4G30170.1	Peroxidase family protein	EVVVLTGGPSYPVELGR	[Y11]	Root, RT, RTUZ
		IYNFSPTTR	[Y2]	Root
		TGFYQNSCPNVETIVR	[Y4]	Root, RT
AT1G05240.1	Peroxidase superfamily protein	GDSDPSMNPSYVR	[Y11]	RT, RTTP, RTUZ
AT2G37130.1	Peroxidase superfamily protein	PTPDPNAVLYSR	[Y10]	RT, RTUZ
		QQVETLYYK	[Y8]	RT, RTTP, RTUZ
AT3G01190.1	Peroxidase superfamily protein	TFDLSYFTLVAK	[Y6]	RT, RTUZ
AT5G17820.1	Peroxidase superfamily protein	DSVALAGGPSYSIPTGR	[Y11]	Root, RT
		VGFYSQSCPQAETIVR	[Y4]	RT
AT1G79550.1	Phosphoglycerate kinase	YSLKPLVPRLSELLGVEVVMANDSIGEEVQK	[Y1]	RT
AT4G20260.4	Plasma-membrane associated cation-binding protein 1	VVETYEATSAEVK	[Y5]	Root
AT2G47540.1	Pollen Ole e 1 allergen and extensin family protein	GISGAILQNYR	[Y10]	Root
AT5G05500.1	Pollen Ole e 1 allergen and extensin family protein	TDSYGHFYGELK	[Y4]	RT, RTTP, RTUZ
AT4G14060.1	Polyketide cyclase/dehydrase and lipid transport superfamily protein	VYDTILQFIQK	[Y2]	Root
		ATSGTYVTEVPLKGSAEK	[Y6]	Root
AT4G23680.1	Polyketide cyclase/dehydrase and lipid transport superfamily protein	VYDVVYQFIPK	[Y2]	Root
AT2G19760.1	Profilin 1	TNQALVFGFYDEPMTGGQCNLVVER	[Y10]	RTTOF
AT4G02270.1	Root hair specific 13	VDAYGNELVPISILSSK	[Y4]	Root, RTTP, RTUZ
AT4G26220.1	S-adenosyl-L-methionine-dependent methyltransferases	GLLKSEELYKYILETSVYPR	[Y9]	RTTP
AT1G58270.1	TRAF-like family protein	FLDSYTSDSFSSGGR	[Y5]	Root
AT1G45201.1	Triacylglycerol lipase-like 1	FVYNNDVVPR	[Y3]	Root
AT3G55440.1	Triosephosphate isomerase	IIYGGSVNGGNCK	[Y3]	Root
AT4G30270.1	Xyloglucan endotransglucosylase/hydrolase 24	NYESLGVLFPK	[Y2]	RT
		LVPGNSAGTVTTFYLK	[Y14]	RTTP

Protein Accession and Description, sequence of iodinated peptide and iodination site have been reported. In the case of peptide sequences in which more than one iodinated residues were identified, the asterisk indicates the iodination site identified with the highest score. The datasets in which the iodinated peptides were identified have been indicated.

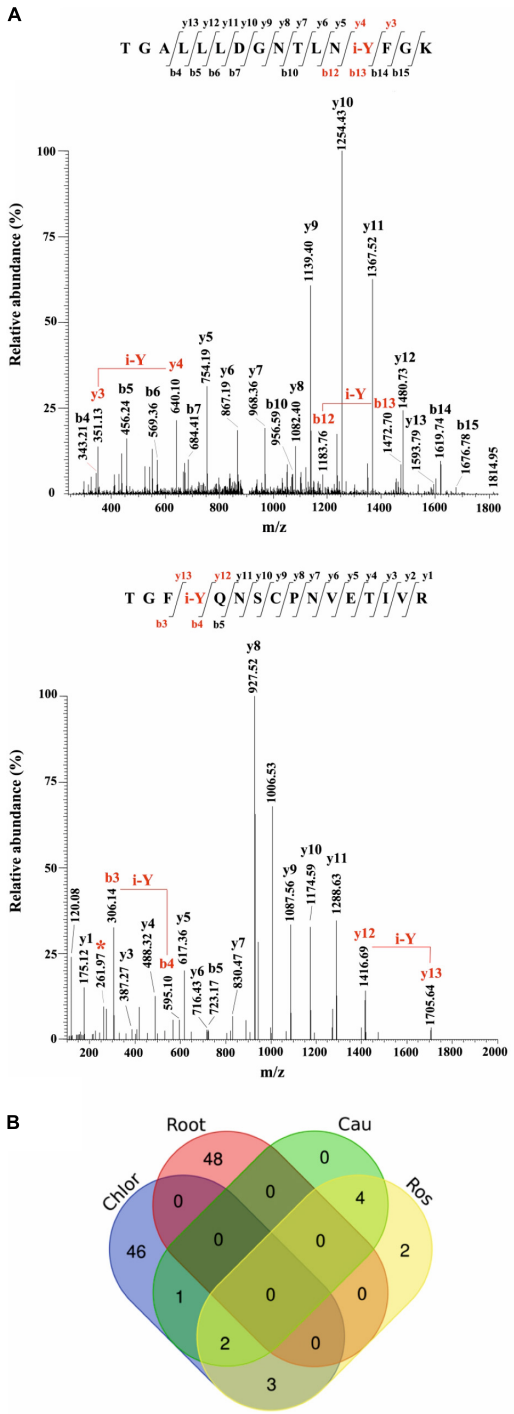


FIGURE 6 | Iodination in *A. thaliana* proteins identified by database searching of nano-LC-ESI-MS/MS raw data from a public repository (PRIDE). **(A)** Unambiguous assignment of iodination sites by MS/MS analysis in two peptides from chloroplast (light harvesting complex of photosystem II 5, AT4G10340.1), upper panel, and roots (peroxidase superfamily protein, AT4G30170.1), lower panel. The peptides are identified by both y, and b ions. Red labels in the spectra evidence the mass shift corresponding to the iodinated tyrosine (i-Y). **(B)** Venn Diagram showing the iodinated peptide sequences identified in the datasets of chloroplasts (Chlor), cauline (Cau), rosette (Ros), and roots (Root).

barley (Borst Pauwels, 1961) and wheat (Cakmak et al., 2017). In tomato, Lehr et al. (1958) demonstrated that treatments with iodine accelerated plant growth, causing early flowering associated with an increase in yield. Similarly, Umaly and Poel (1970) found that the addition of 4 μM KI to the nutrient solution stimulated tomato plants to produce flowers 2–3 days earlier than the control, whereas the use of iodine at a higher concentration (80 μM KI) delayed flower formation and reduced the number of inflorescences. It must be noted that in most biofortification studies with iodine, its native occurrence in nutrient solution or soil of the control plants is not always reported; where iodine concentrations in leaf or root tissue in control plants are reported, these always indicate that iodine was available for uptake and accumulation, regardless of the exogenous administrations (e.g., Borst Pauwels, 1961; Cakmak et al., 2017).

Flowering is a complex physiological process affected by a multitude of internal and external factors, and its hastening may represent an evolutionary adaptive mechanism to guarantee species survival, by optimising the seed set in the case of biotic or abiotic stresses (Ionescu et al., 2017). In Arabidopsis, heat and drought stress are correlated with early flowering, which in turn is generally associated with a reduction in plant growth (Balasubramanian et al., 2006; Schmalenbach et al., 2014). In our study, 10 μM iodate or iodide promoted flowering without negatively impacting on biomass production (**Figures 1**, **2**), which was increased by KIO_3, thus suggesting the specific flowering-promoting role of iodine in the process.

Our transcriptomic analysis of plants treated with 10 μM KI, NaI, or KBr for 48 h showed that several genes were specifically regulated by iodine, as the large part of DEGs similarly responded to KI and NaI, but not to KBr (**Figure 3**). This was more evident in root than in shoot tissues, probably because iodine was added to the nutrient solution and was used first by roots before the green parts. Interestingly, transcripts specifically regulated by iodine in the roots were mostly involved in the plant response to biotic and/or abiotic stresses (**Figure 4** and **Supplementary Tables S6–S8**) and the selective regulation of iodine on these groups of genes was also observed in the shoots (**Supplementary Tables S4, S5** and **Supplementary Figure S4**).

Although no previous data are available on the response of Arabidopsis to iodine at the transcriptomic level, the induction of *HALIDE ION METHYLTRANSFERASE*, *SALICYLIC ACID CARBOXYL METHYLTRANSFERASE*, and *SALICYLIC ACID 3-HYDROXYLASE* genes by aromatic iodine compounds, indicating a possible involvement of iodine in the SA metabolism, has already been described in tomato plants (Halka et al., 2019). SA is a signalling molecule involved in local defence reactions at infection sites and the induction of systemic resistance (Vlot et al., 2009).

Iodine likely has an indirect effect on plant resistance given that iodine treatments induce the biosynthesis of several enzymatic or non-enzymatic compounds involved in the plant response to environmental stresses (Leyva et al., 2011; Blasco et al., 2013; Gupta et al., 2015). The antioxidant response induced by increasing KI and KIO_3 levels was found to be strongly associated with the synthesis of phenolic compounds (Incrocci et al., 2019; Kiferle et al., 2019), in agreement with

our transcriptomic data (**Figure 4** and **Supplementary Table S8**). Iodine treatments have also been associated with the modulation of the essential oil composition in basil plants (Kiferle et al., 2019), which plays a key role in defensive and attraction mechanisms in response to the environment (Cseke et al., 2007; Bakkali et al., 2008).

In our study, the relationship between iodine and plant resistance to stress was also suggested by the activation of GO terms associated with hypoxia (**Figure 4** and **Supplementary Table S8**) and the over-representation of data points related to calcium (Ca) regulation (**Supplementary Figure S3A**). Ca plays a central role in the plant perception of stress by activating a general defence mechanism, which relies on a Ca spiking mechanism and thus on the battery of Ca-dependent proteins that sense Ca and transduce the signal to downstream targets (Dodd et al., 2010; Pucciariello et al., 2012). Our microarray results did not provide evidence that iodine regulated the expression of anaerobic core genes, such as *PYRUVATE DECARBOXYLASE 1* or *ALCOHOL DEHYDROGENASE* (Mustroph et al., 2010). This suggests that the regulation of hypoxic genes by iodine was not associated with limiting O_2 levels but with an unspecific plant response to an environmental/biotic stress, as it is also highlighted by the activation of enzyme families associated with antioxidant response and xenobiotic detoxification, such as peroxidases, cytochrome P450 or glutathione S-transferases (**Supplementary Figure S3B**; Mittler et al., 2004; Jouili et al., 2011; Pandian et al., 2020).

At very low doses, iodine thus activates a general defence response which takes place before any biotic or abiotic danger and thus may prepare the plant for a possible future attack or environmentally unfavourable conditions.

The impact of iodine on the transcriptome related to defence was impressive. For evaluation of iodine as a plant nutrient the possible influence on growth and development is also important, and this appeared to be sustained by more scattered elements, requiring further studies. For instance, we found iodine-driven modulation in the shoots of the expression of specific genes that are known to regulate flowering (Xing et al., 2013; Trapalis et al., 2017). This is line with our phenotypical data that indicate that iodine promotes early blooming (**Figures 1B**, **2A**).

Iodine Is Incorporated Into Plant Proteins

Using radiolabelled iodine, we observed iodine incorporation into leaf and root proteins in various plant species, with a good level of conservation of the molecular mass values (**Figure 5**), suggesting that iodination plays a functional role in specific proteins. The absence of radioactive bands in maize leaf extracts may be due to a specific characteristic of the species: maize was the only C4 plant analysed in our study.

Under alkaline conditions, iodine is known to react *in vitro* with free amino acids, such as Tyr and His, possibly leading to the formation of several I-labelled proteins (Scott, 1954). In our experiments, however, no radioactive signals were present when ^{125}I was added to shoot and root control samples after protein extraction, indicating that protein iodination occurred *in vivo*.

To the best of our knowledge, the presence of naturally occurring iodinated proteins in higher plants has never been described before, although it is well known in seaweed. For instance, the fraction of iodine bound to proteins in *Sargassum kjellanianum* accounts for 65.5% of the total element content of this organism (Hou et al., 2000). In addition, 1D and 2D gel-based electrophoresis combined with laser ablation ICP-MS highlighted several iodinated proteins in Nori seaweed, although no further analyses were conducted to identify them (Romarís-Hortas et al., 2014).

In this study, we identified several iodinated peptides from several high-quality proteomic datasets on plants grown without intentional enrichment of the growing media with iodine, but accumulating the iodine naturally present in soil and water or in MS media. Interestingly, these iodinated peptides belong to proteins, which appeared to be involved in well-defined biological contexts within the plant (**Tables 1**, **2** and **Supplementary Table S10**).

In roots, some of the iodinated protein networks that have been identified belong to various class III peroxidases (EC 1.11.17). These are a large molecular family of isozymes present in higher plants, which catalyse redox processes between H_2O_2 and reductants and are involved in growth, cell wall differentiation and the response to various biotic/abiotic stresses (Moerschbacher, 1992; Hiraga et al., 2001). They are abundant in root tissues, in which high concentrations of H_2O_2 occur during root development (Dunand et al., 2007). In the presence of low concentrations of iodide, various peroxidases catalytically degrade H_2O_2 at neutral pH values, generating hypoiodous acid (HIO) (Davies et al., 2008; Vlasova, 2018), a strong iodinating agent that can modify proteins in the environment surrounding the site of its generation, also inducing modification at Tyr. Our findings thus suggest that the class III peroxidases involved in the neutralisation of H_2O_2 present in root tissues, in the presence of iodide and resulting HIO, become themselves the targets of iodination, which in our study occurred at different Tyr residues in their structure. In fact we also found that Tyr iodination occurred in other proteins that directly/indirectly interact with or are functionally linked to class III peroxidases, and/or are present at high levels in root tissues (**Supplementary Figure S7A** and **Supplementary Table S11**).

Regarding leaves, we identified a number of iodinated peptides from proteins in proteomic datasets from Arabidopsis chloroplast, cauline and rosette extracts (**Figure 6B**). Most of these proteins are well-known constitutive subunits of molecular complexes (PSII, PSI, Cytb6f and ATPase) present in the plant photosynthetic machinery (Dekker and Boekema, 2005; Nevo et al., 2012). In *in vitro* labelling experiments (Machold and Aurich, 1981) demonstrated that some of them can be iodinated.

The above-mentioned macromolecular assemblies are involved in the generation and transfer of reactive electrons, from their early formation up to the coupling reactions, where their chemical potential allows the generation of plant ATP, NADP and carbohydrates (Foyer, 2018). In this context, high light intensity is one of the major stress factors in green plant tissues, which leads to the production of highly reactive oxygen species (ROS) ($^1O_2$, $O_2^{\cdot -}$, H_2O_2), and hydroxyl radicals (Schmitt et al., 2014; Foyer, 2018). These reactions also occur during normal photosynthetic conditions and, whenever not

controlled by dedicated endogenous antioxidants, can impact on photosynthetic efficiency.

The principal target of light stress is the chloroplast, which is the preferential site of iodine accumulation in the leaf (Weng et al., 2013), and PSI and PSII are the main sites of $O_2^{\cdot -}$ and $^1O_2$ production, respectively. High light illumination and the corresponding generation of ROS cause photoinhibition of PSII as well as the modification of other photosynthetic complexes, and induce an accelerated turnover of components of these molecular machineries (Li et al., 2018). The latter phenomenon is generally accomplished through the rapid degradation of photo-damaged proteins and concomitant substitution of them with newly synthetised functional copies (Aro et al., 2005; Yamamoto et al., 2014). This oxidative modification is also known to affect redox-regulated enzymes involved in the Calvin cycle. Proteomic studies have already characterised the nature and the sites of various oxidative and nitrosative modifications at Tyr, Trp and His residues in components of PSII, PSI, Cytb6f and ATP synthase complexes in thylakoid membranes from plants exposed to intense illumination (Galetskiy et al., 2011). These modifications were induced by ROS and/or other reactive nitrogen species, e.g., peroxinitrite, which are formed after the reaction of ROS with nitric oxide and other plant nitrogenous species (Bachi et al., 2013; Lu and Yao, 2018).

Given that such oxidised and nitrated proteins coincide with those found iodinated in our study, ROS likely also react with iodo-containing ions present in the chloroplasts to generate iodinating species that affect Tyr and His residues. We found that iodination processes also affected other proteins functionally related to subunits of PSII, PSI, Cytb6f and ATP synthase complexes, such as those involved in the Calvin Cycle, which are present at high concentrations in the same subcellular district, and have already been reported to directly/indirectly interact with the above-mentioned photosynthetic assemblies (**Supplementary Figure S6A** and **Supplementary Table S11**).

The addition of $^1O_2$ to I^- forms peroxyiodide, which decomposes into highly reactive iodine and iodo-containing radicals during dye-mediated photodynamic bacterial inactivation in the presence of potassium iodide (Wen et al., 2017). This process is fundamental for antimicrobial photodynamic therapy (Hamblin and Abrahamse, 2018). Thus, in the presence of iodide, the above-mentioned photoactivated reactions or their possible process variants may have contributed to generate highly reactive iodo-containing molecules and/or radicals, thereby leading to the formation of the iodinated proteins observed in this study. The possible functional meaning of these is certainly worth studying.

CONCLUSION

We demonstrated that very low amounts of iodine (between 0.20 and 10 μM, i.e., in the range of the concentrations required by plants for several micro-nutrients) improved plant growth and development thus promoting both biomass production and early flowering, and that this effect could not be achieved by another halogen most resembling iodine (Br). Secondly, we found that iodine was able to modulate gene expression in a specific way, activating multiple pathways, mostly involved in defence responses. Finally, we demonstrated that iodine can be a structural component of several different proteins, and conserved iodinated proteins are synthesised in both the roots and shoots of phylogenetically distant species.

These three lines of evidence highlight that iodine has a nutritional role in plants. This means that the influence of iodine on plants is not merely the result of an indirect priming effect by a potentially phytotoxic compound. Considering that plant nutrients are chemical elements that are components of biological molecules and/or influence essential metabolic functions, iodine matches at least the first part of this definition. Further studies on the importance of organification of iodine in proteins on their catalytic and/or regulatory function will help to complete the picture on the functional role of iodine as a plant nutrient.

DATA AVAILABILITY STATEMENT

The datasets presented in this study can be found in online repositories. The names of the repository/repositories and accession number(s) can be found below: https://www.ncbi.nlm.nih.gov/geo/, GSE157643.

AUTHOR CONTRIBUTIONS

PP, CK, MM, KH, and HTH: conceived the project. CK, MM, and SB: experiments on plant phenotype and transcriptomic. PS, CK, and MM: experiments on radioactive feeding. AMS: bioinformatics analysis of mass spectrometry-based proteomics data sets. CK and AMS: data analysis and figures preparation. CK, AMS, AS, and SG: writing—original draft preparation. PP, AS, SG, PS, KH, and HTH: general discussion and revision of the article. All authors read and contributed to previous versions and approved the final version.

FUNDING

This work was supported by the Scuola Superiore Sant'Anna and SQM International N.V. The funder was not involved in the study design, collection, analysis, interpretation of data, the writing of this article or the decision to submit it for publication.

ACKNOWLEDGMENTS

This manuscript has been released as a pre-print at BiorXiv (Kiferle et al., 2020).

SUPPLEMENTARY MATERIAL

The Supplementary Material for this article can be found online at: https://www.frontiersin.org/articles/10.3389/fpls.2021.616868/full#supplementary-material

REFERENCES

Aro, E. M., Suorsa, M., Rokka, A., Allahverdiyeva, Y., Paakkarinen, V., Saleem, A., et al. (2005). Dynamics of photosystem II: A proteomic approach to thylakoid protein complexes. *J. Exp. Bot.* 56, 347–356. doi: 10.1093/jxb/eri\&041

Ashworth, D. J. (2009). "Transfers of Iodine in the soil-plant-air System: Solid-Liquid Partitioning, Migration, Plant Uptake and Volatilization," in *Comprehensive Handbook of Iodine*, eds V. R. Preedy, G. N. Burrow, and R. Ross Watson (Cambridge: Academic Press), 107–118.

Bachi, A., Dalle-Donne, I., and Scaloni, A. (2013). Redox proteomics: chemical principles, methodological approaches and biological/biomedical promises. *Chem. Rev.* 113, 596–698. doi: 10.1021/cr300073p

Bakkali, F., Averbeck, S., Averbeck, D., and Idaomar, M. (2008). Biological effects of essential oils – A review. *Food Chem. Toxicol.* 46, 446–475. doi: 10.1016/j.fct.2007.09.106

Balasubramanian, S., Sureshkumar, S., Lempe, J., and Weigel, D. (2006). Potent induction of Arabidopsis thaliana flowering by elevated growth temperature. *PLoS Genet.* 2:0980–0989. doi: 10.1371/journal.pgen.0020106

Blasco, B., Leyva, R., Romero, L., and Ruiz, J. M. (2013). Iodine effects on phenolic metabolism in lettuce plants under salt stress. *J. Agric. Food. Chem.* 61, 2591–2596. doi: 10.1021/jf303917n

Borst Pauwels, G. W. F. H. (1961). Iodine as a micronutrient for plants. *Plant Soil* 14, 377–392. doi: 10.1007/BF01666295

Brahmachari, U., Guo, Z., Konecny, S. E., Obi, E. N. C., and Barry, B. A. (2018). Engineering proton transfer in photosynthetic oxygen evolution: Chloride, Nitrate, and Trehalose reorganize a hydrogen-bonding network. *J. Phys. Chem. B* 122, 6702–6711. doi: 10.1021/acs.jpcb.8b02856

Cakmak, I., Prom-u-thai, C., Guilherme, L. R. G., Rashid, A., Hora, K. H., Yazici, A., et al. (2017). Iodine biofortification of wheat, rice and maize through fertilizer strategy. *Plant Soil* 418, 319–335. doi: 10.1007/s11104-017-3295-9

Cseke, L. J., Kaufman, P. B., and Kirakosyan, A. (2007). The biology of essential oils in the pollination of flowers. *Nat. Prod. Commun.* 2, 1317–1336. doi: 10.1177/1934578X0700201225

Davies, M. J., Hawkins, C. L., Pattison, D. I., and Rees, M. D. (2008). Mammalian heme peroxidases: From molecular mechanisms to health implications. *Antioxid. Redox Signal.* 10, 1199–1234. doi: 10.1089/ars.2007.1927

Dekker, J. P., and Boekema, E. J. (2005). Supramolecular organization of thylakoid membrane proteins in green plants. *Biochim. Biophys. Acta Bioen.* 1706, 12–39. doi: 10.1016/j.bbabio.2004.09.009

Dodd, A. N., Kudla, J., and Sanders, D. (2010). The language of calcium signaling. *Annu. Rev. Plant Biol.* 61, 593–620. doi: 10.1146/annurev-arplant-070109-104628

Dunand, C., Crèvecoeur, M., and Penel, C. (2007). Distribution of superoxide and hydrogen peroxide in Arabidopsis root and their influence on root development: possible interaction with peroxidases. *N. Phytol.* 174, 332–341. doi: 10.1111/j.1469-8137.2007.01995.x

Eales, J. G. (1997). Iodine metabolism and thyroid-related functions in organisms lacking thyroid follicles: Are thyroid hormones also vitamins? *Exp. Biol. Med.* 214, 302–317. doi: 10.3181/00379727-214-44098

Foyer, C. H. (2018). Reactive oxygen species, oxidative signaling and the regulation of photosynthesis. *Environ. Exp. Bot.* 154, 134–142. doi: 10.1016/j.envexpbot.2018.05.003

Fuge, R., and Johnson, C. C. (1986). The geochemistry of iodine - a review. *Environ. Geochem. Health* 8, 31–54. doi: 10.1007/BF02311063

Galetskiy, D., Lohscheider, J. N., Kononikhin, A. S., Popov, I. A., Nikolaev, E. N., and Adamska, I. (2011). Mass spectrometric characterization of photooxidative protein modifications in Arabidopsis thaliana thylakoid membranes. *Rapid Commun. Mass Spectrom* 25, 184–190. doi: 10.1002/rcm.4855

Gonzali, S., Kiferle, C., and Perata, P. (2017). Iodine biofortification of crops: agronomic biofortification, metabolic engineering and iodine bioavailability. *Curr. Opin. Biotechnol.* 44, 16–26. doi: 10.1016/j.copbio.2016.10.004

Gupta, N., Bajpai, M., Majumdar, R., and Mishra, P. (2015). Response of iodine on antioxidant levels of Glycine max L. grown under Cadmium stress. *Adv. Biol. Res.* 9, 40–48. doi: 10.5829/idosi.abr.2015.9.1.9183

Halka, M., Smoleń, S., Czernicka, M., Klimek-Chodacka, M., Pitala, J., and Tutaj, K. (2019). Iodine biofortification through expression of HMT, SAMT and S3H genes in Solanum lycopersicum L. *Plant Physiol. Biochem.* 144, 35–48. doi: 10.1016/j.plaphy.2019.09.028

Hamblin, M. R., and Abrahamse, H. (2018). Inorganic salts and antimicrobial photodynamic therapy: mechanistic conundrums? *Molecules* 23, 1–18. doi: 10.3390/molecules23123190

Hiraga, S., Sasaki, K., Ito, H., Ohashi, Y., and Matsui, H. (2001). A large family of class III plant peroxidases. *Plant Cell Physiol.* 42, 462–468. doi: 10.1093/pcp/pce061

Hou, X., Yan, X., and Chai, C. (2000). Chemical species of iodine in some seaweeds II. Iodine-bound biological macromolecules. *J. Radioanal. Nucl. Chem.* 245, 461–467. doi: 10.1023/A:1006728420096

Incrocci, L., Carmassi, G., Maggini, R., Poli, C., Saidov, D., Tamburini, C., et al. (2019). Iodine accumulation and tolerance in Sweet basil (Ocimum basilicum L.) with green or purple leaves grown in floating system technique. *Front. Plant. Sci.* 10:1–15. doi: 10.3389/fpls.2019.01494

Ionescu, I. A., Møller, B. L., and Sánchez-Pérez, R. (2017). Chemical control of flowering time. *J. Experim. Bot.* 68, 369–382. doi: 10.1093/jxb/erw427

Jouili, H., Bouazizi, H., and El Ferjani, E. (2011). Plant peroxidases: biomarkers of metallic stress. *Acta Physiol. Plant.* 33, 2075–2082. doi: 10.1007/s11738-011-0780-2

Kiferle, C., Ascrizzi, R., Martinelli, M., Gonzali, S., Mariotti, L., Pistelli, L., et al. (2019). Effect of Iodine treatments on Ocimum basilicum L.: Biofortification, phenolics production and essential oil composition. *PLoS One* 14:e0226559. doi: 10.1371/journal.pone.0226559

Kiferle, C., Martinelli, M., Salzano, A. M., Gonzali, S., Beltrami, S., Salvadori, P. A., et al. (2020). Evidences for a nutritional role of iodine in plants. *BiorXiv* preprint.

Kouzai, Y., Noutoshi, Y., Inoue, K., Shimizu, M., Onda, Y., and Mochida, K. (2018). Benzothiadiazole, a plant defense inducer, negatively regulates sheath blight resistance in Brachypodium distachyon. *Sci. Rep.* 8, 1–7. doi: 10.1038/s41598-018-35790-w

Lehr, J. J., Wybenga, J. M., and Rosanow, M. (1958). Iodine as a micronutrient for tomatoes. *Plant Physiol.* 33, 421–427. doi: 10.1104/pp.33.6.421

Leyva, R., Sánchez-Rodríguez, E., Ríos, J. J., Rubio-Wilhelmi, M. M., Romero, L., Ruiz, J. M., et al. (2011). Beneficial effects of exogenous iodine in lettuce plants subjected to salinity stress. *Plant Sci.* 181, 195–202. doi: 10.1016/j.plantsci.2011.05.007

Li, L., Aro, E. M., and Millar, A. H. (2018). Mechanisms of photodamage and protein turnover in photoinhibition. *Trends Plant Sci.* 23, 667–676. doi: 10.1016/j.tplants.2018.05.004

Li, R., Wang, Z. J., Wang, L., Ma, B. C., Ghasimi, S., Lu, H., et al. (2016). Photocatalytic selective bromination of electron-rich aromatic compounds using microporous organic polymers with visible light. *ACS Catal.* 6, 1113–1121. doi: 10.1021/acscatal.5b02490

Loreti, E., Poggi, A., Novi, G., Alpi, A., and Perata, P. (2005). A genome-wide analysis of the effects of sucrose on gene expression in arabidopsis seedlings under anoxia. *Plant Physiol.* 137, 1130–1138. doi: 10.1104/pp.104.057299

Lu, Y., and Yao, J. (2018). Chloroplasts at the crossroad of photosynthesis, pathogen infection and plant defense. *Int. J. Mol. Sci.* 19, 1–37. doi: 10.3390/ijms19123900

Machold, O., and Aurich, O. (1981). Thylakoid membrane proteins of higher plant chloroplasts II. Application of lactoperoxidase catalyzed iodination to study species specific differences and membrane topography. Biochem. *Physiol. Pflanz.* 176, 549–561. doi: 10.1016/s0015-3796(81)80028-5

Medrano-Macías, J., Leija-Martínez, P., González-Morales, S., Juárez-Maldonado, A., and Benavides-Mendoza, A. (2016). Use of iodine to biofortify and promote growth and stress tolerance in crops. *Front. Plant Sci.* 7:1–20. doi: 10.3389/fpls.2016.01146

Mengel, K., and Kirkby, E. A. (2001). "Plant Nutrients," in *Principles of Plant Nutrition*, eds K. Mengel, E. A. Kirkby, H. Kosegarten, and T. Appel (Dordrecht: Kluwer Academic Publishers), 1–13.

Mittler, R., Vanderauwera, S., Gollery, M., and Van Breusegem, F. (2004). Reactive oxygen gene network of plants. *Trends Plant Sci.* 9, 490–498. doi: 10.1016/j.tplants.2004.08.009

Moerschbacher, B. M. (1992). "Plant peroxidases involvement in response to pathogen," in *Plant Peroxidases 1980–1990*, eds C. Panel, T. Gaspar, and H. Greppin (Geneva: University of Geneva Press), 91–99.

Murashige, T., and Skoog, F. (1962). A revised medium for rapid growth and bio assays with tobacco tissue cultures. *Physiol. Plant* 15, 473–497. doi: 10.1111/j.1399-3054.1962.tb08052.x

Mustroph, A., Lee, S. C., Oosumi, T., Zanetti, M. E., Yang, H., Ma, K., et al. (2010). Cross-kingdom comparison of transcriptomic adjustments to low-oxygen stress highlights conserved and plant-specific responses. *Plant Physiol.* 152, 1484–1500. doi: 10.1104/pp.109.151845

Nevo, R., Charuvi, D., Tsabari, O., and Reich, Z. (2012). Composition, architecture and dynamics of the photosynthetic apparatus in higher plants. *Plant J.* 70, 157–176. doi: 10.1111/j.1365-313X.2011.04876.x

Pandian, B. A., Sathishraj, R., Djanaguiraman, M., Prasad, P. V. V., and Jugulam, M. (2020). Role of cytochrome P450 enzymes in plant stress response. *Antioxid* 9:454. doi: 10.3390/antiox9050454

Perata, P., Matsukura, C., Vernieri, P., and Yamaguchi, J. (1997). Sugar repression of a gibberellin-dependent signaling pathway in barley embryos. *Plant Cell* 9, 2197–2208. doi: 10.1105/tpc.9.12.2197

Perez-Riverol, Y., Csordas, A., Bai, J., Bernal-Llinares, M., Hewapathirana, S., Kundu, D. J., et al. (2019). The PRIDE database and related tools and resources in 2019: Improving support for quantification data. *Nucl. Acids Res.* 47, D442–D450. doi: 10.1093/nar/gky1106

Pucciariello, C., Parlanti, S., Banti, V., Novi, G., and Perata, P. (2012). Reactive oxygen species-driven transcription in Arabidopsis under oxygen deprivation. *Plant Physiol.* 159, 184–196. doi: 10.1104/pp.111.191122

Ramachandran, L. K. (1956). Protein-iodine interaction. *Chem. Rev.* 56, 199–218. doi: 10.1021/cr50008a001

Romarís-Hortas, V., Bianga, J., Moreda-Piñeiro, A., Bermejo-Barrera, P., and Szpunar, J. (2014). Speciation of iodine-containing proteins in Nori seaweed by gel electrophoresis laser ablation ICP-MS. *Talanta* 127, 175–180. doi: 10.1016/j.talanta.2014.04.003

Schmalenbach, I., Zhang, L., Reymond, M., and Jiménez-Gómez, J. M. (2014). The relationship between flowering time and growth responses to drought in the Arabidopsis Landsberg erecta x Antwerp-1 population. *Front. Plant Sci.* 5:1–9. doi: 10.3389/fpls.2014.00609

Schmitt, F. J., Renger, G., Friedrich, T., Kreslavski, V. D., Zharmukhamedov, S. K., Los, D. A., et al. (2014). Reactive oxygen species: Re-evaluation of generation, monitoring and role in stress-signaling in phototrophic organisms. *Biochim. Biophys. Acta Bioen.* 1837, 835–848. doi: 10.1016/j.bbabio.2014.02.005

Scott, R. (1954). Observations on the iodo-amino-acids of marine algae using iodine-131. *Nature* 173, 1098–1099. doi: 10.1038/1731098b0

Smoleń, S., Kowalska, I., Halka, M., Ledwozyw-Smoleń, I., Grzanka, M., Skoczylas, Ł et al. (2020). Selected aspects of iodate and iodosalicylate metabolism in lettuce including the activity of vanadium dependent haloperoxidases as affected by exogenous vanadium. *Agronomy* 10:10010001. doi: 10.3390/agronomy10010001

Sonneveld, C. (2002). "Composition of nutrient solutions," in *Hydroponic Production of Vegetables and Ornamentals*, eds D. Savvas and H. C. Passam (Athens: Embryo Publications), 179–210.

Trapalis, M., Li, S. F., and Parish, R. W. (2017). The Arabidopsis GASA10 gene encodes a cell wall protein strongly expressed in developing anthers and seeds. *Plant Sci.* 260, 71–79. doi: 10.1016/j.plantsci.2017.04.003

Umaly, R. C., and Poel, L. W. (1970). Effects of various concentrations of iodine as potassium iodide on the growth of barley, tomato and pea in nutrient solution culture. *Ann. Bot.* 34, 919–926. doi: 10.1093/oxfordjournals.aob.a084423

Vlasova, I. I. (2018). Peroxidase activity of human hemoproteins: keeping the fire under control. *Molecules* 23, 1–27. doi: 10.3390/molecules23102561

Vlot, A. C., Dempsey, D. A., and Klessig, D. F. (2009). Salicylic acid, a multifaceted hormone to combat disease. *Annu. Rev. Phytopathol.* 47, 177–206. doi: 10.1146/annurev.phyto.050908.135202

Voogt, W., Holwerda, H. T., and Khodabaks, R. (2010). Biofortification of lettuce (Lactuca sativa L.) with iodine: the effect of iodine form and concentration in the nutrient solution on growth, development and iodine uptake of lettuce grown in water culture. *J. Sci. Food Agric.* 90, 906–913. doi: 10.1002/jsfa.3902

Wang, L., Zhou, X., Fredimoses, M., Liao, S., and Liu, Y. (2014). Naturally occurring organoiodines. *RSC Adv.* 4, 57350–57376. doi: 10.1039/c4ra09833a

Welch, R. M., and Shuman, L. (1995). Micronutrient Nutrition of Plants. *CRC Crit. Rev. Plant Sci.* 14, 49–82. doi: 10.1080/07352689509701922

Wen, X., Zhang, X., Szewczyk, G., El-Hussein, A., Huang, Y. Y., Sarna, T., et al. (2017). Potassium iodide potentiates antimicrobial photodynamic inactivation mediated by Rose bengal in in vitro and in vivo studies. *Antimicrob. Agents Chemother.* 61:17. doi: 10.1128/AAC.00467-17

Weng, H. X., Hong, C. L., Xia, T. H., Bao, L. T., Liu, H. P., and Li, D. W. (2013). Iodine biofortification of vegetable plants-An innovative method for iodine supplementation. *Chin. Sci. Bull.* 58, 2066–2072. doi: 10.1007/s11434-013-5709-2

Weng, H. X., Yan, A. L., Hong, C. L., Xie, L. L., Qin, Y. C., and Cheng, C. Q. (2008). Uptake of different species of iodine by water spinach and its effect to growth. *Biol. Trace Elem. Res.* 124, 184–194.

Xing, J. H., Wang, F. R., Jia, J., Zhang, J., Li, L., Chen, Z., et al. (2013). Mutations in AP22.65 accelerate flowering in Arabidopsis thaliana. *J. Plant Biol.* 56, 49–58. doi: 10.1007/s12374-012-0379-1

Yamamoto, Y., Kai, S., Ohnishi, A., Tsumura, N., Ishikawa, T., Hori, H., et al. (2014). Quality control of PSII: Behavior of PSII in the highly crowded grana thylakoids under excessive light. *Plant Cell Physiol.* 55, 1206–1215. doi: 10.1093/pcp/pcu043

Zhu, Y. G., Huang, Y. Z., Hu, Y., and Liu, Y. X. (2003). Iodine uptake by spinach (Spinacia oleracea L.) plants grown in solution culture: Effects of iodine species and solution concentrations. *Environ. Int.* 29, 33–37. doi: 10.1016/S0160-4120(02)00129-0

Zimmermann, M. B., Jooste, P. L., and Pandav, C. S. (2008). Iodine-deficiency disorders. *Lancet* 372, 1251–1262. doi: 10.1016/S0140-6736(08)61005-3

Conflict of Interest: KH and HH were employees of SQM International N.V., a company active in the sector of fertilisers.

The remaining authors declare that the research was conducted in the absence of any commercial or financial relationships that could be construed as a potential conflict of interest.

Copyright © 2021 Kiferle, Martinelli, Salzano, Gonzali, Beltrami, Salvadori, Hora, Holwerda, Scaloni and Perata. This is an open-access article distributed under the terms of the Creative Commons Attribution License (CC BY). The use, distribution or reproduction in other forums is permitted, provided the original author(s) and the copyright owner(s) are credited and that the original publication in this journal is cited, in accordance with accepted academic practice. No use, distribution or reproduction is permitted which does not comply with these terms.

frontiers in Plant Science

REVIEW
published: 22 February 2021
doi: 10.3389/fpls.2021.620018

Advances in Mineral Nutrition Transport and Signal Transduction in Rosaceae Fruit Quality and Postharvest Storage

*Qian Bai, Yuanyue Shen and Yun Huang**

Beijing Key Laboratory for Agricultural Application and New Technique, College of Plant Science and Technology, Beijing University of Agriculture, Beijing, China

Mineral nutrition, taken up from the soil or foliar sprayed, plays fundamental roles in plant growth and development. Among of at least 14 mineral elements, the macronutrients nitrogen (N), potassium (K), phosphorus (P), and calcium (Ca) and the micronutrient iron (Fe) are essential to Rosaceae fruit yield and quality. Deficiencies in minerals strongly affect metabolism with subsequent impacts on the growth and development of fruit trees. This ultimately affects the yield, nutritional value, and quality of fruit. Especially, the main reason of the postharvest storage loss caused by physiological disorders is the improper proportion of mineral nutrient elements. In recent years, many important mineral transport proteins and their regulatory components are increasingly revealed, which make drastic progress in understanding the molecular mechanisms for mineral nutrition (N, P, K, Ca, and Fe) in various aspects including plant growth, fruit development, quality, nutrition, and postharvest storage. Importantly, many studies have found that mineral nutrition, such as N, P, and Fe, not only affects fruit quality directly but also influences the absorption and the content of other nutrient elements. In this review, we provide insights of the mineral nutrients into their function, transport, signal transduction associated with Rosaceae fruit quality, and postharvest storage at physiological and molecular levels. These studies will contribute to provide theoretical basis to improve fertilizer efficient utilization and fruit industry sustainable development.

Keywords: mineral nutrition, Rosaceae fruit, fruit development, quality formation, postharvest storage

OPEN ACCESS

Edited by:
Nikos Tzortzakis, Cyprus University of Technology, Cyprus

Reviewed by:
Athanassios Molassiotis, Aristotle University of Thessaloniki, Greece
Matthew John Milner, National Institute of Agricultural Botany (NIAB), United Kingdom

****Correspondence:***
Yun Huang
yunhuang@bua.edu.cn

Specialty section:
This article was submitted to Plant Nutrition, a section of the journal Frontiers in Plant Science

Received: *11 November 2020*
Accepted: *11 January 2021*
Published: *22 February 2021*

Citation:
Bai Q, Shen Y and Huang Y (2021) Advances in Mineral Nutrition Transport and Signal Transduction in Rosaceae Fruit Quality and Postharvest Storage. Front. Plant Sci. 12:620018. doi: 10.3389/fpls.2021.620018

INTRODUCTION

Many species of Rosaceae are rich in economic value, such as apple, pear, peach, apricot, plum, cherry, loquat, mango, almond, and strawberry. Fruits are rich in vitamins, sugars, and organic acids, as well as many kinds of health-benefit compounds (Mahmood et al., 2012). These compounds, including anthocyanins and vitamins, may have anti-inflammatory and antioxidant effects, and thus fruits are usually used to maintain a balanced diet (Kumari et al., 2017). In addition, dry fruits, such as almond, are especially abundant in nutrition and also are widely cultivated in the world (Maguire et al., 2004). Fruits not only can be eaten directly but also can be used for food industry in the production of wine, juice, jam, and so on.

Thus, fruits are important components in our life, and improvement of fruit quality is going on all the time in orchard management.

It is well known that mineral nutrients, especially macronutrients nitrogen (N), phosphorus (P), potassium (K), and calcium (Ca) as well as micronutrient iron (Fe), are essential for plant growth, fruit yield, and quality (Falchi et al., 2020; Singh et al., 2020). In recent years, many studies have strengthen our insights into the influence and the molecular mechanisms for mineral nutrition (N, P, K, Ca, and Fe) in Rosaceae plant growth, fruit development, quality, and preservation, especially highlighting N in fruit yield and P and K in fruit quality. Mineral nutrition, such as N, P, and Fe, not only affects fruit quality directly but also affects the absorption of other nutrient elements.

In this review, we integrated many previously defined signaling components linked to mineral nutrition transport and signal transduction in the regulation of fruit quality at physiological and molecular levels. This review will not only contribute to provide the theoretical basis to improve fertilizer efficient utilization and fruit industry sustainable development but also highlight the important aims of future work.

TWO FACES OF NITROGEN APPLICATION IN FRUIT YIELD AND QUALITY

Nitrogen (N) is a ubiquitous element that constituted nucleic acids, amino acids, proteins, chlorophyll, as well as many other metabolites in plants. Therefore, it is an indispensable important nutrient element for plant growth and development. Plants acquire inorganic N from the soil, mainly in the form of ammonium and nitrate, and low or excessive N level has a serious influence on fruit yield and quality.

When strawberries were treated with three levels of NO_3^- (9, 12, and 15 mol/m^3), the highest NO_3^- concentration of nutrient solution produced the maximum yield, but the nutraceutical quality, such as antioxidant capacity and phenolic compounds, significantly declined (Preciado-Rangel et al., 2020). Under sufficient soil moisture, the application of N fertilizer to potted apple trees caused an increase in stomatal conductance, which decreased water use efficiency (WUE; Qu et al., 2000). Under soil drought, the WUE of apple trees under nitrogen fertilizer was significantly higher than that of the control, owing to the promotion of mesophyll capacity and photosynthesis (Qu et al., 2000).

As the increasing of N supply in apple (*Malus domestica* Borkh.) trees, the concentrations of sucrose (Suc), glucose (Glc), fructose (Fru), and total nonstructural carbohydrates (TNC) decreased (Cheng et al., 2004), resulting in the production of organic acids. It is confirmed that in strawberries, applying high nitrogen amounts could lead to an increase in citric acid content and conceal fruit sweet flavor, whereas low nitrogen levels could decrease acidity and result in an observably lower content of ascorbic acid and higher fruit firmness (Cardeñosa et al., 2015).

Anthocyanin and chlorophyll are remarked signs for fruit quality, and many research studies suggest that increasing N supply decreases anthocyanin synthesis but induces chlorophyll content in fruits. Under high N nutrition in apple trees, shoot growth was enhanced, and the activity of phenylalanine ammonia lyase, a key enzyme involved in flavonoid biosynthesis, seemed to be downregulated, resulting in a generally decreased flavonoid accumulation (Strissel et al., 2005). N fertilization could be used to suppress anthocyanin formation in green apple cultivars, such as "Granny Smith," in that red blush was undesirable (Ritenour and Khemira, 2007). High N could lead to higher chlorophyll concentration of fruit skin, thus increasing fruit greenness; on the contrary, nitrate deficiency suppressed nitrate absorption and assimilation and inhibited the transformation of 5-aminolevulinic acid (ALA) into porphobilinogen (PBG), thus suppressing chlorophyll synthesis in apple (Wen et al., 2019). Peach fruit from the higher N rates was greener and had higher total soluble solids than fruit from the trees under low N (Rubio Ames et al., 2020).

The application of the nitrification inhibitor, 3,4-dimethylpyrazole phosphate (DMPP) and abscisic acid (ABA), could effectively improve the problem of poor fruit coloring caused by excessive N fertilizer application used in apple trees (Wang et al., 2020a,b). DMPP reduced the capacity of N absorption and N accumulation in fruits and whole apple plant, whereas it increased fruit anthocyanin and soluble solid content (SSC), and it had no significant effect on fruit yield (Wang et al., 2020a). An appropriate ABA concentration could promote the expression of anthocyanin synthesis genes and transcription factors, as well as the anthocyanin content of the "Red Fuji" apple peel. More than that, exogenous ABA reduced the accumulation of N and increased the contents of sugar and carbon in fruits (Wang et al., 2020b).

To improve the anthocyanin content and accordingly the quality and market value of important agricultural commodities, it can be a powerful tool to supply nutrient strategically. In particular, the precise application of N fertilizer should not only improve fruit yield but also positively influence fruit quality including anthocyanin content (Jezek et al., 2018).

Molecular Mechanisms of Nitrogen Assimilate, Transport, and Action

Thirteen ammonium transporters of *AMT1* subfamily in the apple rootstock *Malus robusta* Rehd were grouped into four clusters: clade I (*MrAMT1;1* and *MrAMT1;3*), clade II (*MrAMT1;4*), clade III (*MrAMT1;2*), and clade IV (*MrAMT1;5*). All the *AMT1s*, except *MrAMT1;4*, were highly expressed in vegetative organs and significantly responded to different nitrogen supplies. The ammonium absorption activities of these *AMT1s* were confirmed in the AMT-defective mutant yeast system, though their NH_4^+ uptake kinetics varied (Li et al., 2017).

There were 73 NPF (Nitrate Transporter 1/Peptide Transporter Family) genes in apple that were organized into eight major groups (Wang et al., 2018b). *MdNPF6.5* was strongly induced by both low-nitrate and high-nitrate levels, and the overexpression of *MdNPF6.5* in apple calli enhanced the tolerance to low-N stress, suggesting that MdNPF6.5 has greater nitrogen uptake

activity (Wang et al., 2018b). Under low N treatment, the expression of nitrate transporter *MdNRT2.4* is higher in high nitrogen-use efficiency (NUE) apple cultivars than in low NUE apple (Wang et al., 2019a), which may explain the NUE differences among apple cultivars.

Anion channel PbrSLAH3 of pear (*Pyrus bretschneideri*) could rescue the ammonium toxicity phenomenon of *slah3* mutant grown in high-ammonium/low-nitrate conditions, which was activated by phosphorylation by calcium-dependent protein kinase PbrCPK32 (Chen et al., 2019b). The overexpression of autophagy proteins *MdATG18a* and *MdATG9* enhanced the tolerance to N-deficiency stress and the Suc concentration in apple callus (Sun et al., 2018b; Huo et al., 2020). MdATG18a played a role in nitrate uptake and assimilation by the upregulation of nitrate reductase (NR) MdNIA2 and nitrate transporters MdNRT2.1/2.4/2.5 (Sun et al., 2018b). MdATG9 regulated the expression of *MdNRT1.1*, *MdNRT2.5*, *MdNIA1*, and *MdNIA2* in response to N starvation in apple (Huo et al., 2020). Overexpressing *MdHY5* (transcription factor LONG HYPOCOTYL 5) in apple callus induced the expression of N acquisition-related genes and increased the activity of NR, finally improving nitrate contents (An et al., 2017).

PHOSPHORUS FERTILIZER IMPROVES FRUIT YIELD, QUALITY, AND POSTHARVEST STORAGE QUALITY

Phosphorus (P) supplementation has become a primary agricultural management aspect of fruit production, because P not only affects fruit yield but also modulates the production of the soluble solid and secondary metabolites, such as ascorbic acid and flavonoids, which are closely related to fruit quality.

When appropriate phosphorus was added, the weight of strawberry fruits increased notably (Afroz et al., 2016). The SSC was lower in fruits from P shortage strawberries, indicating that P deficiency could negatively affect sugar biosynthesis (Valentinuzzi et al., 2015a). SSC in strawberry fruits was positively related to the phosphorus content, and P fertilizer could effectively increase SSC in strawberry fruit (Cao et al., 2015). Meanwhile, P content, WUE, and photosynthetic rate (Pn) increased in phosphoric acid-treated strawberry fruits (Cao et al., 2015).

P starvation resulted in a significant change of bioactive compounds in strawberry fruits. The contents of vitamin C, malic acid, galactaric acid, proline, lysine, sorbitol-6-phosphate, malate, and citrate were also inhibited when P was deficient (Valentinuzzi et al., 2015b; Afroz et al., 2016; Zhang et al., 2020), whereas anthocyanin contents were higher (Valentinuzzi et al., 2015a). However, field experiments had shown that the application of phosphite (Phi), a salt of phosphorous acid absorbed and transferred in a way similar to inorganic P, increased the anthocyanin content of strawberry (Estrada-Ortiz et al., 2013). Therefore, the effect of fruit quality formation varies with the type and timing of P fertilizer application (Jezek et al., 2018).

P deficiency also changes other ion contents in plants. The fruit firmness of strawberry fruits under P deficiency increased 60% compared with that of the control, which may be because of the higher concentration of Ca (Valentinuzzi et al., 2015a). Moreover, low P alleviated the Fe deficiency phenotype in apples and improved the ferric-chelated reductase activity of the rhizosphere, because P shortage promotes proton exocytosis and organic acids exudation and enhances Fe absorption, thus increasing the Fe content in both the shoots and roots under Fe deficiency in apples (Zhang et al., 2020). For another, the limited elongation of the main roots under low inorganic phosphate (Pi) conditions may be results of the Fe accumulation in the apical meristem (Zhang et al., 2020).

Many plants can utilize phosphate from places outside the nutrient-depleted zone through symbiotic arbuscular mycorrhizal fungi (AMF; Ezawa and Saito, 2018). The colonization by AMF and appropriate P supplementation of traditional (TF) or organic (OF) fertilizer was regarded as the main approach to raise the yield and quality of strawberry fruits in acidic soils with low P availability (Parada et al., 2019). There was a highly positive correlation between the concentration of P in apple rootstocks and the bacterial genera *Bacillus* (Chai et al., 2020). The P-efficient hybrid apple lines had better growth characteristics and stronger root structure, as well as more abundant *Bacillus* in the rhizosphere, than the P-inefficient hybrid line plants (Chai et al., 2020). However, according to some reports, there is no correlation between the AMF association and low P tolerance when plants are grown under optimal nutrient conditions (Cockerton et al., 2020).

Trisodium phosphate (TSP) treatment could maintain the postharvest quality of apple fruit by inhibiting respiration intensity, delaying weight loss, and inhibiting the decline of flesh firmness, ascorbic acid, titratable acid, and SSC (Ge et al., 2019). The TSP treatment also delayed the decrease of the content of ADP, ATP, and energy charge in apple fruit (Ge et al., 2019).

Molecular Pathways of Phosphate Signal in Rosaceae Species

Roots uptake Pi from the soil mainly by PHT1 family transporters that are located in the plasma membrane (Shin et al., 2004; Wang et al., 2020c). The PHT2-type carriers are plastid envelope-located, and the PHT3-type carriers are inner mitochondrial membrane-located (Rausch and Bucher, 2002). Trans-Golgi-located PHT4;6 proteins function as transporters that can release Pi from the Golgi apparatus (Guo et al., 2008; Hassler et al., 2012). The free phosphate is mainly stored in the plant vacuole, and the Arabidopsis VPT1 (PHT5;1) proteins have been identified as vacuolar Pi influx transporters (Liu et al., 2015). OsVPE1 and OsVPE2 are responsible for *Oryza sativa* vacuolar Pi efflux (Xu et al., 2019).

Phosphate starvation response 1 (PHR1) is a key transcription factor involved in Pi-starvation signaling binding to a cis-element named PHR1-binding sequence (P1BS) and significantly regulates Pi starvation-induced (PSI) genes, including Pi transporters (*PHT1*) and *miR399* (Chiou and Lin, 2011). *miR399* could suppress the expression of ubiquitin-conjugating E2 enzyme PHO2 and therefore release PHT1 and PHO1, involved in phosphate transduction from root to shoot, thus promoting Pi acquisition and transport in Arabidopsis (Chiou and Lin, 2011).

However, only a few phosphate transporters and signal transduction components were reported in Rosaceae species.

A total of 37 putative phosphate transporters in apple were identified into five clusters (MdPHT1, MdPHT2, MdPHT3, MdPHT1, and MdPHT5; *M. domestica*), and their expression was tissue specific and significantly regulated by low P treatment (Sun et al., 2017). The overexpression of *MdMYB2* could regulate the expression levels of PSI genes and further promote the assimilation and utilization of phosphate in apple (Yang et al., 2020). The levels of SUMOylation and *MdSIZ1*, a (SUMO) E3 ligase encoding gene, were induced by Pi-deficient conditions, suggesting that *MdPHR1* and *MdMYB2* might be targets for the SUMO protein (Zhang et al., 2019a).

Some important components involved in phosphate transport and signal regulation have been reported in strawberry. The expression level of *FaPHO1;H9*, homologous with *PHO1* from *Arabidopsis thaliana*, was related to P content in fruits during different developmental stages and under different P fertilizer supplements (Cao et al., 2017). The overexpression of *FvPHR1* and *FvmiR399a* in woodland strawberries significantly increased fruit quality (Wang and Wu, 2017; Wang et al., 2019b). FvPHR1 was found to directly bind to the promoter of *FvmiR399a* and positively regulate its expression (Wang et al., 2019b). PHR1-miR399 participates in the phosphate signaling pathway and maintains the phosphorus homeostatic state of woodland strawberry (Wang and Wu, 2017; Wang et al., 2019b). A tonoplast phosphate transporter FaVPT1 induced by Suc was identified to regulate fruit ripening and quality in strawberry (Huang et al., 2019). The overexpression of *FaVPT1* in strawberry fruits promoted ripening and increased the contents of P, sugar, and anthocyanin, decreased fruit firmness, and affected the expression of ripening-related genes (Huang et al., 2019).

APPROPRIATE POTASSIUM FERTILIZER IMPROVES FRUIT YIELD, QUALITY, AND PLANT STRESS RESISTANCE

Potassium (K) affects the growth of plant and fruit yield, quality, and nutrient content of apple, strawberry, pear, sweet cherry, and almond (Kumar and Ahmed, 2014; Lu et al., 2015; Wang et al., 2018b; Zhang et al., 2018b; Shen et al., 2019; Hüseyin and Ömer, 2020; Preciado-Rangel et al., 2020). Furthermore, the application of K fertilizer at different periods may affect utilization efficiency. For example, 50% K fertilizer at post-anthesis + 50% at the expansion stage decreased the content of Ca in "Fuji" apple fruits significantly, which was detrimental to fruits postharvest storage (Lu et al., 2015). In the orchard, the best period for K fertilizer application was the basal and expansion period equally (Lu et al., 2015).

Fruits from K fertilizer application treatment had higher SSC, and the activities of sugar metabolic enzymes significantly increased in apple (Zhang et al., 2018b). The biomass and K^+ content of root decreased significantly of pear seedlings was affected by K deficiency treatment (Wang et al., 2018c). Appropriate K supply promoted the transport of nutrients and sugar, by which increased the content of sugar in "Huangguan" pear fruits (Shen et al., 2019).

K fertilizer application treatment not only promotes greater fruit quality but also affects the utilization of nitrogen and the transport of other cations. The deficit or excess of K inhibited the uptake and utilization of nitrogen (N), whereas appropriate K supply could promote photosynthesis, enhance the activity of NR, and then increase the nitrogen absorption of *Malus hupehensis* (Tian et al., 2017; Xu et al., 2020). Ca^{2+} concentration increased with increasing K fertilization levels during apple fruit development (Zhang et al., 2018b). The Mg transporters increased under low K, whereas these decreased under medium and high K in pear tree, indicating that Mg had an obvious compensation effect on K, and K had an obvious antagonistic effect on Mg (Shen et al., 2019).

Elevated external K fertilization supply alleviated both biological and abiotic stresses in fruit trees (Araujo et al., 2015; Song et al., 2015a; Peng et al., 2016). K fertilization supply enhanced antioxidant defense systems, by which reducing Zn toxicity of peach seedlings (Song et al., 2015a). Increasing K content in apple trees enhanced resistance to *Valsa* canker, one of the most destructive diseases of apple, pathogen colonization, and establishment, so improved management of K fertilization could effectively control the disease incidence and development of *Valsa* canker (Peng et al., 2016). Spraying the plants with K Phi would induce the phenylpropanoid pathway of mango plants to reduce internal necrosis and the disease development of *Ceratocystis fimbriata* (Araujo et al., 2015).

Molecular Pathways of K Transporters and Channels in Rosaceae Species

K^+ usability, uptake efficiency, and transfer efficiency remarkably affect the performance of plants. In order to maintain optimal K^+ homeostasis, more than 71 K^+ transporters and channels, including three channel families and three transporter families, have already been identified in *A. thaliana* (Wang and Wu, 2017; Wang et al., 2020c). They are involved in K^+ absorption by roots, ion transport between organs and tissues, and K^+ storage in vacuoles (Gierth and Mäser, 2007; Chanroj et al., 2012; Gomez-Porras et al., 2012).

Selective K^+ channels contain three families: Shaker, TPK, and Kir-like. The Shaker K^+ channels display six transmembrane segments (TMS). TPK channels (Tandem-Pore K^+ Channels) display a hydrophobic core composed of four TMS. Plant Kir-like channels are associated with animal Kir (K^+ inward rectifier) channels, displaying two TMS. There are three different families of plasma membrane K^+ transport systems: the HAK/KUP/KT K^+ transporters (Gierth and Mäser, 2007), the HKT high-affinity K^+ transporters (Rodríguez-Navarro and Rubio, 2006), and the CPA2 subfamily, including K^+ efflux (KEA) H^+/K^+ antiporters and the cation/H^+ exchanger (Mäser et al., 2001).

Some K^+ channels and transporters have been reported, but there is far less information in Rosaceae species. Thirty-six Shaker K^+ channel genes from Rosaceae species were divided into five subgroups, including a K^+ channel protein PbrKAT1 that may play a role in regulating salt tolerance of pear, because its activity was inhibited by external sodium ions (Chen et al., 2019a). Similarly, a strawberry K^+ channel, FaKAT1, serves as a positive regulator in the regulation of fruit ripening in an

ABA-dependent manner (Song et al., 2017). K^+ channel AKT1 is activated and phosphorylated by calcineurin B-like protein (CBL)-interacting protein kinases (CIPKs; Xu et al., 2006). *FaAKT1* encoded a highly K^+-selective channel and showed upregulated expression in strawberry "Camarosa" upon salt stress (Garriga et al., 2017). The overexpression of *FaTPK1*, a strawberry tonoplast K channel, promoted the expression of fruit ripening-related genes and the contents of anthocyanin, soluble sugars, and ABA (Wang et al., 2018c). FaTPK1 could not only regulate fruit ripening and quality formation but also enhance fruit resistance to *Botrytis cinerea* (Wang et al., 2018c).

Sixteen KT/HAK/KUP family K transporters in peach (*Prunus persica*) were identified and highly expressed in fruit and flower, indicating that these transporters may play important roles in K^+ uptake and transport as well as fruit development in peach (Song et al., 2015b). *PbrHAK1* and *PbrHAK12/16* were obviously increased under K^+ deficiency, suggesting their significant roles in K^+ uptake of pear, especially in response to K^+ starvation (Wang et al., 2018d). HKT genes and CPA genes were identified in five Rosaceae species, involving *Fragaria vesca*, *Pyrus communis*, *M. domestica*, *P. persica*, and *Prunus mume*, and *HKT* genes of woodland strawberry were responding to the salt stress (Zhang et al., 2019b). FaHKT1 could transport Na^+ selectively, and the increased expression of *FaHKT1* in roots correlates with the higher tolerance to salinity of the strawberry genotype (Garriga et al., 2017). CPA genes of pear were mainly expressed in pollen tubes and fruits, which suggested that CPAs may play significant roles in the growth of pollen tubes (Zhou et al., 2016).

Signal network of K regulating fruit enlargement and ripening was studied in "Huangguan" pear (Shen et al., 2017). K contents in the pear leaves and fruits were significantly reduced under low-K treatment. According to the transcriptome sequencing data, AKT1 and HAK/KUP/KT genes may play a vital role on K^+ transport in leaves and fruits under K deficiency. High K level could promote photosynthesis and modify the distribution of the carbohydrate and nutrient from leaves to fruits, whereas carbohydrate metabolism was inhibited by low K during maturation. Two Suc synthase (SUS) genes were remarkably downregulated in fruits, and this change may be the reason for the decrease Suc concentration of leaves and fruit under low K. Genes associated with ethylene, cytokinin (CK), jasmonic acid (JA), auxin, and ABA were induced by low K, but the genes encoding transporters of auxin, CK, and brassinosteroid were significantly downregulated under low-K treatment in leaves and fruit (Shen et al., 2017).

Studying the signal network of different K applications on plant growth and fruit development and the molecular mechanism of K application on improving fruit quality can provide scientific basis for improving fruit quality by reasonable fertilizer.

CALCIUM FERTILIZER REGULATES FRUIT RIPENING AND POSTHARVEST QUALITY

Calcium (Ca) is considered to be one of the most important mineral elements to determine fruit quality, and many research studies focus on the function of Ca. Studies have confirmed that Ca has a central role in cell wall interactions, plant signaling, and water relations (Hocking et al., 2016). Since Ca is an important part of cell wall structure, it can affect the integrity of the cell membrane as well as affect a key role in membrane function (Fallahi et al., 1997).

Localized Ca deficiencies observed in particular species or varieties can lead to leakage of membranes, irregular softening of the cell walls, and abnormal development of fruit. It is reported that high concentrations of Ca inhibited ethylene production in apple slices, by delaying the conversion of 1-aminocyclopropane-l-carboxylic acid (ACC) to ethylene (Lieberman and Wang, 1982; Han et al., 2020). The de-esterification of pectin and Ca crosslinking resulted in the changes of the physical properties of the cell wall, which eventually lead to fruit softening (Hocking et al., 2016).

Ca deficiencies in fruits may also cause pathological and physiological disorders (Hocking et al., 2016). Ca^{2+} deficiency contributed to the occurrence of skin browning spot, which is an important physiology disorder in Huangguan (*P. bretschneideri* × *Pyrus pyrifolia*) pear fruit (Dong et al., 2015). The Ca^{2+} imbalance of pear fruit would lead to the development of hard end disorder (Wang et al., 2018e). Calcium application during sweet cherry development and ripening caused a reduction in respiration rate and water-induced fruit cracking, which was accompanied by numerous changes in the polar/non-polar primary and secondary metabolites according to the metabolome profiling (Michailidis et al., 2020).

Abnormal Ca content, partitioning, and distribution are the major factors related to bitter-pit (BP; De Freitas et al., 2015). Almost all factors that influence BP incidence in preharvest fruits could be directly or indirectly associated with Ca content in apple fruit (Ferguson et al., 1999). It is studied that the main reason for the decrease of BP of apple (*M. domestica*) is the change of K/Ca ratio (Guerra and Casquero, 2010). Ca-containing fertilizers, such as $CaCl_2$, $Ca(NO_3)_2$, or $Ca(HCOO)_2$, were applied in preharvest apple, in order to improve fruit quality, because as the Ca content increased, the BP was reduced (Yu et al., 2018).

Ca-containing substances are widely used to maintain the quality of fruit after harvest. Treatment with $CaCl_2$ or ultrasound and calcium (U + Ca) boosted fruit total phenolics content in strawberry by stimulating the genes expression involving anthocyanin structure (Xu et al., 2014), preventing the decrease in firmness of strawberries to maintain better fruit quality (Zhang et al., 2018a). Sprays of $CaCl_2$ and $Ca(NO_3)_2$ effectively reduced respiration rate, spoilage, and physiological weight loss, but maintained fruit firmness, palatability, acidity, and pectin methylesterase (PME) activity during storage of peach, apple, apricot, sweet berry, and plum fruits, which helped fruits to be stored longer with acceptable edible quality (Gupta, 2011; Mauro et al., 2016; Liu et al., 2017; Michailidis et al., 2019; Sinha et al., 2019; Han et al., 2020). The combination of calcium propionate (CP) and sodium chlorite (SC) could increase the firmness of apple slices and inhibited apple browning and the growth of *Escherichia coli* and yeast on fresh-cut apple slices (Guan and Fan, 2010). However, it is recently reported that postharvest calcium dipping, including $CaCl_2$ and $Ca(NO_3)_2$ treatment, in apples caused an increase in lenticel breakdown, the damage during storage appearing as discrete tissue deterioration surrounding the lenticels (Singh et al., 2016, 2021).

Ca nutrition also increases plant resistance to both biological and abiotic stresses. The supplement of Ca^{2+} could restrict the growth of fungal pathogen *B. cinerea* in strawberry (Langer et al., 2019). In addition, Ca^{2+} was reported to enhance resistance to *Botryosphaeria dothidea*, which is one of the most serious diseases for pear, by increasing autophagic activity and salicylic acid (SA) accumulation (Sun et al., 2020b). Transcriptome and proteome results showed that the application of Ca alleviated the temperature response of apple tree and salinity stress response of pear plants (Xu et al., 2015; Li et al., 2017).

Molecular Pathways of Ca in Rosaceae Species

Ca^{2+} is a ubiquitous second messenger related to plant cell signaling processes and enables the development as well as biotic and abiotic stress responses in plants. The change of the intracellular free Ca^{2+} content is one of the earliest events during perceiving changes of plants in the environment. Ca^{2+} sensors calmodulin (CaM), Ca^{2+}-dependent protein kinases (CDPKs), calmodulin-like proteins (CMLs), and CBLs play important roles in the process that convert Ca^{2+} signals into appropriate responses (Aldon et al., 2018). In addition to the components of the classical Ca signaling pathway, FaAnn5s and FaAnn8, plant Ca^{2+}-binding proteins, were downstream of Ca signaling during strawberry fruit ripening (Chen et al., 2016). Recently, Ca^{2+}/H^{+} exchangers MdCAX11 and MdCAX5, tonoplast located Ca^{2+} transport proteins, were suggested to mediate the influx of Ca from the cytosol into vacuoles, which may be related to the occurrence of BP in apple fruit, because their expression increased as the severity of BP increased (Liu et al., 2021).

A total of 4 *MdCaM* and 58 *MdCML* genes were identified in apple (*Malus* × *domestica*), and *MdCaMs*/*MdCMLs* were expressed in shoots, roots, mature leaves, flowers, and fruits (Li et al., 2019). The overexpression of *MdCML3* observably improved the salt tolerance of apple callus (Li et al., 2019). *FvCaM* and *FvCML* genes in strawberry were identified (Zhang et al., 2016). The overexpression of four *FvCaMs* and *FvCMLs* could enhance the resistance of *Nicotiana benthamiana* leaves to *Agrobacterium tumefaciens* (Zhang et al., 2016). *PbCBL1* gene, from the birch-leaf pear, is induced by gibberellic acid (GA), ABA, SA, methyl jasmonate (MeJA), and several abiotic stresses (Xu et al., 2015).

In five Rosaceae species, involving strawberry, apple, peach, pear, and plum, a total of 123 CPK genes were identified (Wei et al., 2016). Eleven out of 30 MdCPKs were regulated by pathogen infection (Kanchiswamy et al., 2013). The overexpression of *MdCIPK6L* could improve the salt tolerance in transgenic Arabidopsis and tomatoes (Wang et al., 2012). The expression of *FaCDPK* affected strawberry fruit development and ripening and also responded to salt and drought stresses, as well as ABA treatment (Crizel et al., 2020).

Transcriptome and proteome were used to determine the changes after calcium treatment during fruit development and postharvest senescence in sweet cherry (Michailidis et al., 2019, 2020). The expression of several genes involved in tricarboxylic acid (TCA) cycle, pectin degradation, as well as amino acids and sugar metabolism was affected by Ca treatment in sweet cherry (Michailidis et al., 2019). Ca specifically increased the amounts of proteins that were classified as oxidoreductases, transferases, hydrolases, lyases, and ligases during postharvest storage (Michailidis et al., 2020).

IRON FERTILIZER IMPROVES PHOTOSYNTHESIS, FRUIT YIELD, AND QUALITY

Iron (Fe) deficiency not only reduced biomass, chlorophyll, and photosynthesis but also increased oxidative stress response and leaf chlorosis in both peach and strawberry (Eichert et al., 2010; Gama et al., 2016; Kaya and Ashraf, 2019). However, other effects of Fe deficiency on the growth, fruit quality, and yield of different Rosaceae species were varied.

In peach, Fe deficiency led to decreased fruit production and fruit quality, because of the lower total sugar/total organic acid ratios and the less anthocyanin accumulation, and to a slight improvement of phenolic compounds and vitamin C (Alvarez-Fernández et al., 2003). It not only induced leaf chlorosis in peach but also reduced WUE, because normal stomatal functioning was disturbed in chlorotic leaves (Eichert et al., 2010).

In strawberry, deficiency of Fe resulted in a lower N assimilation, photosynthesis, and antioxidant activity, while higher amounts of bioactive compounds, including phenols and anthocyanin (Valentinuzzi et al., 2015a,b). It was shown that increased nitric oxide (NO) in the root system, root ferrous uptake activity, and indole-3-acetic acid (IAA) content in the shoot apex may enhance tolerance to Fe deficiency in *Malus xiaojinensis* and strawberry (Wu et al., 2012; Zha et al., 2014; Zhai et al., 2016; Kaya et al., 2019).

To improve the tolerance to Fe deficiency in Rosaceae plants, many measures have been taken. Studies have shown that exogenous Suc could enhance tolerance to Fe deficiency through regulating chlorophyll biosynthesis in *Malus halliana* (Guo et al., 2020). Additionally, foliar spraying with amino acid-Fe compound fertilizer remarkably increased fresh weights, Fe accumulation, total chlorophyll content, photosynthesis, and stomatal conductance of leaves in peach (*P. persica* L. Batsch; Sheng et al., 2020).

Pre-treatments with 24-epibrassinolide (EB) improved Fe deficiency tolerance *via* improving Fe^{2+} and antioxidant enzyme activities in leaves, thus causing an elevation in NR in strawberry (Kaya et al., 2020). The NO donor, sodium nitroprusside (SNP), restored Fe deficiency response in *M. xiaojinensis* (Zhai et al., 2016), and exogenously applied NO effectively reduced electrolyte leakage (EL), malondialdehyde (MDA), and H_2O_2 of seedlings in strawberry (*Fragaria* × *ananassa* cv. Camarosa) suffering Fe deficiency (Kaya et al., 2019).

The symptoms of Fe deficiency, such as lower chlorophyll contents in young leaves, were decreased by application of sodium hydrosulfide (NaHS), as it could improve endogenous H_2S and antioxidant enzyme activities, as well as reduce the H_2O_2 and MDA generation under Fe deficiency, eventually enhancing the uptake and activation of Fe (Kaya and Ashraf, 2019).

Molecular Pathways of Fe in Rosaceae Species

Fe is a crucial element in plants, and Fe deficiency would lead to common nutritional disorders. Fe deficiency limits the

yield of fruit trees, reducing fruit quality, particularly for the pear trees growing in calcareous soil (Donnini et al., 2011). When subjected to Fe deficiency, a series of adaptive responses in plants is induced. For example, H^+ secretion of the rhizosphere increased and led to soil acidification, promoting the conversion from Fe^{3+} to Fe^{2+}, which allowed the apple tree to absorb Fe better (Zhang et al., 2020). Currently, the signal mechanism of Rosaceae responding to different Fe supplies is mainly studied in *Malus* plants.

The uptake and transport of Fe mainly depend on transporters. Fe-regulated transporter 1 (*Mx IRT1*), an Fe transporter that was highly effectively inducible in *M. xiaojinensis*, could rescue the phenotype of Arabidopsis *irt1* mutant and restore the growth defect of Fe-limit yeast mutant *DEY1453* (*fet3fet4*; Zhang et al., 2014). In genus *Malus*, a mutant allele of *IRT1* showed increased expression of *IRT1*, which allows apple to adapt to Fe deficiency (Zhang et al., 2017). In apple, 18 Fe-regulated transporter-like protein (ZIP) family genes were identified (Ma et al., 2019). MdZIP10 could not only rescue the growth of Fe^{2+} uptake defective yeast mutants but also increase the Fe content and alleviate Fe deficiency symptoms by inducing the expression of Fe uptake and transport-related genes in *MdZIP10* overexpression *A. thaliana* transgenic plants (Ma et al., 2019).

Transcription factors play important roles in Rosaceae species' responses to Fe deficiency. In the case of Fe deficiency, *MxIRO2*, a novel basic helix-loop-helix Fe-related transcription factor, was upregulated in *M. xiaojinensis* leaves and roots (Yin et al., 2013). MdbHLH104 was identified to play a key role in toleration to Fe deficiency in both transgenic apple plants and callus by directly regulating the expression of *MdAHA8* to increase the plasma membrane (PM) H (+)-ATPase activity and Fe uptake (Zhao et al., 2016a). Additionally, MdbHLH104 was degraded by MdBT2 and MdSIZ1 (a SIZ/PIAS-type SUMO E3 ligase) dependent SUMOylation and ubiquitination through the 26S proteasome pathway in apple (*M. domestica*; Zhao et al., 2016b; Zhou et al., 2019).

Fe deficiency response transcription factor *MxFIT* was induced in roots during Fe deficiency, and the overexpression of *MxFIT* in Arabidopsis enhanced toleration to Fe deficiency, indicating that it may play roles in Fe uptake and Fe deficiency response (Yin et al., 2014). In addition, ethylene response factor MxERF4 could inhibit *MxIRT1* expression *via* binding to its promoter in *M. xiaojinensis*, which suggested that ethylene regulated the Fe deficiency response *via* MxERF4-related Fe acquisition (Liu et al., 2018). *MbERF4* and *MbERF72* were highly expressed in Fe deficiency-sensitive *Malus baccata*, whereas they were lowly expressed in Fe deficiency-tolerant *M. xiaojinensis*, and they repressed the expression of *MbHA2* directly, thus increasing the rhizosphere pH in response to Fe deficiency in *M. baccata* (Zhang et al., 2020).

With overexpressing *MdMYB58*, Fe deficiency-inducible MYB transcription factor, both apple calli and transgenic Arabidopsis could accumulate Fe under low Fe stress (Wang et al., 2018a). MdMYB58 directly repressed the expression of *MdMATE43* and *MdFRD3* in Arabidopsis, but it was competitively attenuated by MdSAT1, a member of bHLH transcription factors, through protein-protein interaction (Wang et al., 2018a). Under both deficient and normal Fe conditions, the content of Fe in transgenic Arabidopsis expressing *MxMYB1* was lower than that of wild type, that may be because of the lower expression of Fe transporter *AtIRT1* and an Fe storage protein ferritin *AtFER1* in plants (Shen et al., 2008).

Besides the transport proteins and transcription factors, MxNRAMP1 (natural resistance-associated macrophage protein), MxNas1 (nicotianamine synthase), and lncRNA MSTRG.85814.11 from *M. xiaojinensis* and *M. domestica* play important roles in Fe deficiency (Pan et al., 2015; Sun et al., 2018a, 2020a). *MxNRAMP1* overexpression could accelerate Fe absorption and accumulation and increase the resistance of plants against Fe deficiency stress (Pan et al., 2015). *MxNAS1* overexpression in transgenic tobacco cells could increase the content of active Fe and Na under Fe sufficiency, while related to the redistribution of Fe in *M. xiaojinensis* under Fe deficiency (Sun et al., 2018a). lncRNA MSTRG.85814.11 positively modulated the small auxin upregulated gene SAUR32 and increased the expression of *AHA10*, a plasma membrane proton ATPase, which activated proton extrusion involved in response to Fe deficiency (Sun et al., 2020a).

M. halliana, which is an apple rootstock with Fe deficiency resistance, is used to evaluate short-term molecular response under Fe deficiency treatment by RNA sequencing (RNA-Seq) analyses (Hu et al., 2018; Wang et al., 2018f). Fe deficiency induced genes involved in photosynthesis, pigment regulation, and glycolysis pathways, which suggested that Fe deficiency can also affect the synthesis and metabolism of sugar in the *M. halliana* leaves and roots (Hu et al., 2018; Wang et al., 2018f).

CONCLUSION AND FUTURE PERSPECTIVES

In this review, we focused on the effect of mineral nutrition on Rosaceae species' fruit yield, quality, and postharvest storage and, on the one hand, on the mechanisms by which Rosaceae absorbed, utilized, and transmitted nutritional signals. In conclusion, nitrogen supply mainly affects fruit yield, anthocyanin synthesis, and chlorophyll degradation in the fruit. Phosphorus (P) supplementation affects the production of SSC and secondary metabolites, such as flavonoids and ascorbic acid. Potassium (K) not only affects fruit quality but also induces both biological and abiotic stress tolerance in fruit trees. Calcium (Ca) deficiency is a major factor associated with fruit softening and BP. Iron (Fe) deficiency reduced biomass and photosynthesis, whereas it increased oxidative stress response and the activities of antioxidant enzymes. Many important transport proteins, transcription factors, and other regulators were reported and shown in **Figure 1**. However, there are still many significant questions to be investigated in the future.

First of all, more comprehensive understanding of the uptake and translocation system in Rosaceae species for mineral elements is required. Compared with the model plant Arabidopsis and crops, the transport and regulation system of mineral elements in Rosaceae species are far from fully understood. Although some transporters have been identified through bioinformatics, their function should be verified through more physiological and molecular experiments in the future.

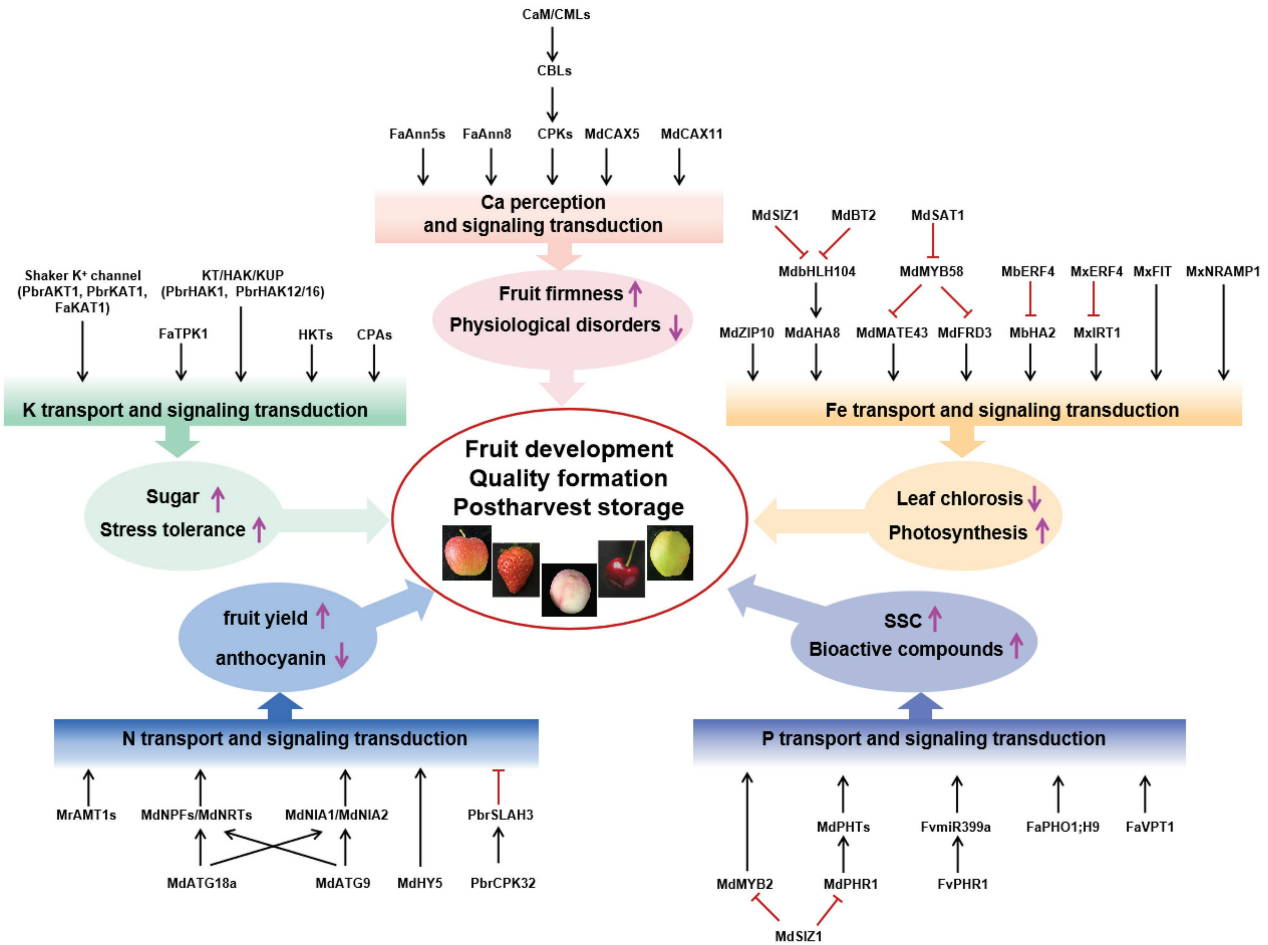


FIGURE 1 | Signal components involved in the regulation of fruit yield, quality, and postharvest storage by N, P, K, Ca, and Fe. Mineral nutrients nitrogen (N; blue box), phosphorus (P; purple box), potassium (K; green box), calcium (Ca; pink box), and iron (Fe; orange box) regulate fruit development, quality formation, and postharvest storage. Black arrows represent positive interactions or regulation, whereas red bars represent repression. Ammonium transporter AMT1 in the apple rootstock *Malus robusta* Rehd, anion channel PbrSLAH3 of pear, nitrate transporter 1/peptide transporter family, NR MdNIA1/MdNIA2, and autophagy protein MdATG18a/MdATG9 from *Malus domestica* are identified in N transport or signal transduction, which mainly affect fruit yield and anthocyanin synthesis. Phosphate transporters SUMO E3 ligase MdSIZ1, MdPHR1, and MdMYB2 in apple and FaPHO1;H9, FaVPT1, FvPHR1, and FvmiR399a in strawberry are identified to change the content of soluble solid (SSC) and bioactive compounds. Shaker K^+ channel, KT/HAK/KUP family K transporters, HKT and CPA transport proteins in five Rosaceae species, and FaKAT1 and FaTPK1 in strawberry were identified, improving sugar content and stress tolerance. MdCaM, MdCML, MdCAX5, and MdCAX11 in apple; FvCaMs, FvCMLs, FaAnn5s, and FaAnn8 in strawberry; PbCBL1 from the birch-leaf pear; and CPK family from five Rosaceae species are identified to be associated with regulating fruit firmness, keeping plants from physiological disorders, and improving sugar content and stress tolerance. Iron-regulated transporters (MxIRT1 and MdZIP), transcription factors (MxIRO2, MdbHLH104, MbERF72, MxFIT, MxERF4, MdSAT1, MdMYB58, and MxMYB1), E3 ligases (MdBT2 and MdSIZ1), and MxNRAMP1 are identified in Fe transport or signal transduction, which promoted photosynthesis and prevented leaf chlorosis.

Second, as the change of fertilization of some mineral nutrient elements will affect the absorption and utilization of other elements and the plants would communicate with rhizosphere microorganisms to improve the absorption and utilization of nutrients, we should pay more attention to the molecular mechanisms of the interactions between different nutrients or plants and microbes and take advantage of them.

Third, as it is difficult for the public to accept transgenic plants, especially transgenic fruits, we need to find more natural variations and refine the gene editing techniques to apply in Rosaceae, in order to improve fruit yield and quality.

AUTHOR CONTRIBUTIONS

YH, YS, and QB wrote the review. QB collected the references. YH designed the model and revised the review. All authors contributed to the article and approved the submitted version.

FUNDING

This study was supported by the National Natural Science Foundation of China (projects 32030100; 31672125), the

Scientific Research Project of Beijing Educational Committee (KM202110020006), the Opening Project of Beijing Key Laboratory of New Technology in Agricultural Application (kf2020021), and the Sichuan Lomon Biotechnology Co., Ltd. (2018001).

ACKNOWLEDGMENTS

We are very grateful to Prof. Chen Yi-Fang (China Agricultural University) for her advice on the role of P in fruit ripening.

REFERENCES

Afroz, C. A., Shimul, M. A. H., Ikrum, M., Siddiky, M. A., and Razzaque, M. A. (2016). Effects of nitrogen phosphorus potassium and sulphur on growth yield and nutrient content of strawberry (*Fragaria ananassa*). *J. Environ. Sci. Nat. Resour.* 9, 99–108. doi: 10.3329/jesnr.v9i1.30300

Aldon, D., Mbengue, M., Mazars, C., and Galaud, J. P. (2018). Calcium signalling in plant biotic interactions. *Int. J. Mol. Sci.* 19:665. doi: 10.3390/ijms19030665

Alvarez-Fernández, A., Paniagua, P., Abadía, J., and Abadía, A. (2003). Effects of Fe deficiency chlorosis on yield and fruit quality in peach (*Prunus persica* L. Batsch). *J. Agric. Food Chem.* 51, 5738–5744. doi: 10.1021/jf034402c

An, J. P., Qu, F. J., Yao, J. F., Wang, X. N., You, C. X., Wang, X. F., et al. (2017). The bZIP transcription factor MdHY5 regulates anthocyanin accumulation and nitrate assimilation in apple. *Hortic. Res.* 4, 1–9. doi: 10.1038/hortres.2017.23

Araujo, L., Bispo, W. S., Rios, V. S., Fernandes, S. A., and Rodrigues, F. A. (2015). Induction of the phenylpropanoid pathway by acibenzolar-S-methyl and potassium phosphite increases mango resistance to *Ceratocystis fimbriata* infection. *Plant Dis.* 99, 447–459. doi: 10.1094/PDIS-08-14-0788-RE

Cao, F., Guan, C., Dai, H., Li, X., and Zhang, Z. (2015). Soluble solids content is positively correlated with phosphorus content in ripening strawberry fruits. *Sci. Hortic.* 195, 183–187. doi: 10.1016/j.scienta.2015.09.018

Cao, F., Li, H., Wang, S., Li, X., Dai, H., and Zhang, Z. (2017). Expression and functional analysis of *FaPHO1;H9* gene of strawberry (*Fragaria* × *ananassa*). *J. Integr. Agric.* 16, 580–590. doi: 10.1016/S2095-3119(16)61433-8

Cardeñosa, V., Medrano, E., Lorenzo, P., Sánchez-Guerrero, M. C., Cuevas, F., Pradas, I., et al. (2015). Effects of salinity and nitrogen supply on the quality and health-related compounds of strawberry fruits (*Fragaria* × *ananassa* cv. Primoris). *J. Sci. Food Agric.* 95, 2924–2930. doi: 10.1002/jsfa.7034

Chai, X., Xie, L., Wang, X., Wang, H., Zhang, J., Han, Z., et al. (2020). Apple rootstocks with different phosphorus efficiency exhibit alterations in rhizosphere bacterial structure. *J. Appl. Microbiol.* 128, 1460–1471. doi: 10.1111/jam.14547

Chanroj, S., Wang, G., Venema, K., Zhang, M. W., Delwiche, C. F., and Sze, H. (2012). Conserved and diversified gene families of monovalent cation/H+ antiporters from algae to flowering plants. *Front. Plant Sci.* 3:25. doi: 10.3389/fpls.2012.00025

Chen, G., Chen, Q., Qi, K., Xie, Z., Yin, H., Wang, P., et al. (2019a). Identification of shaker K^+ channel family members in Rosaceae and a functional exploration of PbrKAT1. *Planta* 250, 1911–1925. doi: 10.1007/s00425-019-03275-3

Chen, J., Mao, L., Mi, H., Lu, W., Ying, T., and Luo, Z. (2016). Involvement of three annexin genes in the ripening of strawberry fruit regulated by phytohormone and calcium signal transduction. *Plant Cell Rep.* 35, 733–743. doi: 10.1007/s00299-015-1915-5

Chen, G., Wang, L., Chen, Q., Qi, K., Yin, H., Cao, P., et al. (2019b). PbrSLAH3 is a nitrate-selective anion channel which is modulated by calcium-dependent protein kinase 32 in pear. *BMC Plant Biol.* 19:190. doi: 10.1186/s12870-019-1813-z

Cheng, L., Ma, F., and Ranwala, D. (2004). Nitrogen storage and its interaction with carbohydrates of young apple trees in response to nitrogen supply. *Tree Physiol.* 24, 91–98. doi: 10.1093/treephys/24.1.91

Chiou, T. J., and Lin, S. I. (2011). Signaling network in sensing phosphate availability in plants. *Annu. Rev. Plant Biol.* 62, 185–206. doi: 10.1146/annurev-arplant-042110-103849

Cockerton, H. M., Li, B., Stavridou, E., Johnson, A., Karlström, A., Armitage, A. D., et al. (2020). Genetic and phenotypic associations between root architecture, arbuscular mycorrhizal fungi colonisation and low phosphate tolerance in strawberry (*Fragaria* × *ananassa*). *BMC Plant Biol.* 20:154. doi: 10.1186/s12870-020-02347-x

Crizel, R. L., Perin, E. C., Vighi, I. L., Woloski, R., Seixas, A., da Silva Pinto, L., et al. (2020). Genome-wide identification, and characterization of the CDPK gene family reveal their involvement in abiotic stress response in *Fragaria* x *ananassa*. *Sci. Rep.* 10:11040. doi: 10.1038/s41598-020-67957-9

De Freitas, S. T., do Amarante, C. V. T., and Mitcham, E. J. (2015). Mechanisms regulating apple cultivar susceptibility to bitter pit. *Sci. Hortic.* 186, 54–60. doi: 10.1016/j.scienta.2015.01.039

Dong, Y., Guan, J. F., Ma, S. J., Liu, L. L., Feng, Y. X., and Cheng, Y. D. (2015). Calcium content and its correlated distribution with skin browning spot in bagged Huangguan pear. *Protoplasma* 252, 165–171. doi: 10.1007/s00709-014-0665-5

Donnini, S., Dell'Orto, M., and Zocchi, G. (2011). Oxidative stress responses and root lignification induced by Fe deficiency conditions in pear and quince genotypes. *Tree Physiol.* 31, 102–113. doi: 10.1093/treephys/tpq105

Eichert, T., Peguero-Pina, J. J., Gil-Pelegrín, E., Heredia, A., and Fernández, V. (2010). Effects of iron chlorosis and iron resupply on leaf xylem architecture, water relations, gas exchange and stomatal performance of field-grown peach (*Prunus persica*). *Physiol. Plant.* 138, 48–59. doi: 10.1111/j.1399-3054.2009.01295.x

Estrada-Ortiz, E., Trejo-Tellez, L. I., Gomez-Merino, F. C., Nunez-Escobar, R., and Sandoval-Villa, M. (2013). The effects of phosphite on strawberry yield and fruit quality. *J. Soil Sci. Plant Nutr.* 13, 612–620. doi: 10.4067/S0718-95162013005000049

Ezawa, T., and Saito, K. (2018). How do arbuscular mycorrhizal fungi handle phosphate? New insight into fine-tuning of phosphate metabolism. *New Phytol.* 220, 1116–1121. doi: 10.1111/nph.15187

Falchi, R., Bonghi, C., Drincovich, M. F., Famiani, F., Lara, M. V., Walker, R. P., et al. (2020). Sugar metabolism in stone fruit: source-sink relationships and environmental and agronomical effects. *Front. Plant Sci.* 11:573982. doi: 10.3389/fpls.2020.573982

Fallahi, E., Conway, W. S., Hickey, K. D., and Sams, C. E. (1997). The role of calcium and nitrogen in postharvest quality and disease resistance of apples. *Hortic. Sci.* 32, 831–835. doi: 10.1023/A:1008607100742

Ferguson, I., Volz, R., and Woolf, A. (1999). Preharvest factors affecting physiological disorders of fruit. *Postharvest Biol. Technol.* 15, 255–262. doi: 10.1016/S0925-5214(98)00089-1

Gama, F., Saavedra, T., Da Silva, J. P., Miguel, M. G., de Varennes, A., Correia, P. J., et al. (2016). The memory of iron stress in strawberry plants. *Plant Physiol. Biochem.* 104, 36–44. doi: 10.1016/j.plaphy.2016.03.019

Garriga, M., Raddatz, N., Véry, A. A., Sentenac, H., Rubio-Meléndez, M. E., González, W., et al. (2017). Cloning and functional characterization of *HKT1* and *AKT1* genes of *Fragaria spp.*-relationship to plant response to salt stress. *J. Plant Physiol.* 210, 9–17. doi: 10.1016/j.jplph.2016.12.007

Ge, Y., Chen, Y., Li, C., Wei, M., Li, X., Li, S., et al. (2019). Effect of trisodium phosphate dipping treatment on the quality and energy metabolism of apples. *Food Chem.* 274, 324–329. doi: 10.1016/j.foodchem.2018.08.142

Gierth, M., and Mäser, P. (2007). Potassium transporters in plants--involvement in K^+ acquisition, redistribution and homeostasis. *FEBS Lett.* 581, 2348–2356. doi: 10.1016/j.febslet.2007.03.035

Gomez-Porras, J. L., Riaño Pachón, D. M., Benito, B., Haro, R., Sklodowski, K., Rodríguez-Navarro, A., et al. (2012). Phylogenetic analysis of k(+) transporters in bryophytes, lycophytes, and flowering plants indicates a specialization of vascular plants. *Front. Plant Sci.* 3:167. doi: 10.3389/fpls.2012.00167

Guan, W., and Fan, X. (2010). Combination of sodium chlorite and calcium propionate reduces enzymatic browning and microbial population of fresh-cut "Granny Smith" apples. *J. Food Sci.* 75, M72–M77. doi: 10.1111/j.1750-3841.2009.01470.x

Guerra, M., and Casquero, P. A. (2010). Summer pruning: an ecological alternative to postharvest calcium treatment to improve storability of high quality apple cv. 'Reinette du Canada'. *Food Sci. Technol. Int.* 16, 343–350. doi: 10.1177/1082013210366977

Guo, A., Hu, Y., Shi, M., Wang, H., Wu, Y., and Wang, Y. (2020). Effects of iron deficiency and exogenous sucrose on the intermediates of chlorophyll

biosynthesis in *Malus halliana*. *PLoS One* 15:e0232694. doi: 10.1371/journal.pone.0232694

Guo, B., Jin, Y., Wussler, C., Blancaflor, E. B., Motes, C. M., and Versaw, W. K. (2008). Functional analysis of the *Arabidopsis* PHT4 family of intracellular phosphate transporters. *New Phytol.* 177, 889–898. doi: 10.1111/j.1469-8137.2007.02331.x

Gupta, S. (2011). An in vitro study of Diffusibility and degradation of three calcium hydroxide pastes. *Int. J. Clin. Pediatr. Dent.* 4, 15–23. doi: 10.5005/jp-journals-10005-1075

Han, S., Liu, H., Han, Y., He, Y., Nan, Y., Qu, W., et al. (2020). Effects of calcium treatment on malate metabolism and γ-aminobutyric acid (GABA) pathway in postharvest apple fruit. *Food Chem.* 334:127479. doi: 10.1016/j.foodchem.2020.127479

Hassler, S., Lemke, L., Jung, B., Möhlmann, T., Krüger, F., Schumacher, K., et al. (2012). Lack of the Golgi phosphate transporter PHT4;6 causes strong developmental defects, constitutively activated disease resistance mechanisms and altered intracellular phosphate compartmentation in *Arabidopsis*. *Plant J.* 72, 732–744. doi: 10.1111/j.1365-313X.2012.05106.x

Hocking, B., Tyerman, S. D., Burton, R. A., and Gilliham, M. (2016). Fruit calcium: transport and physiology. *Front. Plant Sci.* 29:569. doi: 10.3389/fpls.2016.00569

Hu, Y., Zhu, Y. F., Guo, A. X., Jia, X. M., Cheng, L., Zhao, T., et al. (2018). Transcriptome analysis in *Malus halliana* roots in response to iron deficiency reveals insight into sugar regulation. *Mol. Gen. Genomics.* 293, 1523–1534. doi: 10.1007/s00438-018-1479-5

Huang, Y., Xu, P. H., Hou, B. Z., and Shen, Y. Y. (2019). Strawberry tonoplast transporter, FaVPT1, controls phosphate accumulation and fruit quality. *Plant Cell Environ.* 42, 2715–2729. doi: 10.1111/pce.13598

Huo, L., Guo, Z., Zhang, Z., Jia, X., Sun, Y., Sun, X., et al. (2020). The apple autophagy-related gene *MdATG9* confers tolerance to low nitrogen in transgenic apple callus. *Front. Plant Sci.* 11:423. doi: 10.3389/fpls.2020.00423

Hüseyin, Y., and Ömer, A. (2020). Effects of potassium fertilization on leaf nutrient content and quality attributes of sweet cherry fruits (*Prunus avium* L.). *J. Plant Nutr.* 1, 1–12. doi: 10.1080/01904167.2020.1862203

Jezek, M., Zörb, C., Merkt, N., and Geilfus, C. M. (2018). Anthocyanin Management in Fruits by fertilization. *J. Agric. Food Chem.* 66, 753–764. doi: 10.1021/acs.jafc.7b03813

Kanchiswamy, C. N., Mohanta, T. K., Capuzzo, A., Occhipinti, A., Verrillo, F., Maffei, M. E., et al. (2013). Differential expression of CPKs and cytosolic Ca^{2+} variation in resistant and susceptible apple cultivars (*Malus* × *domestica*) in response to the pathogen Erwinia amylovora and mechanical wounding. *BMC Genomics* 14:760. doi: 10.1186/1471-2164-14-760

Kaya, C., Akram, N. A., and Ashraf, M. (2019). Influence of exogenously applied nitric oxide on strawberry (*Fragaria* × *ananassa*) plants grown under iron deficiency and/or saline stress. *Physiol. Plant.* 165, 247–263. doi: 10.1111/ppl.12818

Kaya, C., and Ashraf, M. (2019). The mechanism of hydrogen sulfide mitigation of iron deficiency-induced chlorosis in strawberry (*Fragaria* × *ananassa*) plants. *Protoplasma* 256, 371–382. doi: 10.1007/s00709-018-1298-x

Kaya, C., Ashraf, M., Alyemeni, M. N., and Ahmad, P. (2020). Nitrate reductase rather than nitric oxide synthase activity is involved in 24-epibrassinolide-induced nitric oxide synthesis to improve tolerance to iron deficiency in strawberry (*Fragaria* × *annassa*) by up-regulating the ascorbate-glutathione cycle. *Plant Physiol. Biochem.* 151, 486–499. doi: 10.1016/j.plaphy.2020.04.002

Kumar, D., and Ahmed, N. (2014). Response of nitrogen and potassium fertigation to "Waris" almond (*Prunus dulcis*) under northwestern Himalayan region of India. *Sci. World J.* 2014:141328. doi: 10.1155/2014/141328

Kumari, A., Parida, A. K., Rangani, J., and Panda, A. (2017). Antioxidant activities, metabolic seconda, proximate analysis, mineral nutrient composition of *Salvadora persica* fruit unravel a potential functional food and a natural source of pharmaceuticals. *Front. Pharmacol.* 8:61. doi: 10.3389/fphar.2017.00061

Langer, S. E., Marina, M., Burgos, J. L., Martínez, G. A., Civello, P. M., and Villarreal, N. M. (2019). Calcium chloride treatment modifies cell wall metabolism and activates defense responses in strawberry fruit (*Fragaria* × *ananassa*, Duch). *J. Sci. Food Agric.* 99, 4003–4010. doi: 10.1002/jsfa.9626

Li, C., Meng, D., Zhang, J., and Cheng, L. (2019). Genome-wide identification and expression analysis of calmodulin and calmodulin-like genes in apple (*Malus* × *domestica*). *Plant Physiol. Biochem.* 139, 600–612. doi: 10.1016/j.plaphy.2019.04.014

Li, H., Yang, Q. S., Liu, W., Lin, J., and Chang, Y. H. (2017). The *AMT1* family genes from *Malus robusta* display differential transcription features and ammonium transport abilities. *Mol. Biol. Rep.* 44, 379–390. doi: 10.1007/s11033-017-4119-y

Lieberman, M., and Wang, S. Y. (1982). Influence of calcium and magnesium on ethylene production by apple tissue slices. *Plant Physiol.* 69, 1150–1155. doi: 10.1104/pp.69.5.1150

Liu, H., Chen, F., Lai, S., Tao, J., Yang, H., and Jiao, Z. (2017). Effects of calcium treatment and low temperature storage on cell wall polysaccharide nanostructures and quality of postharvest apricot (*Prunus armeniaca*). *Food Chem.* 225, 87–97. doi: 10.1016/j.foodchem.2017.01.008

Liu, J., Jiang, Z., Qi, Y., Liu, Y., Ding, Y., Tian, X., et al. (2021). MdCAX affects the development of the 'Honeycrisp' bitter pit by influencing abnormal Ca distribution. *Postharvest Biol. Technol.* 171:111341. doi: 10.1016/j.postharvbio.2020.111341

Liu, W., Wu, T., Li, Q., Zhang, X., Xu, X., Li, T., et al. (2018). An ethylene response factor (*MxERF4*) functions as a repressor of Fe acquisition in *Malus xiaojinensis*. *Sci. Rep.* 8, 1–13. doi: 10.1038/s41598-018-19518-4

Liu, J., Yang, L., Luan, M., Wang, Y., Zhang, C., Zhang, B., et al. (2015). A vacuolar phosphate transporter essential for phosphate homeostasis in *Arabidopsis*. *Proc. Natl. Acad. Sci. U. S. A.* 112, E6571–E6578. doi: 10.1073/pnas.1514598112

Lu, Y. L., Yang, X. L., Li, R., Li, S. L., and Tong, Y. A. (2015). Effects of different potassium fertilizer application periods on the yield and quality of Fuji apple. *Ying Yong Sheng Tai Xue Bao* 26, 1179–1185. doi: 10.13287/j.1001-9332.2015.0030

Ma, X., Liu, H., Cao, H., Qi, R., Yang, K., Zhao, R., et al. (2019). Genome-wide analysis of zinc- and iron-regulated transporter-like protein family members in apple and functional validation of *ZIP10*. *Biometals* 32, 657–669. doi: 10.1007/s10534-019-00203-6

Maguire, L. S., O'Sullivan, S. M., Galvin, K., O'Connor, T. P., and O'Brien, N. M. (2004). Fatty acid profile, tocopherol, squalene and phytosterol content of walnuts, almonds, peanuts, hazelnuts and the macadamia nut. *Int. J. Food Sci. Nutr.* 55, 171–178. doi: 10.1080/09637480410001725175

Mahmood, T., Anwar, F., Abbas, M., Boyce, M. C., and Saari, N. (2012). Compositional variation in sugars and organic acids at different maturity stages in selected small fruits from Pakistan. *Int. J. Mol. Sci.* 13, 1380–1392. doi: 10.3390/ijms13021380

Mäser, P., Thomine, S., Schroeder, J. I., Ward, J. M., Hirschi, K., Sze, H., et al. (2001). Phylogenetic relationships within cation transporter families of *Arabidopsis*. *Plant Physiol.* 126, 1646–1667. doi: 10.1104/pp.126.4.1646

Mauro, M. A., Dellarosa, N., Tylewicz, U., Tappi, S., Laghi, L., Rocculi, P., et al. (2016). Calcium and ascorbic acid affect cellular structure and water mobility in apple tissue during osmotic dehydration in sucrose solutions. *Food Chem.* 195, 19–28. doi: 10.1016/j.foodchem.2015.04.096

Michailidis, M., Karagiannis, E., Tanou, G., Sarrou, E., Stavridou, E., Ganopoulos, I., et al. (2019). An integrated metabolomic and gene expression analysis identifies heat and calcium metabolic networks underlying postharvest sweet cherry fruit senescence. *Planta.* 250, 2009–2022. doi: 10.1007/s00425-019-03272-6

Michailidis, M., Karagiannis, E., Tanou, G. M., Samiotaki, G. T., Eirini, S., George, S., et al. (2020). Novel insights into the calcium action in cherry fruit development revealed by high-throughput mapping. *Plant Mol. Biol.* 104, 597–614. doi: 10.1007/s11103-020-01063-2

Pan, H., Wang, Y., Zha, Q., Yuan, M., Yin, L., Wu, T., et al. (2015). Iron deficiency stress can induce MxNRAMP1 protein endocytosis in *M. xiaojinensis*. *Gene* 567, 225–234. doi: 10.1016/j.gene.2015.05.002

Parada, J., Valenzuela, T., Gómez, F., Tereucán, G., García, S., Cornejo, P., et al. (2019). Effect of fertilization and arbuscular mycorrhizal fungal inoculation on antioxidant profiles and activities in *Fragaria ananassa* fruit. *J. Sci. Food Agric.* 99, 1397–1404. doi: 10.1002/jsfa.9316

Peng, H. X., Wei, X. Y., Xiao, Y. X., Sun, Y., Biggs, A. R., Gleason, M. L., et al. (2016). Management of valsa canker on apple with adjustments to potassium nutrition. *Plant Dis.* 100, 884–889. doi: 10.1094/PDIS-09-15-0970-RE

Preciado-Rangel, P., Troyo-Diéguez, E., Valdez-Aguilar, L. A., García-Hernández, J. L., and Luna-Ortega, J. G. (2020). Interactive effects of the potassium and

nitrogen relationship on yield and quality of strawberry grown under soilless conditions. *Plants* 9:441. doi: 10.3390/plants9040441

Qu, G., Wang, H., and Shu, H. (2000). Effect of nitrogen on water use efficiency of apple tree. *Ying Yong Sheng Tai Xue Bao* 11, 199–201.

Rausch, C., and Bucher, M. (2002). Molecular mechanisms of phosphate transport in plants. *Planta* 216, 23–37. doi: 10.1007/s00425-002-0921-3

Ritenour, M., and Khemira, H. (2007). *Red color development of apple: A literature review*. Pullman, WA: Washington State University – Tree Fruit Research and Extension Center.

Rodríguez-Navarro, A., and Rubio, F. (2006). High-affinity potassium and sodium transport systems in plants. *J. Exp. Bot.* 57, 1149–1160. doi: 10.1093/jxb/erj068

Rubio Ames, Z., Brecht, J. K., and Olmstead, M. A. (2020). Nitrogen fertilization rates in a subtropical peach orchard: effects on tree vigor and fruit quality. *J. Sci. Food Agric.* 100, 527–539. doi: 10.1002/jsfa.10031

Shen, C., Shi, X., Xie, C., Li, Y., Yang, H., Mei, X., et al. (2019). The change in microstructure of petioles and peduncles and transporter gene expression by potassium influences the distribution of nutrients and sugars in pear leaves and fruit. *J. Plant Physiol.* 232, 320–333. doi: 10.1016/j.jplph.2018.11.025

Shen, C., Wang, J., Shi, X., Kang, Y., Xie, C., Peng, L., et al. (2017). Transcriptome analysis of differentially expressed genes induced by low and high potassium levels provides insight into fruit sugar metabolism of pear. *Front. Plant Sci.* 8:938. doi: 10.3389/fpls.2017.00938

Shen, J., Xu, X., Li, T., Cao, D., and Han, Z. (2008). An MYB transcription factor from *Malus xiaojinensis* has a potential role in iron nutrition. *J. Integr. Plant Biol.* 50, 1300–1306. doi: 10.1111/j.1744-7909.2008.00761.x

Sheng, Y., Cheng, H., Wang, L., Shen, J., Tang, M., Liang, M., et al. (2020). Foliar spraying with compound amino acid-Iron fertilizer increases leaf fresh weight, photosynthesis, and Fe-S cluster gene expression in peach (*Prunus persica* (L.) Batsch). *Biomed. Res. Int.* 2020:2854795. doi: 10.1155/2020/2854795

Shin, H., Shin, H. S., Dewbre, G. R., and Harrison, M. J. (2004). Phosphate transport in *Arabidopsis*: Pht1;1 and Pht1;4 play a major role in phosphate acquisition from both low- and high-phosphate environments. *Plant J.* 39, 629–642. doi: 10.1111/j.1365-313X.2004.02161.x

Singh, V., Gamrasni, D., Ben Arie, R., Naschitz, S., and Friedman, H. (2016). Identification of open lenticels in apples after harvest in relation to lenticel breakdown development during storage. *Postharvest Biol. Technol.* 121, 160–170. doi: 10.1016/j. postharvbio.2016.06.004

Singh, V., Gamrasni, D., Parimi, P., Kochanek, B., Naschitz, S., Zemach, H., et al. (2021). Postharvest calcium treatment of apple fruit increased lenticel breakdown and altered cuticle structure. *Postharvest Biol. Technol.* 171:111331. doi: 10.1016/j.postharvbio.2020.111331

Singh, G., Kachwaya, D. S., Kuchi, V. S., Singh, M., Singh, J., and Singh, B. (2020). Influence of foliar application of mineral nutrients on vegetative and fruit quality of strawberry (*Fragaria* × *ananassa* Duch.) cv. Chandler. *J. Plant Sci. Res.* 36, 323–328. doi: 10.32381/JPSR.2020.36.1-2.41

Sinha, A., Jawandha, S. K., Gill, P. P. S., and Singh, H. (2019). Influence of pre-harvest sprays of calcium nitrate on storability and quality attributes of plum fruits. *J. Food Sci. Technol.* 56, 1427–1437. doi: 10.1007/s13197-019-03621-z

Song, Z. Z., Duan, C. L., Guo, S. L., Yang, Y., Feng, Y. F., Ma, R. J., et al. (2015a). Potassium contributes to zinc stress tolerance in peach (*Prunus persica*) seedlings by enhancing photosynthesis and the antioxidant defense system. *Genet. Mol. Res.* 14, 8338–8351. doi: 10.4238/2015.July.27.22

Song, Z. Z., Ma, R. J., and Yu, M. L. (2015b). Genome-wide analysis and identification of KT/HAK/KUP potassium transporter gene family in peach (*Prunus persica*). *Genet. Mol. Res.* 14, 774–787. doi: 10.4238/2015.January.30.21

Song, M., Wang, S., Chai, L., Zhang, S., and Shen, Y. (2017). Characterization of an ABA-induced and K^+ channel gene FaKAT1 that regulates strawberry fruit ripening. *J. Plant Growth Regul.* 36, 312–322. doi: 10.1007/s00344-016-9641-y

Strissel, T., Halbwirth, H., Hoyer, U., Zistler, C., Stich, K., and Treutter, D. (2005). Growth-promoting nitrogen nutrition affects flavonoid biosynthesis in young apple (*Malus domestica* Borkh.) leaves. *Plant Biol.* 7, 677–685. doi: 10.1055/s-2005-872989

Sun, Y., Hao, P., Lv, X., Tian, J., Wang, Y., Zhang, X., et al. (2020a). A long non-coding apple RNA, MSTRG.85814.11, acts as a transcriptional enhancer of *SAUR32* and contributes to the Fe-deficiency response. *Plant J.* 103, 53–67. doi: 10.1111/tpj.14706

Sun, X., Jia, X., Huo, L., Che, R., Gong, X., Wang, P., et al. (2018b). *MdATG18a* overexpression improves tolerance to nitrogen deficiency and regulates anthocyanin accumulation through increased autophagy in transgenic apple. *Plant Cell Environ.* 41, 469–480. doi: 10.1111/pce.13110

Sun, T., Li, M., Shao, Y., Yu, L., and Ma, F. (2017). Comprehensive genomic identification and expression analysis of the phosphate transporter (PHT) gene family in apple. *Front. Plant Sci.* 8:426. doi: 10.3389/fpls.2017.00426

Sun, X., Pan, B., Wang, Y., Xu, W., and Zhang, S. (2020b). Exogenous calcium improved resistance to botryosphaeria dothidea by increasing autophagy activity and salicylic acid level in pear. *Mol. Plant-Microbe Interact.* 33, 1150–1160. doi: 10.1094/MPMI-04-20-0101-R

Sun, C., Yuan, M., Zhai, L., Li, D., Zhang, X., Wu, T., et al. (2018a). Iron deficiency stress can induce MxNAS1 protein expression to facilitate iron redistribution in *Malus xiaojinensis*. *Plant Biol.* 20, 29–38. doi: 10.1111/plb.12630

Tian, G., Wang, F., Peng, L., He, L., Jiang, Y. M., and Ge, S. F. (2017). Effects of different potassium levels on growth and NO_3^- uptake and utilization of *Malus hupehensis* seedlings. *Ying Yong Sheng Tai Xue Bao* 28, 2254–2260. doi: 10.13287/j.1001-9332.201707.009

Valentinuzzi, F., Mason, M., Scampicchio, M., Andreotti, C., Cesco, S., and Mimmo, T. (2015a). Enhancement of the bioactive compound content in strawberry fruits grown under iron and phosphorus deficiency. *J. Sci. Food Agric.* 95, 2088–2094. doi: 10.1002/jsfa.6924

Valentinuzzi, F., Pii, Y., Vigani, G., Lehmann, M., Cesco, S., and Mimmo, T. (2015b). Phosphorus and iron deficiencies induce a metabolic reprogramming and affect the exudation traits of the woody plant *Fragaria* x *ananassa*. *J. Exp. Bot.* 66, 6483–6495. doi: 10.1093/jxb/erv364

Wang, Y., Chen, Y. F., and Wu, W. H. (2020c). Potassium and phosphorus transport and signaling in plants. *J. Integr. Plant Biol.* 63, 34–52. doi: 10.1111/jipb.13053

Wang, Y. X., Hu, Y., Zhu, Y. F., Baloch, A. W., Jia, X. M., and Guo, A. X. (2018f). Transcriptional and physiological analyses of short-term Iron deficiency response in apple seedlings provide insight into the regulation involved in photosynthesis. *BMC Genomics* 19:461. doi: 10.1186/s12864-018-4846-z

Wang, R. K., Li, L. L., Cao, Z. H., Zhao, Q., Li, M., Zhang, L. Y., et al. (2012). Molecular cloning and functional characterization of a novel apple *MdCIPK6L* gene reveals its involvement in multiple abiotic stress tolerance in transgenic plants. *Plant Mol. Biol.* 79, 123–135. doi: 10.1007/s11103-012-9899-9

Wang, Q., Liu, C., Dong, Q., Huang, D., Li, C., Li, P., et al. (2018b). Genome-wide identification and analysis of apple NITRATE TRANSPORTER 1/PEPTIDE TRANSPORTER family (NPF) genes reveals *MdNPF6.5* confers high capacity for nitrogen uptake under low-nitrogen conditions. *Int. J. Mol. Sci.* 19:2761. doi: 10.3390/ijms19092761

Wang, Q., Liu, C., Huang, D., Dong, Q., Li, P., and Ma, F. (2019a). High-efficient utilization and uptake of N contribute to higher NUE of 'Qinguan' apple under drought and N-deficient conditions compared with 'Honeycrisp'. *Tree Physiol.* 39, 1880–1895. doi: 10.1093/treephys/tpz093

Wang, Y., Lü, J., Chen, D., Zhang, J., Qi, K., Cheng, R., et al. (2018d). Genome-wide identification, evolution, and expression analysis of the *KT/HAK/KUP* family in pear. *Genome* 61, 755–765. doi: 10.1139/gen-2017-0254

Wang, F., Sha, J., Chen, Q., Xu, X., Zhu, Z., Ge, S., et al. (2020b). Exogenous abscisic acid regulates distribution of ^{13}C and ^{15}N and anthocyanin synthesis in 'Red Fuji' apple fruit under high nitrogen supply. *Front. Plant Sci.* 10:1738. doi: 10.3389/fpls.2019.01738

Wang, S., Song, M., Guo, J., Huang, Y., Zhang, F., Xu, C., et al. (2018c). The potassium channel *FaTPK1* plays a critical role in fruit quality formation in strawberry (*Fragaria* × *ananassa*). *Plant Biotechnol. J.* 16, 737–748. doi: 10.1111/pbi.12824

Wang, F. P., Wang, X. F., Zhang, J., Ma, F., and Hao, Y. J. (2018a). MdMYB58 modulates Fe homeostasis by directly binding to the MdMATE43 promoter in plants. *Plant Cell Physiol.* 59, 2476–2489. doi: 10.1093/pcp/pcy168

Wang, Y., and Wu, W. H. (2017). Regulation of potassium transport and signaling in plants. *Curr. Opin. Plant Biol.* 39, 123–128. doi: 10.1016/j.pbi.2017.06.006

Wang, F., Xu, X., Jia, Z., Hou, X., Chen, Q., Sha, J., et al. (2020a). Nitrification inhibitor 3,4-Dimethylpyrazole phosphate application during the later stage of apple fruit expansion regulates soil mineral nitrogen and tree carbon-

nitrogen nutrition, and improves fruit quality. *Front. Plant Sci.* 11:764. doi: 10.3389/fpls.2020.00764

Wang, Y., Zhang, F., Cui, W., Chen, K., Zhao, R., and Zhang, Z. (2019b). The *FvPHR1* transcription factor control phosphate homeostasis by transcriptionally regulating miR399a in woodland strawberry. *Plant Sci.* 280, 258–268. doi: 10.1016/j.plantsci.2018.12.025

Wang, Y., Zhang, X., Wang, Y., Yang, S., and Qu, H. (2018e). The changes of intracellular calcium concentration and distribution in the hard end pear (*Pyrus pyrifolia* cv. 'Whangkeumbae') fruit. *Cell Calcium* 71, 15–23. doi: 10.1016/j.ceca.2017.11.002

Wei, M., Wang, S., Dong, H., Cai, B., and Tao, J. (2016). Characterization and comparison of the *CPK* gene family in the apple (*Malus* × *domestica*) and other Rosaceae species and its response to *Alternaria alternata* infection. *PLoS One* 11:e0155590. doi: 10.1371/journal.pone.0155590

Wen, B., Li, C., Fu, X., Li, D., Li, L., Chen, X., et al. (2019). Effects of nitrate deficiency on nitrate assimilation and chlorophyll synthesis of detached apple leaves. *Plant Physiol. Biochem.* 142, 363–371. doi: 10.1016/j.plaphy.2019.07.007

Wu, T., Zhang, H. T., Wang, Y., Jia, W. S., Xu, X. F., Zhang, X. Z., et al. (2012). Induction of root Fe(lll) reductase activity and proton extrusion by iron deficiency is mediated by auxin-based systemic signalling in *Malus xiaojinensis*. *J. Exp. Bot.* 63, 859–870. doi: 10.1093/jxb/err314

Xu, X., Du, X., Wang, F., Sha, J., Chen, Q., Tian, G., et al. (2020). Effects of potassium levels on plant growth, accumulation and distribution of carbon, and nitrate metabolism in apple dwarf rootstock seedlings. *Front. Plant Sci.* 11:904. doi: 10.3389/fpls.2020.00904

Xu, J., Li, H. D., Chen, L. Q., Wang, Y., Liu, L. L., He, L., et al. (2006). A protein kinase, interacting with two calcineurin B-like proteins, regulates K+ transporter AKT1 in *Arabidopsis*. *Cell* 125, 1347–1360. doi: 10.1016/j.cell.2006.06.011

Xu, Y., Li, X., Lin, J., Wang, Z., Yang, Q., and Chang, Y. (2015). Transcriptome sequencing and analysis of major genes involved in calcium signaling pathways in pear plants (*Pyrus calleryana* Decne.). *BMC Genomics* 16:738. doi: 10.1186/s12864-015-1887-4

Xu, W., Peng, H., Yang, T., Whitaker, B., Huang, L., Sun, J., et al. (2014). Effect of calcium on strawberry fruit flavonoid pathway gene expression and anthocyanin accumulation. *Plant Physiol. Biochem.* 82, 289–298. doi: 10.1016/j.plaphy.2014.06.015

Xu, L., Zhao, H., Wan, R., Liu, Y., Xu, Z., Tian, W., et al. (2019). Identification of vacuolar phosphate efflux transporters in land plants. *Nat. Plants* 5, 84–94. doi: 10.1038/s41477-018-0334-3

Yang, Y. Y., Ren, Y. R., Zheng, P. F., Qu, F. J., Song, L. Q., You, C. X., et al. (2020). Functional identification of apple *MdMYB2* gene in phosphate-starvation response. *J. Plant Physiol.* 244:153089. doi: 10.1016/j.jplph.2019.153089

Yin, L., Wang, Y., Yan, M., Zhang, X., Pan, H., Xu, X., et al. (2013). Molecular cloning, polyclonal antibody preparation, and characterization of a functional iron-related transcription factor IRO2 from *Malus xiaojinensis*. *Plant Physiol. Biochem.* 67, 63–70. doi: 10.1016/j.plaphy.2013.02.021

Yin, L., Wang, Y., Yuan, M., Zhang, X., Xu, X., and Han, Z. (2014). Characterization of *MxFIT*, an iron deficiency induced transcriptional factor in *Malus xiaojinensis*. *Plant Physiol. Biochem.* 75, 89–95. doi: 10.1016/j.plaphy.2013.12.007

Yu, X. M., Wang, J. Z., Nie, P. X., Xue, X. M., Wang, G. P., and An, M. (2018). Control efficacy of Ca-containing foliar fertilizers on bitter pit in bagged 'Fuji' apple and effects on the Ca and N contents of apple fruits and leaves. *J. Sci. Food Agric.* 98, 5435–5443. doi: 10.1002/jsfa.9087

Zha, Q., Wang, Y., Zhang, X. Z., and Han, Z. H. (2014). Both immanently high active iron contents and increased root ferrous uptake in response to low iron stress contribute to the iron deficiency tolerance in *Malus xiaojinensis*. *Plant Sci.* 214, 47–56. doi: 10.1016/j.plantsci.2013.10.002

Zhai, L., Xiao, D., Sun, C., Wu, T., Han, Z., Zhang, X., et al. (2016). Nitric oxide signaling is involved in the response to iron deficiency in the woody plant *Malus xiaojinensis*. *Plant Physiol. Biochem.* 109, 515–524. doi: 10.1016/j.plaphy.2016.11.005

Zhang, G., Liu, W., Feng, Y., Li, D., Li, K., Sun, Q., et al. (2020). Ethylene response factors *MbERF4* and *MbERF72* suppress iron uptake in woody apple plants by modulating rhizosphere pH. *Plant Cell Physiol.* 61, 699–711. doi: 10.1093/pcp/pcz234

Zhang, M., Lv, Y., Wang, Y., Rose, J. K., Shen, F., Han, Z., et al. (2017). TATA box insertion provides a selection mechanism underpinning adaptations to Fe deficiency. *Plant Physiol.* 173, 715–727. doi: 10.1104/pp.16.01504

Zhang, P., Tan, S., Berry, J. O., Li, P., Ren, N., Li, S., et al. (2014). An uncleaved signal peptide directs the Malus xiaojinensis iron transporter protein mx IRT1 into the ER for the PM secretory pathway. *Int. J. Mol. Sci.* 15, 20413–20433. doi: 10.3390/ijms151120413

Zhang, S., Tong, Y., Li, Y., Cheng, Z. M., and Zhong, Y. (2019b). Genome-wide identification of the *HKT* genes in five Rosaceae species and expression analysis of *HKT* genes in response to salt-stress in *Fragaria vesca*. *Genes Genomics* 41, 325–336. doi: 10.1007/s13258-018-0767-0

Zhang, K., Yue, D., Wei, W., Hu, Y., Feng, J., and Zou, Z. (2016). Characterization and functional analysis of calmodulin and calmodulin-like genes in *Fragaria vesca*. *Front. Plant Sci.* 7:1820. doi: 10.3389/fpls.2016.01820

Zhang, W., Zhang, X., Wang, Y., Zhang, N., Guo, Y., Ren, X., et al. (2018b). Potassium fertilization arrests malate accumulation and alters soluble sugar metabolism in apple fruit. *Biol. Open* 7:bio024745. doi: 10.1242/bio.024745

Zhang, L., Zhao, S., Lai, S., Chen, F., and Yang, H. (2018a). Combined effects of ultrasound and calcium on the chelate-soluble pectin and quality of strawberries during storage. *Carbohydr. Polym.* 200, 427–435. doi: 10.1016/j.carbpol.2018.08.013

Zhang, R. F., Zhou, L. J., Li, Y. Y., You, C. X., Sha, G. L., and Hao, Y. J. (2019a). Apple SUMO E3 ligase MdSIZ1 is involved in the response to phosphate deficiency. *J. Plant Physiol.* 232, 216–225. doi: 10.1016/j.jplph.2018.11.012

Zhao, Q., Ren, Y. R., Wang, Q. J., Wang, X. F., You, C. X., and Hao, Y. J. (2016b). Ubiquitination-related MdBT scaffold proteins target a *bHLH* transcription factor for iron homeostasis. *Plant Physiol.* 172, 1973–1988. doi: 10.1104/pp.16.01323

Zhao, Q., Ren, Y. R., Wang, Q. J., Yao, Y. X., You, C. X., and Hao, Y. J. (2016a). Overexpression of *MdbHLH104* gene enhances the tolerance to iron deficiency in apple. *Plant Biotechnol. J.* 14, 1633–1645. doi: 10.1111/pbi.12526

Zhou, H., Qi, K., Liu, X., Yin, H., Wang, P., Chen, J., et al. (2016). Genome-wide identification and comparative analysis of the cation proton antiporters family in pear and four other Rosaceae species. *Mol. Gen. Genomics.* 291, 1727–1742. doi: 10.1007/s00438-016-1215-y

Zhou, L. J., Zhang, C. L., Zhang, R. F., Wang, G. L., Li, Y. Y., and Hao, Y. J. (2019). The SUMO E3 ligase MdSIZ1 targets *MdbHLH104* to regulate plasma membrane H+-ATPase activity and iron homeostasis. *Plant Physiol.* 179, 88–106. doi: 10.1104/pp.18.00289

Conflict of Interest: The authors declare that the research was conducted in the absence of any commercial or financial relationships that could be construed as a potential conflict of interest.

Copyright © 2021 Bai, Shen and Huang. This is an open-access article distributed under the terms of the Creative Commons Attribution License (CC BY). The use, distribution or reproduction in other forums is permitted, provided the original author(s) and the copyright owner(s) are credited and that the original publication in this journal is cited, in accordance with accepted academic practice. No use, distribution or reproduction is permitted which does not comply with these terms.

frontiers in Plant Science

ORIGINAL RESEARCH
published: 16 April 2021
doi: 10.3389/fpls.2021.653168

New Aspects of Uptake and Metabolism of Non-organic and Organic Iodine Compounds—The Role of Vanadium and Plant-Derived Thyroid Hormone Analogs in Lettuce

Sylwester Smoleń[1†], Małgorzata Czernicka[1†], Iwona Kowalska[1†], Kinga Kęska[1†], Maria Halka[1†], Dariusz Grzebelus[1†], Marlena Grzanka[1†], Łukasz Skoczylas[2†], Joanna Pitala[3†], Aneta Koronowicz[4†] and Peter Kováčik[5†]*

[1] Department of Plant Biology and Biotechnology, Faculty of Biotechnology and Horticulture, University of Agriculture in Krakow, Kraków, Poland, [2] Department of Plant Product Technology and Nutrition Hygiene, Faculty of Food Technology, University of Agriculture in Krakow, Kraków, Poland, [3] Laboratory of Mass Spectrometry, Faculty of Biotechnology and Horticulture, University of Agriculture in Krakow, Kraków, Poland, [4] Department of Human Nutrition and Dietetics, Faculty of Food Technology, University of Agriculture in Krakow, Kraków, Poland, [5] Department of Agrochemistry and Plant Nutrition, Slovak University of Agriculture in Nitra, Nitra, Slovakia

The process of uptake and translocation of non-organic iodine (I) ions, I^- and IO_3^-, has been relatively well-described in literature. The situation is different for low-molecular-weight organic aromatic I compounds, as data on their uptake or metabolic pathway is only fragmentary. The aim of this study was to determine the process of uptake, transport, and metabolism of I applied to lettuce plants by fertigation as KIO_3, KIO_3 + salicylic acid (KIO_3+SA), and iodosalicylates, 5-iodosalicylic acid (5-ISA) and 3,5-diiodosalicylic acid (3,5-diISA), depending on whether additional fertilization with vanadium (V) was used. Each I compound was applied at a dose of 10 μM, SA at a dose of 10 μM, and V at a dose of 0.1 μM. Three independent 2-year-long experiments were carried out with lettuce; two with pot systems using a peat substrate and mineral soil and one with hydroponic lettuce. The effectiveness of I uptake and translocation from the roots to leaves was as follows: 5-ISA > 3,5-diISA > KIO_3. Iodosalicylates, 5-ISA and 3,5-diISA, were naturally synthesized in plants, similarly to other organic iodine metabolites, i.e., iodotyrosine, as well as plant-derived thyroid hormone analogs (PDTHA), triiodothyronine (T3) and thyroxine (T4). T3 and T4 were synthesized in roots with the participation of endogenous and exogenous 5-ISA and 3,5-diISA and then transported to leaves. The level of plant enrichment in I was safe for consumers. Several genes were shown to perform physiological functions, i.e., *per64-like*, *samdmt*, *msams5*, and *cipk6.*

Keywords: 5-iodosalicylic acid, 3,5-diiodosalicylic acid, vHPO, CBL-interacting serine/threonine-protein kinase 6, plant-derived thyroid hormone analogs

OPEN ACCESS

Edited by:
Francesco Di Gioia, Pennsylvania State University (PSU), United States

Reviewed by:
Luca Incrocci, University of Pisa, Italy
Rosario Paolo Mauro, University of Catania, Italy

***Correspondence:**
Sylwester Smoleń
sylwester.smolen@urk.edu.pl

†ORCID:
Sylwester Smoleń
orcid.org/0000-0001-8093-3801
Małgorzata Czernicka
orcid.org/0000-0001-5768-5758
Iwona Kowalska
orcid.org/0000-0002-0012-6143
Kinga Kęska
orcid.org/0000-0002-4329-1499
Maria Halka
orcid.org/0000-0002-3502-8930
Dariusz Grzebelus
orcid.org/0000-0001-6999-913X
Marlena Grzanka
orcid.org/0000-0002-3810-6906
Łukasz Skoczylas
orcid.org/0000-0002-8349-4477
Joanna Pitala
orcid.org/0000-0001-5906-4402
Aneta Koronowicz
orcid.org/0000-0002-1653-2867
Peter Kováčik
orcid.org/0000-0002-0185-3342

Specialty section:
This article was submitted to Plant Nutrition, a section of the journal Frontiers in Plant Science

Received: *13 January 2021*
Accepted: *19 March 2021*
Published: *16 April 2021*

INTRODUCTION

Iodine in Plants

Iodine (I) is a beneficial element for plants and studies have determine the effectiveness of iodide (I^-) or iodate (IO_3^-) uptake by plants through roots or leaves (upon foliar application) and their potential translocation (Medrano-Macías et al., 2016; Antonyak et al., 2018). The effectiveness of I ion accumulation has been determined for a number of species of plants. The majority of the studies have been performed in the context of I biofortification of plants. They were conducted with the aim to prepare an I deficiency prevention program, other than through the consumption of kitchen salt based on plant enrichment with I (White and Broadley, 2009). Among the papers published within the last 15 years, there has been research on species such as kohlrabi (Golob et al., 2020), strawberry (Budke et al., 2020), lettuce (Blasco et al., 2008; Dávila-Rangel et al., 2020), basil (Incrocci et al., 2019; Kiferle et al., 2019), green bean, lettuce (Dobosy et al., 2020), cabbage, cowpea (Ojok et al., 2019), broccoli raab, curly kale, mizuna, and red mustard (Gonnella et al., 2019). There was also research devoted to the I uptake mechanism (Kato et al., 2013; Humphrey et al., 2019).

Another subject of research was the impact of I on oxyreduction, e.g., in lettuce (Blasco et al., 2008; Dávila-Rangel et al., 2020), the process of photosynthesis in kohlrabi (Golob et al., 2020) and basil (Kiferle et al., 2019), nitrate (V) content in four *Brassica* genotypes (Gonnella et al., 2019), and changes in the content of macro- and microelements in green bean and lettuce (Dobosy et al., 2020). Furthermore, there was also research devoted to the efficacy of I^- and/or IO_3^- uptake by plants, depending on the additional application of other elements, such as selenium in kohlrabi (Golob et al., 2020), zinc, selenium, and iron in wheat (Zou et al., 2019), and zinc and selenium in wheat and rice (Cakmak et al., 2020). The impact of I on the induction of plant resistance to diseases was also analyzed (Ajiwe et al., 2019). There are also works focused on the process of methylation, i.e., volatilization to the atmosphere, of volatile I forms (Leblanc et al., 2006; Itoh et al., 2009).

There were also studies that tackled a unique subject of the plants' ability to take up I applied in the form of organic compounds, e.g., iodoacetate anion (Weng et al., 2008) or organic I complexes. For instance, Dávila-Rangel et al. (2020) showed that the application of the chitosan-I complex enhanced I uptake by lettuce. The ability of tomato plants to take up organic I compounds was also determined, in which I was bound with the aromatic ring (Halka et al., 2019). The conclusion for lettuce was that the effectiveness of I biofortification with 5-ISA was higher than upon application with KIO_3 (Smoleń et al., 2017). Smoleń et al. (2020) showed the enrichment of lettuce with I using KIO_3, 5-ISA, and 3,5-diISA; however, they did not study the molecular mechanisms associated with the process of uptake and metabolism of these three I compounds.

Previous literature on physiology and/or biochemistry of plants has not considered the issue of activity and function of plant-derived thyroid hormone analogs (PDTHA), which are compounds that contain I; hence, the scarcity of scientific data on the subject. Fowden (1959) demonstrated that radioactive I binds to I organic compounds, e.g., T3 in bean, barley, aster, and Salicornia plants. Lima et al. (2012) presented general information on the potential presence of PDTHA compounds in plants. Based on their model research, Pessoa et al. (2010) concluded that in *Arabidopsis thaliana* exogenous T4 may be bound by the transthyretin-like protein. Plants were observed to produce transthyretins, i.e., proteins that may potentially act as T3 and/or T4 transporters (Eneqvist et al., 2003). However, in the available literature, it is unclear whether T3/T4 receptors might be present in plants, and descriptions of the potential genes that might encode such proteins is lacking. Obtaining information on the issue seems crucial for the determination of functionality and mechanism of PDTHA activity in plants.

Vanadium vs. Iodine

Vanadium is classified as a beneficial element for plants (Welch and Huffman, 1973; Mengel and Kirkby, 1996) and is also beneficial for animals and humans (Anke et al., 2002). In the human body, V regulates the activity of a number of enzymes (WHO, 2001; Anke et al., 2002; Gruzewska et al., 2014). It also improves thyroid function (Afkhami et al., 2009). There is no recommended dietary allowance (RDA) established for humans (Trumbo et al., 2001). The official information on the effect of V on humans was issued by WHO (World Health Organization) several decades ago and only contains rough suggestions concerning V doses for humans (10 $\mu g\ V \cdot 24\ h^{-1}$).

A positive impact of V on the growth and development of plants was observed at low doses < 0.04 mg $V \cdot dm^{-3}$ in the nutrient solution (Kaplan et al., 1990; Pilbeam and Drihem, 2007). Such doses have been observed to have a synergistic effect on the uptake of selected macroelements by plants or to increase the foliar content of photosynthetically active pigments (Kaplan et al., 1990; Pilbeam and Drihem, 2007). Higher photosynthetic activity following V application results in the accumulation of sugars in sweetcorn (Sentíes-Herrera et al., 2018), leading to larger biomass growth in the aboveground parts of the plants (Basiouny, 1984).

In hydroponic systems, the availability of V for roots is higher than that in the soil. Therefore, the V tolerance/harmfulness for plants (Gil et al., 1995; Chongkid et al., 2007; Vachirapatama et al., 2011) is much lower than that in the soil (Zhang et al., 2012; Akoumianaki-Ioannidou et al., 2016; Imtiaz et al., 2018). Next to the dose, the plants' response to V also depends on I oxidation and is a generic property of plants (Kaplan et al., 1990; Gil et al., 1995; Vachirapatama et al., 2011). The low root absorbability of V is due to its poor mobility in the soil (Cappuyns and Swennen, 2014). The process of V sorption is related to the fact that VO_2^+ very easily reacts with humic acids in soil organic matter (SOM), making V not easily available to plants (Pilbeam and Drihem, 2007). Vanadium has not been commonly included in the process of preparing nutrient solutions for hydroponic systems (Jones, 2016). The conducted research made it possible to determine the plant's response to the interaction between the simultaneous fertilization of plants with I and V.

In marine algae, V functions in I uptake into cells. This functionality of V is attributed to its presence at the active

site of iodoperoxidase and other haloperoxidases (vHPO), i.e., V-dependent bromoperoxidase or chloroperoxidase (Leblanc et al., 2006). The structure, regulatory activity, and functionality of vHPO was described, owing to research on a number of marine alga species (Almeida et al., 2000; Colin et al., 2003; Kongkiattikajorn and Pongdam, 2006; Leblanc et al., 2006). Haloperoxidases (HPOs) are responsible for the oxidation of halogens that was conducted in the presence of H_2O_2 (Colin et al., 2005).

The process of cell I uptake by marine algae, catalyzed by vHPO, consisted of the oxidation of I^- to HIO, which was further transformed to molecular I_2. HIO and I_2 are produced within the cell wall. Being more lipophilic than I^-, they easily penetrate through the wall to the cytosol (Leblanc et al., 2006). Medrano-Macías et al. (2016) reported that there is likely a relationship between I and V in terrestrial plants. However, the function of vHPO in domesticated plants is not known. Smoleń et al. (2020) identified vHPO-like enzyme activity in lettuce and a relationship between its activity and I root uptake in the setting of trace I content in the rhizosphere. Thus far, no gene in the genome of lettuce has been assigned the function of vHPO.

The response of plants to I and V application on physiological and biochemical properties has not been diagnosed. The issue has been, to a limited extent, described in preliminary research by Smoleń et al. (2020). This situation is different for marine algae, as these plants actively take up I, accumulate it in their tissues, and carry out methylation (Leblanc et al., 2006; Keng et al., 2020). The methylation process (I volatilization) has also been described for selected terrestrial plant species (Attieh et al., 2000; Nagatoshi and Nakamura, 2007; Itoh et al., 2009). Among the studies conducted were biotechnological studies on deactivation of the process in *A. thaliana* (Landini et al., 2012). Iodovolatilization is carried out with the participation of vHPO. In contrast, the methylation of iodic hydrocarbons (CH_xI_x) is carried out with the participation of S-adenosyl-l-methionine (SAM)-dependent halide methyltransferase (HMT) or SAM-dependent halide/thiol methyltransferase (HTMT). These enzymes use iodide as a substrate (Medrano-Macías et al., 2016; Gonzali et al., 2017). No gene encoding HMT or HTMT has been identified in the genome of lettuce.

Salicylic Acid (SA) and SA-Derivatives vs. Iodine

A volatile ester of methyl salicylic acid (MeSA) can be volatilized in roots and leaves. MeSA is produced in the process of esterification of salicylic acid, during which CH_3 is joined to the SA carboxylic group (Taiz and Zeiger, 2010; Zhang et al., 2013). In tomatoes, MeSA is synthesized by an enzyme named salicylic acid carboxyl methyltransferase (SAMT) (Tieman et al., 2010). This volatile ester participates in SAR (systemic acquired resistance) in plants (Gao et al., 2014). SA is classified as a plant phytohormone (Gust and Nürnberger, 2012) or as a phytohormone-like compound (Hayat et al., 2010). Literature lacks information on whether endogenous and exogenous iodosalicylates, such as 5-ISA and 3,5-diISA, in plants may undergo further catabolic reactions. No enzymes related to the catabolism of 5-ISA and 3,5-diISA have been identified to date in plants. Additionally, there is no data indicating whether SAMT can participate in the methylation of 5-ISA, 3,5-diISA, or the SA produced as a result of the potential degradation of these iodosalicylates. Moreover, genes encoding proteins with a SAMT-like function in lettuce have not been found.

The aim of this study was to determine the process of uptake and metabolism of I applied to plants as KIO_3 and iodosalicylates. Additionally, the study aimed to determine the effect of V on these processes. Another objective was to document the selected molecular processes in the metabolism of non-organic and organic I compounds in roots and leaves of lettuce, considering aspects related to the synthesis of PDTHA.

A novelty in this study, when compared with previously published ones, was research on the plants' ability to take up non-organic and organic I compounds (iodosalicylates) through the roots, as well as whether and to what extent these compounds can be metabolized and transported within the plants' roots-leaves system. Additionally, selected genes were examined and assigned a potential putative role for encoding enzyme proteins demonstrating functions typical of vHPO, SAMT, and HMT/HTMT.

MATERIALS AND METHODS

Plant Material and Treatments

Lactuca sativa L. var. *capitata* cv. "Melodion" was planted in two pot studies and one hydroponic study. This research was performed within the camp of the University of Agriculture in Kraków (50°05′04.1″N 19°57′02.1″E).

A nutrient film technique (NFT) was used for the hydroponic system in a greenhouse setting. The hydroponic experiment was named Experiment 1 (**Table 1**). The pot studies were in turn conducted in a foil tunnel with the plants being farmed in 2 types of substrate, a peat substrate as organic soil (Experiment 2) and loam soil as an example of a heavy mineral soil (Experiment 3). Each of the 3 experiments was repeated twice in the spring season during 2 consecutive years of the study in 2018 and 2019.

The subject of this study was plant fertilization with I (**Table 1**), that is, with potassium iodate (KIO_3), 5-iodosalicylic acid (5-ISA), and 3,5-diiodosalicylic acid (3,5-diISA), as well as with ammonium metavanadate (V). An additional application of salicylic acid (SA) was also used to compare the effects of both iodosalicylic acids. The same configuration of the combinations tested was used in all 3 experiments: (1) Control; (2) SA; (3) KIO_3; (4) KIO_3+SA; (5) 5-ISA; (6) 3,5-diISA; (7) KIO_3 + V; (8) KIO_3 + SA + V; (9) 5-ISA + V; and (10) 3,5-diISA + V. In each experiment, application started at the rosette stage (5–6 true leaves). The following concentrations were used: 10 μM for all I compounds (molar mass equivalents), 10 μM for SA, and 0.1 μM for V. The experiments differed in the frequency of application. In hydroponic systems, the nutrient solution (containing the compounds tested) was applied continually (fixed concentration). A different application strategy was used in the pot systems. The I and V compounds and SA were applied to the soil once a week through manual fertigation (manual

watering with solutions of the compounds studied, at a dose of 100 mL·pot^{-1} (one plant^{-1}). In total, in Experiments 2 and 3, plants were fertilized with I, V, and SA 8 times. This research strategy was planned purposefully. Our aim was to avoid the risk of accumulation of I concentrations that would be toxic to plants in either the peat substrate or mineral soil. When designing the study, we had no information on whether or to what extent iodosalicylates applied to the soil would be taken up by the plants. Additionally, the aim was to measure the effectiveness of biofortification of lettuce using different I compounds with or without V, depending on the method of cultivation and substrate.

In a hydroponic system, it was possible to obtain the entire root system for chemical analyses without damaging it, among other things. This allowed model research on the uptake and transport of different forms of I in the roots-leaves system. In the pot system, it was impossible to isolate roots from the soil because the root system outgrew the volume of soil in the pots. Therefore, in Experiments 2 and 3, roots were not subjected to chemical analyses.

In each year of the study, seeds were sown in early March (13 March 2018 and 4 March 2019). They were sown in multi-pallets filled with substrate, that is, with peat substrate and sand 1:1 (V/V). The multi-pallets had 112 cells (14 rows × 8 cells), each sized 3.2 × 3.2 × 4 cm. Young plants in the phase of 4–5 true leaves were replanted to the NFT hydroponic system (in Experiment 1) or to pots (in Experiments 2 and 3; 10 April 2018 and 2 April 2019). The plants were potted together with the entire root ball in either peat substrate or heavy mineral soil. The volume of substrate in pots was 1.5 dm^3. The chemical properties of the peat substrate and heavy mineral soil before cultivation are presented in **Table 2**; a detailed description of methods used for chemical analysis of soil is reported in the **Supplementary Material**. No fertilization was performed before or during lettuce cultivation in either of the two pot experiments. This was because the nutrient content, pH, and EC (electrical conductivity) were optimal for growing this species in the peat substrate or heavy mineral soil I (Sady, 2000; **Table 2**).

In the NFT hydroponic system, target replanting was preceded by thorough rinsing of the substrate between the seedlings'

TABLE 1 | Design and method of conducting experiments with lettuce cultivation in the hydroponics NFT Experiment No. 1 as well as in pot experiments: Experiment Nos. 2 and 3.

Treatments	Hydroponics NFT Experiment No. 1					
	Dose of I compounds and dose of I	Dose of V as ammonium metavanadate	Dose of SA	I, V, and/or SA application from the rosette phase	Amount of I applied for one plant (μ mol I·plant^{-1})	Amount of V applied for one plant (μ mol V·plant^{-1})
Control	–*	–*	–	–	13.2	0.09
SA	–*	–*	10 μM	Permanent	13.2	0.09
KIO_3	10 μM (10 μM I)	–	–	Permanent	100	0.09
KIO_3+SA	10 μM (10 μM I)	–	10 μM	Permanent	100	0.09
5-ISA	10 μM (10 μM I)	–	–	Permanent	100	0.09
3,5-diISA	10 μM (20 μM I)	–	–	Permanent	200	0.09
KIO_3+V	10 μM (10 μM I)	0.1 μM V	–	Permanent	100	0.98
KIO_3+SA+V	10 μM (10 μM I)	0.1 μM V	10 μM	Permanent	100	0.98
5-ISA+V	10 μM (10 μM I)	0.1 μM V	–	Permanent	100	0.98
3,5-diISA+V	10 μM (20 μM I)	0.1 μM V	–	Permanent	200	0.98
	Pot experiments: Peat substrate Experiment No. 2 and mineral soil Experiment No. 3					
Control	–**	–**	–	–	–****	–****
SA	–**	–**	10 μM	8 times***	–****	–****
KIO_3	10 μM (10 μM I)	–	–	8 times***	2.67	–****
KIO_3+SA	10 μM (10 μM I)	–	10 μM	8 times***	2.67	–****
5-ISA	10 μM (10 μM I)	–	–	8 times***	2.67	–****
3,5-diISA	10 μM (20 μM I)	–	–	8 times***	5.34	–****
KIO_3+V	10 μM (10 μM I)	0.1 μM V	–	8 times***	2.67	0.027
KIO_3+SA+V	10 μM (10 μM I)	0.1 μM V	10 μM	8 times***	2.67	0.027
5-ISA+V	10 μM (10 μM I)	0.1 μM V	–	8 times***	2.67	0.027
3,5-diISA+V	10 μM (20 μM I)	0.1 μM V	–	8 times***	5.34	0.027

Trace concentration of I and V in nutrient solution: **0.0204 μM I and **0.009 μM V** of nutrient solution (I and V from tap water and fertilizers).*

***Without I and V fertilization—the natural content of I and V in peat substrate and mineral soil prior to the Experiments No 2 and 3 was presented in **Table 2**.*

****8 times every 7 days.*

*****The determined I and V content (in TMAH and metricconverterProductID1 M1 M HCl extracts, respectively see **Table 2**) do not allow estimating the amount of available I and V for plants in the soil solution of peat substrate (organic soil) and mineral soil. It is also not possible to accurately estimate the changes in the content of I and V in the soil solution during the whole period of lettuce cultivation using other methods of soil extraction.*

roots with tap water. Seedlings were placed in the openings (spaced 25 cm apart) in Styrofoam slabs filling the NFT beds. No substrate was used in slabs. Once planted, seedlings in the NFT system were watered during the day. Each experiment consisted of four replicates in a randomized block design. In hydroponic Experiment 1, there were 15 plants per replicate and 60 plants per combination (600 plants per experiment). In pot Experiments 2 and 3, there were 7 plants per replicate and 28 plants per combination (a total of 560 plants in both pot experiments).

The type of nutrient solution, its preparation (content of macro- and microelements), regulation of pH and EC, and type of fertilizers in the NFT were the same as in our previous studies with lettuce in the same hydroponic system (Smoleń et al., 2019b). The I used in the base nutrient solutions (control) was iodide I^- (25.52 μg $I \cdot dm^{-3}$) and iodate IO_3^- (0.29 μg $I \cdot dm^{-3}$). The content of I was natural (from water and dissolved fertilizers).

Once planted in spacers in the NFT systems, the plants were watered during the day between 5 am and 7 pm and at night between 1 and 2 am, for 1 min at 5-min intervals. In pot experiments, the plants were watered with tap water using drip irrigation. A single dose of water was about 100 $mL \cdot plant^{-1}$ (pot^{-1}). The frequency of watering was adjusted to weather conditions and sizes of the plants; factors that determined the rate of substrate drying involved controlling watering by the irrigation computer with the option to sum the amount of solar radiation to start irrigation. The adopted watering strategy made it possible to eliminate water leaching from pots. On the days when the compound solutions were applied to the substrate in pot Experiments 2 and 3, the plants were not watered through the drip system.

Plants were harvested at the phase of head development, that is on 15 May 2018 and 7 May 2019 in hydroponic Experiment 1, and on 9 May 2018 and 16 May 2019 in pot Experiments 2 and 3. Then, the heads (lettuce leaves) were weighed. Hydroponic Experiment 1 was the only experiment where lettuce leaf harvesting was immediately followed by pipette collection of a secretion produced as a result of root pressure [white secretion (RootSec) on the surface of the root neck, visible after cutting the heads at collar level (lettuce leaves), as shown in **Supplementary Figure 1**]. The secretion was collected for the determination of the chemical forms of I, transported from roots to the aboveground parts of plants. A total of two samples were collected for each combination, each containing 5 mL of root secretion. Immediately after collection, the secretion was 1:1 mixed with buffer (20 mM Tris HCl buffer, pH 8.5). Then, the samples were frozen at −20°C and stored until analyzed using two mass spectrometry techniques. Iodides (I^-) and iodates (IO_3^-) were analyzed using high-performance liquid chromatography with inductively coupled plasma mass spectrometry (HPLC-ICP-MS)/MS, while organic I compounds were analyzed using liquid chromatography-mass spectrometry (LC-MS)/MS. Methodologic details are presented in the following subsections.

In Experiment 1, the collection of root secretions was followed by the measurement of lettuce root biomass, while in pot Experiments 2 and 3 these measurements were abandoned, as the root biomass could not be separated from the soil without damaging the roots. Chemical analyses were performed on roots of all plants from the hydroponic system, and on four randomly selected heads from each biological replicate in all three experiments.

TABLE 2 | Selected chemical properties of the soil prior to the Experiments Nos. 2 and 3.

Physicochemical soil characteristic	Peat substrate—Experiment 2	Mineral soil—Experiment 3
pH_{H_2O}	5.50	6.70
$pH_{(KCl)}$	5.33	6.28
EC ($mS \cdot cm^{-1}$)	1.18	1.46
Eh(mV)	270.1	221.6
Macroelements:		
$N\text{-}NH_4$ ($mg \cdot dm^{-3}$)	158.7	68.2
$N\text{-}NO_3$ ($mg \cdot dm^{-3}$)	103.1	205.9
$N\text{-}NH_4$+ $N\text{-}NO_3$ ($mg \cdot dm^{-3}$)	261.8	274.1
P ($mg \cdot dm^{-3}$)	125.1	94.5
K ($mg \cdot dm^{-3}$)	316.8	122.2
Mg ($mg \cdot dm^{-3}$)	180.0	175.4
Ca ($mg \cdot dm^{-3}$)	2 046.2	1 686.8
S ($mg \cdot dm^{-3}$)	227.8	287.4
Na ($mg \cdot dm^{-3}$)	20.6	55.9
Iodine ($mg\ I \cdot kg^{-1}$)	6.25	5.56
Vanadium ($mg\ V \cdot kg^{-1}$)	0.84	6.57
Al-hydroxides ($mg \cdot kg^{-1}$)	145.8	400.53
Fe-hydroxides ($mg \cdot kg^{-1}$)	624.3	5 118.0
Mn-hydroxides ($mg \cdot kg^{-1}$)	15.4	433.7
BeA ($mg \cdot kg^{-1}$)	1.768	0.864
SA ($mg \cdot kg^{-1}$)	0.156	0.034
5-ISA ($mg \cdot kg^{-1}$)	0.0125	0.0036
3,5-diISA ($mg \cdot kg^{-1}$)	0.008	0.008
2-IBeA ($mg \cdot kg^{-1}$)	0.028	0.013
4-IBeA ($mg \cdot kg^{-1}$)	0.001	0.002
2,3,5-triIBeA ($mg \cdot kg^{-1}$)	0.013	0.026
Exchange hydrolytic acidity ($me \cdot 100\ g^{-1}$)	0.99	22.13
Cation exchange capacity ($me \cdot 100\ g^{-1}$)	21.03	47.62
Total soil sorption capacity ($me \cdot 100\ g^{-1}$)	22.02	69.74
Soil organic matter (%)	100	1.92
Soil texture (according to the ISSS classification).	Peat soil (organic soil)	Loam soil 35 sand 28 % silt 37% clay

Where: benzoic acid (BeA), salicylic acid (SA), 5-iodosalicylic acid (5-ISA), 3,5-diiodosalicylic acid (3,5-diISA), 2-iodobenzoic acid (2-IBeA), 4-iodobenzoic acid (4-IBeA), 2,3,5-triiodobenzoic acid (2,3,5-triIBeA).

Activity of Vanadium-Dependent Haloperoxidases

Fresh leaf samples collected in all three experiments and root samples from Experiment 1 were used to measure the

total activity of vHPO enzymes. The analysis was performed with a method adapted for lettuce by Smoleń et al. (2020) based on that for marine algae. The activity of vHPO was calculated based on the increase in absorbance within 20 min (wavelength: 620 nm) and converted into $U \cdot mg^{-1} \cdot min^{-1}$ protein. Protein content in enzyme extracts was measured using the Lowry method (Waterborg, 2002). Bovine serum albumin was used as a standard.

Freeze-Drying of Samples

Fresh root and leaf samples (lettuce) were washed in tap and distilled water. Samples of lettuce heads were vacuum-dried. Each head was halved (leaves were peeled in each growth phase) and mixed thoroughly as part of each replicate. Root and leaf samples were frozen at −20°C. The freeze-drying of frozen samples was performed with the Christ Alpha 1–4 unit (Martin Christ Gefriertrocknungsanlagen GmbH, Germany). Vacuum-dried samples of roots and leaves were ground in a lab mill (FRITSCH Pulverisette 14; FRITSCH GmbH, Weimar, Germany) and stored in sealed polyethylene bags until further chemical analyses (described in the next three sections).

Analysis of Total Iodine and Vanadium in Dry Samples of Roots and Leaves

The analysis of I content in samples of lettuce leaves and roots was performed by inductively coupled plasma mass spectrometry (ICP-MS/MS) with a triple quadruple spectrometer (iCAP TQ ICP-MS Thermo Fisher Scientific, Bremen, Germany), preceded by alkaline extraction of 0.2 g samples by tetramethylammonium hydroxide (TMAH; Smoleń et al., 2019a,c; based on Pn-En 15111, 2008).

Vanadium content in leaf and root samples was measured using inductively coupled plasma optical emission spectrometry (ICP-OES) (Prodigy Spectrometer, Leeman Labs, New Hampshire, MA, United States). The mineralization and measurement procedures were consistent with the method described by Smoleń et al. (2020).

The results of I and V content in the plant samples and biomass measurements were used to calculate I uptake (I-uptake) and V uptake (V-uptake) by plants.

Analysis of Iodides (I^-) and Iodates (IO_3^-) in Roots and Leaves by HPLC-ICP-MS/MS

The content of iodides (I^-) and iodates (IO_3^-) was only determined in root and leaf samples of hydroponic lettuce (Experiment 1); in pot experiments, there was no possibility to collect root samples for analysis. The content of these I ions was measured using a modified extraction procedure described by Smoleń et al. (2016). Briefly, a 0.05 g analytic portion of air-dried, ground plant samples was extracted (in 7 mL polypropylene tubes) using a solution containing 4 mL 25% TMAH (Sigma-Aldrich, St. Louis, MO, United States) and 10 mL 0.1 M NaOH (Chempur, Piekary Śląskie, Poland) dissolved to a final volume of 1 L with demineralized water. Once mixed, the samples were incubated for 1 h at 50°C in an ultrasonic bath, then cooled to approximately 20°C, mixed thoroughly, and centrifuged for 15 min at 4,500 rpm. The supernatants were filtered through a 0.22 μm syringe filter. The content of I ions in filtered samples was analyzed using HPLC-ICP-MS/MS. For I^- and IO_3^- speciation forms, HPLC (Thermo Scientific Ultimate 3000; Thermo Fisher Scientific, Bremen, Germany) was coupled to ICP-MS/MS (iCAP TQ). This method employed a strong anion exchange column [Thermo Fisher Scientific; Dionex IonPac AS11 (4 × 250 mm)] and a precolumn [Thermo Fisher Scientific; Dionex IonPac AG11 (4 × 50 mm)]. The column temperature was set to 30°C. Demineralized water, 50 mM NaOH, and 0.5% TMAH were used as eluents. To separate both I ions, a mobile phase, containing 2.5 mM NaOH and 0.125% TMAH at an isocratic flow, was used. The flow-rate was 1.5 mL/min, with an injection volume of 10 μL and total analysis time of 7 min (**Supplementary Figures 2**, **3**). The HPLC-column effluent was introduced directly into ICP-MS/MS (iCAP TQ ICP-MS). Iodine was determined at 127I.16O isotope, using S-TQ-O2 mode. Standards were prepared through dissolution of KI and KIO_3 (Sigma-Aldrich, St. Louis, MO, United States) in demineralized water.

To ensure correct iodide and I measurements, a "standard addition method" was used; it was applied independently for each leaf and root sample from each of the 10 combinations (**Supplementary Figures 4–6**). The standard addition method has been applied because that the alternative and easier "standard series method," which is described in numerous publications, would not provide correct analytical results. The difficulty to obtain reliable assaying results with the standard series method was due to the different matrix effects of root and leaf extracts obtained from each of the 10 combinations tested in Experiment 1. The effect could be eliminated through the use of the standard addition method, which allowed us to obtain correct analytic results.

Determination of Salicylic Acid, Benzoic Acid, Iodosalicylates, Iodobenzoates, and Plant-Derived Thyroid Hormone Analogs

Roots of plants from the hydroponic system (Experiment 1) and lettuce leaves in all three experiments were tested using LC-MS/MS to measure the content of SA, BeA (benzoic acid), 5-ISA, 3,5-diISA, 2-iodobenzoic acid (2-IBeA), 4-iodobenzoic acid (4-IBeA), 2,3,5-triiodobenzoic acid (2,3,5-triIBeA), iodotyrosine (I-Tyr), sodium salt triiodothyronine (T3-Na), triiodothyronine (T3), and thyroxine (T4) (**Supplementary Figure 7**). The root and leaf content of these compounds was analyzed in extracts prepared with 75% ethanol containing 50 $ng \cdot mL^{-1}$ of deuterated salicylic acid (SA-d4, Sigma-Aldrich). Sample extraction and filtration procedures were the same as described in our previous research (Smoleń et al., 2020).

The compounds were also measured in **RootSec** after lettuce harvesting. The **RootSec** were mixed with 20 mM Tris HCl buffer (pH 8.5). The collection and storage of **RootSec** is described in section "Plant Material and Treatments."

Root secretions stored in the TRIS-HCl buffer were mixed in vortex prior to analysis and centrifuged at 5°C for 15 min at 4,500 rpm. Then, the supernatant was filtered with a 0.22 μm nylon syringe filters (FilterBio NY Syringe Filter, Phenomenex, Torrance, CA, United States) and analyzed using LC-MS/MS according to Smoleń et al. (2020).

Biofortification Target and the Safety of Iodine-Enriched Lettuce Consumers

The results of I measurements in lettuce leaves were used in each of the experiments to calculate the following coefficients: (1) recommended daily allowance of iodine (% RDA-I) and (2) hazard quotient for iodine (HQ-iodine). They were calculated for 100 g of fresh lettuce leaves, considering the daily I requirement of adults of 150 μg. The % RDA-I and HQ-iodine coefficients were calculated using mathematical formulas described in detail by Smoleń et al. (2019a).

Gene Expression Analysis

Plants cultivated in the hydroponic NFT system (Experiment 1) were used as material for gene expression analysis. Leaves and roots for RNA extraction were collected directly before harvest. The leaf and root samples were collected from 8 plants (2 plants from each of the 4 replications), separately for each of the 10 treatments. The third youngest leaf and root samples (portions of 5–10 cm, with tips) were collected for each plant. The samples were immediately frozen in liquid nitrogen and stored at −80°C until isolation of RNA. Total RNA extraction was carried out with a Direct-zol^{TM} RNA MiniPrep Plus RNA isolation kit (Zymo Research, Irvine, CA, United States), according to the manufacturer's instructions. RNA samples were treated with 1 U μl^{-1} RNase-free Dnase I (Ambion Inc., Austin, TX, United States) and 40 U μl^{-1} RiboLock RNase Inhibitor (Thermo Fisher Scientific, Wilmington, DE, United States) to avoid contamination by DNA and RNA degradation. The quality and integrity of RNA samples were verified by electrophoresis in 1% agarose gel in denaturing conditions. The concentration and quality of RNA were evaluated spectrophotometrically using NanoDrop 2000c (Thermo Fisher Scientific, Wilmington, DE, United States) at 230, 260, and 280 nm. cDNA synthesis was conducted in four biological replicates, each comprising two plants. One microgram of RNA from each sample was transcribed into cDNA using the iScript cDNA synthesis kit (BioRad laboratories, Hemel Hempstead, United Kingdom), according to the manufacturer's instructions. The cDNA was frozen at −20°C until it was used as a template in real-time qPCR using the StepOnePlus^{TM} Real-Time PCR System (Applied Biosystems, Foster City, CA, United States), according to the following steps: denaturation at 95°C for 10 min; 40 cycles at 95°C for 15 s, 60°C for 30 s, and 72°C for 30 s. The melting curves were obtained by melting the amplicons from 60 to 95°C for 15 s; the temperature was increased by 0.3°C per cycle.

For expression analysis, five genes possibly related to selected metabolic pathways for I and/or iodosalicylates in lettuce, i.e., *per12-like*, *per-64-like*, *samdmt*, *cipk6,* and *msams5*, were chosen (**Supplementary Table 1**). Moreover, differential expression patterns of those genes were shown by RNA-seq in leaves and roots of *L. sativa* "Melodion" of control plants and supplemented with SA, KIO_3 and KIO_3+V (data unpublished). Gene-specific primers for real-time qPCR were designed using Primer3Plus[1] based on *L. sativa* var. *capitata* "Melodion" transcript sequences *de novo* assembled from RNAseq, deposited in the NCBI GeneBank (Acc. No MT649253, MT649254, MT663549-MT663551) and Lettuce Genome Resource[2] (**Supplementary Table 1**).

The absence of primer-dimer and hairpin structures was determined using IDT-OligoAnalyzer 3.1[3]. The utility of the designed primers was validated in a reverse-transcriptase polymerase chain reaction (RT-PCR) and confirmed by electrophoresis in 1% agarose gel (**Supplementary Figure 8**). Primer specificity was verified by observing single peaks in all melting curves. The total volume of the reaction mixture was 25 μL. The mixture included 12.5 μL Maxima SYBR Green/ROX qPCR Master Mix (2X) (Thermo Fisher Scientific), 0.7 μM of (5 μM) each primer (forward and reverse), 2 μL of a 5-fold diluted template cDNA, and a total volume of 25 μL made up with nuclease-free DEPC-treated water (diethylpyrocarbonate; Thermo Fisher Scientific, Wilmington, DE, United States). qPCR reactions were conducted in four biological and three technical replicates. No template controls were included. Amplification efficiencies for all primer pairs were evaluated using serial 10-fold dilutions of pooled cDNA. The efficiency of each primer pair was calculated from the slope of the standard curve using the formula $E = 10^{-1/slope}$ and converted into percentage values according to the following formula: $\%E = (E - 1) \times 100\%$.

Actin (*act*) (Smoleń et al., 2016) and protein phosphatase 2A regulatory subunit A3 (*pp2aa3*) (Sgamma et al., 2016) were used as endogenous reference genes. As *Pp2aa3* expression was more stable than that of *act* (**Supplementary Figure 9**), relative quantification of gene expression was calculated using the $2^{-\Delta\ \Delta\ C(T)}$ method (Livak and Schmittgen, 2001) with Ct value normalization to *pp2aa3*. In the case of *per64-like*, *per12-like*, *cipk6*, and *msams5*, the relative gene expression was compared with control samples from roots, whereas in *samdmt*, it was compared to control samples from leaves, since expression of *samdmt* in root control samples was not detectable (**Supplementary Figure 8**).

Statistical Analyses

All data were statistically verified using one-way analysis of variance (ANOVA) in the Statistica 12.0 PL (StatSoft Inc., Tulsa, OK 74104, United States)[4] program at a significance level of $p < 0.05$. In the case of significant effects, homogenous groups were distinguished on the basis of a *post-hoc* Tukey HSD test. The results obtained were verified statistically by one-way ANOVA and *post-hoc* Tukey HSD test, separately for each of the three experiments and separately for leaves and roots of lettuce in Experiment 1.

[1]https://primer3plus.com/cgi-bin/dev/primer3plus.cgi
[2]https://lgr.genomecenter.ucdavis.edu
[3]https://eu.idtdna.com/calc/analyzer
[4]https://www.tibco.com/products/data-science

RESULTS

Plant Biomass

Hydroponic Experiment 1 was the only experiment where the application of 5-ISA and 3,5-diISA (without or with V) caused a reduction in the weight of leaves and whole plants (roots + leaves) compared with the control (**Table 3**). No negative impact of 3,5-diISA and 3,5-diISA+V on the weight of roots was observed. A comparable increase in root weight was observed for the application of 5-ISA and 5-ISA+V, compared with the control. In this experiment, combined fertilization with V and KIO_3, KIO_3+SA, 5-ISA, and 3,5-diISA had no effect on the weight of roots and heads (leaves) of lettuce, compared with the application of these compounds without V.

None of the combinations of SA, V, and I compounds had a significant impact on the weight of lettuce heads in either of the two pot experiments (Experiments 2 and 3).

Gene Expression in Roots and Leaves of Plants Cultivated in a Hydroponic System (Experiment 1)

I compounds, V, and SA applied to the nutrient solution had a statistically significant impact on the expression of the following genes in lettuce roots and leaves: *per64-like*, *per12-like*, *samdmt*, *cipk6*, and *msams5* (**Figures 1A–E**). Basically, the expression of *per64-like* in leaves and *samdmt* in roots was relatively very low compared with roots and leaves, respectively. As for the remaining three genes (*per12-like*, *cipk6*, and *msams5*), their expression in roots was higher than in leaves.

Compared with the control, all combinations with the application of I, I+SA, and V, caused increased expression of all five genes, i.e., *per64-like*, *per12-like*, *samdmt*, *cipk6*, and *msams5*, in roots (**Figures 1A–E**). The highest expression level of *per64-like* in roots was observed after application of KIO_3+SA and 5-ISA. Additionally, exogenous 5-ISA in roots caused the highest expression of *cipk6* and *msams5;* application of 3,5-diISA led to the most pronounced expression of *per12-like*, while plants fertilized with KIO_3 had the highest expression of *samdmt.* Foliar activity of these five genes in lettuce was completely different that in roots compared with the control. The highest foliar expression of individual genes was as follows: *per64-like* following the application of exogenous 3,5-diISA, *per12-like* following the application of 5-ISA+V, *samdmt* following the application of SA, *cipk6* following the application of exogenous 5-ISA, and *msams5* following the application of KIO_3.

Iodine Accumulation and Uptake by Lettuce

Inorganic (IO_3^-) and organic (5-ISA, 3,5-diISA) I accumulated in larger amounts in roots than in leaves (**Figures 2A,B**; hydroponic Experiment 1). Root accumulation of I upon the application of both iodosalicylates was higher than upon using KIO_3 as a fertilizer. Vanadium added to the nutrient solution caused a significant reduction of I content in roots for the combination of KIO_3+SA+V vs. KIO_3+SA. Additionally, V caused a significant increase in I content in roots for the combination 5-ISA+V vs. 5-ISA, and for 3,5-diISA+V vs. 3,5-diISA (**Figure 2B**).

Compared with the control and SA, application of each I compound (without V, with V, and with KIO_3+SA) caused a significant increase in foliar I content (**Figures 2A,C**), RDA-I%, and HQ-iodine, as well as I uptake by a single lettuce head (leaves from one plant) in all three Experiments (**Supplementary Table 2**).

The highest foliar I content, RDA-I%, and HQ-iodine, as well as I uptake by a single lettuce head, was found in plants with applied 5-ISA in all three experiments (**Figures 2A,C** and **Supplementary Table 2**). Adding V to the compound (5-ISA+V vs. 5-ISA) reduced foliar I content in both pot experiments (Experiments 2 and 3) but not in the hydroponic system (Experiment 1). Consequently, RDA-I%, HQ-iodine, and I uptake by

TABLE 3 | Fresh weight of roots, leaves /lettuce head/ and whole plants /roots+leaves/ in hydroponic NFT Experiment No. 1 as well as in lettuce leaves /head/ in pot Experiment Nos. 2 and 3.

Treatments	Hydroponics NFT Experiment No. 1			Peat substrate Experiment No. 2	Mineral soil Experiment No. 3
	FW of leaves/lettuce head/(g)	FW of roots from one plant (g)	FW of whole plants /roots+leaves/(g)	FW of leaves/lettuce head/(g)	FW of leaves/lettuce head/(g)
Control	291.4 ± 35.2b	31.7 ± 4.5a	323.1 ± 39.6b	174.1 ± 12.2a	186.6 ± 22.8a
SA	291.3 ± 29.5b	33.1 ± 3.7ab	324.4 ± 33.2b	169.3 ± 14.4a	168.5 ± 16.1a
KIO_3	296.8 ± 34.1b	34.6 ± 3.8ab	331.4 ± 37.7b	169.8 ± 12.2a	180.5 ± 23.1a
KIO_3+SA	276.5 ± 42.2b	32.6 ± 3.8ab	309.1 ± 45.9b	161.3 ± 14.3a	176.9 ± 23.6a
5-ISA	171.1 ± 35.7a	39.4 ± 6.1bc	210.5 ± 41.8a	167.7 ± 10.5a	194.7 ± 18.5a
3,5-diISA	147.7 ± 37.8a	30.1 ± 5.2a	177.8 ± 42.9a	171.9 ± 13.9a	185.5 ± 20.3a
KIO_3+V	305.9 ± 33.0b	35.2 ± 3.2ab	341.1 ± 36.1b	167.9 ± 10.7a	186.5 ± 19.4a
KIO_3+SA+V	305.6 ± 28.0b	33.1 ± 4.1ab	338.7 ± 32.0b	163.7 ± 13.3a	171.7 ± 21.9a
5-ISA+V	160.7 ± 35.8a	42.9 ± 5.8c	203.6 ± 41.4a	173.7 ± 9.8a	172.5 ± 18.8a
3,5-diISA+V	152.0 ± 41.1a	33.1 ± 6.3ab	185.1 ± 47.3a	168.3 ± 10.5a	180.2 ± 21.6a

Means in the column followed by different letters separately for each experiments differ significantly at $P < 0.05$ (n = 8).

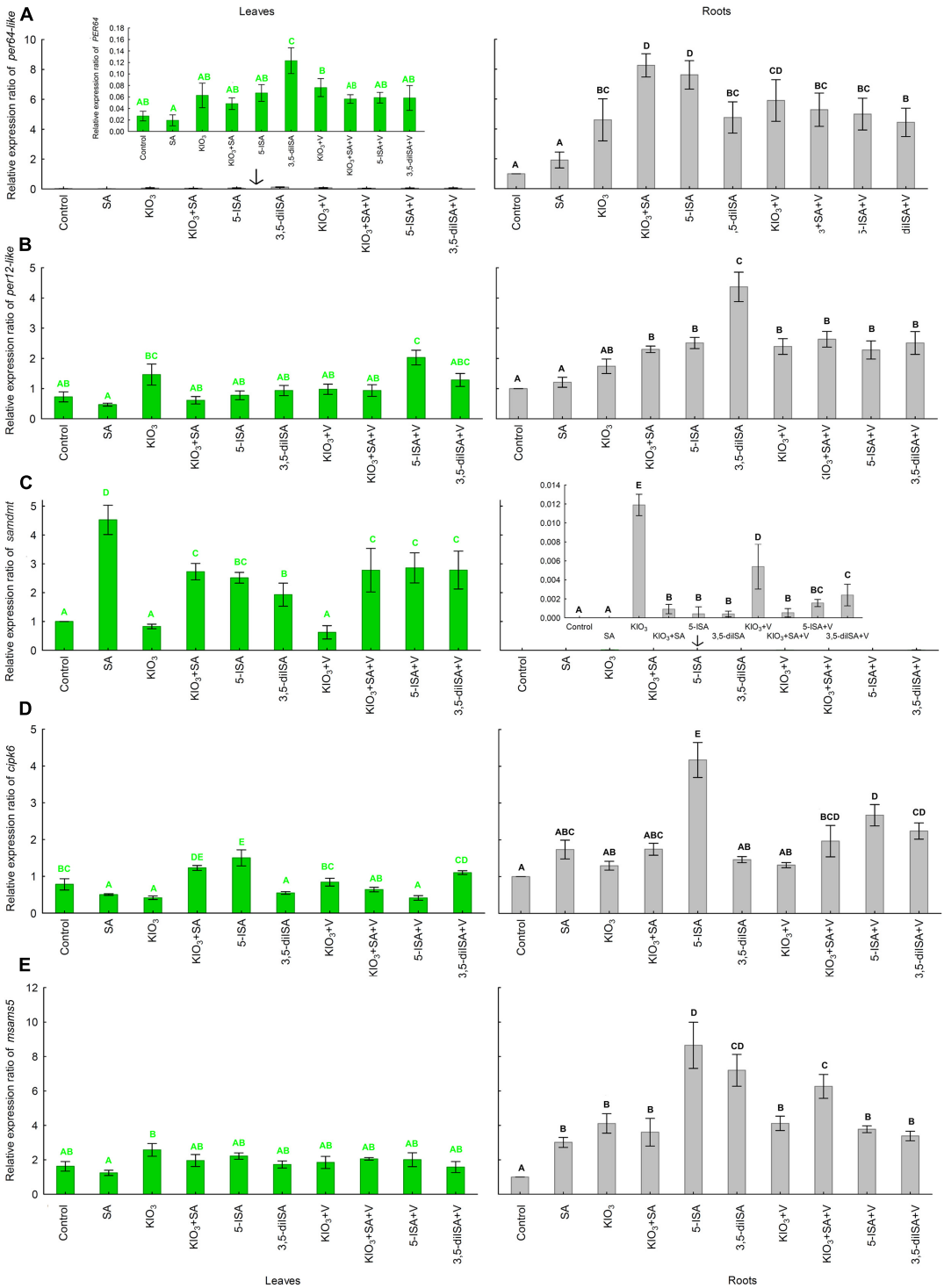


FIGURE 1 | Relative expression of *per64-like* **(A)**, *per12-like* **(B)**, *samdmt* **(C)**, *cipk6* **(D)**, and *msams5* **(E)** genes in leaves and roots of lettuce plants cultivated in hydroponic NFT Experiment No. 1. Means followed by different letters for treatments differ significantly at $P < 0.05$. Bars indicate standard error ($n = 4$).

a single lettuce head was significantly lowered for 5-ISA+V vs. 5-ISA in both pot experiments (**Supplementary Tables 2**, **3**).

Combined fertilization with KIO_3+V had no impact on leaf I content in any of the three experiments, compared with KIO_3 without V. As for the application of 3,5-diISA+V (compared with

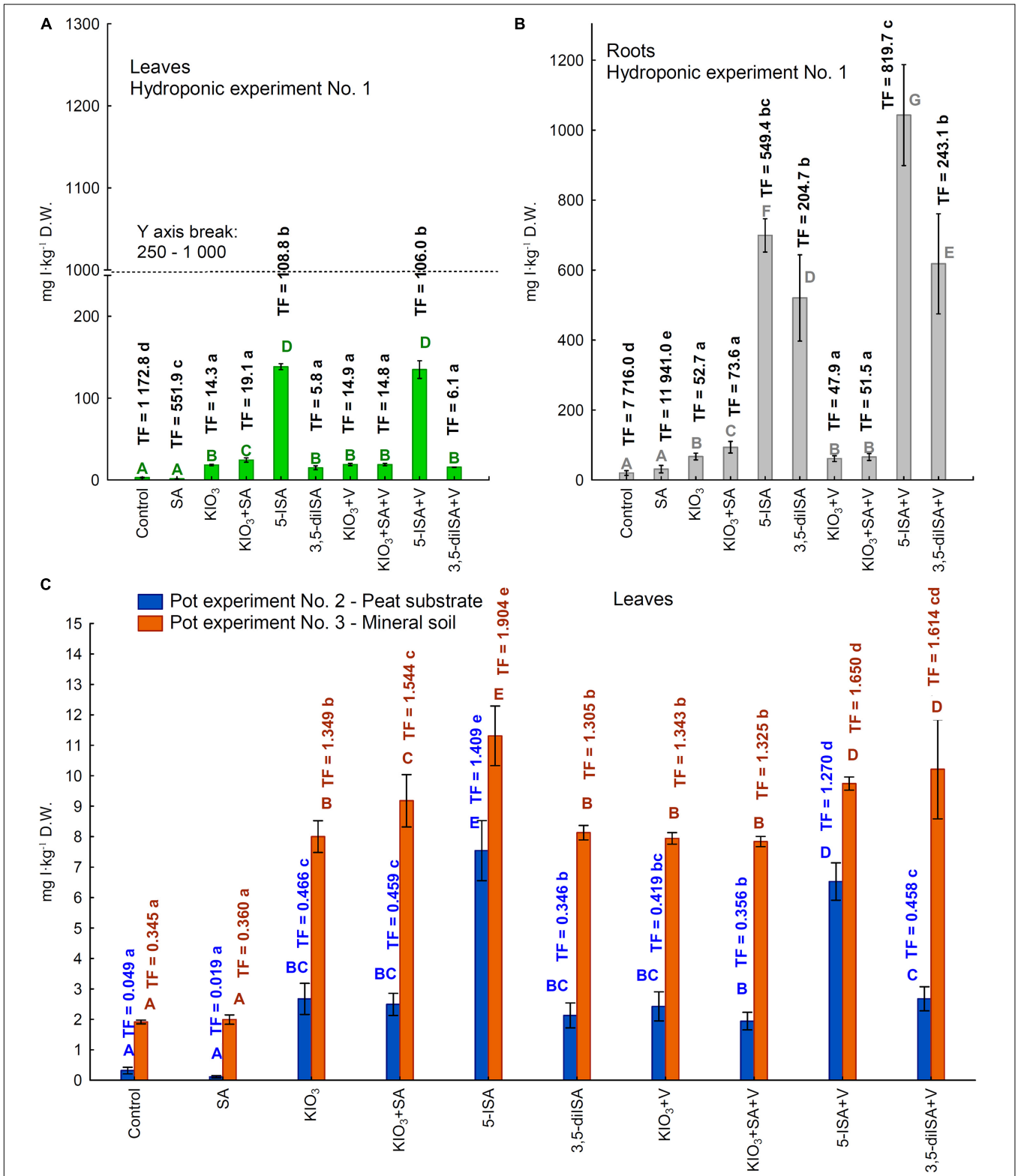


FIGURE 2 | Concentrations of iodine in leaves /heads/ **(A)** and roots of lettuce **(B)** cultivated in hydroponic NFT Experiment No. 1 as well as in leaves of plants cultivated in pot Experiment No. 2 and 3 **(C)**. Transfer factor /TF/ of iodine to roots and leaves /heads/ in the all experiments. Means followed by different letters for treatments, separately for each experiments differ significantly at $P < 0.05$. Color-coded capital letters for iodine content (green and gray for leaves and roots in Experiment 1 and blue and orange for leaves in Experiments 2 and 3); lowercase letters in the same colors for the TF factor in these experiments. Bars indicate standard error ($n = 8$).

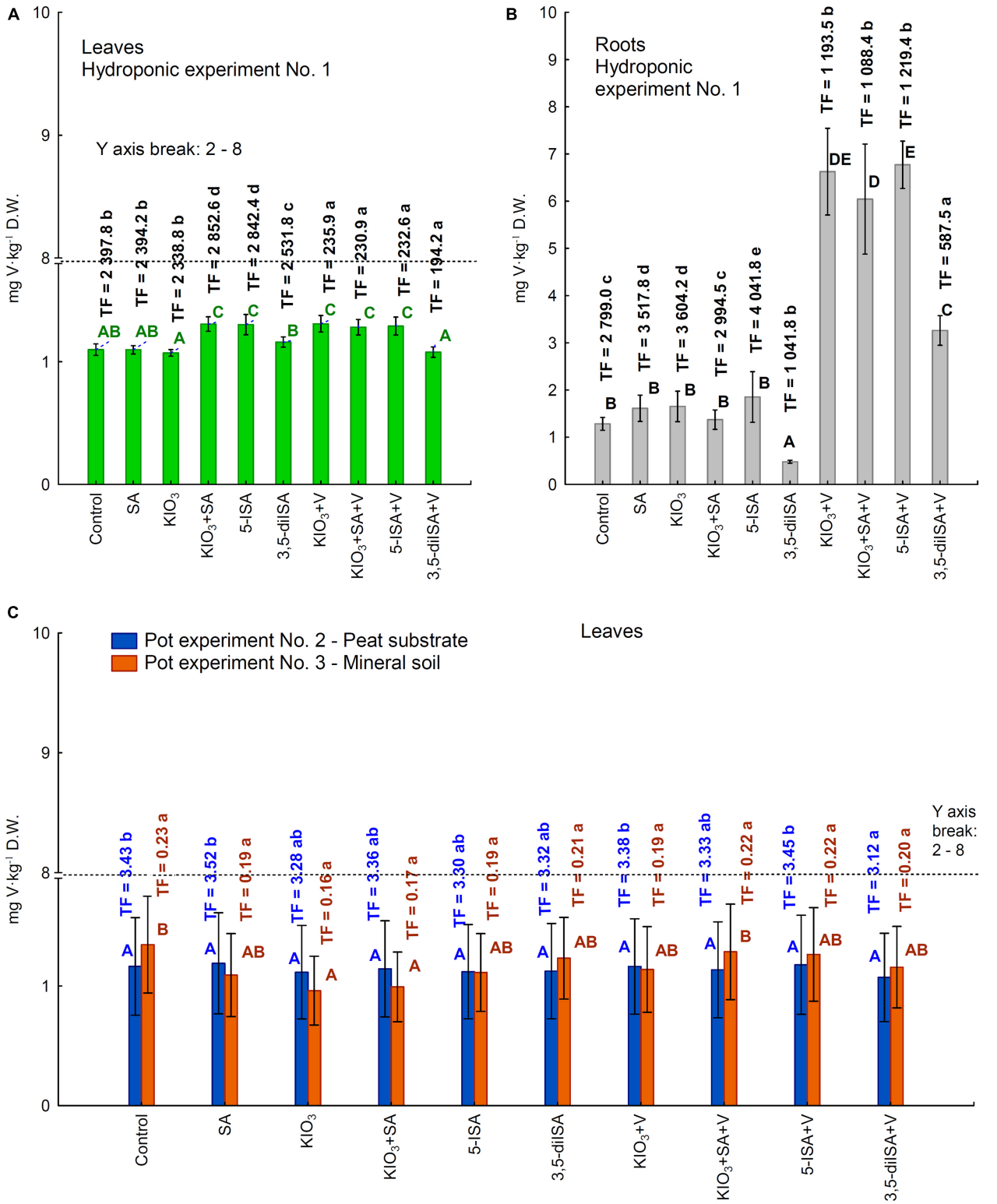


FIGURE 3 | Concentrations of vanadium in leaves /heads/**(A)** and roots of lettuce **(B)** cultivated in hydroponic NFT Experiment No. 1 as well as in leaves of plants cultivated in pot Experiment No. 2 and 3 **(C)**. Transfer factor /TF/ of vanadium to roots and leaves /heads/ in the all experiments. Means followed by different letters for treatments, separately for each experiments differ significantly at $P < 0.05$. Color-coded capital letters for vanadium content (green and gray for leaves and roots in Experiment 1 and blue and orange for leaves in Experiments 2 and 3); lowercase letters in the same colors for the TF factor in these experiments. Bars indicate standard error ($n = 8$).

3,5-diISA without V), only Experiment 3 with a peat substrate showed a significant increase in leaf I content, RDA-I%, HQ-iodine, and I uptake by a single lettuce head (**Supplementary Tables 2**, **3**).

In all three experiments, the calculated TFs for I uptake were significantly modified by application of the I compounds tested, as well as SA and V (**Figures 2A–C**). The TF values reflected I uptake by plants (I content in roots or leaves) depending on its availability in the rhizosphere, i.e., in the nutrient solution in the hydroponic system (Experiment 1) or mineral soil or peat substrate (Experiments 2 and 3).

Vanadium Uptake and Accumulation by Lettuce

In hydroponic Experiment 1, V was accumulated in larger amounts in roots than in leaves (**Figures 3A,B**). Fertilization with V combined with KIO_3, KIO_3+SA, and 5-ISA caused an approximately 4-fold increase in V content in roots compared with the control (**Figure 3B**). Following fertilization with 3,5-diISA without applying ammonium metavanadate, the content of V in roots was lower than in the control (**Figure 3B**); V uptake by roots of a single plant and by whole plants (roots + head) was consequently lower (**Supplementary Table 3**). Application of 3,5-diISA+V resulted in a significant increase in V content in roots and V uptake by roots of a single plant and by whole plants (roots + head) compared with 3,5-diISA without V. However, the increase in root V content and in V uptake by roots and whole plants was less effective for fertilization with 3,5-diISA+V than for KIO_3+V, KIO_3+SA+V, and 5-ISA+V than for 3,5-diISA, KIO_3, KIO_3+SA, and 5-ISA, respectively. This was confirmed by TF values in roots for the respective combinations with and without V fertilization.

Following the application of KIO_3+V, KIO_3+SA+V, and 5-ISA+V, the foliar content of V for hydroponic Experiment 1 was significantly higher than that for the control (**Figure 3A**); however, it was still at the same level as following the application of KIO_3+SA and 5-ISA without ammonium metavanadate. Additionally, in Experiment 1, the combination of KIO_3+V was the only one for which V uptake by a single head in Experiment 1 was significantly higher than that for KIO_3 without ammonium metavanadate (**Supplementary Table 3**).

In the two pot experiments with lettuce, foliar V content (**Figure 3C**) and V uptake by a single head (leaves from one plant) (**Supplementary Table 3**) were significantly lower than in the control but only for the KIO_3 and KIO_3+SA combination in Experiment 3. For the remaining combinations, the content of V and V uptake by a single head was the same as in the control in both pot experiments (**Figure 3C** and **Supplementary Table 3**).

In Experiment 3, the TF for foliar V was about 20-fold lower than in Experiment 2 (**Figure 3C**), which was due to lower V content in the peat substrate than in mineral soil (**Table 2**).

vHPO Activity in Lettuce

The activity of vHPO in roots (Experiment 1) and leaves of lettuce in all three experiments was significantly modified by the application of the compounds studied to the nutrient solution or substrate in the pots (**Figures 4A–C**). In hydroponic Experiment 1, the vHPO activity measured in roots was 2.5- to 4.0-fold higher than that in leaves (**Figures 4A,B**). Foliar activity of vHPO in all three experiments was in the range between 0.08 and 1.43 $U{\cdot}ng^{-1}$ protein.

The root activity of vHPO following the application of KIO_3+SA and 5-ISA (**Figure 4B**) in the hydroponic system was significantly higher than that in the control. These two combinations also produced a significantly higher foliar activity of vHPO than that in the control (**Figure 4A**). For all four combinations with ammonium metavanadate fertilization and 3,5-diISA (without V), the root activity of vHPO was lower than in the control, while foliar activity of vHPO was significantly higher than that in the control (**Figures 4A,B**). Furthermore, 3,5-diISA (vs. 3,5-diISA+V) was the only combination where the activity of vHPO in both roots and leaves was the same. Additional fertilization with V together with KIO_3, KIO_3+SA, and 5-ISA caused a significant increase in vHPO in leaves and a decrease in the roots compared with the application of these compounds without V.

In each of the three experiments, the highest vHPO activity was measured in leaves of plants representing different combinations: 3,5-diISA+V in Experiment 1 (1.27 $U{\cdot}ng^{-1}$ protein), 5-ISA+V in Experiment 2 (0.49 $U{\cdot}ng^{-1}$ protein), and 5-ISA+V in Experiment 3 (1.43 $U{\cdot}ng^{-1}$ protein) (**Figures 4A,C**). The lowest foliar activity of vHPO was identified in the control in Experiment 1 (0.21 $U{\cdot}ng^{-1}$ protein) and for SA in Experiments 2 and 3 (0.08 $U{\cdot}ng^{-1}$ protein in each experiment).

BeA, SA, and Iodine Metabolites in Secretions Collected as a Result of Root Pressure

The contents of I^-, IO_3^-, BeA, SA, 5-ISA, 2-IBeA, 4-IBeA, 2,3,5-triIBeA, I-Tyr, T3-Na, T3, and T4 measured in root secretions collected as a result of root pressure (**RootSec**) from plants in Experiment 1 differed significantly between the combinations studied (**Table 4**).

Compared with the control and SA application in all remaining combinations, I content is RootSec was markedly higher. The highest content of I^- was found after the application of 5-ISA (without V); it was 9.7-fold higher than when KIO_3 was applied to the nutrient solution alone (**Table 4**). Compared with the control, a significant increase of IO_3^- was observed in RootSec following the application of KIO_3, KIO_3+SA, 5-ISA+V, and 3,5-diISA+V, with the highest RootSec content of IO_3^- being observed for fertilization with KIO_3+SA.

3,5-diISA was detected in RootSec exclusively after the application of 3,5-diISA (with or without V). Additionally, the RootSec content of 5-ISA was on average 6.2-fold higher for these two combinations than for the control. However, the highest content of 5-ISA in RootSec (25- to 46-fold higher than in the control) was demonstrated following its application to the nutrient solution. Plants treated with exogenous 5-ISA were characterized by the highest content of T3 and T4 and the

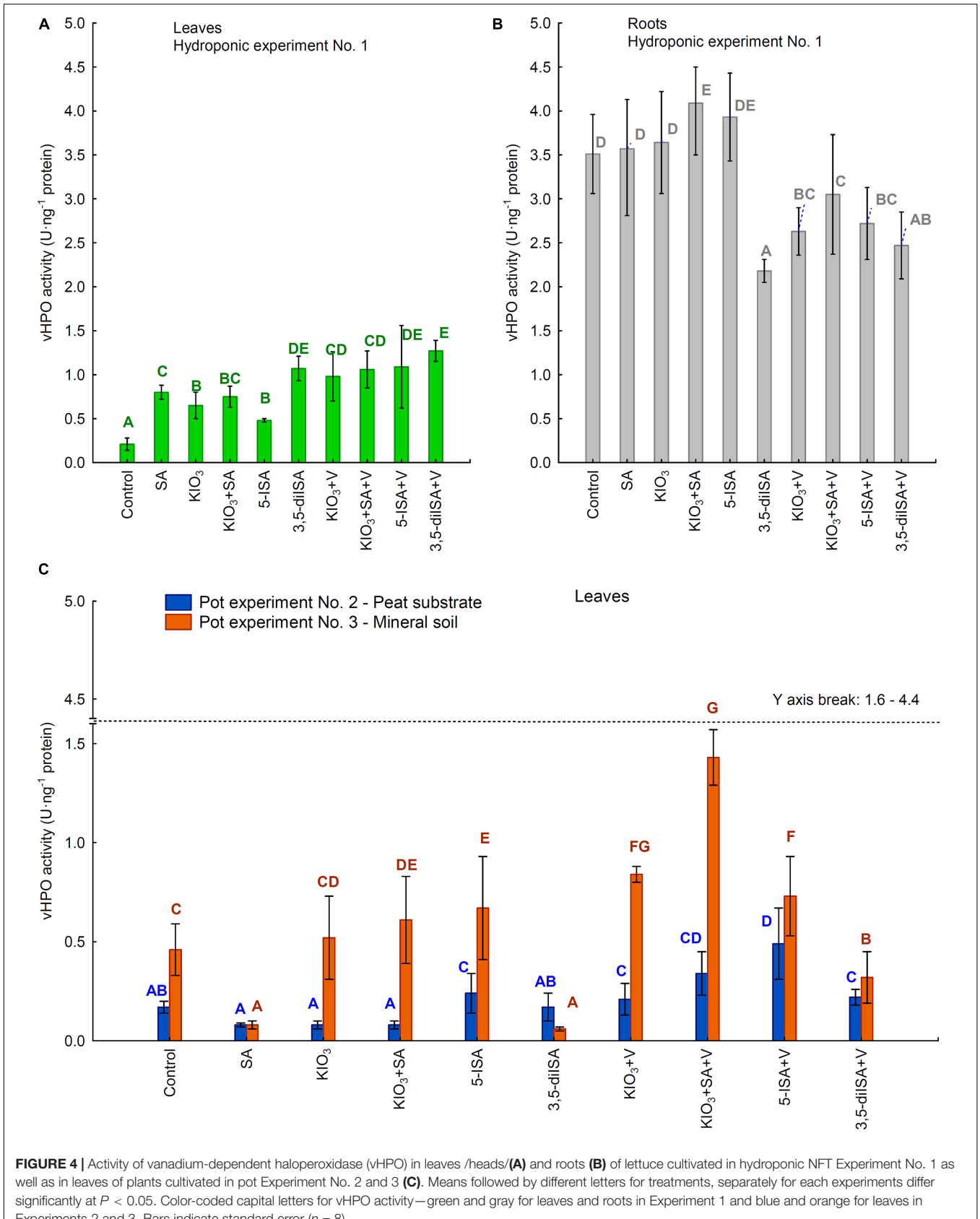


FIGURE 4 | Activity of vanadium-dependent haloperoxidase (vHPO) in leaves /heads/**(A)** and roots **(B)** of lettuce cultivated in hydroponic NFT Experiment No. 1 as well as in leaves of plants cultivated in pot Experiment No. 2 and 3 **(C)**. Means followed by different letters for treatments, separately for each experiments differ significantly at $P < 0.05$. Color-coded capital letters for vHPO activity—green and gray for leaves and roots in Experiment 1 and blue and orange for leaves in Experiments 2 and 3. Bars indicate standard error ($n = 8$).

lowest content of BeA and 2,3,5-triIBeA in RootSec. The RootSec content of T4 was equally high for fertilization using 3,5-diISA.

For all combinations with fertilization using ammonium metavanadate, application of the compound caused a reduction in T3 content in RootSec; the comparison encompassed combinations with KIO_3, KIO_3+SA, 3,5-diISA, 5-ISA without and with V (**Table 4**). The application of 5-ISA+V vs. 5-ISA (without V) had a reduced content of SA, 5-ISA, T3, and T4 and increased 2-IBeA in RootSec. When it comes to fertilization using 3,5-diISA+V vs. 3,5-diISA (without V), it caused a significant increase in BeA, 2-IBeA, and 4-IBeA and a decrease in the content of 5-ISA, T3, and T4 in RootSec.

Application of exogenous SA to the nutrient solution caused a significant increase in the RootSec content of 2,3,5-triIBeA compared with all the remaining combinations (**Table 4**).

Determination of Iodides (I^-) and Iodates (IO_3^-) in Roots and Leaves of Lettuce in a Hydroponic System (Experiment 1)

Roots and leaves had a higher content of iodides (I^-) than iodates (IO_3^-), from 12.5 times in roots for SA treatment to 53,750 times in leaves for 5-ISA+V treatment (**Table 5**). There were trace amounts of IO_3^-

TABLE 4 | Results of the determination of iodides, iodates, organic acids, and iodine metabolites in secretions collected as a result of root pressure (RootSec)—this is in white secretion on the surface of the root neck after cutting the heads (lettuce leaves).

Treatments	($\mu g \cdot dm^{-3}$)*				
	Iodides (I^-)	**Iodates (IO_3^-)**	**BeA**	**SA**	
Control	16.1 ± 0.25a	1.08 ± 0.07ab	68 ± 9.0b	638.6 ± 10.0b	
SA	10.4 ± 0.37a	0.74 ± 0.15ab	98 ± 0.6cd	214.6 ± 18.3a	
KIO_3	184.3 ± 3.69b	2.02 ± 0.05c	116 ± 9.9cde	2 163.0 ± 100.0c	
KIO_3+SA	215.2 ± 19.76bc	2.94 ± 0.71d	88 ± 10.0bcd	118.2 ± 18.9a	
5-ISA	1 789.9 ± 18.29e	0.70 ± 0.11ab	2 ± 1.0a	740.6 ± 4.0b	
3,5-diISA	291.2 ± 23.36c	0.67 ± 0.02ab	128 ± 10.0de	258.4 ± 51.1a	
KIO_3+V	203.5 ± 3.34b	0.28 ± 0.07a	10 ± 1.4a	106.6 ± 5.4a	
KIO_3+SA+V	169.8 ± 15.74b	0.65 ± 0.30ab	74 ± 9.8bc	104.3 ± 1.3a	
5-ISA+V	389.6 ± 70.51d	1.54 ± 0.06bc	132 ± 10.0de	254.0 ± 82.9a	
3,5-diISA+V	171.2 ± 10.99b	2.13 ± 0.32cd	138 ± 10.0e	221.3 ± 49.3a	
	5-ISA	**3,5-diISA**	**2-IBeA**	**4-IBeA**	
Control	8.4 ± 0.82a	<LOQ**	0.05 ± 0.01abc	0.04 ± 0.01a	
SA	8.3 ± 0.57a	<LOQ	0.15 ± 0.01d	0.19 ± 0.01c	
KIO_3	8.7 ± 0.73a	<LOQ	0.07 ± 0.01abc	0.10 ± 0.01abc	
KIO_3+SA	7.2 ± 0.24a	<LOQ	0.26 ± 0.03e	0.08 ± 0.01ab	
5-ISA	386.1 ± 11.45d	<LOQ	0.02 ± 0.01ab	0.06 ± 0.01ab	
3,5-diISA	58.6 ± 0.67b	63.9 ± 6.07a	0.01 ± 0.00a	0.06 ± 0.01ab	
KIO_3+V	7.4 ± 0.36a	<LOQ	0.08 ± 0.01bc	0.11 ± 0.03abc	
KIO_3+SA+V	7.7 ± 1.10a	<LOQ	0.06 ± 0.01abc	0.16 ± 0.02bc	
5-ISA+V	215.7 ± 97.09c	<LOQ	0.09 ± 0.02cd	0.08 ± 0.01ab	
3,5-diISA+V	46.2 ± 1.48b	83.6 ± 3.64b	0.10 ± 0.01cd	0.36 ± 0.05d	
	2,3,5-triIBeA	**I-Tyr iodotyrosine**	**T3-Na**	**T3**	**T4**
Control	0.25 ± 0.01a	0.52 ± 0.08bc	484.1 ± 40.5ab	2.81 ± 0.10d	0.22 ± 0.01ab
SA	2.67 ± 0.46b	0.56 ± 0.02bc	422.4 ± 41.6ab	1.31 ± 0.01b	1.83 ± 0.10cd
KIO_3	0.45 ± 0.10a	0.55 ± 0.06bc	746.7 ± 58.6c	2.84 ± 0.10d	0.01 ± 0.00a
KIO_3+SA	0.17 ± 0.07a	0.71 ± 0.06c	608.9 ± 77.5bc	3.46 ± 0.10e	0.64 ± 0.09b
5-ISA	0.01 ± 0.002a	0.52 ± 0.24bc	342.0 ± 3.4ab	5.00 ± 0.06f	4.78 ± 0.10h
3,5-diISA	0.09 ± 0.01a	0.16 ± 0.01ab	285.2 ± 36.1a	2.10 ± 0.10c	4.04 ± 0.15g
KIO_3+V	0.08 ± 0.02a	2.17 ± 0.10d	270.6 ± 60.5a	0.16 ± 0.01a	2.34 ± 0.21de
KIO_3+SA+V	0.08 ± 0.01a	2.26 ± 0.01d	409.7 ± 1.6ab	1.34 ± 0.10b	0.15 ± 0.01ab
5-ISA+V	0.17 ± 0.02a	0.50 ± 0.08bc	225.3 ± 2.0a	3.83 ± 0.10e	1.63 ± 0.10c
3,5-diISA+V	0.13 ± 0.02a	0.01 ± 0.00a	591.3 ± 109.0bc	1.16 ± 0.01b	3.14 ± 0.10f

**The content of the following compounds was analyzed: iodides (I^-), iodates (IO_3^-), benzoic acid (BeA), salicylic acid (SA), 5-iodosalicylic acid (5-ISA), 3,5-diiodosalicylic acid (3,5-diISA), 2-iodobenzoic acid (2-IBeA), 4-iodobenzoic acid (4-IBeA), 2,3,5-triiodobenzoic acid (2,3,5-trilBeA), iodotyrosine (I-Tyr), sodium salt triiodothyronine (T3-Na), triiodothyronine (T3), and thyroxine (T4).*

***Limit of quantification (LOQ) for 3,5-diISA was 2.748.*

TABLE 5 | Concentrations of iodides (I^-) and iodates (IO_3^-) in roots and leaves of lettuce in hydroponics NFT Experiment No. 1 (speciation of iodine analyzed HPLC-ICP-MS/MS) as well percentage of the iodides and iodates in relation to the total iodine.

Experiment No. 1. Hydroponic NFT/Part of plant	Treatments	(mg·kg^{-1} D.W.)			Percentage of the sum of iodides and iodates in relation to the total I content* (%)	Percentage of the sum of analyzed organic-I** in relation to the total I content* (%)	Theoretical percentage share of the content of other unanalyzed organic or inorganic I compounds in the total I content (%)
		Iodides (I^-)	Iodates (IO_3^-)	The sum of two forms of I: I^- and IO_3^-			
Leaves	Control	2.34 ± 0.005b	0.0272 ± 0.0008d	2.365 ± 0.005b	57.7 ± 0.80c	3.26 ± 0.11d	39.0
	SA	0.97 ± 0.006a	0.0293 ± 0.0009d	0.998 ± 0.006a	56.3 ± 0.53c	2.39 ± 0.26c	41.4
	KIO_3	15.06 ± 0.042f	0.0146 ± 0.0006b	15.078 ± 0.042f	73.4 ± 0.64f	0.71 ± 0.05b	25.9
	KIO_3+SA	17.49 ± 0.140g	0.0139 ± 0.0001b	17.504 ± 0.140g	56.0 ± 0.33c	0.16 ± 0.02a	43.9
	5-ISA	97.06 ± 0.189i	0.0488 ± 0.0006f	97.113 ± 0.189i	67.6 ± 1.77e	0.25 ± 0.01ab	32.1
	3,5-diISA	8.63 ± 0.044d	0.0002 ± 0.0001a	8.625 ± 0.044d	5.3 ± 0.60a	0.75 ± 0.01b	93.9
	KIO_3+V	14.12 ± 0.041e	0.0215 ± 0.0004c	14.143 ± 0.041e	63.1 ± 0.36d	0.30 ± 0.06ab	36.6
	KIO_3+SA+V	18.92 ± 0.229h	0.0023 ± 0.0001a	18.918 ± 0.229h	84.1 ± 1.20h	0.66 ± 0.01ab	15.3
	5-ISA+V	118.25 ± 0.623j	0.0022 ± 0.0001a	118.252 ± 0.624j	72.4 ± 0.12f	0.31 ± 0.01ab	27.3
	3,5-diISA+V	3.46 ± 0.009c	0.0428 ± 0.0017e	3.507 ± 0.010c	23.6 ± 0.20b	7.01 ± 0.12f	69.4
Roots	Control	7.70 ± 0.0187b	0.8780 ± 0.0007e	8.577 ± 0.019b	22.7 ± 0.32g	2.41 ± 0.04	74.9
	SA	0.16 ± 0.0025a	0.0137 ± 0.0001a	0.169 ± 0.002a	0.3 ± 0.01a	0.70 ± 0.02	99.0
	KIO_3	10.87 ± 0.0131c	0.9914 ± 0.0006ef	11.866 ± 0.013c	12.8 ± 0.12d	0.55 ± 0.05	86.7
	KIO_3+SA	34.99 ± 0.4050e	0.2436 ± 0.0037d	35.235 ± 0.408e	25.6 ± 0.24h	0.40 ± 0.04	74.0
	5-ISA	72.58 ± 0.0764f	1.7800 ± 0.0428g	80.364 ± 0.119f	14.0 ± 0.23e	0.86 ± 0.03	85.1
	3,5-diISA	8.12 ± 0.0183b	0.9589 ± 0.0005f	9.080 ± 0.018b	1.1 ± 0.01ab	9.18 ± 0.10	89.8
	KIO_3+V	13.53 ± 0.0426d	0.0531 ± 0.0004ab	13.583 ± 0.042d	16.4 ± 0.15f	1.32 ± 0.06	82.3
	KIO_3+SA+V	11.27 ± 0.0564c	0.1136 ± 0.0009c	11.382 ± 0.057c	12.5 ± 0.23d	2.10 ± 0.06	85.4
	5-ISA+V	119.26 ± 1.6836g	0.9511 ± 0.0266ef	120.212 ± 1.710g	6.2 ± 0.08c	0.44 ± 0.00	93.4
	3,5-diISA+V	11.59 ± 0.0606c	0.0695 ± 0.0003bc	11.661 ± 0.060c	1.2 ± 0.01b	7.99 ± 0.14	90.8

Total I content determinate after TMAH extraction (see **Figure 1).*

***Organic-I—I in all organic I compounds analyzed in roots and leaves of lettuce from hydroponic Experiment No. 1 (see **Supplementary Table 4**, 5). Sum content of I in form: 5-ISA, 3,5-diISA, I-Tyr, T3-Na, T3, 2-IBeA, 4-IBeA, 2,3,5-triIBeA in relation to the total I content.*

Means in the column followed by different letters separately for each experiments differ significantly at $P < 0.05$.

in leaves and roots in all combinations subjected to analysis. Even in roots and leaves of plants fertilized with KIO_3, the content of IO_3^- was lower than or similar to the control.

The lowest root and leaf content of I^- (lower than in the control) was detected in plants treated with exogenous SA (**Table 5**). The highest content of I^- in roots and leaves was found in plants treated with 5-ISA+V; it was significantly higher than in combinations where 5-ISA was used alone.

A comparison of combinations with I applied to the nutrient solution shows the following quantitative root content of I^- (**Table 5**): 5-ISA+V > 5-ISA > KIO_3+SA > KIO_3+V > 3,5-diISA+V = KIO_3+SA+V = KIO_3 > 3,5-diISA. The quantitative content of I^- in leaves was as follows: 5-ISA+V > 5-ISA > KIO_3+SA+V > KIO_3+SA > KIO_3 > KIO_3+V > 3,5-diISA > 3,5-diISA+V.

An additional application of V together with KIO_3, KIO_3+SA, 5-ISA, and 3,5-diISA in each of these four combinations had a different impact on the I^- content in leaves and roots (**Table 5**) and resulted in an increase or decrease in I^- content in leaves and roots, compared with application of exogenous I compounds without V.

The percentage of the sum of iodides (I^-) and iodates (IO_3^-) in relation to total I content was within the range from 0.3 for SA to 25.6 for KIO_3+SA in roots, and from 5.3 for 3,5-diISA to 84.1 for KIO_3+SA+V in leaves (**Table 5**).

In the supporting information files were included the results of content of BeA, SA, iodine metabolites in roots and leaves (**Supplementary Tables 4**, **5**) as well as content of I and V in soil after lettuce cultivation (**Supplementary Table 6**).

DISCUSSION

The aim of research on I biofortification of plants is to establish biofortification regimens, define the threshold of I toxicity for plants, and optimize I biofortification

of plants to make it safe and adequate to consumers' needs (Lawson et al., 2016). Research on I biofortification must be connected with research targeted at expanding knowledge on biochemical, physiologic, and molecular aspects of the functions of trace elements in plants (White and Broadley, 2009).

Plant Biomass and Iodine Biofortification Efficiency Depending on the Chemical Form of Iodine, Vanadium Application, and Type of Cultivation

The dose of I in the hydroponic system was 37.5-fold higher than that in both pot experiments. In consequence, the I compounds (particularly as 5-ISA and secondarily as 3,5-diISA) were applied at a concentration that was too high, negatively impacting plants (reduced yield) in hydroponic Experiment 1. Smoleń et al. (2017) showed that in the hydroponic system, 5-ISA was toxic to lettuce when applied at a dose of 40.0 μM I; the symptoms were not reported after application of 5-ISA at a dose of 1.6 and 8.0 μM I. The authors did not conduct research on 3,5-diISA. Based on the results of a study by Smoleń et al. (2017) and the reduced lettuce biomass shown in this study (Experiment 1), we presume that the threshold of transition from harmful to toxic I activity in lettuce is somewhere between the dose of 8.0 μM and 10.0 μM of I applied as 5-ISA. Because only one dose of 3,5-diISA was tested, it was impossible to establish an exact threshold of harmfulness/toxicity of exogenous 3,5-diISA on lettuce, as was done for 5-ISA.

Welch and Huffman (1973) did not report a significant impact of 1 μM V (as NH_4VO_3) on the yield of lettuce or tomato compared with the control without V fertilization, for doses ranging from 0.05 to 0.40 μM V. In the three experiments described in the publication, simultaneous fertilization with KIO_3, 5-ISA, and 3,5-diISA plus V at a dose of 0.1 μM V (vs. no V) had no negative impact on the biomass of lettuce.

The highest efficacy of I biofortification on lettuce following the application of 5-ISA (in each of the three experiments) compared with 3,5-diISA and KIO_3 was justified in research by Smoleń et al. (2017). The authors demonstrated that 5-ISA at a dose of 8.0 μM I was enough to achieve a similar effect of I biofortification in lettuce leaves, as in the case of using KIO_3 at a dose of 40.0 μM I. In Experiment 1, the dose of 5-ISA (or, to a lesser extent, 3,5-diISA and KIO_3) was too high in the context of a need to balance I content in the daily diet of consumers. This is indicated by the RDA for I (%) in a 100 g portion of fresh lettuce leaves $>$ 480% and HQ $>$ 0.66; the compound would be harmful to consumers if HQ exceeded 1.0. The two iodosalicylates mentioned above, as well as 2-IBeA, 4-IBeA, 2,3,5-triIBeA, and I-Tyr, and T3 were naturally synthesized in lettuce, which further confirms the results of previous studies on lettuce (Smoleń et al., 2020). Halka et al. (2019) showed that these organic I compounds were present in tomato fruits and willow bark. The problem with defining a "target range" for I biofortification of lettuce with non-organic I compounds (KI and KIO_3), as well as the determination of human demand of I and estimations of lettuce consumption by the general population were addressed in a study by Lawson et al. (2016). Vegetables enriched with KI and KIO_3 have been found to be safe both for humans (Tonacchera et al., 2013) and laboratory rats (Piątkowska et al., 2016). In our studies, exogenous 5-ISA and 3,5-diISA caused a significantly higher accumulation of these compounds in leaves and roots. This information may provoke questions on consumer safety where iodosalicylates are used for I enrichment of plants. There is no direct data on the effect of exogenous iodosalicylates used in vegetable growth on animals or humans. We presume that exogenous iodosalicylates may increase health-promoting effects of domesticated plants. This is because the fertilization of plants using inorganic KI or KIO_3 compounds increases synthesis and accumulation of organic I metabolites in plants, as confirmed in research on lettuce (Smoleń et al., 2020) and tomato (Halka et al., 2019). Even though organic I metabolites, including T3, are present in marine algae in much higher amounts than in lettuce (Fenical, 1975), marine algae are still consumed by a number of people worldwide (González et al., 2019).

In hydroponic Experiment 1 with lettuce, I enrichment of plants was higher than in both pot experiments. This was probably because I taken up directly from the nutrient solution was more readily available to roots and because the dose of I per plant was higher than in Experiments 2 and 3. The effectiveness of I biofortification in plants is much higher in hydroponic and soilless systems than when soil fertilization is used (Blasco et al., 2008). This is due to high I sorption by soil, a phenomenon that is absent in hydroponic nutrient solutions. Iodine sorption in soil is attributable to the mineral fractions and SOM (Kashparov et al., 2005), especially the humified aromatic ring of organic matter but not fresh organic matter (Schlegel et al., 2006). After SOM, the following compounds also participate in I sorption by mineral soils: hydroxides Fe/Al (Yoshida et al., 1992), Cu(I)-Fe (III)-sulfides and Cu(I)-sulfides (Lefèvre et al., 2003), as well as Cu/Cr and Cu/Al (Pless et al., 2007). Additionally, I desorption by soil is very slow, which inhibits I uptake by roots (Dai et al., 2004). The SOM also contains SA and its derivatives (Hue et al., 1986). Molecular I or its non-organic anions in the soil may react with aromatic rings of compounds included in SOM (Yamada et al., 1996). Endogenous iodosalicylates and iodobenzoates were identified in the soil prior to lettuce cultivation. The peat substrate was richer in BeA, SA, 5-ISA, and 2-IBeA than mineral soil. In both pot experiments, lettuce heads grown in the peat substrate accumulated less I than those grown in mineral soil. The sorption of I anions (IO_3^-) by organic soils was higher than in mineral soils (Yamaguchi et al., 2005). This has also been confirmed by the results of analyses of the peat substrate and mineral soil after lettuce cultivation. Post-cultivation I content in the peat substrate was on average 1.5-fold higher than in mineral soil. The highest efficacy of I enrichment of lettuce following the application of 5-ISA in the peat substrate and mineral soil may have resulted from the low degradation or conversion of low-molecular-weight organic aromatic I compounds in soil, which then may be taken up by roots.

Relative Expression of Analyzed Genes vs. Iodine Uptake. Iodine Metabolism in Lettuce

The absence of impact or insignificant increase in V content in leaves following ammonium metavanadate fertilization reported in the three experiments was also confirmed in the literature. When V is applied through a soil fertilizer or nutrient solution, it accumulates in roots and its transport to aboveground parts of the plants is very limited. This was also reported for the cultivation of tomato, Chinese green mustard (Vachirapatama et al., 2011), soybean (Kaplan et al., 1990), rice (Chongkid et al., 2007), and lettuce (Gil et al., 1995). Increased V transfer to the aboveground parts of plants is possible if high concentrations of the element, which are potentially toxic to plants, are used in fertilization (Chongkid et al., 2007; Vachirapatama et al., 2011).

Peroxidases are linked to a number of physiological functions. These include the removal of H_2O_2, oxidation of toxic reductants, biosynthesis and degradation of lignin, and participation in many other biochemical processes (additional descriptions in **Supplementary Data 1**). The ion Ca^{2+} has been described as a cofactor for peroxidase (Pandey et al., 2017). Enzymes from the group of V-dependent haloperoxidases (vHPO) contain the bare metal oxide vanadate, as a prosthetic group (Wever and Hemrika, 2001) (see also **Supplementary Data 1**). In the presence of H_2O_2, they oxidize halides (I, Be, Cl) in the following reaction: $H_2O_2 + X^- + H^+ \rightarrow H_2O + HOX$, where X represents Cl^-, Br^-, or I^- (Wever and Hemrika, 2001; Leblanc et al., 2006). The function of vHPO is well-described for marine algae (Leblanc et al., 2006; Verhaeghe et al., 2008). In marine algae, the vHPO enzyme plays a dual function. It can participate in the process of I uptake into cells and is involved in the process of I excretion from cells to the environment in the form of I_2 (Leblanc et al., 2006).

An additional application of V with different I compounds and SA had no definitive impact on the expression of *per64-like*, *per12-like*, *samdmt*, *cipk6*, or *msams5* in either roots or leaves. *per64-like* was the only gene whose expression decreased in the roots of plants treated with KIO_3+SA+V, 5-ISA+V, and 3,5-diISA+V (in nutrient solution) when compared to the application of the same compounds without V. For these very same combinations (with and without V), the root activity of vHPO was reported to decrease. Therefore, the level of expression of the *per64-like* gene was correlated with the activity of vHPO in roots. The decreased activity of vHPO was accompanied by a lower expression of *per64-like* in plants treated with KIO_3+SA+V, 5-ISA+V, and 3,5-diISA+V. These results are sufficient to assign vHPO-like activity to an enzyme encoded by *per64*-like, rather than the one encoded by *per12-like*. Perhaps peroxidase encoded by *per64-like* may have vHPO-like function (may be a V-dependent enzyme). The results of pairwise alignment of protein sequences of *A. thaliana* PER12 and PER64 with vIPO1 *L. digitata* and vBPO *C. officinalis* and *A. nodosum* showed common regions between them (see also **Supplementary Data 1**). Further *in-silico* research is needed to this end or research directed at isolating PER64-like enzyme to be able to examine its structure and functionality depending on the application of V.

Colin et al. (2005) proved that the *in-vitro* activity of vHPO isolated from *Laminaria digitata* grew intensively within the range 0–10 mM KI and dropped suddenly when KI > 20 mM was used. In the three experiments conducted as part of our study, exogenous KIO_3, 5-ISA, and 3,5-diISA (applied without V) had a different effect on root and foliar activity of vHPO. Before its uptake by roots or immediately thereafter, IO_3^- must be reduced to I^- (Kato et al., 2013). Surprisingly, there was no significant difference in vHPO activity in the roots of plants treated with KIO_3 alone (Experiment 1) compared with the control, despite a simultaneous 2.6-fold increase in the expression of the *per64-like* gene. The results indirectly indicate that other molecular and biochemical mechanisms than vHPO must be involved in the process of root uptake and transport of I^- produced following IO_3^- reduction. These mechanisms are probably responsible for chloride transport. The transport of I^- within root cells and to the xylem is analogous to the translocation of Cl^- ions and takes the form of symport (H^+/anion) or antiport (Na:K/Cl) or is effected through I channels that are permeable to Cl^-/I^- (White and Broadley, 2001; Roberts, 2006; Colmenero-Flores et al., 2007).

The three experiments share the observation that none of the tested I compounds silenced foliar activity of vHPO. 3,5-diISA was the only compound that reduced the activity of vHPO in roots, an observation consistent with Smoleń et al. (2020). This may be because of the specific effect of 3,5-diISA on vHPO, which inhibited the activity of the enzyme (already at a dose of 10 μM; or 20 μM I) but did not suppress the expression of the *per64-like* gene, which has been linked with vHPO-like functions. Notably, lower expression of *per64-like* was reported in the roots of plants treated with 3,5-diISA but only compared with KIO_3+SA and 5-ISA, with a simultaneous increase in gene expression in comparison with the control. 5-ISA increased the foliar activity of vHPO in all three experiments compared with the control, which translated into the highest I accumulation in lettuce leaves. The potential mechanism most likely to stimulate foliar activity of vHPO through 5-ISA and 3,5-diISA is not fully understood. It could be a result of catabolism in both iodosalicylates to I^-, as only in this form could I be taken up intracellularly with the aid of vHPO in a mechanism resembling the one described for marine algae by Leblanc et al. (2006).

The activity of vHPO and expression of *per64-like* in leaves and roots were determined at the final stage of cultivation (shortly before lettuce harvesting), which means that the measurements were made after the plants have been exposed to exogenous V and I compounds for an extended time. While theoretically it may seem that V fertilization should increase the activity of vHPO in plants, due to the higher availability of the enzyme's cofactor, lettuce fertilization with V caused decreased activity of vHPO and expression of the *per64-like* gene. Reduction in vHPO activity following test fertilization with I compounds + V is consistent with the previous findings of Smoleń et al. (2020). The authors showed that fertilization with V without the simultaneous use of I (plant cultivation with trace amounts of I in the nutrient solution) significantly enhanced the activity of vHPO. Given these results, the assignment of a vHPO-like function to the protein encoded by *per64-like* seems to be substantively justified.

Fertilization with V did not cause an increase in foliar V content in any of the experiments conducted as part of this research (except for KIO_3+V vs. KIO_3 in Experiment 1). However, a considerable increase in root V content following V fertilization was observed. The results were consistent with the literature. V fertilization of Chinese greens, at a dose of 0.39, 0.79, and 1.57 mM, caused a proportional increase in V content in the plants, with the following preserved concentration gradient: roots > stems > leaves system (Vachirapatama et al., 2011). A similar V concentration gradient was obtained by Akoumianaki-Ioannidou et al. (2016) for sweet basil fertilized with NH_4VO_3. The rate of transfer of V from roots to leaves can only be increased if it is used at very high doses, which may be harmful to plants. The negative effect of V on plants also depends on its chemical form. Findings for soybean showed that a harmful dose of $VOSO_4$ was 1.2 mM V (Kaplan et al., 1990). A dose of 0.39 mM V was reported to be harmful for rice (Chongkid et al., 2007). The adverse effects of V may include root darkening, decreased number of secondary roots, decreased turgor pressure, loss of leaf firmness, and plastid degradation in plants (Gil et al., 1995). In Experiment 1, we did not observe any negative impact of V on the development of roots, which was demonstrated by the biomass obtained from the roots of one of the plants.

Expression of *cipk6* Gene

The available literature describes the likely biochemical mechanisms of PDTHA activity in plants by comparing their function to thyroid hormones (T3 or T4) in humans. Eneqvist et al. (2003) stated that higher plants can produce a protein homologous to human transthyretin, which is responsible for T3 and T4 transport (TransThy-T3/T4trans). Additionally, the TransThy-T3/T4trans protein from higher plants, including *A. thaliana*, tomato, and potato was more closely related in the phylogenetic tree of the transthyretin protein family to the protein found in *Homo sapiens* than to TransThy-T3/T4trans from bacteria or fungi. In model research, Pessoa et al. (2010) showed that exogenous T4 can be bound by transthyretin-like protein in *A. thaliana*. Furthermore, Power et al. (2000) showed that transthyretin in humans belongs to the group of proteins that includes thyroxine-binding globulin and albumin. The chemical bond is responsible for transporting thyroid hormones in blood. Davis et al. (2000) showed that in humans, T4 can activate signal transduction proteins, such as mitogen-activated protein kinase (MAPK). Additionally, T4 can enhance the activity of several nuclear transactivator proteins, through serine phosphorylation by MAPK. A similar complex mechanism may exist in lettuce. Findings show that the protein encoded by *cipk6* can likely perform the function of a T3 and/or T4 receptor (see the functional annotation of the *cipk6* gene in **Supplementary Data 2**). This assumption is justified by results of chemical analyses of roots and RootSec. The synthesis of T3 and T4 (and possibly other isomers of these PDTHAs) probably occurs, with the participation of iodobenzoates and/or iodosalicylates (5-ISA and 3,5-diISA) as the substrates of PDTHA (**Figures 5**, **6**). The results showed that the process occurs primarily in roots. T3 and T4 are then transported to the aboveground parts of plants (**Figures 5**, **6**). The observation of root synthesis of T3 are consistent with the outcome of our previous study (Smoleń et al., 2020). In the present study, we measured T4 directly in leaves and roots. The key problem with T3 and T4 measurements in plant tissues is that there are no analytical protocols dedicated to the analysis of PDTHA content in plants. However, the content of T4 was measured directly in RootSec. Therefore, it is important that we postulate the need to search for and elaborate on the optimum methods or analytical procedures that would enable measurements of the total T4/T3 and other PDTHAs in the tissue of plants. We believe that the results of our analyses of non-organic and organic I metabolites (particularly T3 and T4) in roots, RootSec, and leaves, provide grounds to assign the function of a T3 and/or T4 receptor in lettuce to a protein encoded by *cipk6*. For *cipk6*, a significant correlation coefficient was reported between its expression vs.: 1) the content of T3 (r = 0.30*), 5-ISA (r = 0.72*), and total content of I (r = 0.84*) directly in roots and 2) the content of T3 (r = *0.60**), T4 (r = *0.58**), 5-ISA (r = 0.89*), and total content of I (r = 0.89*) in RootSec. A statistically significant correlation between the expression of *cipk6* and total I content (r = 0.26*) was found in leaves; however, no correlation was reported between the expression of *cipk6* and the content of T3 or 5-ISA. This led us to the conclusion that the root activity of *cipk6* is closely related to the presence of PDTHA. The effect of PDTHA on *cipk6* gene expression in leaves was smaller. This may be proof that the function of the dominant PDTHA receptor in aboveground parts of plants may be performed by a protein encoded by another gene/group of genes. However, the results of research presented herein are insufficient to thoroughly describe the physiological function of PDTHA in lettuce.

The highest expression of *cipk6* in roots and leaves of plants treated with 5-ISA was unequivocally associated with I uptake and metabolism in these plants. The plants were found to demonstrate the highest I-uptake and total I content, and had increased 5-ISA, 2-IBeA, 3,5-diISA, I^-, and IO_3^- levels in roots and leaves. In addition, RootSec from plants where 5-ISA had been applied were also found to have the highest content of 5-ISA and I metabolites, such as I^-, T3, and T4. The results clearly showed that there is a close interdependence between a larger preference to take up 5-ISA (compared with IO_3^- and 3,5-diISA) and the metabolism of I compounds which, among others, induces the synthesis of PDTHA and increases the expression of *cipk6*, a gene of the T3 and/or T4 receptor.

Expression of the *msams5* Gene

The functions of S-adenosyl-l-methionine (SAM)-dependent halide methyltransferase (HMT) or SAM-dependent halide/thiol methyltransferase (HTMT), enzymes responsible for I volatilization to CH_3I or CH_2I_2, are subject to a complex control mechanism and are typical of a number of marine algae species (Keng et al., 2020) and terrestrial plants (Attieh et al., 2000; Nagatoshi and Nakamura, 2007; Itoh et al., 2009; Landini et al., 2012). These enzymes are not specific for I as a substrate but can also participate in the methylation of other group-17 elements (halogens) from the periodic table. A different, complicated affinity in the substrate-enzyme system is as follows: $I^- > Br^- > Cl^-$ (Manley, 2002; Murphy, 2003). In *B. oleracea*,

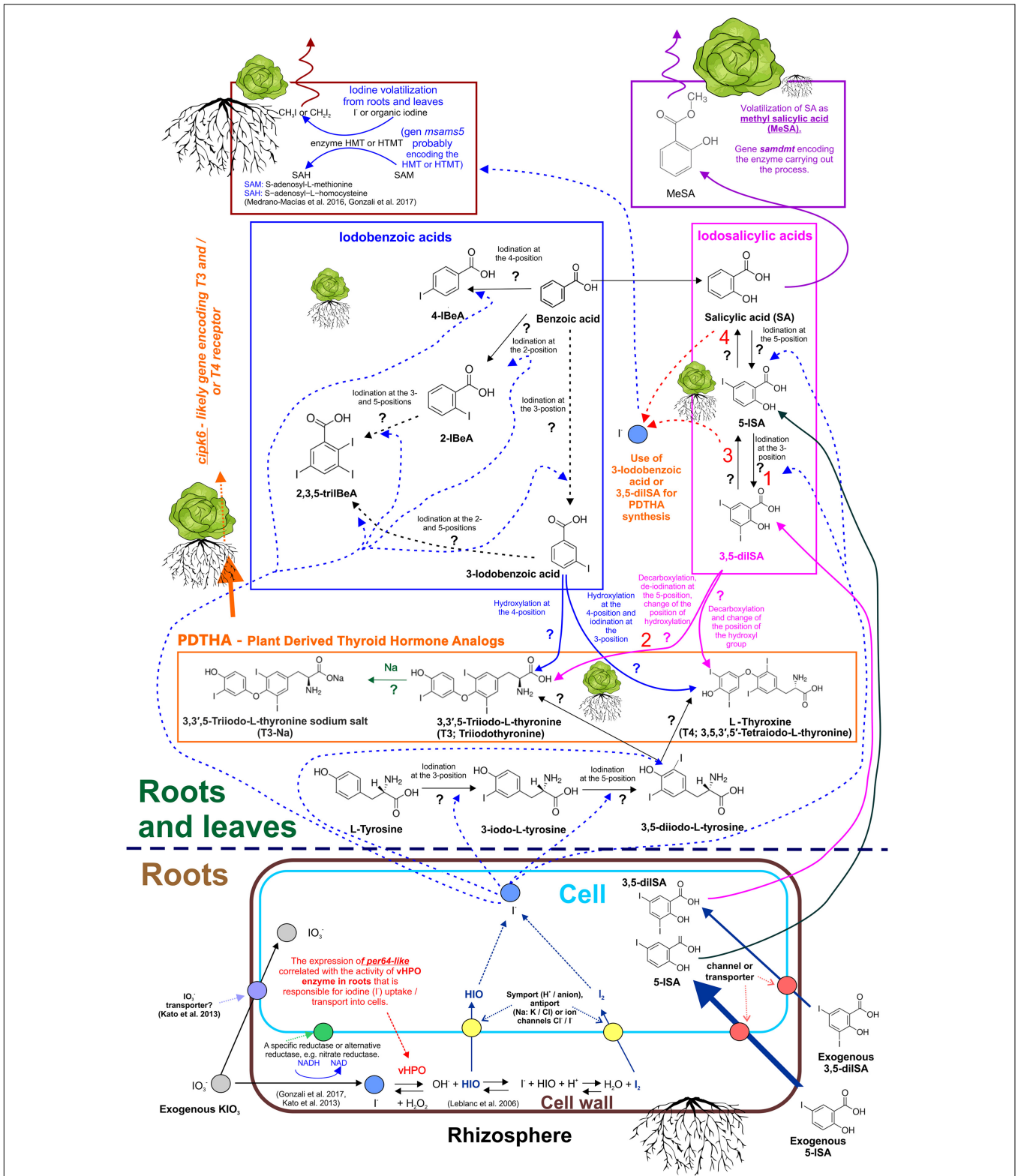


FIGURE 5 | Mechanism of uptake of non-organic and organic iodine compounds. Theoretical metabolic pathway of iodosalicylates, iodobenzoates, and plant-derived thyroid hormone analogs (PDTHA) in lettuce—summary of the study and literature data. 1 and 2—Processes that mainly occur in roots. Foliar activity intensifies after application of 5-ISA and 3,5-diISA. 3—Deiodination of 3,5-diISA. Observed increased content of 5-ISA following exogenous application of 3,5-diISA. 4—Deiodination of 5-diSA. Observed increased content of SA following exogenous application of 5-diSA and 3,5-diISA. **?**—Undefined enzymatic/metabolic processes that carry out these reactions.

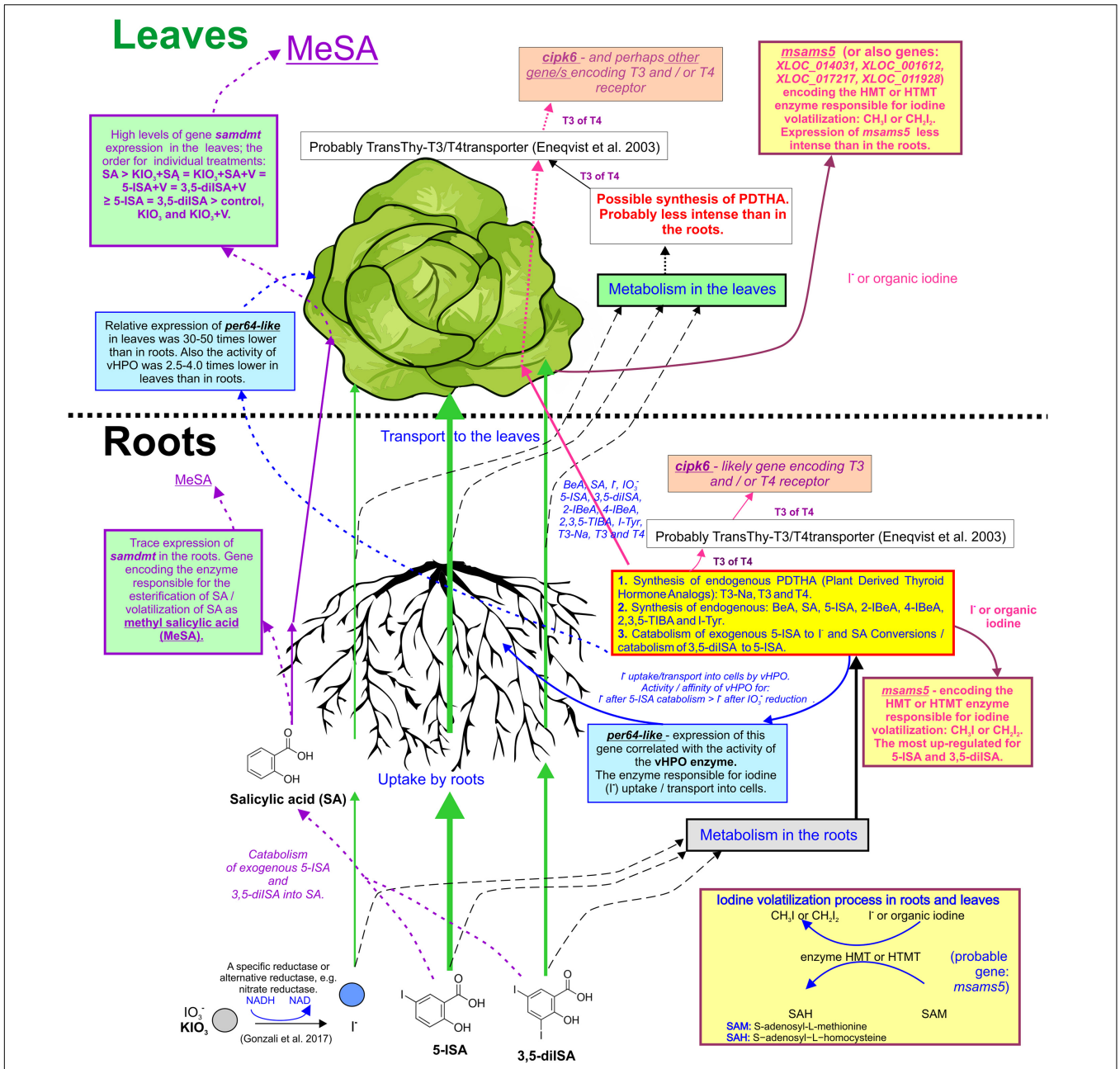


FIGURE 6 | Graphic summary of study outcomes: uptake, transport, and metabolic pathways of iodine compounds and SA. Genes with described activity and function: *Peroxidase 64-like (per64-like)*: the gene's activity has been linked to the activity/functionality of V-dependent haloperoxidase (vHPO) in roots and leaves of lettuce. *Peroxidase 12-like (per12-like)*: no correlation has been found between the gene's expression and vHPO activity in roots. *S-adenosyl-L-methionine-dependent methyltransferase (samdmt)*: gene that possibly encodes an enzyme that conducts the process of esterification/volatilization of methyl salicylic acid (MeSA). *CBL-interacting serine/threonine-protein kinase 6 (cipk6):* gene that likely encodes triiodothyronine (T3) and/or thyroxine (T4) receptors. *S-adenosylmethionine synthase 5 (msams5):* gene that possibly encodes an enzyme responsible for I volatilization in the process of methylation (synthesis of CH_3I or CH_2I_2).

HTMT was also involved in the process of methylation of [SH]- and [SCN]- groups to CH_3SH (Attieh et al., 2000).

The available literature does not name the specific gene(s) responsible for I methylation in lettuce. The results justify the assignment of the potential HMT or HTMT function to an enzyme, S-adenosylmethionine synthase 5, encoded by the *msams5* gene. Characteristics of the *L. sativa* MSAMS5 protein are shown in **Supplementary Data 3**. Significant overexpression (about 8.5-fold higher than the control) of the *msams5* gene in the roots of plants treated with exogenous 5-ISA was detected. These results and, indirectly, the total root content of I and iodine metabolites show that a protein of the

msams5-encoded enzyme may be immediately associated with I methylation by lettuce roots. Iodine volatilization through roots (with the participation of *msams5*-encoded enzyme) was higher following the application of iodosalicylates than when using KIO_3. This indicates that the enzyme protein encoded by *msams5* might have played a dominant role in I methylation in roots but not in leaves. Compared with the control, foliar expression of *msams5* was slightly, yet significantly, increased only following the application of KIO_3. Therefore, foliar expression of the *msams5* gene did not reflect the reported accumulation of I or its organic or non-organic compounds. The process of methylation (volatilization) of gaseous I from leaves probably occurred with the participation of the enzyme(s) encoded by a gene(s) other than *msams5*. On the basis of the transcriptome analysis (Kęska et al., 2019), we were able to identify other genes in lettuce leaves that may potentially be associated with synthesis of enzymes with HMT- or HTMT-like function, i.e., with the synthesis of CH_3I or CH_2I_2. The list includes the following genes described in the genome of lettuce: *S-adenosylmethionine synthase (XLOC_014031)* (Lsat_1_v5_gn_6_117861.1), *lysine-specific demethylase REF6 methyltransferase (XLOC_001612)* (Lsat_1_v5_gn_1_28820.1), *probable methyltransferase At1g27930 (XLOC_017217)* (Lsat_1_v5_gn_8_148061.1), and *histone-lysine N-methyltransferase (XLOC_011928)* (Lsat_1_v5_gn_5_154240.1).

Notably, *in vitro* emission of CH_3I, CH_3Br, and CH_3Cl by rice depended on the stadium of the plants' development (Redeker et al., 2004). Secretion of CH_3I by rice during the day was nearly twice that observed at night (Muramatsu and Yoshida, 1995; Muramatsu et al., 1995). Gonzali et al. (2017) suggested that because the structure of HMT or HTMT and other methyltransferases is homologic, they are probably involved in plant salinity tolerance or play a role in the protection of plants against diseases. The interpretation assumed in the literature is that the process of I methylation (synthesis of CH_3I or CH_2I_2) serves to detoxify plants from excess I content in tissues (Landini et al., 2012; Medrano-Macías et al., 2016; Gonzali et al., 2017). The results justify the presumption that the process of volatilization of gaseous I compounds, i.e., CH_3I or CH_2I_2 (associated with HMT- or HTMT-like enzymatic activity) may also perform a different physiological function that is not yet described in the literature.

The activity of S-adenosylmethionine synthases, including those encoded by *msams5*, requires divalent cations, such as Mg^{2+}, Mn^{2+}, or Ca^{2+}, and monovalent cations, such as K^+ or Na^+ (**Supplementary Data 3**). The V cation (VO^{2+}) may replace divalent cations at the active site of this type of enzyme (Chasteen, 1995). Morrell et al. (1986) showed that biotransformation (oxidation) of V from vanadate (VO_3^-) to vanadyl (VO_2^+) during its uptake by plants is possible. In the three experiments conducted as part of the research, V was applied as VO_3^-. The research results obtained imply that VO_3^- transformation to VO_2^+ was weaker in the presence of exogenous 5-ISA and 3,5-diISA. This is indicated by reduced activity of *msams5*, which encodes an enzyme dependent on VO_2^+ and not on VO_3^-, and decreased V uptake by roots and leaves, in particular for the 3,5-diISA+V combination (in Experiment 1).

Expression of *samdmt* Gene

The process of methylation (volatilization of methyl salicylic acid ester [MeSA]) occurs with the participation of an enzyme called salicylic acid carboxyl methyltransferase (SAMT) (Tieman et al., 2010). The synthesis of MeSA is one of the many processes in the production of SA derivatives in plants. MeSA participates in processes responsible for SAR. MeSA is volatilized from roots and overground parts of plants and can be transported by the phloem (Gao et al., 2014). The process of biosynthesis of MeSA is catalyzed by SA methyltransferases (SAMT/BSMT); the reconversion of MeSA back to SA by methyl esterase (MES, SABP2) is also possible (Park et al., 2009; Gao et al., 2014).

In our study the expression of the *S-adenosyl-L-methionine-dependent methyltransferase* gene (*samdmt)* (**Supplementary Data 4**) in lettuce leaves was clearly associated with application of exogenous SA, SA + KIO_3 (KIO_3+SA, KIO_3+SA+V), and both iodosalicylates, 5-ISA and 3,5-diISA, with or without V. We reported a significant correlation between the foliar activity of *samdmt* and (1) the **RootSec** content of SA transported from roots to leaves ($r = 0.80^*$) and (2) the foliar content of SA and 5-ISA ($r = 0.72^*$ for SA and $r = 0.77^*$ for 5-ISA). Additionally, the results of measurements of all organic I metabolites and SA in roots and leaves showed that exogenous 5-ISA and 3,5-diISA underwent at least a 2-way transformation (**Figures 5**, **6**). Conversely, 5-ISA and 3,5-diISA served as substrates in PDTHA synthesis, while they underwent a catabolic/decomposition reaction: (1) to I^- ions that could be used as substrates in CH_3I or CH_2I_2 synthesis with the participation of the *msams5*-encoded enzyme or (2) to the SA molecule. This is indicated by the elevated SA content in roots and leaves and, consequently, by an increased foliar expression of *samdmt* in plants treated with exogenous 5-ISA or 3,5-diISA. Therefore, the results justify the assignment of a SAMTase-like function (esterification of SA; volatilization of MeSA) to the *samdmt* gene. The process was probably far more intense in leaves than in roots. This was exemplified by the relatively high expression of *samdmt* in leaves and trace functionality of the gene in the roots. For this very reason, no significant correlation was found between the activity of *samdmt* and root content of SA, 5-ISA, and 3,5- diISA.

CONCLUSION

The direction of metabolic conversion of KIO_3, 5-ISA, and 3,5-diISA in plants was documented. Both iodosalicylates were applied exogenously and underwent degradation inside the plants to I ions or served as precursors of synthesis of T3 and T4, classified as PDTHAs. The assignment of the role of encoding protein receptor T3 or T4, mainly in lettuce roots, to *cipk6* was proposed.

There are reasons to believe that the *per64-like,* rather than the *per12-like* gene, may act as a V-dependent haloperoxidase (vHPO), an enzyme that participates in I uptake (expression of

per64-like gene in roots > leaves). The expression of *msams5* was sufficiently specific to link the gene to the functions of HMT/HTMT enzymes. This gene was overexpressed in roots in systems where exogenous iodosalicylates were applied. The expression of *samdmt*, in turn, makes it naturally shortlisted for the role of a gene encoding the enzyme responsible for esterification/volatilization of ethyl salicylic acid (activity: leaves > roots).

V added to the nutrient solution caused a significant reduction and growth of I content in roots, but not in leaves, for the combination of: KIO_3+SA+V vs. KIO_3+SA and 3,5-diISA+V vs. 3,5-diISA, respectively. V was mostly accumulated in roots, with its transfer to leaves being limited. The level of *per64-like* expression was correlated with root activity of vHPO.

Plant enrichment with I through 5-ISA and 3,5-diISA was more effective than that through KIO_3. The results of pot experiments indicated that the I compounds tested, including 5-ISA and 3,5-diISA, in particular, may be used in I enrichment of plants through fertigation without the fear of harming the plants. The level of plant enrichment in I was safe for consumers. This is implied by the fact that the highest HQ-I in pot studies was 0.071. Consumers' safety would be at risk if the HQ exceeded 1.0. In Experiment 1 (hydroponic system), the efficacy of I uptake from the nutrient solution was higher than in the mineral soil or peat substrate. However, in the context of balancing the reference daily allowance of I for humans, the achieved level of I accumulation (especially following application of 5-ISA) was too high [as shown by RDA-I (%) > 480%, HQ > 0.66]. This means that doses < 10 μM of I compounds can be recommended for hydroponic systems, especially where both iodosalicylates are used.

I-enriched lettuce strongly reduces the *in vitro* development of cancerous cells in colon cancer (Koronowicz et al., 2016). It seems appropriate to study the use of lettuce enriched with 5-ISA and 3,5-diISA in nutrigenomics.

DATA AVAILABILITY STATEMENT

The datasets presented in this study can be found in the online repositories. The names of the repository/repositories and accession number(s) can be found in the article/ **Supplementary Material**.

AUTHOR CONTRIBUTIONS

SS, MC, IK, and JP: methodology. SS, MC, and KK: formal analysis. SS: funding acquisition. SS, IK, MH, MG, ŁS, JP, and AK: investigation of lettuce cultivation and chemical analyses of plant, nutrient solution, and soil samples. MC, KK, and DG: investigation of molecular analyses of lettuce. SS, MC, IK, and KK: resources. SS and MC: supervision. SS, MC, and KK: writing—original draft. SS, MC, IK, KK, MH, MG, DG, ŁS, and PK: writing—review and editing. All authors contributed to the article and approved the submitted version.

FUNDING

This research was financed by the National Science Centre, Poland (Grant No. UMO-2017/25/B/NZ9/00312), "Molecular and physiological mechanisms of vanadium influence on the uptake of iodates and iodosalicylates by lettuce and its anticancer effect tested on human cell lines."

ACKNOWLEDGMENTS

The method of enriching plants with I, i.e., with 5-iodosalicylic acid and 3,5-diiodosalicylic acid, is patented by the Polish Patent Office. Patent number P.410806 (November 20, 2017).

SUPPLEMENTARY MATERIAL

The Supplementary Material for this article can be found online at: https://www.frontiersin.org/articles/10.3389/fpls.2021.653168/full#supplementary-material

Supplementary Data 1 | The functional annotation of *per12-like i per64-like* genes.

Supplementary Data 2 | The functional annotation of *cipk6* gene.

Supplementary Data 3 | The functional annotation of *msams5* gene.

Supplementary Data 4 | The functional annotation of *samdmt* gene.

REFERENCES

Afkhami, A. M., Karimi, M., Nourian, F., and SoheyL. (2009). Comparison of the effects of sodium metavanadate and zinc sulfate supplementation on lipid and glucose in patients with type 2 diabetes. *Iranian J. Diab. Obesit.* 1, 22–29.

Ajiwe, S. T., Popoola, A. R., Afolabi, C. G., Oduwaye, O. A., Ganiyu, S. A., Fajinmi, O. B., et al. (2019). Effect of iodine biofortification on incidence and severity of Fusarium wilt and yield of tomato (*Solanum lycopersicum* L.). *Nigerian J. Biotechnol.* 36, 146–151. doi: 10.4314/njb.v36i1.19

Akoumianaki-Ioannidou, A., Barouchas, P. E., Ilia, E., Kyramariou, A., and Moustakas, N. K. (2016). Effect of vanadium on dry matter and nutrient concentration in sweet basil ('*Ocimum basilicum*' L.). *Aust. J. Crop. Sci.* 10, 199–206.

Almeida, M. G., Humanes, M., Melo, R., Silva, J. A., Da Silva, J. F., and Wever, R. (2000). Purification and characterisation of vanadium haloperoxidases from the brown alga *Pelvetia canaliculata*. *Phytochemistry* 54, 5–11. doi: 10.1016/S0031-9422(99)00602-0

Anke, M., Illing-Günther, H., Gürtler, H., Holzinger, S., Jaritz, M., Anke, S., et al. (2002). Vanadium—an essential element for animals and humans? *Trace Elem. Man Anim.* 10, 221–225.

Antonyak, H. L., Panas, N. E., Pershyn, O. I, Polishchuk, A. I., and Hoyvanovych, N. K. (2018). Iodine in abiotic and biotic environments. *Biol. Stud.* 12, 117–134. doi: 10.30970/sbi.1202.567

Attieh, J., Sparace, S. A., and Saini, H. S. (2000). Purification and properties of multiple isoforms of a novel thiol methyltransferase involved in the production of volatile sulfur compounds from *Brassica oleracea*. *Arch. Biochem. Biophys.* 380, 257–[[4051]]266. doi: 10.1006/abbi.2000.1896

Basiouny, F. M. (1984). Distribution of vanadium and its influence on chlorophyll formation and iron metabolism in tomato plants. *J. Plant Nutr.* 7, 1059–1073. doi: 10.1080/01904168409363265

Blasco, B., Riosm, J. J., Cervillam, L. M., Sánchez-Rodrigezm, E., Ruizm, J. M., and Romero, L. (2008). Iodine biofortification and antioxidant capacity of lettuce: potential benefits for cultivation and human health. *Ann. Appl. Biol.* 152, 289–299. doi: 10.1111/j.1744-7348.2008.00217.x

Budke, C., thor Straten, S., Mühling, K. H., Broll, G., and Daum, D. (2020). Iodine biofortification of field-grown strawberries–APPROACHES and their limitations. *Sci. Hort.* 269:109317. doi: 10.1016/j.scienta.2020.109317

Cakmak, I., Marzorati, M., Van den Abbeele, P., Hora, K., Holwerda, H. T., Yazici, M. A., et al. (2020). Fate and bioaccessibility of iodine in food prepared from agronomically biofortified wheat and rice and impact of cofertilization with zinc and selenium. *J. Agricult. Food Chem.* 68, 1525–1535. doi: 10.1021/acs.jafc.9b05912

Cappuyns, V., and Swennen, R. (2014). Release of vanadium from oxidized sediments: insights from different extraction and leaching procedures. *Environ. Sci. Pollut. Res. Int.* 21, 2272–2282. doi: 10.1007/s11356-013-2149-0

Chasteen, N. D. (1995). Vanadium-protein interactions. *Met. Ions Biol. Syst.* 31, 231–231.

Chongkid, B., Vachirapattama, N., and Jirakiattikul, Y. (2007). Effects of vanadium on rice growth and vanadium accumulation in rice tissues. *Kasetsart J. Nat. Sci.* 41, 28–33.

Colin, C., Leblanc, C., Michel, G., Wagner, E., Leize-Wagner, E., Van Dorsselaer, A., et al. (2005). Vanadium-dependent iodoperoxidases in *Laminaria digitata*, a novel biochemical function diverging from brown algal bromoperoxidases. *JBIC J. Biol. Inor. Chem.* 10, 156–166. doi: 10.1007/s00775-005-0626-8

Colin, C., Leblanc, C., Wagner, E., Delage, L., Leize-Wagner, E., Van Dorsselaer, A., et al. (2003). The brown algal kelp *Laminaria digitata* features distinct bromoperoxidase and iodoperoxidase activities. *J. Biol. Chem.* 278, 23545–23552. doi: 10.1074/jbc.M300247200

Colmenero-Flores, J. M., Martínez, G., Gamba, G., Vázquez, N., Iglesias, D. J., Brumós, J., et al. (2007). Identification and functional characterization of cation-chloride cotransporters in plants. *Plant J.* 50, 278–292. doi: 10.1111/j.1365-313X.2007.03048.x

Dai, J. L., Zhang, M., and Zhu, Y. G. (2004). Adsorption and desorption of iodine by various Chinese soils. I Iodate. *Environ. Int.* 30, 525–530. doi: 10.1016/j.envint.2003.10.007

Dávila-Rangel, I. E., Trejo Téllez, L. I., Ortega Ortiz, H., Juárez Maldonado, A., González Morales, S., Companioni González, B., et al. (2020). Comparison of iodide, iodate, and iodine-chitosan complexes for the biofortification of lettuce. *Appl. Sci.* 10:2378. doi: 10.3390/app10072378

Davis, P. J., Shih, A., Lin, H. Y., Martino, L. J., and Davis, F. B. (2000). Thyroxine promotes association of mitogen-activated protein kinase and nuclear thyroid hormone receptor (TR) and causes serine phosphorylation of TR. *J. Biol. Chem.* 275, 38032–38039. doi: 10.1074/jbc.M002560200

Dobosy, P., Kröpfl, K., Óvári, M., Sandil, S., Németh, K., Engloner, A., et al. (2020). Biofortification of green bean (*Phaseolus vulgaris* L.) and lettuce (*Lactuca sativa* L.) with iodine in a plant-calcareous sandy soil system irrigated with water containing KI. *J. Food. Compos. Anal.* 88:103434. doi: 10.1016/j.jfca.2020.103434

Eneqvist, T., Lundberg, E., Nilsson, L., Abagyan, R., and Sauer-Eriksson, A. E. (2003). The transthyretin-related protein family. *Eur. J. Biochem.* 270, 518–532. doi: 10.1046/j.1432-1033.2003.03408.x

Fenical, W. (1975). Halogenation in the rhodophyta 1, 2 a review. *J. Phycol.* 11, 245–259. doi: 10.1111/j.1529-8817.1975.tb02775.x

Fowden, L. (1959). Radioactive iodine incorporation into organic compounds of various angiosperms. *Physiol. Plant.* 12, 657–664. doi: 10.1111/j.1399-3054.1959.tb08900.x

Gao, Q. M., Kachroo, A., and Kachroo, P. (2014). Chemical inducers of systemic immunity in plants. *J. Exp. Bot.* 65, 1849–1855. doi: 10.1093/jxb/eru010

Gil, J., Álvarez, C. E., Martinez, M. C., and Pérez, N. (1995). Effect of vanadium on lettuce growth, cationic nutrition, and yield. *J. Environ. Sci. Health Part A* 30, 73–87. doi: 10.1080/10934529509376186

Golob, A., Novak, T., Maršić, N. K., Šircelj, H., Stibilj, V., Jerše, A., et al. (2020). Biofortification with selenium and iodine changes morphological properties of *Brassica oleracea* L. var. *gongylodes*) and increases their contents in tubers. *Plant Physiol. Biochem.* 150, 234–243. doi: 10.1016/j.plaphy.2020.02.044

Gonnella, M., Renna, M., D'Imperio, M., Santamaria, P., and Serio, F. (2019). Iodine biofortification of four brassica genotypes is effective already at low rates of potassium iodate. *Nutrients* 11:451. doi: 10.3390/nu11020451

González, A., Paz, S., Rubio, C., Gutiérrez, ÁJ., and Hardisson, A. (2019). Human exposure to iodine from the consumption of edible seaweeds. *Biol. Trace Elem. Res.* 197, 361–366. doi: 10.1007/s12011-019-01996-w

Gonzali, S., Kiferle, C., and Perata, P. (2017). Iodine biofortification of crops: agronomic biofortification, metabolic engineering and iodine bioavailability. *Curr. Opin. Biotechnol.* 44, 16–26. doi: 10.1016/j.copbio.2016.10.004

Gruzewska, K., Michno, A., Pawelczyk, T., and Bielarczyk, H. (2014). Essentiality and toxicity of vanadium supplements in health and pathology. *J. Physiol. Pharmacol.* 65, 603–611.

Gust, A. A., and Nürnberger, T. (2012). From plant immunology: a life or death switch. *Nature* 486, 198–199. doi: 10.1038/486198a

Halka, M., Smoleń, S., Czernicka, M., Klimek-Chodacka, M., Pitala, J., and Tutaj, K. (2019). Iodine biofortification through expression of HMT, SAMT and S3H genes in *Solanum lycopersicum* L. *Plant Physiol. Biochem.* 144, 35–48. doi: 10.1016/j.plaphy.2019.09.028

Hayat, Q., Hakat, S., Irfan, M., and Ahmad, A. (2010). Effect of exogenous salicylic acid under changing environment: a review. *Environ. Exp. Bot.* 68, 14–25. doi: 10.1016/j.envexpbot.2009.08.005

Hue, N. V., Craddock, G. R., and Adams, F. (1986). Effect of organic acids on aluminum toxicity in subsoils. *Soil Sci. Soc. Am. J.* 50, 28–34. doi: 10.2136/sssaj1986.03615995005000010006x

Humphrey, O. S., Young, S. D., Bailey, E. H., Crout, N. M. J., Ander, E. L., Hamilton, E. M., et al. (2019). Iodine uptake, storage and translocation mechanisms in spinach (*Spinacia oleracea* L.). *Environ. Geochem. Health* 41, 2145–2156. doi: 10.1007/s10653-019-00272-z

Imtiaz, M., Ashraf, M., Rizwan, M. S., Nawaz, M. A., Rizwan, M., Mehmood, S., et al. (2018). Vanadium toxicity in chickpea (*Cicer arietinum* L.) grown in red soil: effects on cell death, ROS and antioxidative systems. *Ecotox. Environ. Safe* 158, 139–144. doi: 10.1016/j.ecoenv.2018.04.022

Incrocci, L., Carmassi, G., Maggini, R., Poli, C., Saidov, D., Tamburini, C., et al. (2019). Iodine accumulation and tolerance in sweet basil (*Ocimum basilicum* L.) with green or purple leaves grown in floating system technique. *Front Plant Sci.* 10:1494. doi: 10.3389/fpls.2019.01494

Itoh, N., Toda, H., Matsuda, M., Negishi, T., Taniguchi, T., and Ohsawa, N. (2009). Involvement of S-adenosylmethionine-dependent halide/thiol methyltransferase (HTMT) in methyl halide emissions from agricultural plants: isolation and characterization of an HTMT-coding gene from *Raphanus sativus* (Daikon radish). *BMC Plant Biol.* 9:116. doi: 10.1186/1471-2229-9-116

Jones, J. B. Jr. (2016). *Hydroponics: A Practical Guide for the Soilless Grower*, 2nd Edn. Boca Raton, FL: CRC press.

Kaplan, D. I., Adriano, D. C., Carlson, C. L., and Sajwan, K. S. (1990). Vanadium: toxicity and accumulation by beans. *Water Air Soil Pollut.* 49, 81–91. doi: 10.1007/BF00279512

Kashparov, V., Colle, C., Zvarich, S., Yoschenko, V., Levchuk, S., and Lundin, S. (2005). Soil-to-plant halogens transfer studiem 1. Root uptake of radioiodine by plants. *J. Environ. Radioact.* 79, 187–204. doi: 10.1016/j.jenvrad.2004.06.005

Kato, S., Wachi, T., Yoshihira, K., Nakagawa, T., Ishikawa, A., Takagi, D., et al. (2013). Rice (*Oryza sativa* L.) roots have iodate reduction activity in response to iodine. *Front. Plant Sci.* 4:227. doi: 10.3389/fpls.2013.00227

Keng, F. S. L., Phang, S. M., Abd Rahman, N., Elvidge, E. C. L., Malin, G., and Sturges, W. T. (2020). The emission of volatile halocarbons by seaweeds and their response towards environmental changes. *J. Appl. Phycol.* 32, 1377–1394. doi: 10.1007/s10811-019-02026-x

Kęska, K., Czernicka, M., Smoleń, S., and Kowalska, I. (2019). "Uptake of iodine in the form of KIO_3 depending on the vanadium application in lettuce: transcriptomic approach," in *Proceedings of the PLANT BIOLOGY CS 2019 Conference 27-30.08.2019*, České Budějovice.

Kiferle, C., Ascrizzi, R., Martinelli, M., Gonzali, S., Mariotti, L., Pistelli, L., et al. (2019). Effect of iodine treatments on *Ocimum basilicum* L.: biofortification, phenolics production and essential oil composition. *PLoS One* 15:e0229016. doi: 10.1371/journal.pone.0226559

Kongkiattikajorn, J., and Pongdam, S. (2006). Vanadium haloperoxidase from the red alga Gracilaria fisheri. *Sci. Asia* 32, 25–30. doi: 10.2306/scienceasia1513-1874.2006.32(s1).025

Koronowicz, A., Kopeć, A., Master, A., Smoleń, S., Piątkowska, E., Bieżanowska-Kopeć, R., et al. (2016). Transcriptome profiling of Caco-2 cancer cell line following treatment with extracts from iodine-biofortified lettuce (*Lactuca sativa* L.). *PLoS One* 11:e0147336. doi: 10.1371/journal.pone.0147336

Landini, M., Gonzali, S., Kiferle, C., Tonacchera, M., Agretti, P., Dimida, A., et al. (2012). Metabolic engineering of the iodine content in *Arabidopsis*. *Sci. Rep.* 2:338. doi: 10.1038/srep00338

Lawson, P. G., Daum, D., Czauderna, R., and Vorsatz, C. (2016). Factors influencing the efficacy of iodine foliar sprays used for biofortifying butterhead lettuce (*Lactuca sativa*). *J. Plant Nutri. Soil Sci.* 179, 661–669. doi: 10.1002/jpln.201600213

Leblanc, C., Colin, C., Cosse, A., Delage, L., La Barre, S., Morin, P., et al. (2006). Iodine transfers in the coastal marine environment: the key role of brown algae and of their vanadium-dependent haloperoxidases. *Biochemie* 88, 1773–1785. doi: 10.1016/j.biochi.2006.09.001

Lefèvre, G., Bessière, J., Ehrhardt, J. J., and Walcarius, A. (2003). Immobilization of iodide on copper (I) sulfide minerals. *J. Eviron. Radioactiv.* 70, 73–83. doi: 10.1016/S0265-931X(03)00119-X

Lima, S. T. C., Merrigan, T. L., and Rodrigues, E. D. (2012). "Synthetic and plant derived thyroid hormone analogs," in *Thyroid and Parathyroid Diseases–New Insights into Some Old and Some New Issues*, ed. L. S. Ward (London: IntechOpen), 221.

Livak, K. J., and Schmittgen, T. D. (2001). Analysis of relative gene expression data using real-time quantitative PCR and the $2^{-\Delta\Delta ct}$ method. *Methods* 25, 402–408.

Manley, S. L. (2002). Phytogenesis of halomethanes: a product of selection or a metabolic accident? *Biogeochemistry* 60, 163–180. doi: 10.1023/A:1019859922489

Medrano-Macías, J., Leija-Martínez, P., González-Morales, S., Juárez-Maldonado, A., and Benavides-Mendoza, A. (2016). Use of iodine to biofortify and promote growth and stress tolerance in crops. *Front. Plant Sci.* 7:1146. doi: 10.3389/fpls.2016.01146

Mengel, K., and Kirkby, E. A. (1996). *Principles of Plant Nutrition*. Bern: International Potash Institute.

Morrell, B. G., Lepp, N. W., and Phipps, D. A. (1986). Vanadium uptake by higher plants: some recent developments. *Environ. Geochem. Health* 8, 14–18. doi: 10.1007/BF02280116

Muramatsu, Y., and Yoshida, S. (1995). Volatilization of methyl iodide from the soil-plant system. *Atmosph. Environ.* 29, 21–25. doi: 10.1016/1352-2310(94)00220-F

Muramatsu, Y., Yoshida, S., and Bannai, T. (1995). Tracer experiments on the behaviour of radioiodine in the soil-plant-atmosphere system. *J. Radioanal. Nuclear Chem.* 194, 303–310. doi: 10.1007/BF02038428

Murphy, C. (2003). New frontiers in biological halogenation. *J. Appl. Microbiol.* 94, 539–548. doi: 10.1046/j.1365-2672.2003.01900.x

Nagatoshi, Y., and Nakamura, T. (2007). Characterization of three halide methyltransferases in *Arabidopsis thaliana*. *Plant Biotechnol.* 24, 503–506. doi: 10.5511/plantbiotechnology.24.503

Ojok, J., Omara, P., Opolot, E., Odongo, W., Olum, S., Gijs, D. L., et al. (2019). Iodine agronomic biofortification of cabbage (*Brassica oleracea* var. *capitata*) and Cowpea (*Vigna unguiculata* L.) is effective under farmer field conditions. *Agronomy* 9:797. doi: 10.3390/agronomy9120797

Pandey, V. P., Awasthi, M., Singh, S., Tiwari, S., and Dwivedi, U. N. (2017). A comprehensive review on function and application of plant peroxidases. *Biochem. Anal. Biochem.* 6, 1–16. doi: 10.4172/2161-1009.1000308

Park, S. W., Liu, P. P., Forouhar, F., Vlot, A. C., Tong, L., Tietjen, K., et al. (2009). Use of a synthetic salicylic acid analog to investigate the roles of methyl salicylate and its esterases in plant disease resistance. *J. Biol. Chem.* 284, 7307–7317. doi: 10.1074/jbc.M807968200

Pessoa, J., Sárkány, Z., Ferreira-da-Silva, F., Martins, S., Almeida, M. R., Li, J., et al. (2010). Functional characterization of *Arabidopsis thaliana* transthyretin-like protein. *BMC Plant Biol.* 10:30. doi: 10.1186/1471-2229-10-30

Piątkowska, E., Kopeć, A., Bieżanowska-Kopeć, R., Pysz, P., Kapusta-Duch, J., Koronowicz, A., et al. (2016). The impact of carrot enriched in iodine through soil fertilization on iodine concentration and selected biochemical parameters in Wistar rats. *PLoS One* 11:e0152680. doi: 10.1371/journal.pone.0152680

Pilbeam, D. J., and Drihem, K. (2007). "Vanadium," in *Handbook of Plant Nutrition*, eds A. V. Barker and D. J. Pilbeam (Boca Raton, FL: CRC Press), 585–596.

Pless, J. D., Chwirka, J. B., and Krumhansl, J. L. (2007). Iodine sequestration using delafossites and layered hydroxides. *Environ. Chem. Lett.* 5, 85–89. doi: 10.1007/s10311-006-0084-8

Pn-En 15111 (2008). *Foodstuffs – Determination of Trace Elements – Determination of Iodine by ICP-MS (Inductively Coupled Plasma Mass Spectrometry)*. Warsaw: Polish Committee of Standardization.

Power, D. M., Elias, N. P., Richardson, S. J., Mendes, J., Soares, C. M., and Santos, C. R. A. (2000). Evolution of the thyroid hormone-binding protein, transthyretin. *Gen. Comp. Endocr.* 119, 241–255. doi: 10.1006/gcen.2000.7520

Redeker, K. R., Manley, S. L., Walser, M., and Cicerone, R. J. (2004). Physiological and biochemical controls over methyl halide emissions from rice plants. *Glob. Biogeochem. Cycle* 18:GB1007. doi: 10.1029/2003GB002042

Roberts, S. K. (2006). Plasma membrane anion channels in higher plants and their putative functions in roots. *New Phytol.* 169, 647–666. doi: 10.1111/j.1469-8137.2006.01639.x

Sady, W. (2000). *Fertilizing Field Vegetables*. Krako: Plantpress.

Schlegel, M. L., Reiller, P., Mercier-Bion, F., Barré, N., and Moulin, V. (2006). Molecular environment of iodine in naturally iodinated humic substances: insight from X-ray absorption spectroscopy. *Geochim. Cosmochim. Acta* 70, 5536–5551. doi: 10.1016/j.gca.2006.08.026

Sentíes-Herrera, H. E., Trejo-Téllez, L. I., Volke-Haller, V. H., Cadena-Íñiguez, J., Sánchez-García, P., and Gómez-Merino, F. C. (2018). Iodine, silicon, and vanadium differentially affect growth, flowering, and quality components of stalks in sugarcane. *Sugar Tech.* 20, 518–533. doi: 10.1007/s12355-017-0572-0

Sgamma, T., Pape, J., Massiah, A., and Jackson, S. (2016). Selection of reference genes for diurnal and developmental time-course real-time PCR expression analyses in lettuce. *Plant Methods* 12:21. doi: 10.1186/s13007-016-0121-y

Smoleń, S., Baranski, R., Ledwożyw-Smoleń, I., Skoczylas, Ł, and Sady, W. (2019a). Combined biofortification of carrot with iodine and selenium. *Food Chem.* 300:125202. doi: 10.1016/j.foodchem.2019.125202

Smoleń, S., Kowalska, I., Czernicka, M., Halka, M., Kęska, K., and Sady, W. (2016). Iodine and selenium biofortification with additional application of salicylic acid affects yield, selected molecular parameters and chemical composition of lettuce plants (*Lactuca sativa* L. var. *capitata*). *Front. Plant Sci.* 7:1553. doi: 10.3389/fpls.2016.01553

Smoleń, S., Kowalska, I., Halka, M., Ledwożyw-Smoleń, I., Grzanka, M., Skoczylas, Ł, et al. (2020). Selected aspects of iodate and iodosalicylate metabolism in lettuce including the activity of vanadium dependent haloperoxidases as affected by exogenous vanadium. *Agronomy* 10, 1–21. doi: 10.3390/agronomy10010001

Smoleń, S., Kowalska, I., Kováčik, P., Halka, M., and Sady, W. (2019b). Biofortification of six varieties of lettuce (*Lactuca sativa* L.) with iodine and selenium in combination with the application of salicylic acid. *Front. Plant Sci.* 10:143. doi: 10.3389/fpls.2019.00143

Smoleń, S., Kowalska, I., Kováèik, P., Sady, W., Grzanka, M., and Kutman, U. B. (2019c). Changes in the chemical composition of six lettuce cultivars (*Lactuca sativa* L.) in response to biofortification with iodine and selenium combined with salicylic acid application. *Agronomy* 9:660. doi: 10.3390/agronomy9100660

Smoleń, S., Ledwożyw-Smoleń, I., Halka, M., Sady, W., and Kováčik, P. (2017). The absorption of iodine from 5-iodosalicylic acid by hydroponically grown lettuce. *Sci. Hortic.* 225, 716–725. doi: 10.1016/j.scienta.2017.08.009

Taiz, L., and Zeiger, E. (2010). "Plant physiology," in *The Benjamin Cummings Publishing Company*, 3rd Edn (Redwood City, CA: The Benjamin Cummings Publishing Company).

Tieman, D., Zeigler, M., Schmelz, E., Taylor, M. G., Rushing, S., Jones, J. B., et al. (2010). Functional analysis of a tomato salicylic acid methyl transferase and its role in synthesis of the flavor volatile methyl salicylate. *Plant J.* 62, 113–123. doi: 10.1111/j.1365-313X.2010.04128.x

Tonacchera, M., Dimida, A., De Servi, M., Frigeri, M., Ferrarini, E., De Marco, G., et al. (2013). Iodine fortification of vegetables improves human iodine nutrition: in vivo evidence for a new model of iodine prophylaxis. *J. Clin. Endoc. Methods* 98, E694–E697. doi: 10.1210/jc.2012-3509

Trumbo, P., Yates, A. A., Schlicker, S., and Poos, M. (2001). Dietary reference intakes: vitamin A, vitamin K, arsenic, boron, chromium, copper, iodine, iron, manganese, molybdenum, nickel, silicon, vanadium, and zinc. *J. Acad. Nutr. Diet* 101, 294–301.

Vachirapatama, N., Jirakiattiku, Y., Dicinoski, G. W., Townsend, A. T., and Haddad, P. R. (2011). Effect of vanadium on plant growth and its accumulation in plant tissues. *Songklanakarin J. Sci. Technol.* 33, 255–261.

Verhaeghe, E., Buisson, D., Zekri, E., Leblanc, C., Potin, P., and Ambroise, Y. (2008). A colorimetric assay for steady-state analyses of iodo-and bromoperoxidase activities. *Anal. Biochem.* 379, 60–65. doi: 10.1016/j.ab.2008.04.041

Waterborg, J. H. (2002). "The lowry method for protein quantitation," in *The Protein Protocols Handbook*, ed. J. M. Walker (Totowa, NJ: Humana Press).

Welch, R. M., and Huffman, E. W. (1973). Vanadium and plant nutrition: the growth of lettuce (*Lactuca sativa* L.) and tomato (*Lycopersicon esculentum* Mill.) plants in nutrient solutions low in vanadium. *Plant Physiol.* 52, 183–185. doi: 10.1104/pp.52.2.183

Weng, H. X., Yan, A. L., Hong, C. L., Xie, L. L., Qin, Y. C., and Cheng, C. Q. (2008). Uptake of different species of iodine by water spinach and its effect to growth. *Biol. Trace Elem. Res.* 124, 184–194. doi: 10.1007/s12011-008-8137-4

Wever, R., and Hemrika, W. (2001). "Vanadium haloperoxidases," in *Handbook of Metalloproteins*, eds A. Messerschmidt, R. Huber, T. Poulos, and K. Wieghardt (Chichester: John Wiley & Sons, Ltd).

White, P. J., and Broadley, M. R. (2001). Chloride in soils and its uptake and movement within the plant: a review. *Ann. Bot.* 88, 967–988. doi: 10.1006/anbo.2001.1540

White, P. J., and Broadley, M. R. (2009). Biofortification of crops with seven mineral elements often lacking in human diets – iron, zinc, copper, calcium, magnesium, selenium and iodine. *New Phytol.* 182, 49–84.

WHO (2001). *Vanadium Pentoxide and Other Inorganic Vanadium Compounds*. Geneva: The World Health Organization.

Yamada, H., Sugahara, M., Kosaka, H., Katayama, A., Takahashi, K., and Yonebayashi, K. (1996). Determination of total and water soluble iodine in soil by high performance liquid chromatography. *Soil Sci. Plant Nutr.* 42, 367–374. doi: 10.1080/00380768.1996.10415107

Yamaguchi, N., Nakano, M., and Tanida, H. (2005). *Transformation of Iodine Species in Soil Under Upland Field and Submerged Paddy Field Conditions*. Hyogo: Spring-8.

Yoshida, S., Muramatsu, Y., and Uchida, S. (1992). Studies on the sorption of I^- (iodide) and IO_3^- (iodate) onto andosols. *Water Air Soil Pollut.* 63, 321–329. doi: 10.1007/BF00475499

Zhang, K., Halitschke, R., Yin, C., Liu, C. J., and Gan, S. S. (2013). Salicylic acid 3-hydroxylase regulates *Arabidopsis* leaf longevity by mediating salicylic acid catabolism. *Proc. Natl. Acad. Sci. U.S.A.* 110, 14807–14812. doi: 10.1073/pnas.1302702110

Zhang, L., Mao, X., and Xia, Z. (2012). Effects of sodium metavanadate and germination on the sprouting of chickpeas and its content of vanadium, formononetin and biochanin a in the sprouts. *J. Diet Suppl.* 9, 34–44. doi: 10.3109/19390211.2011.639858

Zou, C., Du, Y., Rashid, A., Ram, H., Savasli, E., Pieterse, P. J., et al. (2019). Simultaneous biofortification of wheat with zinc, iodine, selenium, and iron through foliar treatment of a micronutrient cocktail in six countries. *J. Agr. Food Chem.* 67, 8096–8106.

Conflict of Interest: The authors declare that the research was conducted in the absence of any commercial or financial relationships that could be construed as a potential conflict of interest.

Citation: Smoleń S, Czernicka M, Kowalska I, Kęska K, Halka M, Grzebelus D, Grzanka M, Skoczylas Ł, Pitala J, Koronowicz A and Kováčik P (2021) New Aspects of Uptake and Metabolism of Non-organic and Organic Iodine Compounds—The Role of Vanadium and Plant-Derived Thyroid Hormone Analogs in Lettuce. Front. Plant Sci. 12:653168. doi: 10.3389/fpls.2021.653168

Copyright © 2021 Smoleń, Czernicka, Kowalska, Kęska, Halka, Grzebelus, Grzanka, Skoczylas, Pitala, Koronowicz and Kováčik. This is an open-access article distributed under the terms of the Creative Commons Attribution License (CC BY). The use, distribution or reproduction in other forums is permitted, provided the original author(s) and the copyright owner(s) are credited and that the original publication in this journal is cited, in accordance with accepted academic practice. No use, distribution or reproduction is permitted which does not comply with these terms.

GLOSSARY

2,3,5-triIBeA = 2,3,5-triiodobenzoic acid
2-IBeA = 2-iodobenzoic acid
3,5-diISA = 3,5-diiodosalicylic acid
4-IBeA = 4-iodobenzoic acid
5-ISA = 5-iodosalicylic acid
BeA = benzoic acid
HMT = halide methyltransferase
HPLC-ICP-MS)/MS = high-performance liquid chromatography with inductively coupled plasma mass spectrometry
HPOs = haloperoxidases
HTMT = SAM-dependent halide/thiol methyltransferase
ICP-OES = inductively coupled plasma optical emission spectrometry
I-Tyr = iodotyrosine
LC-MS/MS = liquid chromatography-mass spectrometry
MAPK = mitogen-activated protein kinase
MeSA = volatile ester of methyl salicylic acid
NFT = nutrient film technique
PDTHA = plant-derived thyroid hormone analogs
RDA = recommended dietary allowance
RootSec = secretion produced as a result of root pressure
SA = salicylic acid
SAM = S-adenosyl-l-methionine
SAMT = salicylic acid carboxyl methyltransferase
SAR = Systemic Acquired Resistance
SOM = soil organic matter
T3 = triiodothyronine
T3-Na = sodium salt triiodothyronine
T4 = thyroxine
TF = transfer factor
TMAH = tetramethylammonium hydroxide
TransThy-T3/T4trans = transthyretin, responsible for T3 and T4 transport
vHPO = vanadium-dependent haloperoxidases
per64-like = Peroxidase 64-like
per12-like = Peroxidase 12-like.
samdmt = S-adenosyl-L-methionine-dependent methyltransferase
cipk6 = CBL-interacting serine/threonine-protein kinase 6
msams5 = S-adenosylmethionine synthase 5

frontiers in Plant Science

ORIGINAL RESEARCH
published: 21 May 2021
doi: 10.3389/fpls.2021.656283

Effectiveness of Foliar Biofortification of Carrot With Iodine and Selenium in a Field Condition

Roksana Rakoczy-Lelek[1]†, Sylwester Smoleń[2,3]†, Marlena Grzanka[1,2]†, Krzysztof Ambroziak[1]†, Joanna Pitala[3]†, Łukasz Skoczylas[4]†, Marta Liszka-Skoczylas[5]† and Hubert Kardasz[1]*

[1] Intermag Sp. z o.o., Olkusz, Poland, [2] Department of Plant Biology and Biotechnology, Faculty of Biotechnology and Horticulture, University of Agriculture in Kraków, Kraków, Poland, [3] Laboratory of Mass Spectrometry, Faculty of Biotechnology and Horticulture, University of Agriculture in Kraków, Kraków, Poland, [4] Department of Plant Product Technology and Nutrition Hygiene, Faculty of Food Technology, University of Agriculture in Kraków, Kraków, Poland, [5] Department of Engineering and Machinery for Food Industry, Faculty of Food Technology, University of Agriculture in Kraków, Kraków, Poland

Iodine (I) and selenium (Se) are essential to human and animal development. There is a worldwide deficit of I and Se in the diet of humans, as well as in animals. It is advisable to enrich plants with these elements to ensure adequate uptake in animals and humans. The aim of this study was to determine the efficacy of the application of I and Se in the cultivation of carrot crops, to better understand the metabolic pathways and processes of I applied through foliar spray. Carrots were fertilized with 4-fold foliar applications of I and Se, which were applied as the liquid fertilizers "I + Se", "Solo iodine" and "Solo selenium", all containing an organic stabilizer, in two field trials. Foliar nutrient applications of I and Se were translocated by the plant for storage in the roots. The level of enriched I and Se in the roots was considered safe for the consumer. The Recommended Daily Allowance values for I and Se in the roots of 100 g of fresh carrots are 4.16% and 4.37%, respectively. Furthermore, I and Se accumulated in the roots to a level that was physiologically tolerated by carrot. Biofortification through foliar feeding did not impact negatively on the yield or quality of the carrot crop. Iodides applied via foliar application were the dominant form of I in the plant tissues and were included in the metabolic process of the synthesis of iodosalicylates, iodobenzoates, iodotyrosine (I-Tyr), and plant-derived thyroid hormone analogs. No synergistic or antagonistic interaction between I and Se, with respect to the effectiveness of biofortification in roots, was observed in any treatments. The molar ratio of I:Se in the roots after foliar application of both elements was approximately 1.6:1 and was similar to the control (1.35:1).

Keywords: selenium, iodine, biofortification, carrot, foliar application dates

OPEN ACCESS

Edited by:
Spyridon Alexandros Petropoulos, University of Thessaly, Greece

Reviewed by:
Debjyoti Sen Gupta, Indian Institute of Pulses Research (ICAR), India
Massimiliano D'Imperio, Institute of Sciences of Food Production, Italian National Research Council, Italy

***Correspondence:**
Roksana Rakoczy-Lelek
roksana.rakoczy@intermag.pl

†ORCID:
Roksana Rakoczy-Lelek
orcid.org/0000-0002-9782-3200
Sylwester Smoleń
orcid.org/0000-0001-8093-3801
Marlena Grzanka
orcid.org/0000-0002-3810-6906
Joanna Pitala
orcid.org/0000-0001-5906-4402
Łukasz Skoczylas
orcid.org/0000-0002-8349-4477
Marta Liszka-Skoczylas
orcid.org/0000-0001-7281-3711
Krzysztof Ambroziak
orcid.org/0000-0001-7978-2866

Specialty section:
This article was submitted to Plant Nutrition, a section of the journal Frontiers in Plant Science

Received: *20 January 2021*
Accepted: *23 March 2021*
Published: *21 May 2021*

Citation:
Rakoczy-Lelek R, Smoleń S, Grzanka M, Ambroziak K, Pitala J, Skoczylas Ł, Liszka-Skoczylas M and Kardasz H (2021) Effectiveness of Foliar Biofortification of Carrot With Iodine and Selenium in a Field Condition. Front. Plant Sci. 12:656283. doi: 10.3389/fpls.2021.656283

Abbreviations: I-Tyr, iodotyrosine; PDTHA, plant-derived thyroid hormone analogs; RDA, Recommended Daily Allowance; RDA-I, Recommended Daily Allowance for iodine; RDA-Se, Recommended Daily Allowance for selenium; HQ, hazard quotient; SA, salicylic acid; BeA, benzoic acid; 5-ISA, 5-iodosalicylic acid; 3,5-diISA, 3,5-diiodosalicylic acid; 2-IBeA, 2-iodobenzoic acid; 4-IBeA, 4-iodobenzoic acid; 2,3,5-triIBeA, 2,3,5-triiodobenzoic acid; T3, triiodothyronine; T4, thyroxine; D.W., dry weight; F.W., fresh weight.

INTRODUCTION

Iodine (I) and selenium (Se) are micronutrients that are essential for proper functioning of humans and animals (Gonzali et al., 2017; Márquez et al., 2020). Both of these microelements are required for the optimal synthesis of the thyroid hormones, thyroxine (T4) and triiodothyronine (T3) (Zimmermann, 2011; Mehdi et al., 2013). I deficiency causes severe health problems that affect approximately 1.5 billion people worldwide (White and Broadley, 2005; Blasco et al., 2012; Choudhry and Nasrullah, 2018). Roughly 15% of the global population is afflicted with diseases caused by Se deficiency, and 500 million to 1 billion people are exposed to a Se-deficient diet (Athar et al., 2020; Márquez et al., 2020). The Recommended Daily Allowance (RDA) for I and Se depends on age and gender and amounts to 90–250 μg I per day (Gonzali et al., 2017) and 60–70 μg Se per day (Mehdi et al., 2013).

I and Se are considered beneficial plant elements. However, they are not classified as essential for the metabolism of vascular plants (Pilon-Smits et al., 2009; Gonzali et al., 2017). Se is the only essential micronutrient for plants classified as a hyperaccumulator of Se (Pilon-Smits et al., 2009). This positive effect of Se was confirmed in studies on ryegrass, tomato, and lettuce, which are crop plants that are not Se hyperaccumulators (Hartikainen, 2005; Pilon-Smits et al., 2009). In contrast to I, Se is effective in stimulating growth and plant development (Xue et al., 2001; Hartikainen, 2005). Se protects cell membranes against lipid peroxidation influences on tocopherol levels (Xue et al., 2001; Hartikainen, 2005), increases the activity of glutathione peroxidase (GPX) (Xue et al., 2001; Hartikainen, 2005; Pilon-Smits et al., 2009), and increases resistance to ultraviolet light (Mostafa and Hassan, 2015). Indian mustard (*Brassica juncea*) plants grown with Se showed repellent properties against herbivory by caterpillars (*Pieris rapae*) (Hanson et al., 2003).

Both inorganic and organic forms of Se are taken up by plants (Sors et al., 2005; Winkel et al., 2015; Smoleń et al., 2016b). The inorganic form of Se is selenate (SeO_4^{2-}), which is effectively taken up by the roots, transported through the phloem and xylem, and accumulated in shoots and leaves (Winkel et al., 2015). Selenate levels are reduced after being absorbed by the leaves, and Se is involved in protein metabolism, resulting in the production of selenoproteins (Sors et al., 2005; Mehdi et al., 2013). Selenate and its organic combinations are bioavailable forms and are actively taken up via the sulfate pathway by sulfate transporters (Sors et al., 2005; Pilon-Smits et al., 2009; White and Broadley, 2009).

The uptake of I from the soil is not as effective as in the case of Se. I is present in the soil in the form of inorganic salts, such as iodide (I^-), iodate (IO_3^-), and organic molecules (White and Broadley, 2009). The availability and mobility of I in the soil depend on the soil conditions and its physicochemical properties (Amachi, 2008). In most of the types of soil, I is not available for the plants. Soils that are fertile and rich in organic matter (humus) have a significant effect on limiting the bioavailability of inorganic I present in the soil (White and Broadley, 2005; Dai et al., 2009). Acidic soils containing aluminum and iron ions also reduce the bioavailability of I. Mainly soils with a neutral pH provide the best conditions for I mobility. The forms in which I occurs in the soil depend on the soil conditions. Iodides dominate in low pH and redox conditions, whereas iodates are common in oxidative conditions and soils with a neutral to alkaline pH (White and Broadley, 2009; Blasco et al., 2012).

Another important limiting factor in the enrichment of plants with I is low I mobility in the phloem that results in difficulties in the effective enriching of cereals, rice, and maize and low I accumulation in grain (Blasco et al., 2012). The most effective accumulation of I is observed when I is transported by xylem. Therefore, enrichment with I is most effective in leafy vegetables (Mackowiak and Grossl, 1999; Blasco et al., 2012).

Generally, the uptake of I by the roots from the soil and transport to the generative plants organs is limited. Therefore, various agrotechnical methods for biofortification with I and Se of crops have been developed. One of these methods is foliar application, which is more effective than soil fertilization.

Signore et al. (2018) showed that foliar application of high doses of I (500 mg · L^{-1}) did not have phytotoxic effects on the leaves of carrots cultivated in the field. Foliar fertilization with potassium iodate (KIO_3) (at a high dose of 500 mg · L^{-1}) of carrots cultivated in a greenhouse did not show the significant I enrichment effect seen in foliar application of the same dose in carrots cultivated in the field. However, the addition of KIO_3 in lower doses (50 mg · L^{-3}) to the nutrient solution resulted in significant enrichment of I in carrot roots, as well as in visible phytotoxic properties present on the leaves.

Research in a field of biofortification of plants with simultaneous applications of I and Se has been undertaken in several crops such as lettuce (Sahin, 2020), buckwheat and pumpkin sprouts (Germ et al., 2015), kohlrabi (Golob et al., 2020), and Indian mustard (Golubkina et al., 2018). The experiments were carried out in pots, using hydroponic systems under field conditions. Most of the research was focused on enriching plants with I and Se through soil fertilization or hydroponic system with a nutrient solution. There was no effect on the uptake and accumulation of these elements by plants, based on the simultaneous application of I and Se (Zhu et al., 2004; Sahin, 2020).

Foliar biofortification of cereals (including wheat and rice) with I and Se has been widely studied (Zou et al., 2019; Cakmak et al., 2020). Protocols for carrot biofortification through soil fertilization with I and Se have been also compiled (Smoleń et al., 2016a, 2019). However, little is known about carrot enrichment with I and Se via foliar application. Additionally, the organic I metabolites that may be present in the leaves and roots of the carrot plant have not yet been determined.

In this article, the efficacy of carrot biofortification with I and Se through foliar application has been studied.

This study was aimed at determining the effect of the foliar application of both I and Se on the biofortification efficiency in the roots of the carrot plant. The efficacy of I and Se accumulation was assessed in the carrot plant after the foliar application of the formulations "Solo iodine" containing only I, "Solo selenium" containing only Se, and the newly developed fertilizer "I + Se". Hypothesis whether I and Se could be uptaken by the leaves and effectively transported to the storage root has been investigated.

The extent to which organic forms of I, such as iodosalicylates, iodobenzoates, and iodotyrosine (I-Tyr), as well as plant-derived thyroid hormone analogs (PDTHAs), such as T3 and T4, were metabolized in the carrot after foliar application of I and Se was investigated.

PLANT MATERIAL AND TREATMENTS

Study Design

Two field trials were undertaken in 2019 and 2020, respectively, for the carrot (*Daucus carota* L.) cultivar "Octavo F_1". The carrots were cultivated on a farm specializing in the cultivation of root vegetables in southeastern Poland. This carrot variety is harvested in autumn for the fresh market. Wheat was the forecrop each year, and carrots were cultivated in a soil with high clay content (**Table 1**). The soil was characterized by a low electrical conductivity (EC) and low levels of mineral nitrogen (N) before cultivation. The soil had low potassium (K) levels and optimal magnesium (Mg) levels for cultivation of carrots over both years. In 2020, the content of calcium (Ca) and organic matter was naturally higher than in 2019. Each year, NPK was added as a fertilizer to the soil before sowing (applied at levels of 100 mg N · dm^{-3}, 80 mg phosphorus (P) · dm^{-3}, 200 mg K · dm^{-3}), to supplement the levels of N, P, and K, which are essential elements for optimal growth of carrots (Sady, 2006). Commercially available fertilizers were used, which comprised 50% of K as potassium sulfate (Siarkopol Tarnobrzeg, Poland) and 50% of K as potassium chloride (Zakład Obrotu Towarami Sp. z o.o., Dwikozy, Poland), Polifoska 5 (Grupa Azoty, Zakłady Chemiczne Police SA, Poland), and the N fertilizer Sulfamo, with 23% N (Timac Agro, Roullier Group, France). Chemical plant protection against weeds, diseases, and pests was applied in accordance with the current plant protection program in Poland. Carrots were sowed in raised beds in single rows, 40 cm wide and 30 cm high, at a seeding rate of approximately 1.6 million seeds per hectare. The seeds were sown on April 30, 2019, and April 15, 2020.

The study included foliar biofortification of carrots with I and Se (applied together and separately), using the newly developed water-soluble liquid concentrate fertilizers "I + Se", "Solo iodine" and "Solo selenium" (**Table 2**). An untreated crop was included as the control in the experiments. The methods for conducting the experiment are described in **Table 2**. Four foliar applications of fertilizers were applied to the carrot crop at the following doses: 200 g I + 10 g Se · ha^{-1}, 400 g I + 20 g Se · ha^{-1}, 200 g I · ha^{-1}, 400 g I · ha^{-1}, 5 g Se · ha^{-1}, and 10 g Se · ha^{-1}. The field trials were conducted in a split-plot design with four repetitions per treatment and a plot size of 10 m^2. Foliar fertilization was applied in the morning during fine weather.

In the study, 5 g I and 10 g Se · ha^{-1} were tested using an application of "Solo selenium" (Se-alone fertilizer). Doses of 10 g and 20 g Se · ha^{-1} were used for the combined application of I and Se, whereas the 5 g Se · ha^{-1} dose was not tested. In screening test carried out in the greenhouse on carrot plants, it was observed that the foliar application of Se in doses of 10 and 20 g of Se combined with I had a similar effect on Se accumulation in plants as the foliar application of Se in doses of 5 and 10 g Se · ha^{-1} (the obtained results are presented in the **Supplementary Table 1**). Field trials were conducted under commercial conditions at the agricultural research farm over 2 years to determine the effects on carrot plants.

The fertilizers used in the field trials were developed based on the research project called "Modern agrochemical preparations based on biodegradable ligands and other natural compounds stimulating resistance, enabling plant biofortification, intended to be used as a part of Integrated Plant Production", which was co-financed by the European Union via the European Regional Development Fund under the Smart Growth Operational Program 2014–2020. The project was implemented under the National Centre for Research and Development: Szybka Ścieżka, project no. POIR.01.01.01-00-0024/15 (Intermag Sp. z o.o., Olkusz, Poland). The studies described in the publication were preceded by the formulation of an appropriate concentration of I and Se in liquid fertilizers, with addition of an organic stabilizer/enhancer® (biodegradable stabilizer). The research and development for the formulation consisted of screening test on carrot and the determination of safe concentrations of I and Se in working solution for plants. The results of the test made it possible to develop a protocol of foliar biofortification of carrot plants with I and Se, which detail the safe dosage per hectare, required concentrations of I and Se in working solution, and recommended application dates. This study describes the final stage of research and testing for the efficacy of fertilizers for carrot biofortification (enrichment) with I and Se.

The total yield of leaves and roots harvested, as well as the average weight of roots and leaves from single plants, was measured (**Table 2**). Roots were sorted into marketable and non-marketable yields, according to the criteria described by Smoleń et al. (2019). At harvest, samples of approximately 5 kg of carrot roots of marketable yield were chosen from each plot for laboratory analysis (allowing for repetition). Samples of healthy, fully developed leaves with a mass of approximately 0.2 kg were collected from each replicate.

TABLE 1 | The chemical properties of the soil prior to carrot cultivation.

Physicochemical soil characteristic	Year 2019	Year 2020
$pH_{(H2O)}$	6.48	7.50
EC (mS · cm^{-1})	0.48	0.14
Macroelements:		
N-NH_4 (mg · dm^{-3})	6.0	0.29
N-NO_3 (mg · dm^{-3})	3.0	8.81
N-NH_4 + N-NO_3 (mg · dm^{-3})	9.0	9.0
P (mg · dm^{-3})	60.0	33.2
K (mg · dm^{-3})	134.0	136.9
Mg (mg · dm^{-3})	70.0	105.5
Ca (mg · dm^{-3})	1,520.0	4,585.2
Soil organic matter (%)	0.80	1.72
Type of soil	Heavy soil	Heavy soil

TABLE 2 | Experimental treatments of foliar application (foliar biofortification) of carrot with iodine and selenium–the methodological information.

Treatments of foliar application: the total dose of I and/or Se in four applications	**Type of fertilizer[1] and way dosage of I and Se**
Control	Without fertilizer–spray only with water
200 g I + 10 g Se · ha^{-1}	0.25 dm^3 "I + Se^{2}" · ha^{-1} per one application × four applications = 1.0 dm^3 "I + Se" · ha^{-1} "I + Se" liquid fertilizer containing iodine and selenium in the form I^- and SeO_4^{2-} with organic stabilizer/enhancer®. Concentration of iodine and selenium in "I + Se", respectively, 15.7% wt/vol and 0.79% wt/vol Molar mass ratio of I:Se in the fertilizer = 12.4:1
400 g I + 20 g Se · ha^{-1}	0.5 dm^3 "I + Se" · ha^{-1} per one application × four applications = 2.0 dm^3 "I + Se" · ha^{-1}. Other information as above
200 g I · ha^{-1}	0.25 dm^3 "Solo $iodine^{2}$" · ha^{-1} per one application × four applications = 1.0 dm^3 "Solo iodine" · ha^{-1} "Solo iodine": liquid iodine fertilizer in form I^- with organic stabilizer/enhancer Concentration of iodine 16.6% wt/vol
400 g I · ha^{-1}	0.5 dm^3 "Solo iodine" · ha^{-1} per one application × four applications = 2.0 dm^3 "Solo iodine" · ha^{-1} Other information as above
5 g Se · ha^{-1}	0.125 dm^3 "Solo $selenium^{2}$" · ha^{-1} per one application × four applications = 0.5 dm^3 "Solo selenium" · ha^{-1} "Solo $selenium^{2}$": liquid selenium fertilizer in form SeO_4^{2-} with organic stabilizer/enhancer Concentration of selenium 0.95% wt/vol
10 g Se · ha^{-1}	0.25 dm^3 "Solo $selenium^{2}$" · ha^{-1} per one application × four applications = 1.0 dm^3 "Solo selenium" · ha^{-1} Other information as above
Schedule and method of foliar application for each treatment of foliar application	
Quantity and dates (growth phase) of foliar application in 2019 and 2020	1st BBCH 16–first decade of July 2nd BBCH 21–end of July 3rd BBCH 35–mid August 4th BBCH 42–end of August
The amount of working solutions	500 dm^{-3} · ha^{-1}–tap water was used in the control and tested combinations
Sprayer type	Foliar treatments on plots performed with a manual, pneumatic pressure sprayer
Date of completion of the field experiment—carrot harvest	First half of September of 2019 and 2020; BBCH 46-48 phase. Carrot harvest, yield evaluation and sampling of leaves and roots for chemical analysis

1: Surfactants ADITENS MAX (Intermag Sp. z o.o., Olkusz, Poland) were used in the control and in each treatment with the foliar application of iodine and/or selenium.
2: "I + Se", "Solo iodine" and "Solo selenium"–experimental liquid fertilizers for foliar feeding developed in the project entitled "Modern agrochemical preparations based on biodegradable ligands and other natural compounds stimulating resistance, enabling plant biofortification, intended to be used as a part of Integrated Plant Production," which was co-financed by the European Union from the European Regional Development Fund under Smart Growth Operational Program 2014–2020. Project implemented as part of the competition of the National Centre for Research and Development: Szybka Ścieżka, project no. POIR.01.01.01-00-0024/15, implemented by Intermag Sp. z o.o., Olkusz, Poland. Fertilizers at the registration stage. Fertilizers are stable and maintain the initial content of I and/or Se during storage over 2 years' time in a tightly closed containers.
Organic stabilizer/enhancer® (the same stabilizer for iodine and selenium) is proprietary, the know-how of the producer of these fertilizers, i.e., Intermag Sp. z o.o., Olkusz, Poland. Stabilizer/enhancer® of I and Se is based on a mixture of organic compounds occurring exogenously in the plants.

Plant Analyses

The leaves and roots were washed in tap water before analysis. The samples of fresh roots and leaves were then homogenized. The dry weight content in these samples was determined using the oven-drying method, at 105°C. The content of total carotenoids in the fresh homogenized roots, extracted with acetone/n-hexane (4:6), was determined using spectrophotometry. Total dissolved solids (% Brix) in roots were measured using the Atago Palette PR-32, a digital refractometer. The analyses were performed using the methods described by Smoleń et al. (2014b, 2019).

Total sugars, as a sum of glucose, fructose, and sucrose, were measured in the ethanol extracts, using the reverse capillary electrophoresis technique with the PA 800 Plus system (Beckman Coulter, United States). Capillaries of ø 50 μm and total length of 60 cm (10 cm for detection) were used. A positive power supply of 15 kV was applied, and the temperature was set at 25°C. The running buffer solution comprised 20.0 mmol/L sorbic acid, 0.20 mmol/L CTAB, and 40 mmol/L NaOH, pH 12.2 (Rizelio et al., 2012).

In addition, approximately 400 g (fresh weight) of a homogenized sample of leaves and roots was frozen at −20°C and then dried by lyophilization. A freeze dryer was used, namely, the PG90-Lx4/14 type LIOex-4/330-A4 (ARTVAC-Plus, Męcina, Krzeszowice, Poland). After drying, the samples were ground in a laboratory mill using a Pulverisette 14 Fritsch (Idar-Oberstein, Germany) variable speed rotor mill, with a 0.5-mm sieve. The Se and I content of the dried leaves and roots was analyzed with an inductively coupled plasma–tandem mass spectrometry (ICP-MS/MS) triple quadruple spectrometer (iCAP TQ ICP-MS

Thermo Fisher Scientific, Bremen, Germany). The Se content was determined after microwave mineralization. Samples (0.1 g) were placed into 55 mL TFM vessels and were mineralized in 10 mL 65% super pure HNO_3 (Merck no. 100443.2500), in a Mars 5 Xpress (CEM, United States) microwave digestion system (Kalisz et al., 2019). The I content was determined after extraction using tetramethylammonium hydroxide (TMAH) (Sigma–Aldrich Co., LLC, St. Louis, MO, United States), according to the Polish Standard-European Standard procedure (European Standard Norme Européenne Europäische Norm, 2008) with modifications described by Smoleń et al. (2019).

Speciation of I, i.e., iodides and iodates, was analyzed in the dried samples of roots and leaves, using high-performance liquid chromatography (HPLC)–ICP-MS/MS. The content of these two I ions was measured using a modified extraction procedure described by Smoleń et al. (2016c), whereby 0.05 g of air-dried, ground plant samples were mixed with an extraction solution containing 4 cm^3 of 25% TMAH (Sigma–Aldrich Co., LLC) and 10 cm^3 0.1 M NaOH (Chempur, Piekary Śląskie, Poland), in 1 dm^3 of demineralized water. The samples were placed in 7-mL polypropylene tubes, whereupon 5 mL of the extraction mixture was added. Once mixed, the samples were incubated for 1 h at 50°C in an ultrasonic bath and then cooled to approximately 20°C, mixed thoroughly, and centrifuged for 15 min at 4,500 revolutions/min. The supernatants were filtered through a 0.22-μm syringe filter. The content of I ions in filtered samples was analyzed using HPLC–ICP-MS/MS. For I^- and IO_3^- speciation forms, HPLC (Thermo Scientific Ultimate 3000; Thermo Fisher Scientific, Bremen, Germany) was coupled to ICP-MS/MS (iCAP TQ). This method employed a strong anion exchange column (Thermo Scientific; Dionex IonPac AS11 [4 × 250 mm]) and a pre-column (Thermo Scientific; Dionex IonPac AG11 [4 × 50 mm]). The column temperature was set to 30°C. Demineralized water, 50 mM NaOH, and 0.5% TMAH were used as eluents. To separate both I ions, a mobile phase was used, containing 2.5 mM NaOH and 0.125% TMAH with an isocratic flow. The flow rate was 1.5 mL/min, with an injection volume of 10 μL, and total analysis time of 7 min. The 127I.16O isotope of I was determined, using the S-TQ-O2 mode. Standards were prepared through dissolution of KI and KIO_3 (Sigma–Aldrich Co., LLC) in demineralized water.

Leaves and roots were analyzed for salicylic acid (SA), benzoic acid (BeA), iodosalicylates [5-iodosalicylic acid (5-ISA) and 3,5-diiodosalicylic acid (3,5-diISA)], iodobenzoates [2-iodobenzoic acid (2-IBeA), 4-iodobenzoic acid (4-IBeA), 2,3,5-triiodobenzoic acid (2,3,5-triIBeA)], I-Tyr, and PDTHA such as T3 and T4, using the liquid chromatography (LC)–MS/MS system after extraction with 75% ethanol (Smoleń et al., 2020). Measurements were made using the HPLC Ultimate 3000 system (Thermo Scientific) and an LC-MS/MS: 4500 Qtrap, Sciex spectrometer. Chromatographic separation was carried out on a Luna 3 μm phenyl-hexyl 100 Å (150 × 3 mm, internal diameter 3 μm) column (Phenomenex, Torrance, CA, United States). Electrospray ionization in negative ion mode was used. MS/MS was performed for quantitative analysis. The transitions monitored for SA, BeA, 5-ISA, 3,5-diISA, 2-IBeA, 4-IBeA, 2,3,5-triIBeA, I-Tyr, TransThy-T3/T4trans (T3 and T4 proteins), and for SA-d4 were 136.8/93.1, 120.9/76.9, 262.9/126.7, 388.8/126.7, 246.9/126.6, 246.9/144.7, 498.7/454.4, 306.1/126.8, 649.9/632.7, 775.7/574.6, and 141/96.8, respectively. The LC-MS/MS system was controlled using Analyst 1.7 with HotFix 3 software, which was also used for data processing. Analysis of the content of SA and BeA, I derivatives of these acids, and PDTHA in leaves and roots was performed for three selected treatments, i.e., the control and foliar application of "I + Se" (200 g I + 10 g Se · ha^{-1}) and "Solo iodine" (200 g I · ha^{-1}). These treatments were selected to determine the preferred pathways of I metabolism in plants after foliar application of this element. In addition, these treatments were selected to determine whether, and to what extent, the additional application of Se affects metabolism of I in leaves and roots.

The transmittance method in the CIE*Lab* system was used to measure the color of roots of carrot plants (Wrolstad and Smith, 2017), using a Konica Minolta CM-3500d spectrophotometer (Konica Minolta Sensing, Osaka, Japan). This system used the reflectance method, with the illuminant D65 in a Petri dish (6 cm in diameter and 4 cm in height), at an observer angle of 10°. This allowed for measurement of values for the parameters of L^* (lightness), a^* (redness), and b^* (yellowness). The indices ΔE^* (total color difference), ΔC^* (total saturation difference), and ΔH^* (total hue difference) were also calculated.

Color changes between the biofortified and unfortified samples of carrot roots were expressed as the total color difference (ΔE^*). This parameter was calculated as the Euclidean distance between two points in the three-dimensional space determined by L^*, a^*, and b^* using the following formula:

$$\Delta E^*_{ab} = \sqrt{\Delta a^{*2} + \Delta b^{*2} + \Delta L^{*2}}$$

where Δa^*, Δb^*, and ΔL^* are the differences between the reference and analyzed sample. The quantitative attribute of color is Chroma (C^*), which was calculated using following equation:

$$C^* = \sqrt{a^{*2} + b^{*2}}$$

whereas ΔC^* is the difference between the C^* parameter value obtained for the analyzed sample and the reference.

Total hue difference (ΔH^*) was determined according to the following formula:

$$\Delta H^* = \sqrt{(\Delta E^*)^2 - (\Delta L^*)^2 - (\Delta C^*)^2}$$

that calculated the indices of color, averaged over 20 measurements for each replication of each experimental treatment.

The results of the color parameters were interpreted in accordance with the criteria established by the International Commission on Illumination (CIE) (Hutchings, 1999).

Eight individual soil samples were randomly collected from the study area. Soil samples were taken from the 0- to 30-cm layer, to allow for characterization of the chemical properties of the soil prior to the start of the study (**Table 1**). The description of these results is presented in section "Results".

The following procedures were used for soil samples analyses: pH was measured potentiometrically in soil samples mixed with

water (1:2 vol/vol, soil:H_2O), and the EC was analyzed using a conductivity meter. After extraction with 0.03 M acetic acid, the concentrations of P, K, Mg, and Ca were determined with the ICP-OES technique (Nowosielski, 1988). The extracts were also used to determine the concentrations of N minerals in the form of N-NH_4 and N-NO_3 using the AQ2 discrete analyzer (SEAL Analytical, Mequon, WI, United States), based on the protocol developed by the manufacturer. The organic matter in the soil was determined using the Tiurin method (Nowosielski, 1988; Komornicki et al., 1991).

Meteorological Data

The average daily temperature from April to September in 2019 and 2020 was similar. In the 2019, the warmest month was June, and in 2020, it was August (**Table 3**). The largest difference in the average daily temperature between 2019 and 2020 was in June. Rainfall from April to September in the 2019 was higher by 64.8 mm (17%), compared to 2020. In the 2020, rainfall was evenly distributed from April to September. In 2019, June had the lowest average rainfall (14.5 mm), and May and August had the highest rainfall, with 131.7 and 128.7 mm, respectively.

Biofortification Targets Based on Consumer Safety for I and Se Enriched Carrots

The percentage of the RDA for I (RDA-I) and Se (RDA-Se) in 100-g portions of the roots of fresh carrots was calculated, based on chemical analyses of the roots. In addition, the molar ratio of I:Se in fresh carrot roots was calculated, dependent on the foliar application of I, as well as the hazard quotient (HQ). The intake of I and Se was calculated based on the consumption of 100 g of fresh carrot roots by adults (average of 70-kg body weight). All of the calculations were based on the methods described by Smoleń et al. (2019).

TABLE 3 | Meteorological data for the carrot cultivation period in 2019 and 2020.

Month	Monthly mean daily air temperature (°C)	
	Year 2019	Year 2020
April	8.49	6.08
May	11.44	10.25
June	20.33	17.09
July	18.54	18.19
August	17.27	19.42
September	13.69	14.47
Mean	14.96	14.25
	Monthly sum of rainfall (mm)	
April	59.1	23.0
May	131.7	76.2
June	14.5	71.8
July	22.0	55.7
August	128.7	82.9
September	78.4	60.0
Sum	434.4	369.6

Data Analysis

TIBCO Software Inc. (2017). Statistica (data analysis software system), version 13.3 PL https://www.statsoft.pl/, was used for analysis of variance (ANOVA) by ANOVA module. The Tukey test was used for determining the significance between the means at $p < 0.05$.

RESULTS

Carrot Yield

No statistically significant effects of foliar applications of I, Se, and I + Se, applied in two doses, were observed for the yield of leaves and roots, the marketable yield as a percentage of the total yield, or the average weight of roots and leaves from one plant, compared to the control (**Table 4**).

Content of I and Se in the Carrot Plants and Consumer Safety

Foliar application of the I fertilizer "Solo iodine" and the I-Se fertilizer "I + Se" resulted in a significant increase in the total content of I (I-total) and of iodide (I^-) ions in the leaves and roots of carrot plants (**Figure 1**). When a higher I dose of 400 g I · ha^{-1}, rather than 200 g I · ha^{-1}, of both fertilizers was applied, there was a proportional increase in the accumulation of I-total and I^- in the leaves and roots. Similar increases in I-total and I^- accumulation were observed in the roots after the application of the same doses of I (200 and 400 g I · ha^{-1}, respectively) with the "I + Se" and "Solo iodine" fertilizers. A significant increase in the accumulation of I-total and I^- was observed in the leaves after application of "I + Se" (400 g I · ha^{-1}), which was approximately 17% greater than was observed after the application of "Solo iodine". This was not the case when doses of 200 g I · ha^{-1} were applied. The levels of I-total in all foliar applications of "I + Se" and "Solo iodine" were 10–20 times higher in the leaves than in the roots.

There was a significant increase in the levels of Se in the leaves and roots compared to the control, after the plants were sprayed with the "I + Se" and "Solo selenium" fertilizers (**Figure 1**). The Se content in leaves and roots increased proportionally to increasing concentrations of Se (5 and 10 g of Se · ha^{-1}), applied as the fertilizer "Solo selenium". Application of 10 g Se · ha^{-1} with "Solo selenium" and "I + Se" had similar effectiveness in enriching the roots and leaves with Se. The use of the "I + Se" at a dosage of 20 g Se · ha^{-1}, compared with 10 g Se · ha^{-1}, resulted in a 2-fold increase in the levels of Se in leaves and roots. The levels of Se in the roots were approximately 4.5-fold lower than in the leaves in plants treated with the foliar fertilizers "Solo selenium" and "I + Se".

Foliar applications of "Solo selenium" and "Solo iodine" did not show any significant changes in the levels of I and Se in leaves and roots, respectively, when compared to the control (**Figure 1**).

Consumption of 100 g of fresh carrot roots from plants enriched with I from the fertilizer "I + Se" could provide between 1.96 and 4.19% of RDA-I and 1.98 and 4.37% of RDA-Se for the lower and higher doses of the fertilizer, respectively (**Table 5**).

TABLE 4 | Yield of leaves and storage roots, share of the marketable yield in the total yield, and average weight of single storage roots and leaves from one plant, depending on the foliar application of iodine and selenium.

Foliar application	Yield of carrot leaves (t · ha^{-1})	Total yield of carrot storage roots (t · ha^{-1})	Marketable yield of carrot roots (t · ha^{-1})	Non-marketable yield of carrot roots (t · ha^{-1})
Control	39.6 ± 8.68a	100.4 ± 8.18a	85.2 ± 4.25a	15.2 ± 4.48a
200 g I + 10 g Se	37.5 ± 7.00a	95.5 ± 4.78a	81.5 ± 2.87a	14.0 ± 4.23a
400 g I + 20 g Se	38.2 ± 7.67a	100.2 ± 6.21a	84.2 ± 3.31a	16.0 ± 4.27a
200 g I	34.6 ± 6.56a	100.2 ± 7.51a	83.8 ± 3.09a	16.4 ± 4.63a
400 g I	38.1 ± 7.33a	106.3 ± 10.22a	93.8 ± 7.02a	12.5 ± 4.45a
5 g Se	37.8 ± 7.83a	101.6 ± 9.17a	85.9 ± 6.59a	15.7 ± 5.70a
10 g Se	34.0 ± 5.55a	97.1 ± 6.76a	79.4 ± 4.47a	17.7 ± 4.20a
Test *F* for foliar application	n.s.	n.s.	n.s.	n.s.
Test *F* for foliar application × year of study	n.s.	n.s.	n.s.	n.s.

	Share of the marketable yield in the total yield of storage roots (%)	Total biological yield (roots + leaves) (t · ha^{-1})	Average weight of single storage roots (g · plants^{-1})	Average weight of leaves from one plant (g · plants^{-1})
Control	86.7 ± 3.46a	140.0 ± 16.53a	63.9 ± 3.97a	27.0 ± 1.64a
200 g I + 10 g Se	86.3 ± 3.70a	133.0 ± 11.25a	63.8 ± 3.58a	25.0 ± 0.28a
400 g I + 20 g Se	85.2 ± 3.50a	138.4 ± 13.44a	66.7 ± 4.14a	24.0 ± 1.25a
200 g I	85.3 ± 3.24a	134.8 ± 13.43a	67.3 ± 6.49a	23.6 ± 1.14a
400 g I	89.8 ± 2.93a	144.4 ± 17.35a	58.6 ± 3.07a	23.6 ± 0.63a
5 g Se	86.1 ± 4.87a	139.4 ± 16.01a	63.6 ± 3.29a	23.0 ± 0.67a
10 g Se	82.9 ± 3.50a	131.1 ± 12.04a	67.2 ± 7.55a	24.4 ± 1.35a
Test *F* for foliar application	n.s.	n.s.	n.s.	n.s.
Test *F* for foliar application × year of study	n.s.	n.s.	n.s.	n.s.

Application 200 g I + 10 g Se · ha^{-1} and 400 g I + 20 g Se · ha^{-1} by "I + Se" fertilizer, application of 200 g and 400 I · ha^{-1} by "Solo iodine" fertilizer, and application 5 and 10 g Se · ha^{-1} by "Solo selenium"·fertilizer.
Means followed by the same letters are not significantly different for $p < 0.05$. ±, standard error (n = 8); n.s., not significant for $p < 0.05$. Average for the years 2019–2020.

Percentages of RDA-I and RDA-Se from plants enriched with the "Solo iodine" and "Solo selenium" fertilizers were similar to the equivalent doses of I and Se applied with "I + Se". The HQ-I and HQ-Se coefficients were significantly lower than 1.0 for all tested treatments. I and Se could potentially harm the consumer if both the HQ coefficients were ≥1.0. The highest value of HQ-I and HQ-Se occurred after the application of a higher dose of "I + Se" (400 g I + 20 g Se · ha^{-1}) and was 0.0074 for HQ-I and 0.00638 for HQ-Se.

The ratio of I and Se in fresh carrot roots (converted to the molar mass of both elements) after applying the "I + Se" fertilizer in both doses was similar to the control (**Table 5**). After applying the fertilizer "Solo selenium" at both doses, the molar content ratio of I:Se in the roots was significantly lower than in the control. However, after application of "Solo iodine", a significant extension of this ratio in favor of I was observed.

Levels of Iodates, SA, BeA, and Their I Derivatives

When compared to the control treatment, the fertilizers "I + Se" and "Solo iodine" caused a decrease of 20% in the levels of BeA in the roots and increased the levels of 3,5-diISA by 20% in the leaves (**Table 6**). "I + Se" caused a significant increase in the levels of 2,3,5-triIBeA (3-fold) and I-Tyr (2-fold) and a significant decrease in BeA (1.7-fold) and 2-IBeA (3-fold) in the leaves. It caused a significant increase in IO_3^- ions (5.2-fold) in the roots. The application of "Solo iodine" resulted in a significant increase in the levels of 5-ISA (2.2-fold), 2,3,5-triIBeA (12.0-fold), and I-Tyr (3.5-fold) and a 2-fold decrease in 4-IBeA and T3 in the leaves compared to that in the untreated control (**Table 6**). This fertilizer also caused a significant increase in the content of 5-ISA (1.9-fold), 4-IBeA (8.3-fold), 2,3,5-triIBeA (1.18-fold), T4 (1.9-fold), and I-Tyr (1.8-fold) in the roots. I and Se applied together as "I + Se" (200 g I + 10 g Se · ha^{-1}), compared to I-alone "Solo iodine" (200 g I · ha^{-1}), caused a significant decrease in the levels of 5-ISA (3.3-fold) 2-IBeA (1.27-fold), 2,3,5-triIBeA (3.8-fold), and I-Tyr (1.6-fold) in the leaves (**Table 6**). In the roots, it caused a significant decrease of 5-ISA (1.5-fold), 3,5-diISA (2.7-fold), 4-IBeA (2.5-fold), 2,3,5-triIBeA (1.26-fold), and T4 (1.4-fold).

None of the treatments resulted in statistically significant changes in levels of IO_3^-, SA, and T4 in the leaves and SA and 2-IBeA in the roots when compared to the control.

Leaf and Root Dry Matter Content and Content of Total Dissolved Solids (Brix %), Sugars, and Carotenoids in Roots

The foliar application of "I + Se", "Solo iodine" and "Solo selenium" (in all doses) had no significant effect on dry weight (**Table 7**), the Brix percentage, glucose, fructose, sucrose, total

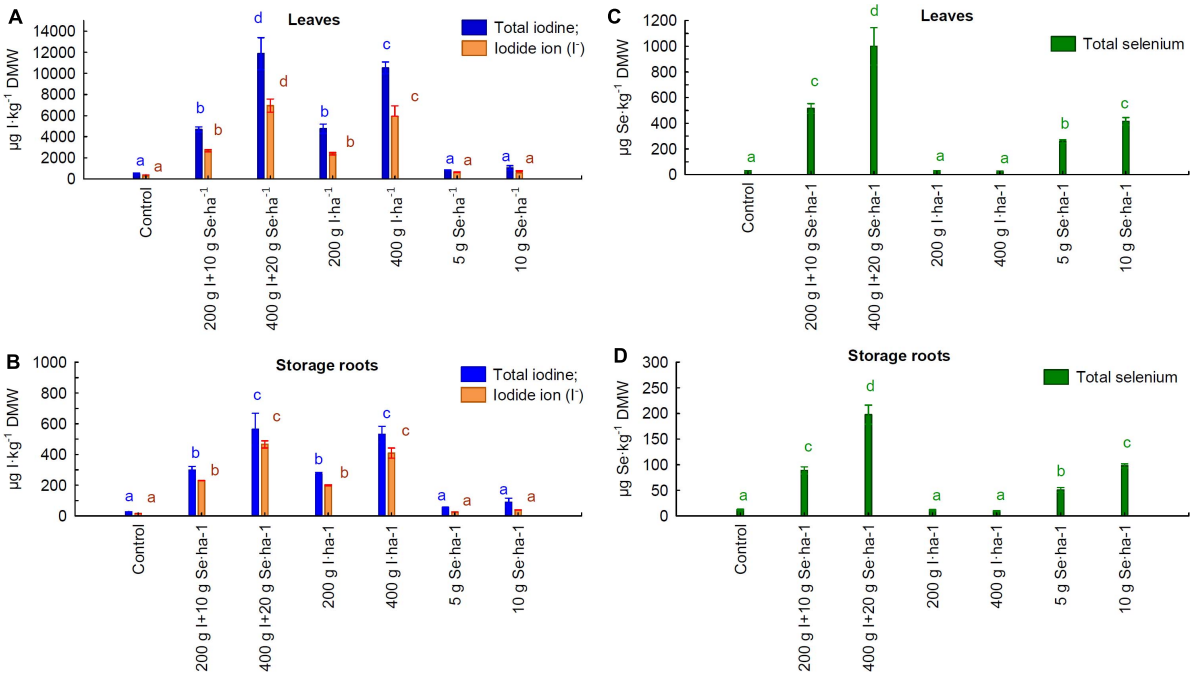


FIGURE 1 | Total iodine, iodide ion (I^-) **(A,B)**, and total selenium **(C,D)** contents in carrot leaves **(A,C)** and storage roots **(B,D)**, depending on the foliar application of both elements. Application 200 g I + 10 g Se · ha^{-1} and 400 g I + 20 g Se · ha^{-1} by "I + Se" fertilizer, application of 200 g and 400 I · ha^{-1} by "Solo iodine" fertilizer, and application 5 g and 10 g Se · ha^{-1} by "Solo selenium"·fertilizer. The results of the test *F* for "foliar application" for all qualitative features in panels **(A–D)** were statistically significant. The results of the test *F* for "foliar application × year of study" for all qualitative features in panels **(A–D)** were not statistically significant. Means followed by the same letters are not significantly different for $p < 0.05$; bars indicate standard error ($n = 8$). Average for the years 2019–2020.

TABLE 5 | Percentage of Recommended Daily Allowance (RDA) for iodine (RDA-I) and selenium (RDA-Se) in 100-g portion of fresh carrot roots, I:Se molar ratio in fresh carrot roots, and hazard quotient (HQ) for intake of I and Se through the consumption of 100 g of fresh carrot roots by adults (70-kg body weight), depending on the foliar application of iodine and selenium.

	Storage roots				
Foliar application	**Percent RDA-I in 100 g of fresh carrot roots (%)***	**HQ-iodine for 100 g of fresh carrot roots**	**Percent RDA-Se in 100 g of fresh carrot roots (%)***	**HQ-selenium for 100 g of fresh carrot roots**	**Molar mass ratio of I:Se in fresh carrot roots**
Control	0.21 ± 0.03a	0.0003 ± 0.0001a	0.27 ± 0.03a	0.00033 ± 0.00003a	1.35:1 (±0.15:1)b
200 g I + 10 g Se	1.96 ± 0.30b	0.0030 ± 0.0005b	1.98 ± 0.19c	0.00283 ± 0.00026c	1.63:1 (±0.14:1)b
400 g I + 20 g Se	4.19 ± 0.58c	0.0074 ± 0.0016d	4.37 ± 0.45d	0.00638 ± 0.00082d	1.60:1 (±0.12:1)b
200 g I	1.95 ± 0.16b	0.0030 ± 0.0003b	0.26 ± 0.03a	0.00027 ± 0.00002a	13.50:1 (±1.23:1)c
400 g I	3.55 ± 0.44c	0.0053 ± 0.0007c	0.21 ± 0.02a	0.00027 ± 0.00002a	31.11:1 (±5.97:1)c
5 g Se	0.26 ± 0.07a	0.0004 ± 0.0001a	1.13 ± 0.12b	0.00150 ± 0.00011b	0.37:1 (±0.10:1)a
10 g Se	0.45 ± 0.15a	0.0007 ± 0.0003a	2.18 ± 0.12c	0.00319 ± 0.00024c	0.33:1 (±0.10:1)a
Test *F* for foliar application	*	*	*	*	*
Test *F* for foliar application × year of study	n.s.	n.s.	n.s.	n.s.	n.s.

Application 200 g I + 10 g Se · ha^{-1} and 400 g I + 20 g Se · ha^{-1} by "I + Se" fertilizer, application of 200 g and 400 I · ha^{-1} by "Solo iodine" fertilizer, and application of 5 and 10 g Se · ha^{-1} by "Solo selenium"·fertilizer.
*Means followed by the same letters are not significantly different for $p < 0.05$; ±, standard error ($n = 8$). *Statistically significant; n.s., not significant for $p < 0.05$. The hazard to consumer exists when the value of HQ exceeds 1.0. Average for the years 2019–2020.*

sugars, and carotenoids in carrots when compared to the control (**Table 8**). There were significant differences in the levels of total soluble solids between the treatments. The highest value of Brix (9.30%) was observed in carrot roots after the plant was sprayed with "I + Se" at a dosage of 400 g I + 20 g Se · ha^{-1}. Alternatively, the highest concentration of all sugars was observed in the roots

TABLE 6 | Content of iodates (IO_3^-), salicylic acid (SA), benzoic acid (BeA), iodosalicylates [5-iodosalicylic acid (5-ISA) and 3,5-diiodosalicylic acid (3,5-diISA)], iodobenzoates [2-iodobenzoic acid (2-IBeA), 4-iodobenzoic acid (4-IBeA), 2,3,5-triiodobenzoic acid (2,3,5-triIBeA)], iodotyrosine (I-Tyr), and plant-derived thyroid hormone analogs (PDTHAs), i.e., triiodothyronine (T3) and thyroxine (T4) in carrot storage roots–results only from 1 year of study.

Foliar application	Part of plants	(mg · kg^{-1} DW)					
		IO_3^-	SA	BeA	5-ISA	3,5-diISA	2-IBeA
Control	Leaves	0.0276 ± 0.008a	0.35 ± 0.032a	1.43 ± 0.22c	0.0018 ± 0.0003a	0.109 ± 0.015a	0.038 ± 0.002c
200 g I + 10 g Se		0.0231 ± 0.005a	0.37 ± 0.081a	0.84 ± 0.13a	0.0012 ± 0.0002a	0.129 ± 0.017b	0.011 ± 0.001a
200 g I		0.0402 ± 0.007a	0.32 ± 0.011a	1.22 ± 0,14bc	0.0040 ± 0.0003b	0.137 ± 0.012b	0.014 ± 0.004b
Test *F* for foliar application		n.s.	n.s.	*	*	*	*
Control	Roots	0.0062 ± 0.001ab	0.04 ± 0.005a	0.56 ± 0.07b	0.0038 ± 0.0007a	0.017 ± 0.003ab	0.015 ± 0.003a
200 g I + 10 g Se		0.0326 ± 0.016c	0.05 ± 0.004a	0.45 ± 0.07a	0.0047 ± 0.0006a	0.009 ± 0.001a	0.014 ± 0.001a
200 g I		0.0125 ± 0.008bc	0.07 ± 0.003a	0.44 ± 0.09a	0.0075 ± 0.0009b	0.025 ± 0.008b	0.015 ± 0.002a
Test *F* for foliar application		*	n.s.	*	*	*	n.s.

		4-IBeA	2,3,5-triIBeA	T3	T4	I-Tyr
Control	Leaves	0.012 ± 0.002b	0.010 ± 0.002a	0.012 ± 0.004b	0.0070 ± 0.0002a	0.0031 ± 0.0004a
200 g I + 10 g Se		0.019 ± 0.002b	0.031 ± 0.005b	0.011 ± 0.003b	0.0074 ± 0.0002a	0.0066 ± 0.0010b
200 g I		0.005 ± 0.001a	0.120 ± 0.007c	0.006 ± 0.000a	0.0073 ± 0.0004a	0.0111 ± 0.0006c
Test *F* for foliar application		*	*		n.s.	*
Control	Roots	0.003 ± 0.001a	0.092 ± 0.007a	0.002 ± 0.001a	0.0106 ± 0.0011a	0.0036 ± 0.0014a
200 g I + 10 g Se		0.010 ± 0.003b	0.086 ± 0.004a	0.011 ± 0.002b	0.0137 ± 0.0003a	0.0051 ± 0.0004ab
200 g I		0.025 ± 0.002c	0.109 ± 0.007b	0.011 ± 0.003b	0.0202 ± 0.0026b	0.0065 ± 0.0008b
Test *F* for foliar application		*	*	*	*	*

Application 200 g I + 10 g Se · ha^{-1} and 400 g I + 20 g Se · ha^{-1} by "I + Se" fertilizer, and application of 200 g and 400 I · ha^{-1} by "Solo iodine" fertilizer.
*Means followed by the same letters separately for each part of plants are not significantly different for $p < 0.05$; ±, standard error (n = 4). *Statistically significant; n.s., not significant for $p < 0.05$. Results only from 2019.*

of plants sprayed with "Solo iodine" at a dose of 200 g I · ha^{-1} and then with "Solo selenium" at a dose of 20 g Se · ha^{-1}, as well as with "I + Se" at a dose of 400 g I + 20 g Se · ha^{-1}.

Color of the Carrot Roots

Statistical analysis showed no differences in the L^* parameter, i.e., the brightness of the color of the roots (**Table 9**). The values of the remaining parameters a^*, b^*, and C^* showed significant differences, depending on the fertilizer used. The roots of the untreated carrot showed the lowest mean values for the color parameters a^*, b^*, and C^*. However, the highest values for these parameters were observed in carrots treated with the "Solo selenium" fertilizer, applied at a dose of 5 g Se · ha^{-1}. There were no significant differences in the a^*, b^*, and C^* color parameters for applications with higher and lower doses of "I + Se", "Solo iodine" and "Solo selenium" fertilizers.

According to the guidelines of the CIE, a total color difference was not recognized for the roots of plants treated with the fertilizers "I + Se" at a dose of 400 g I + 20 g Se · ha^{-1} and "Solo iodine" at a dose of 200 g I · ha^{-1} (value $\Delta E^* < 2$) (**Figure 2**). For the other treatments, the parameter was between 2 and 5, which is a color difference that is recognized by a specialist. The total saturation difference (ΔC^*) for plants sprayed with "Solo iodine" at a dose of 200 g I · ha^{-1} had the lowest value. For this parameter, there were no differences visible to the eye in the roots of plants treated with "Solo selenium" (10 g Se · ha^{-1}). No value greater than 2 was observed for total hue difference (ΔH^*) in any of the treatments, which is interpreted as no visible differences in the hue of the roots.

TABLE 7 | Content of dry weight in leaves and storage roots of carrot, depending on the foliar application of iodine and selenium.

Foliar application	% D.W. in leaves	% D.W. in storage roots
Control	14.8 ± 0.79a	13.5 ± 0.84a
200 g I + 10 g Se	14.6 ± 0.60a	13.3 ± 0.84a
400 g I + 20 g Se	14.4 ± 0.65a	15.1 ± 1.76b
200 g I	14.6 ± 0.74a	13.4 ± 0.67a
400 g I	14.7 ± 0.72a	13.0 ± 0.58a
5 g Se	14.2 ± 0.57a	13.1 ± 0.62a
10 g Se	14.9 ± 0.86a	13.5 ± 0.65a
Test *F* for foliar application	n.s.	n.s.
Test *F* for foliar application × year of study	n.s.	n.s.

Application 200 g I + 10 g Se · ha^{-1} and 400 g I + 20 g Se · ha^{-1} by "I + Se" fertilizer, application of 200 g and 400 I · ha^{-1} by "Solo iodine" fertilizer, and application 5 and 10 g Se · ha^{-1} by "Solo selenium"·fertilizer.
Means followed by the same letters are not significantly different for $p < 0.05$; ±, standard error (n = 8); n.s., not significant for $p < 0.05$. Average for the years 2019–2020.

DISCUSSION

Simultaneous biofortification of crops with I and Se in agriculture is recommended because of the benefits of these elements for human and animal health, due to the deficiency of both

TABLE 8 | Content of and total soluble solids (Brix %); glucose, fructose, sucrose, and total sugars (the sum of the three sugars); and carotenoids in storage roots, depending on the foliar application of iodine and selenium.

Foliar application	Brix (%)[1]	Glucose (mg · 100 g^{-1} f.w.)	Fructose (mg · 100 g^{-1} f.w.)	Sucrose (mg · 100 g^{-1} f.w.)	Total sugars (mg · 100 g^{-1} f.w.)	Carotenoids (mg · 100 g^{-1} f.w.)
Control	9.15 ± 0.09abc	262.8 ± 32.2a	322.9 ± 121.0a	2,819.4 ± 536.4abc	3,405.0 ± 668.6ab	13.3 ± 0.59a
200 g I + 10 g Se	9.10 ± 0.07abc	297.3 ± 82.7ab	363.0 ± 130.8ab	2,736.0 ± 216.1ab	3,396.3 ± 319.5a	13.7 ± 0.39a
400 g I + 20 g Se	9.30 ± 0.04c	326.6 ± 84.1abc	400.2 ± 73.4bc	3,166.9 ± 350.6bc	3,893.7 ± 361.4bc	14.6 ± 0.31a
200 g I	9.05 ± 0.02ab	545.7 ± 79.1d	587.6 ± 210.6d	3,009.01674.8c	4,142.3 ± 159.3c	14.0 ± 0.76a
400 g I	9.10 ± 0.04abc	261.9 ± 49.4a	335.3 ± 82.4a	2,463.7 ± 776.7a	3,060.9 ± 820.8a	15.6 ± 1.30a
5 g Se	8.95 ± 0.13a	343.2 ± 21.8bc	405.7 ± 167.7bc	2,617.5 ± 846.7a	3,366.4 ± 1014.5a	14.6 ± 1.23a
10 g Se	9.25 ± 0.02bc	384.2 ± 92.8c	453.2 ± 57.4c	3,190.7 ± 485.1c	4,028.1 ± 459.8c	14.6 ± 0.79a
Test *F* for foliar application	*	*	*	*	*	n.s.
Test *F* for foliar application × year of study	–	n.s.	n.s.	n.s.	n.s.	n.s.

1: Results of Brix and carotenoids are only from 2020, results of all sugars are average for the years 2019–2020.
Application 200 g I + 10 g Se · ha^{-1} and 400 g I + 20 g Se · ha^{-1} by "I + Se" fertilizer, application of 200 g and 400 I · ha^{-1} by "Solo iodine" fertilizer, and application 5 and 10 g Se · ha^{-1} by "Solo selenium"·fertilizer.
*Means followed by the same letters are not significantly different for $p < 0.05$; ±, standard error (n = 8). *Statistically significant; n.s., not significant for $p < 0.05$.*

elements in many regions of the world (Germ et al., 2015; Gonzali et al., 2017; Márquez et al., 2020). In addition, the combined application of I and Se in low doses can influence the plant positively. This effect can be observed in the crop yields and/or in the concentrations of nutrients, bioactive compounds, and nutraceuticals (Germ et al., 2015; Medrano-Macías et al., 2018).

Mao et al. (2014) conducted research with soil fertilization, using I and Se. They showed that the effectiveness of I and Se biofortification of wheat, maize, soybean, potato, canola, and cabbage was similar, regardless of whether the elements were applied independently or in combination. Foliar fertilization is considered more effective than soil fertilization for enriching plants with I and Se (Lawson et al., 2015).

TABLE 9 | Color parameters of carrot storage roots, depending on the foliar application of iodine and selenium–results only from 1 year of study.

Foliar application	*L**	*a**	*b**	*C**
Control	45.85a	27.34a	37.96a	46.78
200 g I + 10 g Se	46.95a	29.77c	39.89bc	49.77
400 g I + 20 g Se	46.16a	29.26c	39.77bc	49.37
200 g I	46.39a	27.66ab	38.53ab	47.42
400 g I	46.56a	28.69bc	39.57bc	48.88
5 g Se	46.96a	29.41c	40.68c	50.20
10 g Se	47.36a	28.59abc	38.76ab	48.16
Test *F* for foliar application	n.s.	*	*	n.c.

Application 200 g I + 10 g Se · ha^{-1} and 400 g I + 20 g Se · ha^{-1} by "I + Se" fertilizer, application of 200 g and 400 I · ha^{-1} by "Solo iodine" fertilizer, and application 5 and 10 g Se · ha^{-1} by "Solo selenium"·fertilizer.
*Means followed by the same letters are not significantly different for $p < 0.05$; ±, standard error (n = 4). *Statistically significant; n.s., not significant for $p < 0.05$; n.c., this parameter is not statistically calculated. All results were obtained from the trials carried in 2020.*
L indicates color lightness (L* = 0 black, L* = 100 white).*
a, contribution of green (a* < 0) or red (a* > 0) color.*
b, contribution of blue (b* < 0) or yellow (b* > 0) color.*

The research presented in this article adds to the body of research currently being undertaken across the world. The effectiveness of enriching wheat and rice grains with these elements by foliar application was shown in experiments in several different countries (Zou et al., 2019; Cakmak et al., 2020). The effectiveness of foliar biofortification of I in plants depends on whether this element is applied alone or in combination with other minerals. Foliar application of a "cocktail" of three elements, I + Zn + Se resulted in a significant decrease in I accumulation in wheat grain, in comparison to the application of I alone (Cakmak et al., 2020). A similar decrease in the levels of I in wheat grains was observed with the application of a "cocktail" of I + Zn + Fe + Se, versus I alone (Zou et al., 2019). This research indicated that levels of Se were determined in the control plants and in the plants treated with the "cocktail," but analysis for Se was not performed on plants treated with I. Golubkina et al. (2018) undertook similar studies on the Indian mustard and did not show a negative effect for the foliar application of I + Se (KI + Na_2SeO_4) on the accumulation of Se in plants when compared to the foliar application of Se alone (Na_2SeO_4). However, there was a noticeable decrease in the accumulation of I in the Indian mustard after the application of I + Se, compared to that in plants treated with I alone. The research is helpful in identifying the interactions for uptake and translocation of I and Se in various crops after foliar application of these elements, when applied "Solo" or in combination with other elements.

Foliar biofortification of plants with I and Se occurs because of transportation of these elements through the phloem, despite the relatively low mobility of I through phloem compared to more effective transportation through xylem. I and Se are translocated through the phloem from the leaves to other aerial parts of plants, including to grains or seeds (Cakmak et al., 2017) and fruits such

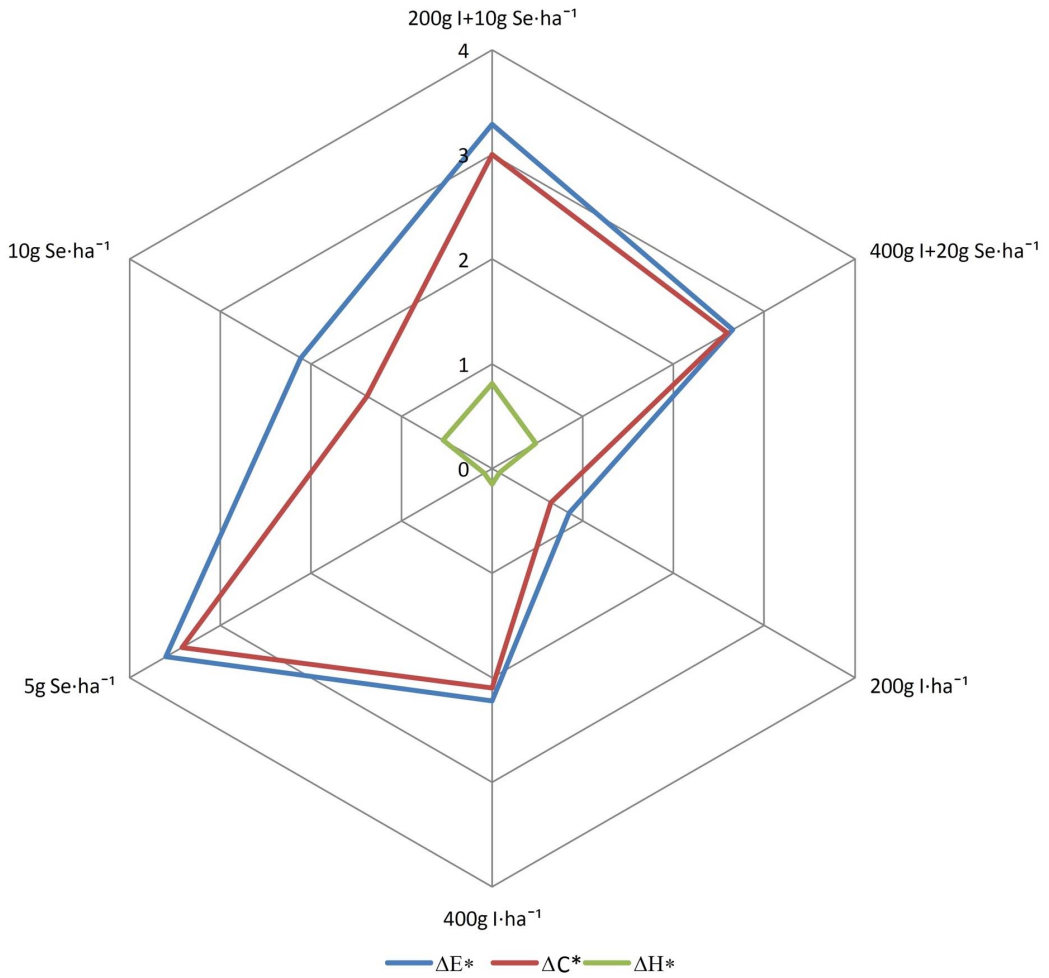


FIGURE 2 | Effect of biofortification on color indices: ΔE^*, ΔC^*, ΔH^*. The mentioned parameters are calculated using the results of the average values of the basic parameters (L^*, a^*, b^*, C^*). In accordance to the guidelines of International Commission on Illumination, the parameter values of ΔE^*, ΔC^*, and ΔH^* less than 2 indicate the lack of recognizable differences in the color by the observer; greater than 5 indicates the differences are clear and visible to any observer. Where ΔE^*, total color difference; ΔC^*, total saturation difference; ΔH^*, total hue difference. Application 200 g I + 10 g Se · ha^{-1} and 400 g I + 20 g Se · ha^{-1} by "I + Se" fertilizer, application of 200 g and 400 I · ha^{-1} by "Solo iodine" fertilizer, and application 5 g and 10 g Se · ha^{-1} by "Solo selenium"·fertilizer.

as strawberries (Budke et al., 2020b), apples (Budke et al., 2020a), and tomatoes (Landini et al., 2011). Some authors indicate that despite the success of plants enrichment with I, redistribution of this element from the leaves to fruits, grains, or seeds by the phloem is limited (Muramatsu et al., 1995; Shinonaga et al., 2000; Salau et al., 2008). The enrichment of underground parts of plants, such as the roots of carrots or potato tubers with I or Se, is possible because of the transportation of these elements through the phloem from the leaves to underground tissues. This effect was demonstrated in studies on biofortification with I in the cultivation of carrots (Signore et al., 2018) and potatoes (Ledwożyw-Smoleń et al., 2020), as well as in research on biofortification with Se in carrots (Oliveira et al., 2018) and potatoes (Zhang et al., 2019). There are no data on whether the foliar application of I and Se simultaneously will enrich carrot roots. The research showed that both elements, applied as I^- and SeO_4^{2-}, were transported through the phloem from the leaves to the roots after foliar application. There was no interaction between the elements with respect to the level of the enrichment of the roots with I and Se. In case of the leaves, it was observed that combined application of I with Se (400 g I + 20 g Se · ha^{-1}), compared to the application of I alone (400 g I · ha^{-1}), had a synergistic effect on increasing the uptake and accumulation of I. However, no interaction was observed in the accumulation of Se in the leaves after foliar application of Se alone, and I + Se. The interaction between I and Se in foliar applications is most likely dependent on the plant species and the chemical form in which these elements are applied. In lettuce cultivation, foliar application of KIO_3 had a synergistic effect on the uptake of SeO_4^{2-}, whereas Se in this form had no effect on the level of I accumulation in leaves after the plants were sprayed with KIO_3 (Smoleń et al., 2014a).

Biofortification of I and Se in the roots of carrots does not have a negative effect on the yield of leaves and roots (total,

marketable, and non-marketable yield); or on the dry weight in leaves and roots; or on the levels of total dissolved solids, sugars, and carotenoids in the carrot roots. Foliar application of I alone (200 g I · ha^{-1}) caused a significant increase in sugar content in the roots. No plant damage was observed after foliar application of I, Se, and I + Se in the study. The study was not investigating ways to increase yield but rather to enhance the accumulation of I and Se in carrots. Similar effects were found by Smoleń et al. (2019) when soils were fertilized with I + Se (4 kg I · ha^{-1} as KI and 0.25 kg Se · ha^{-1} as Na_2SeO_4). There was no effect on yield, but enrichment of the four carrot varieties with I and Se was achieved.

Color assessment is one of the basic parameters assessed in the context of the quality of raw materials. It is the first and often decisive parameter in the choice of consumers. Instrumental assessment of color, thanks to the recommendations of the CIE, allows determining whether the color difference will be visible to the naked eye. In the presented research, it was found that the enrichment had a slight but statistically significant effect on the color of carrot roots. Gonnella et al. (2019) found no differences in the color of the leaves of different cabbage cultivars after the use of I fortification. Similar conclusions from the research were obtained by Montesano et al. (2016) and D'Imperio et al. (2016) for green peas and six species of leaf vegetables fortified with silicon compounds. Statistical differences in color after the use of Se fortification were also not found by Mimmo et al. (2017) study for strawberry fruit, although the results suggest that these differences should be visible to the naked eye. In the case of the cited data, the color parameters of the tested raw materials depend mainly on the content of chlorophylls and polyphenolic compounds, which do not always change under the influence of fortification (Smoleń et al., 2014a). Carotenoids determine the color of carrot roots. In the literature, information on the effect of I and Se biofortification on the content of these compounds in carrot roots could be found (Vanuze Costa de Oliveira et al. Oliveira et al., 2018; Smoleń et al., 2019). The results of the carotenoids content obtained in the experiment were not statistically significant what they comply with cited literature.

The results of this study show that the doses and types of foliar fertilizers ("I + Se", "Solo iodine" and "Solo selenium") allowed for enrichment of carrot roots with I and Se safely during cultivation. The plants were physiologically able to tolerate the doses of I and Se applied. Furthermore, the chemical form of I^- and Se (SeO_4^{2-}), when combined with an organic stabilizer/enhancer®, allowed for a higher uptake of I and Se by the epidermis of leaves and better transport through the phloem to the roots. Evidence was also provided that the foliar application of I in the form of I^- ions stabilized by organic stabilizer/enhancer® allowed for uptake, transport, and metabolization in the whole carrot plant. The results of the analysis in this study showed the levels of I, ions I^-, and organic metabolites of I compounds in leaves and roots. The dominant form of I in the roots and leaves were iodides (IO_3^-), which were taken up from the soil. On average, I^- represented 77.4% of total level of I in the roots for treatments with fertilizers "I + Se" and "Solo iodine", and 50.1% for the untreated control and for plants treated with "Solo selenium". On average, I^- represented 55.5% of the total content of I in the leaves for plants treated "I + Se" and "Solo iodine" and 63.6% for the control and "Solo selenium" treatment.

These results demonstrate the effective translocation of I^- ions from the leaves to the roots of carrot plants. Chemical analysis also showed that iodides were utilized in carrot plants in metabolic pathways for the synthesis of iodosalicylates, iodobenzoates, I-Tyr, and PDTHA. Similar results were found for lettuce plants (Smoleń et al., 2020). I can also be incorporated into other groups of compounds, such as polysaccharides, lipids, polyphenols, and proteins (Millard, 1988; Hou, 2009).

As already mentioned, no significant differences were found in the levels of total I accumulation in the leaves and roots when doses of 200 g I + 10 g Se · ha^{-1} were applied as "I + Se" versus 200 g I · ha^{-1} as "Solo iodine". However, significant interactions between I and Se in plants were observed for the levels of I metabolites in carrots. The results showed that combined applications of I + Se, opposed to the use of I alone, had significant impacts at a biochemical level. First, a decreasing synthesis/accumulation of 5-ISA, 2-IBeA, 2,3,5-triIBeA, and I-Tyr and an increasing synthesis/accumulation of 4-IBeA, T3 were found in the leaves. Second, a decreasing synthesis/accumulation of 5-ISA, 3,5-diISA, 4-IBeA, 2,3,5-triIBeA, and T4 was found in the roots. One of the most important findings of the study was that the organic metabolites of I, namely I-Tyr, 5-ISA, and 2,3,5-triIBeA, were synthesized and accumulated in higher levels in the carrot plant after foliar application of I. While these compounds were found in plants not treated with I in studies on tomatoes (Halka et al., 2019) and lettuce plants (Smoleń et al., 2020), fertilization with I increased their levels in these plants (Halka et al., 2019; Smoleń et al., 2020), which was also confirmed in this study.

It is noteworthy that the synthesis of two of iodosalicylates (5-ISA 3,5-diISA) decreased in carrots after the combined application of I and Se, compared to when I alone was applied. These are PDTHA precursors in plants (Smoleń et al., 2020). However, the application of I alone in contrast to the application of I and Se together caused a significant reduction of the content of T3 (but not T4) and simultaneously increased the content of I-Tyr in carrot leaves, compared to the control. I-Tyr is an I amino acid that most likely acts to store I in the plant. This amino acid also participates in the complex mechanism of PDTHA synthesis (Smoleń et al., 2020). The physiological and biochemical functions and range of actions of PDTHA in plants have not yet been described in the literature. There are studies that show that the proteins T3 and T4 synthesized in plants are homologous to human proteins (Eneqvist et al., 2003). The T3 and T4 proteins that occur in cereals, tomatoes, potatoes and in *Arabidopsis thaliana* are more closely related to the protein present in the *Homo sapiens* organism than to those in bacteria and fungi. In *A. thaliana*, exogenous T4 is bound by the transthyretin-like protein (Pessoa et al., 2010). In the human body, transthyretin-like proteins belong to the group of proteins that include T4-binding globulin and albumin (Power et al., 2000). Based on this, it can be assumed that PDTHA may have a regulatory function in plants.

5-iodosalicylic acid is the primary iodosalicylate in plants and one of the three metabolites most synthesized in carrot plants after foliar application of I (Smoleń et al., 2020). The results indicate that 5-ISA was transported from the leaves to the roots of carrot plants, where it was converted to 3,5-diISA. The direction of transformations of 5-ISA to 3.5-diISA is consistent with reports in the literature (Halka et al., 2019; Smoleń et al., 2020).

An important issue is an increase of the synthesis of 2,3,5-triIBeA, subsequent to the application of fertilizers containing I. In the literature, 2,3,5-triIBeA is regarded as an auxin inhibitor (Saniewski et al., 2014). Despite the fact that the levels of 2,3,5-triIBeA (especially in leaves) increased after foliar application of I, compared to the control, this did not have a negative effect on the functioning of auxins in carrots. However, there is a lack of influence related to the effect of fertilizers containing I ("I + Se" and "Solo iodine") on the yield of carrot roots and leaves.

The application of trace elements with organic stabilizers is an acceptable plant biofortification strategy in the cultivation of plants. The stabilizer/enhancer® contained in all three fertilizers used in this study is based on organic compounds naturally present in plants, which makes it safe for the plants and consumers. For example, Dávila Rangel et al. (2020) tested the application of chitosan-I complex (Cs-KIO_3, Ch-KI) to enrich lettuce with I successfully.

The optimal molar ratio of I:Se for the daily intake by the consumer is within the range of 4.4–8.8:1. This range is based on the RDA-I and RDA-Se for consumers in various age groups, namely, children, adolescents, adults, and breastfeeding mothers (Institute of Medicine, 2000; Andersson et al., 2007). Therefore, plant biofortification protocols should aim to enrich plants with I and Se to obtain a molar ratio for both elements in the range of 4.4–8.8:1. The upper levels of biofortification of the edible parts of crop plants must be safe for the consumer, indicating the need for values of I and Se of HQ < 1.0.

It is not easy to achieve optimum ratios of I:Se in cereal yields when simultaneously enriching with I and Se. Research by Cakmak et al. (2020) in wheat cultivation showed that foliar application with 2.3 mM I + 15.9 mM zinc + 0.05 mM Se (molar ratio of I:Se = 46:1) resulted in grains with a molar ratio of I:Se = 0.23:1, whereas application of I alone resulted in a molar ratio of I:Se in grains of 4.35:1. Zou et al. (2019) enriched wheat grains with both elements using foliar application of I + Se in a ratio of 50:1, but the resultant molar ratio of I:Se in grains was 0.45:1. Mao et al. (2014) applied fertilizers with a mixture of I + Ze + Se in a ratio of I:Se 2.8:1. The result was enrichment of plants with I and Se, achieving a molar ratio of I:Se for wheat and maize grains of 0.0027:1 and 0.0067:1, respectively; of 0.021:1 for potato tubers; and of 0.037:1 for cabbages. Similarly, as in the case of the cereals, potatoes, and cabbages mentioned above (Mao et al., 2014; Zou et al., 2019; Cakmak et al., 2020), the molar ratio of I:Se in fertilizers did not translate into similar molar ratios of I:Se in the roots. Smoleń et al. (2019) applied pre-sowing fertilization with I and Se in the ratio of 9.9:1 for four carrot varieties. Biofortification was obtained, but the molar ratio of I:Se in the roots was 0.24:1. This resulted from better absorption of I than Se in the soil and differences in the rate of uptake and transport from the roots to leaves, as well as metabolism in plants (Smoleń et al., 2019). A better ratio of I:Se biofortification in the roots of carrots was achieved when applying pre-sowing and top dressing in soil fertilization (Smoleń et al., 2016a), rather than pre-sowing application only (Smoleń et al., 2019).

The molar mass ratio of I:Se in the "I + Se" fertilizer is 12.4:1. Foliar application of this fertilizer allowed for molar concentrations of approximately 1.6:1 of I:Se in the roots. The ratio of the molar content deviated from the optimal level, resulting from the values of RDA-I and RDA-Se. Despite the significantly increased accumulation of I and Se, the foliar application of "I + Se" fertilizer allowed for an I:Se ratio at a similar level to the one observed in the control plants. Therefore, it can be concluded that the metabolic processes of I and Se in carrots after foliar application of "I + Se" allowed for maintenance of the equilibrium state of biofortification with I:Se, as was observed in the control plants. We assumed that there were mechanisms for self-regulation of the physiological concentration (accumulation) of I and Se, which is based on the methylation process of I in the plants (Itoh et al., 2009; Izydorczyk et al., 2020) and Se (Kápolna et al., 2009; Sors et al., 2009).

CONCLUSION

The effect of biofortification of carrot roots with I and Se after foliar application of the fertilizers "I + Se" (I-Se fertilizer), "Solo iodine" and "Solo selenium" was studied. The foliar biofortification strategy had no negative impact on the yield of leaf biomass and roots (total and marketable yield) in carrot plants or the nutritional value of carrots. Elements applied as foliar applications had no influence on the content of total dissolved solids, sugars, and carotenoids in roots or on dry weight of roots and leaves. The fluctuations in the color of the roots were negligible and not noticeable to the human eye.

The results proved that foliar application is an effective way to biofortify roots with I and Se, which were transported from the leaves to the roots, probably through the phloem. No interaction (synergistic or antagonistic) was identified between the applied elements with regard to the effectiveness of biofortification of roots in any of the treatments.

The accumulation level of I metabolites in leaves and roots when compared to the control, in the light of applications of I + Se, is important from the perspective of plant biochemistry and physiology. This provides information about plant nutrition and I metabolism in carrot plants. The levels of organic I metabolites and PDTHA content in roots can be considered safe for consumers as the value of the HQ-I index was lower than 1.0, and the percentage of the RDA-I in 100 g of fresh carrot roots was a maximum of 4.16% (for treatment with 400 g I + 20 g Se $\cdot$ ha^{-1}). The HQ-Se values also indicated that the Se-enriched carrot was safe for the consumer. The percentage of RDA-Se in 100 g of fresh carrot roots was a maximum of 4.37% in the combination treatment with 400 g I + 20 g Se $\cdot$ ha^{-1}. This study has allowed for the development of foliar spraying protocols for the biofortification of carrot plants with I and Se.

DATA AVAILABILITY STATEMENT

The original contributions presented in the study are included in the article/**Supplementary Material**, further inquiries can be directed to the corresponding author/s.

AUTHOR CONTRIBUTIONS

RR-L, MG, KA, HK, and SS conceived and designed the field experiments. SS and MG conducted the field experiments and wrote the manuscript, together with RR-L and KA. JP, ŁS, and ML-S conducted the analytical investigations. SS and RR-L supervised the analytical investigations. SS provided resources to conduct the field experiments and analytical investigations. SS and ŁS analyzed and supervised the statistical data analysis. All authors contributed to manuscript revision, reading, and approved the submitted version.

FUNDING

This research was financed by the project entitled "Modern agrochemical preparations based on biodegradable ligands and other natural compounds stimulating resistance, enabling plant biofortification, intended to be used as a part of Integrated Plant Production" which was co-financed by the European Union from the European Regional Development Fund under Smart Growth Operational Program 2014–2020. The project was implemented as part of the competition of the National Center for Research and Development: Szybka Ścieżka, project no. POIR.01.01.01-00-0024/15, implemented by Intermag Sp. z o.o., Olkusz, Poland.

ACKNOWLEDGMENTS

We would like to thank Marceli Jaros and Damian Micyk for allowing us to conduct studies with carrot cultivation on the production plantation on their farms. We would also like to thank the students of the Faculty of Biotechnology and Horticulture, University of Agriculture in Kraków for their help in harvesting carrot.

SUPPLEMENTARY MATERIAL

The Supplementary Material for this article can be found online at: https://www.frontiersin.org/articles/10.3389/fpls.2021.656283/full#supplementary-material

REFERENCES

Amachi, S. (2008). Microbial contribution to global iodine cycling: Volatilization, accumulation, reduction, oxidation and sorption of iodine. *Microbes Environ.* 23, 269–276. doi: 10.1264/jsme2.me08548

Andersson, M., de Benoist, B., Darnton-Hill, I., and Delange, F. (2007). *Iodine Deficiency in Europe: A Continuing Public Health Problem*. Geneva: World Health Organization.

Athar, T., Khan, M. K., Pandey, A., Yilmaz, F. G., Hamurcu, M., Hakki, E. E., et al. (2020). Biofortification and the involved modern approaches. *J. Elem.* 25, 717–731. doi: 10.5601/jelem.2020.25.1.1911

Blasco, B., Rıos, J. J., Sanchez-Rodrıguez, E., Rubio-Wilhelmi, M. M., Leyva, R., Romero, L., et al. (2012). Study of the interactions between iodine and mineral nutrients in lettuce plants. *J. Plant Nutr.* 35, 1958–1969. doi: 10.1080/01904167.2012.716889

Budke, C., Thor Straten, S., Mühling, K. H., and Daum, D. (2020b). Iodine biofortification of field-grown strawberries-Approaches and their limitations. *Sci. Hortic.* 269:109317. doi: 10.1016/j.scienta.2020.109317

Budke, C., Mühling, K. H., and Daum, D. (2020a). Iodine uptake and translocation in apple trees grown under protected cultivation. *J. Plant Nutr. Soil Sci.* 183, 468–481. doi: 10.1002/jpln.202000099

Cakmak, I., Marzorati, M., Van den Abbeele, P., Hora, K., Holwerda, H. T., Yazici, et al. (2020). Fate and Bioaccessibility of Iodine in Food Prepared from Agronomically Biofortified Wheat and Rice and Impact of Cofertilization with Zinc and Selenium. *J. Agric. Food Chem.* 68, 1525–1535. doi: 10.1021/acs.jafc.9b05912

Cakmak, I., Prom-u-thai, C., Guilherme, L. R. G., Rashid, A., Hora, K. H., Yazici, A., et al. (2017). Iodine biofortification of wheat, rice and maize through fertilizer strategy. *Plant Soil.* 418, 319–335. doi: 10.1007/s11104-017-3295-9

Choudhry, H., and Nasrullah, M. D. (2018). Iodine consumption and cognitive performance: Confirmation of adequate consumption. *Food Sci. Nutr.* 6, 134–1351. doi: 10.1002/fsn3.694

Dai, J. L., Zang, M., Hu, Q. H., Huang, Y. Z., Wang, R. Q., and Zhu, Y. G. (2009). Adsorption and desorption of iodine by various Chinese soil: II. Iodine and iodate. *Geoderma* 153, 130–135.

Dávila Rangel, I. E., Trejo Téllez, L. I., Ortega Ortiz, H., Juárez Maldonado, A., González Morales, S., Companioni González, B., et al. (2020). Comparison of iodide, iodate, and iodine-chitosan complexes for the biofortification of lettuce. *Appl. Sci.* 10:2378. doi: 10.3390/app10072378

D'Imperio, M., Renna, M., Cardinali, A., Buttaro, D., Santamaria, P., and Serio, F. (2016). Silicon biofortification of leafy vegetables and its bioaccessibility in the edible parts. *J. Sci. Food Agric.* 96, 751–756.

Eneqvist, T., Lundberg, E., Nilsson, L., Abagyan, R., and Sauer-Eriksson, A. E. (2003). The transthyretin-related protein family. *Eur. J. Biochem.* 270, 518–532. doi: 10.1046/j.1432-1033.2003.03408.x

European Standard Norme Européenne Europäische Norm (2008). *PN-EN 15111 2008. Foodstuffs - Determination of trace elements - Determination of iodine by ICP-MS (inductively coupled plasma mass spectrometry)*. Warsaw: Polish Committee of Standardization.

Germ, M., Maršića, N. K., Turka, J., Pirca, M., Goloba, A., Jeršeb, A., et al. (2015). The effect of different compounds of selenium and iodine on selected biochemical and physiological characteristics in common buckwheat and pumpkin sprouts. *Acta Biol. Slovenica.* 58, 35–44.

Golob, A., Novak, T., Maršić, N. K., Šircelj, H., Stibilj, V., and Jerše, A. (2020). Biofortification with selenium and iodine changes morphological properties of *Brassica oleracea* L. var. gongylodes) and increases their contents in tubers. *Plant Physiol. Bioch.* 150, 234–243. doi: 10.1016/j.plaphy.2020.02.044

Golubkina, N., Kekina, H., and Caruso, G. (2018). Yield, quality and antioxidant properties of Indian mustard (*Brassica juncea* L.) in response to foliar biofortification with selenium and iodine. *Plants* 7:80. doi: 10.3390/plants7040080

Gonnella, M., Renna, M., D'Imperio, M., Santamaria, P., and Serio, F. (2019). Iodine biofortification of four brassica genotypes is effective already at low rates of potassium iodate. *Nutrients* 11:451. doi: 10.3390/nu11020451

Gonzali, S., Kiferle, C., and Perata, P. (2017). Iodine biofortification of crops: agronomic biofortification, metabolic engineering and iodine bioavailability. *Curr. Opin. Biotechnol.* 44, 16–26. doi: 10.1016/j.copbio.2016.10.004

Halka, M., Smoleń, S., Czernicka, M., Klimek-Chodacka, M., Pitala, J., and Tutaj, K. (2019). Iodine biofortification through expression of HMT, SAMT and S3H genes in *Solanum lycopersicum* L. *Plant Physiol. Bioch.* 144, 35–48. doi: 10.1016/j.plaphy.2019.09.028

Hanson, B., Garifullina, G. F., Lindblom, S. D., Wangeline, A., Ackley, A., Kramer, K., et al. (2003). Selenium accumulation protects *Brassica juncea* from

invertebrate herbivory and fungal infection. *New Phytol.* 159, 461–469. doi: 10.1046/j.1469-8137.2003.00786.x

Hartikainen, H. (2005). Biogeochemistry of selenium and its impact on food chain quality and human health. *J. Trace Elem. Med. Biol.* 18, 309–318. doi: 10.1016/j.jtemb.2005.02.009

Hou, X. (2009). "Iodine speciation in foodstuffs, tissues, and environmental samples: iodine species and analytical method," in *Comprehensive handbook of iodine*, eds V. Preedy, G. Burrow, and R. Watson (Amsterdam: Elsevier Academic Press), 139–150. doi: 10.1016/B978-0-12-374135-6.00015-7

Hutchings, J. B. (1999). *Food Color and Appearance*. Gaithersburg, MD: Aspen Publishers.

Institute of Medicine (2000). *Food and nutrition board dietary reference intakes: Vitamin C, vitamin E, selenium, and carotenoids*. Washington, DC: National Academy Press.

Itoh, N., Toda, H., Matsuda, M., Negishi, T., Taniguchi, T., and Ohsawa, N. (2009). Involvement of S-adenosylmethionine-dependent halide/thiol methyltransferase (HTMT) in methyl halide emissions from agricultural plants: isolation and characterization of an HTMT-coding gene from Raphanus sativus (*Daikon radish*). *BMC Plant Biol.* 9:116. doi: 10.1186/1471-2229-9-116

Izydorczyk, G., Ligas, B., Mikula, K., Witek-Krowiak, A., Moustakas, K., and Chojnacka, K. (2020). Biofortification of edible plants with selenium and iodine-A systematic literature review. *Sci. Tot. Environ.* 754:141983. doi: 10.1016/j.scitotenv.2020.141983

Kalisz, A., Sękara, A., Smoleń, S., Grabowska, A., Gil, J., Komorowska, M., et al. (2019). Survey of 17 elements, including rare earth elements, in chilled and non-chilled cauliflower cultivars. *Sci. Rep.* 9, 1–14. doi: 10.1038/s41598-019-41946-z

Kápolna, E., Hillestrøm, P. R., Laursen, K. H., Husted, S., and Larsen, E. H. (2009). Effect of foliar application of selenium on its uptake and speciation in carrot. *Food Chem.* 115, 1357–1363. doi: 10.1016/j.foodchem.2009.01.054

Komornicki, T., Oleksynowa, K., Tokaj, J., and Jakubiec, J. (1991). *Guide for Soil Science and Geology Experiments. Part 2. Methods of Soil Analysis*. Kraków: Agricultural University in Cracow.

Landini, M., Gonzali, S., and Perata, P. (2011). Iodine biofortification in tomato. *J. Plant Nutr. Soil Sci.* 174, 480–486. doi: 10.1002/jpln.201000395

Lawson, P. G., Daum, D., Czauderna, R., Meuser, H., and Härtling, J. W. (2015). Soil versus foliar iodine fertilization as a biofortification strategy for field-grown vegetables. *Front. Plant Sci.* 6:450. doi: 10.3389/fpls.2015.00450

Ledwożyw-Smoleń, I., Smoleń, S., Rożek, S., Sady, W., and Strzetelski, P. (2020). Iodine biofortification of potato (*Solanum tuberosum* L.) grown in field. *Agronomy* 10:1916. doi: 10.3390/agronomy10121916

Mackowiak, C. L., and Grossl, P. R. (1999). Iodate and iodide effects on iodine uptake and partitioning in rice (*Oryza sativa* L.) grown in solution culture. *Plant Soil.* 212, 135–143. doi: 10.1023/a:1004666607330

Mao, H., Wang, J., Wang, Z., Zan, Y., Lyons, G., and Zou, C. (2014). Using agronomic biofortification to boost zinc, selenium, and iodine concentrations of food crops grown on the loess plateau in China. *J. Soil Sci. Plant. Nutr.* 14, 459–470.

Márquez, V. G., Moreno, A. M., Mendoza, A. B., and Medrano Macías, J. (2020). Ionic Selenium and Nanoselenium as Biofortifiers and Stimulators of Plant Metabolism. *Agronomy* 10:1399. doi: 10.3390/agronomy10091399

Medrano-Macías, J., Mendoza-Villarreal, R., Robledo-Torres, V., Fuentes-Lara, L. O., Ramírez-Godina, F., Pérez-Rodríguez, M. Á, et al. (2018). The Use of Iodine, Selenium, and Silicon in Plant Nutrition for the Increase of Antioxidants in Fruits and Vegetables. *Antioxid. Foods Appl.* 2018, 155–168. doi: 10.5772/intechopen.75069

Mehdi, Y., Hornick, J. L., Istasse, L., and Dufrasne, I. (2013). Selenium in the Environment, Metabolism and Involvement in Body Functions. *Molecules* 18, 3292–3311. doi: 10.3390/molecules18033292

Millard, M. M. (1988). Lactoperoxidase-Catalyzed Iodination of Plasmamembrane Lipids and Proteins in *Arabidopsis* Protoplasts. *Plant Cell Physiol.* 29, 901–990.

Mimmo, T., Tiziani, R., Valentinuzzi, F., Lucini, L., Nicoletto, C., Sambo, P., et al. (2017). Selenium biofortification in Fragaria × ananassa: implications on strawberry fruits quality, content of bioactive health beneficial compounds and metabolomic profile. *Front. Plant Sci.* 8:1887.

Montesano, F. F., D'Imperio, M., Parente, A., Cardinali, A., Renna, M., and Serio, F. (2016). Green bean biofortification for Si through soilless cultivation: plant response and si bioaccessibility. *Sci. Rep.* 6:31662.

Mostafa, E., and Hassan, A. (2015). The ameliorative effect of selenium on Azolla caroliniana grown under UV-B stress. *Phytoprotection* 95, 20–26. doi: 10.7202/1031954ar

Muramatsu, Y., Yoshida, S., and Bannai, T. (1995). Tracer experiments on the behaviourof radioiodine in the soil-plant-atmosphere system. *J. Radioanal. Nucl. Chem.* 194, 303–310. doi: 10.1007/BF02038428

Nowosielski, O. (1988). *The Rules in Development of Fertilizing Strategies in Horticulture*. Poland: PWRiL Publisher.

Oliveira, V. C. D., Faquin, V., Guimarães, K. C., Andrade, F. R., Pereira, J., and Guilherme, L. R. G. (2018). Agronomic biofortification of carrot with selenium. *Ciência e Agrotecnol.* 42, 138–147.

Pessoa, J., Sárkány, Z., Ferreira-da-Silva, F., Martins, S., Almeida, M. R., Li, J., et al. (2010). Functional characterization of Arabidopsis thaliana transthyretin-like protein. *BMC Plant Biol.* 10:30. doi: 10.1186/1471-2229-10-30

Pilon-Smits, E. A. H., Quinn, C. F., Tapken, W., Malagoli, M., and Schiavon, M. (2009). Physiological functions of beneficial elements. *Curr. Opin. Plant Biol.* 12, 267–274. doi: 10.1016/j.pbi.2009.04.009

Power, D. M., Elias, N. P., Richardson, S. J., Mendes, J., Soares, C. M., and Santos, C. R. A. (2000). Evolution of the thyroid hormone-binding protein, transthyretin. *Gen. Comp. Endocr.* 119, 241–255. doi: 10.1006/gcen.2000.7520

Rizelio, V. M., Tenfen, L., Da Silveira, R., Gonzaga, L. V., Costa, A. C. O., and Fett, R. (2012). Development of a fast capillary electrophoresis method for determination of carbohydrates in honey samples. *Talanta* 93, 62–66.

Sady, W. (2006). *Fertilization of field vegetables*. Kraków: Plantpress, 70–71.

Sahin, O. (2020). Combined biofortification of soilless grown lettuce with iodine, selenium and zinc and its effect on essential and non-essential elemental composition. *J. Plant Nutr.* 2020, 1–7.

Salau, B. A., Ketiku, A. O., Ajani, E. O., Ezima, E. N., Idowu, G. O., and Soladoye, M. O. (2008). Iodine contents of some selected roots/tubers, cereals and legumes consumed in Nigeria. *Afr. J. Biotechnol.* 7, 4328–4330.

Saniewski, M., Góraj, J., Węgrzynowicz-Lesiak, E., Miyamoto, K., and Ueda, J. (2014). Differential of auxin polar transport inhibitors on rooting in some Crassulaceae species. *Acta Agrobot.* 67, 85–92. doi: 10.5586/aa.2014.028

Shinonaga, T., Casta, J., Muck, K., and Gerzabek, M. H. (2000). Determination of iodinein cereal grains and standard reference materials by neutron activationanalysis. *Int. J. Environ. Anal. Chem.* 78, 175–184. doi: 10.1080/03067310008044409

Signore, A., Renna, M., D'Imperio, M., Serio, F., and Santamaria, P. (2018). Preliminary Evidences of Biofortification with Iodine of "Carota di Polignano", An Italian Carrot Landrace. *Front. Plant Sci.* 9:170. doi: 10.3389/fpls.2018.00170

Smoleń, S., Baranski, R., Ledwożyw-Smoleń, I., Skoczylas, Ł, and Sady, W. (2019). Combined biofortification of carrot with iodine and selenium. *Food Chem.* 300, 1–8. doi: 10.1016/j.foodchem.2019.125202

Smoleń, S., Kowalska, I., Halka, M., Ledwożyw-Smoleń, I., Grzanka, M., Skoczylas, Ł, et al. (2020). Selected aspects of iodate and iodosalicylate metabolism in lettuce including the activity of vanadium dependent haloperoxidases as affected by exogenous vanadium. *Agronomy* 10, 1–21. doi: 10.3390/agronomy10010001

Smoleń, S., Kowalska, I., and Sady, W. (2014a). Assessment of biofortification with iodine and selenium of lettuce cultivated in the NFT hydroponic system. *Sci. Hortic.* 166, 9–16. doi: 10.1016/j.scienta.2013.11.011

Smoleń, S., Sady, W., Ledwożyw-Smoleń, I., Strzetelski, P., Liszka-Skoczylas, M., and Rożek, S. (2014b). Quality of fresh and stored carrot depending on iodine and nitrogen fertilization. *Food Chem.* 159, 316–322. doi: 10.1016/j.foodchem.2014.03.024

Smoleń, S., Skoczylas, Ł, Ledwożyw-Smoleń, I., Rakoczy, R., Kopeć, A., Piątkowska, E., et al. (2016b). Iodine and selenium biofortification of lettuce (*Lactuca sativa* L.) by soil fertilization with various compounds of these elements. *Acta Sci. Polon Hort. Cult.* 15, 69–91.

Smoleń, S., Skoczylas, Ł, Ledwożyw-Smoleń, I., Rakoczy, R., Kopeć, A., Piątkowska, E., et al. (2016a). Biofortification of carrot (*Daucus carota* L.) with iodine and selenium in a field experiment. *Front. Plant Sci.* 7:730. doi: 10.3389/fpls.2016.00730

Smoleń, S., Ledwożyw-Smoleń, I., and Sady, W. (2016c). The role of exogenous humic and fulvic acids in iodine biofortification in spinach (*Spinacia oleracea* L.). *Plant Soil.* 402, 129–143.

Sors, T. G., Ellis, D. R., and Salt, D. E. (2005). Selenium uptake, translocation, assimilation and metabolic fate in plants. *Photosynthesis Res.* 86, 373–389. doi: 10.1007/s11120-005-5222-9

Sors, T. G., Martin, C. P., and Salt, D. E. (2009). Characterization of selenocysteine methyltransferases from Astragalus species with contrasting selenium accumulation capacity. *Plant J.* 59, 110–122.

Vanuze Costa de Oliveira, V., Faquin, V., Guimarães, K. C., Andrade, F. R., Pereira, J., et al. (2018). Agronomic biofortification of carrot with selenium. *Ciência e Agrotecnol.* 42, 138–147. doi: 10.1590/1413-70542018422031217

White, P. J., and Broadley, M. R. (2005). Biofortifying crops with essential mineral elements. *Trends Plant Sci.* 10, 586–593.

White, P. J., and Broadley, M. R. (2009). Biofortification of crops with seven mineral elements often lacking in human diets - iron, zinc, copper, calcium, magnesium, selenium and iodine. *New Phytol.* 182, 49–84. doi: 10.1111/j.1469-8137.2008.02738.x

Winkel, L. H., Vriens, B., Jones, G. D., Schneider, L. S., Pilon-Smits, E., and Bañuelos, G. S. (2015). Selenium cycling across soil-plant-atmosphere interfaces: acritical review. *Nutrients* 7, 4199–4239. doi: 10.3390/nu7064199

Wrolstad, R., and Smith, D. (2017). Color Analysis. *Food Analy.* 2017, 545–555. doi: 10.1007/978-3-319-45776-5-31

Xue, T., Hartikainen, H., and Piironen, V. (2001). Antioxidative and growth-promoting effect of selenium on senescing lettuce. *Plant Soil* 237, 55–61. doi: 10.1023/A:1013369804867

Zhang, H., Zhao, Z., Zhang, X., Zhang, W., Huang, L., Zhang, Z., et al. (2019). Effects of foliar application of selenate and selenite at different growth stages on Selenium accumulation and speciation in potato (*Solanum tuberosum* L.). *Food Chem.* 286, 550–556.

Zhu, Y. G., Huang, Y., Hu, Y., Liu, Y., and Christie, P. (2004). Interactions between selenium and iodine uptake by spinach (*Spinacia oleracea* L.) in solution culture. *Plant Soil.* 261, 99–105.

Zimmermann, M. B. (2011). The role of iodine in human growth and development. *Sem. Cell Devel. Biol.* 22, 645–652. doi: 10.1016/j.semcdb.2011.07.009

Zou, C., Du, Y., Rashid, A., Ram, H., Savasli, E., Pieterse, P. J., et al. (2019). Simultaneous biofortification of wheat with zinc, iodine, selenium, and iron through foliar treatment of a micronutrient cocktail in six countries. *J. Agric. Food Chem.* 67, 8096–8106. doi: 10.1021/acs.jafc.9b01829

Conflict of Interest: HK is CEO of Intermag. KA is Director of R&D at Intermag. RR-L and MG are employees of Intermag Sp. z o.o., Olkusz, Poland, a company active in the sector of fertilizers and biostimulants.

The remaining authors declare that the research was conducted in the absence of any commercial or financial relationships that could be construed as a potential conflict of interest.

Copyright © 2021 Rakoczy-Lelek, Smoleń;, Grzanka, Ambroziak, Pitala, Skoczylas, Liszka-Skoczylas and Kardasz. This is an open-access article distributed under the terms of the Creative Commons Attribution License (CC BY). The use, distribution or reproduction in other forums is permitted, provided the original author(s) and the copyright owner(s) are credited and that the original publication in this journal is cited, in accordance with accepted academic practice. No use, distribution or reproduction is permitted which does not comply with these terms.

frontiers in Plant Science

ORIGINAL RESEARCH
published: 14 June 2021
doi: 10.3389/fpls.2021.658892

Effect of the Boron Concentration in Irrigation Water on the Elemental Composition of Edible Parts of Tomato, Green Bean, Potato, and Cabbage Grown on Soils With Different Textures

Márk Rékási[1], Péter Ragályi[1], Anna Füzy[1], Nikolett Uzinger[1], Péter Dobosy[2], Gyula Záray[2], Nóra Szűcs-Vásárhelyi[1], András Makó[1] and Tünde Takács[1]*

[1]Institute for Soil Sciences, Centre for Agricultural Research, Budapest, Hungary, [2]Institute of Aquatic Ecology, Centre for Ecological Research, Budapest, Hungary

The most important environmental source of boron (B) contamination is irrigation water. The data on the effect of B on the elemental composition in the edible parts of vegetables are scarce. A greenhouse pot experiment investigated the effect of irrigation water containing 0.1 and 0.5 mg/L B on the biomass, elemental (e.g., B, Mg, K, Fe, Cu, and Zn) composition, and photosynthetic parameters of tomato (*Solanum lycopersicum*), green bean (*Phaseolus vulgaris*), potato (*Solanum tuberosum*), and cabbage (*Brassica oleracea*) plants grown on 10 kg of sand, silty sand, or silty soil. The biomass of the edible part was unaffected by B treatment. The soil type determined the effect of B irrigation on the elemental composition of vegetables. The B content increased by 19% in tomatoes grown on silty soil. The 0.1 mg/L B treatment facilitated tomato fruit ripening on all soils, and the 0.5 mg/L B treatment doubled its chlorophyll content index (CCI) on silty soil. The 0.5 mg/L B treatment negatively affected the nutritional value of green beans on all soils, decreasing the Fe and K contents by an average of 83 and 34%, respectively. The elemental composition of potato was unaffected by the treatments, but the CCI of potato leaves increased in the 0.5 mg/L B treatment by 26%. The B content was increased by 39% in cabbages grown on light-textured soils. In conclusion, B concentration of up to 0.5 mg/L in irrigation water had no significant beneficial or adverse effect on the investigated vegetables, but 0.1 mg/L B treatment could shorten tomato fruit maturation time on B-poor soils. The B levels in vegetables remained suitable for human consumption.

Keywords: irrigation, element uptake, translocation, vegetables, nutritional value

OPEN ACCESS

Edited by:
Spyridon Alexandros Petropoulos, University of Thessaly, Greece

Reviewed by:
Georgios Liakopoulos, Agricultural University of Athens, Greece
Sukamal Sarkar, Bidhan Chandra Krishi Viswavidyalaya, India
Rilner Flores, Universidade Federal de Goiás, Brazil

***Correspondence:**
Péter Ragályi
ragalyi.peter@atk.hu

Specialty section:
This article was submitted to Plant Nutrition, a section of the journal Frontiers in Plant Science

Received: *26 January 2021*
Accepted: *19 May 2021*
Published: *14 June 2021*

Citation:
Rékási M, Ragályi P, Füzy A, Uzinger N, Dobosy P, Záray G, Szűcs-Vásárhelyi N, Makó A and Takács T (2021) Effect of the Boron Concentration in Irrigation Water on the Elemental Composition of Edible Parts of Tomato, Green Bean, Potato, and Cabbage Grown on Soils With Different Textures. Front. Plant Sci. 12:658892. doi: 10.3389/fpls.2021.658892

INTRODUCTION

The three quality criteria for irrigation water are decisive for the potential threat to crop production, namely, salinity, sodicity, and toxicity. Regarding the third criterion, the main characteristic water components that may cause adverse physiological effects in plants are chloride and boron (B; Rhoades, 1972). On the one hand, the application of B-rich irrigation water (B irrigation) is a global issue and the most important B pollution source in the environment (Türker et al., 2019). On the other hand, a study by FAO revealed that B deficiency is a worldwide problem, affecting about 8 million ha (Tariq and Mott, 2007).

Boron (B) is both a potential hazard and an essential micronutrient for vascular plants. It is not classified as an essential nutrient in the human diet (Naghii et al., 1996; Rainey et al., 1999), but B deficiency affects the skeleton and brain physiology and modifies the metabolism of several nutrients (Nielsen, 1996). The daily intake ranges from 0.02 to >9 mg/day; the consumption of B above 10 mg/day may be toxic (Rainey et al., 1999; EFSA, 2018), but an intake of at least 1 mg B/day is recommended (Nielsen, 1997). The major B sources are legumes, fresh vegetables, and fruits (Naghii et al., 1996).

In plants, B deficiency causes biochemical, physiological, and anatomical aberrations. B plays a role in carbohydrate transport, cell wall and membrane synthesis and function, nucleic acid and hormone metabolism, and the growth of the apical meristem (Howe, 1998; Bolaños et al., 2004; Pereira et al., 2021). Of all the nutrients, B has the narrowest optimal concentration in a range between toxicity and deficiency (Rees et al., 2011). The tolerance of plants to B is highly dependent on soil properties and irrigation management, which influence the availability of B (Bingham, 1973). Vascular plants absorb B mostly by passive diffusion, especially in the case of adequate or high availability of B. Under these circumstances, the absorption of B is mostly determined by the B concentration in the soil solution and the transpiration rate. However, if the availability of B is low, the transportation of active membrane will also occur in the plants (Dannel et al., 2002).

For plants, the main source of B is the soil, the B content of which depends mostly on the elemental composition of the parent material. The total B concentration in soils ranges from 1 to 467 mg/kg, with an average value of 9–85 mg/kg. B may be adsorbed on either organic or inorganic surfaces in the soil, but these bonds are weak (Kabata-Pendias and Pendias, 2001). In addition, B in mineral forms is not readily available for plants (Nable et al., 1997). In soils with higher $CaCO_3$ content and pH value, B is less available for plants, probably due mainly to the pH that facilitates the formation of the tetrahedral anionic form of boric acid (Goldberg, 1997; Parks and Edwards, 2005). Soils with high organic matter (OM) content and a pH of less than 7.3 may contain more available B than that is required for plant nutrition (Berger and Truog, 1939). The soil texture, moisture content, and temperature also affect the availability of B. The higher soil clay content results in a higher adsorption capacity of B, which increases with increasing pH and reaches its maximum at pH 8 (Goldberg, 1997). Thus, the addition of B with irrigation water may influence the elemental composition and growth of plants in different ways on different soils.

The amount of B available in the soil determines the plant uptake of B, which in turn influences the elemental composition of the plant and thus the nutritional value of edible plant parts. The data on the B tolerance of various crops are available in the literature, but information on the effect of B irrigation on elemental composition, and hence, the nutritional value of edible plant parts is scarce. The other shortcoming of the available literature is that most experiments were performed under hydroponic conditions or on artificial growth media, thus preventing investigations on the effect of soil properties that may modify the availability of B. Parks et al. (1944) found that, on quartz sand, the elemental composition of tomato leaves changed as a function of B supplies. The sign of changes in element contents of plants was dependent on the soil B concentration. Eggert and von Wirén (2016) demonstrated that B fertilization may improve the microelement uptake of oilseed rape seedlings in growth media that are poor in B. Tariq and Mott (2006) reported the increases in the concentration of B, Zn, and Cu and the decreases in Fe, Mn, and Mo in radish plants that are grown on acid-washed sand as the B concentration of the nutrient solution rose. The leaves of tobacco grown on peat growth medium showed an increase in Mn and Fe concentration and a decrease in Cu and Zn concentration as a function of the B concentration in the irrigation water (López-Lefebre et al., 2002). The effect of B irrigation on the elemental concentration of maize grown on quartz sand was also demonstrated by Mozafar (1989). Choi et al. (2015) found that insufficient B supplies reduced the Ca content of tomato fruit clusters in water culture after 36 days. Dursun et al. (2010) also investigated the effect of B fertilization on tomato, but this study focused on the elemental composition of the vegetative parts of the plant. Similarly, Eraslan et al. (2007) studied the effect of toxic amounts of B on the vegetative parts of tomatoes on soil media and showed an increase in N, P, and K contents in the plant in parallel with the decrease in biomass. Ghasemidehkordi et al. (2018) studied the B content of leafy vegetables and irrigation water in Iran but did not examine the relationship between these parameters. Lucho-Constantino et al. (2005) studied the effect of irrigation with wastewater with high B concentration in a sample area in Mexico, which showed the risk posed by B, but did not examine the direct relationship between the B content of irrigation water and the elemental composition of plants.

This study aimed to investigate the effect of B irrigation on the elemental composition and the B accumulation in the edible parts in four vegetables (i.e., tomato, potato, cabbage, and green bean) grown on soils of different textural classes. The possible toxicity effect of the treatments was monitored by measuring photosynthetic parameters. The B concentration in the irrigation water (0.1 and 0.5 mg/L) was chosen to avoid acute toxicity and to reveal the effects of B in physiologically healthy plants. These concentrations are below the B threshold values for irrigation water in most countries (Jeong et al., 2016). According to the study by Bingham (1973), potato and tomato can be considered as semi-tolerant plants of B, being

able to tolerate up to 5 mg/L B in the soil solution without negative effects. Cabbage can tolerate B concentrations of up to 10 mg/L. No data appear in the studies available in the literature on the B tolerance of green bean. Wilcox (1960) suggested the critical concentrations of 1–2 and 2–4 mg B/L in the irrigation water for semi-tolerant and tolerant plants, respectively. However, these values are highly dependent on soil properties and irrigation management, which influence the availability of B.

In the study by Fernandez-Jaramillo et al. (2012), chlorophyll fluorescence (Fv/Fm) imaging and the chlorophyll content index (CCI) were used to determine the changes in photosynthetic processes, which are the indicators of plant health and B phytotoxicity, but the reports on the use of quantum efficiency of photosystem II (PSII) photochemistry to determine the toxicity of different B concentrations in tissues are still rare. Most of the studies in the literature focus on the plant physiological processes caused by B deficiency or discuss the simultaneous application of B and other microelements and macroelements (Chapman et al., 1997; Herrera-Rodríguez et al., 2010). Moreover, most of the studies were performed in a hydroponic system. The Fv/Fm ratio significantly decreased in plants due to the effect of B toxicity (Guidi et al., 2011; Landi et al., 2012). The Fv/Fm reduction could be caused by the structural damage in thylakoid membranes, changing the electron transport and inhibiting the photoassimiliation. The photoinhibition is also amplified by the reduction in stomatal conductance under B loading. The stress-induced changes in the quantity and composition of photosynthetic pigments caused variations in the optical features of leaves and plant chlorophyll content, which are the indicators of phytotoxicity (Füzy et al., 2019).

The questions raised in this study were as follows: (i) Does the B concentration of the irrigation water influence the B concentration of plants and the transfer of B from soil to plants and within the plants on different soils? (ii) Does B concentration in irrigation water influence some parameters of the photosynthetic system and biomass of plants grown on different soils? (iii) Does the B concentration of the irrigation water influence the elemental composition of the edible parts of vegetables grown on different soils?

MATERIALS AND METHODS

Experimental Setup

The effect of irrigation with a B solution was investigated in a pot experiment conducted in a greenhouse with two open sides at the Experimental Station of the Centre for Agricultural Research in Őrbottyán, Hungary, using 10-L pots with four holes (Ø 0.5 cm) in the bottom so that leached water could flow out (Dobosy et al., 2020). The bottom of each pot was filled with a 1-cm layer of gravel (4–8 mm) covered with a fine synthetic fiber fabric on which 10 kg of soil was placed (Dobosy et al., 2020). The three topsoils (0–20 cm) investigated were as follows: sand [Mollic Umbrisol (Arenic) from Őrbottyán], silty sand (Luvic Calcic Phaeozem from Gödöllő), and silty soil (Calcic Chernozem from Hatvan). The soil properties are shown in **Table 1**. The total number of pots was measured as follows: three soils × two B doses (i.e., 0.1 and 0.5 mg B/L; actual measured concentrations were 0.134 and 0.506 mg B/L, respectively) + control (i.e., tap water; actual measured B concentration: 0.023 mg B/L) × 4 plant species × 3 replications = 108. The test plants were tomatoes (e.g., *Solanum lycopersicum*, cv. Mano; ZKI), green beans (e.g., *Phaseolus vulgaris*, cv. Golden Goal; Réde), potatoes (e.g., *Solanum tuberosum* L. cv. Balatoni rózsa), and cabbages (e.g., *Brassica oleracea* L. var. *capitata* cv. Zora; Réde). Before the pot experiment was set up, tomato and cabbage seeds and potato tubers were germinated and planted in propagation trays (i.e., 1 seed or tuber/cell) filled with VEGASCA Bio vegetable organic growing medium (i.e., mixture of peat and gray cattle manure compost; OM > 50%; *N* > 0.3%; P_2O_5 > 0.1%; K_2O > 0.1%; pH of 6.8). The seedlings were cultivated in a random arrangement in a growth chamber for 22 days at day/night temperatures and photoperiods of 26/18°C and 16/8 h, respectively, with a photon flux density of 500 μmol/m^2/s and relative humidity of 50–70%. The seedlings were irrigated weekly with 60-ml tap water. The soil-free seedlings were then transplanted into the experimental plastic pots (1 seedling/pot) after a 6-day acclimatization period in the greenhouse. The germinated seeds of green beans were planted directly into the experimental soils (1 seed/pot).

The irrigation water was delivered using individual drip stakes placed in each pot. After planting the seedlings were irrigated with tap water for 3 weeks, but during the growing period, all the plants (including the control) were watered weekly with Hoagland solution (200 ml/pot). Irrigation with B solution (H_3BO_3 diluted with tap water) started 3 weeks after planting. The tap water was stored in 0.5 m^3 tanks (i.e., separate tanks for each irrigation solution) before applying in order to reduce the chlorine concentration. The daily volume of irrigation water was adjusted to the water requirements of the plant species.

TABLE 1 | Selected properties of the applied soils.

Properties	Sand	Silty sand	Silt
pH-H_2O	7.96	6.83	7.34
OM (%)	0.91	1.24	2.12
$CaCO_3$ (%)	1.45	0.08	0.20
CEC (Na meq/100 g)	9	17	37
Total N (%)	0.064	0.092	0.135
NH_4-N (mg/kg)	1.4	2.3	3.9
NO_3-N (mg/kg)	4.7	2.3	14.2
Total K (mg/kg)	3,164	7,250	7,639
AL-K_2O (mg/kg)	74	174	176
Total P (mg/kg)	449	446	412
AL-P_2O_5 (mg/kg)	131	238	81
Total B (mg/kg)	2.63	5.26	9.14
Water-soluble B (mg/kg)	0.102	0.267	0.306
Total Mg (mg/kg)	4,035	3,942	5,399
Total Fe (mg/kg)	10,028	17,875	29,651
Total Cu (mg/kg)	5.00	13.8	20.1
Total Zn (mg/kg)	22.9	49.1	62.1
Clay (<0.002 mm, %)	14	23	34
Silt (0.002–0.02 mm, %)	18	30	50
Sand (0.02–2 mm, %)	69	46	16

AL, ammonium-lactate soluble; total, aqua regia-soluble.

A monitoring system (Sensor: Decagon EC-5) installed at a depth of 10 cm measured the soil moisture content every hour. The irrigation system delivered the set amount of water at 7 AM every day. The irrigation details can be found in **Table 2**.

The experimental area received natural light in a greenhouse, where the climate data (i.e., mean day and night temperature, air humidity, and photon flux density of photosynthetically active radiation) were continuously monitored during the growing period (**Table 3**). Pesticides were applied as necessary.

Chemical Analysis

The plants were harvested and cleaned with deionized water, after which the root, shoot (stem + leaf), and fruit were separated, and the fresh weight (FW) of the plant parts was measured. The shoot and root samples were dried at 40°C for 2 days in a laboratory dryer, while tomato, green bean, and potato fruit samples were freeze-dried at −70°C in Christ Alpha 1 equipment (Martin Christ Gefriertrocknungsanlagen GmbH, Germany; 200 Pa for 72 h), after which the dry mass of the samples was determined. All the samples were homogenized in a household blending machine equipped with plastic housing and a stainless-steel blade. The dried, homogenized samples were mineralized in a microwave-assisted acid digestion system (TopWave, Analytik Jena, Germany). Twelve PTFE bombs were used, 1 for the blank and 11 for the samples, and the blank was measured each time. Dried plant samples (400–500 mg) were digested in a mixture of 7 cm^3 67% HNO_3 and 3 cm^3 30% H_2O_2. After digestion, the internal standards were added to the solutions and the volume was made up to 15 cm^3 with deionized water. The concentrations of B, macroelements, and microelements were measured by inductively coupled plasma mass spectrometer (ICP-MS).

After removing plant residues, the soil samples were dried and sieved through a 2-mm size mesh. The pseudo-total B, K, and P contents of soil samples were determined after digestion with aqua regia in a microwave Teflon bomb (MSZ-21470-50, 2006). The plant-available B fraction of soil samples was measured in 0.5 M NH_4 acetate + 0.02 M ethylenediaminetetraacetic acid (EDTA) extract (Lakanen and Erviö, 1971). The plant-available P and K contents were determined in ammonium acetate–lactate (AL) extract (AL-P_2O_5 and AL-K_2O; Egnér et al., 1960). The element contents were measured using the ICP-MS method. The operating conditions of the ICP-MS instrument are summarized in **Supplementary Table 1**. The total N content was analyzed according to the Kjeldahl method (ISO 11261, 1995), and the mineral N (NH_4-N and NO_3-N) contents were measured from KCl extracts (MSZ-20135, 1999). The soil pH was measured according to the Hungarian Standard (MSZ-08-0206/2, 1978) in a soil:water suspension of 1:2.5 after mixing for 12 h. Soil OM content was determined using the modified Walkley–Black method (MSZ-08-0452, 1980). The soil $CaCO_3$ content was measured by the Scheibler gas-volumetric method (MSZ-08-0206/2, 1978), and the cation exchange capacity (CEC) values were measured by the modified method of Mehlich (MSZ-08-0215, 1978).

TABLE 2 | Irrigation parameters in the greenhouse.

Parameters	Tomato	Green bean	Potato	Cabbage
Growing period (transplanting-harvest)	24 May–21 August	23 May–24 July	24 May–17 July	17 July–25 September
Length of growing period (days)	88	63	55	71
Total irrigation (ml/pot)	36,983	15,645	19,553	22,965
B load in 0.1 mg/L treatment (mg/pot)	2.71	0.78	1.07	1.91
B load in 0.5 mg/L treatment (mg/pot)	13.56	3.88	5.35	9.53

Translocation Coefficient

The translocation coefficient (TC) has been calculated according to Wang et al. (2017). Three steps of translocation have been defined as follows: (i) from soil to root (root/soil total B content including the B added with irrigation); (ii) from root to shoot (shoot/root B content); and (iii) from shoot to fruit (fruit/shoot B content).

Quantum Efficiency of PSII Photochemistry and CCI

The CCI values of potato, tomato, green bean, and cabbage cultivars were measured at the harvesting stage. The CCI values of the youngest adult leaves were determined *in situ* using a CCM-200 plus Chlorophyll Content Meter (Opti-Sciences, Hudson, NY, United States) and calculated from the average of three measurements per plant. The quantum efficiency (Fv/Fm) of PSII photochemistry was measured with Os30p+ handheld chlorophyll fluorometer (Opti-Sciences). To indicate the potential stress caused in the crops by B treatment, Fv/Fm ratios were measured after 15-min dark adaptation.

Statistical Analysis

The data were analyzed for treatment effects using factorial analysis of variance (ANOVA) and Tukey's *post hoc* test. The variance was calculated for soil type and B concentration of the irrigation water. Significant differences between the treatments were calculated at the $p < 0.05$ level. Statistica version 13

TABLE 3 | Greenhouse parameters during the growing period.

Parameters	Tomato	Green bean	Potato	Cabbage
Mean day temperature (°C)	26.6 ± 3.3	25.5 ± 3.3	25.6 ± 3.5	25.5 ± 4
Mean night temperature (°C)	19.1 ± 2.3	18.3 ± 2.3	18.1 ± 2.3	18.2 ± 3.4
Photosynthetically active radiation (μmol/m^2/s)*	982 ± 419	1,045 ± 484	1,097 ± 489	703 ± 197
Air humidity (%)	69.4 ± 8.1	70.3 ± 8.6	69.7 ± 23.3	72.2 ± 23
Soil moisture (% v/v)	22 ± 3	24 ± 3	22 ± 6	22 ± 6

Spectral band: 400–700 nm.

(Statsoft Inc, Palo Alto, CA, USA) software was used for all the statistical evaluations. Data visualization was performed with R statistical software (R Core Team, 2019).

RESULTS

Soil Chemical Properties

Regarding their original B contents, the applied soils can be categorized as B-poor soils as they are in the low end of the natural concentration range (Kabata-Pendias and Pendias, 2001). As a result of irrigation, the total B concentration did not change in the soils. The plant-available B content increased as a function of the B concentration in the irrigation water, but this change was only significant in the case of cabbages, green beans, and tomatoes cultivated on sandy soil (**Supplementary Table 2**). The pH and plant-available N, P, and K contents did not change significantly during the experiment as a function of the B concentration in the irrigation water.

Plant Biomass

Based on the biomass values, none of the irrigation water was toxic to the plants. In the case of tomatoes and potatoes, the treatment did not influence the biomass of the plant organs (i.e., root, shoot, and fruit/tuber; **Supplementary Table 3**). The average FW of tomato fruit was 306 ± 77 g/plant and the dry weight (DW), 19.8 ± 4.6 g/plant. The shoot and root biomass were 26.3 ± 5.5 g and 3.23 ± 0.53 g DW, respectively. The average FW of potato tuber was 179 ± 19 g/plant and its average DW was 34.2 ± 4.4 g/plant, while the average shoot and root DW were 9.38 ± 1.07 g/plant and 2.7 ± 0.6 g/plant, respectively. Neither FW nor DW of the green bean fruits nor the shoot DW (100 ± 23 g/plant, 10.6 ± 3 g/plant, and 12.3 ± 1.8 g/plant, respectively) changed as a function of B treatment on any soil. The dry biomass of green bean roots was also unaffected by B irrigation, being 4.1 ± 0.8 g/plant on sandy soil and 1.84 ± 0.17 g/plant on the other two soils. The irrigation and soil-type combinations did not modify the biomass of cabbage leaves (520 ± 48 g FW/plant and 53 ± 8.4 g DW/plant), but the root DW was increased from the control value of 1.95 g/plant to 4.50 g/plant, applying 0.5 mg B/L irrigation water on sandy soil.

Quantum Efficiency of PSII Photochemistry and CCI

No visible toxic symptoms were observed on B-irrigated plants compared with the control plants (**Table 4**). The Fv/Fm ratio of potato, cabbage, and tomato leaves ranged from 0.667 to 0.83, which was not significantly affected by either the soil type or the B treatment. The lowest Fv/Fm values were measured in the control potato cultivated on sand and the highest values were measured in cabbages grown on silty soil in the control treatment.

Chlorophyll content index was proved to be a more sensitive indicator of the effect of B treatments than Fv/Fm. In comparison with the control, both doses of B significantly increased the CCI value in potatoes on silty soil. Potatoes had significantly higher CCI on silt than on silty sand or sand. On silty soil, the 0.5 mg/L B treatment caused a significant increase in the CCI value of tomato compared with the control. The CCI of cabbage leaves was not affected either by different B doses or by soil type. In the case of green beans, the highest CCI values were observed on silty sand.

Element Content in Edible Parts

The boron treatment had a significant effect on the elemental composition of the edible part of the plants. The B content in the edible parts increased in all the plant species as a result of increasing B concentration in the irrigation water, but in most cases, this change was not significant. The soil type influenced the effect of B irrigation on the element content of edible parts.

In the case of tomatoes, irrigation with B-rich water affected the content of all the elements tested, though the B content of fruit increased significantly (by 18%) only on silty soil in the 0.5 mg B/L treatment (**Figure 1**). On sand and silt substrate, the Mg content in the tomato fruit increased by the B concentration of irrigation water, being 36% higher than the control in the 0.5 mg B/L treatment on sand and 44% higher on silty soil. Only the K content of tomato changed on sand and silty sand as a result of the B treatments, with average decreases of 12 and 18% compared with the control. The Fe content of tomato fruit tripled on sandy soil and doubled on silty sand and silty soil in the 0.1 mg B/L treatment.

TABLE 4 | Chlorophyll content index (CCI) and quantum efficiency of PSII photochemistry (Fv/Fm) of investigated plants.

Soil	Irrigation water	Tomato		Cabbage		Green bean		Potato	
		Fv/Fm	CCI	Fv/Fm	CCI	Fv/Fm	CCI	Fv/Fm	CCI
Sand	Control	0.786 ± 0.009a	12.5 ± 3.1ab	0.831 ± 0.003a	20.9 ± 4.3a	0.735 ± 0.012a	15.5 ± 4.6ab	0.667 ± 0.028a	11.1 ± 1.0a
	0.1 mg B/L	0.780 ± 0.010a	15.6 ± 4.2abc	0.829 ± 0.004a	24.4 ± 7.3a	0.723 ± 0.004a	11.7 ± 2.1a	0.685 ± 0.018a	14.7 ± 3.6ab
	0.5 mg B/L	0.783 ± 0.004a	15.9 ± 1.8abc	0.823 ± 0.016a	31.2 ± 11.6a	0.753 ± 0.015a	16.4 ± 1.6ab	0.718 ± 0.055a	14.2 ± 2.5ab
Silty sand	Control	0.792 ± 0.006a	10.9 ± 5.1abc	0.826 ± 0.012a	24.4 ± 7.2a	0.764 ± 0.033a	20.6 ± 1.5b	0.734 ± 0.045a	13.1 ± 2.2a
	0.1 mg B/L	0.789 ± 0.006a	18.5 ± 5.1abcd	0.825 ± 0.004a	22.4 ± 5.9a	0.787 ± 0.045a	19.0 ± 2.4ab	0.738 ± 0.052a	12.1 ± 1.8a
	0.5 mg B/L	0.794 ± 0.005a	30.2 ± 6.5cd	0.822 ± 0.009a	27.9 ± 11.7a	0.794 ± 0.025a	20.8 ± 1.4b	0.725 ± 0.035a	10.9 ± 0.3a
Silt	Control	0.771 ± 0.025a	16.0 ± 8.5abc	0.835 ± 0.005a	33.0 ± 16.4a	0.773 ± 0.023a	19.1 ± 4.1ab	0.726 ± 0.046a	19.0 ± 2.0b
	0.1 mg B/L	0.791 ± 0.011a	27.5 ± 9.6bcd	0.822 ± 0.010a	25.4 ± 3.5a	0.756 ± 0.039a	18.1 ± 2.7ab	0.736 ± 0.031a	25.9 ± 1.0c
	0.5 mg B/L	0.793 ± 0.012a	33.6 ± 4.0d	0.822 ± 0.011a	30.9 ± 12.6a	0.759 ± 0.039a	16.6 ± 2.5ab	0.706 ± 0.041a	24.6 ± 0.9c

The data are given as mean ± SD of the replicates. Different letters (a–d) indicate significant differences between rows ($p < 0.05$).

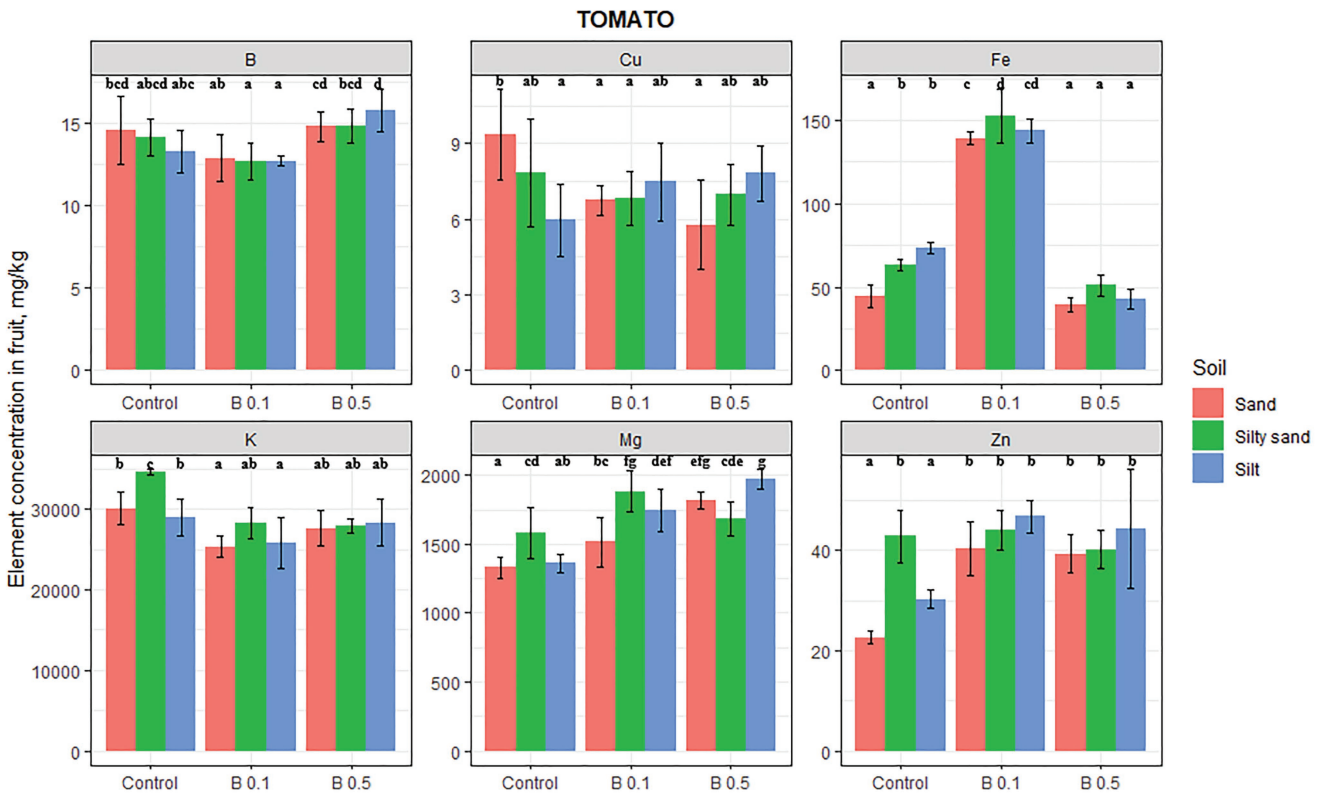


FIGURE 1 | Element contents in tomato fruit in different irrigation water treatments on sand, silty sand, and silty soil (mg/kg DW). The data are means of the replicates. Different letters (a–g) indicate significant differences between treatments ($p < 0.05$).

However, in the 0.5 mg B/L treatments, the Fe content remained at the control level on sandy soil, while it decreased significantly on silty sand and silty soil compared with the control. The Cu content of tomato fruit was only affected by B irrigation on sandy soil, where the Cu content diminished by 33% on average. In contrast, the Zn content in tomato fruit increased significantly in the B treatments on sandy and silty soil by 75 and 50%, respectively. Tomato was the only vegetable studied whose Zn content was increased by the B treatment.

The B content in green beans increased as a function of the B treatments, but this change was not significant (**Figure 2**). Significant changes were recorded only after B irrigation in Mg, K, and Fe. The Mg content decreased on all the soils, but the change was significant only in the 0.1 mg B/L treatment on silty soil (24%). The K content decreased significantly on every soil as a result of B treatment, but there was no difference between the effect of the two B doses, the reduction being 29, 33, and 40% compared with the control on sand, silty sand, and silty soil, respectively. The Fe content in green beans was also negatively affected by B irrigation, decreasing by 75, 83, and 90% on sand, silty sand, and silty soil, respectively, in the 0.5 mg B/L water treatment compared with the control. The Cu and Zn contents of green beans were unaffected by the B treatments.

Among the species tested, the elemental composition in the edible part of potatoes was the least affected by B irrigation (**Figure 3**). The B content in potato tubers increased as a function of B treatment on every soil, but this change was not significant. Similarly, Mg and K contents also increased on lighter textured soils, but this change was not significant either. B treatment had a negative effect on the Fe content on silty soil, with an average decrease of 56%. The only other element significantly influenced by the B treatment was Cu, which exhibited a 55% increase in the 0.1 mg B/L treatment on silty sand compared with the control. There was no change in the Zn content of potato tuber as a function of B treatments.

Boron treatment significantly influenced the B, Mg, K, Fe, and Cu contents of cabbage leaves (**Figure 4**), but the changes were highly dependent on the soil type. The concentration of B of the irrigation water influenced the elemental composition to the greatest extent on sand and silty sand. B, Mg, Fe, and Cu were influenced by B treatment on sandy soil, B, Mg, and K on silty sand, and only Fe on silty soil.

The increase in B content of cabbage leaves in the 0.5 mg B/L treatments was 34 and 39% on sand and silty sand, respectively. An increase of 19% was also observed on silty soil, but this was not significant. On sandy soil, B treatment significantly decreased the Mg content of cabbage leaves (by 14%), while on silty sand and silt, the opposite trend was observed, with a 22 and 8% increase in the 0.5 mg B/L treatment compared with the control, respectively. Although this change in the silty soil was not statistically significant, only the K

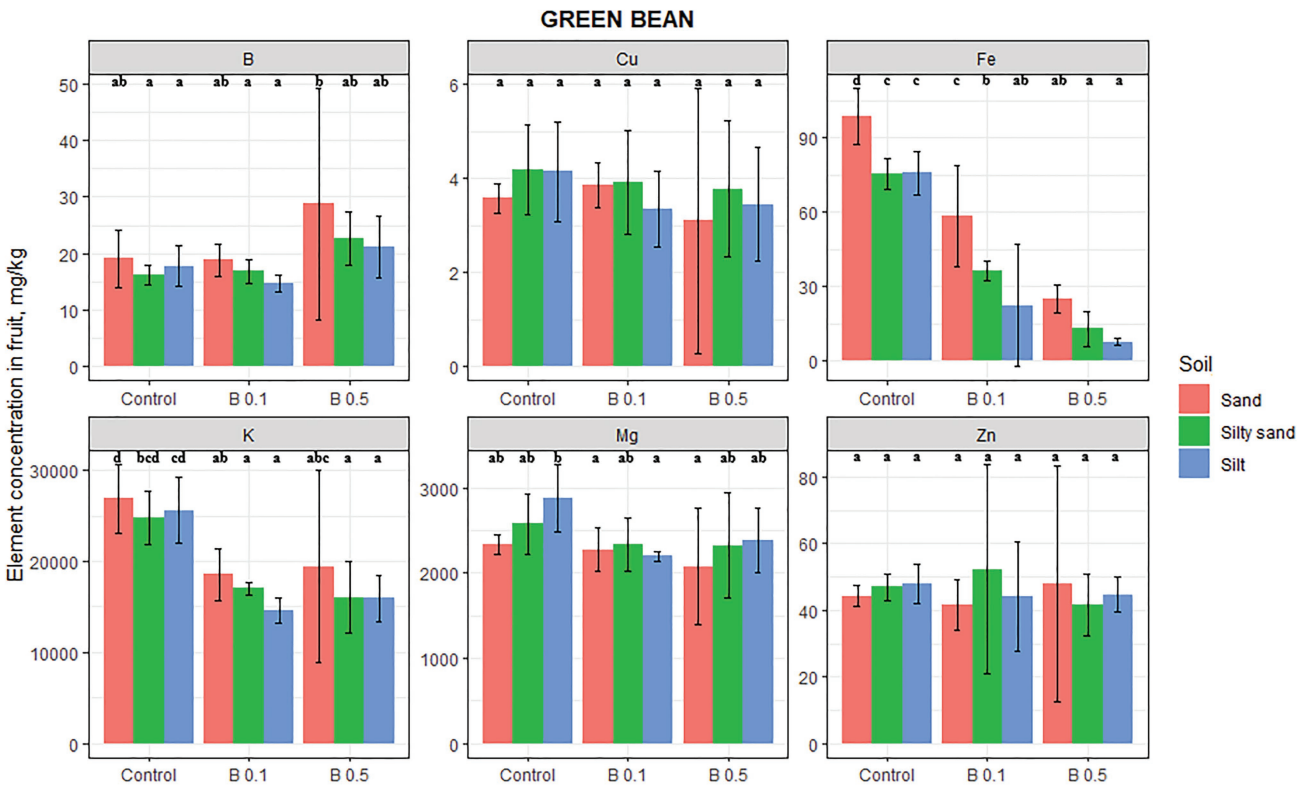


FIGURE 2 | Element contents in green bean fruit in different irrigation water treatments on sand, silty sand, and silty soil (mg/kg DW). The data are means of the replicates. Different letters (a–d) indicate significant differences between treatments ($p < 0.05$).

content in the leaves increased by 20% on silty sand in the 0.5 mg B/L water treatment compared with the control. The K content also increased on silty soil as a function of the B treatment, but the 12% change was not significant. The sign of the change in Fe content varied with the soil type. On sandy soil, it decreased by 28% in the 0.1 mg B/L treatment, but on silty sand, it increased by 30% in the 0.5 mg B/L treatment compared with the control. There was a significant decrease of 28% in the Cu content of cabbage leaves as a result of the 0.1 mg B/L treatment, but Zn was unaffected by the B irrigation on any of the soils.

Boron Translocation

The root/soil B translocation was higher on sandy soil (3.8 on average) than on silty sand (2 on average) and silt (1.4 on average) for all the plant species (**Table 5**). If TC is higher than 1, it means that B accumulates in the given plant part (Sasmaz, 2008). In the case of green beans, the B concentration in the irrigation water did not influence the root/soil TC on any soil. The B translocation to cabbage roots was significantly higher in the 0.1 mg B/L water treatment (2.9) than in the control (2.2) or the 0.5 mg B/L water treatment (2.0) on silty sand. In the case of tomatoes, the 0.1 mg B/L concentration resulted in the lowest root/soil TC on all three soils (1.4 on average). Potatoes had the highest root/soil TC values on average (3.1). The B treatment caused only a significant increase in the potato root/soil TC on sandy soil, from 3.9 (control) to an average value of 5.1 in the B treatments.

The soil type did not influence the shoot/root TC value, which was higher than 1 for all the species, indicating the accumulation of B in the shoot. The shoot/root TC values increased as a function of the B concentration in the irrigation water for all the species on all the soils, but this change was not always significant. The shoot/root TC for tomatoes was 37% higher on average in the B treatments than in the control on every soil. For green bean plants, the shoot/root TC significantly increased as a result of the 0.5 mg B/L treatment compared with the control on sand (2.8 times) and silty sand (1.8 times). For potatoes, the B concentration of the irrigation water did not cause any difference in the B translocation from root to shoot. In the case of cabbages, the 0.5 mg B/L treatment resulted in 1.4 times higher shoot/root TC compared with the control on silty sand, but on other soils, there was no significant increase. Based on the average shoot/root TC values, all three plant species can be considered as B accumulators. Tomatoes accumulated the most B in the shoot compared with the root, followed by potatoes, green beans, and cabbages. The average transfer values were 3.6, 2.9, 1.9, and 1.3, respectively.

The fruit/shoot TC values were below 1, showing that B was not accumulated in the edible parts of tomatoes, potatoes, and green beans.

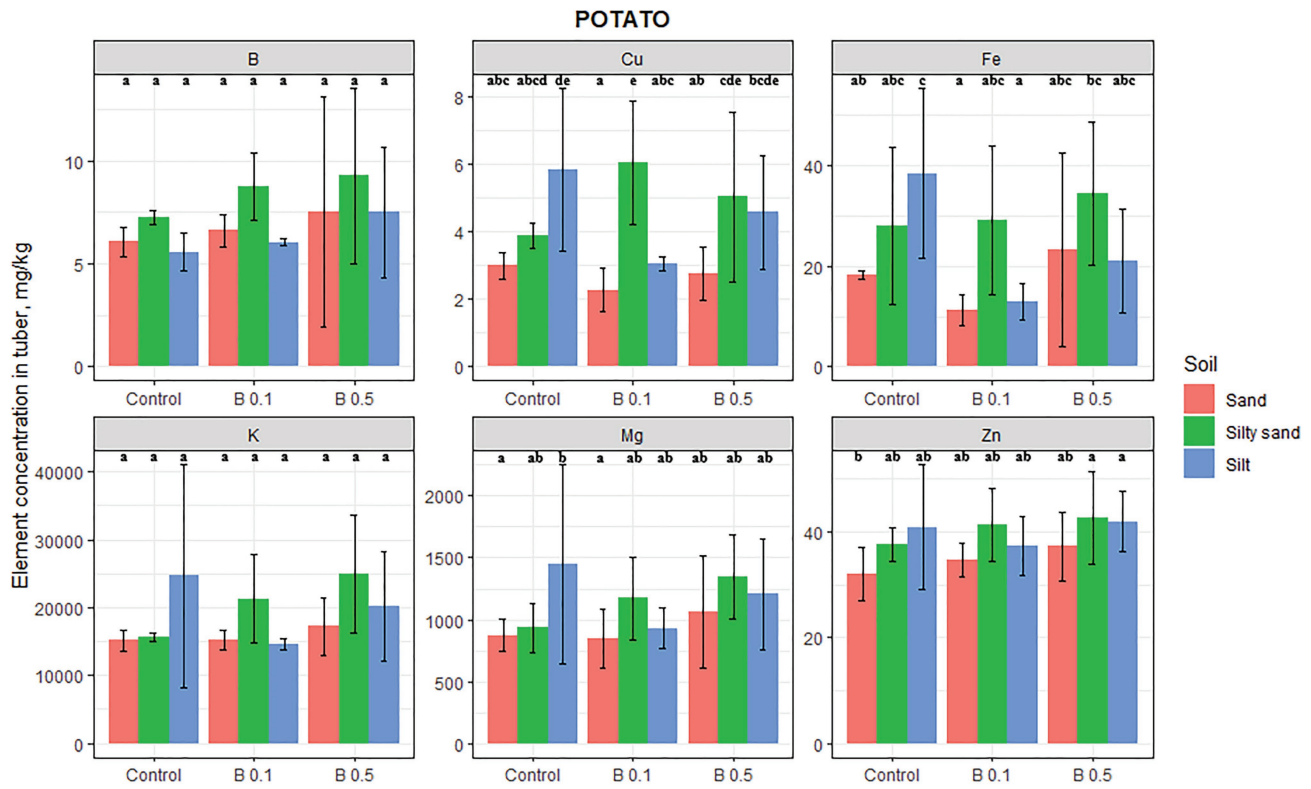


FIGURE 3 | Element contents in potato tuber in different irrigation water treatments on sand, silty sand, and silty soil (mg/kg DW). The data are means of the replicates. Different letters (a–e) indicate significant differences between treatments ($p < 0.05$).

DISCUSSION

Biomass

Boron may either increase or decrease plant yield depending on the circumstances. In this study, the B irrigation had no toxic effect on the plants under the given conditions. One specific symptom of B toxicity is a decrease in leaf and root biomass (Roessner et al., 2006; Turan et al., 2009), which was not observed in this experiment. On B-poor soils B fertilization has been reported to increase plant yield (Sarkar et al., 2018), but this was not confirmed in this study probably due to the low amount of the B applied (Singh and Singh, 1990; Ganie et al., 2014).

Photosynthetic Efficiency and CCI

The high concentrations of B in the plant growth medium or in the irrigation water can result in oxidative damage induced by antioxidant enzyme activity. The maximum quantum yield of Fv/Fm significantly decreased in plants exposed to B toxicity (Landi et al., 2012). Guidi et al. (2011) reported that a B concentration of up to 2 mg/L in the irrigation water caused no change in the Fv/Fm values of tomato leaves. When B stress levels were assessed, the chlorophyll fluorescence was found to be inversely proportional to B toxicity in potato cultivars (Ayvaz et al., 2016). In this study, the B treatments did not have a significant effect on Fv/Fm values (**Table 4**). The optimal Fv/Fm value of all plant species is around 0.8 (Pang et al., 2004). In this experiment, the minimum Fv/Fm values, indicating photoinhibition (0.667–0.718), were observed in the case of potatoes grown on sand.

The CCI values showed no change as a function of B treatments for green beans and cabbages. According to the study of Bingham (1973), cabbages tolerate B without symptoms of phytotoxicity. However, Pandey and Archana (2013) demonstrated that higher B doses (3.3 and 33 mg B/L) may reduce chlorophylls a and b and carotenoids in cabbage leaves. The high concentrations of B (2 and 4 mg B/L) reduced the dry matter, fruit yield, and chlorophyll content of tomatoes (Kaya et al., 2009). In this study, the 0.5 mg/L dose of B had a beneficial effect on the CCI-based chlorophyll content in tomato leaves, which could be attributed to the effect of B on the uptake of microelements, especially Mg (Bohn et al., 2004). The plant physiological measurements indicate that green beans are sensitive to B, which is required for nodule formation and N_2-fixation processes in legumes and is essential for *Rhizobium*-legume signaling and nod-gene expression (Bolanos et al., 1994; Redondo-Nieto et al., 2001). Averaged over each species, the highest CCI values resulted on silty soil, possibly due to the higher concentration of N (**Table 1**). A close correlation has been reported between leaf chlorophyll content and plant N status in many agricultural crops (Liu et al., 2019; Padilla et al., 2019).

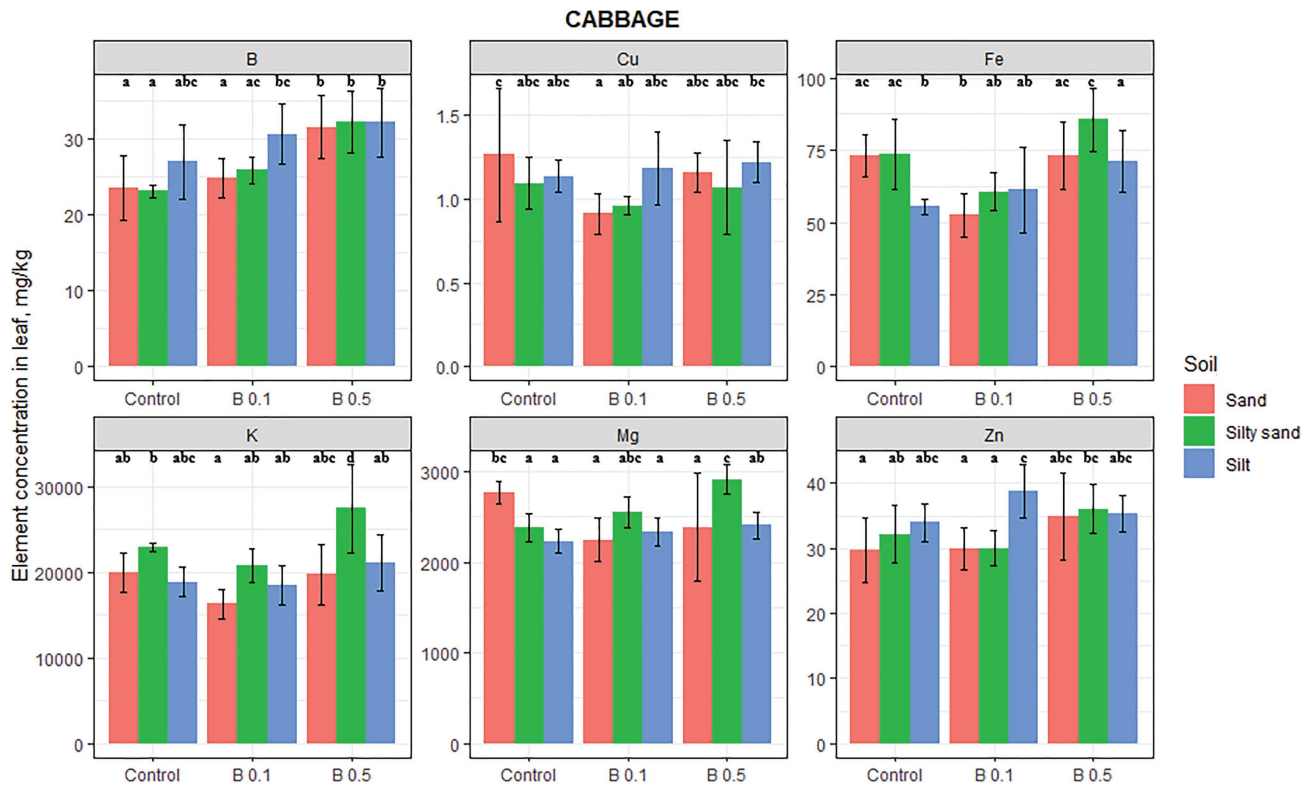


FIGURE 4 | Element contents in cabbage leaf in different irrigation water treatments on sand, silty sand, and silty soil (mg/kg DW). The data are means of the replicates. Different letters (a–d) indicate significant differences between treatments ($p < 0.05$).

Element Contents

The B content of the vegetables remained in the range of values suitable for human consumption even after the treatments. For the required minimum daily intake (1 mg B/day), either 520 g of green beans, 370 g of cabbages, 770 g of potatoes, or 1,110 g of tomatoes should be consumed. In silty soil, a moderate B increment was observed in tomato fruit. Dursun et al. (2010) also reported a significant 7-fold increment of B in tomato fruit after B fertilization with 0.5 mg/kg soil. The element concentrations measured in tomato fruit were within the range reported by Kelly and Bateman (2010), with the exception of Fe in the 0.1 mg B/L treatment. However, Demir et al. (2010) measured similar Fe concentrations in tomatoes grown on clay loam soil. The Fe content of tomato fruit and leaves changes during the ripening process. In the final stage of fruit ripening, the Fe content increases, so the higher Fe content can indicate more ripped fruit (Chohura et al., 2009; Ramesh et al., 2020). According to this, the 0.1 mg B/L dose may have promoted the ripening process, which is shown by the higher Fe content on each soil in this treatment. However, the 0.5 mg B/L treatment on the sandy soil did not affect the ripening process (i.e., Fe content is equal to the control), while, on the other two soils, the lower Fe content compared with the control may indicate inhibited fruit maturation. The increase in Mg content of tomato fruit as a result of B treatment is consistent with the changes in the vegetative parts of tomatoes observed by Eraslan et al. (2007), but contradictory with the results observed by Dursun et al. (2010). The higher Mg content is favorable, since the presence of sufficient Mg in the human diet reduces the risk of cancer (Gile et al., 2020). The Cu content of tomato fruit was in the same range as detected on non-contaminated soil by Ginocchio et al. (2002), who concluded that the Cu content of tomato fruit is determined by the soil Cu content, pH, and CEC. Since these values were not modified by the irrigation water in this experiment, the decrease in the Cu content on sandy soil could be explained by the effect of B addition. To the best of our knowledge, no information is available about the effect of B on the Cu content of tomato fruit, although B fertilization resulted in higher Cu levels in the vegetative parts of tomato ffruit in the experiment performed by Dursun et al. (2010). The results of this study indicate that the application of B may increase the Zn content of tomato fruit. This effect of B has only been demonstrated in the studies in the literature for tomato shoots (Güneş et al., 1999; Dursun et al., 2010). An increase in the Zn content of tomato fruit would be beneficial, since over 25% of the world population lives with the risk of Zn deficiency (Maret and Sandstead, 2006).

Based on the elemental composition, B treatment decreased the nutritional value of green beans on all three soils. According to the studies by Singh and Singh (1990) and Ganie et al. (2014), the optimal B fertilization of green bean is about 1 kg/ha. This value represents about 3 mg/kg content in the

TABLE 5 | Translocation coefficients of B between soil and plant and between different plant parts.

Soil	Irrigation water	Root/Soil				Shoot/Root				Fruit/Shoot			
		Tomato	Green bean	Potato	Cabbage	Tomato	Green bean	Potato	Cabbage	Tomato	Green bean	Potato
Sand	Control	3.02 ± 0.10f	3.98 ± 0.29b	3.89 ± 0.16d	4.22 ± 0.07b	2.74 ± 0.05b	1.15 ± 0.14c	2.52 ± 0.32a	1.05 ± 0.09ab	0.33 ± 0.04a	0.79 ± 0.15b	0.12 ± 0.01a
	0.1 mg B/L	2.27 ± 0.12d	4.02 ± 0.85b	5.23 ± 0.07c	4.22 ± 0.14b	4.37 ± 0.20c	1.35 ± 0.25ac	2.21 ± 0.20a	1.07 ± 0.05ab	0.23 ± 0.01ab	0.66 ± 0.06ab	0.11 ± 0.01a
	0.5 mg B/L	2.77 ± 0.17e	3.41 ± 0.42b	4.92 ± 0.37c	3.75 ± 0.35b	3.58 ± 0.33a	2.70 ± 0.29de	2.40 ± 0.59a	1.35 ± 0.20bc	0.23 ± 0.01ab	0.53 ± 0.08ab	0.11 ± 0.04a
Silty sand	Control	1.69 ± 0.04c	1.82 ± 0.14a	2.70 ± 0.12b	2.21 ± 0.18d	3.05 ± 0.10b	1.52 ± 0.16abc	2.99 ± 0.24ab	1.06 ± 0.10ab	0.28 ± 0.02ab	0.60 ± 0.05ab	0.09 ± 0.01a
	0.1 mg B/L	1.15 ± 0.06ab	1.59 ± 0.23a	2.64 ± 0.20b	2.86 ± 0.15e	3.93 ± 0.10ac	2.11 ± 0.26bde	3.22 ± 0.16ab	0.90 ± 0.07a	0.28 ± 0.01ab	0.51 ± 0.04a	0.10 ± 0.01a
	0.5 mg B/L	1.47 ± 0.03c	1.41 ± 0.06a	2.84 ± 0.30b	1.97 ± 0.20cd	3.88 ± 0.11a	2.76 ± 0.05e	3.91 ± 0.77b	1.52 ± 0.18cd	0.15 ± 0.13b	0.57 ± 0.05ab	0.08 ± 0.02a
Silt	Control	1.18 ± 0.07b	1.44 ± 0.24a	1.75 ± 0.04a	1.29 ± 0.05a	2.79 ± 0.09b	1.53 ± 0.29abc	2.80 ± 0.47ab	1.60 ± 0.18cd	0.31 ± 0.02a	0.64 ± 0.14ab	0.09 ± 0.02a
	0.1 mg B/L	0.93 ± 0.01a	1.29 ± 0.16a	1.83 ± 0.41a	1.50 ± 0.12ac	3.74 ± 0.13a	1.84 ± 0.40ab	2.91 ± 0.59ab	1.53 ± 0.05cd	0.27 ± 0.01ab	0.49 ± 0.12a	0.09 ± 0.01a
	0.5 mg B/L	1.14 ± 0.05ab	1.38 ± 0.11a	1.86 ± 0.04a	1.27 ± 0.04a	3.99 ± 0.17ac	2.03 ± 0.11abd	3.38 ± 0.35ab	1.80 ± 0.13d	0.24 ± 0.01ab	0.56 ± 0.08ab	0.09 ± 0.02a

The data are given as means ± SD of the replicates. Different letters (a–f) indicate significant differences between rows (treatments: soil and irrigation water; $p < 0.05$).

plowed layer, which is about 10 times higher than the B dose in the 0.5 mg B/L treatment (**Table 2**). The B content recorded in green beans in the 0.5 mg B/L treatment can be categorized as high, since it exceeds the range reported by Beebe et al. (2000) based on 1,000 samples (maximum value: 18 mg/kg). The decrease in the K content of green beans fruit contradicts the results suggested by Ganie et al. (2014), who reported an increase in K content after 0.5–1.5 kg/ha B fertilization. The decrease in the K content is unfavorable, because the recommended intake of K is about four times higher than the average consumption of this element in the current diet (Sebastian et al., 2006). The Fe content decreased to half the average value for beans in 0.5 mg B/L treatment, which is unfavorable from a human nutrition point of view, as Fe deficiency is one of the most common health issues in the world (Beebe et al., 2000; Blanco-Rojo and Vaquero, 2019). No results are available on the effect of B fertilization on the Mg content of green beans, but similar decreases in Mg content have been observed in the vegetative parts of tomatoes, cucumbers, peppers, and tobacco after the application of B to the soil (López-Lefebre et al., 2002; Dursun et al., 2010).

The B treatment had less effect on the elemental composition of potato tubers, which may vary greatly depending on the growth conditions such as soil properties, fertilization, and irrigation, and such variation could not be observed in this experiment (White et al., 2009). Even after the changes caused by the application of B, the Fe and Cu contents of potato tubers were still in the range reported by True et al. (1978).

Among the vegetables studied, the response of cabbages to the B treatment showed the most significant differences as a function of soil type. Although B irrigation influenced the B, Mg, K, Fe, and Cu contents, there was no element on which B had a significant effect on all three soils. The application of B only led to a decrease in the nutritional value of cabbage on sandy soil by diminishing the Fe, Cu, and Mg contents. The vegetables from the cruciferous family like cabbage have high B requirements, which explains the increasing B content of cabbage leaves as a function of the B treatment (Choi et al., 2016). According to the ranking suggested by Tariq and Mott (2007), the B content in cabbages can be considered as adequate in all the treatments. Even after the changes caused by the addition of B, the Mg content of cabbages always remained in the range reported by Hara and Sonoda (1981).

Translocation

The soil type influenced the root/soil TC, but it had no effect on the distribution of B (i.e., shoot/root and fruit/shoot TC) in plants. The lighter the soil texture, the more B was absorbed by the roots from irrigation water, which is in accordance with the results suggested by Wear and Patterson (1962). The uptake of B is more influenced by the B content in the soil solution than by the B adsorbed on soil particles (Keren et al., 1985). In the case of adequate B supply, the uptake mechanism is passive diffusion (Dannel et al., 2002). Thus, the higher uptake on sandy soil can be explained by the lower CEC of this soil and the relatively high amount of added B compared with the original B content of the soil.

Within the plants, B mostly moves passively in the xylem *via* the transpiration stream (Landi et al., 2013). Each of the species investigated was able to absorb B from the soil and store it in aboveground parts (Sasmaz, 2008). According to the findings suggested by Choi et al. (2015), the tomato organs that accumulate the most B are the stem and leaves, which is in accordance with the results of this study.

CONCLUSION

The main conclusion can be summarized as follows:

- The B treatment had no effect on the biomass of the edible parts of tomatoes, green beans, potatoes, and cabbages but modified the nutritional value of these vegetables by changing their element contents.
- These changes were influenced by soil type.
- The B content showed a significant increase only in the case of tomatoes grown on silty soil and cabbages grown on light-textured soils irrigated with water containing 0.5 mg/L B.
- The B irrigation had the most significant effect on the elemental composition of tomato fruit, as it affected the B, Mg, K, Fe, Cu, and Zn contents.
- The irrigation water containing 0.1 mg/L B promoted the ripening of tomatoes on all the soils.
- The B treatment decreased the nutritional value of green beans by diminishing its K and Fe contents on all the soils.
- The element content of potatoes was almost unaffected by the B treatments.
- The nutritional value of cabbages was modified only on sandy soil, where the Mg, Fe, and Cu contents of the leaves decreased as a result of the B treatments.

The chlorophyll content index was proved to be a more effective parameter for the indication of the effects of the B irrigation than Fv/Fm. The B treatments applied in this study caused no stress to the plants, and in the case of tomatoes and potatoes, an increase in chlorophyll content was observed on silty soil.

DATA AVAILABILITY STATEMENT

The raw data supporting the conclusions of this article will be made available by the authors, without undue reservation.

AUTHOR CONTRIBUTIONS

MR contributed to the design and implementation of the experiment and prepared the manuscript. PR contributed to the implementation of the experiment and conducted the statistical data analyses. AF conducted the statistical data analyses and proofread the manuscript. NU contributed to the data evaluation and proofread the manuscript. PD was the leader of the project, performed the analytical experimental work, and proofread the manuscript. GZ provided substantial contributions to the conception of the study and proofread the manuscript. NS-V contributed to the implementation of the experiment. AM performed the soil analysis. TT carried out the photosynthetic efficiency and chlorophyll content measurements and prepared and proofread the manuscript. All authors contributed to the article and approved the submitted version.

FUNDING

This research was funded by the National Research Development and Innovation Office (grant no. NVKP_16-1-2016-0044).

SUPPLEMENTARY MATERIAL

The Supplementary Material for this article can be found online at: https://www.frontiersin.org/articles/10.3389/fpls.2021.658892/full#supplementary-material

REFERENCES

Ayvaz, M., Guven, A., Blokhina, O., and Fagerstedt, K. V. (2016). Boron stress, oxidative damage and antioxidant protection in potato cultivars (*Solanum tuberosum* L.). *Acta Agric. Scand. Sec. B Soil Plant Sci.* 66, 302–316. doi: 10.1080/09064710.2015.1109133

Beebe, S., Gonzalez, A. V., and Rengifo, J. (2000). Research on trace minerals in the common bean. *Food Nutr. Bull.* 21, 387–391. doi: 10.1177/156482650002100408

Berger, K. C., and Truog, E. (1939). Boron determination in soils and plants. *Ind. Eng. Chem. Anal. Ed.* 11, 540–545. doi: 10.1021/ac50138a007

Bingham, F. T. (1973). "Boron in cultivated soils and irrigation waters," in *Trace Elements in the Environment*. ed. E. L. Kothnz (Washington, DC, USA: American Chemical Society), 130–138.

Blanco-Rojo, R., and Vaquero, M. P. (2019). Iron bioavailability from food fortification to precision nutrition: a review. *Innov. Food Sci. Emerg. Technol.* 51, 126–138. doi: 10.1016/j.ifset.2018.04.015

Bohn, T., Walczyk, T., Leisibach, S., and Hurrell, R. F. (2004). Chlorophyll-bound magnesium in commonly consumed vegetables and fruits: relevance to magnesium nutrition. *J. Food Sci.* 69, S347–S350. doi: 10.1111/j.1365-2621.2004.tb09947.x

Bolanos, L., Esteban, E., de Lorenzo, C., Fernandez-Pascual, M., de Felipe, M. R., Garate, A., et al. (1994). Essentiality of boron for symbiotic dinitrogen fixation in Pea (*Pisum sativum*) rhizobium nodules. *Plant Physiol.* 104, 85–90. doi: 10.1104/pp.104.1.85

Bolaños, L., Lukaszewski, K., Bonilla, I., and Blevins, D. (2004). Why boron? *Plant Physiol. Biochem.* 42, 907–912. doi: 10.1016/j.plaphy.2004.11.002

Chapman, V. J., Edwards, D. G., Blamey, F. P. C., and Asher, C. J. (1997). "Challenging the dogma of a narrow supply range between deficiency and toxicity of boron," in *Boron in Soils and Plants: Developments in Plant and Soil Sciences*. eds. R. W. Bell and B. Rerkasem (Dordrecht: Springer), 151–155.

Chohura, P., Kolota, E., and Komosa, A. (2009). Effect of fertilization with Fe chelates on the state of iron nutrition of greenhouse tomato. *J. Elem.* 14, 657–664. doi: 10.5601/jelem.2009.14.4.657-664

Choi, E. Y., Jeon, Y. A., Choi, K. Y., and Stangoulis, J. (2016). Physiological and morphological responses to boron deficient Chinese cabbage. *Hortic. Environ. Biotechnol.* 57, 355–363. doi: 10.1007/s13580-016-0023-y

Choi, E. Y., Park, H. I., Ju, J. H., and Yoon, Y. H. (2015). Boron availability alters its distribution in plant parts of tomato. *Hortic. Environ. Biotechnol.* 56, 145–151. doi: 10.1007/s13580-015-0044-y

Dannel, F., Pfeffer, H., and Römheld, V. (2002). Update on boron in higher plants - uptake, primary translocation and compartmentation. *Plant Biol.* 4, 193–204. doi: 10.1055/s-2002-25730

Demir, K., Sahin, O., Kadioglu, Y. K., Pilbeam, D. J., and Gunes, A. (2010). Essential and non-essential element composition of tomato plants fertilized with poultry manure. *Sci. Hortic.* 127, 16–22. doi: 10.1016/j.scienta.2010.08.009

Dobosy, P., Endrédi, A., Sandil, S., Vetési, V., Rékási, M., Takács, T., et al. (2020). Biofortification of potato and carrot with iodine by applying different soils and irrigation with iodine-containing water. *Front. Plant Sci.* 11:593047. doi: 10.3389/fpls.2020.593047

Dursun, A., Turan, M., Ekinci, M., Gunes, A., Ataoglu, N., Esringü, A., et al. (2010). Effects of boron fertilizer on tomato, pepper, and cucumber yields and chemical composition. *Commun. Soil Sci. Plant Anal.* 41, 1576–1593. doi: 10.1080/00103624.2010.485238

EFSA (2018). Overview on Tolerable Upper Intake Levels as derived by the Scientific Committee on Food (SCF) and the EFSA Panel on Dietetic Products, Nutrition and Allergies (NDA). European Food Safety Authority.

Eggert, K., and von Wirén, N. (2016). The role of boron nutrition in seed vigour of oilseed rape (*Brassica napus* L.). *Plant Soil* 402, 63–76. doi: 10.1007/s11104-015-2765-1

Egnér, H., Riehm, H., and Domingo, W. R. (1960). Untersuchungen über die chemische Bodenanalyse als Grundlage für die Beurteilung des Nährstoffzustandes der Böden. II. Chemische Extraktionsmethoden zur Phosphor- und Kaliunibestimmung. *Kungl. Lantbrukshögskolans Annaler* 26, 199–215.

Eraslan, F., Inal, A., Gunes, A., and Alpaslan, M. (2007). Boron toxicity alters nitrate reductase activity, proline accumulation, membrane permeability, and mineral constituents of tomato and pepper plants. *J. Plant Nutr.* 30, 981–994. doi: 10.1080/15226510701373221

Fernandez-Jaramillo, A. A., Duarte-Galvan, C., Contreras-Medina, L. M., Torres-Pacheco, I., Romero-Troncoso, R. D. J., Guevara-Gonzalez, R. G., et al. (2012). Instrumentation in developing chlorophyll fluorescence biosensing: a review. *Sensors* 12, 11853–11869. doi: 10.3390/s120911853

Füzy, A., Kovács, R., Cseresnyés, I., Parádi, I., Szili-Kovács, T., Kelemen, B., et al. (2019). Selection of plant physiological parameters to detect stress effects in pot experiments using principal component analysis. *Acta Physiol. Plant.* 41, 1–10. doi: 10.1007/s11738-019-2842-9

Ganie, M. A., Akhter, F., Najar, G. R., Bhat, M. A., and Mahdi, S. S. (2014). Influence of sulphur and boron supply on nutrient content and uptake of French bean (*Phaseolus vulgaris* L.) under inceptisols of North Kashmir. *Afr. J. Agric. Res.* 9, 230–239.

Ghasemidehkordi, B., Malekirad, A. A., Nazem, H., Fazilati, M., Salavati, H., and Rezaei, M. (2018). Arsenic and boron levels in irrigation water, soil, and green leafy vegetables. *Int. J. Veg. Sci.* 24, 115–121. doi: 10.1080/19315260.2017.1356896

Gile, J., Ruan, G., Abeykoon, J., McMahon, M. M., and Witzig, T. (2020). Magnesium: the overlooked electrolyte in blood cancers? *Blood Rev.* 44:100676. doi: 10.1016/j.blre.2020.100676

Ginocchio, R., Rodríguez, P. H., Badilla-Ohlbaum, R., Allen, H. E., and Lagos, G. E. (2002). Effect of soil copper content and pH on copper uptake of selected vegetables grown under controlled conditions. *Environ. Toxicol. Chem.* 21, 1736–1744. doi: 10.1002/etc.5620210828

Goldberg, S. (1997). Reactions of boron with soils. *Plant Soil* 193, 35–48. doi: 10.1023/A:1004203723343

Guidi, L., Degl'Innocenti, E., Carmassi, G., Massa, D., and Pardossi, A. (2011). Effects of boron on leaf chlorophyll fluorescence of greenhouse tomato grown with saline water. *Environ. Exp. Bot.* 73, 57–63. doi: 10.1016/j.envexpbot.2010.09.017

Güneş, A., Alpaslan, M., Çikili, Y., and Özcan, H. (1999). Effect of zinc on the alleviation of boron toxicity in tomato. *J. Plant Nutr.* 22, 1061–1068. doi: 10.1080/01904169909365695

Hara, T., and Sonoda, Y. (1981). The role of macronutrients in cabbage-head formation. *Soil Sci. Plant Nutr.* 27, 45–54. doi: 10.1080/00380768.1981.10431253

Herrera-Rodríguez, M. B., González-Fontes, A., Rexach, J., Camacho-Cristóbal, J. J., Maldonado, J. M., and Navarro-Gochicoa, M. T. (2010). Role of boron in vascular plants and response mechanisms to boron stresses. *Plant Stress* 4, 115–122.

Howe, P. D. (1998). A review of boron effects in the environment. *Biol. Trace Elem. Res.* 66, 153–166. doi: 10.1007/BF02783135

ISO 11261 (1995). Soil quality - Determination of total nitrogen - Modified Kjeldahl method. International Organization for Standardization.

Jeong, H., Kim, H., and Jang, T. (2016). Irrigation water quality standards for indirect wastewater reuse in agriculture: a contribution toward sustainable wastewater reuse in South Korea. *Water* 8:169. doi: 10.3390/w8040169

Kabata-Pendias, A., and Pendias, H. (2001). *Trace Elements in Soils and Plants*. Boca Raton: CRC Press.

Kaya, C., Tuna, A. L., Dikilitas, M., Ashraf, M., Koskeroglu, S., and Guneri, M. (2009). Supplementary phosphorus can alleviate boron toxicity in tomato. *Sci. Hort.* 121, 284–288. doi: 10.1016/j.scienta.2009.02.011

Kelly, S. D., and Bateman, A. S. (2010). Comparison of mineral concentrations in commercially grown organic and conventional crops – tomatoes (*Lycopersicon esculentum*) and lettuces (*Lactuca sativa*). *Food Chem.* 119, 738–745. doi: 10.1016/j.foodchem.2009.07.022

Keren, R., Bingham, F. T., and Rhoades, J. D. (1985). Plant uptake of boron as affected by boron distribution between liquid and solid phases in soil. *Soil Sci. Soc. Am. J.* 49, 297–302. doi: 10.2136/sssaj1985.03615995004900020004x

Lakanen, E., and Erviö, R. (1971). A comparison of eight extractants for the determination of plant available micronutrients in soils. *Acta Agric. Fenn.* 123, 223–232.

Landi, M., Degl'Innocenti, E., Pardossi, A., and Guidi, L. (2012). Antioxidant and photosynthetic responses in plants under boron toxicity: a review. *Am. J. Agric. Biol. Sci.* 7, 255–270. doi: 10.3844/ajabssp.2012.255.270

Landi, M., Remorini, D., Pardossi, A., and Guidi, L. (2013). Boron excess affects photosynthesis and antioxidant apparatus of greenhouse *Cucurbita pepo* and *Cucumis sativus*. *J. Plant Res.* 126, 775–786. doi: 10.1007/s10265-013-0575-1

Liu, C., Liu, Y., Lu, Y., Liao, Y., Nie, J., Yuan, X., et al. (2019). Use of a leaf chlorophyll content index to improve the prediction of above-ground biomass and productivity. *PeerJ* 6:e6240. doi: 10.7717/peerj.6240

López-Lefebre, L. R., Rivero, R. M., García, P. C., Sánchez, E., Ruiz, J. M., and Romero, L. (2002). Boron effect on mineral nutrients of tobacco. *J. Plant Nutr.* 25, 509–522. doi: 10.1081/PLN-120003379

Lucho-Constantino, C. A., Prieto-García, F., Del Razo, L. M., Rodríguez-Vázquez, R., and Poggi-Varaldo, H. M. (2005). Chemical fractionation of boron and heavy metals in soils irrigated with wastewater in central Mexico. *Agric. Ecosyst. Environ.* 108, 57–71. doi: 10.1016/j.agee.2004.12.013

Maret, W., and Sandstead, H. H. (2006). Zinc requirements and the risks and benefits of zinc supplementation. *J. Trace Elem. Med. Biol.* 20, 3–18. doi: 10.1016/j.jtemb.2006.01.006

Mozafar, A. (1989). Boron effect on mineral nutrients of maize. *Agron. J.* 81, 285–290. doi: 10.2134/agronj1989.00021962008100020029x

MSZ-08-0206/2 (1978). Evaluation of some chemical properties of the soil. Laboratory tests. (pH value, phenolphtalein alkalinity expressed in soda, total water soluble salt content, hydrolytic (y1 value) and exchangeable acidity (y2 value). edited by Hungarian Standard Association. Hungary.

MSZ-08-0215 (1978). Determination of the cation adsorption capacity of the soil. Modified mechlich technique. Hungarian Standard Association.

MSZ-08-0452 (1980). Use of high-capacity analyser systems for soils analyses. Quantitative determination of the organic carbon content of the soil on Contiflo analyzer system. Hungarian Standard Association.

MSZ-20135 (1999). Determination of the soluble nutrient element content of the soil. Hungarian Standard Association.

MSZ-21470-50 (2006). Environmental testing of soils. Determination of total and soluble toxic element, heavy metal and chromium (VI) content. Hungarian Standard Association.

Nable, R. O., Bañuelos, G. S., and Paull, J. G. (1997). Boron toxicity. *Plant Soil* 193, 181–198. doi: 10.1023/A:1004272227886

Naghii, M. R., Wall, P. M., and Samman, S. (1996). The boron content of selected foods and the estimation of its daily intake among free-living subjects. *J. Am. Coll. Nutr.* 15, 614–619. doi: 10.1080/07315724.1996.10718638

Nielsen, F. H. (1996). Evidence for the nutritional essentiality of boron. *J. Trace Elem. Exp. Med.* 9, 215–229. doi: 10.1002/(SICI)1520-670X(1996)9:4<215::AID-JTRA7>3.0.CO;2-P

Nielsen, F. H. (1997). Boron in human and animal nutrition. *Plant Soil* 193, 199–208. doi: 10.1023/A:1004276311956

Padilla, F. M., de Souza, R., Peña-Fleitas, M. T., Grasso, R., Gallardo, M., and Thompson, R. B. (2019). Influence of time of day on measurement with

chlorophyll meters and canopy reflectance sensors of different crop N status. *Precis. Agric.* 20, 1087–1106. doi: 10.1007/s11119-019-09641-1

Pandey, N., and Archana. (2013). Antioxidant responses and water status in Brassica seedlings subjected to boron stress. *Acta Physiol. Plant.* 35, 697–706. doi: 10.1007/s11738-012-1110-z

Pang, J., Zhou, M., Mendham, N., and Shabala, S. (2004). Growth and physiological responses of six barley genotypes to waterlogging and subsequent recovery. *Aust. J. Agric. Res.* 55, 895–906. doi: 10.1071/AR03097

Parks, J. L., and Edwards, M. (2005). Boron in the environment. *Crit. Rev. Environ. Sci. Technol.* 35, 81–114. doi: 10.1080/10643380590900200

Parks, R. Q., Lyon, C. B., and Hood, S. L. (1944). Some effects of boron supply on the chemical composition of tomato leaflets. *Plant Physiol.* 19, 404–419. doi: 10.1104/pp.19.3.404

Pereira, G. L., Siqueira, J. A., Batista-Silva, W., Barcellos Cardoso, F., Nunes-Nesi, A., and Araújo, W. L. (2021). Boron: more than an essential element for land plants? *Front. Plant Sci.* 11:610307. doi: 10.3389/fpls.2020.610307

Rainey, C. J., Nyquist, L. A., Christensen, R. E., Strong, P. L., Culver, B. D., and Coughlin, J. R. (1999). Daily boron intake from the American diet. *J. Am. Diet. Assoc.* 99, 335–340. doi: 10.1016/S0002-8223(99)00085-1

Ramesh, K. V., Paul, V., and Pandey, R. (2020). Dynamics of mineral nutrients in tomato (*Solanum lycopersicum* L.) fruits during ripening: part I—on the plant. *Plant Physiol. Rep.* 26, 23–37. doi: 10.1007/s40502-020-00546-0

R Core Team (2019). R: A Language and Environment for Statistical Computing. Vienna: R Foundation for Statistical Computing.

Redondo-Nieto, M., Rivilla, R., El-Hamdaoui, A., Bonilla, I., and Bolaños, L. (2001). Research note: boron deficiency affects early infection events in the pea-rhizobium symbiotic interaction. *Funct. Plant Biol.* 28, 819–823. doi: 10.1071/PP01020

Rees, R., Robinson, B. H., Menon, M., Lehmann, E., Günthardt-Goerg, M. S., and Schulin, R. (2011). Boron accumulation and toxicity in hybrid poplar (*Populus nigra* × euramericana). *Environ. Sci. Technol.* 45, 10538–10543. doi: 10.1021/es201100b

Rhoades, J. D. (1972). Quality of water for irrigation. *Soil Sci.* 113, 277–284. doi: 10.1097/00010694-197204000-00007

Roessner, U., Patterson, J. H., Forbes, M. G., Fincher, G. B., Langridge, P., and Bacic, A. (2006). An investigation of boron toxicity in barley using metabolomics. *Plant Physiol.* 142, 1087–1101. doi: 10.1104/pp.106.084053

Sarkar, S., Banerjee, H., Ray, K., and Ghosh, D. (2018). Boron fertilization effects in processing grade potato on an inceptisol of West Bengal, India. *J. Plant Nutr.* 41, 1456–1470. doi: 10.1080/01904167.2018.1457685

Sasmaz, A. (2008). Translocation and accumulation of boron in roots and shoots of plants grown in soils of low boron concentration in Turkey's Keban Pb-Zn mining area. *Int. J. Phytorem.* 10, 302–310. doi: 10.1080/15226510802096119

Sebastian, A., Frassetto, L. A., Sellmeyer, D. E., and Morris, R. C. Jr. (2006). The evolution-informed optimal dietary potassium intake of human beings greatly exceeds current and recommended intakes. *Semin. Nephrol.* 26, 447–453. doi: 10.1016/j.semnephrol.2006.10.003

Singh, B. P., and Singh, B. (1990). Response of French bean to phosphorus and boron in acid Alfisols in Meghalaya. *J. Indian Soc. Soil Sci.* 38, 769–771.

Tariq, M., and Mott, C. J. B. (2006). Effect of boron supply on the uptake of micronutrients by radish (*Raphanus sativus* L.). *J. Agric. Biol. Sci.* 1, 1–8.

Tariq, M., and Mott, C. J. B. (2007). The significance of boron in plant nutrition and environment-a review. *J. Agron.* 6, 1–10. doi: 10.3923/ja.2007.1.10

True, R. H., Hogan, J. M., Augustin, J., Johnson, S. J., Teitzel, C., Toma, R. B., et al. (1978). Mineral composition of freshly harvested potatoes. *Am. Potato J.* 55, 511–519. doi: 10.1007/BF02852157

Turan, M. A., Taban, N., and Taban, S. (2009). Effect of calcium on the alleviation of boron toxicity and localization of boron and calcium in cell wall of wheat. *Not. Bot. Hort. Agrobot. Cluj-Napoca* 37, 99–103. doi: 10.15835/nbha3723241

Türker, O. C., Yakar, A., Türe, C., and Saz, Ç. (2019). Cost-effectiveness of boron (B) removal from irrigation water: an economic water treatment model (EWTM) for farmers to prevent boron toxicity. *Environ. Sci. Pollut. Res.* 26, 18777–18789. doi: 10.1007/s11356-019-05268-x

Wang, C., Ji, J., Chen, M., Zhong, C., Yang, Z., and Browne, P. (2017). Atmospheric contribution to boron enrichment in aboveground wheat tissues. *Chemosphere* 174, 655–663. doi: 10.1016/j.chemosphere.2017.01.124

Wear, J. I., and Patterson, R. M. (1962). Effect of soil pH and texture on the availability of water-soluble boron in the soil. *Soil Sci. Soc. Am. J.* 26, 344–346. doi: 10.2136/sssaj1962.03615995002600040011x

White, P. J., Bradshaw, J. E., Finlay, M., Dale, B., Gavin, R., Hammond, J. P., et al. (2009). Relationships between yield and mineral concentrations in potato tubers. *HortScience* 44, 6–11. doi: 10.21273/HORTSCI.44.1.6

Wilcox, L. V. (1960). *Boron Injury to Plants.* Washington, DC: Agricultural Information Bulletin 211, USDA-ARS.

Conflict of Interest: The authors declare that the research was conducted in the absence of any commercial or financial relationships that could be construed as a potential conflict of interest.

Copyright © 2021 Rékási, Ragályi, Füzy, Uzinger, Dobosy, Záray, Szűcs-Vásárhelyi, Makó and Takács. This is an open-access article distributed under the terms of the Creative Commons Attribution License (CC BY). The use, distribution or reproduction in other forums is permitted, provided the original author(s) and the copyright owner(s) are credited and that the original publication in this journal is cited, in accordance with accepted academic practice. No use, distribution or reproduction is permitted which does not comply with these terms.

frontiers in Plant Science

ORIGINAL RESEARCH
published: 02 August 2021
doi: 10.3389/fpls.2021.710093

Iron Deficiency Leads to Chlorosis Through Impacting Chlorophyll Synthesis and Nitrogen Metabolism in *Areca catechu* L.

*Jia Li[1], Xianmei Cao[2], Xiaocheng Jia[1], Liyun Liu[1], Haowei Cao[2], Weiquan Qin[1] and Meng Li[1,3]**

[1] Coconut Research Institute, Chinese Academy of Tropical Agricultural Sciences, Wenchang, China, [2] Hainan Key Laboratory for Sustainable Utilization of Tropical Bioresources, College of Tropical Crops, Hainan University, Haikou, China, [3] College of Life Science and Technology, Central South University of Forestry and Technology, Changsha, China

Deficiency of certain elements can cause leaf chlorosis in *Areca catechu* L. trees, which causes considerable production loss. The linkage between nutrient deficiency and chlorosis phenomenon and physiological defect in *A. catechu* remains unclear. Here, we found that low iron supply is a determinant for chlorosis of *A. catechu* seedling, and excessive iron supply resulted in dark green leaves. We also observed morphological characters of *A. catechu* seedlings under different iron levels and compared their fresh weight, chlorophyll contents, chloroplast structures and photosynthetic activities. Results showed that iron deficiency directly caused chloroplast degeneration and reduced chlorophyll synthesis in chlorosis leaves, while excessive iron treatment can increase chlorophyll contents, chloroplasts sizes, and inflated starch granules. However, both excessive and deficient of iron decreases fresh weight and photosynthetic rate in *A. catechu* seedlings. Therefore, we applied transcriptomic and metabolomic approaches to understand the effect of different iron supply to *A. catechu* seedlings. The genes involved in nitrogen assimilation pathway, such as *NR* (nitrate reductase) and *GOGAT* (glutamate synthase), were significantly down-regulated under both iron deficiency and excessive iron. Moreover, the accumulation of organic acids and flavonoids indicated a potential way for *A. catechu* to endure iron deficiency. On the other hand, the up-regulation of POD-related genes was assumed to be a defense strategy against the excessive iron toxicity. Our data demonstrated that *A. catechu* is an iron-sensitive species, therefore the precise control of iron level is believed to be the key point for *A. catechu* cultivation.

Keywords: iron, chlorosis, chloroplast, nitrogen metabolism, *Areca catechu* L.

OPEN ACCESS

Edited by:
Francesco Di Gioia, The Pennsylvania State University (PSU), United States

Reviewed by:
Serenella Nardi, University of Padua, Italy
Yongxing Zhu, Yangtze University, China

***Correspondence:**
Meng Li
limeng0422@foxmail.com

Specialty section:
This article was submitted to Plant Nutrition, a section of the journal Frontiers in Plant Science

Received: *15 May 2021*
Accepted: *06 July 2021*
Published: *02 August 2021*

Citation:
Li J, Cao X, Jia X, Liu L, Cao H, Qin W and Li M (2021) Iron Deficiency Leads to Chlorosis Through Impacting Chlorophyll Synthesis and Nitrogen Metabolism in Areca catechu L. Front. Plant Sci. 12:710093. doi: 10.3389/fpls.2021.710093

INTRODUCTION

A. catechu is one of the most important tropical industrial crops. It is mainly distributed in Asian countries such as China, India, Malaysia and Indonesia. Extensive documents have demonstrated that betel nut, the fruit of *A. catechu*, has various pharmacological activity, including antiparasitic, antibacterial, antifungal, anti-inflammatory, and analgesic effects. Therefore, betel nut is considered

as not only a chewable snack but also a medicinal material to fight against diverse diseases (Gilani et al., 2004).

In China, more than 95% *A. catechu* cultivation area is located at Hainan province. In the past decades, the planting area of *A. catechu* in Hainan province has increased from 6.66×10^4 acres to 2.85×10^5 acres (from 2010 to 2019) (Public data of government work report, 2020). The total output of betel nut in 2019 is 2.87×10^5 tons, and the total value is \$ 4.92×10^9, which accounts for 7.1% of the Gross Domestic Product (GDP) of Hainan province (Li et al., 2020). Therefore, the development of *A. catechu* industry is vital to the local economy. However, in recent years, leaf chlorosis in *A. catechu* was frequently reported in almost all planting areas in Hainan province, and the proportion of yellowing trees keeps increasing. The latest survey indicated that on average, 4.7% of the current *A. catechu* showed chlorosis symptoms, which will seriously reduce the yield of betel nut (unpublished data). Our previous study demonstrated that the yellowing trees were not infected by pathogens or virus, thus the chlorosis was assumed to be induced by physiological factors. It has been extensively documented that mineral nutrient deficiency or heavy metal stress could lead to physiological chlorosis (van Maarschalkerweerd and Husted, 2015). Leaf chlorosis could be caused by the deficiency of nitrogen, potassium, magnesium or iron in diverse species, but the mechanism might be different (Guerinot and Yi, 1994; Sun et al., 2017; Ueno et al., 2018; de Bang et al., 2020). In *A. catechu*, low levels of nitrogen, phosphorus, potassium, magnesium or zinc, and high calcium/magnesium ratio were reported to cause leaf chlorosis (Mathai, 1986; Cpcri, 1990; Chowdappa et al., 2002). However, *A. catechu* plants showed relatively strong resistance to nutrient deficiency during the cultivation, and these cases were occasional events and did not cause serious consequences. The determinant of the large-scale physiological chlorosis of *A. catechu* remains unclear.

Iron deficiency-induced chlorosis is a common phenomenon in many crops. It was estimated that more than 30% of the crops growing worldwide were threatened by iron deficiency (Imsande, 1998). Iron deficiency is mainly caused by the insoluble ferric hydroxide, the main existing form of iron, in soil, especially calcareous soil (Vose, 1982). The insoluble form of iron cannot be used by plants; thus, the bioavailability is seriously limited (Guerinot and Yi, 1994). For example, the typical symptom caused by iron deficiency is yellowing leaves with green veins in citrus (Fu et al., 2017). Moreover, iron deficiency is often related to the nutrient deficiency of other elements. In Chickpea, leaf chlorosis caused by reduced iron absorption, which was regulated by phosphorus. The phosphates decrease the solubility of iron oxide thus resulted in iron deficiency (Sánchez-Rodríguez et al., 2014).

There are two strategies developed by plants to dissolve and transport iron to adapt the iron deficiency stress (Marschner and Römheld, 1994). One strategy is adopted by dicotyledons and non-gramineae monocotyledons, which reduce ferric ion in soil to ferrous ion by ferric-chelate reductase (FCR) proteins encoded by the *FRO* genes, and they take up iron with transporters encoded by *IRT* genes (Kobayashi et al., 2010). Another strategy was used by most Gramineae species, which secrete iron carrier (PS) to the soil through their roots, and directly integrate ferric ions to absorb it (Kobayashi et al., 2010; Nozoye et al., 2011). For the plant species adopted the first strategy, phenols are often the main components of root exudates in response to iron deficiency (Romheld and Maschner, 1986; Susín et al., 1996; Curie and Briat, 2003; Hell and Stephan, 2003). The phenol compounds have multiple functions including iron chelation and reduction, free radical scavenging, antibacterial activity, and react as a carbon source for microbial growth (Rice-Evans and Miller, 1996; Cao et al., 1997; Blum et al., 2000). These evidences indicated that specific genes, enzymes and metabolites were involved into the response pathway of iron deficiency.

In this study, we identified that iron is a main determinant for physiological chlorosis of *A. catechu*. Thus, we performed comparative analysis at transcription and metabolism level to identify key genes and key metabolites involved in the iron deficiency-induced chlorosis pathway. Our data will provide a theoretical basis to understand the mechanism underlying physiological chlorosis of *A. catechu*, and to improve the adaptability and vitality of *A. catechu* seedlings.

MATERIALS AND METHODS

Plant Materials and Iron Treatments

The seedlings of an *A. catechu* cultivar "Reyan NO.1," bred by the Coconut Research Institute of Chinese Academy of Tropical Agricultural Sciences, were used in this study. All seedlings were grown at the *A. catechu* nursery of the Coconut Research Institute (19°33′N, 110°47′E). The *A. catechu* seedings with three fully expanded leaves (4-month-old) were selected, and each seedling was planted in a 16 cm × 22 cm plastic pot containing 1 kg medium consists of silica sand, perlite and vermiculite with the proportion 1:1:1 (v/v/v). The seedlings were grown in an artificial growth chamber with a constant photoperiod (16 h light/8 h darkness) and an average temperature of 27°C.

An special nutrient solution (Li J. et al., 2019) for *A. catechu* (10 mmol/L NH_4NO_3, 0.625 mmol/L KH_2PO_4, 9 mmol/L KNO_3, 1.5 mmol/L $CaCl_2$, 0.015 mmol/L $ZnSO_4$, 0.75mmol/L $MgSO_4$, 0.05 mmol/L H_3BO_3, 2.5 μmol/L KI, 0.05 mmol/L $MnSO_4.H_2O$, 0.05 μmol/L $CuSO_4$, 0.5 μmol/L Na_2MoO_4, 0.5 μmol/L $CoCl_2$), and 0.5 μM (iron deficiency, ID), 50 μM (normal, CK) and150 μM (excessive iron, EI) Fe-EDTA was applied in this study. The pH of all the nutrient solutions was adjusted to 5.8 with 0.1 mol/L KOH. Totally 20 *A. catechu* seedlings were prepared for each treatment. During the treatment, 400 ml nutrient solution was added to each pot every 3 days, and the excess salt was scavenged with deionized water every 10 days to prevent salt accumulation. The leaf samples of *A. catechu* seedlings were collected at 28 days after treatment, because the obvious chlorosis symptom could be observed at this phase in the seedlings grown under ID. Totally 10 youngest leaves were collected for each sample, which was then mixed and divided into two parts. One part was used for biochemical and physiological measurement, and the other part was immediately frozen in liquid nitrogen and stored at −80°C for transcriptome and metabolome analysis.

Photosynthetic Gas Exchange and Pigments Measurement

Five plants from each treatment were randomly selected for the measurement of gas exchange and pigment contents. Photosynthetic rates were measured through a CIARS-2 portable photosynthesis system (PP systems, Herts, United Kingdom) at an ambient CO_2 concentration under a controlled light intensity of 993–1003 $\mu mol/m^{2}*s$. The samples were measured at between 9 and 11 a.m. on a clear day with the leaf temperature is $28 \pm 0.4°C$ and the relative humidity is $45 \pm 1\%$. Photosynthetic rates were measured in fully expanded leaves of at least five individuals of each treatment, and each sample was measured for three times.

Fresh leaf tissues were collected and used to determine pigment content through a spectrophotometer according to the method of Arnon (1949). Briefly, 0.5 g of leaf tissue were cut into small pieces, marinated in 10 ml of 95% ethanol and held for 48 h in darkness. The supernatants were collected by centrifugation and analyzed using a 752 N UV/Vis Spectrophotometer at 665, 649 and 470 nm, respectively.

Transmission Electron Microscopy (TEM) Observation

Leaf samples were cut into small pieces (1 mm × 1.2 mm), fixed in 2.5% (v/v) glutaraldehyde in 0.1 mol/L phosphate buffer (pH 7.4) at 4°C for 4 h, then rinsed and incubated overnight in a solution of 1% (w/v) OsO_4 at 4°C. The mixtures were subsequently dehydrated using an ethanol series and infiltrated in a gradient series of epoxy resin, and then embedded in the Epon 812 resin. Thin sections were made with a Leica UC7 ultramicrotome, stained in the solution containing 2% (w/v) uranyl acetate and 10 mM lead citrate (pH 12), and the sections were observed and recorded with a HT7700 (Hitachi, Japan) transmission electron microscope.

Leaf Ionomic Concentration Determination

The aerial parts and subterranean parts of *A. catechu* seedlings were harvested and dried at 70°C until their dry weight was unchanged (for at least 48 h). The total nitrogen was determined by an automatic azotometer (KT8200, FOSS, Sweden), through alkaline hydrolysis diffusion. Leaf P, S, K, Ca, Mg, Fe, Mn, Zn, Cu, and B content was assayed by inductively coupled plasma-atomic emission spectrometry (ICP-AES, IRIS-Advan type, Thermo, United States) after digestion with 1 mol/L HCl.

Determination of Enzyme Activity Involved in Nitrogen Assimilation

The enzyme activities of nitrate reductase (NR, EC 1.7.99.4), glutamine synthetase (GS, EC 6.3.1.2) and glutamate synthase (GOGAT, EC 1.4.7.1) were determined in the leaves of *A. catechu* seedlings. NR activity was determined based on a previously described method (Yu and Zhang, 2012). Plant tissues was homogenized in a triturator with prechilled extraction medium containing 25 mM phosphate buffer (pH 7.5), 5 mM cysteine and 5 mM EDTA–Na_2. The enzyme extract was added to assay mixture (KNO_3–phosphate buffer and NADH). The mixture was incubated for 30 min at 30°C. The reaction was stopped by adding 1% 4-aminobenzene sulfonic acid and 0.2% 1-naphthylamine and left standing for 30 min for color development at 30°C. The absorbance of the supernatant was measured at 540 nm immediately; GS activity was assayed according to a previously described method (Yu and Zhang, 2012). Plant tissues were ground in 0.05 M Tris–HCl solution (pH 8.0) containing 2 mM $MgSO_4$, 2 mM DTT and 0.4 M sucrose in an ice-cold mortar with a pestle. The crude enzyme extract was added to assay mixture (0.25 M imidazole–HCl buffer, 0.30 M sodium hydrogen glutamate, 30 mM ATP-Na, and 0.5 M $MgSO_4$). The mixture was incubated for 5 min at 25°C. And then, hydroxylamine hydrochloride (a mixture of 1 M hydroxylamine hydrochloride and 1 M HCl, 1:1) was added and left standing for 15 min. The reaction was stopped by adding $FeCl_3$ solution containing 10% $FeCl_3$, 24% trichloroacetic acid and 50% HCl (1:1:1). The resulting supernatants were measured at 540 nm; and GOGAT activity was measured by the method described by Singh and Srivastava (1986). Tissues were ground and extracted with a medium containing 0.2 M sodium phosphate (pH 7.5), 2 mM EDTA, 50 mM KCI, 0.1% (v/v) β-mercaptoethanol and 0.5% (w/v) Triton X-100. The enzyme was assayed spectrophotometrically following the oxidation of NADH and using 2 control mixtures (minus 2-oxoglutarate and minus glutamine in each case). The assay mixture contained 0.4 ml 20 mM L-glutamine, 0.4 ml 5 mM 2-oxoglutarate, 1 mM EDTA (added in assay buffer), 0.1 ml 100 mM KCI, 0.6 ml 1 mM NADH, and 0.5 ml of the enzyme preparation in a final volume of 3.0 ml completed with 25 mM sodium phosphate (pH 7.5). The reaction was started by adding L-glutamine immediately following the enzyme preparation. The decrease in absorbance was recorded for 5 min at 340 nm in a double beam spectrophotometer. The amount of NADH oxidized was calculated from a standard curve of NADH.

RNA-Seq Analysis

The leaf samples were collected from the *A. catechu* seedlings grown under ID, EI and CK conditions. Each treatment contains three individual samples as biological replicates. The total RNA was extracted using E.Z.N.A. Plant RNA Kit (Omega, R6827-01, United States). The quality of RNA, including degradation and contamination was monitored on 1% agarose gels. RNA concentration and integrity of the total RNA were measured using Nano Photometer® Spectrophotometer (IMPLEN, CA, United States) and Agilent 2100 Bioanalyzer (Agilent Technologies, CA, United States), respectively.

Subsequently, the library preparations were sequenced on the Illumina HiSeq platform to generate raw data. After sequencing, the clean reads were obtained by removing reads containing adaptors, more than 5% unknown bases and low-quality reads (>20% of the bases with a quality score of ≤ 10). Gene function was annotated based on the following databases: NCBI non-redundant protein sequences (NR), clusters of orthologous (KOG/COG), gene ontology (GO), manually annotated and reviewed protein sequence database (Swiss-Prot), Kyoto Encyclopedia of Genes and Genomes (KEGG). Gene

expression levels were represented using fragments per kilobase of transcript per million fragments mapped (FPKM) method. The differentially expressed genes (DEGs) were recruited based on False Discovery Rate (FDR) < 0.05 and $|\log2\text{Fold Change}| \geq 1$. All DEGs were analyzed by GO enrichment using GOseq (1.10.0) (Young et al., 2010) and KEGG enrichment using KOBAS software (Mao et al., 2005; Minoru et al., 2016).

qPCR Analysis

The extracted RNA of normal and albinotic leaf samples were converted into cDNA using PrimeScript^{TM} RT reagent Kit for qPCR (RR047Q, TaKaRa, Japan). Then the cDNA was 10 × diluted and used as templates for qPCR. The qPCR reaction was performed using the PowerUp^{TM} SYBR^{TM} Green Master Mix (A25777, Applied Biosystems, United States) in an ABI real-time instrument (QuantStudio^{TM} 6 Flex System, United States). Three independent biological replicates of each sample with internal technical replicates were used for qPCR analysis. An *A. catechu* gene, *AcActin* (CL9155.Contig7) (Li et al., 2020) was used as the reference gene for data normalization. Primers used in qPCR are shown in **Supplementary Table 1**. The relative expression fold of each sample was calculated by its C_T value normalized to the C_T value of reference gene using the $2^{-\Delta\Delta CT}$ method described by Livak and Schmittgen (2001). The normalized values of relative expression and FPKM values were calculated by log2, respectively, and the values were used to analyze the correlation between qPCR and RNA-seq results.

Metabolite Profiling Analysis

The leaf samples were collected from the *A. catechu* seedlings grown under ID, EI and CK conditions for metabolome analysis. Each treatment contains three individual samples as biological replicates. Sample preparation, metabolite extraction and analysis were carried out as follows. In brief, the 100 mg freeze-dried samples were extracted overnight at 4°C with 1.0 ml 70% aqueous methanol (containing 0.1 mg/L lidocaine). Subsequently, 10,000 g centrifugation for 10 min at 4°C, then the extracts were absorbed and filtered before LC-MS analysis. A quality-control sample was prepared by equal blending of all samples; during the assay, the quality control sample was run every 10 injections to monitor the stability of the analytical conditions. The extracted samples were analyzed using a HPLC system (Shim-pack UFLC SHIMADZU CBM 30A system) equipped with Waters ACQUITY UPLC HSS T3 C18 column (1.8 μm, 2.1 mm × 100 mm). LIT and triple quadrupole (QQQ) scans were acquired on a triple quadrupole-linear ion trap mass spectrometer (Q TRAP), API 6500 Q TRAP LC/MS/MS System, equipped with an ESI Turbo Ion-Spray interface, operating in a positive ion mode and controlled by Analyst 1.6.3 software (AB Sciex). The solvent system, gradient program and ESI source operation parameters were carried out as described by previous research. The qualitative analysis of primary and secondary MS data was performed by searching the internal database using a self-compiled database MWDB (Metware Biotechnology Co., Ltd. Wuhan, China), Data pre-processing and metabolites identification were performed by the standard metabolic procedures, including comparing the m/z values, RT, and the fragmentation patterns with the standards. The variable importance of the projection (VIP) score of the application (O) PLS model was used to filter the best differentiated metabolites between treatments. Metabolites with significant differences in content were set with thresholds of variable importance in projection (VIP) ≥ 1 and fold change ≥ 2 or ≤ 0.5.

Statistical Analysis

All data, including photosynthetic rates, pigment contents, enzyme activity and mineral nutrient concentration analysis were derived from three independent biological replicates. Data were analyzed using a one-way ANOVA analysis of variance, and differences between means were assessed using Duncan's multiple range tests ($P < 0.05$). All statistical analyses were performed with SPSS version 19.0 (SPSS Inc., Chicago, United States).

RESULTS

Morphological and Biochemical Characteristics of *A. catechu* Seedlings With Physiological Chlorosis

In order to clarify the main determinant of leaf chlorosis, we performed nutrient deficiency treatment of different elements, respectively. The results indicated that leaf chlorosis was not observed in the *A. catechu* seedlings grown under nitrogen and zinc deficiency until 80 days (**Supplementary Figures 1, 2**). Similarly, slight chlorosis appeared in the seedlings grown under the deficiency of boron, magnesium (**Supplementary Figures 1, 3**) and potassium (data not shown) after more than 80 days. The symptom of chlorosis could be recognized in 15 days and became obvious after 20-day ID treatment. The chlorosis generally initiated in the youngest leaf and aggravated in the following leaves, which exhibited gradually yellowing colors (**Supplementary Figure 4**). The yellowing seedlings grow very slowly, while keep alive but not develop for a long time. To clarify the mineral nutrient composition variation occurring in the yellowing leaves, we selected seven *A. catechu* planting areas for sampling and performing the element analysis. The yellowing or slight yellowing samples were found and collected in four of these planting areas. The results demonstrated that most mineral elements showed no difference between normal and yellowing leaves except for iron. The iron content was 58.14 and 58.37% on average in yellowing and slight yellowing leaves of that in normal ones, respectively (**Supplementary Table 2**).

Then the *A. catechu* seedlings were treated with different iron levels to investigate whether iron deficiency could directly induce physiological chlorosis. Obvious chlorosis symptom was observed in the seedlings grown under ID, and greener leaves were observed in the seedlings grown under EI (**Figure 1A**). The pigment contents were measured in normal and yellowing leaves. The results showed that all pigments, including chlorophyll *a*, chlorophyll *b* and carotenoids, were significantly reduced in the leaves under ID, and the pigment contents elevated along with the increasing iron levels, indicating that iron level is critical for pigment synthesis in *A. catechu* leaves (**Figure 1B**).

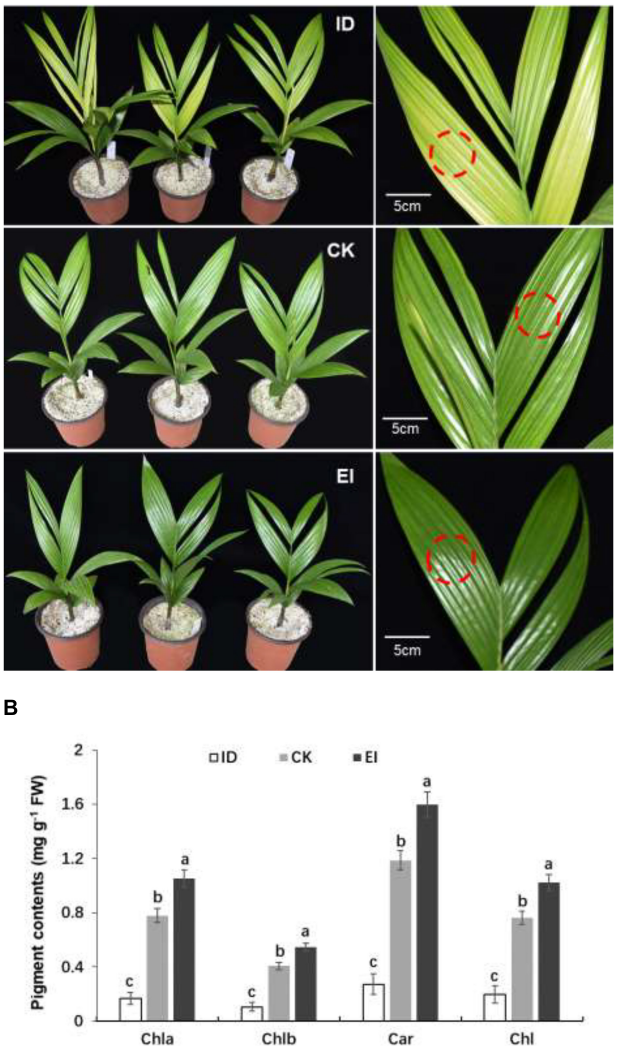


FIGURE 1 | Morphological characteristics **(A)** and pigment content **(B)** of *A. catechu* seedlings grown under ID (0.5 μM Fe-EDTA), CK (50 μM Fe-EDTA), and EI (150 μM Fe-EDTA). ID, iron-deficiency treatment; CK, normal conditions; EI, excessive-iron treatment. Chla, chlorophyll *a*; Chlb, chlorophyll *b*; Car, carotenoid; Chl, chlorophyll *a* + chlorophyll *b*; red dashed circles represent the sampling areas. The small bars show standard deviation. Different letters represent significant differences at $P < 0.05$ according to Duncan's multiple range tests.

The chloroplasts of the leaf cells under different treatments showed obvious structural variations. In the normal cells, the chloroplasts were well-developed, shuttle shaped with complete structure and close to the cell wall. The lamellae structure of grana and matrix was clear, and the thylakoids were stacked and arranged in order. On the contrary, partially disintegrated membrane was observed in the chloroplasts of the cells from yellowing leaves, the lamellae structure was imperfect or vanished, and a lot of osmiophagic granules were generated, indicating that ID seriously impacted the chloroplast structure. However, high iron level also impacted the lamellae structure, altered the chloroplasts into irregular shape, and produced more starch granules with larger size, implying that EI was also deleterious for *A. catechu* leaves (**Figure 2**).

The starch and soluble sugar content were significantly reduced in the leaves of *A. catechu* seedlings grown under ID, indicating that ID inhibited the photosynthesis and carbohydrate accumulation. However, seedlings grown under EI also showed reduced net photosynthetic rate, and reduced fresh weight in subterranean parts (**Figure 3**). This result might be attributed to the high iron toxicity, and indicated that the suitable concentration range of iron for *A. catechu* seedlings is narrow.

The mineral nutrient analysis demonstrated that the nitrogen, iron and manganese levels of *A. catechu* seedlings grown under ID were reduced in aerial part, and the nitrogen, potassium, magnesium and boron levels were reduced in subterranean part. While, the *A. catechu* seedlings grown under EI showed reduced nitrogen and iron levels in aerial part, and reduced potassium, magnesium and copper levels in subterranean part (**Table 1**). We noticed that iron level was accumulated and significantly elevated in the subterranean part of seedlings grown under EI. However, the iron level in the aerial part was reduced to the comparable level of ID, indicating that there is a mechanism of preventing excessive iron ion transport to the aerial part. This results also confirmed that high iron level is unacceptable for *A. catechu* seedlings.

Gene Expression Profiles of *A. catechu* Seedlings Under Different Iron Levels

To identify the key genes involved in the response to either ID or EI in *A. catechu* seedlings, transcriptome analysis was performed. The cDNA libraries for ID, EI and CK were constructed, respectively, and 64.27G clean data was generated (**Supplementary Table 3**). Totally 278,541 transcripts with the average length of 1,251 bp were obtained after assembly. Finally, 224,186 unigenes were obtained with the N50 of 2,461 bp (**Supplementary Tables 4–6**). The raw data of transcriptome sequencing has been deposited to the NCBI Short Reads Archive (SRA) with the accession number PRJNA695119. According to the annotation of unigenes against the Nr database, a high percentage of *A. catechu* transcripts were closely matched to the sequences of *Elaeis guineensis* (54.65%), *Phoenix dactylifera* (27.37%), and *Cephalotus follicularis* (1.5%) (**Supplementary Figure 5**).

Digital Gene Expression Profiling (DGE) analysis identified 454, 1,915, and 2,102 differentially expressed genes (DEGs) from ID vs. CK, EI vs. CK and ID vs. EI, respectively (**Supplementary Figure 6**). The functions of DEGs were classified according to the Gene Ontology (GO) classifications. In total, 454 DEGs from ID vs. CK were enriched into GO pathways, including the cell part, binding, cellular process, catalytic activity, metabolic process, and other functional categories. Between EI and CK, there were 1915 GO-annotated DEGs, which were mainly categorized into the cell part, cellular process, catalytic activity, binding, metabolic process, organelle, and other functional categories (**Figure 4**).

Totally 3,621 DEGs were identified from all the combinations. These genes were classified into six groups according to their

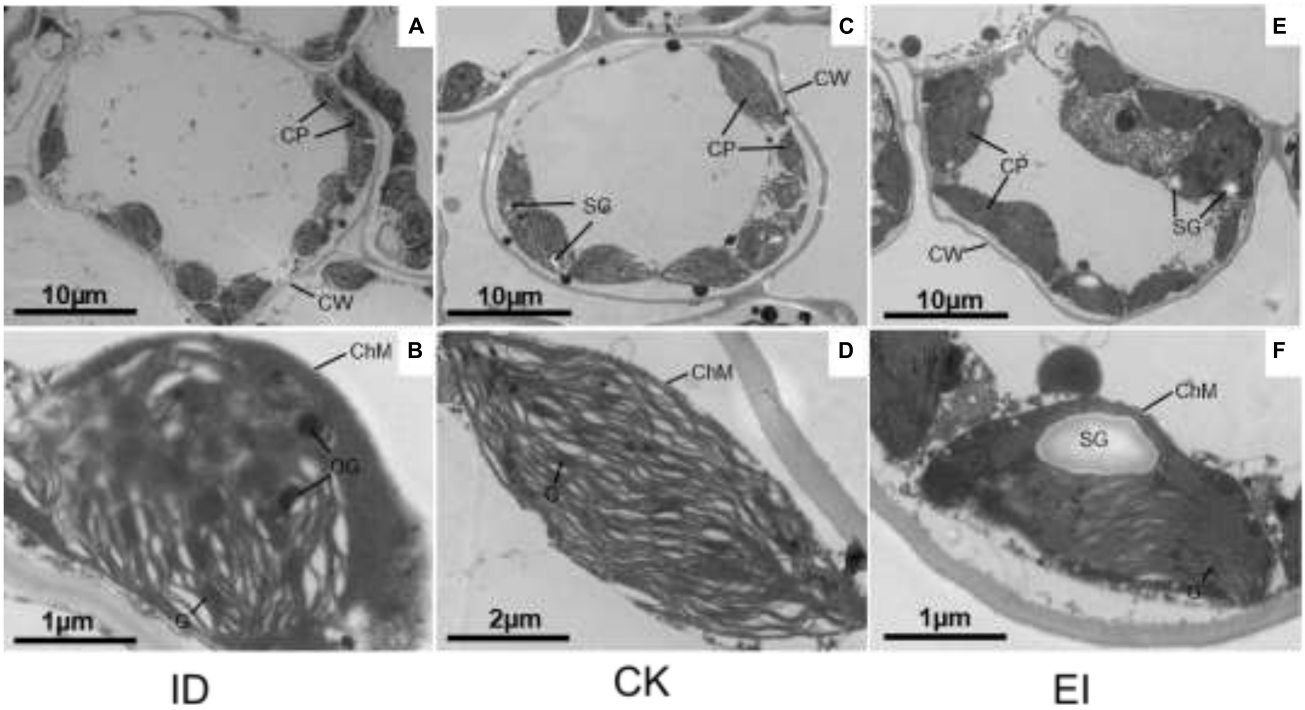


FIGURE 2 | Chloroplast structures in ID, CK and EI leaves of *A. catechu*. **(A,B)** chloroplasts in ID leaf cells; **(C,D)** chloroplasts in CK leaf cells; **(E,F)** chloroplasts in EI leaf cells; CW, Cell wall; CP, Chloroplast; ChM, Chloroplast membrane; OG, Osmiophilic granule; SG, Starch grains.

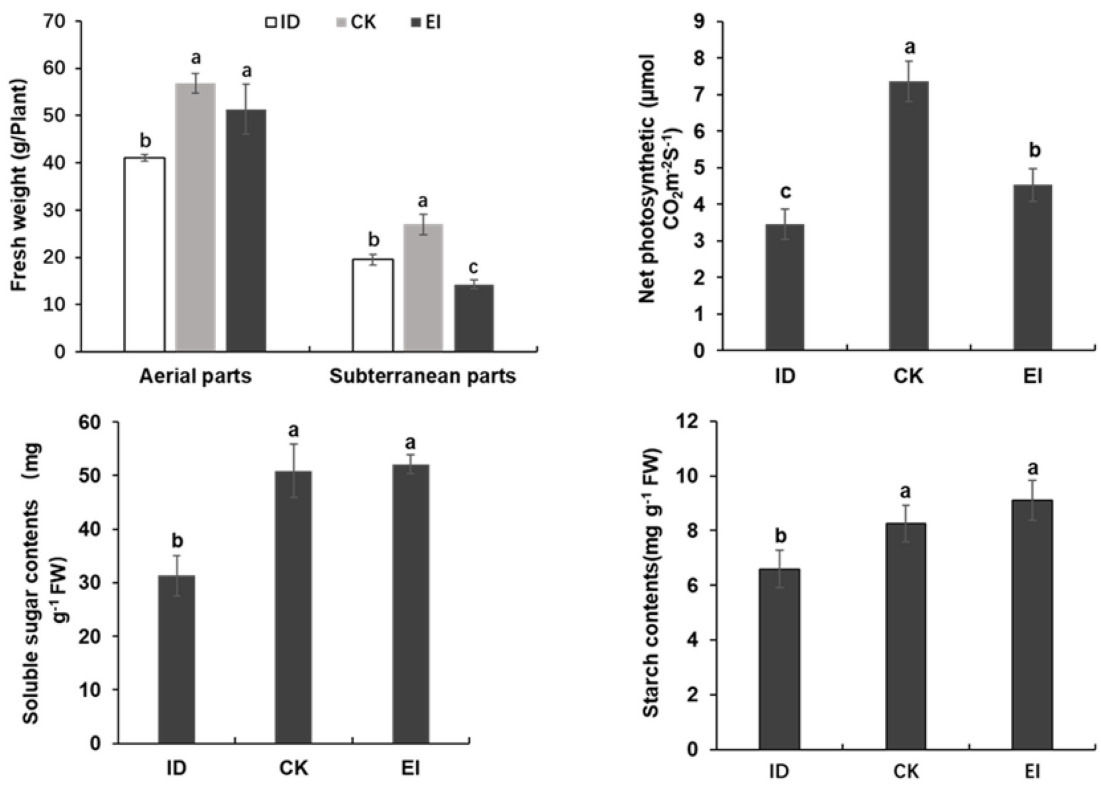


FIGURE 3 | Fresh weight, photosynthetic efficiency and carbon hydrate in ID, CK and EI leaves. The small bars show standard deviation. Different letters represent significant differences at $P < 0.05$ according to Duncan's multiple range tests.

TABLE 1 | Nutrient concentration of aerial parts and subterranean parts in *A. catechu* under different treatments.

	Aerial parts			Subterranean parts		
	ID	CK	EI	ID	CK	EI
N (mg/g)	25.5 ± 0.6c	30.2 ± 1.2a	27.0 ± 1.5b	12.9 ± 1.1b	16.3 ± 0.1a	15.0 ± 0.5a
P (mg/g)	2.1 ± 0.3a	1.6 ± 0.2a	1.8 ± 0.1a	1.2 ± 0.0ab	1.1 ± 0.1b	1.3 ± 0.1a
S (mg/g)	3.5 ± 0.3a	3.2 ± 0.1a	3.2 ± 0.1a	4.0 ± 0.2a	3.4 ± 0.2b	4.1 ± 0.2a
K (mg/g)	27.6 ± 0.5a	24.1 ± 0.1b	25.1 ± 0.9b	19.2 ± 1.4b	26.6 ± 2.7a	21.6 ± 2.0b
Ca (mg/g)	8.2 ± 0.4a	5.2 ± 1.0b	5.1 ± 0.5b	9.0 ± 0.1a	8.1 ± 0.9b	11.8 ± 2.3a
Mg (mg/g)	1.9 ± 0.2a	1.7 ± 0.2ab	1.5 ± 0.1a	2.5 ± 0.1b	3.1 ± 0.2a	2.2 ± 0.1c
Fe (μg/g)	121.1 ± 3.2b	172.2 ± 16.3a	134.1 ± 7.7b	416.4 ± 23.2b	539.4 ± 105.2ab	655.0 ± 132.7a
Mn (μg/g)	53.9 ± 11.7b	61.5 ± 21.3ab	82.7 ± 16.2a	140.8 ± 16.7a	79.6 ± 6.8b	92.1 ± 7.4b
Zn (μg/g)	76.6 ± 6.7a	67.0 ± 6.1a	71.8 ± 15.6a	62.8 ± 4.2b	68.8 ± 1.1ab	71.6 ± 5.6a
Cu (μg/g)	6.5 ± 1.0a	7.4 ± 1.1a	6.3 ± 1.3a	25.5 ± 3.0a	19.9 ± 4.3b	12.5 ± 1.4c
B (μg/g)	1.9 ± 0.2a	2.2 ± 0.2a	2.2 ± 0.8a	0.3 ± 0.1b	2.27 ± 0.3a	1.77 ± 0.7a

Different lowercase letters within each column indicate significant differences between ID, CK, and EI at $P < 0.05$ based on the t-test.

expression patterns (**Figure 5**). We observed that the genes encoding chlorophyll *a-b* binding protein, photosystem I and II protein, ferredoxin, ferritin, metallothionein, fatty acid desaturase, celloluse synthase and flavonoid 3′,5′-hydroxylase showed consistently up-regulation along with the increasing iron level, while the genes encoding chloroplast processing peptide, cysteine-rich receptor protein kinase, wall-associated receptor kinase, early light-induced protein, ferredoxin-dependent glutamate synthase, and glutamate synthase showed consistently down-regulation along with the increasing iron level. Specifically, the genes encoding dehydrogenase, aspartic proteinase, E3 ubiquitin, proteasome activator, protein detoxification and plastid-lipid-associated protein showed up-regulation, and the genes encoding nitrate reductase and chloroplast enhancing stress tolerance protein showed down-regulation in the samples under ID conditions. Moreover, the genes encoding anthocyanidin, expansin, pectin, GDSL esterase, peroxidase, squalene monooxygenase, sucrose synthase, pentatricopeptide repeat-containing protein, protein phosphatase 2C, and cell number regulator showed up-regulation in both ID and EI samples, while the genes encoding actin-related protein, auxin response factor, nitrogen regulatory protein, lipoxygenase, and vacuolar-sorting receptor showed down-regulation in both ID and EI samples (Additional Files 1–3).

Transcription Factors Analysis

The DEGs encoding transcription factors were selected and analyzed separately (**Figure 6**). The results showed that 34 TF (transcription factor)-encoding genes belong to 24 TF or TR (transcription regulator) families were identified between ID and CK. Among them, 1 gene encoding bHLH93 TF showed up-regulation, 1 gene encoding WRKY TF showed down-regulation, and 3 genes encoding NAC TFs showed up-regulation (1 of 3) and down-regulation (2 of 3). Totally 120 TF-encoding genes belong to 34 TF or TR families were identified between EI and CK. The gene family with the highest number of DEGs was bHLH (14.2%, 15 were up-regulated and 2 were down-regulated), followed by WRKY (7.5%, 9 were down-regulated), bZIP (7.5%, 5 were up-regulated and 2 were down-regulated) and NAC (4 were down-regulated). Totally 129 TF-encoding genes belong to 41 TF or TR families were identified between EI and ID. The gene family with the highest number of DEGs was NAC (7.8%, 10 were up-regulated), followed by bHLH (7.0%, 7 were down-regulated and 2 were down-regulated), MYB (6.2%, 4 were up-regulated and 4 were down-regulated) and AP2/ERF (5 were up-regulated and 3 were down-regulated).

Metabolome Analysis in *A. catechu* Seedlings Under Different Iron Levels

In order to reveal the variation of metabolites in *A. catechu* seedlings grown under different iron level, we performed metabolome analysis. Totally 106 metabolites showed significant difference between ID and CK samples, and 69 and 37 of them showed higher and lower content in ID samples than that in CK samples, respectively. Among them, the content of naringenin, butin and hesperetin was increased by more than threefold, while the content of xanthohumol, purine and N-p-coumaroylspermine was decrease by approximately 60%. Totally 116 metabolites showed significant difference between EI and CK samples, and 43 and 73 of them showed higher and lower content in EI samples than that in CK samples, respectively (**Supplementary Figure 6**). Among them, the content of 1,5-Anhydro-D-glucitol increased by more than 800-fold, the content of oxalic acid and nicotinic acid-hexoside increased by more than fourfold, while the content of 5-O-p-coumaroyl shikimic acid O-hexoside, 2-aminoethanesulfonic acid and 5-O-p-Coumaroyl shikimic acid showed more than 90% decrease (Additional Files 4–6).

All the differentially accumulated metabolites (DAMs) were classified into different pathways through KEGG analysis. The 106 DAMs from ID vs. CK were classified into 105 pathways, such as biosynthesis of secondary metabolites (ko01100), flavonoid biosynthesis (ko00941) and biosynthesis of phenylpropanoids (ko00940). The 116 DAMs from EI vs. CK were classified into 72 pathways, such as metabolic pathways (ko01100), biosynthesis of secondary metabolites (ko01100), biosynthesis of amino acids (ko01230) and flavonoid biosynthesis (ko00941) (**Figure 7**).

Overview of the Correlations in Metabolomics and Transcriptomics

The correlation between metabolomics and transcriptome data was analyzed in order to further understand the response

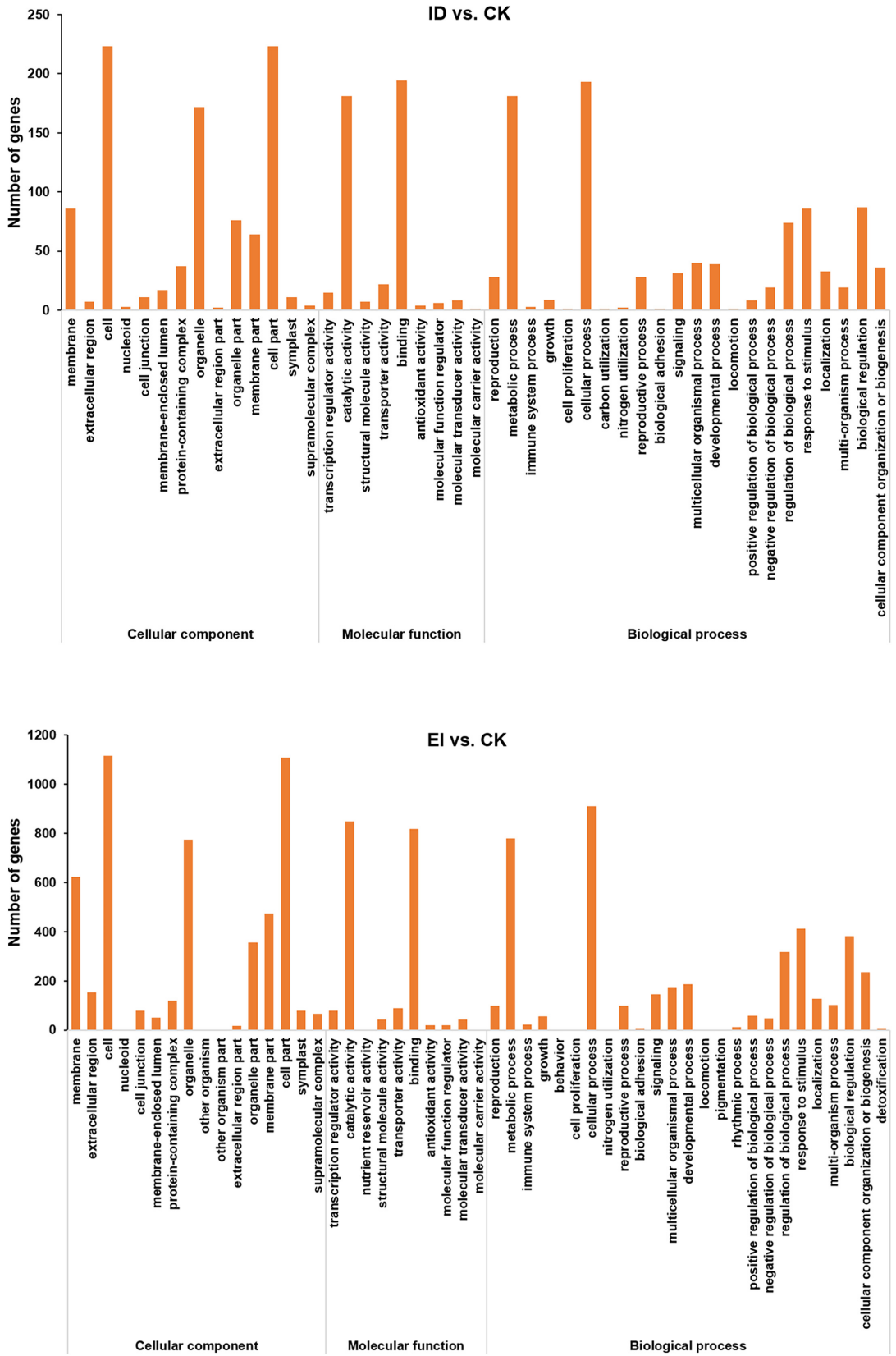


FIGURE 4 | Summary of GO (gene ontology) categories of DEGs. The numerals beside the histogram indicate the number of DEGs.

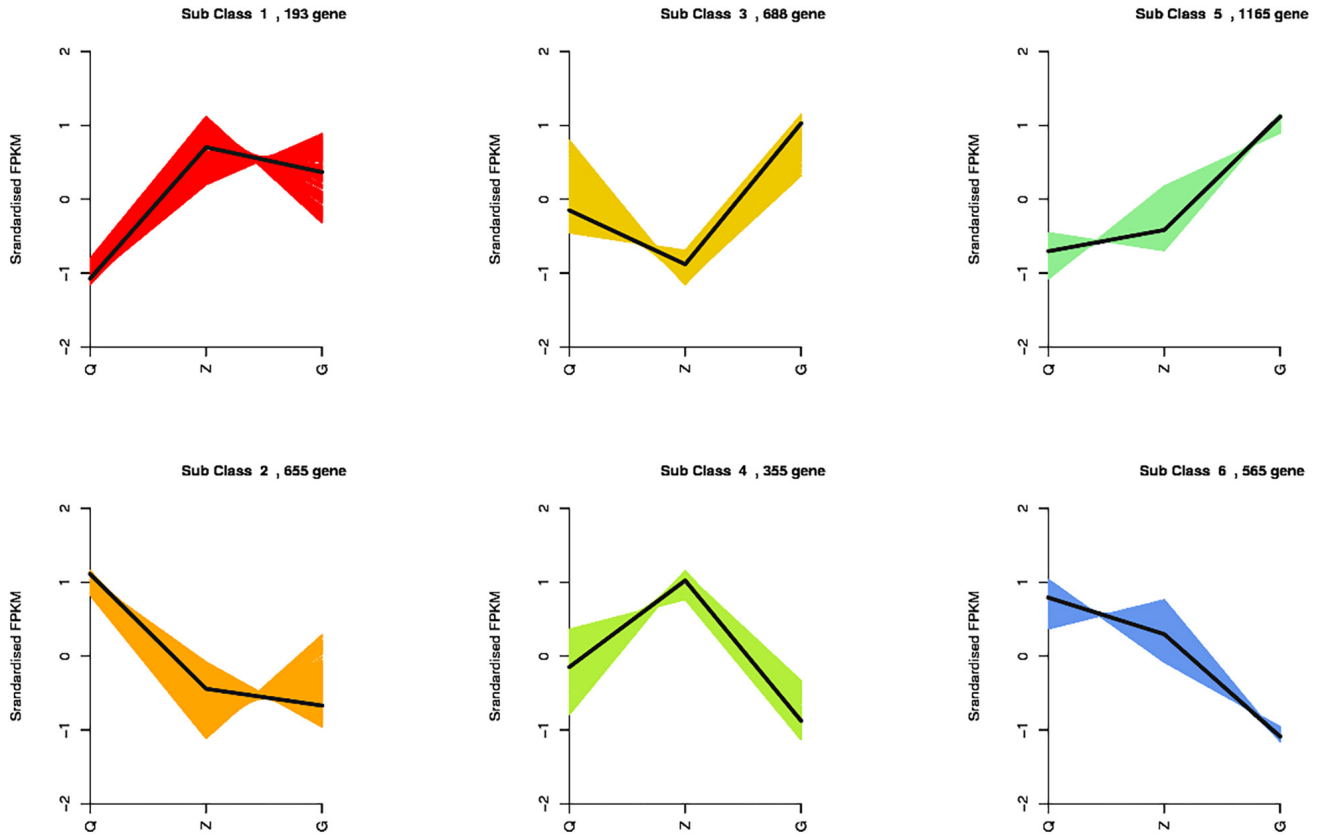


FIGURE 5 | *K*-means clustering analysis of the DEGs into six clusters according to their expression profiles. The cluster names and the number of unigenes for each cluster are indicated.

of *A. catechu* to ID. Among 454 DEGs, the expression profiles of 178 have positive correlation with the content profiles of 109 metabolites, such as p-Coumaryl alcohol, L-phenylalanine, naringenin and butin, between ID and CK. The differentially expressed genes and metabolites were both enriched in some KEGG pathways, including phenylalanine metabolism, biosynthesis of amino acids, pyrimidine metabolism, ABC transporters and glutathione metabolism (**Figure 8**).

Nitrogen Assimilation Was Impacted by Iron Deficiency in *A. catechu* Seedlings

The element analysis showed that the nitrogen level was significantly reduced in the seedlings grown under ID. Moreover, the content of most free amino acids was elevated (**Supplementary Figure 7**), and the genes encoding key enzymes involved into the nitrogen assimilation pathway showed consistent down-regulation indicated by metabolome and transcriptome data. We speculated that ID could affect the nitrogen assimilation in *A. catechu*, therefore, the genes and metabolites involved into this pathway were further studied. We observed that although the expression level of genes encoding ferredoxin up-regulation along with the iron levels increasing, the expression of *NR* (*nitrate reductase*) and *GOGAT* (*glutamate synthase*) genes showed down-regulation in both ID and EI conditions (**Figure 9A**). This result implied that ID and EI could impact the iron-dependent nitrogen assimilation, therefore resulted in chloroplast degeneration. Consistently, the enzymatic activity of NR and GOGAT, as well as the soluble protein content, was reduced under both ID and EI condition (**Figure 9B**).

Phenylpropanoid and Flavonoid Biosynthesis Were Provoked by ID

The strategy of *A. catechu* seedlings to survive the ID conditions was implied by the present results. We identified 16 DEGs involved into the phenylpropanoid biosynthesis pathway. Among them, the genes encoding 4CL (4-coumarate–CoA ligase) and CCR (cinnamoyl-CoA reductase) showed significant down-regulation in both ID and EI. The genes encoding BGLU (beta-glucosidase), HCT (shikimate O-hydroxy cinnamoyl transferase), and COMT (caffeic acid 3-O-methyltransferase) showed significant down-regulation in ID but significant up-regulation in EI. In addition, most genes encoding POD (peroxidase) showed significant up-regulation in EI (**Figure 10A**). For the flavonoid biosynthesis pathway, 2 genes encoding ANS (anthocyanidin synthase) and HCT (shikimate O-hydroxy cinnamoyl transferase), respectively, showed significant up-regulation under ID. Totally 10 metabolites, including catechin, naringenin, xanthohumol, eriodictyol,

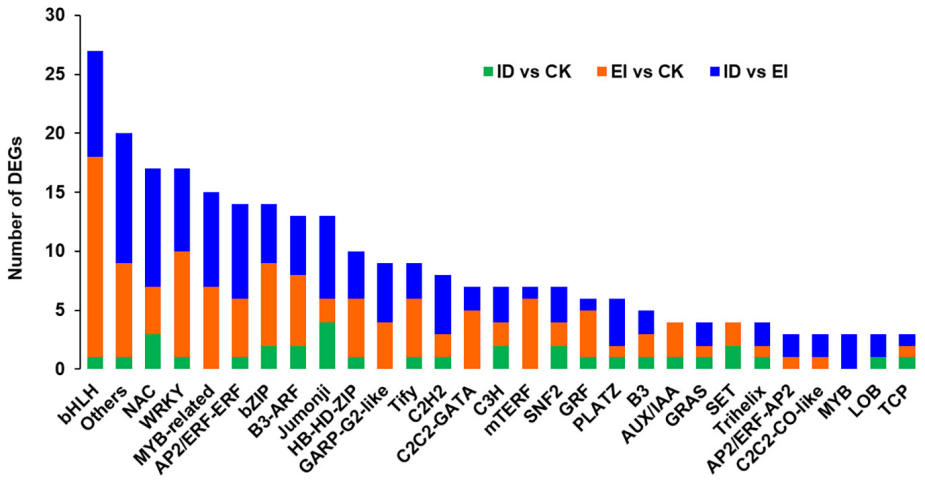


FIGURE 6 | Analysis of transcription factors (TFs) and transcriptional regulators (TRs) in ID, CK and EI.

hesperetin, dihydromyricetin, naringenin chalcone, tricetin, homoeriodictyol, and butin, also showed significant increased content in ID samples (**Figure 10B**).

qPCR Analysis on Selected Key Genes

Totally 27 genes were selected according to the previous analysis for confirming their expression patterns using qPCR. The results showed that the genes encoding 4CL, GOGAT and NRT showed down-regulation in both ID and EI. On the contrary, the genes encoding bHLH transcription factor and expansin showed significant up-regualtion in both ID and EI (**Supplementary Figure 8**). The gene encoding ferritin, WRKY70 and fatty acid export protein were up-regulated, while the gene encoding plant cysteine oxidase, FRO2, isoflavone 2′-hydroxylase and chloroplast processing peptidase were down-regulated along with the increasing iron level (**Supplementary Figure 8**). The qPCR result has a significant correlation with the RNA-seq data (**Supplementary Figure 9**).

DISCUSSION

There are many different causes of leaf chlorosis in plants. While in this study, iron deficiency was proved to be the main determinant for leaf chlorosis in *A. catechu*. The iron deficiency in the soil of *A. catechu* planting area might due to the low availability of the transition from ferric to ferrous (Honetschlägerová et al., 2018). Iron has been extensively documented for its role in chlorophyll biosynthesis (Hänsch and Mendel, 2009). Iron level could also regulate the formation rate of aminoacetylalanine (ALA), which is the precursor for not only chlorophyll but also heme (Pushnik and Miller, 1989). Iron is necessary for the formation of protochlorophyll from magnesium protoporphyrin (Marschner and Marschner, 2012). Moreover, there are 20 iron atoms directly involved in the electron transport chain in the thylakoid membrane. The photosystem I is a strong iron sink (12 iron atoms per complex) compared with PS II (3 iron atoms per complex) and Cyt *bf* complex (5 iron atoms per complex) (Raven et al., 1999). The high requirement of iron for the structural and functional integrity of thylakoid membrane, and the extra iron for ferredoxin and the biosynthesis of chlorophyll could explain the particular sensitivity of chloroplasts, especially endosomes, to iron deficiency. We observed that iron deficiency resulted in chloroplast degeneration in a short period, indicating that iron deficiency also impacted the development of chloroplast. We noticed that the *A. catechu* leaves were very sensitive to iron deficiency, while have relatively strong tolerance to the deficiency of other elements (nitrogen, zinc, magnesium, boron) (**Supplementary Figures 1–3**). These evidences confirmed that iron is one of the critical determinants for physiological chlorosis.

Since iron deficiency is verified to be the main reason for leaf chlorosis, iron supplement was supposed to be an efficient way to recover the *A. catechu* seedlings. We observed obvious dark green leaves in the seedlings grown under excessive iron conditions. It may be related to the promotion of chlorophyll synthesis by EI at the early stage of treatment. However, threefold of normal iron level also resulted in abnormal chloroplast structure, reduced net photosynthetic rate and decreased biomass. This result could be attributed to the high iron toxicity. The toxic damage of iron is caused by its reaction with hydrogen peroxide (H_2O_2) and form hydroxyl radical (OH^-), which is the most active reactive oxygen species (ROS) (Dixon and Stockwell, 2014). The ROS can directly damage cells by destroying biological molecules such as lipids or proteins (Li B. et al., 2019). During the long-term evolution of plants, antioxidant enzymes that scavenge free radicals have been produced. Studies have shown that the activity of POD (peroxidase) enhances with the increase of reducing iron concentration (Wu et al., 2014). On the one hand, POD scavenges H_2O_2 in plants, and prevents Fe^{2+} from entering cells by accelerating cell wall lignification (Wu et al., 2014). In our transcriptome data, most genes encoding POD (10 of 12) were significantly up-regulated under the high iron condition, indicating that the *A. catechu* seedlings were

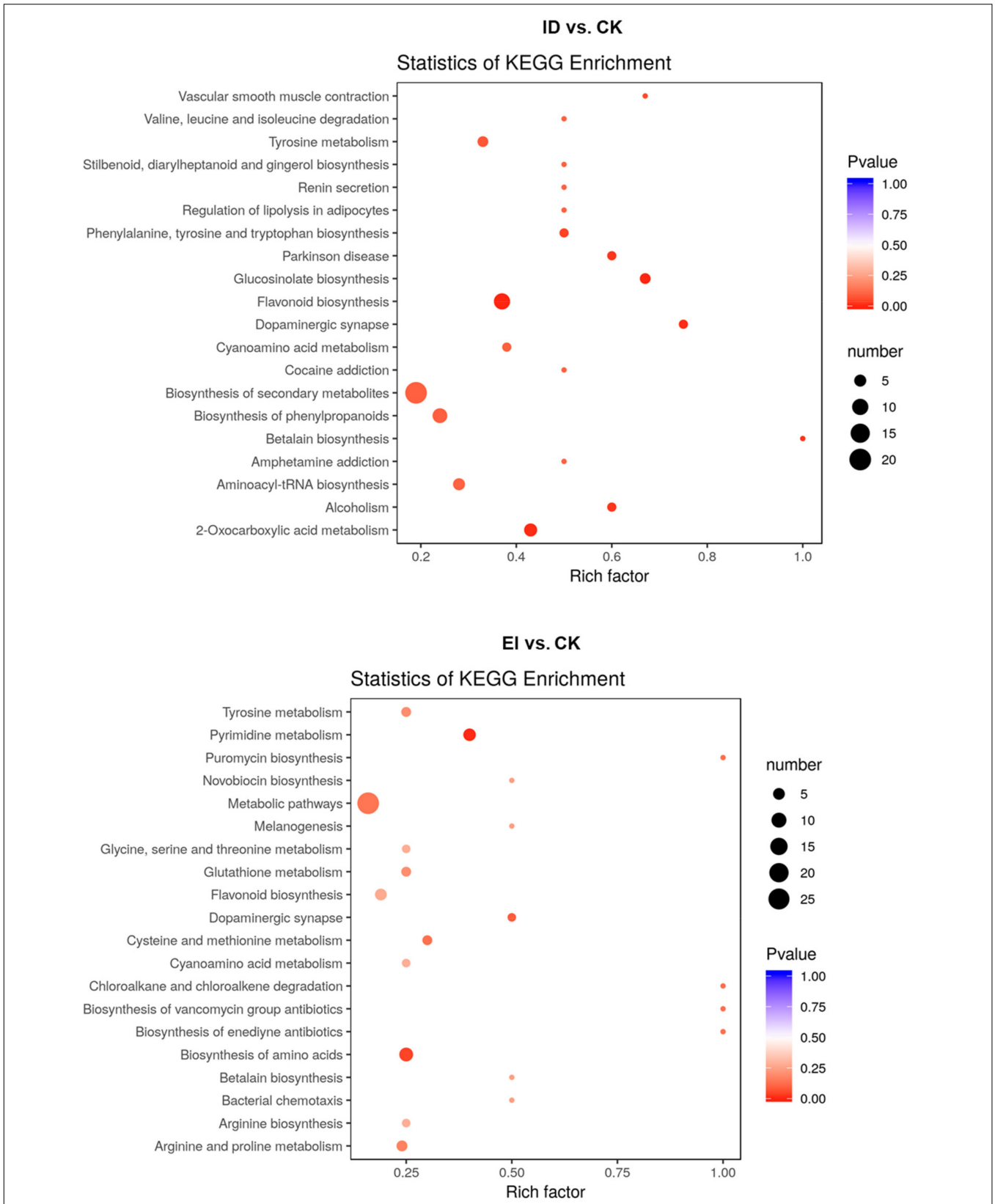


FIGURE 7 | Scatter plot analysis of the DAMs in response to the ID and EI treatment in *A. catechu* seedlings leaves.

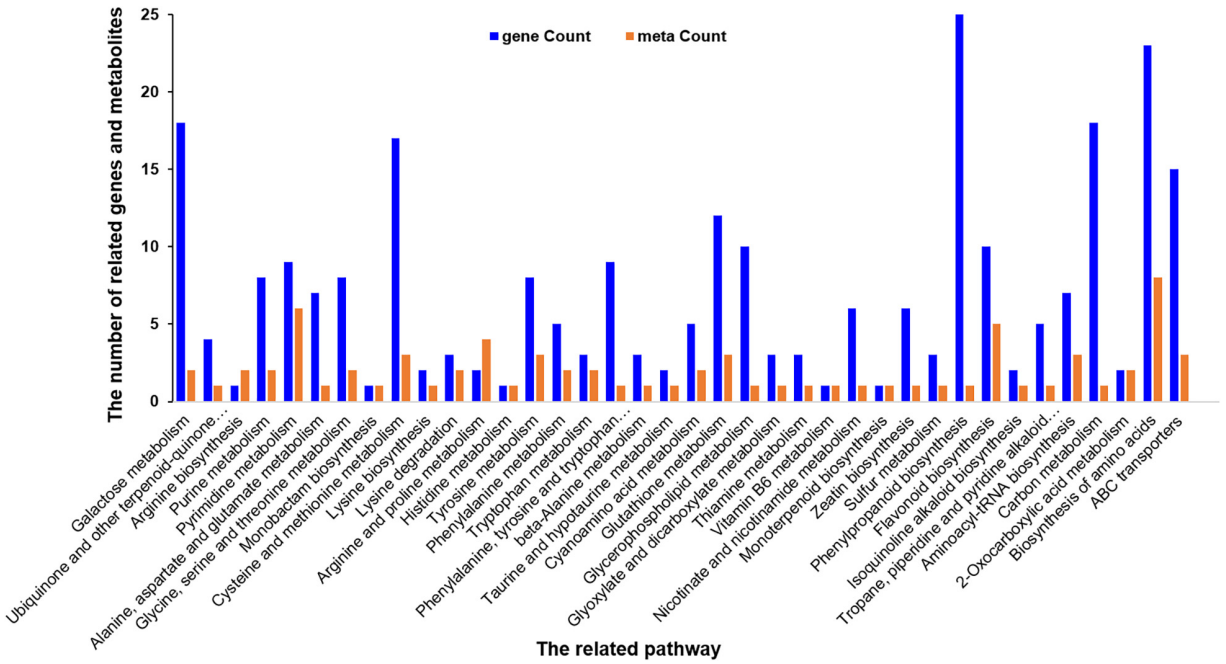


FIGURE 8 | Histogram of the differentially expressed related genes and metabolites in response to ID in *A. catechu* seedlings leaves.

improving the cellular defense mechanism to fight against iron toxicity. In rice (*Oryza sativa*), iron toxicity initiated when the iron concentration was more than 300 mg/kg, and serious iron toxicity occurred when the iron concentration is more than 500 mg/kg (Yamauchi, 1989), which is much higher than the concentration adopted in this study. In addition, although the iron content in the subterranean parts was largely increased in the seedlings grown under EI, the iron content in aerial parts was even reduced, implying that there is a defend mechanism to prevent excessive iron transport to *A. catechu* leaves. These results proved that the range of iron level suitable for the growth of young *A. catechu* seedlings is very narrow, and confirmed again that *A. catechu* is an iron-sensitive plant species.

An intriguing hypothesis proposed that some proteins might be used as a source of amino acids, carbon skeletons and N-NH_4^+ under iron deficiency through an iron-regulated protein degradation machinery (Donnini et al., 2010). In our study, soluble protein content was significantly decreased, and the free amino acid content was largely increased indicated by the metabolome data. The increased amino acids content was in agreement with the down-regulation of *NR* genes, which are iron-dependent (Campbell, 1999; Borlotti et al., 2012). NR is a cytoplasmic enzyme consist of two identical subunits. Each subunit contains three cofactors covalently binding to NR, including adenine dinucleotide (FAD), Heme (heme-Fe), and molybdopterin (a molybdenum containing co-factor). Therefore, the reduction of NR activity might be attributed to both transcription suppression and heme deactivation.

Besides NR, genes encoding GOGAT were also consistently down-regulated by ID. GOGAT is involved in ammonium assimilation. It catalyzes the transfer of amide group ($-NH_2$) from glutamine to 2-oxoglutarate. The conversion of glutamine to glutamate takes place in plastids which have two isoforms of GOGAT. The ferredoxin-linked GOGAT isoform dominates in leaves, which contains an Fe-S cluster transferring electrons during the reductive synthesis of two glutamate molecules from one 2-oxoglutarate and one glutamine molecule. Similar to the case in NR, ID reduced both the transcription level of *GOGAT* and the activity of Fe-S protein. Therefore, our data demonstrated that ID inhibited nitrogen assimilation in *A. catechu* leaves, similar results of which has recently been reported in fragrant citrus (Jin et al., 2017) and soybean (Chu et al., 2019).

The accumulation of flavonoids and flavonols, and the up-regulation of genes involved into the flavonoids and flavonols biosynthesis pathway was assumed to be a critical strategy for *A. catechu* seedlings to survive ID. Plants grown under ID often secrete small molecule organic compounds, including organic acids, phenols and flavonoids, into the rhizosphere to improve the availability of iron (Rodriguez-Celma et al., 2011). For example, dicotyledons such as *Beta vulgaris* and *Medicago truncatula* can secrete flavonoids to reduce trivalent iron in soil to divalent iron with high solubility to improve the availability of iron (Brumbarova et al., 2014). The root exudates, such as low molecular weight organic acids including citric acid, malic acid and oxalic acid, could activate insoluble iron through chelation or acidify rhizosphere to promote iron absorption (Jones and Darrah, 1994). Another kind of compounds secreted by root under ID is phenols, which can directionally reconstruct the microbial community structure of rhizosphere soil, thus indirectly improve the availability

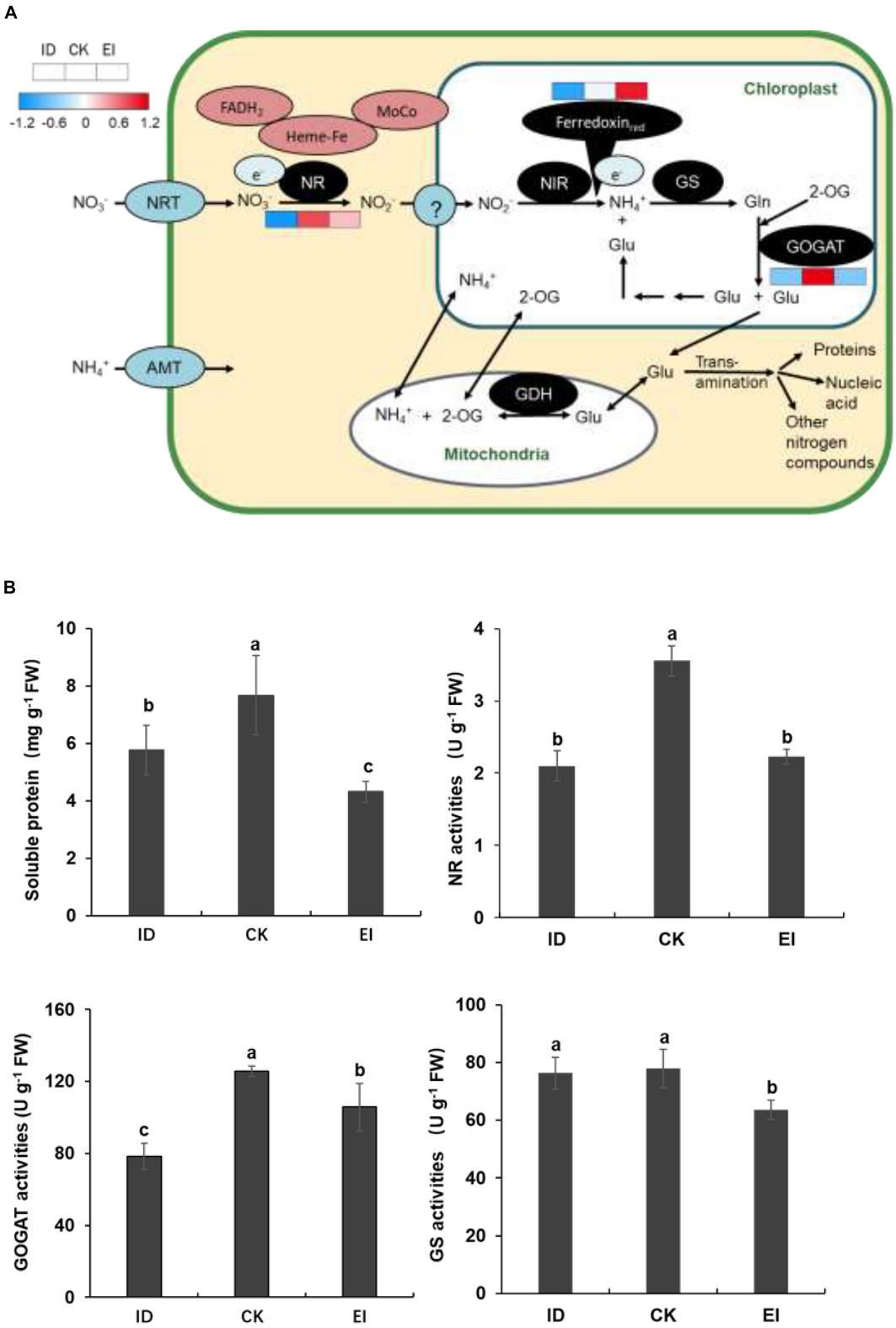


FIGURE 9 | Nitrogen assimilation pathway and activities of key enzymes related with N metabolism in ID, CK, and EI leaves. **(A)** Pathway viewer of main N metabolism in *A. catechu* leaf. Heat maps were drawn using *log2*-transformed FPKM values. **(B)** Comparison of soluble protein, Nitrate reductase (NR), glutamate synthase (GOGAT), and glutamine synthetase (GS). The small bars show standard deviation. Different letters represent significant differences at $P < 0.05$ according to Duncan's multiple range tests.

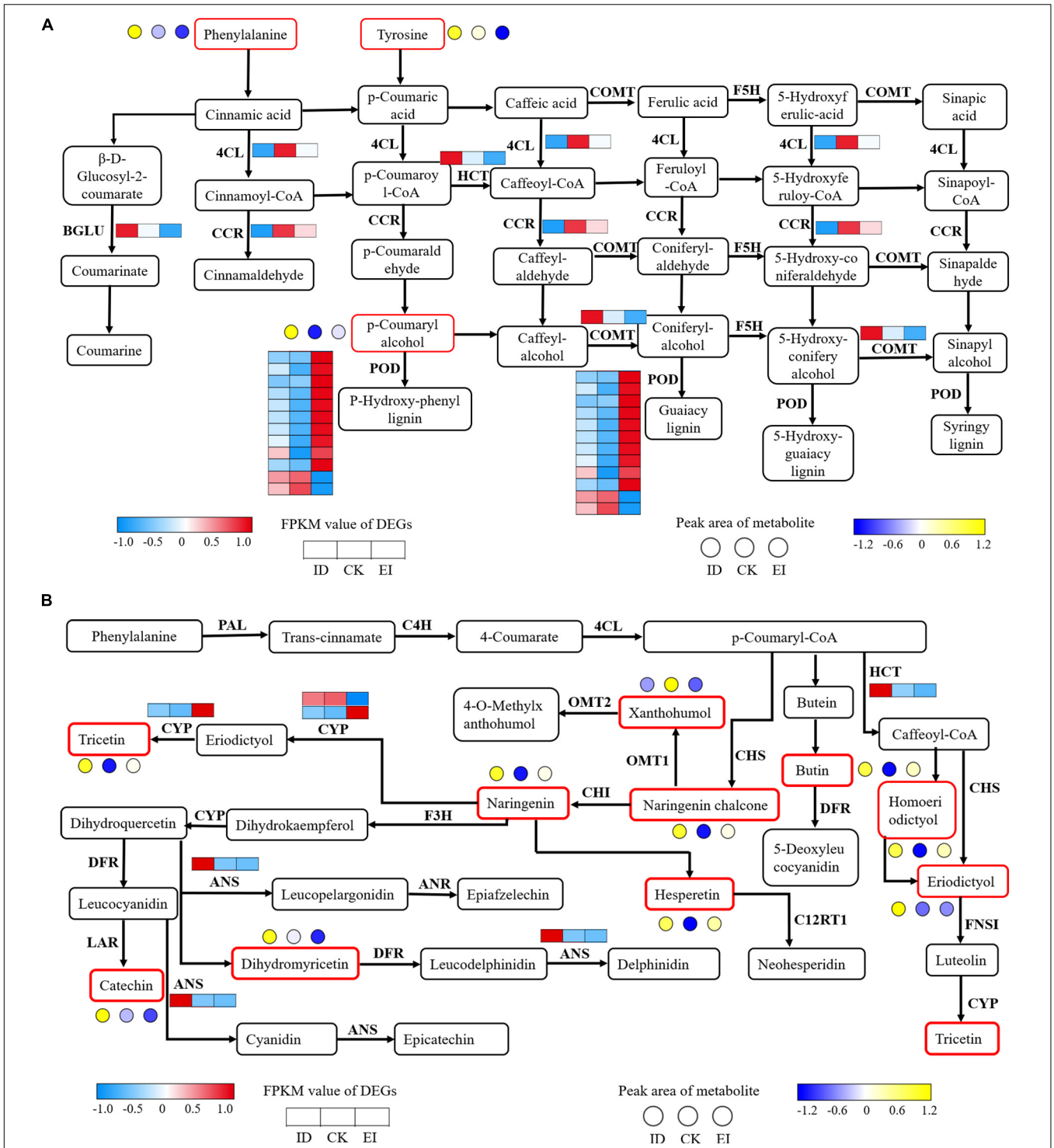


FIGURE 10 | Transcriptomic and metabolomic variation related to phenylpropanoid **(A)** and flavonoid **(B)** metabolism. 4CL, 4-coumarate CoA ligase; BGLU, beta-glucosidase; CCR, cinnamoyl-CoA reductase; COMT, caffeic acid 3-O-methyltransferase; F5H, flavanone 5-hydroxylase; PAL, phenylalanine ammonia-lyase; C4H, cinnamic acid 4-hydroxylase; CHS, chalcone synthase; CHI, chalcone isomerase; F3H, flavanone 3-hydroxylase; DFR, dihydroflavonol 4-reductase; ANS, anthocyanidin synthase; FLS, flavonol synthesis; ANR, anthocyanin reductase.

of iron. Jin et al. (2006) found that phenolic compounds secreted under ID in red clover can inhibit the growth and reproduction of phenol sensitive microorganisms in rhizosphere soil through its antibacterial function. The phenolic compounds can also be used as carbon sources to promote the growth and reproduction of phenol resistant microorganisms. The combined action of these two aspects can form a dominant microbial community which can secrete siderophore in the rhizosphere (Jin et al., 2014). Our data demonstrated that most genes involved in the process of decarboxylation of phenolic acids were also down-regulated in the seedlings grown under ID. The inhibition of decarboxylation activity could result in the accumulation of phenolic acids, which might be an important compound for *A. catechu* seedlings to deal with ID. On the other hand, the phenylalanine pathway is identified as the major target for *A. catechu* to response to ID. The genes including *HCT*, *ANS*, *BGLU,* and *COMT*, and the metabolites including catechin, naringenin, xanthohumol, eriodictyol, hesperetin, dihydromyricetin, naringenin chalcone, tricetin, homoeriodictyol, and butin were important candidates for indicating the ID status of *A. catechu* seedlings.

The bHLH family transcription factors were identified from both ID vs. CK and EI vs. CK. It is known that at least 16 bHLH transcription factors are closely involved into the regulation of plant iron homeostasis through a complex regulatory network (Gao et al., 2019). It was found in Arabidopsis that the *FIT* (*FER-LIKE FE DEFICIENCY-INDUCED TRANSCRIPTION FACTOR*) gene could form a heterodimer with bHLH038, bHLH039, bHLH100, and bHLH101, respectively, and activate the expression of downstream target genes such as *FRO2* and *IRT1* under iron deficiency (Sivitz et al., 2012). The expression of bHLH11 was significantly inhibited under iron deficiency in Arabidopsis (Tanabe et al., 2018). A number of genes encoding WRKY were identified from ID vs. CK. The WRKY transcription factors have been reported to play a role in response to nutrient deficiency (Kasajima et al., 2010; Ding et al., 2013; Su et al., 2015). The WRKY-related cis-element, W-box, was located in the promoter sequences of *IRT* and *NAS4*, which are critical genes response to iron deficiency. A *WRKY46* gene from Arabidopsis was verified to promote Fe translocation from root to shoot by suppressing the expression of a nodulin-like gene (*VIT1-like1*) under iron deficiency (Yan et al., 2016). Moreover, a gene encoding an IDEF2 transcription factor from rice was proved to response to ID. IDEF2 can recognize the iron deficiency-responsive *cis*-acting element 2 (IDE2) thus regulate the genes involved in iron homeostasis. Knocking down of *IDEF2* resulted in abnormal Fe allocation between the shoots and roots (Li Q. et al., 2019). These evidences indicated that the DEGs encoding bHLH, WRKY and NAC identified from our transcriptome data, might be key regulators in the chlorosis process of *A. catechu*.

CONCLUSION

In summary, iron was identified as a determinant for leaf chlorosis in *A. catechu* seedlings. The *A. catechu* seedlings have good adaptability to different nutrients (nitrogen, magnesium, zinc, boron) except for iron. Iron deficiency seriously impacted chloroplast development and nitrogen assimilation in *A. catechu* leaves. *A. catechu* seedlings response to ID through alter the flavonoids and flavonols biosynthesis, and secrete flavones and phenolic acids to the rhizosphere. The transcription factors bHLH, WRKY, and NAC were identified as key regulators under ID. On the other hand, high iron is also deleterious to *A. catechu* seedlings. An unknown mechanism blocks the iron transport and retains iron in the subterranean parts of the plants. The up-regulation of POD-related genes was assumed to be a defense strategy against the excessive iron toxicity. These evidences indicated that *A. catechu* is an iron-sensitive species, therefore we suggest that the precise iron control, including the detection of iron level, the way of iron supplement and the maintenance of suitable iron level, should be taken into account for *A. catechu* cultivation in the future.

DATA AVAILABILITY STATEMENT

The datasets presented in this study can be found in online repositories. The names of the repository/repositories and accession number(s) can be found in the article/ **Supplementary Material**.

AUTHOR CONTRIBUTIONS

JL: conceptualization, methodology, software, investigation, and writing—original draft. XC: investigation and data curation. XJ: software and writing—review. LL: resources and funding acquisition. HC: software. WQ: resources and formal analysis. ML: data curation and writing—review and editing. All authors contributed to the article and approved the submitted version.

FUNDING

This work was supported by the grants from Hainan Major Research Program of Science and Technology (ZDKJ201817), the Central Public-interest Scientific Institution Basal Research Fund for Innovative Research Team Program of CATAS (17CXTD-14), and the Innovation Project of Forestry Science and Technology in Hunan Province (XLK201984).

ACKNOWLEDGMENTS

We are grateful to Dr. Yinglang Wan and Mr. Sai Xie for their valuable suggestions and comments on this manuscript.

SUPPLEMENTARY MATERIAL

The Supplementary Material for this article can be found online at: https://www.frontiersin.org/articles/10.3389/fpls.2021.710093/full#supplementary-material

REFERENCES

Arnon, D. I. (1949). Copper enzymes in isolated chloroplasts. Polyphenoloxidase in beta vulgaris. *Plant Physiol.* 24, 1–15. doi: 10.1104/pp.24.1.1

Blum, U., Staman, K. L., Flint, L. J., and Shafer, S. R. (2000). Induction and/or selection of phenolic acid-utilizing bulk-soil and rhizosphere bacteria and their influence on phenolic acid phytotoxicity. *J. Chem. Ecol.* 26, 2059–2078. doi: 10.1023/A:1005560214222

Borlotti, A., Vigani, G., and Zocchi, G. (2012). Iron deficiency affects nitrogen metabolism in cucumber (Cucumis sativus L.) plants. *BMC Plant Biol.* 12:189. doi: 10.1186/1471-2229-12-189

Brumbarova, T., Bauer, P., and Ivanov, R. (2014). Molecular mechanisms governing Arabidopsis iron uptake. *Trends Plant Sci.* 20, 124–133. doi: 10.1016/j.tplants.2014.11.004

Campbell, W. H. (1999). Nitrate reductase structure, function and regulation: bridging the gap between biochemistry and physiology. *Ann. Rev. Plant Physiol. Plant Mol. Biol.* 50, 277–277. doi: 10.1146/annurev.arplant.50.1.277

Cao, G., Sofic, E., and Prior, R. L. (1997). Antioxidant and prooxidant behavior of flavonoids: structure-activity relationships. *Free Radic. Biol. Med.* 22, 749–760. doi: 10.1016/S0891-5849(96)00351-6

Chowdappa, P., Iyer, R., and Gunasekaran, M. (2002). *Plant pathology research at CPCRI*. Kasaragod, India: Central Plantation Crop Research Institute, 113.

Chu, Q., Sha, Z., Maruyama, H., Yang, L., Pan, G., Xue, L., et al. (2019). Metabolic reprogramming in nodules, roots, and leaves of symbiotic soybean in response to iron deficiency. *Plant Cell Environ.* 42, 3027–3043. doi: 10.1111/pce.13608

Cpcri. (1990). *Central Plantation Crops Research Institute Annual Report 1989-1990*. Kasaragod, India: CPCRI.

Curie, C., and Briat, J. F. (2003). Iron transport and signaling in plants. *Annu. Rev. Plant. Biol.* 54, 183–206. doi: 10.1016/j.inoche.2010.03.022

de Bang, T. C., Husted, S., Laursen, K. H., Persson, D. P., and Schjoerring, J. K. (2020). The molecular-physiological functions of mineral macronutrients and their consequences for deficiency symptoms in plants. *New Phytol.* 5, 2445–2469. doi: 10.1111/NPH.17074

Ding, Z. J., Ya, J. Y., Xu, X. Y., Li, G. X., and Zheng, S. J. (2013). WRKY46 functions as a transcriptional repressor of ALMT1, regulating aluminum-induced malate secretion in Arabidopsis. *Plant J.* 76, 825–883. doi: 10.1111/tpj.12337

Dixon, S. J., and Stockwell, B. R. (2014). The role of iron and reactive oxygen species in cell death. *Nat. Chem. Biol.* 10, 9–17. doi: 10.1038/nchembio.1416

Donnini, S., Prinsi, B., Negri, A. S., Vigani, G., Espen, L., and Zocchi, G. (2010). Proteomic characterization of iron deficiency response in Cucumis sativus L. roots. *BMC Plant Biol.* 10:268. doi: 10.1186/1471-2229-10-268

Fu, L., Zhu, Q., Sun, Y., Wei, D., Pan, Z., and Peng, S. (2017). Physiological and transcriptional changes of three citrus rootstock seedlings under iron deficiency. *Front. Plant Sci.* 8:1104. doi: 10.3389/fpls.2017.01104

Gao, F., Rob, E. K., Gaymard, F., Izquierdo, E., and Dubos, C. (2019). The transcriptional control of iron homeostasis in plants: A tale of bHLH transcription factors? *Front. Plant Sci.* 10:6. doi: 10.3389/fpls.2019.00006

Gilani, A. H., Ghayur, M. N., Saify, Z. S., Ahmed, S. P., Choudhary, M. I., and Khalid, A. (2004). Presence of cholinomimetic and acetylcholinesterase inhibitory constituents in betel nut. *Life Sci.* 75, 2377–2389. doi: 10.1016/j.lfs.2004.03.035

Guerinot, M. L., and Yi, Y. (1994). Iron: Nutritious, noxious, and not readily available. *Plant Physiol.* 104, 815–820. doi: 10.1104/pp.104.3.815

Hänsch, R., and Mendel, R. R. (2009). Physiological functions of mineral micronutrients (Cu, Zn, Mn, Fe, Ni, Mo, B, Cl). *Curr. Opin. Plant Biol.* 12, 259–266. doi: 10.1016/j.pbi.2009.05.006

Hell, R., and Stephan, U. W. (2003). Iron uptake, trafficking and homeostasis in plants. *Planta* 216, 541–551. doi: 10.1007/s00425-002-0920-4

Honetschlägerová, L., Škarohlíd, R., Martinec, M., Šír, M., and Luciano, V. (2018). Interactions of nanoscale zero valent iron and iron reducing bacteria in remediation of trichloroethene. *Int. Biodeterior. Biodegradation.* 127, 241–246. doi: 10.1016/j.ibiod.2017.10.009

Imsande, J. (1998). Iron, sulfur, and chlorophyll deficiencies: a need for an integrative approach in plant physiology. *Plant Physiol.* 103, 139–144. doi: 10.1034/j.1399-3054.1998.1030117.x

Jin, C. W., He, Y. F., Tang, C. X., Wu, P., and Zheng, S. J. (2006). Mechanisms of microbially enhanced Fe acquisition in red clover (Trifolium pratense L.). *Plant Cell Environ.* 29, 888–897. doi: 10.1111/j.1365-3040.2005.01468.x

Jin, C. W., Ye, Y. Q., and Zheng, S. J. (2014). An underground tale: contribution of microbial activity to plant iron acquisition via ecological processes. *Ann. Bot.* 113, 7–18. doi: 10.1093/aob/mct249

Jin, L. F., Liu, Y. Z., Du, W., Fu, L. N., Hussain, S. B., and Peng, S. A. (2017). Physiological and transcriptional analysis reveals pathways involved in iron deficiency chlorosis in fragrant citrus. *Tree Genet. Genomes.* 13:51. doi: 10.1007/s11295-017-1136-x

Jones, D. L., and Darrah, P. R. (1994). Role of root derived organic acids in the mobilization of nutrients from the rhizosphere. *Plant Soil.* 166, 247–257. doi: 10.1007/bf00008338

Kasajima, I., Ide, Y., Hirai, M. Y., and Fujiwara, T. (2010). WRKY6 is involved in the response to boron deficiency in Arabidopsis thaliana. *Plant Physiol.* 139, 80–92. doi: 10.1111/j.1399-3054.2010.01349.x

Kobayashi, T., Nakanishi, H., and Nishizawa, N. K. (2010). Recent insights into iron homeostasis and their application in graminaceous crops. *Proc. Jpn. Acad. Ser. B.* 86, 900–913. doi: 10.2183/pjab.86.900

Li, B., Sun, L., Huang, J., Gschl, C., and Busch, W. (2019). GSNOR provides plant tolerance to iron toxicity via preventing iron-dependent nitrosative and oxidative cytotoxicity. *Nat Commun.* 10:3896.

Li, J., Cao, X., Liu, L., and Niu, Q. (2019). Effects of different magnesium nutrition levels on photosynthetic characteristics and chloroplast ultrastructure of areca palm seedlings. *J. Plant Nutr. Fertil.* 25, 1949–1956.

Li, J., Jia, X. C., Liu, L. Y., Cao, X. M., Xiong, Y. F., Yang, Y. D., et al. (2020). Comparative biochemical and transcriptome analysis provides insights into the regulatory mechanism of striped leaf albinism in arecanut (Areca catechu L.). *Indust. Crops Products* 154:112734. doi: 10.1016/j.indcrop.2020.112734

Li, Q., Lei, C., and Yang, A. (2019). The molecular mechanisms underlying iron deficiency responses in rice. *Int. J. Mol. Sci.* 21:43. doi: 10.3390/ijms21010043

Livak, K. J., and Schmittgen, T. D. (2001). Analysis of relative gene expression data using real-time quantitative PCR and the $2^{-\Delta\Delta CT}$ method. *Methods* 25, 402–408. doi: 10.1006/meth.2001.1262

Mao, X., Tao, C., John, G. O., and Wei, L. (2005). Automated genome annotation and pathway identifcation using the KEGG Orthology (KO) as a controlled vocabulary. *Bioinformatics* 21, 3787–3793. doi: 10.1093/bioinformatics/bti430

Marschner, H., and Marschner, P. (2012). *Marschner's mineral nutrition of higher plants*, 3rd Edn. San Diego: Academic Press.

Marschner, H., and Römheld, V. (1994). Strategies of plants for acquisition of iron. *Plant Soil* 165, 261–274. doi: 10.1007/bf00008069

Mathai, C. K. (1986). Nutritional status and related changes in soil environment with reference to the incidence of yellow leaf disease of arecanut palms. *Indian Cocoa Arecanut Spices J.* 10, 31–33.

Minoru, K., Yoko, S., Masayuki, K., Miho, F., and Mao, T. (2016). KEGG as a reference resource for gene and protein annotation. *Nucleic Acids Res.* 44, D457–D462. doi: 10.1093/nar/gkv1070

Nozoye, T., Nagasaka, S., Kobayashi, T., Takahashi, M., Sato, Y., Sato, Y., et al. (2011). Phytosiderophore efflux transporters are crucial for iron acquisition in gramina-ceous plants. *J. Biol. Chem.* 286, 5446–5454. doi: 10.1074/jbc.M110.180026

Pushnik, J. C., and Miller, G. W. (1989). Iron regulation of chloroplast photosynthetic function: mediation of PS I development. *J. Plant Nutr.* 12, 407–421. doi: 10.1080/01904168909363962

Raven, J. A., Evans, M., and Korb, R. E. (1999). The role of trace metals in photosynthetic electron transport in O_2-evolving organisms. *Photosynth. Res.* 60, 111–150.

Rice-Evans, C. A., and Miller, N. J. (1996). Antioxidant activities of flavonoids as bioactive components of food. *Biochem. Soc. Trans.* 24, 790–795. doi: 10.1042/bst0240790

Rodriguez-Celma, J., Vázquez-Reina, S., Orduna, J., Abadía, A., Abadía, J., Álvarez-Fernández, A., et al. (2011). Characterization of flavins in roots of Fe-deficient strategy I plants, with a focus on medicago truncatula. *Plant Cell Physiol.* 52, 2173–2189. doi: 10.1093/pcp/pcr149

Romheld, V., and Maschner, H. (1986). Mobilization of iron in the rhizosphere of different plant species. *Adv. Plant Nutr.* 2, 155–204.

Sánchez-Rodríguez, A. R., del Campillo, M. C., Torrent, J., and Jones, D. L. (2014). Organic acids alleviate iron chlorosis in chickpea grown on two

p-fertilized soils. *J. Soil Sci. Plant Nutr.* 14, 292–303. doi: 10.4067/S0718-95162014005000024

Singh, R. P., and Srivastava, H. S. (1986). Increase in glutamate synthase (n.d.) activity in maize seedlings in response to nitrate and ammonium nitrogen. *Plant Physiol.* 66, 413–416. doi: 10.1111/j.1399-3054.1986.tb05944.x

Sivitz, A. B., Victor, H., Catherine, C., Grégory, V., and Malcolm, B. (2012). Arabidopsis bHLH100 and bHLH101 control iron homeostasis via a FIT-Independent Pathway. *Plos One* 7:e44843. doi: 10.1371/journal.pone.0044843

Su, T., Xu, Q., Zhang, F. C., Chen, Y., Li, L. Q., Wu, W. H., et al. (2015). WRKY42 modulates phosphate homeostasis through regulating phosphate translocation and acquisition in arabidopsis. *Plant Physiol.* 167, 1579–1591. doi: 10.1104/pp.114.253799

Sun, Y., Yang, R., Li, L., and Huang, J. (2017). The magnesium transporter MGT10 is essential for chloroplast development and photosynthesis in Arabidopsis thaliana. *Mol. Plant* 10, 1584–1587. doi: 10.1016/j.molp.2017.09.017

Susín, S., Abián, J., Sánchez-Baeza, F., Peleato, M. L., Abadía, A., Gelpí, E., et al. (1996). Riboflavin 3′- and 5′-sulphate, two novel flavins accumulating in the roots of iron-deficient sugar beet (Beta vulgaris). *J. Biol. Chem.* 268, 20958–20965. doi: 10.1016/S0021-9258(19)36879-6

Tanabe, N., Noshi, M., Mori, D., Nozawa, K., and Shigeoka, S. (2018). The basic helix-loop-helix transcription factor, bHLH11 functions in the iron-uptake system in Arabidopsis thaliana. *J. Plant Res.* 132, 93–105. doi: 10.1007/s10265-018-1068-z

Ueno, H., Maeda, T., Katsuyama, N., Katou, Y., Matsuo, S., Yano, K., et al. (2018). Cation measurements and gene expression analysis suggest tomato leaf marginal necrosis is caused by a jasmonate signal induced by K^+ starvation in the tip region of leaflets. *Horticult. J.* 87, 206–213. doi: 10.2503/hortj.OKD-101

van Maarschalkerweerd, M., and Husted, S. (2015). Recent developments in fast spectroscopy for plant mineral analysis. *Front. Plant Sci.* 6:169. doi: 10.3389/fpls.2015.00169

Vose, P. B. (1982). Iron nutrition in plants: a world overview. *J. Plant Nutr.* 5, 233–249. doi: 10.1080/01904168209362954

Wu, L. B., Wu, L. B., Shhadi, M. Y., Gregorio, G., Matthus, E., Becker, M., et al. (2014). Genetic and physiological analysis of tolerance to acute iron toxicity in rice. *Rice* 7:8. doi: 10.1186/s12284-014-0008-3

Yamauchi, M. (1989). Rice bronzing in Nigeria caused by nutrient imbalances and its control by potassium sulfate application. *Plant Soil.* 117, 275–286. doi: 10.1007/bf02220722

Yan, J. Y., Li, C. X., Sun, L., Ren, J. Y., Li, G. X., Ding, Z. J., et al. (2016). A WRKY transcription factor regulates Fe translocation under Fe deficiency. *Plant Physiol.* 171, 2017–2027. doi: 10.1104/pp.16.00252

Young, M. D., Wakefeld, M. J., Smyth, G. K., and Oshlack, A. (2010). Gene ontology analysis for RNA-seq: accounting for selection bias. *Genome Biol.* 11:R14. doi: 10.1186/gb-2010-11-2-r14

Yu, X. Z., and Zhang, F. Z. (2012). Activities of nitrate reductase and glutamine synthetase in rice seedlings during cyanide metabolism. *J. Hazard Mater.* 225-226, 190–194. doi: 10.1016/j.jhazmat.2012.05.027

Conflict of Interest: The authors declare that the research was conducted in the absence of any commercial or financial relationships that could be construed as a potential conflict of interest.

Publisher's Note: All claims expressed in this article are solely those of the authors and do not necessarily represent those of their affiliated organizations, or those of the publisher, the editors and the reviewers. Any product that may be evaluated in this article, or claim that may be made by its manufacturer, is not guaranteed or endorsed by the publisher.

Copyright © 2021 Li, Cao, Jia, Liu, Cao, Qin and Li. This is an open-access article distributed under the terms of the Creative Commons Attribution License (CC BY). The use, distribution or reproduction in other forums is permitted, provided the original author(s) and the copyright owner(s) are credited and that the original publication in this journal is cited, in accordance with accepted academic practice. No use, distribution or reproduction is permitted which does not comply with these terms.

frontiers in Plant Science

ORIGINAL RESEARCH
published: 05 August 2021
doi: 10.3389/fpls.2021.716437

Biofortification of Sodium Selenate Improves Dietary Mineral Contents and Antioxidant Capacity of Culinary Herb Microgreens

*Rachel G. Newman[1], Youyoun Moon[2], Carl E. Sams[3], Janet C. Tou[1] and Nicole L. Waterland[2]**

[1] Division of Animal and Nutritional Sciences, West Virginia University, Morgantown, WV, United States, [2] Division of Plant and Soil Sciences, West Virginia University, Morgantown, WV, United States, [3] Department of Plant Sciences, The University of Tennessee, Knoxville, TN, United States

Selenium biofortification of plants has been suggested as a method of enhancing dietary selenium intake to prevent deficiency and chronic disease in humans, while avoiding toxic levels of intake. Popular herbs such as basil (*Ocimum basilicum* L.), cilantro (*Coriandrum sativum* L.), and scallions (*Allium fistulosum* L.) present an opportunity for biofortification as these plants are used for added flavors to meals and are available as microgreens, young plants with increasing popularity in the consumer marketplace. In this study, basil, cilantro, and scallion microgreens were biofortified with sodium selenate under hydroponic conditions at various selenium concentrations to investigate the effects on yield, selenium content, other mineral contents (i.e., sodium, potassium, calcium, magnesium, phosphorus, copper, zinc, iron, manganese, sulfur, and boron), total phenol content, and antioxidant capacity [oxygen radical absorbance capacity (ORAC)]. The results showed that the selenium content increased significantly at all concentrations, with scallions demonstrating the largest increase. The effects on other minerals varied among herb species. Antioxidant capacity and total phenol content increased in all herbs at the highest selenium treatments, but basil and scallions demonstrated a decreased crop yield. Overall, these biofortified culinary herb microgreens are an ideal functional food for enhancing selenium, other dietary minerals, and antioxidants to benefit human health.

Keywords: selenium, biofortification, antioxidants, minerals, herbs, microgreens

OPEN ACCESS

Edited by:
Spyridon Alexandros Petropoulos, University of Thessaly, Greece

Reviewed by:
Szilvia Veres, University of Debrecen, Hungary
Rasim Mogulkoc, Selçuk University, Turkey

***Correspondence:**
Nicole L. Waterland
nicole.waterland@mail.wvu.edu

Specialty section:
This article was submitted to Plant Nutrition, a section of the journal Frontiers in Plant Science

Received: *28 May 2021*
Accepted: *01 July 2021*
Published: *05 August 2021*

Citation:
Newman RG, Moon Y, Sams CE, Tou JC and Waterland NL (2021) Biofortification of Sodium Selenate Improves Dietary Mineral Contents and Antioxidant Capacity of Culinary Herb Microgreens. Front. Plant Sci. 12:716437. doi: 10.3389/fpls.2021.716437

INTRODUCTION

Selenium (Se) is an essential trace mineral in humans and a component of biologically important selenoproteins, such as antioxidant enzymes (Navarro-Alarcon and Cabrera-Vique, 2008). While Se deficiency is uncommon in North America, it is estimated that one in seven people worldwide have inadequate intake of dietary Se, and the prevalence of Se deficiency may increase with climate change (Jones et al., 2017). Supplementation of Se has been suggested for the prevention of chronic disease; however, high-dose supplementation can increase the risk of Se toxicity (Navarro-Alarcon and Cabrera-Vique, 2008). Plants are a major dietary source of Se, and biofortification is a method of enhancing the Se content in plants to improve adequacy of the

human diet (Gupta and Gupta, 2017). Biofortification with selenate demonstrates maximum Se translocation to the edible shoots of plants, whereas selenite accumulates in the roots (Terry et al., 2000; Saha et al., 2017). The use of hydroponic growing conditions further allows for highly controlled Se application (Puccinelli et al., 2017a), making the addition of sodium selenate (Na_2SeO_4) to nutrient solutions an efficient biofortification method.

Different plant species exhibit varying levels of Se tolerance rather than essentiality (Terry et al., 2000). The goal of Se biofortification is to increase the Se content while avoiding significant decreases in the crop yield (Puccinelli et al., 2017a). While this suggests a trade-off between supplying supra-adequate levels of Se to the diet and detrimental effects on plant growth, Navarro-Alarcon and Cabrera-Vique (Navarro-Alarcon and Cabrera-Vique, 2008) noted that plants serve as an effective buffer to Se toxicity in humans because of a decreased yield at high levels. Studies have also reported that Se biofortification can impact other dietary minerals and antioxidant compounds, such as polyphenols, which have anticancer and cardioprotective properties (He et al., 2004; Hawrylak-Nowak, 2008; Boldrin et al., 2013; Saffaryazdi et al., 2012). Therefore, it is imperative that studies investigating Se biofortification include other nutrients that are relevant to human health.

Culinary herbs are added to meals for flavor to replace salt and can increase consumer acceptance of vegetables (Manero et al., 2017). Popular culinary herbs, such as basil (*Ocimum basilicum* L.), cilantro (*Coriandrum sativum* L.), and scallions (*Allium fistulosum* L.), present an opportunity for Se biofortification as small, flavorful additions to meals. Furthermore, microgreens are increasingly popular among consumers for their distinct flavors (Choe et al., 2018). Microgreens are young plants typically consisting of the stem, cotyledons, and a pair of true leaves (Choe et al., 2018), making microgreen herbs a quick and easy crop to biofortify. Few studies have investigated Se biofortification of herb microgreens. The objective of this study was to investigate the effect of Se biofortification on plant yield, total Se content, content of other minerals relevant to human health, and antioxidants in three culinary herb species grown to microgreen stage under hydroponic conditions. This study tests the hypothesis that biofortification of culinary herb microgreens increases the content of Se, other minerals important to human health, and antioxidants. Enhancements in nutrient profiles would enable these herbs to serve as a functional food for improving human nutrition.

MATERIALS AND METHODS

Plant Growth and Harvest

Seeds of basil, cilantro, and scallions were purchased from Johnny's Selected Seeds (Winslow, ME). The seeds were sown in 25.4 × 25.4 × 2.54 cm black growing trays onto Biostrate felt mats (0.35 cm thickness; Grow-Tech, South Portland, ME). The seed density per tray for each species was as follows: 2.8 seeds per cm^2 of basil seeds, 2.8 seeds per cm^2 of cilantro seeds, and 3.4 seeds per cm^2 of scallion seeds. Treatments for all species consisted of 0.5× concentrated Hoagland's modified nutrient solution (PhytoTechnology Labs, Shawnee Mission, KS) prepared in ultrapure water (18.2 MΩ·cm) and supplemented with Na_2SeO_4 (VWR, Radnor, PA) concentrations of 0.0 (control), 2.5, and 5.0 mg/L of Se. Scallions received an additional treatment with 10.0 mg/L of Se as a member of *Allium* plant family which is known for the ability to accumulate Se levels up to 1,000 μg/g dry weight (DW) (Navarro-Alarcon and Cabrera-Vique, 2008).

The treatments were completed with three replicates, where each tray represented a replicate, and mineral contents, total phenolic content (TPC), and oxygen radical absorbance capacity (ORAC) were measured for each replicate. Based on preliminary studies with low yields, scallions were grown in two trays per replicate, which were combined to obtain enough sample for various analyses. The plant yield was analyzed as grams per tray. Each tray received an initial 180 ml of a 0.5× concentrated Hoagland's nutrient solution. The trays were placed into growth chambers (Percival Scientific, Perry, IA) with a photoperiod of 16/8 h light/dark, temperature of 19.7/18.7 ± 1.0/0.8°C day/night, relative humidity of 57.3 ± 0.8%, and photosynthetic photon flux density of 210 ± 7.9 μmol/m^2/s (mean ± standard deviation [SD]). The average value of pH of all nutrient solutions was 5.4 ± 0.1. The plants were sprayed with plain ultrapure water as needed to avoid drying of seeds during germination. Treatment began when 80% of seeds were germinated for each species. The plants were fertigated as needed by adding solutions directly to the growing mats based on the mat saturation within plant species. Each tray within plant species received the same volume of treatment every day. The total volume of treatment per tray for each species over the 25-day treatment period was 2,965, 2,835, and 3,825 mL for basil, scallions, and cilantro, respectively.

Each plant species was harvested on the 25th day of treatment, at which point basil and cilantro had two true leaves and scallions had one true leaf. Microgreens were harvested at the base, approximately 1.0 cm from the growing pad. The seed coats were removed as needed, and fresh weight (FW) per tray was recorded. Microgreens were immediately flash frozen with liquid nitrogen, and stored at −80°C until freeze-dried (Virtus Genesis 35 SQ Super XL, SP Industries, Gardiner, NY). Dried samples were weighed, ground to a fine powder, and stored at −80°C until analyses. The water content of microgreens was determined for each tray by comparing DW with FW. All measured parameters were converted to FW basis, as microgreens are consumed exclusively fresh.

Mineral Analysis

The measurement of minerals was completed according to Barickman et al. (2012). In brief, 0.5 g of lyophilized ground plant tissue was mixed with 10 ml of 70% HNO_3 and was digested in a microwave digestion system (Ethos model, Milestone Inc., Shelton, CT, USA). Digestion procedures for organically based matrixes were followed U.S. Environmental Protection Agency (1996). The digested samples were diluted with 2% HNO_3/0.5% HCl (v/v). The samples were analyzed for Se, sulfur (S), sodium (Na), potassium (K), phosphorus (P), calcium (Ca), magnesium (Mg), copper (Cu), iron (Fe), manganese (Mn), zinc (Zn), and

boron (B) by inductively coupled plasma mass spectrometry (ICP-MS) using an Agilent 7500ce ICP-MS system (Agilent Technologies, Inc., Wilmington, DE, USA) equipped with an ASX-510 (CETAC, Omaha, NE, USA) autosampler.

Determination of Total Phenolic Content

Total phenolics were extracted using the method of Nicolle et al. (2004) with some modifications. In brief, 10 mg of lyophilized ground plant tissue was extracted using 1 ml of methanol–water mixture (60:40, v/v), vortexed for 10 s, and centrifuged at 16,110*g* for 20 min at 4°C. The supernatant was collected, and the extraction process was repeated. Supernatants were combined and stored at −80°C until analysis. TPC was determined with modifications for a 96-well microplate according to Waterland et al. (2019). In brief, 18.2 μL of sample extract or gallic acid standard was plated in duplicates, followed by 90.9 μL of 0.5 N Folin–Ciocalteau reagent (Sigma-Aldrich, St. Louis, MO). The plate was incubated for 5 min, and then 90.9 μL of 0.5 M sodium carbonate was added to each well. The plate was incubated at room temperature in the dark for 1 h. The absorbance was measured at 765 nm with a BioTek Synergy H1 (Winooski, VT) microplate reader. The interassay coefficient of variation was 5.7%. TPC was determined using a gallic acid standard curve and expressed in mg of gallic acid equivalents (GAE) per gram of FW.

Oxygen Radical Absorbance Capacity Assay

Sample preparation for hydrophilic ORAC assay was completed according to Ou et al. (2013). In brief, 10 mg of lyophilized ground plant tissue was added to a microcentrifuge tube with 0.4 mL of acetone–water mixture (50:50, v/v) and vortexed at room temperature for 1 h. The tube was then centrifuged at 16,110*g* for 15 min at 4°C. The supernatant was collected and stored at −20°C until assayed. The sample preparation for the lipophilic assay was completed according to OxiSelect ORAC Activity Assay kit protocol (CellBio Labs, San Diego, CA). In brief, 10 mg of lyophilized ground plant tissue was added to a microcentrifuge tube with 0.4 mL of pure acetone and vortexed at room temperature for 1 h. The tube was stored at −20°C until assayed, and the supernatant was separated from the tissue. The ORAC assays were completed by following the OxiSelect ORAC Activity Assay kit protocol (CellBio Labs, San Diego, CA). Fluorescence was read using a Biotek Synergy H1 (Winooski, VT) microplate reader. The interassay coefficient of variation was 21.0%. Results were expressed in μmol Trolox equivalents per gram of FW. The lipophilic and hydrophilic portions were summed for measuring the total ORAC values.

Statistical Analysis

Due to scallions having an additional treatment group, one-way ANOVA was used to determine the differences among treatment groups for each herb species. *Post hoc* multiple comparison tests were performed using Tukey's test with significance at $P \leq 0.05$. A two-way ANOVA was used to determine potential interaction effects of plant species and Se treatments (excluding 10.0 mg/L Se) on minerals, TPC, and ORAC. To determine the differences in Se content in response to concentrations of Se treatment among fresh scallions, basil, and cilantro, a regression analysis was combined with ANOVA [analysis of covariance (ANCOVA)]. The analyses were performed using JMP and SAS software (JMP, Version 13, SAS Institute Inc., Cary NC; SAS, Version 9.2, SAS Institute Inc., Cary NC).

RESULTS

Selenium Content and Plant Yield

The present study showed an interaction of Se treatment and plant species ($P \leq 0.0001$). Se content increased ($P \leq 0.05$) with increasing Se treatments for all three culinary herbs (**Figure 1**). The Se content of fresh scallions increased 98, 202, and 507 times for doses of 2.5, 5.0, and 10.0 mg/L Se, respectively (**Figure 1A**). The DW values for scallions were 824.9, 1,530.4, and 2,481.4 μg/g Se for 2.5, 5.0, and 10.0 mg/L Se treatments,

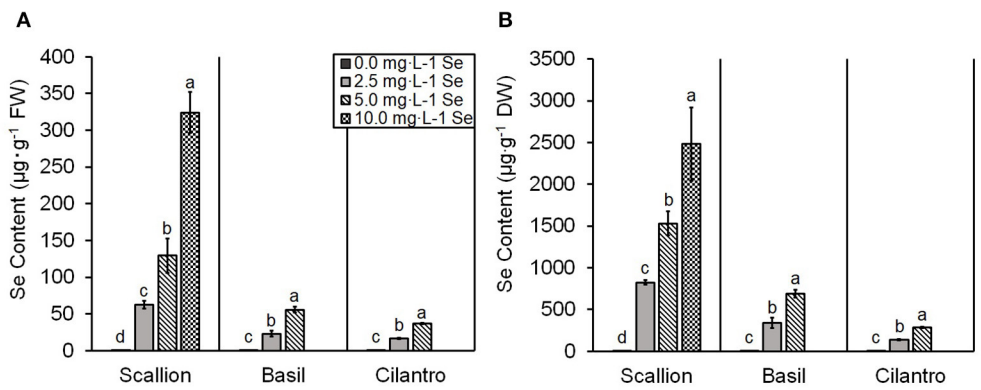


FIGURE 1 | Selenium (Se) content of scallion (*Allium fistulosum* L.), basil (*Ocimum basilicum* L.), and cilantro (*Coriandrum sativum* L.) microgreens treated with various concentrations of Se as sodium selenate, on **(A)** fresh weight (FW) basis and **(B)** dry weight (DW) basis. Bars indicate mean ± standard deviation (SD) for three replicates ($n = 3$) of each plant species. The Tukey's significance at $P \leq 0.05$ among Se treatments is indicated by different letters within the plant species.

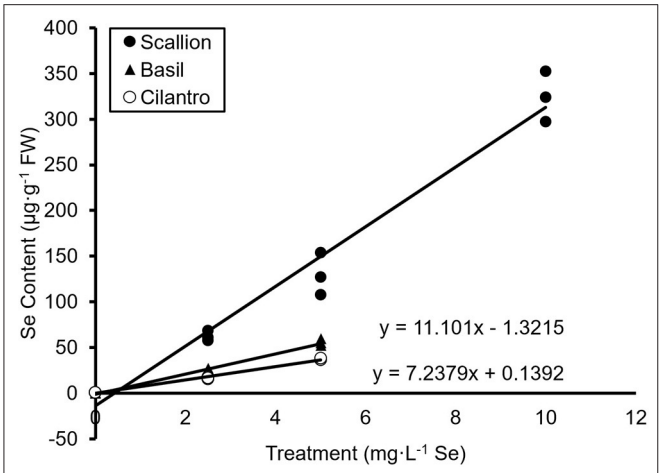


FIGURE 2 | Regression analysis of fresh weight (FW) selenium (Se) content of scallion (*Allium fistulosum* L.), basil (*Ocimum basilicum* L.), and cilantro (*Coriandrum sativum* L.) microgreens treated with various concentrations of Se as sodium selenate ($n = 3$).

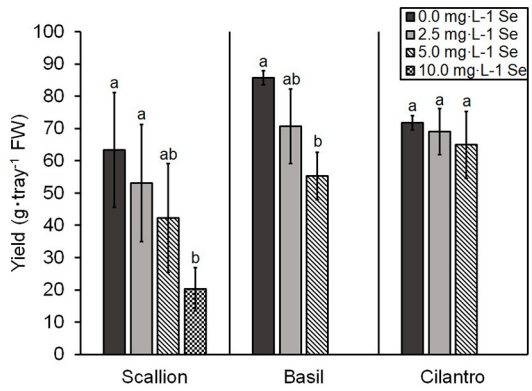


FIGURE 3 | Fresh weight (FW) yield of scallion (*Allium fistulosum* L.), basil (*Ocimum basilicum* L.), and cilantro (*Coriandrum sativum* L.) microgreens treated with various concentrations of selenium (Se) as sodium selenate. Bars indicate mean ± standard deviation (SD) for three replicates ($n = 3$) of basil and cilantro and six replicates ($n = 6$) for scallion. The Tukey's significance at $P \leq 0.05$ among Se treatments is indicated by different letters within the plant species.

respectively (**Figure 1B**). The Se content of fresh basil increased 64 and 155 times at doses of 2.5 and 5.0 mg/L Se (**Figure 1A**) and accumulated 338.6 and 690.0 µg/g Se DW at 2.5 and 5.0 mg/L Se, respectively (**Figure 1B**). The Se content of fresh cilantro increased 18 and 40 times at 2.5 and 5.0 mg/L Se treatments (**Figure 1A**), and cilantro accumulated 136.2 and 287.2 µg/g Se DW at 2.5 and 5.0 mg/L Se, respectively (**Figure 1B**). ANCOVA showed significant effects ($P \leq 0.0001$) of Se treatments, plant species, and interaction of Se content and plant species. The regression analysis for concentrations of Se treatment on the Se content were different among plant species ($\beta = 32.63$, $P \leq 0.0001$ for scallions; $\beta = 11.10$, $P = 0.0001$ for basil; and $\beta = 7.24$, $P = 0.0058$ for cilantro; **Figure 2**). Fresh scallions demonstrated the highest rate of Se accumulation among the plant species ($P \leq 0.0001$). The rates of Se accumulation in basil and cilantro did not differ between these two species ($P = 0.2642$).

The yield of scallion decreased (i.e., 68.0%) at 10.0 mg/L Se but was not significantly affected at 5.0 mg/L Se (**Figure 3**). The yield of basil decreased (i.e., 35.5%) at 5.0 mg/L Se (**Figure 3**). In contrast, the yield of cilantro was not affected by the Se treatments used (**Figure 3**).

Other Dietary Minerals

Se biofortification impacted the content of other minerals relevant to human health in fresh herb microgreens. The current study showed an interaction of Se treatment and plant species ($P \leq 0.0001$) for S content. In cilantro, S content tended to decrease with increasing Se treatments ($P = 0.1027$), while in scallions, S content increased ($P \leq 0.05$) by 124.5, 140.8, and 228.6% at doses of 2.5, 5.0, and 10.0 mg/L Se, respectively. In basil, S content increased by 46.4 and 96.4% at doses of 2.5 and 5.0 mg/L Se, respectively (**Table 1**).

Sodium accumulation demonstrated a trend ($P = 0.0547$) for the interaction of Se treatment and plant species. The addition of Na_2SeO_4 to the nutrient solution increased the Na content in scallions and cilantro ($P \leq 0.05$) but not in basil ($P = 0.0531$) (**Table 1**). The potassium content increased by 91.6% in scallions that were treated with 10.0 mg/L Se, and it increased by 72.2% in basil that were treated with 5.0 mg/L Se (**Table 1**). Biofortification of cilantro did not impact the content of K or other minerals, except for Se and Na. The phosphorus content was significantly increased in scallions by 47.4% at 10.0 mg/L Se and increased in basil by 42.4% at 5.0 mg/L Se (**Table 1**). The contents of Ca and Mg were not affected by Se biofortification in basil or cilantro microgreens; however, both minerals increased in scallions at 10.0 mg/L Se by 59.8% for Ca and 60.6% for Mg (**Table 1**).

A significant increase of Cu in scallions started at the 5.0 mg/L Se treatment and continued to increase at 10.0 mg/L Se (**Table 2**). The contents of Fe, Mn, Zn, and B in scallions were highest ($P \leq 0.05$) in the 10.0 mg/L Se treatment compared with the other Se doses. Basil and cilantro did not demonstrate significant changes in Cu, Fe, Mn, Zn, or B (**Table 2**). Overall, fresh Se-biofortified scallions demonstrated increases in the content of all other minerals that were analyzed, including major and trace minerals in human nutrition. Meanwhile, Se-biofortified basil and cilantro demonstrated increases in only three (S, P and K) and one (Na) minerals, respectively.

Total Phenolic Content and Total Antioxidant Capacity

TPC was significantly higher at the treatment of highest Se concentration in all herb species (**Figure 4**). TPC demonstrated an interaction of Se treatment and plant species ($P = 0.0001$). For basil and cilantro, the highest dose of 5.0 mg/L Se treatment achieved the highest TPC (102.6 and 50.3% increases for basil and cilantro, respectively). For scallions, the TPC of 5.0 mg/L

TABLE 1 | Major mineral content of scallion (*Allium fistulosum* L.), basil (*Ocimum basilicum* L.), and cilantro (*Coriandrum sativum* L.) microgreens treated with various concentrations of selenium as sodium selenate on a fresh weight basis.

Treatment ($mg \cdot L^{-1}$ Se)	S			Na			K			P			Ca			Mg		
	SN	BL	CO	SN	BL	CO	SN	BL	CO	SN	BL	CO	SN	BL	CO	SN	BL	CO
	$mg \cdot g^{-1}$ FW																	
0.0	0.49 c	0.28 c	0.18 a	0.003 b	0.005 a	0.009 c	2.25 b	1.62 b	4.71 a	0.38 b	0.33 b	0.61 a	0.97 b	1.03 a	0.90 a	0.33 b	0.30 a	0.49 a
2.5	1.10 b	0.41 b	0.08 a	0.007 b	0.010 a	0.021 b	2.66 b	2.26 ab	4.30 a	0.38 b	0.43 ab	0.59 a	1.13 b	1.24 a	0.79 a	0.39 b	0.38 a	0.44 a
5.0	1.18 b	0.55 a	0.06 a	0.013 b	0.022 a	0.040 a	2.94 ab	2.79 a	4.88 a	0.38 b	0.47 a	0.66 a	1.12 b	1.32 a	0.76 a	0.39 b	0.39 a	0.46 a
10.0	1.61 a	–	–	0.053 a	–	–	4.31 a	–	–	0.56 a	–	–	1.55 a	–	–	0.53 a	–	–

Values expressed as mean of three replications (n = 3) of each plant species. The Tukey's significance at $P \leq 0.05$ among Se treatments is indicated by different letters within the plant species for each given nutrient.
SN, scallions; BL, basil; CO, cilantro; FW, fresh weight; Se, selenium; S, sulfur; Na, sodium; K, potassium; P, phosphorus; Ca, calcium; Mg, magnesium.

TABLE 2 | Trace mineral content of scallion (*Allium fistulosum* L.), basil (*Ocimum basilicum* L.), and cilantro (*Coriandrum sativum* L.) microgreens treated with various concentrations of selenium as sodium selenate on a fresh weight basis.

Treatment ($mg \cdot L^{-1}$ Se)	Cu			Fe			Mn			Zn			B		
	SN	BL	CO	SN	BL	CO	SN	BL	CO	SN	BL	CO	SN	BL	CO
	$\mu g \cdot g^{-1}$ FW														
0.0	0.25 c	0.34 a	0.48 a	6.71 b	8.90 a	6.73 a	2.78 b	3.71 a	4.40 a	1.57 b	1.49 a	3.52 a	2.23 b	3.78 a	5.44 a
2.5	0.28 c	0.39 a	0.46 a	5.64 b	7.29 a	11.44 a	3.26 b	4.43 a	3.46 a	1.69 b	1.68 a	3.39 a	2.70 b	4.29 a	4.85 a
5.0	0.35 b	0.41 a	0.62 a	8.00 b	7.30 a	10.44 a	3.30 b	5.00 a	4.10 a	1.88 b	1.94 a	4.20 a	2.77 b	3.96 a	5.54 a
10.0	0.48 a	–	–	14.62 a	–	–	5.65 a	–	–	3.10 a	–	–	5.40 a	–	

Values expressed as mean of three replications (n = 3) of each herb species. The Tukey's significance at $P \leq 0.05$ among selenium treatments is indicated by different letters within the plant species for each given nutrient.
SN, scallions; BL, basil; CO, cilantro; FW, fresh weight; Se, selenium; Cu, copper; Fe, iron; Mn, manganese, Zn, zinc; B, boron.

Se treatment was not affected; however, the highest dose of 10.0 mg/L Se treatment resulted in a 113.7% increase of TPC (**Figure 4**).

In terms of total antioxidant capacity for all herb species, the hydrophilic, lipophilic, and total ORAC values were higher ($P \leq 0.05$) at the highest Se treatment (**Figures 5A–C**). Only the lipophilic antioxidant capacity showed an interaction of Se treatment and plant species ($P = 0.0227$). Scallions at the highest dose of 10.0 mg/L Se and basil and cilantro at the highest dose of 5.0 mg/L Se resulted in herbs with the highest total antioxidant capacity determined by ORAC (152.2, 68.6, and 66.0% increases in scallions, basil, and cilantro, respectively) (**Figure 5C**).

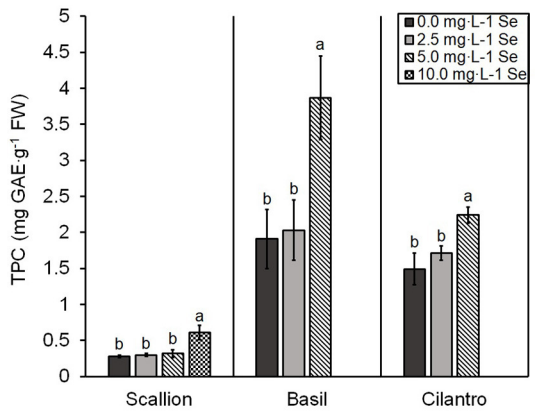


FIGURE 4 | Total phenolic content (TPC) of scallion (*Allium fistulosum* L.), basil (*Ocimum basilicum* L.), and cilantro (*Coriandrum sativum* L.) microgreens treated with various concentrations of selenium (Se) as sodium selenate on a fresh weight (FW) basis. Bars indicate mean ± standard deviation (SD) for three replicates ($n = 3$) of each plant species. The Tukey's significance at $P \leq 0.05$ among Se treatments is indicated by different letters within the plant species.

DISCUSSION

The results confirm the role of scallion as a Se accumulator and indicate hyperaccumulator status as shown by the Se content in levels higher than 1,000 μg/g DW (**Figure 1B**) and superior accumulation capacity (**Figure 2**). It is also noteworthy that despite requiring the least amount of Se treatment volume (2,835 mL), scallions accumulated the highest content of Se at 2.5 and 5.0 mg/L Se treatments compared with basil and cilantro, which required 2,965 and 3,825 mL of treatments, respectively.

Gupta and Gupta (2017) defined secondary accumulators as plant species that are capable of accumulating Se from 100 to 1,000 μg/g DW. Based on this definition, basil and cilantro

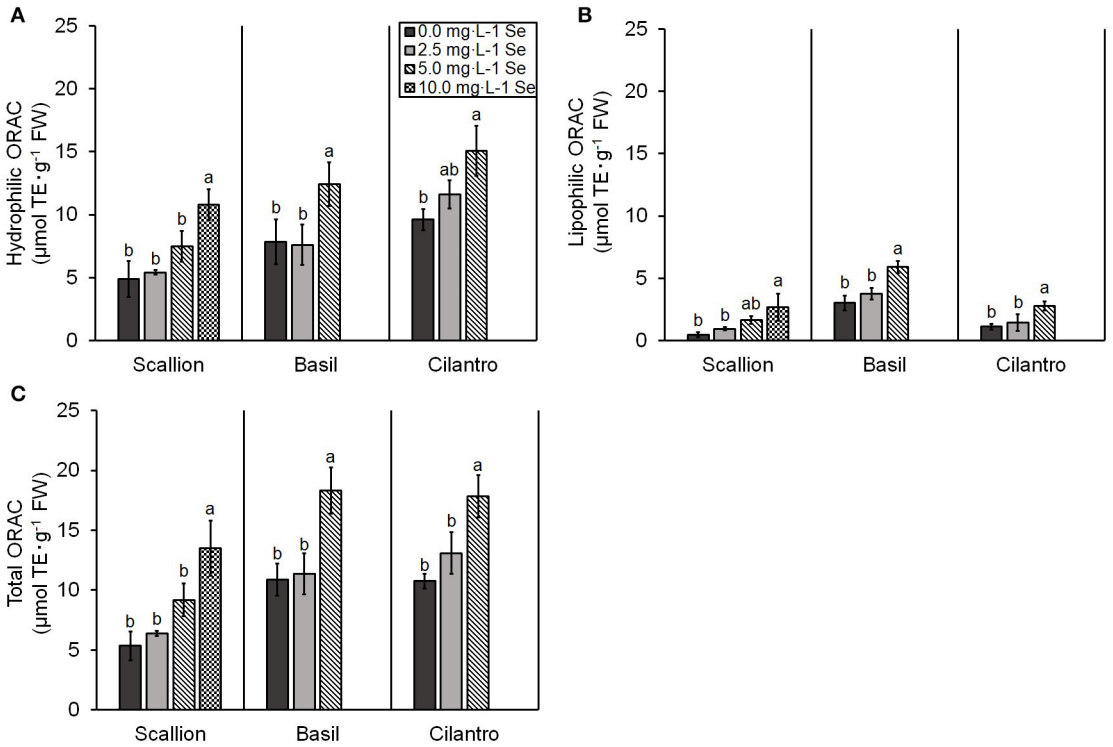


FIGURE 5 | (A) Hydrophilic, **(B)** lipophilic, and **(C)** total oxygen radical absorbance capacity (ORAC) values for scallion (*Allium fistulosum* L.), basil (*Ocimum basilicum* L.), and cilantro (*Coriandrum sativum* L.) microgreens treated with various concentrations of selenium (Se) as sodium selenate on a fresh weight (FW) basis. Bars indicate mean ± standard deviation (SD) for three replicates ($n = 3$) of each plant species. The Tukey's significance at $P \leq 0.05$ among Se treatments is indicated by different letters within the plant species.

can be classified into secondary Se accumulators, given the Se content demonstrated in this study (**Figure 1B**). The total Se uptake in basil plants was higher in the current study compared with the study by Puccinelli et al. (2019), which reported a maximum of 203 μg/g Se DW in basil microgreens grown from the seeds of Se-biofortified parent plants. Kopsell et al. (2009) assessed the Se content of a 32.0 mg/L Se foliar application to adult cilantro plants, yielding 9.3–49.5 μg/g Se DW in cilantro. These lower Se contents compared with those in our study support the efficiency of Se uptake under hydroponic conditions. Additionally, the high Se content of herbs in the current study may be a result of the addition of fresh nutrient solution every day, which provided a constant supply of Se to maximize the uptake in these young plants. Furthermore, the smaller biomass of microgreens may concentrate the Se content, as a "dilution effect" of minerals has been observed as basil plants mature and biomass increases (Puccinelli et al., 2017b). A study by Pannico et al. (2020), which used hydroponics in selenate biofortification of microgreens, demonstrated lower levels of Se content for green basil and cilantro (150.0 and 26.2 μg/g DW, respectively) than our study, likely due to the lower Se dose used (1.26 mg/L Se).

At high Se doses, growth stunting is a common symptom of Se toxicity in plants (Terry et al., 2000). In our study, the highest treatments of Se decreased the yield of both scallions and basil but did not affect cilantro (**Figure 3**). The similarity between Se and S can cause the substitution of S-amino acids with Se-amino acids in proteins and detrimental changes in the tertiary structure of the protein, resulting in Se toxicity in plants (Gupta and Gupta, 2017). The preferential uptake of selenate or sulfate varies among plant species (Terry et al., 2000), and in the present study, an increased S content was observed in scallions and basil but not in cilantro, which may account for the lack of effect on the yield of cilantro. A study on hydroponically grown lettuce shoots biofortified with selenate also demonstrated an increased S content at higher levels of Se application (Hawrylak-Nowak, 2013). This is significant for human nutrition since organic S can be used to increase synthesis of glutathione, the most abundant endogenous non-protein thiol, which has a protective role against free radical damage (Parcell, 2002).

The Dietary Guidelines for Americans (DGAs) recommend restricting Na consumption to <2,300 mg/day (U.S. Department of Agriculture and U.S. Department of Health Human Services, 2020), so the increased Na content of scallions and basil is not favorable. However, the highest amount of Na accumulation was 0.053 mg/g FW in scallions treated with 10.0 mg/L Se (**Table 1**). This translates to ∼1.0 mg of Na for 20 g of fresh scallion microgreens; thus, the amount of Na from fresh scallion

microgreens is negligible. Furthermore, the DGAs suggest the use of herbs and spices instead of salt as a strategy to lower Na intake (U.S. Department of Agriculture and U.S. Department of Health Human Services, 2020). An inadequate K intake can increase the risk for hypertension (Adrogué and Madias, 2014); thus, the increased K content of scallions and basil in this study is beneficial to human health. Previous studies on Se biofortification using microgreen basil and cilantro under hydroponic conditions have demonstrated an increase in K content on a DW basis compared with control plants (Pannico et al., 2020). Other studies using garlic reported a decrease in K content, while biofortification of onion did not demonstrate significant K changes (Põldma et al., 2011, 2013). However, the studies on garlic and onion involved mature plants instead of microgreens. The concentration of K is typically higher in young plant tissues because of the role of K in photosynthesis, respiration, and water homeostasis (Waterland et al., 2017).

Other major minerals of importance in human health are P, Ca, and Mg, which are essential components for bone formation and strength, with deficiencies contributing to the risk for osteoporosis (Bonjour et al., 2009). While P deficiencies in humans are rare due to its ubiquity in food, inadequate Ca intake may result from diets excluding dairy products, and Mg intake is often suboptimal due to its removal during processing of staple foods (Bonjour et al., 2009). Pannico et al. (2020) demonstrated increased P on a DW basis for green basil and cilantro microgreens biofortified with 0.63 and 1.26 mg/L Se as selenate. For cilantro, the lack of effect on P in our study may be a result of the different dosages used for this species between studies. Põldma et al. (2013) further reported a decreased Ca content in onions grown with a foliar spray of 10 and 50 mg/L Se as selenate and an increased Mg content at 50 mg/L Se. In the present study, the increases of P, Ca, and Mg in scallions are beneficial to human health. Overall, biofortification of fresh scallions resulted in enhancements of major minerals in human nutrition involved in fluid balance and bone health.

Trace elements also contribute to bone mineralization, but Cu, Fe, Mn, and Zn are more often studied as cofactors for antioxidant enzymes, such as superoxide dismutase and catalase (Soetan et al., 2010). Micronutrient deficiencies are a major public health concern, with Fe deficiency of specific interest, especially among women and children (Soetan et al., 2010). The enhanced content of Cu, Fe, Mn, and Zn demonstrated in scallion microgreens treated with 10.0 mg/L Se adds to the nutritional benefits of Se-biofortified scallions. Other Se biofortification studies that analyzed trace mineral contents have variable results due to differences in plant species, Se species, application technique, and dosage (He et al., 2004; Boldrin et al., 2013; Pannico et al., 2020). The increased content of B in scallions at 10.0 mg/L Se observed in the present study is also favorable for humans and plants. Boron has several roles in human health including steroid hormone metabolism, bone development, and cell membrane maintenance (Uluisik et al., 2018). In plant nutrition, B is essential for plant growth and phenolic metabolism (Uluisik et al., 2018). This is important since plants are a major source of phenolic compounds in the human diet.

A diet rich in phytochemicals is associated with lower incidence of chronic disease (Zhan et al., 2018). The accumulation of polyphenols in plants increases under stressful growing conditions, such as in the presence of excess Se in the soil (Kulbat, 2016; Saha et al., 2017). The increased TPC in Se-biofortified scallion, basil, and cilantro microgreens in the current study parallels the results of earlier studies in adult basil and onion and microgreen green basil and cilantro (Hawrylak-Nowak, 2008; Põldma et al., 2013; Pannico et al., 2020). Zheng and Wang (2001) reported the TPC of 2.23 mg GAE/g FW for basil, and Zhan et al. (2018) reported 0.20 mg GAE/g FW for scallions. These values are comparable with the control groups in our study (1.91 and 0.29 mg GAE/g FW for control basil and scallions, respectively). Henning et al. (2011) demonstrated the TPC of basil and cilantro at 8.70 and 6.10 mg GAE/g FW, respectively. In comparison, the TPC values were lower in our study for control basil and cilantro at 1.91 and 1.49 mg GAE/g FW, respectively. These lower values may be due to the difference in plant maturity. For instance, McCance et al. (2016) reported a decreased TPC in purple basil at earlier stages of harvest. TPC can also vary depending on the growing conditions and extraction techniques. Enhanced TPC adds to the nutritional benefits of biofortification with 5.0 mg/L Se in basil and cilantro and 10.0 mg/L Se in scallions. The TPC in scallions at 5.0 mg/L Se was not affected, which may be a result of the increased capacity of *Alliums* to resist Se toxicity.

The total antioxidant capacity of foods can be assessed by ORAC and provides a unique *in vitro* assessment of hydrophilic and lipophilic antioxidants, which considers the most common free radical in lipid oxidation *in vivo* (Shahidi and Zhong, 2015). Similar to the results in our study, Guardado-Felix et al. (2017) demonstrated an increase in ORAC for chickpea sprouts treated with increasing Se levels. In the current study, the highest Se treatment increased ORAC but decreased plant yield in scallions and basil. At high treatment doses, Se can act as a prooxidant in plants causing oxidative stress, which contributes to Se toxicity (Saha et al., 2017). To counteract the oxidative stress, plants increase antioxidant defenses (Gupta and Gupta, 2017). However, toxicity symptoms, such as decreased growth, can result if reactive oxygen species (ROS) overwhelms these antioxidant defenses. This may explain the increase in total ORAC occurring alongside a decreased yield for basil and scallions in our study. However, cilantro demonstrated increases in ORAC without decreased plant yield, suggesting antioxidant defenses of cilantro were adequate to quench ROS induced by Se.

CONCLUSION

Sodium selenate biofortification affected the content of dietary minerals, TPC, and total antioxidant capacity in the culinary herb microgreens studied. The Se content, TPC, and total antioxidant capacity increased at the highest Se dose for all herb species. Scallions accumulated the highest total Se, suggesting that scallion microgreens have the greatest potential as a functional food despite decreased crop yield at its highest dose. In populations with adequate Se consumption, increasing Se intake

using Se-rich dietary sources may be more beneficial than over-the-counter supplements which risk toxicity. A realistic serving size of 10 fresh scallion microgreens treated with 10.0 mg/L Se would supplement about 32 μg of Se to the diet. While scallions at 10.0 mg/L Se treatment may be unfavorable from the perspective of a grower due to the decreased crop yield, scallions offer a dietary supplement of Se with added benefits of increased TPC, antioxidant capacity, and content of other minerals important to human health. At the lower 5.0 mg/L Se treatment, scallion yield was not affected; however, other minerals and antioxidants were not increased. Basil and cilantro at 5.0 mg/L Se provided less Se but increased antioxidants. Se-biofortified basil offers the additional benefit of elevated S, K, and P contents, while the absence of decreased crop yield in cilantro can make cilantro preferable to growers. A serving size of 10 fresh microgreens of basil or cilantro at 5.0 mg/L Se would be approximately 19 and 15 μg of Se, respectively. These Se-biofortified herb microgreens can be added to meals for flavor while providing a simple method of enhancing dietary Se intake. Different Se dosages and application techniques impact plant yield and mineral and antioxidant contents of biofortified foods, requiring additional studies that consider a variety of biofortification techniques to generate optimal growing recommendations. The results of this study confirm that sodium selenate biofortification of culinary herb of culinary herb microgreens under hydroponic conditions can produce functional foods by increasing the Se content with additional benefits of enhanced dietary minerals and antioxidants.

DATA AVAILABILITY STATEMENT

The original contributions generated for the study are included in the article/Supplementary Material, further inquiries can be directed to the corresponding author/s.

AUTHOR CONTRIBUTIONS

RN, YM, JT, and NW conceived the project. RN carried out experiment, performed analyses, and wrote the original draft manuscript. CS performed the analysis of mineral contents. RN, YM, CS, JT, and NW assisted with study design and experiments. All authors read and contributed to earlier versions and approved the final version.

FUNDING

Salaries and research support were provided in part by state and federal funds appropriated to the West Virginia Agricultural and Forestry Experiment Station, West Virginia University, Scientific Article, No. 3407 of the West Virginia Agricultural and Forestry Experiment Station, Morgantown, WV.

ACKNOWLEDGMENTS

The authors would like to thank Dr. Ida Holásková for assistance with statistical analyses. This manuscript appeared in its initial version as a graduate thesis (Newman, 2019).

REFERENCES

Adrogué, H. J., and Madias, N. E. (2014). The impact of sodium and potassium on hypertension risk. *Semin. Nephrol.* 34, 257–272. doi: 10.1016/j.semnephrol.2014.04.003

Barickman, T. C., Kopsell, D. A., and Sams, C. E. (2012). Selenium influences glucosinolate and isothiocyanates and increases sulfur uptake in Arabidopsis thaliana and rapid-cycling Brassica oleracea. *J. Agric. Food Chem.* 61, 202–209. doi: 10.1021/jf,3037227

Boldrin, P. F., Faquin, V., Ramos, S. J., Boldrin, K. V. F., Ávila, F. W., and Guilherme L. R. G. (2013). Soil and foliar application of selenium in rice biofortification. *J. Food Compos. Anal.* 31, 238–244. doi: 10.1016/j.jfca.2013.06.002

Bonjour, J. P., Gueguen, L., Palacios, C., Shearer, M. J., and Weaver, C. M. (2009). Minerals and vitamins in bone health: the potential value of dietary enhancement. *Br. J. Nutr.* 101, 1581–1596. doi: 10.1017/S0007114509311721

Choe, U., Yu, L. L., and Wang, T. T. Y. (2018). The science behind microgreens as an exciting new food for the 21st century. *J. Agric. Food Chem.* 66, 11519–11530. doi: 10.1021/acs.jafc.8b03096

Guardado-Felix, D., Serna-Saldivar, S. O., Cuevas-Rodriguez, E. O., Jacobo-Velazquez, D. A., and Gutierrez-Uribe J. A. (2017). Effect of sodium selenite on isoflavonoid contents and antioxidant capacity of chickpea (*Cicer arietinum* L.) sprouts. *Food Chem.* 226, 69–74. doi: 10.1016/j.foodchem.2017.01.046

Gupta, M., and Gupta, S. (2017). An overview of selenium uptake, metabolism, and toxicity in plants. *Front. Plant. Sci.* 7, 2074. doi: 10.3389/fpls.2016.02074

Hawrylak-Nowak, B. (2008). Enhanced selenium content in sweet basil (*Ocimum basilicum*) by foliar fertilization. *Veg. Crop. Res. Bul.* 69, 63–72. doi: 10.2478/v10032-008-0021-4

Hawrylak-Nowak, B. (2013). Comparative effects of selenite and selenate on growth and selenium accumulation in lettuce plants under hydroponic conditions. *Plant. Growth Regul.* 70, 149–157. doi: 10.1007/s10725-013-9788-5

He, P. P., Lv, X. Z., and Wang, G. Y. (2004). Effects of Se and Zn supplementation on the antagonism against Pb and Cd in vegetables. *Environ. Int.* 30, 167–172. doi: 10.1016/S0160-4120(03)00167-3

Henning, S. M., Zhang, Y., Seeram, N. P., Lee, R. -P., Wang, P., Bowerman, S., et al. (2011). Antioxidant capacity and phytochemical content of herbs and spices in dry, fresh, and blended herb paste form. *Int. J. Food Sci. Nutr.* 62, 219–225. doi: 10.3109/09637486.2010.530595

Jones, G. D., Droz, B., Greve, P., Gottschalk, P., Poffet, D., McGrath, S. P., et al. (2017). Selenium deficiency risk predicted to increase under future climate change. *Proc. Natl. Acad. Sci. U. S. A.* 114, 2848–2853. doi: 10.1073/pnas.1611576114

Kopsell, D. A., Sams, C. E., Barickman, T. C., and Deyton, D. E. (2009). Selenization of basil and cilantro through foliar applications of selenate-selenium and selenite-selenium. *HortSci.* 44, 438–442. doi: 10.21273/HORTSCI.44.2.438

Kulbat, K. (2016). The role of phenolic compounds in plant resistance. *Biotech. Food Sci.* 80, 97–108.

Manero, J., Phillips, C., Ellison, B., Lee, S., Nickols-Richarson, S. M., and Chapman-Novakofski, K. M. (2017). Influence of seasoning on vegetable selection, liking and intent to purchase. *Appetite.* 116, 239–245. doi: 10.1016/j.appet.2017.04.035

McCance, K. R., Flanigan, P. M., Quick, M. M., and Niemeyer, E. D. (2016). Influence of plant maturity on anthocyanin concentrations, phenolic composition, and antioxidant properties of 3 purple basil (*Ocimum basilicum* L.) cultivars. *J. Food Compost. Anal.* 53, 30–39. doi: 10.1016/j.jfca.2016.08.009

Navarro-Alarcon, M., and Cabrera-Vique, C. (2008). Selenium in food and the human body: a review. *Sci. Total Environ.* 400, 115–41. doi: 10.1016/j.scitotenv.2008.06.024

Newman, R. G. (2019). *The Effect of Sodium Selenate Biofortification on Plant Yield, Mineral Content, and Antioxidant Capacity of Culinary Herb Microgreens*. Graduate Theses, Dissertations, and Problem Reports. 3870. Available online at: https://researchrepository.wvu.edu/etd/3870 (accessed April 10, 2021).

Nicolle, C., Carnat, A., Fraisse, D., Lamaison, J. –L., Rock, E., Michel, H., et al. (2004). Characterisation and variation of antioxidant micronutrients in lettuce (*Lactuca sativa* folium). *J. Sci. Food Agric.* 84, 2061–2069. doi: 10.1002/jsfa.1916

Ou, B., Chang, T., Huag, D., and Prior, R. L. (2013). Determination of total antioxidant capacity by oxygen radical absorbance capacity (ORAC) using fluorescein as the fluorescence probe: first action 2012.23. *J. AOAC Int*. 96, 1372–1376. doi: 10.5740/jaoacint.13-175

Pannico, A., El-Nakhel, C., Graziani, G., Kyriacou, M. C., Giordano, M., Soteriou, G. A., et al. (2020). Selenium biofortification impacts the nutritive value, polyphenolic content, and bioactive constitution of variable microgreens genotypes. *Antioxidants*. 9, 272. doi: 10.3390/antiox9040272

Parcell, S. W. (2002). Sulfur in human nutrition and applications in medicine. *Altern. Med. Rev.* 7, 22–44.

Põldma, P., Moor, U., Tõnutare, T., Herodes, K., and Rebane, R. (2013). Selenium treatment under field conditions affects mineral nutrition, yield, and antioxidant properties of bulb onion (*Allium cepa* L.). *Acta Sci. Pol. Hortorum. Cultus*. 12, 167–181.

Põldma, P., Tõnutare, T., Viitak, A., Luik, A., and Moor, U. (2011). Effect of selenium treatment on mineral nutrition, bulb size, and antioxidant properties of garlic (*Allium sativum* L.). *J. Agric. Food Chem.* 59, 5498–5503. doi: 10.1021/jf200226p

Puccinelli, M., Malorgio, F., and Pezzarossa, B. (2017a). Selenium enrichment of horticultural crops. *Molecules.* 22:933. doi: 10.3390/molecules22060933

Puccinelli, M., Malorgio, F., Rosellini, I., and Pezzarossa, B. (2017b). Uptake and partitioning of selenium in basil (*Ocimum basilicum* L.) plants grown in hydroponics. *Sci. Hortic*. 225, 271–276. doi: 10.1016/j.scienta.2017.07.014

Puccinelli, M., Malorgio, F., Rosellini, I., and Pezzarossa, B. (2019). Production of selenium-biofortified microgreens from selenium-enriched seeds of basil. *J. Sci. Food Agric.* 99, 5601–5605. doi: 10.1002/jsfa.9826

Saffaryazdi, A., Lahouti, M., Ganjeali, A., and Bayat, H. (2012). Impact of selenium supplementation on growth and selenium accumulation on spinach (Spinacia oleracea L.) plants. *Not. Sci. Biol.* 4, 95–100. doi: 10.15835/nsb448029

Saha, U., Fayiga, A., and Sonon, L. (2017). Selenium in the soil-plant environment: a review. *Int. J. Appl. Agric. Sci.* 3, 1–18. doi: 10.11648/j.ijaas.20170301.11

Shahidi, F., and Zhong, Y. (2015). Measurement of antioxidant activity. *J. Funct. Foods*. 18, 757–781. doi: 10.1016/j.jff.2015.01.047

Soetan, K. O., Olaiya, C. O., and Oyewole, O. E. (2010). The importance of mineral elements for humans and domestic animals and plants: a review. *Afr. J. Food Sci.* 4, 200–222. doi: 10.5897/AJFS.9000287

Terry, N., Zayed, A. M., de Souza, M. P., and Tarun, A. S. (2000). Selenium in higher plants. *Annu. Rev. Plant. Physiol. Plant. Mol. Biol.* 51, 401–432. doi: 10.1146/annurev.arplant.51.1.401

U.S. Department of Agriculture and U.S. Department of Health Human Services (2020). *Dietary Guidelines for Americans, 2020-2025, 9th Edn*. Available online at: DietaryGuidelines.gov (accessed April 15, 2021).

U.S. Environmental Protection Agency (1996). *Method 3052: Microwave Assisted Acid Digestion of Siliceous and Organically Based Matrices*. Washington, DC: U.S. EPA.

Uluisik, I., Karakaya, H. C., and Koc, A. (2018). The importance of boron in biological systems. *J. Trace. Elem. Med. Biol.* 45, 156–162. doi: 10.1016/j.jtemb.2017.10.008

Waterland, N. L., Moon, Y., Tou, J. C., Kim, M. J., Pena-Yewtukhiw, E. M., and Park, S. (2017). Mineral content differs among microgreen, baby leaf, and adult stages in three cultivars of kale. *HortScience.* 52, 566–571. doi: 10.21273/HORTSCI11499-16

Waterland, N. L., Moon, Y., Tou, J. C., Kopsell, D. A., Kim, M. J., and Park, S. (2019). Differences in leaf color and stage of development at harvest influenced phytochemical content in three cultivars of kale (*Brassica oleracea* L. and *B. napus*). *J. Agric. Sci.* 11, 14–21. doi: 10.5539/jas.v11n3p14

Zhan, L., Ma, Y., Zhang, C., Li, L., Pang, L., and Huang, X. (2018). Antioxidants and antioxidant capacity in leafy, stem, and fruit vegetables including 50 species. *J. Food Eng. Technol.* 7, 8–15. Available online at: https://www.xpublication.com/index.php/jfet/article/view/175

Zheng, W., and Wang, S. Y. (2001). Antioxidant activity and phenolic compounds in selected herbs. *J. Agric. Food Chem.* 49, 5165–5170. doi: 10.1021/jf010697n

Conflict of Interest: The authors declare that the research was conducted in the absence of any commercial or financial relationships that could be construed as a potential conflict of interest.

Publisher's Note: All claims expressed in this article are solely those of the authors and do not necessarily represent those of their affiliated organizations, or those of the publisher, the editors and the reviewers. Any product that may be evaluated in this article, or claim that may be made by its manufacturer, is not guaranteed or endorsed by the publisher.

Copyright © 2021 Newman, Moon, Sams, Tou and Waterland. This is an open-access article distributed under the terms of the Creative Commons Attribution License (CC BY). The use, distribution or reproduction in other forums is permitted, provided the original author(s) and the copyright owner(s) are credited and that the original publication in this journal is cited, in accordance with accepted academic practice. No use, distribution or reproduction is permitted which does not comply with these terms.

frontiers in Plant Science

ORIGINAL RESEARCH
published: 11 October 2021
doi: 10.3389/fpls.2021.744843

Migration of Chlorine in Plant–Soil–Leaching System and Its Effects on the Yield and Fruit Quality of Sweet Orange

*Xiaodong Liu[1,2], Chengxiao Hu[1,2], Zongying Zhu[1,2], Muhammad Riaz[3], Xiaoman Liu[1,2], Zhihao Dong[1,2], Yu Liu[1,2], Songwei Wu[1,2], Zhenhua Tan[4] and Qiling Tan[1,2]**

[1] Micro-Element Research Center/Hubei Provincial Engineering Laboratory for New Fertilizers, College of Resources and Environment, Huazhong Agricultural University, Wuhan, China, [2] Key Laboratory of Arable Land Conservation (Middle and Lower Reaches of Yangtze River), Ministry of Agriculture, Huazhong Agricultural University, Wuhan, China, [3] Root Biology Center, College of Natural Resources and Environment, South China Agricultural University, Guangzhou, China, [4] Xiangnan Navel Orange Comprehensive Test Station, Hunan, China

OPEN ACCESS

Edited by:
Spyridon Alexandros Petropoulos, University of Thessaly, Greece

Reviewed by:
Dirceu Mattos Jr., Instituto Agronômico de Campinas (IAC), Brazil
Ricardo A. Cabeza, University of Talca, Chile

***Correspondence:**
Qiling Tan
qltan@mail.hzau.edu.cn

Specialty section:
This article was submitted to Plant Nutrition, a section of the journal Frontiers in Plant Science

Received: 21 July 2021
Accepted: 03 September 2021
Published: 11 October 2021

Citation:
Liu X, Hu C, Zhu Z, Riaz M, Liu X, Dong Z, Liu Y, Wu S, Tan Z and Tan Q (2021) Migration of Chlorine in Plant–Soil–Leaching System and Its Effects on the Yield and Fruit Quality of Sweet Orange. Front. Plant Sci. 12:744843. doi: 10.3389/fpls.2021.744843

Chlorine (Cl) is indispensable for the growth of plants. While rarely systematic reports are available for the effect of Cl-containing fertilizers on citrus production. This study aimed to investigate the impacts of various Cl-containing fertilizers on the nutrients in the leaves, the yield and quality of sweet orange, and the Cl migration in the plant–soil–leaching system. A 5-year field experiment (2016–2020) with five Cl treatments (0, 75, 150, 450, and 900 kg ha^{-1}), and soil core lysimeter test with five Cl levels (0, 150, 225, 300, and 450 kg ha^{-1}) were carried out. The results showed that 77.0% of Cl leached into above 60 cm deeper soil layer, with calcium as the main accompanying ions, resulting in less Cl being absorbed by the citrus plants. The content of Cl in the leaves and soil was enhanced by the increasing input of Cl-containing fertilizer, without yearly increased characteristics, under a mean annual rainfall of 1,474 mm. Chlorine significantly increased the yield (13.24–37.8 9%), fruit weight, and vitamin C (Vc), in addition to enhancing the flavor and the juice yield of sweet orange via improving the absorption of N and K. Moreover, the long-term application of potassium sulfate has elevated the accumulation of sulfur in the soil and in leaves; it is becoming a potential risk factor for citrus production. Taken together, the application of Cl-containing fertilizer in sweet orange is feasible, and trace absorbance of Cl could improve the yield and fruit quality of sweet orange.

Keywords: chlorine-containing fertilizer, chlorine migration, leaf nutrients, citrus yield, fruit quality

HIGHLIGHTS

- About 77.0% of Cl leached into deep soil and was mainly accompanied by Ca^{2+}.
- Cl increased the yield, fruit weight, and Vc in sweet orange.
- Cl improved the flavor and juice yield of citrus *via* enhanced N and K content.
- Sulfur accumulated in the soil and leaves might be a risk factor for citrus production.

INTRODUCTION

Chlorine (Cl) is deemed as an essential micronutrient in plants and participates in a variety of physicochemical processes (Raven, 2017; Colmenero et al., 2019). The Cl requirement is relatively low and is usually met by air, rainfall, soil, and potassium fertilizer (Wang et al., 2020). The content of Cl in most plants is observed in the range of 2–20 g kg^{-1} (Broadley et al., 2012; Colmenero et al., 2019). Chloride primarily accumulates in the vacuoles, reaching concentrations of up to 150 mM, and can serve as a permeable substance to drive water flow (Geilfus, 2018b). Furthermore, the accumulation of Cl could improve the utilization of nitrogen (N) by decreasing the compartmentalization of nitrate ($N\text{-}NO_3$) in the vacuole and promoting its assimilation. In the previous study, it was observed that the utilization of N increased by 0–22% in citrus and olive, and increased by 60–80% in tomato and tobacco when aided by Cl (Rosales et al., 2020).

Chlorine also appears as a toxic element for some specific plants, such as citrus, tobacco, and grapevine, which are defined as Cl sensitive crops (Xu et al., 1999). Long-term use of river water with a salt level of 2.5 dS m^{-1} for irrigation caused the soil salinity to increase linearly;, the citrus yield reduced by 17%, and the trunk-diameter growth slowed down 59% yearly (Prior et al., 2007). The adverse environment and the mismanagement (e.g., saline soils, lower rainfall, excessive fertilizer, and irrigation of saline water) mean it is easy to cause Cl poisoning and stunt plant growth. Farmers have historically failed to define the safe dose of Cl-containing fertilizer for this Cl-sensitive crop. Therefore, citrus production in China has always been based on the use of potassium sulfate (K_2SO_4) as K fertilizer, instead of potassium chloride (KCl). The long-term application of K_2SO_4 has witnessed the sharp rise in soil sulfate (SO_4^{2-}) (Szynkiewicz et al., 2011), leading to strong acidification of the environment and the leaching of SO_4^{2-} resulting in an excess of SO_4^{2-} in the soil (Tabak et al., 2020). Consistently, previous research has increased concerns that further input of sulfur could increase the risk of methylmercury (MeHg) production (a bio-accumulative neurotoxicant), which may enhance the dietary MeHg exposure (Lei et al., 2021). Additionally, excessive sulfur (S) greatly increased the accumulation of cadmium in roots, resulting in a diminished rice yield (Fan et al., 2010). The reckless pursuit of yield leads to the problem of excessive fertilization in most of the citrus-producing areas in China (Liu et al., 2021). Thus, the long-term application of K_2SO_4 caused the increasing S content in the leaves and soil of 'Guanximiyou' pomelo orchards, which exacerbated the acidification of soil and the leaching of calcium (Ca) and Mg (magnesium). Therefore, it is essential to reduce the K_2SO_4 application in production (Lin et al., 2020).

Citrus, an indispensable economic crop, accounts for one-quarter of the total fruit yield in the world (Qi and Qi, 2016), and it is mainly planted in acid soil. At present, excessive application of N, phosphorus (P), and K fertilizer leads to increasingly serious acidification of soil in citrus orchards, which inhibits nitrification and promotes N loss (Quaggio et al., 2014). Soil acidification enhancement has releases other cations (e.g., Ca, K, Mg, Al, Fe), and led to vast amounts of SO_4^{2-} absorbed into soil (Souza et al., 2006), which may advance Cl leaching. The problem of planting citrus in acid soil has become increasingly prominent. It is quite necessary to conduct deep-reaching research and comprehensive analyses of cation and anion movement in acid soil. Therefore, acid soil was selected for this study aiming to investigate the migration characteristics of Cl in plant-soil-leachate and analyze the application potential of Cl-containing fertilizer with the employment of the soil core lysimeter experiments (1); and to identify the effect of Cl on the nutrient content in the leaf and the fruit quality of sweet orange (2).

MATERIALS AND METHODS

Experimental Materials and Design

The field experiment was conducted during 2016–2020 on 7-year-old trees of Newhall sweet orange [*C. sinensis (L.) Osbeck*] grafted onto trifoliate orange [*Poncirus trifoliata (L.) Osbeck*] rootstock. The experimental location was at the experimental orchard of the institute of Xiangnan navel orange comprehensive test station, Yizhang, Chenzhou city, Hunan province, China, which is a semi-humid climate. The annual precipitation was 1,850, 1,238, 1,236, 1,742, and 1,309 mm in 2016, 2017, 2018, 2019, and 2020, respectively. Acid red soil (pH = 4.46) was selected in the experiment and the basic properties were assessed (soil organic matter: 28.79 g kg^{-1}, available N: 81.71 mg kg^{-1}, available P: 74.08 mg kg^{-1}, available K: 241.96 mg kg^{-1}, and Cl: 10.6 mg kg^{-1}). The fertilizer was applied evenly on both sides of trees (on the ditch near the drip line, with a length of 100 cm and a depth of 30 cm). In March, the basic fertilization was applied at 60% of the total fertilization amount, and the remaining 40% was applied as a topdressing in June. Annual application rates of N were 375 kg ha^{-1} as urea, 225 kg ha^{-1} P_2O_5 as triple superphosphate, and 225 kg ha^{-1} K_2O as K_2SO_4 or KCl. Considering that excessive potassium would result in stem blight and the decreased citrus yield (Mattos et al., 2003; Quaggio et al., 2011), the additional amount of Cl was provided by $CaCl_2$ after KCl application had been completed. There were five levels of Cl in the field experiment, including 0 kg ha^{-1}, K_2O was provided by K_2SO_4 (100% K_2SO_4); 75 kg ha^{-1}, replacing 50% of the amount of K_2O in K_2SO_4 with KCl (50% K_2SO_4+ 50% KCl); 150 kg ha^{-1}, where K_2O was all supplied by KCl (100% KCl); 450 kg ha^{-1}, K_2O again completely from KCl and extra Cl was supplied by calcium chloride ($CaCl_2$, 300 kg Cl ha^{-1}, Cl content is twice that of KCl); and 900 kg ha^{-1}, K_2O again all from KCl with extra Cl supplied by $CaCl_2$ (750 kg Cl ha^{-1}, Cl content was 5 times that of KCl). The sites were composed of 3 rows with 22 trees of each, and trees were spaced at 4.0 m × 3.0 m (750 trees ha^{-1}). During the experimental periods, all the evaluations were carried out on 20 central trees, and the treatments were distributed by completely random block design and were replicated three times with four trees of each.

In order to explore the effect of Cl-containing fertilizer on the ion leaching in leachate, a soil core lysimeter experiment was performed to solve the difficult aquisition of leachate. Considering the size of the soil core lysimeter, the 3-year-old Newhall sweet orange [*C. sinensis (L.) Osbeck*] grafted on trifoliate orange [*Poncirus trifoliata (L.) Osbeck*] was selected for

this experiment, which was conducted at Huazhong Agricultural University, Wuhan, China. Therefore, the rate of fertilization has been reduced appropriately. Fertilizer was applied at the total fertilization amount in a circular ditch (30 cm deep and 10 cm wide) near the edge of the lysimeter wall on June 15, 2020. The application rates of N of one season (about 3 months) were 375 kg ha^{-1} as urea, 225 kg ha^{-1} P_2O_5 as triple superphosphate, and K_2O 225 kg ha^{-1} as K_2SO_4 or KCl. There were five levels of Cl set up in the soil core lysimeter: 0 kg ha^{-1}, K_2O was from K_2SO_4 (100% K_2SO_4); 150 kg ha^{-1}, K_2O was all from KCl (100% KCl); 225 kg ha^{-1}, K_2O was all from KCl, supplimented with $CaCl_2$ (75 kg Cl ha^{-1}, Cl content was half of KCl); 300 kg ha^{-1}, K_2O was KCl and supplimented with $CaCl_2$ (150 kg Cl ha^{-1}, Cl content was equal to that of KCl) for extra Cl; 450 kg ha^{-1}, K_2O was from KCl and supplimented with CaCl2 (300 kg Cl ha^{-1}, Cl content was 2 times that of KCl) for extra Cl. The sites were composed of 2 rows with 15 trees of each, and trees were spaced at an area of 0.3 m^2 in a soil column (15,000 trees ha^{-1}). The treatments were distributed by a completely random block design and were replicated three times with two trees of each. The bulk density of the acid yellow-brown soil (pH = 4.60) was 1.275 g cm^{-3}.

The collection of undisturbed soil monolith lysimeters was performed following the rules previously laid out by Cameron et al. (1992) and Zhao et al. (2010). The vertical structure of the design lysimeter used for the large soil core is shown in **Supplementary Figure S1**. Every lysimeter case consisted of a PVC cylinder (600 mm in internal diameter, 630 mm in external diameter, and 700 mm high). A PVC disk (640 mm in internal diameter, 660 mm in external diameter, and 50 mm thick) was used as the base. Three layers of nylon mesh (diameter 0.074 mm) and acid quartz sand (diameter 0.8 mm, depth of 20 mm) were placed on the base disc to filtrate the leaching water. This gravel filter layer was located at the bottom of the lysimeter to ensure an undisturbed water flow.

Sample Preparation

Eight fruits and twelve leaves were randomly collected from the east, south, west, and north of the tree in mid-November every year of the field experiment. Four collected samples were mixed as one repetition. The collected samples were successively washed by a 0.1% aqueous solution of neutral detergent, 0.2% nitric acid solution, and deionized water for 30 s, respectively. The fruits were separated into pulp and peel, and then evenly into two parts after weighing. One part of the peel was used to measure the thickness, and the pulp was juiced and filtered. The filtrate was used for the assessment of total soluble solids (TSS), titratable acidity (TA) concentrations, the TSS/TA ratio, and the concentration of vitamin C (Vc). The leaf and a part of the peel and pulp samples were dried at 105°C in an oven for 30 min to inactivate enzymes, followed by drying at 60°C. Subsequently, the dried samples were smashed and passed through the 60-mesh sieves.

In the field experiment, soil samples were collected in mid-November every year. Three random soil collection points (near the drip line of the selected trees) were chosen per tree at depths of 0–20 cm, 20–40 cm, 40–60 cm. The samples were collected in the vertical direction of each soil extraction point of the selected trees. All the sampling tools were made of stainless steel to avoid any possible contamination. To prevent rain and dust, soil samples from all four trees were mixed and 1 kg of soil was taken to a clean indoor ventilation hood for air drying. After that, soil samples were ground and passed through the 20- and 100-mesh sieves.

The 30 L polyethylene container was used to collect the leachate in the lysimeter. When leachate samples reached a volume of 30 L, 200 ml of leachate samples were collected in polyethylene bottles and stored at 4°C until analysis. The first to eighth samples were collected on June 26, June 30, July 4, July 6, July 11, July 20, August 13, and September 10, respectively.

Analysis of Fruit Quality

The analysis of fruit quality was based on the test method of citrus fresh fruit (GB/T8210-2011, China). Briefly, the fruit weight (FW) was weighed by an electronic balance with an accuracy of 0.01 g. The percentage yield of the juice (JY) was calculated from the volume of the obtained juice. The peel thickness (PT) was measured with a vernier caliper. The titratable acidity (TA) was measured by the standard base titration, and the digital sugar meter (ATAGO PAL-BX/ACID1) was used to analyze the total soluble solids (TSS). The TSS/TA ratio (TSA) is a ratio between the total soluble solids and the titratable acidity. Finally, the content of vitamin C (Vc) was analyzed by the 2, 6-dichlorophenol titration method (Ruck, 1963).

Analysis of the Content of Nutrients in the Plant, Soil, and Leachate Sample

Plant analysis: Analyzed for the content of N, P, K, Ca, Mg, S, Cl according to the methods described by Bao (2000).

Soil analysis: The content of Cl was determined using an automatic potentiometric titrator (ZDJ-3D, China) by silver ion-titration. The content of soil avail-S in phosphate-acetic acid extraction was analyzed by ICP-OES (5110VDV, USA).

Leaching: The concentration of Cl was determined using the silver ion-titration method on an automatic potentiometric titrator (ZDJ-3D, China). A flame photometer (AP1200, China) was used for the determination of K concentration. The concentration of Ca and Mg in the samples digested with HNO_3-$HClO_4$ was determined by the atomic absorption spectrophotometry (Z2000, HITACHI, Japan). UV-Spectrophotometric was used for the determination of N-NO_3 (UV-5200, China). The evaluation of SO_4^{2-} was conducted with the Barium Sulfate Turbidimetry (UV-5200, China).

Chlorine Leaching Factor Calculations

$$\text{Cl leaching factor } (\text{ClLF, \%}) = \frac{(C_T - C_{CK}) * V_1 * 15000}{Cl_r} \times 100\%$$

where C_T and C_{CK} (mg L^{-1}) are the concentrations of chlorine in Cl treated and 0 Cl plots, respectively, V_l (L) represents the volume of leached water, 15,000 is a conversion coefficient representing the planting density in soil core lysimeter experiment, and Cl_r is the amount of Cl applied rate (kg ha^{-1}).

Statistical Analysis

Analysis of variance (ANOVA) and single-factor analyses used Duncan multiple comparisons ($p < 0.05$) with the SPSS 22.0 software. The fruit quality index was plotted with TBtools. The relationship between Cl application rate and the yield of sweet orange was quantified by one-way regression analysis using Origin 2021 software. The correlations matrix ($p < 0.05$) between leaf nutrients and fruit quality was calculated and plotted by R software.

RESULTS

Effects of Cl on Sweet Orange Yield

Chlorine-containing fertilizer and their application rates significantly affected the yield of sweet orange during the growing years with an average increase of 13.2–37.9% compared with 0 kg ha^{-1} (**Figure 1**, $p < 0.05$). Among these, the 450 kg ha^{-1} treatment showed the highest yield every year (21.46 t ha^{-1} for 2017, 9.68 t ha^{-1} for 2018, 17.23 t ha^{-1} for 2019, and 14.94 t ha^{-1} for 2020, respectively). The mean maximum yield with the Cl application rates was 485 kg ha^{-1} (**Figure 1**).

Effects of Cl on Sweet Orange Fruit Quality

The Cl-containing fertilizer improved fruit quality, specifically by increasing FW, JY, TSS, TSA, Vc, and PT. Meanwhile, Cl-containing fertilizer also significantly elevated the TSS and PT in 2018, Vc in 2016 and 2017, JY in 2016, and FW in 2017 and 2020 (**Figure 2**; **Supplementary Table S1**, $p < 0.05$). The JY and FW were significantly associated with the treatments, the TA, TSA, and PT were significantly related to growth years (**Supplementary Table S1**, $p < 0.05$), and the TSS was not only significantly related to years' change but also to treatment, while Vc was related neither to treatment nor years' change (**Supplementary Table S1**, $p < 0.05$).

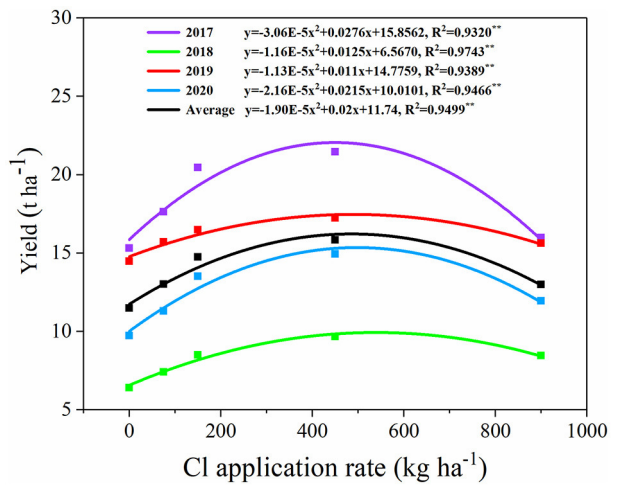


FIGURE 1 | Regressions between annual Cl application rate and yield of sweet orange in the field experiment for 2017–2020.

The Content of Cl in the Leaf, Pulp, and Peel

In the field experiment, the Cl-containing fertilizer significantly increased the content of Cl in the plants (**Figure 3**, $p < 0.05$). However, the leaf Cl content did not increase along with the year of application. There was a low content of Cl in the plant during 2016 and 2019, which appeared to result from the higher rainfall (1,849.5 and 1,742.1 mm) and the lower content of Cl in the soil. The highest Cl accumulation was observed in the treatment of 900 mg Cl ha^{-1} with the value of 1,205 mg kg^{-1} in the leaves (**Figure 3A**), 1,113 mg Cl ha^{-1} in the peel (**Figure 3B**), and 1,027 mg Cl ha^{-1} in the pulp (**Figure 3C**). The content of Cl was ranked as leaf > peel > pulp and leaf Cl was 16.62% higher than peel and was 28.88% higher than pulp (**Figure 3**).

Nutrient Content in the Leaves

The Cl-containing fertilizer had a significant effect on the content of N, K, Ca, and S in the leaves ($p < 0.05$), but no significant effect on the content of P and Mg was noted. The content of N, K, Ca, and S in the leaves were not only significantly related to years' change, but also with the Cl input rate (**Table 1**). The content of N and K in the leaves significantly increased with the Cl input rate. The content of Ca in the treatment with KCl (150 kg Cl ha^{-1}) was significantly lower than that in the treatment with K_2SO_4 (0 kg Cl ha^{-1}), but extra Cl supplied by $CaCl_2$, such as in the 450 kg Cl ha^{-1} and 900 kg Cl ha^{-1} treatments, could increase the content of Ca in the leaves (**Table 1**, $p < 0.05$). Furthermore, the average of S content was higher by 116.9 and 29.4% by application of 100% K_2SO_4 (0 kg Cl ha^{-1}) and 50% K_2SO_4 (75 kg Cl ha^{-1}) respectively, compared with no S-containing fertilizer treatment (the 150, 450, and 900 kg Cl ha^{-1} treatments), meanwhile, the annual average growth rate in the leaves was 30.6 and 18.5%.

Correlations Between Fruit Quality and Mineral Nutrients in the Leaves

The FW had significantly positive correlations with the content of P, Ca, and Cl in the leaves, but negative correlations with the content of N and S (**Figure 4**, $p < 0.05$). There were dramatically positive correlations was found between the TA and the Ca and S in the leaves, but negative correlations with N, P, and K ($p < 0.05$). The TSS only had significantly positive correlations with N and showed negative correlations with P, K, and Mg ($p < 0.05$). The content of Ca and S was found to be negatively correlated with the TSA, which was positively correlated with N ($p < 0.05$). The Vc possessed significantly positive correlations with Cl content and negative correlations with S in the leaves ($p < 0.05$). Similarly, there were remarkable positive correlations between JY and P, K, Mg, and Cl content in the leaves, but negative correlations with S ($p < 0.05$). The PT was prominently negatively correlated with S in the leaves (**Figure 3**; $p < 0.05$). Interestingly, the content of N and K had significantly positive correlations with Cl in the leaves, but negative correlations with the content of S in the leaves.

The Content of Cl and Avail-S in Soil

The Cl-containing and S-containing fertilizer significantly increased the content of Cl and avail-S in the soil (**Figure 5**, $p < 0.05$). The content of Cl in the soil (0–60 cm) increased

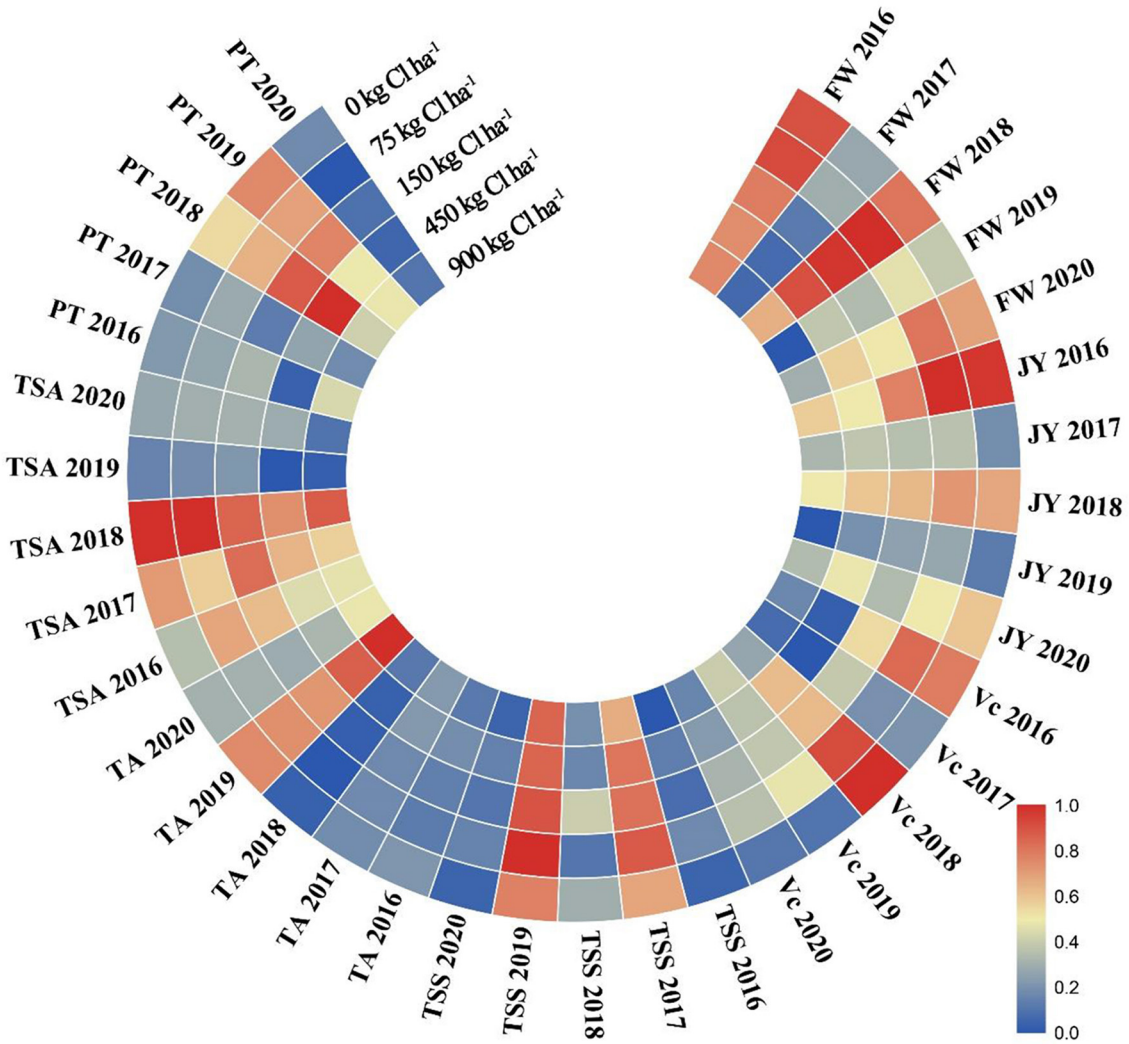


FIGURE 2 | Effects of Cl-containing fertilizer on fruit weight (FW), juice yield (JY), Vc, TSS, TA, TSS/TA (TSA), and peel thickness (PT) of fruit quality in 5-year field experiment from 2016 to 2020. Bars are means of three replicates ± SD. Different letters (a, b, c) in each sub-figure represent significant differences at ($P < 0.05$). The data corresponding to this figure is shown in **Supplementary Table S1**.

significantly as soil depth increased. Specifically, the Cl content in the 40–60 cm soil layer was 21.15 and 14.77% higher than that in the 0–20 and 20–40 cm soil layers, respectively (except for the 0 kg Cl ha^{-1} treatment). Similarly, the content of avail-S in the 40–60 cm soil layer was 65.1 and 24.3% higher than the 0–20 and 20–40 cm layers, respectively with the application of S-containing fertilizer. It can be seen that the content of Cl in the soil in each treatment did not increase with the year of Cl-containing fertilizer, whereas the content of soil avail-S with 2020 had 16.6, 33.3, and 51.7% higher than 2016 in 0–20, 20–40, and 40–60 cm soil layer (except for 150, 450, and 900 kg Cl ha^{-1}). Interestingly, the Cl accumulation in soil may have been affected by rainfall as the content of Cl in the soil was low in 2016 and 2019, which were 2 years with high rainfall (1,849.5 and 1,742.1 mm, respectively). Simultaneously, the dynamic changes in the content of Cl at the 0–60 cm soil layer during 2016–2018 were analyzed (**Supplementary Figure S2**). The variation of soil Cl content showed inverted U-shaped curves. The soil Cl content was ranked as September > December > June, with September being 34.15 and 12.98% higher than June and December, respectively (except 0 kg Cl ha^{-1}).

Anions and Cations in the Leachate

There were a total of eight leaching events during the soil core lysimeter experiment (**Figure 6**). The leachate with Cl-containing fertilizer had 3–11 folds more of average chloride concentrations than non-chlorine treatment, and the average Cl leaching factor was 77.0% in the soil core lysimeter experiment (**Figure 6A**). The concentration of SO_4^{2-} in leachate increased remarkably by use of the K_2SO_4 fertilizer, but no effect was observed in the treatments

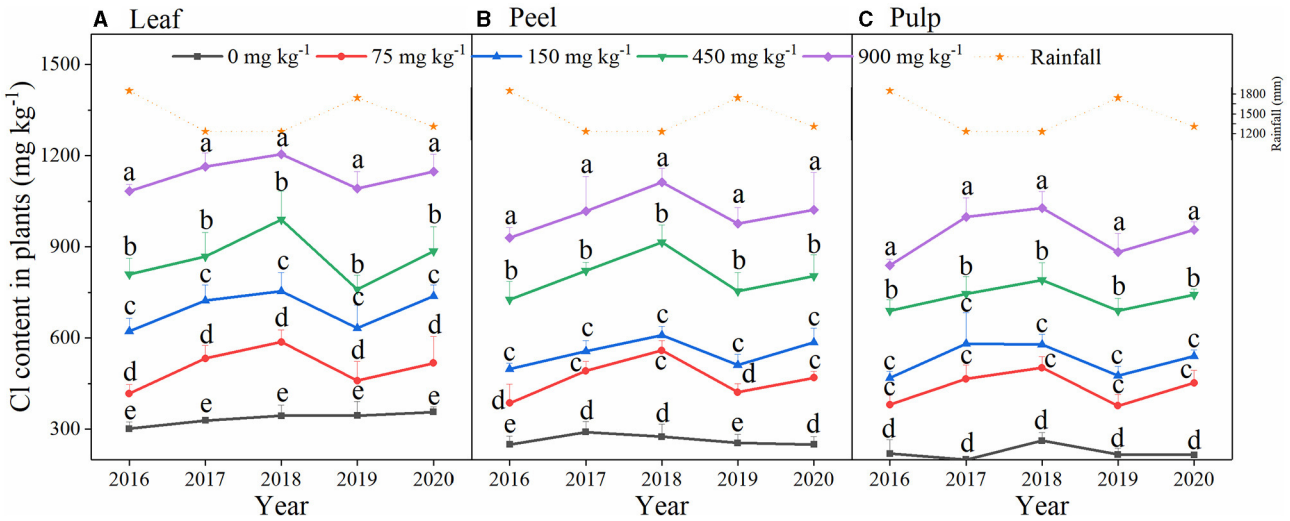


FIGURE 3 | The content of chloride in leaf **(A)**, peel **(B)**, pulp **(C)** in a five-year field experiment from 2016 to 2020. Bars are means of three replicates ± SD. Different letters (a, b, c, d, e) in each sub-figure represent significant differences at ($P < 0.05$).

of Cl (**Figure 6B**). Furthermore, the concentration of N-NO_3 and K^+ treated with K_2SO_4 was higher than in the KCl treatment, the highest content was observed in the treatment of 450 kg Cl ha^{-1}. The Ca^{2+} concentration increased with the Cl application rate, but Mg^{2+} concentration reduced.

DISCUSSION

Application of Cl-Containing Fertilizer on Citrus Is Feasible Under the Premise of Rainfall Higher Than Evaporation

In field trials, we can only observe the dynamic changes of the Cl content in the soil, it is difficult to obtain the soil leaching solution. The soil core lysimeter solved the difficult collection of leachates and can better evaluate the pattern of ion migration (Derby et al., 2002; Di and Cameron, 2005; Zhao et al., 2010).

Chlorine mainly exists in the soil in the form of chloride and was usually considered as a tracer to measure soil water movement (Geilfus, 2018a). When the rainfall exceeds the evaporation, there is a downward movement of Cl. However, the rainfall may lead to the opposite trend of Cl, namely upward movement, resulting in an increasing content of Cl in the soil. Water fluxes are the key factors of Cl migration in soil (Havlin et al., 1985). In our research, despite the Cl content in soil being increased remarkably by Cl-containing fertilizer and soil depth (0–60 cm), the Cl content in soil did not increase with years of consecutive application over 5 years of such application with an average rainfall 1,475 mm in the field experiment (**Figure 5A**). The high rainfall resulted in the rapid dissolution of Cl-containing fertilizer, accompanied by diffusion and leaching. These processes mainly occur in the rainy season from March to August. Within a year, the Cl dissolution rate was higher than the leaching rate during the period from June to September, while the opposite result was observed from September to December, which helps explain the reason for the highest soil Cl content in September (**Supplementary Figure S2**). As explained above, Cl-containing fertilizer underwent a dissolution-diffusion-leaching process in the soil. Similarly, the fact that the ion concentration first rose and then decreased in leachate further supports this process (**Figure 6**). The content of Cl in the soil is affected by rainfall and evaporation (Burns, 1974). Herein, the further research result revealed that the Cl leaching factor reached 77.0% in the soil core lysimeter experiment (**Figure 6A**). In most southern areas of the Yangtze River, the annual rainfall is over 1,000 mm, and the accumulation of Cl in the soil is generally <10%, which is consistent with our research (Mao et al., 2001), illustrating that chloride is easy to migrate since it is not easily adsorbed by soil.

The kinetics of ions is associated with the charge balance in the soil, which in turn depends on the process of ion exchange, nutrient loss caused by soil leaching, and acidification (Souza et al., 2006). The release of K^+, Ca^{2+}, and Mg^{2+}, etc cations increased, and leached loss more easily in acid soil (Quaggio, 2000) with Cl, N-NO_3, and S as the main accompanying anions (Li et al., 2015). The result suggested that the concentration of Cl, N-NO_3, Ca^{2+}, and S were much higher than K^+ and Mg^{2+} concentrations in the leachate (**Figure 6**). The Cl and Ca^{2+} concentration of the leachate conspicuously increased after the application of Cl-containing fertilizer, indicating the contribution rate of Ca^{2+} is greater than K^+ and Mg^{2+}, etc cations in Cl leaching processes.

In general, soil avail-S mainly exist as SO_4^{2-} in the soil, and the different cation migration may result from the low solubility of $CaSO_4$ resulting in the slow migration of SO_4^{2-} h in the soil compared to Cl. Iron and aluminum oxides had a strong

TABLE 1 | Data and statistical analysis of leaf nutrient content in 2016–2020.

Year	Cl rate kg ha^{-1}	N	P	K	Ca	Mg	S
				g kg^{-1}			
2016	0	28.3 ± 1.6b	1.7 ± 0.1a	19.3 ± 1.7a	38.5 ± 3.2a	3.1 ± 0.2a	2.6 ± 0.2a
	75	31.6 ± 1.6a	1.8 ± 0.1a	19.8 ± 0.9a	38.1 ± 3.4a	3.0 ± 0.2a	2.2 ± 0.1a
	150	30.4 ± 0.4ab	1.8 ± 0.1a	20.5 ± 0.7a	33.8 ± 4.9a	2.7 ± 0.1a	2.2 ± 0.2a
	450	29.3 ± 1.5ab	1.8 ± 0.1a	20.2 ± 1.1a	38.5 ± 2.5a	3.0 ± 0.4a	2.1 ± 0.3a
	900	31.07 ± 0.6a	1.8 ± 0.1a	20.6 ± 0.8a	40.3 ± 4.3a	3.2 ± 0.4a	2.2 ± 0.5a
2017	0	27.0 ± 1.0b	1.5 ± 0.0ab	23.2 ± 2.6a	29.2 ± 3.7ab	2.3 ± 0.3a	3.4 ± 0.1a
	75	28.3 ± 0.4ab	1.4 ± 0.1b	24.6 ± 2.9a	27.3 ± 1.1b	2.2 ± 0.1a	2.4 ± 0.1b
	150	27.3 ± 1.2b	1.4 ± 0.0bc	27.1 ± 0.5a	26.8 ± 1.4b	2.0 ± 0.4a	2.2 ± 0.1b
	450	29.2 ± 0.3a	1.5 ± 0.0ab	25.5 ± 3.8a	31.4 ± 3.0ab	2.1 ± 0.4a	2.1 ± 0.1b
	900	27.7 ± 0.6ab	1.5 ± 0.1a	28.3 ± 2.3a	34.0 ± 3.4a	2.3 ± 0.4a	2.2 ± 0.1b
2018	0	23.9 ± 1.0c	1.4 ± 0.1a	17.5 ± 0.9b	34.0 ± 0.4ab	2.1 ± 0.1a	4.8 ± 0.8a
	75	26.4 ± 0.6ab	1.5 ± 0.1a	19.8 ± 1.3a	33.4 ± 2.4ab	2.1 ± 0.3a	2.4 ± 03b
	150	25.5 ± 1.1bc	1.5 ± 0.1a	19.6 ± 0.2a	29.8 ± 2.6b	1.9 ± 0.3a	1.8 ± 0.2b
	450	25.8 ± 0.7bc	1.5 ± 0.1a	19.3 ± 1.0a	33.6 ± 1.9ab	2.1 ± 0.2a	2.0 ± 0.5b
	900	28.1 ± 1.8a	1.4 ± 0.2a	19.6 ± 0.8a	35.0 ± 3.7a	1.9 ± 0.2a	1.7 ± 0.3b
2019	0	24.1 ± 1.4b	1.5 ± 0.2a	18.0 ± 0.4b	37.2 ± 3.3a	2.0 ± 0.1a	5.8 ± 0.6a
	75	25.6 ± 1.0ab	1.4 ± 0.1a	18.9 ± 0.8ab	36.9 ± 5.2a	2.1 ± 0.4a	3.0 ± 0.3b
	150	27.0 ± 1.0a	1.4 ± 0.1a	18.5 ± 1.0ab	35.4 ± 4.0a	2.0 ± 0.3a	2.5 ± 0.1b
	450	25.6 ± 0.8ab	1.4 ± 0.1a	19.5 ± 0.8a	37.8 ± 5.1a	1.9 ± 0.2a	2.2 ± 0.2b
	900	26.9 ± 1.5a	1.4 ± 0.1a	19.6 ± 0.7a	39.6 ± 4.2a	1.9 ± 0.1a	2.2 ± 0.2b
2020	0	26.4 ± 0.8b	1.4 ± 0.1a	18.4 ± 0.8b	34.9 ± 0.2a	2.0 ± 0.4a	7.4 ± 0.5a
	75	30.0 ± 0.6ab	1.4 ± 0.1a	18.8 ± 0.8ab	34.0 ± 0.8ab	2.0 ± 0.6a	4.2 ± 0.1b
	150	30.4 ± 3.6ab	1.4 ± 0.1a	19.7 ± 0.4ab	30.97 ± 3.1b	1.9 ± 0.1a	2.9 ± 0.3c
	450	30.0 ± 1.2ab	1.4 ± 0.1a	20.1 ± 0.2a	34.0 ± 0.9ab	1.9 ± 0.1a	2.5 ± 0.3c
	900	31.6 ± 4.0a	1.4 ± 0.1a	19.3 ± 1.2ab	35.5 ± 2.0a	1.9 ± 0.2a	2.4 ± 0.1c
F test	Rate (R)	8.7***	0.4^{ns}	4.8**	5.3***	1.2^{ns}	174.4***
	Year (Y)	26.0***	53.3***	55.4***	16.2***	36.1***	62.1***
	R*Y	1.0^{ns}	1.3^{ns}	0.8^{ns}	0.3^{ns}	0.4^{ns}	17.1***

*Values are means of three replicates. Values represent means ± SE (n = 3). *p < 0.05, **p < 0.01, and ***p < 0.001. Different letters in each sub-figure represent significant differences at (P < 0.05).*

absorption capacity for SO_4^{2-} in soil, and this absorption capacity was further enhanced in acid soil (Bolan et al., 2003). In the current study, the content of soil avail-S was enhanced yearly by the long-term application of K_2SO_4 (**Figure 5B**). And the concentration of Ca^{2+} in the K_2SO_4 treatment was lower than that of the KCl treatment in leachate (**Figure 6E**). Likewise, about 24.6% of S was adsorbed by soil and reached the maximum at 45–60 cm soil layer, after consecutive application of S-containing fertilizer over 6 years (Saha et al., 2001). Furthermore, Cowling et al. (1992) reported that the reoxidation of metal sulfides will produce hydrogen ions, which would induce soil acidification. Gradually, the long-term application of S-containing fertilizer will cause avail-S to accumulate in soil and lead to more severe soil acidification.

The soil is considered not only one of the important sources of plant nutrition, but also the main reservoir and a source of Cl, which directly affects the uptake of Cl by plants. This 5-year field experiment showed the relatively stable content of Cl in the leaves, peel, and pulp over the 5 years, while S content was scaling up. The Cl content in the leaves of olives and mandarin, which have been using saline irrigation water for a long time, have also not increased continuously, which is consistent with the present results (Melgar et al., 2009; Nicolás et al., 2016). The reasons may be due to (i) Cl is used as the nutritient for plant growth; (ii) a part of Cl was taken away by the fruit; (iii) since most of the Cl is being leached to a deeper soil layer, that reduced the amount of Cl uptake by citrus. Conversely, the content of S in the leaves increased yearly by the application of S-containing fertilizer during 2016–2020, which may be the result of the continuous accumulation of soil avail-S therefore promoting the absorption by citrus (**Table 1**). Excessive S application could improve the availability of heavy metals in soil, meanwhile, promoting the absorption and accumulation of metal sulfide by plants (Zakari et al., 2021), implying that the difference in adsorption capacity of Cl and S by soil resulted in the divergent accumulation of Cl and S in the leaves.

To sum up, in acidic soil, metal cations are released more easily causing more Cl leaching, in which calcium is the main accompanying ion. Therefore, only a small amount of chlorine is absorbed by citrus. However, sulfate will form complexes

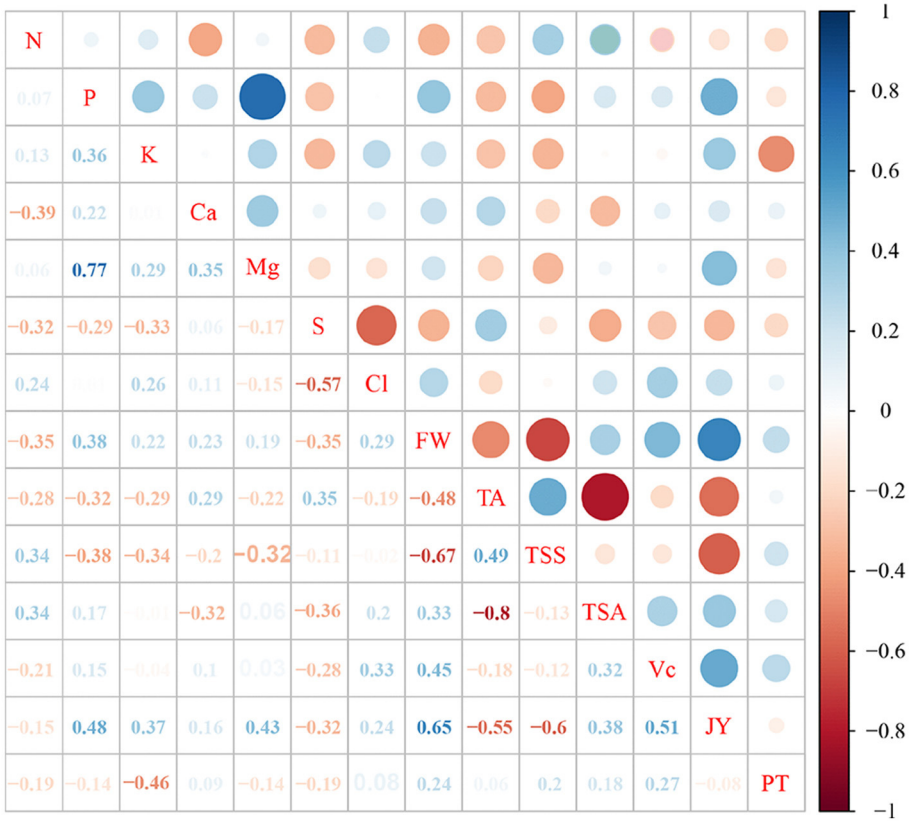


FIGURE 4 | Correlation analyses of leaf mineral nutrients and fruit quality. N, P, K, Ca, Mg, S, and Cl represent the content of N, P, K, Ca, Mg, S, and Cl in the levaes; FW, fruit weight; TA, titratable acid; TSS, total soluble solid; TSA, TSS/TA; Vc, vitamin C; JY, juice yield; PT, peel thickness.

with metal cations (e.g., Ca, Fe, Al, etc.) and cause deposition in the soil and lead to the increase of S absorption by citrus, and produce hydrogen ions resulting in serious acidification of the soil.

Appropriate Application of Cl-Containing Fertilizer Improved Citrus Yield and Fruit Quality

The initiative uptake of Cl by plants was far more than 200–400 mg kg^{-1}. A remarkable improvement of growth and biomass was observed when Cl existing in plants was higher than micronutrient levels (Chen et al., 2010; Franco-Navarro et al., 2016). Through the determination of leaf samples from 670 species of terrestrial plants belonging to 138 families, it was shown that the highest Cl content is about 0.5% (Watanabe et al., 2007; Colmenero et al., 2019). In the present study, the Cl content in the leaves ranging from 335 to 1,138 mg kg^{-1} showed no symptoms of Cl stress and harvested the highest yield at the 485 kg Cl ha^{-1} input rate. The long-term application of KCl increased the yield of sweet orange and lemon in Brazil (Quaggio et al., 2002, 2006, 2011), which is consistent with our conclusion that Cl improved the photosynthetic activity, leaf cell division rates, water use efficiency, and biomass promoting the growth of citrus (Brumos et al., 2010; Franco-Navarro et al., 2019). Meanwhile, the accumulation of Cl subsided the N-NO_3 accumulation efficiency in plants, thereby improving nitrogen use efficiency (Rosales et al., 2020), similar results were obtained in PO_4^{3-} and SO_4^{2-} (Franco-Navarro et al., 2016). Collectively, the Cl content in plants is at a level equivalent to the macronutrient level (302–1,205 mg Cl kg^{-1}) can promote the growth of citrus and improve its yield.

It is still unclear whether the beneficial effect on plants is a result of the direct effect of chloride or the effect of concomitant ions (Flowers, 1988). Despite the fact that the application of Cl-containing fertilizer had no significant effect on fruit quality during 2016–2020, the application of Cl-containing fertilizer did nonetheless cause a slight improvement in fruit quality (**Figure 2**). The correlation between leaf mineral nutrition and fruit quality analysis showed that leaf Cl is positively correlated with the FW, Vc, and JY of sweet orange. Appropriate Cl input conspicuously increased the FW whereas N input rate showed a negative effect on the FW (Quaggio et al., 2002), which agrees with our research. Improving the absorption of Cl extremely increased Vc in the fruit of strawberry (Xu et al., 1999). The JY content of sweet orange increased with the KCl input rate (Quaggio et al., 2011), revealing that Cl improved fruit quality based on enhancing the FW, Vc, and JY of citrus.

Widely, N and K are the important elements for citrus yield and fruit quality (Quaggio et al., 2002). Here, it was found that

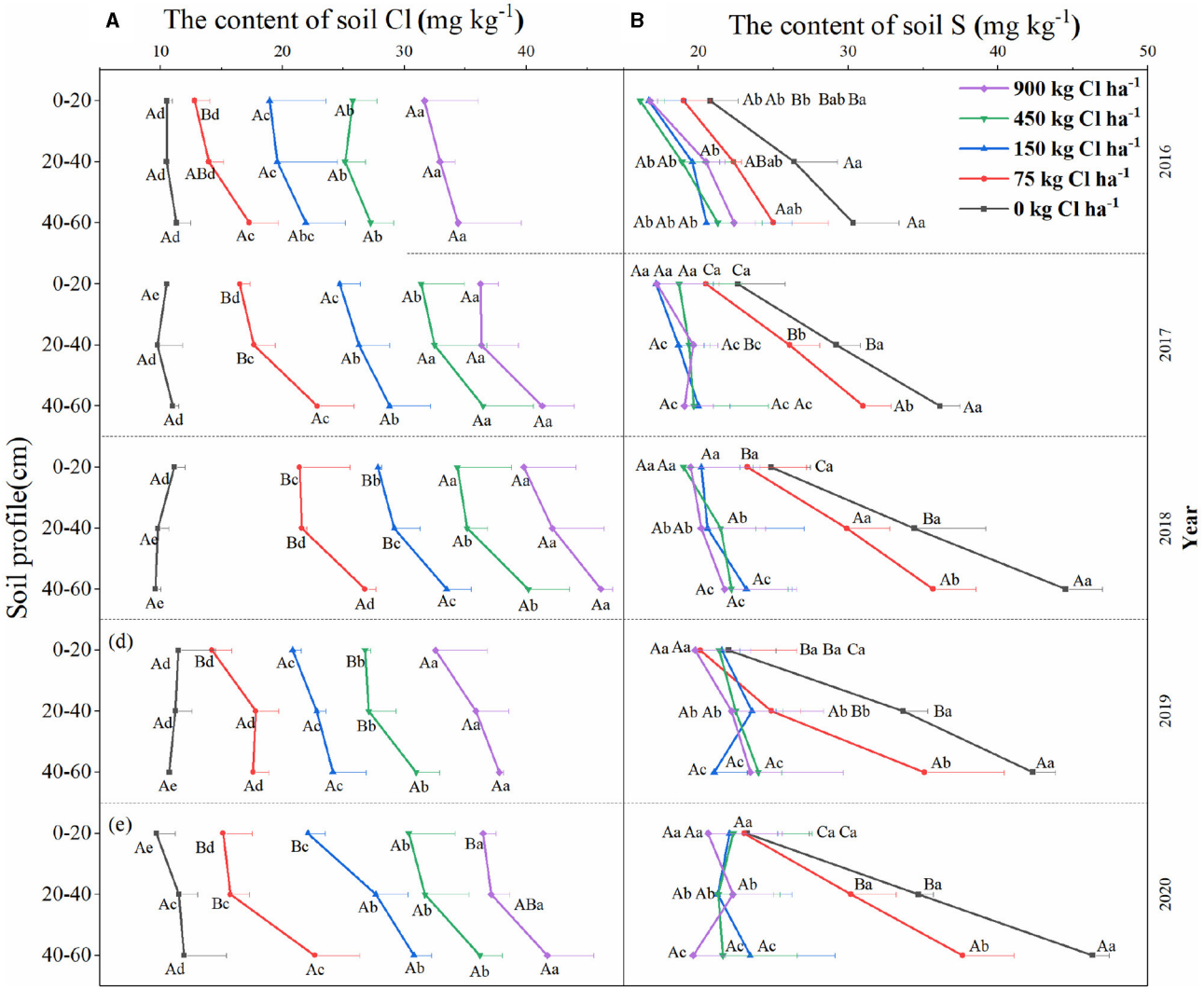


FIGURE 5 | The content of Cl **(A)** and S **(B)** changes in 0–60 cm soil layer in a 5-year field experiment from 2016 to 2020. Bars are means of three replicates ± SD. The different lowercase letters (a, b, c, d, e) indicate significant differences between the Cl treatment at ($P < 0.05$). The different uppercase letters (A, B, C) indicate significant differences between the soil layer at ($P < 0.05$).

Cl content in the leaves is positively correlated with the contents of N and K (**Figure 4**). The content of N and K is greatly higher under the KCl treatment in comparison to the K_2SO_4 treatment (**Table 1**). Chlorine has the tendency of increasing K content in the leaves of citrus seedlings (Xu et al., 1999). Meanwhile, previous reports showed that Cl had no significant effect on the content of N in the leaves, in turn, Cl has decreased N-NO_3 accumulation in the vacuole, promote its assimilation, which improves the utilization of N and plant growth (Rosales et al., 2020). The leaf N content was positively correlated with TSS, while it was passively correlated with TA. He et al. (2003) reported the same correlation between leaf N and TA, TSS in grapefruit, confirming that N reduced TA and increased TSS to improve the citrus flavor. Furthermore, the content of K in the leaves was noticeably positively correlated with JY. The JY content has significantly increased by application of K fertilizer to improve leaf K content in Kinnow (Ashraf et al., 2010), indicating that K improved the internal fruit quality. Therefore, supplying Cl increased the leaf N and K content, which has improved the citrus flavor and JY.

CONCLUSION

The present results showed that Cl experienced a process of dissolution-diffusion-leaching in the soil after the application of Cl-containing fertilizer. Even though the content of Cl in soil elevated with Cl input rate, it did not increase yearly in a 5-year field experiment. Little Cl uptake by citrus and no year-on-year increase might be a result of the leaching of the majority Cl to the deeper soil layers. Simultaneously, Ca^{2+} is the accompanying cation of Cl during its leaching. Chlorine enhanced the yield

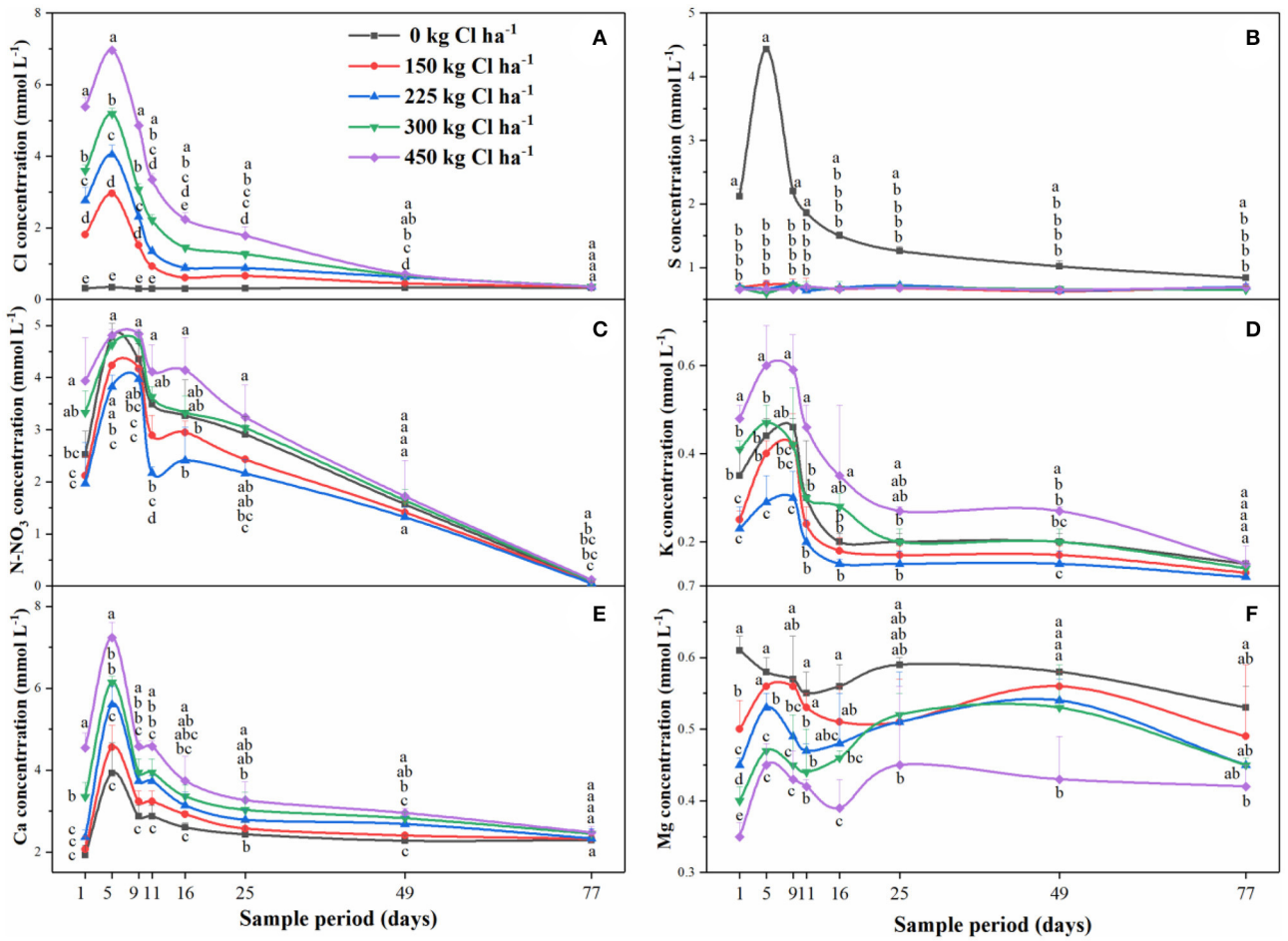


FIGURE 6 | The concentration of Cl **(A)**, S **(B)**, N-NO_3 **(C)**, K **(D)**, Ca **(E)**, and Mg **(F)** dynamics changes in leachate by application of Cl-containing fertilizers on sweet orange. Bars are means of three replicates ± SD. Different letters (a, b, c, d, e) in each sub-figure represent significant differences at ($P < 0.05$).

and FW of sweet orange, and, improved the flavor and JY by promoting the absorption of N and K in the leaves. Furthermore, the content of S in soil and leaf has increased year after year from the long-term application of K_2SO_4 due to SO_4^- being easily complexed with metal cations, resulting in accumulation and accelerated soil acidification that may be adverse for citrus production. Therefore, it was recommended that the application of Cl-containing fertilizer could improve citrus yield and fruit quality, and avoid the risk of excessive S in citrus production.

DATA AVAILABILITY STATEMENT

The original contributions presented in the study are included in the article/**Supplementary Material**, further inquiries can be directed to the corresponding author.

AUTHOR CONTRIBUTIONS

QT and XDL designed and supervised this study. XDL conducted the experiments, performed data interpretation, and drafted the manuscript. ZZ and ZT helped in interpreting the results of the study. YL, XML, and ZD helped in the experiment and determining nutrition concentration. CH, SW, and MR helped to revise the manuscript grammatically. All authors read and approved the final manuscript.

FUNDING

This work was supported by the National Key Research and Development Program of China (2019YFD1001400), the Modern Citrus Industry Technology System of China (CARS-26), and the National Key Research and Development Program of China (2019YFD1000103).

SUPPLEMENTARY MATERIAL

The Supplementary Material for this article can be found online at: https://www.frontiersin.org/articles/10.3389/fpls.2021.744843/full#supplementary-material

REFERENCES

Ashraf, M. Y., Gul, A., Ashraf, M., Hussain, F., and Ebert, G. (2010). Improvement in yield and quality of kinnow (*Citrus deliciosa* × *Citrus nobilis*) by potassium fertilization. *J. Plant Nutr.* 33, 1625–1637. doi: 10.1080/01904167.2010.496887

Bao, S. D. (2000). *Soil and Agricultural Chemistry Analysis*. Beijing: China Agriculture Press, 355–356.

Bolan, N. S., Adriano, D. C., and Curtin, D. (2003). "Soil acidification and liming interactions with nutrient and heavy metal transformation and bioavailability," in *Advances in Agronomy*. (New York, NY: Academic Press), 215–272. doi: 10.1016/S0065-2113(02)78006-1

Broadley, M., Brown, P., Cakmak, I., Rengel, Z., and Zhao, F. (2012). "Chapter 7—Function of Nutrients: Micronutrients," in *Marschner's Mineral Nutrition of Higher Plants 3 edn,* ed P. Marschner (San Diego: Academic Press), 191–248. doi: 10.1016/B978-0-12-384905-2.00007-8

Brumos, J., Talon, M., Bouhlal, R., and Colmenero-Flores, J. M. (2010). Cl-homeostasis in includer and excluder citrus rootstocks: transport mechanisms and identification of candidate genes. *Plant Cell Environ.* 33, 2012–2027. doi: 10.1111/j.1365-3040.2010.02202.x

Burns, I. G. (1974). A model for predicting the redistribution of salts applied to fallow soils after excess rainfall or evaporation. *J. Soil Sci.* 25, 165–178. doi: 10.1111/j.1365-2389.1974.tb01113.x

Cameron, K. C., Smith, N. P., McLay, C. D. A., Fraser, P. M., McPherson, R. J., Harrison, D. F., et al. (1992). Lysimeters without edge flow: an improved design and sampling procedure. *Soil Sci. Soc. Am. J.* 56, 1625–1628. doi: 10.2136/sssaj1992.03615995005600050048x

Chen, W., He, Z. L., Yang, X. E., Mishra, S., and Stoffella, P. J. (2010). Chlorine nutrition of higher plants: progress and perspectives. *J. Plant Nutr.* 33, 943–952. doi: 10.1080/01904160903242417

Colmenero, J., Franco-Navarro, J. D., Cubero-Font, P., Peinado-Torrubia, P., and Rosales, M. (2019). Chloride as a beneficial macronutrient in higher plants: new roles and regulation. *Int. J. Mol. Sci.* 20, 4686. doi: 10.3390/ijms20194686

Cowling, S. J., Gardner, M. J., and Hunt, D. T. E. (1992). Removal of heavy metals from sewage by sulphide precipitation: thermodynamic calculations and tests on a pilot-scale anaerobic reactor. *Environ. Technol.* 13, 281–291. doi: 10.1080/09593339209385155

Derby, N. E., Knighton, R. E., and Montgomery, B. R. (2002). Construction and performance of large soil core lysimeters. *Soil Sci. Soc. Am. J.* 66, 1446–1453. doi: 10.2136/sssaj2002.1446

Di, H. J., and Cameron, K. C. (2005). Reducing environmental impacts of agriculture by using a fine particle suspension nitrification inhibitor to decrease nitrate leaching from grazed pastures. *Agr. Ecosyst. Environ.* 109, 202–212. doi: 10.1016/j.agee.2005.03.006

Fan, J.-L., Hu, Z.-Y., Ziadi, N., Xia, X., and Wu, C.-Y.-H. (2010). Excessive sulfur supply reduces cadmium accumulation in brown rice (*Oryza sativa* L.). *Environ. Pollut.* 158, 409–415. doi: 10.1016/j.envpol.2009.08.042

Flowers, T. (1988). Chloride as a nutrient and as an osmoticum. *Adv. Plant Nutr.* 3, 55–78.

Franco-Navarro, J. D., Brumos, J., Rosales, M. A., Cubero-Font, P., Talon, M., and Colmenero-Flores, J. M. (2016). Chloride regulates leaf cell size and water relations in tobacco plants. *J. Exp. Bot.* 67, 873–891. doi: 10.1093/jxb/erv502

Franco-Navarro, J. D., Rosales, M. A., Cubero-Font, P., Calvo, P., Alvarez, R., Diaz-Espejo, A., et al. (2019). Chloride as a macronutrient increases water-use efficiency by anatomically driven reduced stomatal conductance and increased mesophyll diffusion to CO_2. *Plant J.* 99, 815–831. doi: 10.1111/tpj.14423

Geilfus, C. M. (2018a). Chloride: from nutrient to toxicant. *Plant Cell Physiol.* 59, 877–886. doi: 10.1093/pcp/pcy071

Geilfus, C. M. (2018b). Review on the significance of chlorine for crop yield and quality. *Plant Sci.* 270, 114–122. doi: 10.1016/j.plantsci.2018.02.014

Havlin, J., Beaton, J. D., Tisdale, S. L., and Nelson, W. L. (1985). *Soil Fertility and Fertilizers. An Introduction to Nutrient Management.* Bengaluru: Pearson Education India

He, Z. L., Calvert, D. V., Alva, A. K., Banks, D. J., and Li, Y. C. (2003). Thresholds of leaf nitrogen for optimum fruit production and quality in grapefruit. *Soil Sci. Soc. Am. J.* 67, 583–588. doi: 10.2136/sssaj2003.5830

Lei, P., Tang, C., Wang, Y., Wu, M., Kwong, R. W. M., Jiang, T., et al. (2021). Understanding the effects of sulfur input on mercury methylation in rice paddy soils. *Sci. Total Environ.* 778 :146325. doi: 10.1016/j.scitotenv.2021.146325

Li, J.-Y., Liu, Z.-D., Zhao, W.-Z., Masud, M. M., and Xu, R.-K. (2015). Alkaline slag is more effective than phosphogypsum in the amelioration of subsoil acidity in an Ultisol profile. *Soil Till. Res.* 149, 21–32. doi: 10.1016/j.still.2014.12.017

Lin, W. J., Li, X. B., Lin, F., Zhuang, M. L., Zhu, D. H., Guo, J. X., et al. (2020). Sulfur nutrition status in trees and soils of'Guanximiyou'pomelo orchards. *J. Fruit Sci.* 37, 848–856. doi: 10.13925/j.cnki.gsxb.20190606

Liu, X., Liu, X., Liu, W., Tan, Q., Hu, C., and Li, J. (2021). Nutritional status of different citrus trees and the recommended dosages of N, P and K for citrus production in China. *J. Plant Nutr.* 27, 565–574. doi: 10.11674/zwyf.20457

Mao, Z. G., Li, J. K., He, G. A., and Di, T. L. (2001). "Chapter 1-Chlorine nutrition in plants," in *Chlorine-Containing Fertilizer in China* (Wuhan: China Agriculture Press), 57–105.

Mattos, D. Jr., Quaggio, J. A., Cantarella, H., and Alva, A. K. (2003). Nutrient content of biomass components of Hamlin sweet orange trees. *Sci. Agric.* 60, 155–160. doi: 10.1590/s0103-90162003000100023

Melgar, J. C., Mohamed, Y., Serrano, N., Garcia-Galavis, P. A., Navarro, C., Parra, M. A., et al. (2009). Long term responses of olive trees to salinity. *Agric. Water Manage.* 96, 1105–1113. doi: 10.1016/j.agwat.2009.02.009

Nicolás, E., Alarcón, J. J., Mounzer, O., Pedrero, F., Nortes, P. A., Alcobendas, R., et al. (2016). Long-term physiological and agronomic responses of mandarin trees to irrigation with saline reclaimed water. *Agric. Water Manage.* 166, 1–8. doi: 10.1016/j.agwat.2015.11.017

Prior, L. D., Grieve, A. M., Bevington, K. B., and Slavich, P. G. (2007). Long-term effects of saline irrigation water on Valencia orange trees: relationships between growth and yield, and salt levels in soil and leaves. *Aust. J. Agric. Res.* 58, 349–358. doi: 10.1071/AR06199

Qi, L., and Qi, C. J. A. O. (2016). Status quo and development trend of world's citrus industry. *Agric. Oulook* 12, 46–52. doi: 10.3969/j.issn.1673-3908.2016.12.010

Quaggio, J. A. (2000). *Acidez e calagem em solos tropicais.* Londrina: Instituto Agronômico.

Quaggio, J. A., Mattos, D., and Boaretto, R. M. (2011). Sources and rates of potassium for sweet orange production. *Sci. Agric.* 68, 369–375. doi: 10.1590/S0103-90162011000300015

Quaggio, J. A., Mattos, D., and Cantarella, H. (2006). Fruit yield and quality of sweet oranges affected by nitrogen, phosphorus and potassium fertilization in tropical soils. *Fruits* 61, 293–302. doi: 10.1051/fruits:2006028

Quaggio, J. A., Mattos, D., Cantarella, H., Almeida, E. L. E., and Cardoso, S. A. B. (2002). Lemon yield and fruit quality affected by NPK fertilization. *Sci. Horticult.* 96, 151–162. doi: 10.1016/S0304-4238(02)00121-8

Quaggio, J. A., Souza, T. R., Bachiega Zambrosi, F. C., Marcelli Boaretto, R., and Mattos, D. Jr. (2014). Nitrogen-fertilizer forms affect the nitrogen-use efficiency in fertigated citrus groves. *J. Plant Nutr. Soil Sci.* 177, 404–411. doi: 10.1002/jpln.201300315

Raven, J. A. (2017). Chloride: essential micronutrient and multifunctional beneficial ion. *J. Exp. Bot.* 68, 359–367. doi: 10.1093/jxb/erw421

Rosales, M. A., Franco-Navarro, J. D., Peinado-Torrubia, P., Diaz-Rueda, P., Alvarez, R., and Colmenero-Flores, J. M. (2020). Chloride improves nitrate utilization and nue in plants. *Front. Plant Sci.* 11:13. doi: 10.3389/fpls.2020.00442

Ruck, J. A. (1963). *Chemical Methods for Analysis of Fruit and Vegetable Products*. Ottawa: Canada Department of Agriculture (No. 1154).

Saha, J. K., Singh, A. B., Ganeshamurthy, A. N., Kundu, S., and Biswas, A. K. (2001). Sulfur accumulation in Vertisols due to continuous gypsum application for six years and its effect on yield and biochemical constituents of soybean (*Glycine max* L. Merrill). *J. Plant Nutr. Soil Sci.* 164, 317–320. doi: 10.1002/1522-2624(200106)164:3<317::AID-JPLN317>3.0.CO;2-C

Souza, T. R. D., Quaggio, J. A., and Silva, G. O. (2006). Dinâmica de íons e acidificação do solo nos sistemas de fertirrigação e adubação sólida na citricultura. *Rev. Bras. Fruticult.* 28, 501–505. doi: 10.1590/S0100-29452006000300035

Szynkiewicz, A., Witcher, J. C., Modelska, M., Borrok, D. M., and Pratt, L. M. (2011). Anthropogenic sulfate loads in the Rio Grande, New Mexico (USA). *Chem. Geol.* 283, 194–209. doi: 10.1016/j.chemgeo.2011.01.017

Tabak, M., Lisowska, A., and Filipek-Mazur, B. (2020). Bioavailability of sulfur from waste obtained during biogas desulfurization and the effect of sulfur on soil acidity and biological activity. *Processes* 8, 17. doi: 10.3390/pr807 0863

Wang, L., Xu, J. Y., Jia, W., Chen, Z., and Xu, Z. C. (2020). Chloride salinity in a chloride-sensitive plant: Focusing on photosynthesis, hormone synthesis and transduction in tobacco. *Plant Physiol. Biochem.* 153, 119–130. doi: 10.1016/j.plaphy.2020.05.021

Watanabe, T., Broadley, M. R., Jansen, S., White, P. J., Takada, J., Satake, K., et al. (2007). Evolutionary control of leaf element composition in plants. *New Phytol.* 174, 516–523. doi: 10.1111/j.1469-8137.2007. 02078.x

Xu, G., Magen, H., Tarchitzky, J., and Kafkafi, U. (1999). Advances in chloride nutrition of plants. *Adv. Agron.* 68, 97–150. doi: 10.1016/S0065-2113(08)60844-5

Zakari, S., Jiang, X., Zhu, X., Liu, W., Allakonon, M. G. B., Singh, A. K., et al. (2021). Influence of sulfur amendments on heavy metals phytoextraction from agricultural contaminated soils: a meta-analysis. *Environ. Pollut.* 288, 117820. doi: 10.1016/j.envpol.2021.117820

Zhao, C., Hu, C., Huang, W., Sun, X., Tan, Q., and Di, H. J. (2010). Design, construction and installation of large soil core lysimeters. *Trans. Chin. Soc. Agric. Eng.* 26, 48–53. doilink[10.3969/j.issn.1002-6819.2010.02.009]10.3969/j.issn.1002-6819.2010.02.009

Conflict of Interest: The authors declare that the research was conducted in the absence of any commercial or financial relationships that could be construed as a potential conflict of interest.

Publisher's Note: All claims expressed in this article are solely those of the authors and do not necessarily represent those of their affiliated organizations, or those of the publisher, the editors and the reviewers. Any product that may be evaluated in this article, or claim that may be made by its manufacturer, is not guaranteed or endorsed by the publisher.

Copyright © 2021 Liu, Hu, Zhu, Riaz, Liu, Dong, Liu, Wu, Tan and Tan. This is an open-access article distributed under the terms of the Creative Commons Attribution License (CC BY). The use, distribution or reproduction in other forums is permitted, provided the original author(s) and the copyright owner(s) are credited and that the original publication in this journal is cited, in accordance with accepted academic practice. No use, distribution or reproduction is permitted which does not comply with these terms.

frontiers in Plant Science

ORIGINAL RESEARCH
published: 29 October 2021
doi: 10.3389/fpls.2021.736614

Variability in Physiological Traits Reveals Boron Toxicity Tolerance in Aegilops Species

Mohd. Kamran Khan[1†], Anamika Pandey[1†], Mehmet Hamurcu[1], Zuhal Zeynep Avsaroglu[1], Merve Ozbek[1], Ayse Humeyra Omay[1], Fevzi Elbasan[1], Makbule Rumeysa Omay[1], Fatma Gokmen[1], Ali Topal[2] and Sait Gezgin[1]*

[1] Department of Soil Science and Plant Nutrition, Faculty of Agriculture, Selcuk University, Konya, Turkey, [2] Department of Field Crops, Faculty of Agriculture, Selcuk University, Konya, Turkey

OPEN ACCESS

Edited by:
Antonios Chrysargyris, Cyprus University of Technology, Cyprus

Reviewed by:
Nikolaos Nikoloudakis, Cyprus University of Technology, Cyprus
Shailender Kumar Verma, Central University of Himachal Pradesh, India

***Correspondence:**
Anamika Pandey
anamika.biotech@gmail.com; anamika@selcuk.edu.tr

[†] These authors have contributed equally to this work

Specialty section:
This article was submitted to Plant Nutrition, a section of the journal Frontiers in Plant Science

Received: *05 July 2021*
Accepted: *30 September 2021*
Published: *29 October 2021*

Citation:
Khan MK, Pandey A, Hamurcu M, Avsaroglu ZZ, Ozbek M, Omay AH, Elbasan F, Omay MR, Gokmen F, Topal A and Gezgin S (2021) Variability in Physiological Traits Reveals Boron Toxicity Tolerance in Aegilops Species. Front. Plant Sci. 12:736614. doi: 10.3389/fpls.2021.736614

Boron (B) is an important micronutrient required for the normal growth and development of plants. However, its excess in the soil causes severe damage to plant tissues, which affects the final yield. Wheat, one of the main staple crops, has been reported to be largely affected by B toxicity stress in arid and semi-arid regions of the world. The prevalence of B toxicity stress can be addressed by utilizing wild wheat genotypes with a variant level of stress tolerance. Wild wheat relatives have been identified as a prominent source of several abiotic stress-tolerant genes. However, Aegilops species in the tertiary gene pool of wheat have not been well exploited as a source of B toxicity tolerance. This study explores the root and shoot growth, proline induction, and extent of lipid peroxidation in 19 Aegilops accessions comprising 6 different species and the B-tolerant check wheat cultivar Bolal 2973 grown under Control (3.1 μM B), toxic (1 mM B), and highly toxic (10 mM B) B stress treatment. B toxicity stress had a more decisive impact on growth parameters as compared to the malondialdehyde (MDA) and proline content. The obtained results suggested that even the genotypes with high shoot B (SB) accumulation can be tolerant to B toxicity stress, and the mechanism of B redistribution in leaves should be studied in detail. It has been proposed that the studied Aegilops accessions can be potentially used for genetically improving the B toxicity-tolerance trait due to a high level of variation in the response toward high B toxicity. Though a number of accessions showed suppression in the root and shoot growth, very few accessions with stress adaptive plasticity to B toxicity stress leading to an improvement of shoot growth parameters could be determined. The two accessions, *Aegilops biuncialis* accession TGB 026219 and *Aegilops columnaris* accession TGB 000107, were identified as the potential genotypes with B toxicity stress tolerance and can be utilized for developing a pre-breeding material in B tolerance-based breeding programs.

Keywords: Aegilops, alien introgression, boron toxicity, genetic resources, genetic variation, stress tolerance, wheat, wild species

INTRODUCTION

Boron (B) toxicity is a critical abiotic stress condition that has a detrimental effect on plant growth (Landi et al., 2019), thus limiting the agricultural yield in the different parts of the world, especially arid and semi-arid territories (Brdar-Jokanovic, 2020). The regions suffering from excess B accumulation were commonly reported for high B content in irrigation water and soil with little rainfall and insufficient leaching (Nable et al., 1997; Camacho-Cristóbal et al., 2018). B, which is taken up by plants in the form of boric acid, usually enters *via* passive diffusion in normal B conditions; however, boric acid channels and borate exporters are required for the movement of B within plants under B toxic environment (Pandey et al., 2019).

Though the role of B has been majorly recognized in the case of binding with the pectin polysaccharides present in the cell wall and thus facilitating cell wall stability (Funakawa and Miwa, 2015), its involvement in other metabolic processes has also been constantly highlighted (Hamurcu et al., 2020a). Thus, its excess leads to additional accumulation in apoplastic and symplastic tissues binding with molecules, including sugar molecules, glycoproteins, glycolipids, and ribose containing compounds such as RNA, ATP, and NADPH (Reid et al., 2004), and consequently hampering important processes such as cell division, photosynthesis, and stomatal conductance (Papadakis et al., 2004; Landi et al., 2012).

Along with the hindrance in root growth, the main symptoms of B toxicity include necrosis on leaf tips and chlorosis, which results from the production of reactive oxygen species (ROS) (Cervilla et al., 2007; Wang et al., 2010; Sakamoto et al., 2011). However, the reactions toward B toxicity rely on the capacity of the plant to re-translocate B within the phloem. Though it is thought that genotypes with less B uptake from roots - and consequently lower transport to shoots - can show greater tolerance to B toxicity, some genotypes with a greater B uptake and higher shoot B (SB) concentration can also be tolerant to high B (Reid and Fitzpatrick, 2009). Hence, B toxicity tolerance varies considerably within the species and among different species (Papadakis et al., 2003; Cervilla et al., 2007; Ardic et al., 2009; Landi et al., 2013; Wu et al., 2018). Thus, greater genetic diversity in the gene pool of a plant species is a desirable character that can help to deal with the problem of B toxicity stress.

Wheat is one of the main cereal crops and its yield is largely affected by high soil B either alone or in combination with salinity stress, i.e., BorSal stress (Pandey et al., 2019). A number of studies have reported a differential response of wheat genotypes toward B toxicity stress (Paull, 1990; Yau et al., 1997; Torun et al., 2006). However, these reported variations were dependent on several factors, including the growth stage (young or old plant), a dosage of B treatment, growth environment (hydroponic or soil), genotypes, and the organs in which B concentration is determined (shoot, root, or grains) (Brdar-Jokanovic, 2020). Thus, the B tolerance level of wheat genotypes may vary irrespective of the fact whether B concentration in different tissues is high or low (Yau et al., 1994).

Moreover, despite the attempts to find a correlation between B tolerance and geographical origins of genotypes (Yau et al., 1995; Rerkasem and Jamjod, 1997; Kalayci et al., 1998; Rerkasem et al., 2004; Pallotta et al., 2014; Brdar et al., 2017), no final conclusion could be drawn on the basis of origin (Brdar-Jokanovic, 2020). Though a variation in B toxicity tolerance has been observed in the existing cultivated wheat gene pool, the genetic base of the germplasm is still narrow and needs to be broadened for crop improvement (Rerkasem et al., 2004). To achieve the genotypes that may adjust to a high range of soil B concentration, it is necessary to identify B toxicity-tolerant sources from all the wheat gene pools and to include them in the breeding programs.

Wild wheat relatives have been identified as a potential source of genes providing tolerance to different biotic and abiotic stress conditions (Hairat and Khurana, 2015; Ahmadi et al., 2018; Nazari et al., 2018; Olivera et al., 2018). Aegilops, which is the closest genus to cultivated wheat, have been explored to a certain extent for B toxicity tolerance (Emon et al., 2012). While some of the Aegliops accessions, including *A. tauschii, A. longissima*, and *A. sharonensis,* have shown certain B tolerance, there is scanty information on the status of lipid peroxidation and proline formation in this tertiary wheat gene pool under high B stress.

Thus, we investigated the disparity in the responses of 19 different accessions (**Figure 1**) of 6 different Aegilops species toward a high B supply as compared to the well-recognized B toxicity-tolerant cultivar "Bolal 2973" (Mahboobi et al., 2001; Öz et al., 2014; Pallotta et al., 2014) in terms of root and shoot growth parameters, lipid peroxidation, proline content, and B accumulation. The aim of this study is to determine the level of resilience (most tolerant accession) in these genotypes toward B toxicity, which could contribute to an understanding of its adaptive mechanism under B stress conditions and for the improvement of high B tolerance in wheat breeding programs.

METHODOLOGY

Plant Materials

Aegilops genotypes used in this study consisted of 19 accessions belonging to 6 different species (3 diploid and 3 tetraploid species) (**Table 1**). The materials provided by the Turkish Seed Gene Bank (TSGB), Ankara, and AARI National Gene Bank, İzmir, Turkey were originated from the different sites of Turkey, and their respective gene banks accession numbers are listed in **Table 1**. To refer to a particular accession in the text, their assigned genotype code is used. The Turkish bread wheat cultivar, Bolal 2973, well recognized for its B toxicity tolerance (Mahboobi et al., 2001; Öz et al., 2014; Pallotta et al., 2014), was used as reference material in that study mainly to estimate the extent of damage to the root and shoot tissues in the presence of a high B supply.

Experimental Conditions and Measurement of Growth Parameters

For evaluating the effect of B toxicity stress on the growth of Aegilops accessions, the experiment was conducted in the hydroponic experiment that was adjusted to 45–55% humidity,



FIGURE 1 | Pictures of the 19 Aegilops accessions provided by the Turkish Seed Gene Bank (TSGB), Ankara, and AARI National Gene Bank, İzmir, Turkey. **(a)** Ab1 (*Aegilops biuncialis*1: TGB 026218; 4x); **(b)** Ab2 (*A. biuncialis2*: TGB 026219; 4x); **(c)** Ab3 (*A. biuncialis3*: TGB 037313; 4x); **(d)** Ac1 (*A. columnaris1*: TGB 037373; 4x); **(e)** Ac2 (*A. columnaris2*: TGB 038488; 4x); **(f)** Ac3 (*A. columnaris3*: TGB 037489; 4x); **(g)** Ac4 (*A. columnaris4*: TGB 000107; 4x); **(h)** Ac5 (*A. columnaris5*: TR 57295; 4x); **(i)** As1 (*A. speltoides1*: TGB 037791; 2x); **(j)** As2 (*A. speltoides2*: TR 62174; 2x); **(k)** Al1 (*A. ligustica1*: TGB 000803; 2x); **(l)** Al2 (*A. ligustica2*: TR 39488; 2x); **(m)** At1 (*A. triuncialis1*: TGB 037311; 4x); **(n)** At2 (*A. triuncialis2*: TGB 037355; 4x); **(o)** At3 (*A. triuncialis3*: TGB 037376; 4x); **(p)** At4 (*A. triuncialis4*: TR 72224; 4x); **(q)** Au1 (*A. umbellulata1*: TGB 037353; 2x); **(r)** Au2 (*A. umbellulata2*: TGB 037356; 2x); **(s)** Au3 (*A. umbellulata1*: TR 72200; 2x).

16/8 h light/dark photoperiod, 22 ± 10°C temperature, and 16,000 Lx/day light intensity. All the accessions along with the check cultivar were grown three times in three different treatments [Control (1/5th Hoagland solution containing 3.1 μM B), toxic B (1 mM B), and highly toxic B (10 mM B)] following a randomized design. Seeds used in this experiment were surface sterilized using sodium hypochlorite, 75% ethanol, and water and were further kept in darkness at 22°C for 3 days for germination.

After germination, five seedlings of all the genotypes were transferred to sterile hydroponic pots (containing one-fifth of Hoagland's solution) three times in three different sets (one set for each B treatment). Thus, 1 biological replicate comprised 5 plants, and a total of 15 plants per accession were kept for each B treatment. After 3 days of growth, plants were supplied with Hoagland's solution (Control) and required B concentrations, 1 mM B and 10 mM B. B treatment was given for 7 days, and the nutrient solution was changed after every 3 days.

The root and shoot harvest was done on the 7th day of B treatment when the plants were in the tillering stage (Feekes scale 4–5) (**Supplementary Figure 1**), and the samples for the different analyses were collected in triplicates. Immediately after harvest, the root lengths (RLs) and shoot lengths (SLs) of the plants were measured, and root fresh weight (RFW) and shoot fresh weight (SFW) was weighed (**Supplementary Figures 2A,B**). Further, the root and shoot samples of the plants were kept in an oven at 70°C for 72 h, and further, root dry weights (RDWs) and shoot dry weights (SDWs) were estimated. Additionally, the root and shoot samples were collected for malondialdehyde (MDA), proline, and inductively coupled plasma atomic emission spectrometry (ICP-AES) analysis.

Inductively Coupled Plasma-Atomic Emission Spectrometry Analysis for the Estimation of Root-Shoot B Content

For the ICP-AES analysis, the harvested root and shoot samples were washed with 0.1 N HCl solution and deionized water followed by air-drying of leaf samples at 70°C in a hot air oven. Dried samples were crushed, and 0.15–0.20 g of the powdered sample was dissolved in 5 ml of 65% HNO3 and 2 ml of 35% H2O2 and digested in a closed microwave accelerating reaction system (Cem Marsxpress, Matthews, NC, United States). ICP-AES (Varian, Vista, Palo Alto, CA, United States) was used to determine the nutrient concentration in the stock

TABLE 1 | Abbreviation code, Genbank code, genome, ploidy, and the site of origin of the 19 Aegilops accessions along with the bread wheat cultivar, Bolal 2973 used in this study.

Abbreviation code	Genbank code	Taxon	Genome	Ploidy	Site of origin
Ab1	TGB 026218	*Aegilops biuncialis*	UUMM	4x	Adıyaman, Turkey
Ab2	TGB 026219	*Aegilops biuncialis*	UUMM	4x	Şanlıurfa, Turkey
Ab3	TGB 037313	*Aegilops biuncialis*	UUMM	4x	Gaziantep, Turkey
Ac1	TGB 037373	*Aegilops columnaris*	UUMM	4x	Gaziantep, Turkey
Ac2	TGB 038488	*Aegilops columnaris*	UUMM	4x	Ankara, Turkey
Ac3	TGB 037489	*Aegilops columnaris*	UUMM	4x	Şanlıurfa, Turkey
Ac4	TGB 000107	*Aegilops columnaris*	UUMM	4x	Adıyaman, Turkey
Ac5	TR 57295	*Aegilops columnaris*	UUMM	4x	Van, Turkey
As1	TGB 037791	*Aegilops speltoides*	SS	2x	Şanlıurfa, Turkey
As2	TR 62174	*Aegilops speltoides*	SS	2x	Gaziantep, Turkey
Al1	TGB 000803	*Aegilops ligustica*	SS	2x	Mersin, Turkey
Al2	TR 39488	*Aegilops ligustica*	SS	2x	Şanlıurfa, Turkey
At1	TGB 037311	*Aegilops triuncialis*	CCUU	4x	Şanlıurfa, Turkey
At2	TGB 037355	*Aegilops triuncialis*	CCUU	4x	Adıyaman, Turkey
At3	TGB 037376	*Aegilops triuncialis*	CCUU	4x	Gaziantep, Turkey
At4	TR 72224	*Aegilops triuncialis*	CCUU	4x	Adıyaman, Turkey
Au1	TGB 037353	*Aegilops umbellulata*	UU	2x	Erzincan, Turkey
Au2	TGB 037356	*Aegilops umbellulata*	UU	2x	Şanlıurfa, Turkey
Au3	TR 72200	*Aegilops umbellulata*	UU	2x	Şanlıurfa, Turkey
Bolal	Bolal 2973	*Triticum aestivum*	AABBDD	6x	Turkey

solution (Pandey et al., 2016). The measurement of the elemental concentration was checked by the certified values of a B element in the reference leaf material provided by the National Institute of Standards and Technology (NIST, Gaithersburg, MD, United States).

Lipid Peroxide Estimation

Malondialdehyde is an end product of lipid peroxidation. Thus, a low MDA content shows less lipid peroxidation and consequently less damage in plant tissues under a stress condition. Reduced damage to plant tissues indicates a greater tolerance level of plants (Esim et al., 2013). Hence, the MDA level in the plant is considered a good indicator of plant tolerance to a particular stress condition. Thus, in this study, its level was estimated by employing the thiobarbituric acid method (Rao and Sresty, 2000; Hamurcu et al., 2020a). For MDA estimation, firstly, 0.5 g of the root and shoot samples were homogenized in 2.5 ml of trichloroacetic acid (TCA) (0.1%) followed by centrifugation at 10,000 × *g* for 10 min. After centrifugation, 1 ml supernatant was dissolved with 4 ml of 20% TCA containing 0.5% thiobarbituric acid. The mixture was further heated to 30 min at 95°C and then kept in an ice bath for cooling followed by centrifugation at 10,000 *g* for 15 min. The absorbance of supernatants was estimated at 532 nm, and the final concentration was calculated using an extinction coefficient of 155 mM^{-1} cm^{-1}.

Proline Level Estimation

In many plants, a strong correlation has been established between proline accumulation and abiotic stress tolerance (Hare and Cress, 1997; Kishor et al., 2005; Kavii Kishor and Sreenivasulu, 2014). Thus, it is interesting to observe the level of proline accumulation in tolerant genotypes under toxic B stressed conditions to understand the role of proline content in providing B toxicity tolerance. Thus, for the estimation of the proline content of the treated root and shoot samples, firstly, the acid ninhydrin was freshly prepared by heating 1.25 g ninhydrin in 30 ml glacial acetic acid and 20 ml 6 M phosphoric acid and stored at 4°C for 24 h (Bates et al., 1973; Hamurcu et al., 2020b). Further, about 0.5 g of the sample was homogenized in 3% sulphosalicylic acid and filtered. Afterward, 2 ml of each, acid ninhydrin and glacial acetic acid was added to 2 ml of extracted filtrate and kept at 100°C for 1 h. Further, the reaction was stopped by keeping the sample in an ice bath. The reaction mixture was mixed with 4 ml toluene using a stirrer for 15–20 s. Finally, the absorbance of the aspired part containing toluene was measured at 520 nm.

Data Analysis

To identify the accessions that are tolerant to B toxicity, statistical analysis was performed on the data from the measurements of different traits. The percentage changes in each of the measured physiological traits under 1 mM and 10 mM B treatment as compared to Control (based on three replicates) were estimated using MS Excel 2010. The frequency distribution analysis based on the percentage changes under 10 mM B treatment as compared to Control for all the measured traits was performed using Minitab Statistical software version 16. The normal graph was plotted for all the measured traits (**Supplementary Figure 3**). The obtained data were subjected to two-way ANOVA using the Graphpad prism 9.0 program, where treatments and genotypes were the two factors and the trait observed was the response. The role of genotypes (G), treatments (T), and their (G × T) interaction in the variability

in the expression of traits was considered to be highly significant for the values with $p < 0.001$. The mean differences between the two B treatments as compared to Control were calculated for the different traits using Dunnett's multiple comparisons tests, and the comparisons with $p < 0.001$ were considered to be significantly different. Bar diagrams based on the average of the three replicates with SE mean caps were developed to estimate the extent of the responsiveness of Aegilops accessions under B toxicity stress. Tukey's pairwise comparison using the general linear model of Minitab Statistical software version 16 was employed as a *post hoc* analysis to distinguish any significant differences among the experimental genotypes. A correlation analysis employing a Pearson correlation was conducted using the Minitab v. 16 software to find an association between the relative changes of the studied parameters, and the associations with $p < 0.05$ were considered to be significant. A heatmap employing the average linkage method was generated using the Euclidean distance matrix based on the percentage changes in the trait values. It allowed the clustering of all the experimental genotypes based on their responses toward B toxicity stress and the grouping of the studied traits according to their association with each other.

RESULTS

A set of 19 accessions consisting of diploid (*Aegilops speltoides*, *Aegilops ligustica*, and *Aegilops umbellulata*) and tetraploid (*Aegilops biuncialis, Aegilops columnaris,* and *Aegilops triuncialis*) progenitor species along with the Control wheat cultivar, Bolal 2973, were subjected to two different B toxicity stress conditions to evaluate their responses (**Table 1**). The hydroponic experiment was conducted to observe the changes in growth parameters, B accumulation, MDA, and proline content in the roots and shoots of the treated plants in response to B toxicity stress. The overall aim of this study is to determine a variation in the resilience of these Aegilops accessions under toxic B growth conditions.

ANOVA for All the Studied Traits

ANOVA-based assessment of the effect of B toxicity stress in 19 Aegilops accessions revealed a significant genotypic effect for all the studied traits, except RB and SB accumulation (**Table 2**). These significant variations among the accessions specify a high genetic diversity in the studied accessions. Indeed, the experimental accessions could serve as an appropriate gene pool for the B toxicity tolerance-based breeding programs. B toxicity stress treatment was also contributed significantly as a source of variation for all the studied traits (**Table 2**). However, Dunnett's test revealed that among all the studied traits, the mean difference between Control vs. 1 mM B treatment was significant only for the root malondialdehyde (RMDA) and shoot malondialdehyde (SMDA) and proline content. However, the mean difference between Control vs. 10 mM B treatment was significant for all the studied traits (**Table 2**). Thus, a variation in the measured traits under 10 mM B treatment is mainly focused on while discussing the results of this study.

TABLE 2 | Details of the results obtained from the two-way ANOVA showing the impact of genotypes (G), B toxicity treatments (T), and their interaction (G × T) on individually studied traits representative of plant growth and development.

Studied traits	Code	% of total variation			*P* value			Control vs. 1 mM		Control vs. 10 mM	
		Interaction	Genotypes	Treatment	Interaction	Genotypes	Treatment	Mean difference	Adjusted *P* value	Mean difference	Adjusted *P* value
Root Length	RL	13.1	50.5	22.8	****	****	****	−0.117	ns	8.833	****
Shoot Length	SL	14.7	54.5	4.3	*	****	***	0.450	ns	2.050	****
Root Fresh Weight	RFW	12.4	30.0	23.2	ns	****	****	0.009	ns	0.084	****
Shoot Fresh Weight	SFW	6.9	57.0	15.4	ns	****	****	0.006	ns	0.087	****
Root Dry Weight	RDW	10.3	45.4	19.6	ns	****	****	0.001	ns	0.004	****
Shoot Dry Weight	SDW	9.0	64.8	2.4	ns	****	**	0.000	ns	0.004	**
Root MDA Content	RMDA	17.2	43.0	39.2	****	****	****	−2.132	****	−4.806	****
Shoot MDA Content	SMDA	18.4	41.0	40.5	****	****	****	−7.194	****	−13.290	****
Root Proline Content	Rpro	19.3	57.9	20.6	****	****	****	−0.013	****	−0.020	****
Shoot Proline Content	Spro	19.9	59.7	18.8	****	****	****	−0.013	****	−0.021	****
Root B Accumulation	RB	–	27.1	31.1	-	ns	****	−0.728	ns	−4.649	****
Shoot B Accumulation	SB	–	15.0	58.7	-	ns	****	−13.790	ns	−88.590	****

*Significant differences are indicated as **** for $p < 0.0001$; *** for $p < 0.0005$; ** for $p < 0.005$; * for $p < 0.05$; ns, non-significant.*

Impact of B Toxicity Stress on the Root-Shoot Length

The average RL of Aegilops accessions in the Control group ranged from 9.50 to 35.67 cm, whereas it was from 5.50 to 19.67 cm in 10 mM B treatment (**Supplementary Table 1**). A highly toxic B led to a reduction in RL up to 133% in Aegilops species (shown by the accession At3) and a decrease of 49% of Bolal 2973 as compared to the Control treatment. However, a number of Aegilops accessions, including Ab2, Ac4, As2, Al1, and At2, showed less reduction in RL as compared to the check cultivar, Bolal 2973 under a highly toxic B condition. Among these accessions, Ab2 and Al1 showed the lowest reduction of 14% and 10% in RL, respectively (**Table 3**). In the case of RL, ANOVA showed a significant difference in genotypes (G), B toxicity treatment (T), and their interaction (G × T) (**Table 2**).

The SL of Aegilops accessions varied from 18.66 to 27.00 cm under controlled conditions, whereas it ranged from 16.50 to 23.67 cm under highly toxic B conditions (**Supplementary Table 1**). B toxicity developed due to boric acid led to a 24% reduction in SL in Aegilops species, while the same led to a 38% reduction in the SL of the B-tolerant check cultivar, Bolal 2973. Under highly toxic B stress, a substantial increase of around 11.9% was observed in the SL of Ab2 and Ac4. Ab2 accession also showed the highest increase in RL (**Table 3**). ANOVA showed a significant difference among genotypes (G), B toxicity treatment (T), and their interaction (G × T) in SL (**Table 2**).

Impact of B Toxicity Stress on the Root-Shoot Fresh Weight

Under controlled growth conditions, the highest RFW was observed in Au2 (270 mg) followed by Ac1 (246 mg), which was higher than the B-tolerant cultivar Bolal (140 mg) (**Supplementary Table 1**). However, under a highly toxic B condition, Ac1 showed the highest RFW followed by Ac5, Au2, and Ac4. A minimum reduction (13%) in RFW was observed in Ac4 followed by Ab2 (47%) (**Table 3**). In RFW, the differences in both genotypes and treatment were found to be significant while the interaction (G × T) was found to be insignificant (**Table 2**).

The SFW of Aegilops species ranged from 100 to 394 mg under normal growth conditions, whereas under a highly toxic B supply, it varied between 65 and 266 mg (**Supplementary Table 1**). Though the check cultivar, Bolal showed the highest SFW under 10 mM B treatment, it showed a 30% reduction as compared to the Control treatment. Three Aegilops accessions, Ab1, Ab2, and Ac4, showed a lower reduction in SFW as compared to Bolal. The lowest reduction of around 4% has been observed in Ac4 (**Table 3**). The interaction between the genotypes and stress treatment was not significant in the case of SFW; however, both B toxicity treatment and genotypes individually revealed significant differences (**Table 2**).

Impact of B Toxicity Stress on the Root-Shoot Dry Weight

Root dry weight and shoot dry weight under B toxic growth conditions have been widely considered for the understanding of the level of B tolerance in wheat genotypes (Torun et al., 2006; Metwally et al., 2012; Nejad et al., 2015). Aegilops accessions showed wide variability in RDW under controlled growth conditions ranging from 3 to 15 mg and a highly toxic B growth condition ranging from 2 to 8 mg (**Supplementary Table 1**). The check cultivar Bolal 2973 showed a 52% decrease with 11 mg RDW under normal growth conditions and 7 mg RDW under 10 mM B treatment. Though seven accessions showed less decrease in RDW as compared to the check cultivar, the accessions Ab2 (9%) and Ac4 (13%) showed the lowest decrease (**Table 3**). According to the obtained ANOVA results, both genotypes and treatment significantly act as a source of variation in the case of RDW. However, the interaction of the two was not significant (**Table 2**).

The SDW of B-tolerant cultivar, Bolal remains almost the same both under controlled growth and highly toxic B conditions (53 mg) (**Supplementary Table 1**). However, the three Aegilops accessions, Ab1, Ab2, and Ac4, showed a 6, 31, and 20% increase in SDW under a highly stressed condition, respectively (**Table 3**). The difference in the treatment was significant (<0.01), whereas the difference of genotypes was highly significant (<0.0001) in the case of SDW. The interaction G × T was not significant (**Table 2**).

Impact of B Toxicity Stress on the Root-Shoot Malondialdehyde Content

According to the obtained results, the range of MDA content in roots is found to be less than the shoots. While RMDA content varied from 5.60 to 12.61 nmol g^{-1} FW under the Control treatment, it changed from 8.04 to 16.78 nmol g^{-1} FW under 10 mM B treatment (**Supplementary Table 2**). Among Aegilops accessions, Ac4 showed the least increment of only 13% under a highly toxic B environment as compared to Control, whereas the check cultivar, Bolal 2973 showed an increase of only 9% as compared to control (**Table 3**).

The SMDA content of Aegilops accessions varied from 7.28 to 21.55 nmol g^{-1} FW under a normal growth condition, whereas the same was in the range between 15.60 and 49.18 nmol g^{-1} FW under highly toxic B treatment (**Supplementary Table 2**). In highly toxic B supply, though most of the genotypes showed an increase in SMDA content as compared to the check cultivar Bolal, the increment was least in the accession, Al1. Among Aegilops accessions, Ac1 and Ac2 showed the lowest (15.6 nmol g^{-1} FW) and highest (49.1 nmol g^{-1} FW) SMDA content under a highly toxic B environment (**Table 3**). In the case of MDA, all of the three [genotypes (G), treatment (T), and their interaction (G × T)] acted as a significant source of variation in both roots and shoots (**Table 2**).

Impact of B Toxicity Stress on the Root-Shoot Proline Content

The root proline (RProline) content of Aegilops accessions ranged from 0.013 to 0.060 nmol g^{-1} FW and 0.024 to 0.085 nmol g^{-1} FW under Control and 10 mM B treatment, respectively (**Supplementary Table 2**). With a decrease of 26%

TABLE 3 | The percentage change in the studied traits of 19 Aegilops accessions and the B-tolerant check cultivar, Bolal 2973 is highly toxic B (10 mM B) treatment as compared to Control.

Code	SL	RL	SFW	RFW	SDW	RDW	S_MDA	R_MDA	S_Proline	R_Proline	S_B	R_B
Ab1	−1.6	−42.5	−21.6	−92.3	6.1	−28.0	47.3	33.2	28.6	33.2	99.26	98.08
Ab2	11.9	−14.0	−8.5	−47.1	30.6	−8.7	33.3	31.1	46.9	51.7	99.61	98.18
Ab3	−1.4	−87.9	−35.1	−114.3	−0.3	−47.2	61.2	21.0	31.3	40.6	99.50	99.36
Ac1	−16.1	−117.3	−48.2	−185.0	−6.6	−91.6	51.3	50.4	−5.4	55.7	99.20	90.11
Ac2	−20.8	−65.9	−98.0	−175.0	−20.2	−75.9	56.2	45.7	25.0	54.4	99.58	97.29
Ac3	−19.5	−117.2	−89.5	−403.1	−47.9	−192.3	46.6	31.1	77.6	41.7	99.17	93.70
Ac4	12.0	−31.8	−4.6	−13.6	20.0	−13.0	47.3	13.6	61.1	43.5	99.81	99.08
Ac5	−9.0	−81.6	−95.5	−109.0	−29.7	−79.1	49.2	43.4	57.0	23.2	98.64	91.35
As1	−6.5	−68.5	−125.3	−356.0	−81.9	−206.1	45.7	25.6	31.6	42.8	99.43	94.02
As2	−2.0	−19.5	−66.2	−134.6	−27.0	−89.8	60.0	31.8	68.3	57.7	99.03	90.12
Al1	6.8	−10.5	−36.5	−100.0	−18.7	−20.0	13.9	36.8	16.9	47.0	98.95	96.66
Al2	−23.7	−67.0	−187.9	−404.4	−98.4	−193.5	60.9	15.8	72.8	7.2	98.91	86.93
At1	−24.1	−65.9	−80.2	−204.4	−53.8	−131.4	62.8	63.4	54.4	48.1	99.09	97.48
At2	−19.4	−40.6	−30.7	−83.4	−4.0	−28.1	47.3	24.3	36.7	45.5	99.02	94.73
At3	−20.8	−133.8	−109.4	−447.8	−70.7	−148.5	53.0	57.8	65.8	69.4	98.94	96.28
At4	−0.7	−81.4	−33.0	−192.2	−27.5	−174.8	50.3	56.2	19.7	29.0	99.15	96.20
Au1	−9.6	−102.6	−51.5	−178.7	−5.6	−49.1	41.4	46.1	46.3	55.9	99.56	96.07
Au2	0.8	−73.4	−50.1	−262.8	−20.0	−148.1	49.4	60.6	14.0	42.5	99.72	97.99
Au3	−13.1	−90.0	−67.2	−232.5	−19.0	−95.7	42.3	49.7	−89.8	−26.1	99.46	92.57
Bolal	−38.2	−49.5	−30.0	−108.4	−0.3	−52.6	33.2	8.9	68.0	68.4	99.09	91.34

and an increase of only 7%, the Aegilops accessions, Au3 and Al2, respectively, showed the least increment in RProline content. The Aegilops accession, At3 (69%), and the check cultivar, Bolal 2973 (68%), showed a maximum increase in RProline content under 10 mM B treatment as compared to Control (**Table 3**).

A huge variation in the shoot proline (SProline) content of Aegilops accessions was observed under both Control (0.009–0.063 nmol g^{-1} FW) and 10 mM B treatment (0.011–0.089 nmol g^{-1} FW). While Au3 showed an 89% decrement in the proline content under a highly toxic B condition as compared to Control, Ac3 revealed the highest increase (78%) in proline content as compared to Control (**Table 3**).

Similar to MDA, in the case of proline also, all of the three (genotypes, treatment, and their interaction) acted as a significant source of variation in both roots and shoots. However, the genotypes showed a much greater contribution to the variability as compared to treatments (**Table 2**).

Impact of B Toxicity Stress on the Root-Shoot B Accumulation

In root B (RB) accumulation, Ab3 and Ac4 showed a maximum increase of 99.36 and 99.08% under highly toxic B treatment as compared to Control (**Table 3**). The check cultivar Bolal showed a 91.34% increase in B accumulation under 10 mM B treatment as compared to Control. In 10 mM B treatment, Ab1 (16.97 μg^{-1} DW) and Ab3 (17.80 μg^{-1} DW) showed the maximum, and Al1 (0.75 $\mu g\ g^{-1}$ DW) and Al2 (0.98 $\mu g\ g^{-1}$ DW) demonstrated minimum RB accumulation (**Supplementary Table 2**).

The accumulated B content in the shoot of Aegilops accessions ranged from 0.28 to 0.81 $\mu g\ g^{-1}$ DW under the Control treatment, whereas the same varied from 30.52 to 295.62 $\mu g\ g^{-1}$ DW under highly toxic B treatment (**Supplementary Table 2**). While Ac4 showed a maximum increase in B accumulation (99.81%) as compared to Control, Ac5 revealed a minimum increase (98.64%) (**Table 3**). As2 and Al1 showed a minimum SB accumulation of 30.52 and 42.65 $\mu g\ g^{-1}$ DW (**Supplementary Table 2**). In the case of RB and SB content, differences in the treatment were found to be significant, which contribute to a 59% variation in shoots and a 31% variation in roots whereas the differences in the genotypes were found to be non-significant (**Table 2**).

Correlation Between the Measured Traits of Aegilops Accessions Grown Under B Toxic Condition

The association between the relative changes in the different studied traits was estimated using a Pearson correlation. The analysis revealed significant positive correlations between the biomass (SDW and RDW) and the growth parameters (SL and RL) (**Table 4**). The RProline and SProline content were not significantly associated with any of the growth parameters or MDA content; however, a significant positive correlation was found between the RProline and SProline content. The RMDA and SMDA content were mostly negatively correlated with all the growth parameters; however, these correlations were not significant except SL. Interestingly, RB showed a significant positive correlation with all the shoot-based traits, including SL, SFW, SDW, and SB. This directs toward the role of B uptake from the roots in SB accumulation and consequently affecting the shoot growth in terms of length and dry weight. SB was found to be significantly and positively associated with SDW only. Other than this, no significant

TABLE 4 | Pearson's correlation and its significance summarizing the association between the percentage changes in the studied parameters under highly toxic B (10 mM B) treatment as compared to Control.

	SMDA	RMDA	SPro	RPro	SL	RL	SFW	RFW	SDW	RDW	SB
RMDA	0.05										
p-value	0.837										
SPro	0.27	−0.33									
p-value	0.265	0.169									
RPro	0.01	0.10	0.56*								
p-value	0.967	0.698	0.013								
SL	−0.51*	−0.27	−0.05	0.08							
p-value	0.026	0.266	0.825	0.739							
RL	−0.35	−0.44	0.10	0.04	0.59**						
p-value	0.138	0.063	0.684	0.887	0.008						
SFW	−0.40	0.01	−0.23	0.21	0.68**	0.37					
p-value	0.094	0.973	0.335	0.379	0.002	0.115					
RFW	−0.27	−0.22	−0.12	0.09	0.61**	0.65	0.78**				
p-value	0.256	0.375	0.612	0.727	0.006	0.003	0.000				
SDW	−0.34	−0.10	−0.25	0.14	0.62**	0.38	0.91**	0.86**			
p-value	0.153	0.677	0.306	0.575	0.005	0.107	0.000	0.000			
RDW	−0.40	−0.25	−0.12	0.17	0.49*	0.53*	0.72**	0.88**	0.85**		
p-value	0.091	0.304	0.623	0.484	0.033	0.020	0.000	0.000	0.000		
SB	−0.071	−0.092	−0.273	0.065	0.427	0.096	0.421	0.229	0.492*	0.234	
p-value	0.773	0.708	0.257	0.792	0.068	0.695	0.073	0.345	0.032	0.336	
RB	−0.22	0.12	−0.01	0.35	0.46*	0.19	0.63**	0.39	0.52*	0.42	0.57*
p-value	0.365	0.618	0.965	0.143	0.049	0.439	0.004	0.100	0.023	0.072	0.011

Associations with $p < 0.05$ and $p < 0.01$ were considered to be significant (*) and highly significant (**), respectively.

correlation was observed between SB and the measured traits (**Table 4**).

B Toxicity-Tolerant Aegilops Accessions

The cluster analysis-based heat map presented in **Figure 2** depicts the physiological responses of 19 Aegilops accessions toward B toxicity stress. Three main clusters with distinguished genetic profiles were identified based on the percentage changes in the studied traits in response to a high B supply. Cluster 1 comprises six Aegilops accessions and one B-tolerant check cultivar, Bolal. The accessions in Cluster 1 had mostly higher SL, RL, SFW, RFW, SDW, and RDW in response to highly toxic B stress in comparison with Clusters 2 and 3 and thus classified as tolerant genotypes. In this cluster, two genotypes, Ab2 and Ac4, were categorized as the most tolerant genotypes as they showed a maximum increment or least decrement in all the growth parameters, including RL and SL and biomass production (RDW and SDW). The eight genotypes in Cluster 2 were considered as moderate genotypes based on their responses toward high B. These accessions mostly showed lower SL, RL, SFW, RFW, SDW, and RDW in response to highly toxic B stress as compared to the accessions in Cluster 1 but higher values than the accessions in Cluster 3. The third group comprises four accessions, which showed lower SL, RL, SFW, RFW, SDW, and RDW in response to highly toxic B stress as compared to both Clusters 1 and 2. Moreover, the heat map also grouped the studied traits into two clusters, where most of the growth parameters, including SL, RL, SFW, SDW, and RDW, are clustered together. In addition, SB and RB were grouped together. These groupings were consistent with the results obtained in Pearson correlation analysis, and the traits showing a significant association were clustered together in a heat map as well.

It can be observed from the heat map (**Figure 2**) that Cluster 1 contains the most tolerant accessions, comprising the genotypes from all the species, including *A. biuncialis, A. triuncialis, A. columnaris, A. ligustica*, and Bolal. However, the other genotypes of the same species were also present in Clusters 2 and 3 that did not show symptoms of B toxicity tolerance. Thus, it cannot be concluded that high tolerance was specific to any of the species. Similarly, although most of the genotypes in the tolerant Cluster 1 were tetraploid, one of the genotypes, Al1 was diploid. Moreover, Clusters 2 and 3 are also comprised the genotypes with all the ploidy levels. Thus, it will not be appropriate to conclude that the high tolerance characteristics were related to the ploidy level. Consequently, it can be concluded that B toxicity tolerance in the experiment was not correlated to any ploidy or species but was genotype-dependent.

DISCUSSION

The process of domestication has narrowed the genetic variability of the genes responsible for the different valuable traits in wheat. Aegilops, the closest wheat relative, can serve as an important source of novel alleles, which can contribute to increasing this genetic diversity in wheat. Although most of the Aegilops species belong to the tertiary gene pool of wheat and thus face the challenges of incompatibility and crossability, a number of

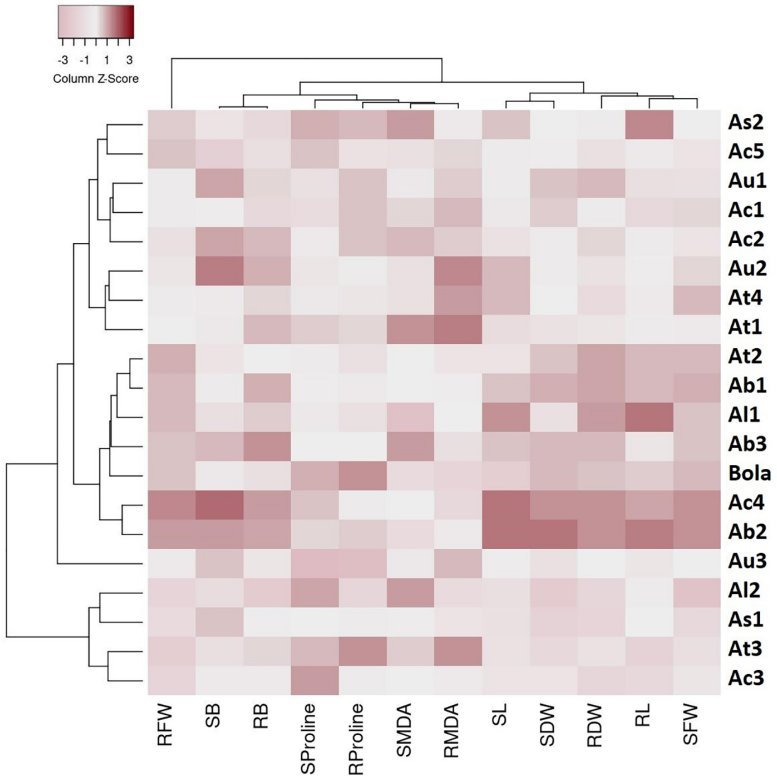


FIGURE 2 | A heat map describing the boron (B) toxicity stress-induced genetic variability in traits among 19 Aegilops accessions and the check cultivar, Bolal 2973 grown under B toxicity in the hydroponic system. The color code signifies the *Z* score for each genotype: dark color specifies an increase in the percentage of the trait values of the genotypes under B toxicity as compared to Control, whereas a lighter shade specifies the decrease in the percentage of the trait values of the genotypes under B toxicity as compared to Control. The genotypes were clustered into three different groups (C1–C3) based on their response to B toxicity stress in terms of different traits, including root length (RL), shoot length (SL), RFW (root fresh weight), shoot fresh weight (SFW), root dry weight (RDW), shoot dry weight (SDW), root malondialdehyde (RMDA), shoot malondialdehyde (SMDA), root proline (RProline), shoot proline (SProline), root boron (RB accumulation), and shoot boron (SB accumulation).

Aegilops genes have been utilized for wheat improvement in terms of biotic/abiotic stresses and nutritional development.

Aegilops have been extensively identified or utilized for different biotic stress conditions, including powdery mildew resistance (Tang et al., 2018), cereal cyst nematodes (CCN) resistance (Ali et al., 2019), leaf rust (Millet et al., 2014; Lee et al., 2020; Rani et al., 2020), stem rust (Yu et al., 2015; Edae et al., 2016; Huang et al., 2018; Olivera et al., 2018), stripe rust (Millet et al., 2014), green bug (Crespo-Herrera et al., 2013), and hessian fly (Martin-Sanchez et al., 2003; Kishii, 2019), and fusarium head blight (Brisco et al., 2017). Other than biotic stress, the utility of Aegilops species for abiotic stress, including drought (Djanaguiraman et al., 2019; Suneja et al., 2019), heat (Awlachew et al., 2016; Green et al., 2018), salinity stress (Kiani et al., 2015), has also been determined. Aegilops genes related to not only stress conditions but also to the grain protein content and grain quality of wheat have been reported (Neelam et al., 2012; Ma et al., 2013; Zhou et al., 2014; Garg et al., 2016; Du and Zhang, 2017; Rakszegi et al., 2017).

The effect of B toxicity stress on 19 Aegilops accessions from 6 different species to understand their adaptive mechanism and to identify the most tolerant accessions to B toxicity stress. The aim of this study was to identify the degree of tolerance in the screened accessions and to determine whether appropriate Aegilops accessions could be found and can be employed as genetic sources to improve B toxicity tolerance in cultivated wheat.

Impact of B Toxicity Stress on the Root-Shoot Growth Parameters

A number of studies have considered RL as the criteria for B toxicity tolerance (Schnurbusch et al., 2008; Pallotta et al., 2014). Genotypes showing an increment or a less decrement in RL under B toxic growth conditions as compared to Control can be selected as B tolerant (**Figure 3A**). In this study, the noticeable least decrement in terms of root development (RL and RDW) (**Figures 3A,C**) and a clear increment in terms of shoot development (SL and SDW) have been observed in some of the Aegilops accessions under highly toxic B growth conditions as compared to Control (**Figures 3B,D**). Ab2, Ac4, As2, Al1, and At2 showed less reduction in RL as compared to the check cultivar, Bolal. Similar to our study, Pallotta et al. (2014) found less reduction in the RL of the B-tolerant cultivar, Halbred under

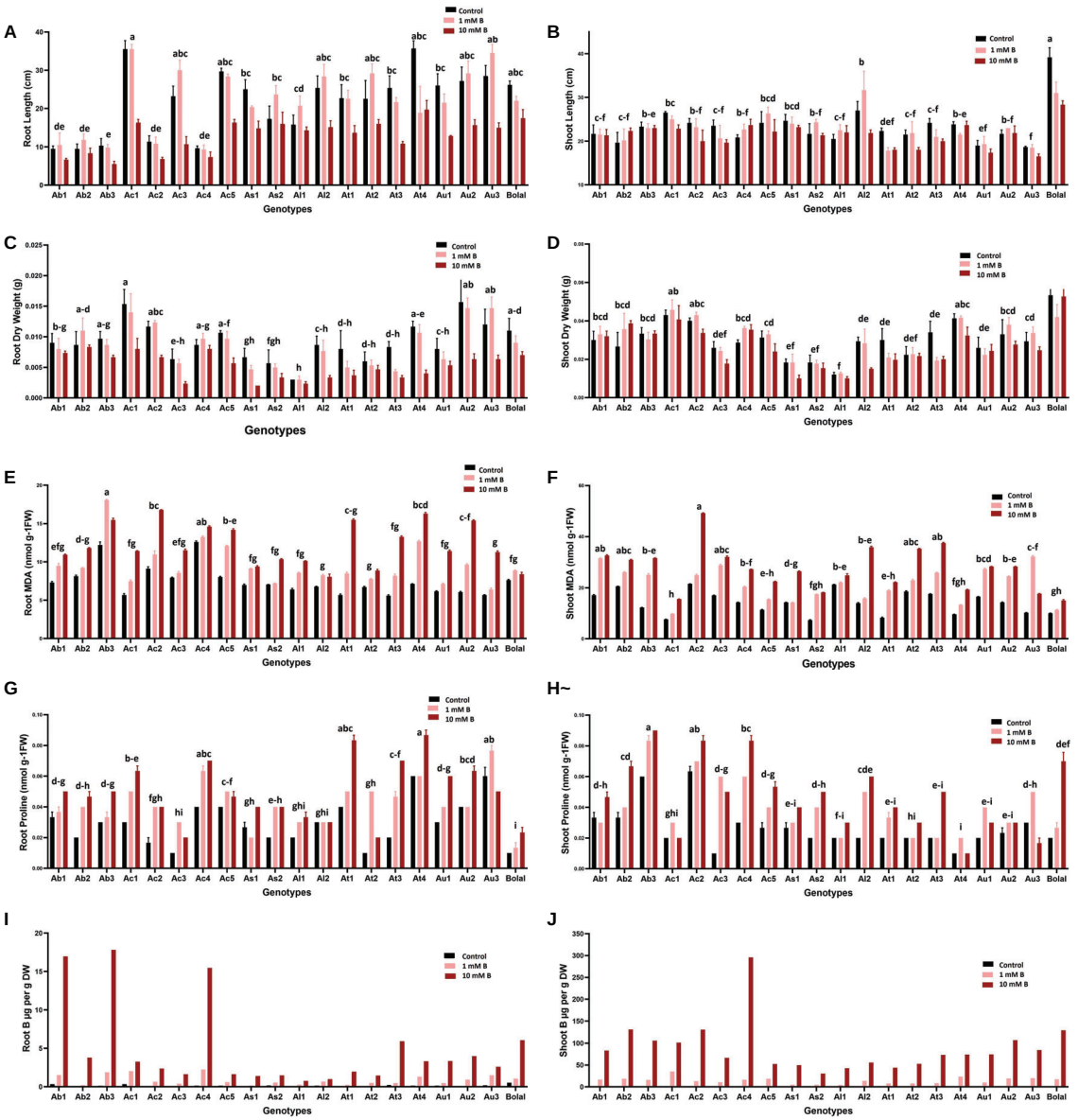


FIGURE 3 | Variability in the **(A)** RL **(B)** SL **(C)** RDW **(D)** SDW **(E)** RMDA **(F)** SMDA **(G)** RProline **(H)** SProline **(I)** RB accumulation and **(J)** SB accumulation of 19 Aegilops accessions and the B-tolerant check cultivar, Bolal 2973 grown under Control (3.1 µM B), toxic B (1 mM B), and highly toxic B (10 mM B). Data represent means ± SE. Tukey's pairwise comparison using the general linear model was employed to distinguish any significant differences among the experimental genotypes. Genotypes that do not share a letter are significantly different.

B toxic conditions as compared to the intolerant genotype, Cranbrook and Langdon.

Similar to RL, B toxicity may also negatively affect SL. However, in our study, despite having a general detrimental effect on the SL of the studied accessions, a very few accessions (Ab2, Ac4, and Al1) could tolerate the highly toxic B supply and showed a significant increase in SL (**Figure 3B**). Though a few studies reported no effect of B toxicity on SL (Yau and Saxena, 1997; Brdar-Jokanovic, 2020), others reported a significant negative effect of high B on the SL of wheat cultivars (Coskun et al., 2014). These differences in the results of the RL and SL direct toward a major role of genotypic variation in response to B toxicity. Thus, the accessions with less or no detrimental effects of high B on both RL and SL should be definitely considered for further studies to understand the mechanism behind B toxicity tolerance and for the B toxicity improvement in breeding programs.

Dry matter production, especially shoots under B toxicity, has also been accepted as a basis for the selection of the tolerant wheat genotypes (Torun et al., 2006; Metwally et al., 2012). In this study, Ab1, Ab2, and Ac4 showed an increment in SDW under a high B supply as compared to Control (**Figure 3D**). These results were consistent with the findings of Torun et al. (2006) where the

genotypes with an increase in SDW were selected as tolerant. In the case of RDW, Ab2 and Ac4 showed less decrement under high B toxicity as compared to the check cultivar, Bolal (**Figure 3C**). It was similar to the results obtained by Nejad et al. (2015) where the varieties with a higher RDW than other varieties under the B toxic condition were accepted as tolerant. The damaging effect of B in our study was greater on RDWs as compared to the SDWs (20 and 2%, respectively). Similar observations were recorded by Kalayci et al. (1998) on wheat cultivars.

Impact of B Toxicity Stress on the Root-Shoot Malondialdehyde Content

Malondialdehyde, a product of lipid peroxidation, has been consistently used as a marker to understand the extent of oxidative damage in plants due to abiotic stresses (Davey et al., 2005; Morales and Munné-Bosch, 2019). An increase in the RMDA and SMDA content in our study under a highly toxic B supply was consistent with a number of studies (Karabal et al., 2003; Esim et al., 2013; Mohamed et al., 2016; Choudhary et al., 2020). The percentage increase in the RMDA and SMDA content of Aegilops accessions was up to 63% under highly toxic B treatment as compared to Control (**Table 3**).

In roots, the lowest percentage increase in MDA content (9%) was observed in the tolerant check cultivar, Bolal showing the lowest oxidative damage in its roots. This might be responsible for a reduced decrease in its RL and dry weight under high toxic B in comparison with a maximum decrement obtained in the Aegilops accessions. Among Aegilops, the least increase (13%) in Ac4 accession reveals less lipid peroxidation in its roots (**Figure 3E**). As lipid peroxidation could be responsible for cell damage, a reduced increase of it seems to be accountable for the less damage and least decrement in its RDW.

In shoots, more than 30% increase has been observed in the MDA content of all the Aegilops accessions (except Al1, 13.5%) under 10 mM B treatment, which shows a significant level of lipid peroxidation due to high B toxicity (**Figure 3F**). However, Ab2 accession showed a 33% increase in SMDA content under highly toxic B, which was similar to the check cultivar Bolal. Similarly, an increase in the MDA content of Ac4 accession under a high B supply was also not too much (47%) as compared to the maximum increase (**Table 3**). This shows lesser oxidative damage in the shoots of these two accessions, and this could be a reason for an increase in their SL and dry weight in 10 mM B treatment.

Impact of B Toxicity Stress on the Root-Shoot Proline Content

Proline is an osmoprotectant known for its role in plants in protecting the proteins from denaturation, the detoxification of hydroxyl radicals, and the stabilization of phospholipids especially under abiotic stress conditions (Cervilla et al., 2012). However, the effect of B toxicity on its accumulation in plants is still controversial (Pandey et al., 2019). While a few studies reported a significant increase in proline content under B toxic condition (Eraslan et al., 2007a; Kaya et al., 2018; Samet and Çıkılı, 2019), others discussed insignificant changes in its accumulation under B toxicity (Karabal et al., 2003; Molassiotis et al., 2006; Eraslan et al., 2007b).

In this study, the effect of B toxicity on proline accumulation and also its role in regulating lipid peroxidation is not conclusive. In general, the proline accumulation increased in both roots and shoots of the studied accessions under highly toxic B treatment. However, some of the accessions showed a decrease in the root (Au3) and shoot (Ac1 and Au3) proline content under a highly toxic B supply (**Figures 3G,H**).

It has been considered in several studies that under B toxic conditions, proline forms a complex with ROS and detoxifies their function with a detrimental effect on lipid peroxidation (Hong et al., 2000). Thus, a decrease in proline accumulation may lead to a higher extent of lipid peroxidation increasing the MDA content in the stressed tissues (Molassiotis et al., 2006). In contrary to this argument, in our study, the accessions with a maximum decrement in proline content did not show a maximum increase in MDA content. Thus, an association between proline accumulation and MDA content could not be concluded, which was in line with the findings of Karabal et al. (2003).

Interestingly, when the RProline and SProline content of the two Aegilops accessions, Ab2 and Ac4 (which demonstrated tolerance in root and shoot growth parameters), were observed under a high B supply, both accessions showed a proline content closer to a higher end in the range (although it was not the highest) (**Supplementary Table 2**). This directs toward the controlled oxidative tissue damage in them and further demonstrate either positive or less detrimental effect on their RL and SL and dry weights.

Impact of B Toxicity Stress on the Root-Shoot B Accumulation

Variability in RB and SB accumulation in the studied Aegilops accessions under the two toxic B treatments can be observed in **Figures 3I,J**. In general, B toxicity tolerance in plants is considered to be associated with its capacity to maintain low B concentrations in the tissues (Cartwright et al., 1986; Nable, 1988; Nable et al., 1990, 1997; Moody et al., 1993; Hayes and Reid, 2004; Rehman et al., 2006; Sutton et al., 2007; Ghaffari Nejad et al., 2015). However, this argument has been rejected by a number of studies where the differences in the behavior toward B toxicity are not associated with B concentration in the tissues (Mahalakshmi et al., 1995; Yau et al., 1995; Torun et al., 2002; Brdar-Jokanovic, 2020). Moreover, tolerant genotypes with higher SB concentrations have also been determined (Torun et al., 2006), and this tolerance is attributed to the plant's own ability to tolerate high B concentrations (Babaoğlu et al., 2004).

The decreased accumulation of B in shoot tissues is partially attributed to the efflux of B from the roots, which is regulated by the increased expression of a gene encoding the B efflux transporter in roots (Hayes and Reid, 2004; Sutton et al., 2007). Reid and Fitzpatrick (2009) demonstrated that the upregulation of the same gene in leaves, and consequently the B efflux led to the redistribution of B from the intracellular phase to the apoplast, which is comparatively less susceptible to B toxicity. This can be

a reason for a poor correlation between SB concentrations and B toxicity symptoms in leaves. However, still, a deep understanding of the mechanism behind this tolerance is required and should be studied in detail focusing on these tolerant genotypes.

Genetic Dissimilarity Among the Aegilops Accessions Based on the Response Toward B Toxicity Stress

Large variations in terms of root and shoot growth parameters have been observed in the studied Aegilops accessions under highly toxic B growth conditions (**Figures 3A–D** and **Supplementary Figures 1A,B**). A similar level of genetic variation in root-shoot growth parameters was observed in previous studies on durum and bread wheat genotypes (Yau et al., 1995; Jamjod, 1996; Kalayci et al., 1998; Torun et al., 2006). Such differences in the response of Aegilops accessions toward B toxicity should be utilized to develop B-tolerant prebreeding material. The genetic profile of the Aegilops accessions can be a major contributor to these variations in response to B toxicity stress. Interestingly, both the genotypes identified as tolerant were tetraploid with the genome UUMM. Moreover, as all the tetraploid genotypes in Cluster 1 consist of the U genome (either along with C or M genome), it might be mis-concluded that the U genome has some contributions in providing B toxicity tolerance. However, it cannot be considered as a favorable conclusion because other tetraploid genotypes containing the U genome are also present in Clusters 2 and 3, which did not show B toxicity tolerance symptoms. Moreover, *A. umbellulata* that only contains the U genome did not show any symptoms of B toxicity tolerance. Thus, based on the results, it can be concluded that B toxicity tolerance in the experiment was not correlated to any ploidy or species but was adhered to specific genotypes.

CONCLUSION

In summary, the effect of B toxicity stress on the growth of 19 Aegilops accessions belonging to 6 different species was explored to identify the level of genetic variability in their tolerance to high B toxicity. Our findings suggested that (i) B toxicity stress had a more conclusive impact on growth parameters as compared to MDA and proline content, (ii) The impact of B toxicity stress was more on shoots as compared to roots, (iii) Some of the Aegilops accessions may have greater levels of B toxicity tolerance as compared to the existing B-tolerant wheat cultivars, and the mechanisms providing them the tolerance needs to be thoroughly studied. The two accessions, Ab2 (*A. biuncialis* accession TGB 026219) and Ac4 (*A. columnaris* accession TGB 000107), were considered to be tolerant in this study can be employed for developing the introgression lines or a pre-breeding material for B tolerance-based breeding programs, (iv) B tolerance level is not always associated with the lower SB accumulation. The accessions with the higher RB and SB accumulation can also be tolerant to toxic B levels. This strengthens the argument of the existence of some additional mechanisms other than the B efflux from roots. The redistribution mechanism of B in leaves suggested by Reid and Fitzpatrick (2009) can be taken into account as well. However, it needs to be confirmed by estimating the B concentration of intracellular tissues and apoplast of leaves separately. More detailed research based on antioxidant and molecular analyses is required to understand the other underlying mechanisms of B toxicity tolerance, and the two Aegilops accessions identified as tolerant in this study can be preferred for such further research.

DATA AVAILABILITY STATEMENT

The original contributions presented in the study are included in the article/**Supplementary Material**, further inquiries can be directed to the corresponding author.

AUTHOR CONTRIBUTIONS

MKK and AP conceived, wrote, and edited the manuscript. MKK, AP, MH, ZZA, MO, AHO, FE, and MRO conducted the experiment and analysis. MKK arranged **Figure 1**, which comprises the original spike pictures of all the studied Aegilops accessions. FG, AT, and SG made an intellectual contribution to the manuscript. All authors have read and agreed to the content.

FUNDING

The authors acknowledge the TUBITAK 1001 (No. 119O455) project for the funding provided to conduct this research work.

ACKNOWLEDGMENTS

The authors acknowledge TSGB, Ankara, and AARI National Gene Bank, İzmir, Turkey for providing the Aegilops accessions used in this study.

SUPPLEMENTARY MATERIAL

The Supplementary Material for this article can be found online at: https://www.frontiersin.org/articles/10.3389/fpls.2021.736614/full#supplementary-material

REFERENCES

Ahmadi, J., Pour-Aboughadareh, A., Ourang, S. F., Mehrabi, A. A., and Siddique, K. H. M. (2018). Wild relatives of wheat: Aegilops–Triticum accessions disclose differential antioxidative and physiological responses to water stress. *Acta Physiol. Plant.* 40, 2673–2670. doi: 10.1007/s11738-018-2673-0

Ali, M. A., Shahzadi, M., Zahoor, A., Dababat, A. A., Toktay, H., Bakhsh, A., et al. (2019). Resistance to cereal cyst nematodes in wheat and barley: an emphasis on classical and modern approaches. *Int. J. Mol. Sci.* 20:432. doi: 10.3390/ijms20020432

Ardic, M., Sekmen, A. H., Tokur, S., Ozdemir, F., and Turkan, I. (2009). Antioxidant responses of chickpea plants subjected to boron

toxicity. *Plant Biol.* 11, 328–338. doi: 10.1111/j.1438-8677.2008.00132.x

Awlachew, Z. T., Singh, R., Kaur, S., Bains, N. S., and Chhuneja, P. (2016). Transfer and mapping of the heat tolerance component traits of Aegilops speltoides in tetraploid wheat Triticum durum. *Mol. Breed.* 36, 1–15. doi: 10.1007/s11032-016-0499-2

Babaoğlu, M., GezgiN, S., Topal, A., Sade, B., and Dural, H. (2004). Gypsophila sphaerocephala Fenzl ex Tchihat.: a boron hyperaccumulator plant species that may phytoremediate soils with toxic B levels. *Turk. J. Bot.* 28, 273–278.

Bates, L. S., Waldren, R. P., and Teare, I. (1973). Rapid determination of free proline for water-stress studies. *Plant Soil* 39, 205–207. doi: 10.1007/BF00018060

Brdar, J. M., Zoric, M., Kondic, S. A., Maksimovic, I., Kobiljski, B., and Kraljevic, B. M. (2017). Boron tolerance in wheat accessions of different origin estimated in controlled and field conditions. *J. Agricult. Sci. Technol.* 19, 345–356.

Brdar-Jokanovic, M. (2020). Boron Toxicity and Deficiency in Agricultural Plants. *Int. J. Mol. Sci.* 21:1424. doi: 10.3390/ijms21041424

Brisco, E. I., Brown, L. K., and Olson, E. L. (2017). Fusarium head blight resistance in Aegilops tauschii. *Genet. Resour. Crop Evolut.* 64, 2049–2058. doi: 10.1007/s10722-017-0495-3

Camacho-Cristóbal, J. J., Navarro-Gochicoa, M. T., Rexach, J., González-Fontes, A., and Herrera-Rodríguez, M. B. (2018). "Chapter 6 - Plant Response to Boron Deficiency and Boron Use Efficiency in Crop Plants," in *Plant Micronutrient Use Efficiency*, eds M. A. Hossain, T. Kamiya, D. J. Burritt, L.-S. Phan Tran, and T. Fujiwara (Florida, FL: Academic Press), 109–121. doi: 10.1016/B978-0-12-812104-7.00007-1

Cartwright, B., Zarcinas, B., and Spouncer, L. (1986). Boron toxicity in South Australian barley crops. *Austral. J. Agricult. Res.* 37, 351–359. doi: 10.1071/AR9860351

Cervilla, L. M., Blasco, B., Rios, J. J., Romero, L., and Ruiz, J. M. (2007). Oxidative stress and antioxidants in tomato (Solanum lycopersicum) plants subjected to boron toxicity. *Ann. Bot.* 100, 747–756. doi: 10.1093/aob/mcm156

Cervilla, L. M., Blasco, B., Rios, J. J., Rosales, M. A., Sánchez-Rodríguez, E., Rubio-Wilhelmi, M. M., et al. (2012). Parameters Symptomatic for Boron Toxicity in Leaves of Tomato Plants. *J. Bot.* 2012, 1–17. doi: 10.1155/2012/726206

Choudhary, S., Zehra, A., Naeem, M., Khan, M. M. A., and Aftab, T. (2020). Effects of boron toxicity on growth, oxidative damage, antioxidant enzymes and essential oil fingerprinting in Mentha arvensis and Cymbopogon flexuosus. *Chem. Biol. Technol. Agricult.* 7:8. doi: 10.1186/s40538-019-0175-y

Coskun, Y., Olgunsoy, P., Karatas, N., Bulut, F., and Yarar, F. (2014). Mannitol application alleviates boron toxicity in wheat seedlings. *Communicat. Soil Sci. Plant Anal.* 45, 944–952. doi: 10.1080/00103624.2013.867054

Crespo-Herrera, L. A., Smith, C. M., Singh, R. P., and Åhman, I. (2013). Resistance to multiple cereal aphids in wheat–alien substitution and translocation lines. *Arthropod Plant Interact.* 7, 535–545. doi: 10.1007/s11829-013-9267-y

Davey, M., Stals, E., Panis, B., Keulemans, J., and Swennen, R. (2005). High-throughput determination of malondialdehyde in plant tissues. *Analyt. Biochem.* 347, 201–207. doi: 10.1016/j.ab.2005.09.041

Djanaguiraman, M., Prasad, P., Kumari, J., and Rengel, Z. (2019). Root length and root lipid composition contribute to drought tolerance of winter and spring wheat. *Plant Soil* 439, 57–73. doi: 10.1007/s11104-018-3794-3

Du, X., and Zhang, X. (2017). Molecular cloning and functional characterization of two novel high molecular weight glutenin subunit genes in Aegilops markgrafii. *J. Genet.* 96, 563–570. doi: 10.1007/s12041-017-0799-2

Edae, E. A., Olivera, P. D., Jin, Y., Poland, J. A., and Rouse, M. N. (2016). Genotype-by-sequencing facilitates genetic mapping of a stem rust resistance locus in Aegilops umbellulata, a wild relative of cultivated wheat. *BMC Genomics* 17:1–10. doi: 10.1186/s12864-016-3370-2

Emon, R., Gustafson, K., Bebeli, P., Jahiruddin, M., Haque, M., Ross, K., et al. (2012). Screening Aegilops-Triticum species for Boron tolerance. *Afr. J. Agricult. Res.* 7, 1631–1936. doi: 10.5897/AJAR11.2084

Eraslan, F., Inal, A., Gunes, A., and Alpaslan, M. (2007a). Impact of exogenous salicylic acid on the growth, antioxidant activity and physiology of carrot plants subjected to combined salinity and boron toxicity. *Sci. Horticult.* 113, 120–128. doi: 10.1016/j.scienta.2007.03.012

Eraslan, F., Inal, A., Savasturk, O., and Gunes, A. (2007b). Changes in antioxidative system and membrane damage of lettuce in response to salinity and boron toxicity. *Sci. Horticult.* 114, 5–10. doi: 10.1016/j.scienta.2007.05.002

Esim, N., Tiryaki, D., Karadagoglu, O., and Atici, O. (2013). Toxic effects of boron on growth and antioxidant system parameters of maize (Zea mays L.) roots. *Toxicol. Ind. Health* 29, 800–805. doi: 10.1177/0748233712442729

Funakawa, H., and Miwa, K. (2015). Synthesis of borate cross-linked rhamnogalacturonan II. *Front. Plant Sci.* 6:223. doi: 10.3389/fpls.2015.00223

Garg, M., Tsujimoto, H., Gupta, R. K., Kumar, A., Kaur, N., Kumar, R., et al. (2016). Chromosome specific substitution lines of Aegilops geniculata alter parameters of bread making quality of wheat. *PLoS One* 11:e0162350. doi: 10.1371/journal.pone.0162350

Ghaffari Nejad, S. A., Savaghebi, G. R., Farahbakhsh, M., Maali Amiri, R., and Rezaei, H. (2015). Tolerance of some wheat varieties to boron toxicity. *Cereal Res. Communicat.* 43, 384–393. doi: 10.1556/0806.43.2015.009

Green, A., Friebe, B., Prasad, P., and Fritz, A. (2018). Evaluating heat tolerance of a complete set of wheat-Aegilops geniculata chromosome addition lines. *J. Agronomy Crop Sci.* 204, 588–593. doi: 10.1111/jac.12282

Hairat, S., and Khurana, P. (2015). Evaluation of Aegilops tauschii and Aegilops speltoides for acquired thermotolerance: Implications in wheat breeding programmes. *Plant Physiol. Biochem.* 95, 65–74. doi: 10.1016/j.plaphy.2015.07.009

Hamurcu, M., Khan, K., Pandey, A., Avşaroğlu, Z. Z., Elbasan, F., and Gezgin, S. (2020a). Boron stress exposes differential antioxidant responses in maize cultivars (Zea mays L.). *J. Elementol.* 25, 1291–1304.

Hamurcu, M., Khan, M. K., Pandey, A., Ozdemir, C., Avsaroglu, Z. Z., Elbasan, F., et al. (2020b). Nitric oxide regulates watermelon (Citrullus lanatus) responses to drought stress. *3 Biotech* 10, 1–14. doi: 10.1007/s13205-020-02479-9

Hare, P. D., and Cress, W. A. (1997). Metabolic implications of stress-induced proline accumulation in plants. *Plant Growth Regulat.* 21, 79–102. doi: 10.1023/A:1005703923347

Hayes, J. E., and Reid, R. J. (2004). Boron tolerance in barley is mediated by efflux of boron from the roots. *Plant Physiol.* 136, 3376–3382. doi: 10.1104/pp.103.037028

Hong, Z., Lakkineni, K., Zhang, Z., and Verma, D. P. S. (2000). Removal of Feedback Inhibition of Δ1-Pyrroline-5-Carboxylate Synthetase Results in Increased Proline Accumulation and Protection of Plants from Osmotic Stress1. *Plant Physiol.* 122, 1129–1136. doi: 10.1104/pp.122.4.1129

Huang, S., Steffenson, B. J., Sela, H., and Stinebaugh, K. (2018). Resistance of Aegilops longissima to the rusts of wheat. *Plant Dis.* 102, 1124–1135. doi: 10.1094/PDIS-06-17-0880-RE

Jamjod, S. (1996). *Genetics of boron tolerance in durum wheat*. Adelaide: University of Adelaide.

Kalayci, M., Alkan, A., Cakmak, I., Bayramoğlu, O., Yilmaz, A., Aydin, M., et al. (1998). Studies on differential response of wheat cultivars to boron toxicity. *Euphytica* 100, 123–129. doi: 10.1023/A:1018312124300

Karabal, E., Yücel, M., and Öktem, H. A. (2003). Antioxidant responses of tolerant and sensitive barley cultivars to boron toxicity. *Plant Sci.* 164, 925–933. doi: 10.1016/S0168-9452(03)00067-0

Kavii Kishor, P. B., and Sreenivasulu, N. (2014). Is proline accumulation per se correlated with stress tolerance or is proline homeostasis a more critical issue? *Plant Cell Environ.* 37, 300–311. doi: 10.1111/pce.12157

Kaya, C., Akram, N. A., and Ashraf, M. (2018). Kinetin and indole acetic acid promote antioxidant defense system and reduce oxidative stress in maize (Zea mays L.) plants grown at boron toxicity. *J. Plant Growth Regulat.* 37, 1258–1266. doi: 10.1007/s00344-018-9827-6

Kiani, R., Arzani, A., and Habibi, F. (2015). Physiology of salinity tolerance in Aegilops cylindrica. *Acta Physiol. Plant.* 37, 1–10. doi: 10.1007/s11738-015-1881-0

Kishii, M. (2019). An update of recent use of Aegilops species in wheat breeding. *Front. Plant Sci.* 10:585. doi: 10.3389/fpls.2019.00585

Kishor, P. B. K., Sangam, S., Amrutha, R. N., Laxmi, P. S., Naidu, K. R., Rao, K. R. S. S., et al. (2005). Regulation of proline biosynthesis, degradation, uptake and transport in higher plants: Its implications in plant growth and abiotic stress tolerance. *Curr. Sci.* 88, 424–438.

Landi, M., Degl'Innocenti, E., Pardossi, A., and Guidi, L. (2012). Antioxidant and Photosynthetic Responses in Plants under Boron Toxicity: A Review. *Am. J. Agricult. Biol. Sci.* 7, 255–270. doi: 10.3844/ajabssp.2012.255.270

Landi, M., Margaritopoulou, T., Papadakis, I. E., and Araniti, F. (2019). Boron toxicity in higher plants: an update. *Planta* 250, 1011–1032. doi: 10.1007/s00425-019-03220-4

Landi, M., Remorini, D., Pardossi, A., and Guidi, L. (2013). Boron excess affects photosynthesis and antioxidant apparatus of greenhouse Cucurbita pepo and Cucumis sativus. *J. Plant Res.* 126, 775–786. doi: 10.1007/s10265-013-0575-1

Lee, A., Trinh, C. S., Lee, W. J., Kim, M., Lee, H., Pathiraja, D., et al. (2020). Characterization of two leaf rust-resistant Aegilops tauschii accessions for the synthetic wheat development. *Appl. Biol. Chem.* 63:13. doi: 10.1186/s13765-020-00496-z

Ma, C., Yang, Y., Li, X., Ge, P., Guo, G., Subburaj, S., et al. (2013). Molecular cloning and characterization of six novel HMW-GS genes from A egilops speltoides and A egilops kotschyi. *Plant Breeding* 132, 284–289. doi: 10.1111/pbr.12046

Mahalakshmi, V., Yau, S. K., Ryan, J., and Peacock, J. M. (1995). Boron toxicity in barley (Hordeum vulgare L.) seedlings in relation to soil temperature. *Plant Soil* 177, 151–156. doi: 10.1007/BF00010121

Mahboobi, H., Yucel, M., and Öktem, H. A. (2001). CELL WALL URONIC ACID CONCENTRATIONS OF RESISTANT AND SENSITIVE CULTIVARS OF WHEAT AND BARLEY UNDER BORON TOXICITY. *J. Plant Nutrit.* 24, 1965–1973. doi: 10.1081/PLN-100107608

Martin-Sanchez, J., Gomez-Colmenarejo, M., Del Moral, J., Sin, E., Montes, M., Gonzalez-Belinchon, C., et al. (2003). A new Hessian fly resistance gene (H30) transferred from the wild grass Aegilops triuncialis to hexaploid wheat. *Theoret. Appl. Genet.* 106, 1248–1255. doi: 10.1007/s00122-002-1182-z

Metwally, A., El-Shazoly, R., and Hamada, A. M. (2012). Effect of boron on growth criteria of some wheat cultivars. *J. Biol. Earth Sci.* 2, B1–B9.

Millet, E., Manisterski, J., Ben-Yehuda, P., Distelfeld, A., Deek, J., Wan, A., et al. (2014). Introgression of leaf rust and stripe rust resistance from Sharon goatgrass (Aegilops sharonensis Eig) into bread wheat (Triticum aestivum L.). *Genome* 57, 309–316. doi: 10.1139/gen-2014-0004

Mohamed, A. K., Qayyum, M. F., Shahzad, A. N., Gul, M., and Wakeel, A. (2016). Interactive Effect of Boron and Salinity on Growth, Physiological and Biochemical Attributes of Wheat (Triticum aestivum). *Int. J. Agricult. Biol.* 18, 238–244. doi: 10.17957/IJAB/15.0032

Molassiotis, A., Sotiropoulos, T., Tanou, G., Diamantidis, G., and Therios, I. (2006). Boron-induced oxidative damage and antioxidant and nucleolytic responses in shoot tips culture of the apple rootstock EM 9 (Malus domestica Borkh). *Environ. Exp. Bot.* 56, 54–62. doi: 10.1016/j.envexpbot.2005.01.002

Moody, D. B., Rathjen, A. J., and Cartwright, B. (1993). "Yield evaluation of a gene for boron tolerance using backcross-derived lines," in *Genetic Aspects of Plant Mineral Nutrition: The Fourth International Symposium on Genetic Aspects of Plant Mineral Nutrition, 30 September – 4 October 1991, Canberra, Australia*, eds P. J. Randall, E. Delhaize, R. A. Richards, and R. Munns (Dordrecht: Springer Netherlands), 363–366. doi: 10.1007/978-94-011-1650-3_45

Morales, M., and Munné-Bosch, S. (2019). Malondialdehyde: facts and artifacts. *Plant Physiol.* 180, 1246–1250. doi: 10.1104/pp.19.00405

Nable, R. O. (1988). Resistance to boron toxicity amongst several barley and wheat cultivars: a preliminary examination of the resistance mechanism. *Plant Soil* 112, 45–52. doi: 10.1007/BF02181751

Nable, R. O., Bañuelos, G. S., and Paull, J. G. (1997). Boron toxicity. *Plant Soil* 193, 181–198. doi: 10.1023/A:1004272227886

Nable, R. O., Cartwright, B., and Lance, R. C. (1990). "Genotypic differences in boron accumulation in barley: relative susceptibilities to boron deficiency and toxicity," in *Genetic aspects of plant mineral nutrition*, eds N. El Bassam, M. Dambroth, and B. C. Loughman (Berlin: Springer), 243–251. doi: 10.1007/978-94-009-2053-8_38

Nazari, M., Moosavi, S. S., and Maleki, M. (2018). Morpho-physiological and proteomic responses of Aegilops tauschii to imposed moisture stress. *Plant Physiol. Biochem.* 132, 445–452. doi: 10.1016/j.plaphy.2018.09.031

Neelam, K., Rawat, N., Tiwari, V., Prasad, R., Tripathi, S., Randhawa, G., et al. (2012). Evaluation and identification of wheat-Aegilops addition lines controlling high grain iron and zinc concentration and mugineic acid production. *Cereal Res. Communicat.* 40, 53–61. doi: 10.1556/CRC.40.2012.1.7

Nejad, S. G., Savaghebi, G., Farahbakhsh, M., Amiri, R. M., and Rezaei, H. (2015). Tolerance of some wheat varieties to boron toxicity. *Cereal Res. Commun.* 43, 384–393.

Olivera, P. D., Rouse, M. N., and Jin, Y. (2018). Identification of New Sources of Resistance to Wheat Stem Rust in Aegilops spp. in the Tertiary Genepool of Wheat. *Front. Plant Sci.* 9:1719. doi: 10.3389/fpls.2018.01719

Öz, M. T., Turan, Ö, Kayihan, C., Eyidoğan, F., Ekmekçi, Y., Yücel, M., et al. (2014). Evaluation of photosynthetic performance of wheat cultivars exposed to boron toxicity by the JIP fluorescence test. *Photosynthetica* 52, 555–563. doi: 10.1007/s11099-014-0065-2

Pallotta, M., Schnurbusch, T., Hayes, J., Hay, A., Baumann, U., Paull, J., et al. (2014). Molecular basis of adaptation to high soil boron in wheat landraces and elite cultivars. *Nature* 514, 88–91. doi: 10.1038/nature13538

Pandey, A., Khan, M. K., Hakki, E. E., Gezgin, S., and Hamurcu, M. (2019). Combined Boron Toxicity and Salinity Stress-An Insight into Its Interaction in Plants. *Plants* 8:364. doi: 10.3390/plants8100364

Pandey, A., Khan, M. K., Hakki, E. E., Thomas, G., Hamurcu, M., Gezgin, S., et al. (2016). Assessment of genetic variability for grain nutrients from diverse regions: potential for wheat improvement. *SpringerPlus* 5:1912. doi: 10.1186/s40064-016-3586-2

Papadakis, I. E., Dimassi, K. N., Bosabalidis, A. M., Therios, I. N., Patakas, A., and Giannakoula, A. (2004). Boron toxicity in 'Clementine' mandarin plants grafted on two rootstocks. *Plant Sci.* 166, 539–547. doi: 10.1016/j.plantsci.2003.10.027

Papadakis, I., Dimassi, K., and Therios, I. (2003). Response of two citrus genotypes to six boron concentrations: concentration and distribution of nutrients, total absorption, and nutrient use efficiency. *Austral. J. Agricult. Res.* 54, 571–580. doi: 10.1071/AR02163

Paull, J. G. (1990). *Genetic studies on the tolerance of wheat to high concentrations of boron*. Ph. D. thesis. Adelaide: University of Adelaide. doi: 10.1007/978-94-009-2053-8_54

Rakszegi, M., Molnár, I., Lovegrove, A., Darkó, É, Farkas, A., Láng, L., et al. (2017). Addition of Aegilops U and M chromosomes affects protein and dietary fiber content of wholemeal wheat flour. *Front. Plant Sci.* 8:1529. doi: 10.3389/fpls.2017.01529

Rani, K., Raghu, B. R., Jha, S. K., Agarwal, P., Mallick, N., Niranjana, M., et al. (2020). A novel leaf rust resistance gene introgressed from Aegilops markgrafii maps on chromosome arm 2AS of wheat. *Theoret. Appl. Genet.* 133, 2685–2694. doi: 10.1007/s00122-020-03625-w

Rao, K. M., and Sresty, T. (2000). Antioxidative parameters in the seedlings of pigeonpea (Cajanus cajan (L.) Millspaugh) in response to Zn and Ni stresses. *Plant Sci.* 157, 113–128. doi: 10.1016/S0168-9452(00)00273-9

Rehman, S., Park, T. I., Kim, Y. J., Seo, Y. W., and Yun, S. J. (2006). Inverse relationship between boron toxicity tolerance and boron contents of barley seed and root. *J. Plant Nutrit.* 29, 1779–1789. doi: 10.1080/01904160600897521

Reid, R. J., Hayes, J. E., Post, A., Stangoulis, J. C. R., and Graham, R. D. (2004). A critical analysis of the causes of boron toxicity in plants. *Plant Cell Environ.* 27, 1405–1414. doi: 10.1111/j.1365-3040.2004.01243.x

Reid, R., and Fitzpatrick, K. L. (2009). Redistribution of boron in leaves reduces boron toxicity. *Plant Signal. Behav.* 4, 1091–1093. doi: 10.4161/psb.4.11.9798

Rerkasem, B., and Jamjod, S. (1997). Genotypic variation in plant response to low boron and implications for plant breeding. *Plant Soil* 193, 169–180. doi: 10.1023/A:1004220226977

Rerkasem, B., Nirantrayagul, S., and Jamjod, S. (2004). Increasing boron efficiency in international bread wheat, durum wheat, triticale and barley germplasm will boost production on soils low in boron. *Field Crops Res.* 86, 175–184. doi: 10.1016/j.fcr.2003.08.009

Sakamoto, T., Inui, Y. T., Uraguchi, S., Yoshizumi, T., Matsunaga, S., Mastui, M., et al. (2011). Condensin II alleviates DNA damage and is essential for tolerance of boron overload stress in Arabidopsis. *Plant Cell* 23, 3533–3546. doi: 10.1105/tpc.111.086314

Samet, H., and Çıkılı, Y. (2019). Response of purslane (Portulaca oleracea L.) to excess boron and salinity: Physiological approach. *Russ. J. Plant Physiol.* 66, 316–325. doi: 10.1134/S1021443719020110

Schnurbusch, T., Langridge, P., and Sutton, T. (2008). The Bo1-specific PCR marker AWW5L7 is predictive of boron tolerance status in a range of exotic durum and bread wheats. *Genome* 51, 963–971. doi: 10.1139/G08-084

Suneja, Y., Gupta, A. K., and Bains, N. S. (2019). Stress Adaptive Plasticity: Aegilops tauschii and Triticum dicoccoides as Potential Donors of Drought Associated Morpho-Physiological Traits in Wheat. *Front. Plant Sci.* 10:211. doi: 10.3389/fpls.2019.00211

Sutton, T., Baumann, U., Hayes, J., Collins, N. C., Shi, B. J., Schnurbusch, T., et al. (2007). Boron-toxicity tolerance in barley arising from efflux transporter amplification. *Science* 318, 1446–1449. doi: 10.1126/science.1146853

Tang, S., Hu, Y., Zhong, S., and Luo, P. (2018). The potential role of powdery mildew-resistance gene Pm40 in Chinese wheat-breeding programs in the post-Pm21 Era. *Engineering* 4, 500–506. doi: 10.1016/j.eng.2018.06.004

Torun, A. A., Yazici, A., Erdem, H., and Çakmak, I. (2006). Genotypic variation in tolerance to boron toxicity in 70 durum wheat genotypes. *Turk. J. Agricult. For.* 30, 49–58.

Torun, B., Kalayci, M., Ozturk, L., Torun, A., Aydin, M., and Cakmak, I. (2002). Differences in Shoot Boron Concentrations, Leaf Symptoms, and Yield of Turkish Barley Cultivars Grown on Boron-Toxic Soil in Field. *J. Plant Nutrit.* 26, 1735–1747. doi: 10.1081/PLN-120023279

Wang, B.-L., Shi, L., Li, Y.-X., and Zhang, W.-H. (2010). Boron toxicity is alleviated by hydrogen sulfide in cucumber (Cucumis sativus L.) seedlings. *Planta* 231, 1301–1309. doi: 10.1007/s00425-010-1134-9

Wu, X., Lu, X., Riaz, M., Yan, L., and Jiang, C. (2018). Boron deficiency and toxicity altered the subcellular structure and cell wall composition architecture in two citrus rootstocks. *Sci. Horticult.* 238, 147–154. doi: 10.1016/j.scienta.2018.04.057

Yau, S. K., and Saxena, M. C. (1997). Variation in growth, development, and yield of durum wheat in response to high soil boron. I. Average effects. *Austral. J. Agricult. Res.* 48, 945–950. doi: 10.1071/A96144

Yau, S., Hamblin, J., and Ryan, J. (1994). *Phenotypic variation in boron toxicity tolerance in barley, durum and bread wheat [Hordeum vulgare, Triticum aestivum, Triticum durum]*. Haryana: Barley and Wheat Newsletter.

Yau, S., Nachit, M., Ryan, J., and Hamblin, J. (1995). Phenotypic variation in boron-toxicity tolerance at seedling stage in durum wheat (Triticum durum). *Euphytica* 83, 185–191. doi: 10.1007/BF01678128

Yau, S.-K., Nachit, M. M., and Ryan, J. (1997). "Variation in boron-toxicity tolerance in a durum wheat core collection," in *Boron in Soils and Plants*, eds R. W. Bell and B. Rerkasem (Berlin: Springer), 117–120. doi: 10.1007/978-94-011-5564-9_22

Yu, G., Zhang, Q., Friesen, T. L., Rouse, M. N., Jin, Y., Zhong, S., et al. (2015). Identification and mapping of Sr46 from Aegilops tauschii accession CIae 25 conferring resistance to race TTKSK (Ug99) of wheat stem rust pathogen. *Theoret. Appl. Genet.* 128, 431–443. doi: 10.1007/s00122-014-2442-4

Zhou, J., Yao, C., Yang, E., Yin, M., Liu, C., and Ren, Z. (2014). Characterization of a new wheat-Aegilops biuncialis addition line conferring quality-associated HMW glutenin subunits. *Genet. Mol. Res.* 13, 660–669. doi: 10.4238/2014.January.28.11

Conflict of Interest: The authors declare that the research was conducted in the absence of any commercial or financial relationships that could be construed as a potential conflict of interest.

Publisher's Note: All claims expressed in this article are solely those of the authors and do not necessarily represent those of their affiliated organizations, or those of the publisher, the editors and the reviewers. Any product that may be evaluated in this article, or claim that may be made by its manufacturer, is not guaranteed or endorsed by the publisher.

Copyright © 2021 Khan, Pandey, Hamurcu, Avsaroglu, Ozbek, Omay, Elbasan, Omay, Gokmen, Topal and Gezgin. This is an open-access article distributed under the terms of the Creative Commons Attribution License (CC BY). The use, distribution or reproduction in other forums is permitted, provided the original author(s) and the copyright owner(s) are credited and that the original publication in this journal is cited, in accordance with accepted academic practice. No use, distribution or reproduction is permitted which does not comply with these terms.

frontiers in Plant Science

ORIGINAL RESEARCH
published: 02 November 2021
doi: 10.3389/fpls.2021.719504

Insights Into Manganese Solubilizing *Bacillus* spp. for Improving Plant Growth and Manganese Uptake in Maize

Ayesha Ijaz[1], Muhammad Zahid Mumtaz[1], Xiukang Wang[2]*, Maqshoof Ahmad[3]*, Muhammad Saqib[4], Hira Maqbool[1], Ahmad Zaheer[1], Wenqiang Wang[2]* and Adnan Mustafa[5]*

[1] Institute of Molecular Biology and Biotechnology, The University of Lahore, Lahore, Pakistan, [2] College of Life Sciences, Yan'an University, Yan'an, China, [3] Department of Soil Science, The Islamia University of Bahawalpur, Bahawalpur, Pakistan, [4] Institute of Soil and Environmental Sciences, University of Agriculture, Faisalabad, Pakistan, [5] SoWa Research Infrastructure, Biology Centre CAS, České Budějovice, Czechia

OPEN ACCESS

Edited by:
Monica Höfte, Ghent University, Belgium

Reviewed by:
Amílcar Duarte, University of Algarve, Portugal
Nikos Tzortzakis, Cyprus University of Technology, Cyprus

***Correspondence:**
Muhammad Zahid Mumtaz
zahidses@gmail.com
Xiukang Wang
wangxiukang@yau.edu.cn
Maqshoof Ahmad
maqshoof_ahmad@yahoo.com
Wenqiang Wang
wenqiangwang@yau.edu.cn

Specialty section:
This article was submitted to Plant Nutrition, a section of the journal Frontiers in Plant Science

Received: *14 June 2021*
Accepted: *08 October 2021*
Published: *02 November 2021*

Citation:
Ijaz A, Mumtaz MZ, Wang X, Ahmad M, Saqib M, Maqbool H, Zaheer A, Wang W and Mustafa A (2021) Insights Into Manganese Solubilizing Bacillus spp. for Improving Plant Growth and Manganese Uptake in Maize. Front. Plant Sci. 12:719504. doi: 10.3389/fpls.2021.719504

Manganese (Mn) is an essential micronutrient for plant growth that is involved in the structure of photosynthetic proteins and enzymes. Mn deficiency is widespread mainly in dry, calcareous, and sandy soil, which leads to a significant decrease in crop yield. Mn-reducing bacteria promote the solubilization of Mn minerals, thus increasing Mn availability in soil. The present study aimed to assess the Mn solubilizing ability and plant growth-promoting potential of *Bacillus* spp. strains for maize plants with insoluble Mn compounds. Several Mn-solubilizing bacterial (MSB) strains were isolated from the maize rhizosphere using nutrient agar media amended with 50 mM MnO_2. These strains were screened based on qualitative and quantitative solubilization of Mn, phosphorus, potassium, and zinc and production of ammonia. The majority of MSB strains were positive for catalase, protease, amylase, and oxidase activity, while more than 60% of tested strains were positive for lipase activity, and the production of indole-3-acetic acid and siderophores. Forty-five percent of the tested strains also showed solubilization of potassium. All the MSB strains were evaluated for their ability to promote plant growth and Mn uptake in the presence of MnO_2 under axenic sand culture conditions. The results revealed that inoculation with MSB strains under sand culture significantly improved the growth of maize seedlings except for strains ASH7, ASH10, and ASH12. Comparatively, strains ASH6, ASH11, ASH19, ASH20, and ASH22 demonstrated a better increase in plant growth, fresh and dry biomass, and Mn uptake in roots and shoots than the other strains tested. All of these strains were identified as *Bacillus* spp. through 16S rRNA partial gene sequencing. Maize inoculation with these selected identified MSB strains also resulted in an increase in maize growth and nutrient uptake in maize roots and shoots under soil culture conditions in the presence of native soil Mn. The current study highlights the importance of MSB strain inoculation which could be a potential bioinoculants to promote plant growth under Mn deficiency.

Keywords: ***Bacillus* spp., manganese oxide, manganese reducing bacteria, minerals solubilization, rhizobacteria, *Zea mays***

INTRODUCTION

Plant health is of ultimate significance to agricultural productivity and prominently depends on a series of processes affecting physiological functioning. Plants cope with changes in environmental and edaphic factors and nutrient deficiency by adjusting metabolite compositions (Schöttler and Tóth, 2014). According to the classical Liebig law of the minimum, deficiency of any essential nutrients cannot be compensated by any other nutrients, which is why a balanced supply of essential plant nutrients is required for optimal plant growth (Whitcomb et al., 2014).

Manganese (Mn) is an essential micronutrient with many functional roles in plant physiology, especially in electron transport in photosystem II (PSII), chloroplast structure, and N metabolism (Campbell and Nable, 1988). Mn acts as an activator and cofactor of various metalloenzymes and catalyzes various enzyme reactions including redox reactions, phosphorylation, decarboxylation, and hydrolysis (Schmidt and Husted, 2019). Mn activates more than 35 enzymes, including phenylalanine ammonia-lyase decarboxylases, dehydrogenases, and different glycosyltransferases (White et al., 1993). Mn deficiency causes oxidative stress and a reduction in photosynthetic electron transport, water use efficiency, and root functioning (Schmidt et al., 2016). Its deficiency causes a reduction in the wealth of PSII light-harvesting complex II supercomplexes and D1 together with PSII membrane extrinsic proteins PsbP and PsbQ (Schmidt et al., 2015). In aging mesophyll cells of wheat, Mn deficiency causes an increase in Mn-superoxide dismutase activity from base to tip in leaves due to the production of reactive oxygen species in peroxisomes or the respiratory chain in mitochondria (Leonowicz et al., 2018). In maize (*Zea mays* L.), a deficiency of Mn disturbs N metabolism by restricting NO_3^- uptake and transportation by the production of inhibiting enzymes, *viz.* glutamine synthase, nitrate reductase, and glutamic-oxaloacetic transaminase cause a decline in chlorophyll synthesis and protein solubility (Gong et al., 2011).

Manganese biogeochemistry is complex in soil and exists in three oxidation states *viz.* Mn(II), Mn(III), and Mn(IV). Plants take up only the divalent form (Mn^{2+}) of Mn, while Mn(IV) is highly insoluble and precipitates in soil solution. Mn availability to plants is greatly influenced by soil pH and redox conditions as an increase in soil pH causes a reduction in its availability by forming MnO_2 complexes, while its availability increases under reduced O_2 conditions in terms of soil compaction and flooding (Schmidt et al., 2016; Schmidt and Husted, 2019). Its deficiency symptoms frequently appear patchy due to the irregular distribution of Mn-oxidizing and reducing soil conditions. Globally, Mn deficiency is a widespread problem mainly in dry, calcareous, and sandy soils (Hebbern et al., 2005; Schmidt et al., 2013). A significant reduction in crop yield was observed in Mn-deficient regions, while Mn deficiency in severe winters caused complete crop loss (Schmidt et al., 2013). The agronomic effectiveness of various inorganic and organic Mn fertilizers is greatly influenced by their solubility in water, application method, soil properties, and nature of any macronutrient carrier. Manganous sulfate is mostly applied to the soil and in foliar sprays to address Mn deficiency in crops; however, its efficiency is lower in alkaline and dry soils (Martens and Westermann, 1991).

Manganese (IV) is reduced to Mn(II) through biological or chemical processes due to the presence of protons and electron-carrying reducing agents produced by plant roots, microorganisms, or through organic matter decomposition (Uren, 1981). Various Mn-reducing microorganisms, e.g., *Arthrobacter*, *Acinetobacter*, *Achromobacter*, *Aspergillus*, *Bacillus*, *Clostridium*, *Enterobacter*, *Lysinibacillus*, *Micrococcus*, *Pseudomonas*, and *Staphylococcus*, have been reported in the literature (Baglin et al., 1992; Das et al., 2012; Ghosh et al., 2016). Inoculation with Mn-reducing microorganisms, especially bacteria, can improve Mn uptake and plant growth in Mn-deficient soil (Huber and McCay-Buis, 1993). Mn-reducing bacteria can be termed Mn-solubilizing bacterial (MSB) that promote Mn dissolution through protonation of metal anions and production of organic acids that form a soluble complex of Mn ligands (Wei et al., 2012). Recently, Tang et al. (2020) reported plant growth promotion and Mn accumulation in *Myriophyllum verticillatum* through inoculation with Mn-resistant *Bacillus cereus* WSE01. Numerous other researchers also reported an increase in Mn availability, uptake and plant growth promotion through inoculation of various mycorrhizae and soil bacterial strains (Bromfield and David, 1976; Nogueira et al., 2007).

Therefore, we investigated the effect of various *Bacillus* strains possessing multiple plant growth-promoting (PGP) characteristics with importance for maize growth promotion and Mn uptake under Mn-insoluble compounds. We proposed that bacterial strains with the ability to solubilize Mn compounds *in vitro* and possess multiple PGP attributes could improve maize growth and Mn uptake compared to the uninoculated control in the presence of insoluble Mn compounds. Our main goals were to (i) evaluate the *in vitro* Mn-solubilizing ability of various isolated bacterial strains; (ii) determine the bacterial ability to solubilize phosphorus (P), potassium (K), and zinc (Zn) *in vitro*; (iii) screen the bacterial strains for *in vitro* PGP characterization; and (iv) assess the impact of Mn-solubilizing strain inoculation on growth and Mn uptake in maize plants in the presence of insoluble Mn compounds.

MATERIALS AND METHODS

Isolation of Manganese-Tolerant Rhizobacteria

Manganese-tolerant rhizobacteria were isolated from the rhizosphere of maize grown in different farm fields located in Sargodha and Sheikhupura, Punjab, Pakistan. Rhizospheric samples were collected by uprooting maize seedlings in a sterile plastic polythene bag and transferred to the Laboratory of Microbiology, Institute of Molecular Biology and Biotechnology (IMBB), The University of Lahore (UOL), Lahore, Pakistan. The maize roots along with adhered soil were dipped in sterilized distilled water under aseptic conditions, and the resulting soil suspension was used for isolation of rhizobacterial isolates

through the serial dilution method. Nutrient agar (HiMedia Laboratories, India) media amended with 50 mM manganese oxide (MnO_2; Alfa Aesar, United States) was used for the isolation of Mn-resistant rhizobacteria. The serially diluted soil suspension was spread on nutrient agar plates by a glass spreader and inoculated at 30 ± 1°C for 48 h. The resulting fast-growing colonies with distinct morphological appearances were purified through the streak plate method and preserved at −20°C in 50% glycerol stock.

Manganese-Solubilization Assay

The Mn-tolerant isolates were screened for Mn solubilization by using nutrient agar media modified with MnO_2 (50 mM) (Sanket et al., 2017). The freshly grown isolates were spot inoculated on Mn-amended nutrient agar and plates were incubated at 30 ± 1°C for 72 h to observe the lightening of the dark brown color around the colonies. After incubation, the plates were flooded with iodine solution as an indicator to record clear zone diameter. The Mn-solubilizing diameter and bacterial growth diameter were taken using a meter rod on a mm scale, with five readings taken from each replication and averaged. The degree of Mn solubilization was determined by measuring the clearing halo zone around the colonies, and the Mn-solubilization index (MSI) and Mn-solubilization efficiency (MSE) were calculated using Formulas 1 and 2, respectively. Such rhizobacterial isolates were termed MSB strains and were selected to be evaluated for their multifunctional PGP characterization.

$$Mn\ solubilization\ index\ (MSI) = \frac{Mn\ solubilization\ diameter\ +\ Bacterial\ Colony\ Diameter}{Bacterial\ colony\ diameter} \quad (1)$$

$$Mn\ Solubilization\ Efficiency\ (MSE\ \%) = \frac{Mn\ Solubilization\ Diameter}{Bacterial\ Colony\ Diameter} \times 100 \quad (2)$$

The Mn-solubilized concentration by MSB strains was quantified by performing a quantitative Mn solubilization assay. Nutrient broth (HiMedia Laboratories, India) amended with 50 mM MnO_2 was inoculated with freshly grown strains and incubated with shaking (100 rpm) at 30 ± 1°C for 48 h. For comparison, uninoculated control nutrient broth amended with MnO_2 was also maintained simultaneously. After incubation, broth cultures were filtered with sterile Whatman No. 01 filter paper and wet digested to determine Mn concentration by following the method of Horwitz (2010). A measured volume of culture filtrate along with HNO_3 (2 mL) and HCl (10 mL) was taken in a conical flask and covered with a ribbed watch glass. The solution was placed on a hot plate and heated at 350°C to reduce the volume to 25 mL. Then digest was cooled, filtered, and diluted to 100 mL. The filtered digest was read using inductively coupled plasma optical emission spectroscopy (ICP-OES; Optima 7000DV, Perkin Elmer, United States) from the commercial service of Fish Quality Control Labs, Fisheries Research and Training Institute, Manawan, Lahore, Pakistan. The solubilized Mn concentration was determined by drawing calibration of Mn standard solutions of 0, 50, 100, 150, and 200 $\mu g\ L^{-1}$. To confirm the results of qualitative and quantitative Mn-solubilization, both assays were repeated twice in triplicate.

Mineral Solubilization Assays

Manganese-solubilizing strains were screened to evaluate their ability to solubilize P, K, and Zn using insoluble sources. These nutrient solubilization assays were performed by conducting qualitative and quantitative tests and repeated twice in triplicate. For P solubilization, freshly grown Mn-solubilizing strains were spot-inoculated on modified Pikovskaya (PVK) agar media (Pikovskaya, 1948) and incubated at 30 ± 1°C for 72 h. After incubation, the appearance of solubilization zones around spot inoculation was observed and measured through a meter rod on a mm scale. The P solubilization index (PSI) was calculated using the solubilization zone and bacterial growth diameter as reported by Ahmad et al. (2019). The P solubilization efficiency (PSE) was determined by multiplying the ratio of P-solubilizing diameter and bacterial colony diameter with factor of 100 (Ahmad et al., 2019). The P-solubilized concentration was quantified by inoculating Mn-solubilizing strains in PVK broth and incubated in a shaking incubator at 100 rpm and 30 ± 1°C for 72 h. After incubation, broth culture was centrifuged, and culture filtrate (10 mL) was taken in a 100 mL volumetric flask. Ammonium vanadate-molybdate reagent (10 mL) was added to a volumetric flask containing culture filtrate and diluted with distilled water up to the mark on the flask. A blank containing 10 mL ammonium vanadate-molybdate reagent was also added along with samples. The solutions were read through a spectrophotometer (Model G6860A, Agilent Technologies Cary 60 UV-Vis, Australia) at 420 nm (Ryan et al., 2001).

The MSB strains were screened for qualitative Zn solubilization by using Bunt and Rovira agar media amended with 1.24 g L^{-1} bulk insoluble zinc oxide (ZnO) powder (0.1% Zn) (Bunt and Rovira, 1955; Mumtaz et al., 2017, 2019). The MSB strains were spot inoculated for 7 days at 30 ± 1°C, and the Zn-solubilization zone was observed visually. The Zn solubilization index (ZSI) and Zn solubilization efficiency (ZSE) of MSB strains were calculated by measuring the Zn solubilization diameter and bacterial growth diameter by using the formula reported by Ahmad et al. (2019). A quantitative Zn solubilization assay was also performed by inoculating freshly grown MSB strains in Bunt and Rovira broth medium amended with 1.24 g L^{-1} ZnO and incubated at 30 ± 1°C for 7 days under 100 rpm shaking. After incubation, the bacterial culture was filtered and wet digested by following the method of Horwitz (2010). The filtered digest was read using ICP-OES, and the Zn concentration was estimated by drawing a calibration curve. The MSB strains were also screened for K solubilization using the spot inoculation method on modified Aleksandrov agar media amended with insoluble mouse powder (3.0 g L^{-1}) (Parmar and Sindhu, 2013). After 7 days of incubation at 30 ± 1°C, agar media was flooded with an iodine solution to observe the visual solubilization zone. The K solubilization zone and bacterial growth diameter were measured, and the K solubilization index (KSI) and K solubilization efficiency (KSE) were calculated as reported by Setiawati and Mutmainnah (2016).

In vitro Screening for Plant Growth-Promoting Characteristics

The MSB strains were characterized for indole-3-acetic acid (IAA) production in the presence of L-tryptophan by following the method of Bric et al. (1991). Strains with an optical density of 0.5 at 600 nm were inoculated in Dworkin and Foster (DF) minimal salt broth amended with 1.0 g L^{-1} L-tryptophan and incubated at 30 ± 1°C for 48 h. After incubation, bacterial culture was filtered and Salkowski reagent was added. Then, the OD of a mixer at 600 nm was recorded through a spectrophotometer, and the auxin concentration was determined by plotting the standard curve of the IAA standard solution. Siderophore production by MSB strains was determined by using a blue agar chrome azurol S (CAS) assay as reported by Louden et al. (2011). The strains were spot inoculated on blue agar CAS medium and incubated at 30 ± 1°C for 48 h. The production of orange halo zones around bacterial growth was observed and was considered siderophore positive. For ammonia (NH_3) production, strains were inoculated in peptone broth and incubated at 30 ± 1°C for 48 h. After incubation, culture filtrates were treated with Nessler's reagent, the production of yellow to brown color was observed (Cappuccino and Welsh, 2017), and OD at 530 nm was recorded through a spectrophotometer (Agilent Technologies, Australia). The extracellular enzymes *viz*. catalase, oxidase, amylase, protease, and lipase activities were determined by following the standard method of Cappuccino and Welsh (2017). The cell and colony morphology of MSB strains were also determined by following the protocol reported by Breakwell et al. (2007).

Screening for Maize Growth Promotion

A sand culture pot trial was conducted to screen the ability of the MSB strain to promote maize growth and Mn uptake in the presence of an insoluble Mn source in a sterilized pure sand culture. Pure sieved (2 mm) sand was amended with 50 mM MnO_2 and used to fill plastic pots (length 11 cm; top diameter 11 cm; and bottom diameter 6 cm). These pots were moistened with half-strength Mn-deficient Hoagland solution and autoclaved. To prevent oxidation, ferrous sulfate solution in water was autoclaved separately in a headspace of nitrogen in a tube with a fixed stopper and mixed with other contents of Hoagland solution after autoclaving. The MSB strains were cultured in DF minimal salt broth at 30 ± 1°C in a shaking incubator for 48 h. Maize seeds of variety Afghoi SG-2002 were disinfected by dipping in 95% ethanol for 5 min and then dipped in 0.2% mercury chloride ($HgCl_2$) solution for 3 min. Seeds were then washed several times with sterile distilled water. The surface-sterilized maize seeds were inoculated with bacterial cultures for 30 min. A total of six seeds were sown in each plastic pot and upon germination of maize, three maize seedling were maintained in each pot. For the control treatment, maize seeds were sown after soaking in DF minimal salt broth without bacterial inoculum. The pots were arranged in completely randomized design having three replications in the growth room under optimum conditions of 28 ± 2°C temperature along with 16 h of light and 8 h of a dark period. The pots were irrigated with an equal volume of half-strength Mn-deficient Hoagland solution. After 3 weeks of incubation, harvesting was performed, and growth parameters of plants, including shoot and root length, shoot fresh and dry biomass, and root fresh and dry biomass were recorded by following the standard methods reported by Mumtaz et al. (2017). Maize shoot and root samples were oven-dried and ground into a powder. One gram of maize shoot and root were wet digested by following the method reported in the above section of Mn concentration determination. The digested sample was diluted up to 50 mL and filtered. The digested samples were read using ICP-OES and the Mn concentration was calculated after plotting the calibration curve from the Mn standard solution (Horwitz, 2010).

Identification of Selected Manganese-Solubilizing Bacterial Strains

The MSB strains ASH6, ASH11, ASH19, ASH20, and ASH22 were selected based on their minerals solubilization and maize growth-promoting ability. The method of Cheneby et al. (2004) was adopted to extract the genomic DNA of selected strains through proteinase K treatment. The genomic DNA (2.5 μL) was amplified through a thermocycler (Eppendorf, United States) using universal primers targeting the 16S rRNA gene following the program reported by Mumtaz et al. (2017). The amplified PCR product was confirmed on a 1% agarose gel and subjected to sequencing from the commercial service of Macrogen (Seoul, South Korea). The resulting sequences were blasted using the MegaBlast service on NCBI servers. Closely matched sequences of strains were retrieved from a database, and a neighbor-joining phylogenetic tree was created using MEGA 7.0.14 software (Kumar et al., 2016). The sequences were submitted to the NCBI gene bank, and accession numbers of the MSB strains were obtained.

Pot Experiment

A soil culture pot experiment was performed to evaluate the effect of selected MSB strains *viz*. ASH6, ASH11, ASH19, ASH20, and ASH22 inoculation on maize growth and nutrient uptake. Bacterial cultures were prepared by growing them in nutrient broth amended with 50 mM MnO_2 in a shaking incubator at 30 ± 1°C and 100 rpm for 48 h of incubation. Maize seeds of the Afghoi SG-2002 variety were soaked in bacterial inoculum for 30 min. The uninoculated control treatment was prepared by soaking maize seeds in a similar MnO_2-amended nutrient broth but without bacterial inoculation. A total of six maize seeds inoculated with respective bacterial strains were sown in each pot and three maize seedling after germination were maintained for the experiment. This pot trial was conducted in a greenhouse of IMBB, UOL, Pakistan, located at Latitude: 31.39N, Longitude: 74.24E, and 206 meters elevation above sea level under natural climatic conditions. The soil was collected from farmer fields and analyzed for physicochemical characteristics (Ryan et al., 2001). The soil used for the experiment was sandy loam texture, 8.1 pH, 0.43 dS m^{-1} electrical conductivity, 0.30% organic matter, 0.02% total N, 5.5 mg kg^{-1} available P, 175 mg kg^{-1} extractable K, 14.36 mg kg^{-1} extractable Mn, and 26.90 mg kg^{-1} total Mn concentration. Pots 30.5 cm in width were filled with 10 kg of sieved soil, and maize seeds were sown. The pots were arranged in

completely randomized design, and treatments were replicated in triplicate. The plants were fertilized with two equal doses of 0.54 g of N in the form of urea and applied at the V2 and anthesis stages. The P (0.81 g) and K (0.54 g) were applied in each pot in the form of diammonium phosphate and sulfate of potash, respectively, at the time of sowing. Pots were irrigated with good-quality tap water, and thinning was performed after seed germination. At the cob formation stage, the chlorophyll contents of the second top leaf were recorded through a SPAD chlorophyll meter (Hansatech Instruments, England). At physiological maturity, the growth attributes, *viz*., plant height, root length, shoot dry weight, and root dry weight were recorded. Maize root and shoot samples were wet digested as reported in the above sections (Horwitz, 2010) and analyzed for N, P, K, and Mn concentrations. The plant digested samples were analyzed for the determination of total N through the Kjeldahl method, P concentration through a colorimetric method, and K concentration through a flame photometer (BWB Technologies, United Kingdom; Jackson, 1962). The plant digested samples were also analyzed for Mn concentration using ICP-OES as reported in the above section.

Statistical Analysis

A statistical method was employed to characterize and predict the ability of the MSB strain to promote maize growth. The MSB strain characterization and pot trial data were subjected to one-way analysis of variance (ANOVA) by employing a model completely randomized design with the computer software Statistix v. 8.1. The standard error of three replications in each MSB treatment was calculated by dividing the standard deviation by the square root of three by using Microsoft Excel 2019. The treatment means were compared through the least significant difference (LSD) test at a 5% probability level (Steel et al., 1997). The pairwise Pearson correlation analysis between the nutrient concentration in roots and shoots of maize in soil culture pot trial was performed using computer software Origin Pro 2021 (OriginLab Corporation, Northampton, MA, United States).

RESULTS

Isolation of Manganese-Solubilizing Bacterial Strains

In the present study, a total of 50 Mn-tolerant isolates were isolated from the maize rhizosphere and were coded A1, A2, A3 . . .A50. These isolates were screened for Mn solubilization by growing on nutrient agar amended with insoluble MnO_2. Thirteen Mn-tolerant isolates showing solubilization of Mn were coded as ASH4, ASH6, ASH7, ASH8, ASH9, ASH10, ASH11, ASH12, ASH17, ASH19, ASH20, ASH22, and ASH24. The qualitative Mn solubilization ability of these strains is presented in **Table 1** and **Figure 1**. *In vitro* screening of selected strains for MnO_2 solubilization showed that the Mn solubilization diameter ranged from 7.5 ± 0.03 mm to 35.5 ± 1.06 mm, while the bacterial growth diameter ranged from 7.0 ± 0.01 mm to 19.0 ± 0.70 mm. The maximum Mn solubilization diameter and bacterial growth diameter were reported by strain ASH22. Strain ASH20 showed a comparatively lower growth diameter; however, strain ASH20 showed a better solubilization diameter after strain ASH22 and was non-significant to strain ASH10. The lowest Mn solubilization diameter was obtained with strain ASH9.

The data regarding MSI and MSE calculated through Mn solubilization diameter and bacterial growth diameter showed

TABLE 1 | Qualitative and quantitative solubilization of manganese by rhizobacterial strains isolated from maize rhizosphere.

Strains	MSD (mm)	BGD (mm)	MSI	MSE (%)	SMC (μg mL^{-1})
Control	ND	ND	ND	ND	3.42 ± 0.11^{e}
ASH4	26.00 ± 0.70^{c}	10.50 ± 0.35^{b-e}	3.47 ± 0.01^{b}	247.73 ± 1.60^{b}	3.59 ± 0.02^{e}
ASH6	25.54 ± 0.35^{cd}	14.00 ± 1.41^{b}	2.86 ± 0.07^{b}	186.46 ± 21.36^{b}	10.73 ± 0.59^{a}
ASH7	9.50 ± 0.03^{g}	8.45 ± 0.03^{cde}	2.12 ± 0.03^{b}	111.80 ± 0.49^{b}	3.66 ± 0.12^{e}
ASH8	8.05 ± 0.01^{g}	7.02 ± 0.01^{e}	2.14 ± 0.01^{b}	114.30 ± 0.01^{b}	3.80 ± 0.17^{e}
ASH9	7.50 ± 0.03^{g}	6.50 ± 0.03^{e}	2.15 ± 0.02^{b}	115.50 ± 0.84^{b}	3.69 ± 0.04^{e}
ASH10	29.50 ± 0.35^{b}	12.21 ± 1.41^{bcd}	3.52 ± 0.12^{b}	252.14 ± 26.76^{b}	3.79 ± 0.14^{e}
ASH11	12.45 ± 0.03^{f}	11.00 ± 0.02^{b-e}	2.14 ± 0.03^{b}	113.60 ± 3.21^{b}	6.58 ± 0.27^{b}
ASH12	26.00 ± 0.01^{c}	13.00 ± 0.21^{bc}	3.11 ± 0.13^{b}	211.73 ± 34.47^{b}	3.80 ± 0.02^{e}
ASH17	23.55 ± 1.06^{d}	13.50 ± 0.35^{b}	2.74 ± 0.06^{b}	173.90 ± 3.30^{b}	3.56 ± 0.13^{e}
ASH19	14.03 ± 0.01^{ef}	12.00 ± 0.01^{bc}	2.17 ± 0.02^{b}	116.70 ± 0.02^{b}	4.89 ± 0.06^{c}
ASH20	29.00 ± 0.70^{b}	7.50 ± 2.47^{de}	5.86 ± 1.26^{a}	486.36 ± 151.06^{a}	10.08 ± 0.35^{a}
ASH22	35.51 ± 1.06^{a}	19.00 ± 0.70^{a}	2.87 ± 0.05^{b}	186.94 ± 1.37^{b}	5.87 ± 0.13^{bc}
ASH24	16.01 ± 0.01^{e}	9.50 ± 1.06^{b-e}	2.73 ± 0.08^{b}	172.73 ± 19.28^{b}	3.59 ± 0.12^{e}
LSD	1.09	2.27	0.89	88.72	0.31

The strains showed qualitative and quantitative solubilization of manganese (Mn) and were termed Mn-solubilizing bacterial (MSB) strains; qualitative Mn solubilization by MSB strains was determined by spot inoculating bacterial biomass on MnO_2-amended nutrient agar media and Mn solubilization diameter (MSD) was recorded after 48 h of incubation; Mn solubilization index (MSI) and Mn solubilization efficiency (MSE) were calculated by using MSD and bacterial growth diameter (BGD); quantitative Mn solubilization was estimated through inoculating the strains in MnO_2-amended nutrient broth media and solubilized Mn concentration (SMC) was detected through inductively coupled plasma optical emission spectroscopy; data presented are the mean of three replications ± standard error and least significant difference (LSD) test was performed at 5% ($p \leq 0.05$) probability level; the means in a vertical line for each attributes sharing common letters were considered statistically similar to each other; ND, not detected.

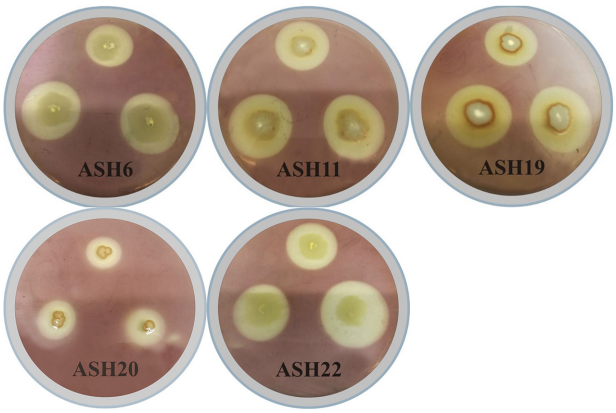


FIGURE 1 | Solubilization of manganese oxide (MnO_2) by manganese solubilizing bacterial (MSB) strains *viz*. ASH6, ASH11, ASH19, ASH20, and ASH22 on MnO_2-amended nutrient agar medium for 48 h; After incubation, dilute iodine solution was flooded on agar medium and appearance of manganese solubilization zone around bacterial growth was considered positive for solubilization of MnO_2.

that the most efficient strain was ASH20 which reported 5.86 ± 1.26 MSI and 486.4 ± 151.06% MSE (**Table 1**). The strains ASH4, ASH10, and ASH12 also showed better MSI and MSE and were non-significant to each other and other tested strains except strain ASH20. The strains ASH7, ASH8, and ASH9 showed the lowest MSI and MSE. The strains ASH6 (10.73 ± 0.59 μg mL^{-1}) and ASH20 (10.08 ± 0.35 μg mL^{-1}) reported maximum Mn solubilized concentration and were non-significant to each other. Following these strains, ASH11 (6.58 ± 0.27 μg mL^{-1}) and ASH22 (5.87 ± 0.13 μg mL^{-1}) also showed better Mn solubilized concentrations and were non-significant to each other. The control broth showed a Mn concentration of 3.42 ± 0.11 μg mL^{-1} and was non-significant with the solubilized Mn concentration by strains ASH4, ASH7, ASH8, ASH9, ASH12, ASH17, and ASH24.

In vitro Mineral Solubilization by Manganese-Solubilizing Bacterial Strains

A qualitative P solubilization assay revealed that all the MSB strains were positive for P solubilization (**Table 2** and **Figure 2**). The maximum P solubilization diameter (25.7 ± 0.72 mm) and bacterial growth diameter (21.7 ± 0.72 mm) were shown by strain ASH17. The strains ASH12, ASH19, and ASH20 also showed better P solubilization diameters and bacterial growth diameters and were non-significant to each other but significant to the other tested strains. The minimum P solubilization diameter (10.0 ± 0.09 mm) and bacterial growth diameter (4.3 ± 0.27 mm) were reported by strain ASH6. Strains ASH6, ASH8, and ASH11 showed maximum PSIs (3.33 ± 0.10, 3.11 ± 0.07, and 3.28 ± 0.11, respectively) and PSEs (232.9 ± 13.61, 211.0 ± 9.07, and 227.8 ± 12.02, respectively) and were non-significant to each other but significant from the other tested strains. Quantitative P solubilization revealed that the maximum solubilized P concentration was obtained from strain ASH12 (6.67 ± 0.69 μg mL^{-1}), followed by strain ASH22 (4.26 ± 0.07 μg mL^{-1}). The uninoculated control broth reported a P concentration of 0.43 ± 0.02 μg mL^{-1} (**Table 2**).

A qualitative assay for Zn solubilization revealed that all the tested bacterial strains were positive for Zn solubilization and data are given in **Table 3** and **Figure 2**. Strain ASH4 a

TABLE 2 | Qualitative and quantitative solubilization of phosphorus by manganese solubilizing bacterial strains isolated from maize rhizosphere.

Strains	PSD (mm)	BGD (mm)	PSI	PSE (%)	SPC (μg mL^{-1})
Control	ND	ND	ND	ND	0.43 ± 0.02^{e}
ASH4	13.67 ± 0.27^{de}	9.33 ± 0.27^{f}	2.47 ± 0.03^{c}	147.16 ± 3.78^{c}	1.67 ± 0.12^{cd}
ASH6	10.00 ± 0.09^{f}	4.33 ± 0.27^{g}	3.33 ± 0.10^{a}	232.93 ± 13.61^{a}	2.27 ± 0.24^{c}
ASH7	11.33 ± 0.54^{ef}	6.33 ± 0.54^{g}	2.80 ± 0.02^{b}	180.95 ± 7.77^{b}	1.93 ± 0.26^{cd}
ASH8	14.00 ± 0.94^{d}	6.65 ± 0.54^{g}	3.11 ± 0.07^{a}	211.11 ± 9.07^{a}	2.50 ± 0.79^{c}
ASH9	18.66 ± 0.27^{c}	12.67 ± 0.27^{de}	2.47 ± 0.01^{c}	147.44 ± 1.04^{c}	1.80 ± 0.32^{cd}
ASH10	12.10 ± 0.47^{def}	6.65 ± 0.27^{g}	2.82 ± 0.12^{b}	181.75 ± 14.64^{b}	0.63 ± 0.05^{d}
ASH11	11.33 ± 1.08^{ef}	5.00 ± 0.47^{g}	3.28 ± 0.11^{a}	227.78 ± 12.02^{a}	1.83 ± 0.21^{cd}
ASH12	23.00 ± 0.81^{b}	15.66 ± 1.18^{bc}	2.48 ± 0.05^{c}	148.29 ± 6.68^{c}	6.67 ± 0.69^{a}
ASH17	25.67 ± 0.72^{a}	21.67 ± 0.72^{a}	2.19 ± 0.07^{d}	118.12 ± 0.63^{d}	2.50 ± 0.41^{c}
ASH19	22.33 ± 1.18^{b}	18.00 ± 0.94^{b}	2.24 ± 0.09^{cd}	124.07 ± 0.75^{cd}	1.83 ± 0.59^{cd}
ASH20	21.67 ± 0.72^{b}	17.33 ± 0.98^{bc}	2.25 ± 0.06^{cd}	125.54 ± 3.19^{cd}	0.73 ± 0.09^{d}
ASH22	18.00 ± 0.47^{c}	15.00 ± 0.81^{cd}	2.21 ± 0.04^{cd}	120.07 ± 4.37^{cd}	4.26 ± 0.07^{b}
ASH24	14.00 ± 0.47^{d}	11.33 ± 0.54^{ef}	2.24 ± 0.03^{cd}	122.89 ± 3.17^{cd}	0.80 ± 0.08^{d}
LSD	1.21	1.16	0.14	13.48	0.67

Manganese solubilizing bacterial (MSB) strains were screened for qualitative solubilization of phosphorus (P) by spot inoculating bacterial biomass on Pikovskaya (PVK) agar media; P solubilization diameter (PSD) and bacterial growth diameter (BGD) were recorded after 7 days of incubation; the P solubilization index (PSI) and P solubilization efficiency (PSE) were calculated through using PSD and BGD; the quantitative P solubilization was determined by inoculating PVK broth for 7 days and solubilized P concentration (SPC) was detected through a colorimetric method by using a spectrophotometer; data presented are the mean of three replications ± standard error and least significant difference (LSD) test was performed at 5% ($p \leq 0.05$) probability level; the means in a vertical line for each attributes sharing common letters were considered statistically similar to each other; ND, not detected.

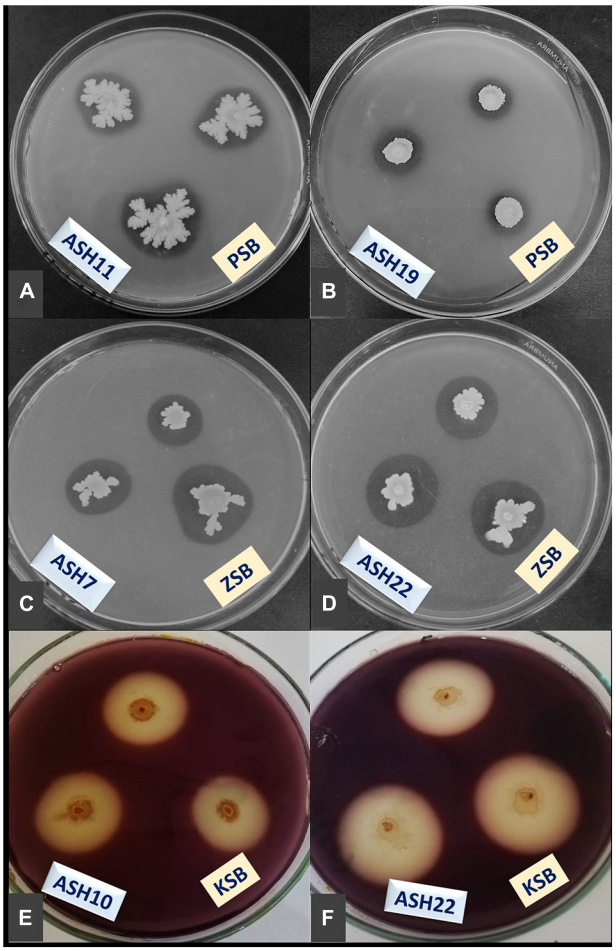


FIGURE 2 | Demonstration of minerals solubilization; phosphorus (P) by ASH11 **(A)** and ASH19 **(B)**, zinc (Zn) by ASH7 **(C)** and ASH22 **(D)**, and potassium (K) by ASH10 **(E)** and ASH22 **(F)**; manganese solubilizing bacterial (MSB) strains were spot inoculated on Pikovskaya agar amended with tri-calcium phosphate and tris-minimal salt agar amended with zinc oxide for P and Zn solubilization; K solubilization was determined by inoculating MSB strains on mica-amended Aleksandrov agar media; these solubilization assays were incubated for 7 days and appearance of solubilization zones were considered positive for respective mineral solubilization; K solubilization zones were observed through diluting agar media with dilute iodine solution for 10 min; PSB, P solubilizing bacteria; ZSB, Zn solubilizing bacteria; KSB, K solubilizing bacteria.

reported maximum growth diameter of 19.0 ± 2.12 mm and Zn solubilization diameter of 28.5 ± 1.76 mm. Strains ASH7, ASH10, and ASH20 also showed better Zn solubilization diameters of 22.0 ± 1.41 mm, 20.0 ± 0.65 mm, and 22.2 ± 0.35 mm, respectively, and were non-significant to each other; however, they were significant to the other tested strains. For ZSI and ZSE values, ASH19 was the leading strain having maximum values of 4.73 ± 0.33 for ZSI and 372.3 ± 37.12% for ZSE followed by strain ASH8, having 4.63 ± 0.08 for ZSI and 361.8 ± 8.83% for ZSE. The better qualitative Zn solubilizing strains ASH6, ASH11, ASH19, ASH20, and ASH22 were tested in a quantitative assay for solubilization of Zn, and data are presented in **Table 3**. The uninoculated control was composed of 0.12 ± 0.01 μg mL^{-1} Zn. Strain ASH19 reported a maximum solubilized Zn concentration of 23.17 ± 0.21 μg mL^{-1}, followed by strain ASH22, which solubilized Zn concentrations up to 22.05 ± 0.19 μg mL^{-1}. The MSB strains were also screened for qualitative K solubilization, and the data are reported in **Table 4** and **Figure 2**. The results revealed that six bacterial strains (ASH4, ASH10, ASH12, ASH17, ASH20, and ASH22) out of 13 tested MSB strains showed K solubilization. Strain ASH22 gave a maximum K solubilization diameter of 25.5 ± 1.76 mm having bacterial growth diameter of 3.5 ± 0.35 mm followed by ASH4 which reported 25 ± 1.41 mm of K solubilization diameter and 5.0 ± 0.70 mm of bacterial growth diameter. Strain ASH22 reported a maximum KSI of 8.33 ± 0.20 and KSE of 733.2 ± 23.57%, followed by strain ASH12, which had a KSI of 8.04 ± 0.87 and KSE of 704.4 ± 91.33%. Both of these strains were non-significant for ASH4 and ASH10 (**Table 4**).

In vitro Characterization of Manganese-Solubilizing Bacterial Strains

The MSB strains were evaluated *in vitro* for PGP characteristics and enzymatic activities, and findings are depicted in **Table 5**. The MSB strains were tested for IAA production in the presence of L-tryptophan, and the results revealed that eight out of thirteen strains were able to produce IAA. The maximum IAA of 24.76 ± 0.42 μg mL^{-1} was produced by strain ASH17 followed by strain ASH10 which had 23.13 ± 1.73 μg mL^{-1} IAA. Both of these strains were non-significant to each other but significantly different from the other tested strains. The strains ASH11 (19.99 ± 0.28 μg mL^{-1}) and ASH19 (18.73 ± 0.12 μg mL^{-1}) also showed significantly better IAA production and were statistically similar to each other. NH_3 production in terms of OD revealed that strains ASH4 and ASH10 were statistically similar to each and reported maximum ODs of 1.57 ± 0.15 and 1.36 ± 0.06, respectively. Strains ASH9 and ASH11 also showed better NH_3 production up to 1.16 ± 0.04 and 1.11 ± 0.08, respectively, while the uninoculated control reported minimum NH_3 production (0.46 ± 0.04). Siderophore production was recorded in terms of the appearance of the halo zone around bacterial growth on CAS agar medium as shown in **Supplementary Figure 1**. Eight out of thirteen MSB strains were positive for siderophore production (**Supplementary Figure 2**). The amylase, lipase, and protease activities were determined by inoculating strains on respective agar media, and the results were observed in terms of the appearance of a halo zone around bacterial growth, as shown in **Supplementary Figure 3**. All the tested strains were positive for protease activity except strain ASH24, while strains ASH7, ASH8, and ASH19 were unable to perform amylase activity. The majority of MSB strains were also positive for lipase activity, while, strains ASH6, ASH9, and ASH12 were negative for catalase activity. All the strains were also positive for oxidase activity except strains ASH6, ASH9, and ASH19. A bacterial morphological chart was made by observing different morphological characteristics in terms of color, texture, margin, elevation, and form (**Supplementary Table 1**). Morphological observation revealed that most of the tested strain colonies

TABLE 3 | Qualitative and quantitative solubilization of zinc by manganese solubilizing bacterial strains isolated from maize rhizosphere.

Strains	ZSD (mm)	BGD (mm)	ZSI	ZSE (%)	SZC ($\mu g\ mL^{-1}$)
Control	ND	ND	ND	ND	0.12 ± 0.01^{f}
ASH4	28.50 ± 1.76^{a}	19.00 ± 2.12^{a}	3.52 ± 0.13^{cde}	151.37 ± 7.63^{cde}	NT
ASH6	18.50 ± 0.03^{cde}	10.00 ± 0.70^{bc}	2.86 ± 0.02^{cd}	185.86 ± 9.64^{cd}	16.54 ± 0.14^{d}
ASH7	22.00 ± 1.41^{bc}	11.50 ± 1.06^{bc}	2.92 ± 0.05^{c}	192.13 ± 5.43^{c}	NT
ASH8	14.50 ± 0.35^{fgh}	4.00 ± 0.01^{e}	4.63 ± 0.08^{ab}	361.80 ± 8.83^{ab}	NT
ASH9	13.00 ± 1.41^{gh}	9.00 ± 0.70^{cd}	2.44 ± 0.11^{cde}	143.15 ± 4.41^{cde}	NT
ASH10	20.00 ± 0.65^{bcd}	12.00 ± 0.02^{bc}	2.67 ± 0.40^{cde}	166.36 ± 0.02^{cde}	NT
ASH11	12.50 ± 0.35^{h}	4.00 ± 0.01^{e}	4.13 ± 0.08^{b}	311.90 ± 8.83^{b}	17.86 ± 0.25^{c}
ASH12	$16.00 \pm 0.01^{e-h}$	12.50 ± 0.35^{bc}	2.28 ± 0.06^{e}	128.02 ± 3.62^{e}	NT
ASH17	17.45 ± 0.35^{def}	13.00 ± 0.70^{b}	2.35 ± 0.02^{de}	135.42 ± 4.62^{de}	NT
ASH19	$16.50 \pm 0.35^{d-g}$	4.50 ± 0.35^{e}	4.73 ± 0.33^{a}	372.30 ± 37.12^{a}	23.17 ± 0.21^{a}
ASH20	22.20 ± 0.35^{b}	12.00 ± 0.70^{bc}	2.88 ± 0.01^{cd}	188.14 ± 8.15^{cd}	12.20 ± 0.31^{e}
ASH22	8.50 ± 0.35^{i}	6.00 ± 0.04^{de}	2.42 ± 0.05^{cde}	141.07 ± 5.89^{cde}	22.05 ± 0.19^{b}
LSD	1.63	1.62	0.25	24.97	0.42

Manganese solubilizing bacterial (MSB) strains were screened for qualitative solubilization of zinc (Zn) by spot inoculating bacterial biomass on ZnO_2-amended tris-minimal salt agar media. Zn solubilization diameter (ZSD) and bacterial growth diameter (BGD) were recorded after 7 days of incubation; the Zn solubilization index (ZSI) and Zn solubilization efficiency (ZSE) were calculated through using ZSD and BGD; the quantitative Zn solubilization was determined by inoculating the ZnO_2-amended tris-minimal salt broth for 7 days and solubilized Zn concentration (SZC) was detected through inductively coupled plasma optical emission spectroscopy; data presented here are the mean of three replications ± standard error and least significant difference (LSD) test was performed at 5% ($p \leq 0.05$) probability level; the means in a vertical line for each attributes sharing common letters were considered statistically similar to each other; NT, not tested.

TABLE 4 | Qualitative solubilization of potassium by manganese solubilizing bacterial strains isolated from maize rhizosphere.

Strains	KSD (mm)	BGD (mm)	KSI	KSE (%)
ASH4	25.00 ± 1.41^{a}	5.00 ± 0.70^{b}	6.13 ± 0.37^{ab}	512.50 ± 44.19^{ab}
ASH6	ND	ND	ND	ND
ASH7	ND	ND	ND	ND
ASH8	ND	ND	ND	ND
ASH9	ND	ND	ND	ND
ASH10	23.50 ± 1.06^{a}	5.00 ± 0.70^{b}	5.96 ± 0.84^{ab}	495.83 ± 91.33^{ab}
ASH11	ND	ND	ND	ND
ASH12	24.00 ± 0.70^{a}	3.50 ± 0.35^{b}	8.04 ± 0.87^{a}	704.17 ± 91.33^{a}
ASH17	22.00 ± 1.41^{a}	8.00 ± 0.70^{a}	3.76 ± 0.02^{bc}	276.19 ± 6.73^{bc}
ASH19	ND	ND	ND	ND
ASH20	8.00 ± 0.01^{b}	4.50 ± 0.35^{b}	2.80 ± 0.10^{c}	180.00 ± 14.14^{c}
ASH22	25.50 ± 1.76^{a}	3.50 ± 0.35^{b}	8.33 ± 0.20^{a}	733.33 ± 23.57^{a}
ASH24	ND	ND	ND	ND
LSD	2.42	1.12	1.14	113.84

Manganese solubilizing bacterial strains (MSB); the MSB strains were screened for qualitative solubilization of potassium (K) by spot inoculating bacterial biomass on mica-amended Aleksandrov agar media for 7 days and K solubilization diameter (KSD) and bacterial growth diameter (BGD) were recorded; the K solubilization index (KSI) and K solubilization efficiency (KSE) were calculated through using KSD and BGD; data presented here are the mean of three replications ± standard error and least significant difference (LSD) test was performed at 5% ($p \leq 0.05$) probability level; the means in a vertical line for each attributes sharing common letters were considered statistically similar to each other; ND, not detected.

were of white to yellow in color, circular in shape, smooth in appearance with raised elevation and entire margin.

Promotion of Maize Growth Under the Axenic Condition

The MSB strains were screened for their ability to promote maize growth and Mn uptake under axenic conditions in a pure sand culture amended with a MnO_2 pot trial. The maize seeds inoculated with MSB strains having the ability to solubilize Mn and other minerals significantly promoted maize growth after 21 days of germination (**Figures 3**, **4**). The uninoculated control reported minimum shoot length (29.66 ± 1.18 cm), root length (18.66 ± 0.72 cm), shoot fresh biomass (0.76 ± 0.07 g), root fresh biomass (0.51 ± 0.03 g), shoot dry biomass (0.15 ± 0.01 g), root dry biomass (0.22 ± 0.03 g), total fresh biomass (1.28 ± 0.10 g), and total dry biomass (0.37 ± 0.04 g) (**Figures 5**, **6**). Compared to the uninoculated control, the majority of MSB strains promoted maize growth attributes in the presence of an insoluble source of Mn; however strains ASH7, ASH10, and ASH12 were unable to promote maize growth compared to the uninoculated control and were considered non-PGP MSB strains. The effect of MSB

TABLE 5 | Plant growth-promoting characteristics and enzymatic activities by manganese solubilizing strains isolated from maize rhizosphere.

Strains	IAA Prod. ($\mu g\ mL^{-1}$)	NH_3 Prod.	Siderophores	Catalase activity	Protease activity	Amylase activity	Lipase activity	Oxidase activity
Control	4.92 ± 0.22^{f}	0.46 ± 0.04^{g}	ND	ND	ND	ND	ND	ND
ASH4	7.86 ± 0.59^{e}	1.57 ± 0.15^{a}	+ve	+ve	+ve	+ve	+ve	+ve
ASH6	16.99 ± 1.74^{c}	0.56 ± 0.05^{fg}	−ve	−ve	+ve	+ve	+ve	−ve
ASH7	ND	0.88 ± 0.05^{de}	−ve	+ve	+ve	−ve	+ve	+ve
ASH8	ND	0.42 ± 0.03^{g}	+ve	+ve	+ve	−ve	+ve	+ve
ASH9	ND	1.16 ± 0.04^{bc}	−ve	−ve	+ve	+ve	−ve	−ve
ASH10	23.13 ± 1.73^{a}	1.36 ± 0.06^{ab}	+ve	+ve	+ve	+ve	−ve	+ve
ASH11	19.99 ± 0.28^{b}	1.11 ± 0.08^{bcd}	+ve	+ve	+ve	+ve	+ve	+ve
ASH12	ND	0.58 ± 0.08^{fg}	+ve	−ve	+ve	+ve	+ve	+ve
ASH17	24.76 ± 0.42^{a}	1.11 ± 0.03^{cd}	+ve	+ve	+ve	+ve	+ve	+ve
ASH19	18.73 ± 0.12^{bc}	0.78 ± 0.02^{ef}	−ve	+ve	+ve	−ve	−ve	−ve
ASH20	12.56 ± 0.61^{d}	0.41 ± 0.01^{g}	+ve	+ve	+ve	+ve	−ve	+ve
ASH22	10.13 ± 0.59^{de}	1.08 ± 0.09^{cd}	−ve	+ve	+ve	+ve	−ve	+ve
ASH24	ND	1.22 ± 0.08^{bc}	+ve	+ve	−ve	+ve	+ve	+ve
LSD	1.31	0.12	ND	ND	ND	ND	ND	ND

Manganese solubilizing bacterial (MSB) strains were screened for various biochemical characterization responsible for plant growth promotion and enzymatic activities; data presented are the mean of three replications ± standard error; the means in a vertical line for each attributes sharing common letters were considered statistical similar to each other and least significant difference (LSD) test was performed at 5% ($p \leq 0.05$) probability level.
The symbol, +ve represents the presence of the traits while the symbol, −ve shows the absence of the trait; ND, not detected.

strains on shoot growth is shown in **Supplementary Figure 4**. The highest shoot length of 57.08 ± 0.24 cm with an increase up to 92% over uninoculated control was shown by strain ASH19. Strain ASH19 was statistically similar to strains ASH4, ASH6, ASH11, ASH17, ASH20, and ASH22, however, these strains were statistically significant compared to other tested strains and the uninoculated control. The shoot lengths due to strains ASH7, ASH10, and ASH12 were 16.83 ± 0.91 cm, 21.50 ± 1.02 cm, and 15.00 ± 0.58 cm, respectively, which were non-significant and/or lower than the shoot length of the uninoculated control (**Figure 5A**). **Figure 4** demonstrates a significant increase in root length of maize in the presence of an insoluble source of Mn, however, strains ASH7, ASH8, ASH10, and ASH12 reported non-significant root lengths of 14.16 ± 0.49 cm, 19.03 ± 1.41 cm, 21.33 ± 1.51 cm, and 17.50 ± 0.02 cm, respectively, over the uninoculated control (**Figure 5B**). The strain ASH19 reported a maximum root length of 41.00 ± 1.17 cm with an increase up to 120% the over uninoculated control. The strains ASH6, ASH20, and ASH22 also showed a better increase in root length of maize up to 38.02 ± 0.94 cm, 38.16 ± 1.62 cm, and 37.33 ± 1.50 cm, respectively, and were non-significant to each other and with strain ASH19 but significantly different from other tested strains and uninoculated control.



FIGURE 3 | Effect of manganese solubilizing bacterial (MSB) strains to increase maize growth and uptake of manganese (Mn) in shoots and roots; the pot experiment was conducted through sowing MSB strains inoculated maize seeds in pure sand culture amended with manganese oxide (MnO_2; 50 mM); Maize seedling was grown up to 21 days after germination under 16 h of light and 8 h of darkness by arranging the pots in complete randomized design in triplicate.

The data for maize fresh and dry biomasses are presented in **Figures 5**, **6** which show a significant increase due to seed inoculation with MSB strains. The maximum shoot fresh biomass of 2.85 ± 0.11 g was reported by strain ASH20 with an increase of up to 275% compared to the uninoculated control and was statistically similar to strain ASH11 which had 2.55 ± 0.11 g of shoot length with an increase of up to 236% compared to the uninoculated control. Strain ASH11 also showed a maximum increase of up to 193% compared to the uninoculated control, as shown by a shoot dry weight of 0.44 ± 0.03 g, which was non-significant to strains ASH6 and ASH20; however, these strains were highly significant to the other tested strains and the uninoculated control. Strains ASH6 and ASH20 also showed better shoot dry biomass of 0.37 ± 0.03 g and 0.38 ± 0.01 g with increases of up to 147 and 153%, respectively, than the uninoculated control. The highest root fresh biomass and root dry biomass were shown by strains ASH19 and ASH22 compared to the uninoculated control. Strain ASH19 reported 2.00 ± 0.03 g



FIGURE 4 | Effect of manganese solubilizing bacterial strains on root length of maize under pure sand culture amended with manganese oxide in pot experimental conditions.

of root fresh biomass and 0.58 ± 0.05 g of root dry biomass with an increase up to 292 and 164%, respectively, over uninoculated control. The strains ASH22 reported 1.81 ± 0.02 g of root fresh biomass and 0.65 ± 0.08 g of root dry biomass with increases of up to 255 and 196%, respectively, compared to the uninoculated control. Both of these strains in root fresh and root dry biomass were non-significant, however, they were highly significant to the uninoculated control and other test strains. The strains ASH19, ASH20, and ASH22 reported significantly maximum total fresh biomass of 4.26 ± 0.11 g, 4.43 ± 0.22 g, and 4.25 ± 0.23 g with an increase up to 232, 246, and 232%, respectively, compared to uninoculated control and these strains were statistically similar to each other. The maximum total dry biomass of 0.84 ± 0.04 g, 0.90 ± 0.08 g, 0.90 ± 0.06 g, and 0.99 ± 0.11 g with an increase up to 127, 143, 143, and 168%, respectively, was reported by strains ASH6, ASH11, ASH19, and ASH20, respectively, compared to the uninoculated control (**Figures 6A,B**).

The MSB strains significantly promoted Mn concentrations in the shoots compared to the uninoculated control (**Figure 6D**). The maximum increases of up to 1209% in Mn concentration of 11.26 ± 0.21 μg mL^{-1} in the shoot were reported due to inoculation with strain ASH7 compared to the uninoculated control. Strain ASH8 and ASH20 also reported better Mn concentrations in shoots, with increases of up to 527 and 572%, respectively, than the uninoculated control. The uninoculated control and inoculation of strains with ASH9, ASH10, ASH22, and ASH24 reported the lowest Mn concentrations in the shoots and were non-significant to each other. The Mn concentration in roots was better than the Mn concentration in shoots. Strain ASH20 reported a significantly maximum Mn concentration of 54.91 ± 0.16 μg mL^{-1} in roots with increase of up to 2632% compared to uninoculated control. Strain ASH11 also reported a better increase of up to 2260% in Mn concentration of 47.43 ± 0.31 μg mL^{-1} in the root, than the uninoculated control. Strain ASH17 was not able to promote Mn concentrations in roots and showed statistically similar Mn concentrations in roots to the uninoculated control (**Figure 6C**). Five best PGP MSB strains *viz.* ASH6, ASH11, ASH19, ASH20, and ASH22 were selected based on their performance to promote maize growth and biomass. A phylogenetic tree of these strains is demonstrated in **Figure 7** which shows that all the identified strains belonged to *Bacillus* spp. with accession numbers MT071447, MT071448, MT071449, MT071450, and MT071451, respectively.

Promotion of Maize Growth and Nutrient Concentrations in Soil Culture Pot Experiment

The MSB strains significantly promoted maize growth and nutrient uptake in soil culture pot experiment with native soil Mn concentrations. The increase in plant growth due to the application of MSB strains was observed in terms of chlorophyll contents, plant height, root length, and shoot and root dry weight of maize (**Table 6**). The uninoculated control showed minimum chlorophyll contents, plant height, root length, and shoot and root dry weight. The maximum increase of up to 26% in chlorophyll contents was reported by strain ASH19 over the uninoculated control and was statistically similar to strains ASH6 and ASH20 which reported 22 and 23% higher chlorophyll contents as compared to uninoculated control. Strain ASH19 reported a maximum increase up to 18% in plant height compared to the uninoculated control and was statistically similar to other MSB strains except for strain ASH22. Strain ASH19 also reported a significant maximum increase of up to 34% in root length over the uninoculated control. The maximum shoot dry weight was reported by strains ASH11, ASH19, and ASH6, with increases of up to 17, 14, and 12%, respectively, over the uninoculated control. These strains were statistically similar to each other, however, produced significantly different shoot dry weight as compared to uninoculated control. The increase in root dry weight due to the application of MSB strains was statistically similar to each other, however, they showed a statistically higher root dry weight than the uninoculated control. The maximum increase of up to 21% in root dry weight was reported by strain ASH20 over the uninoculated control.

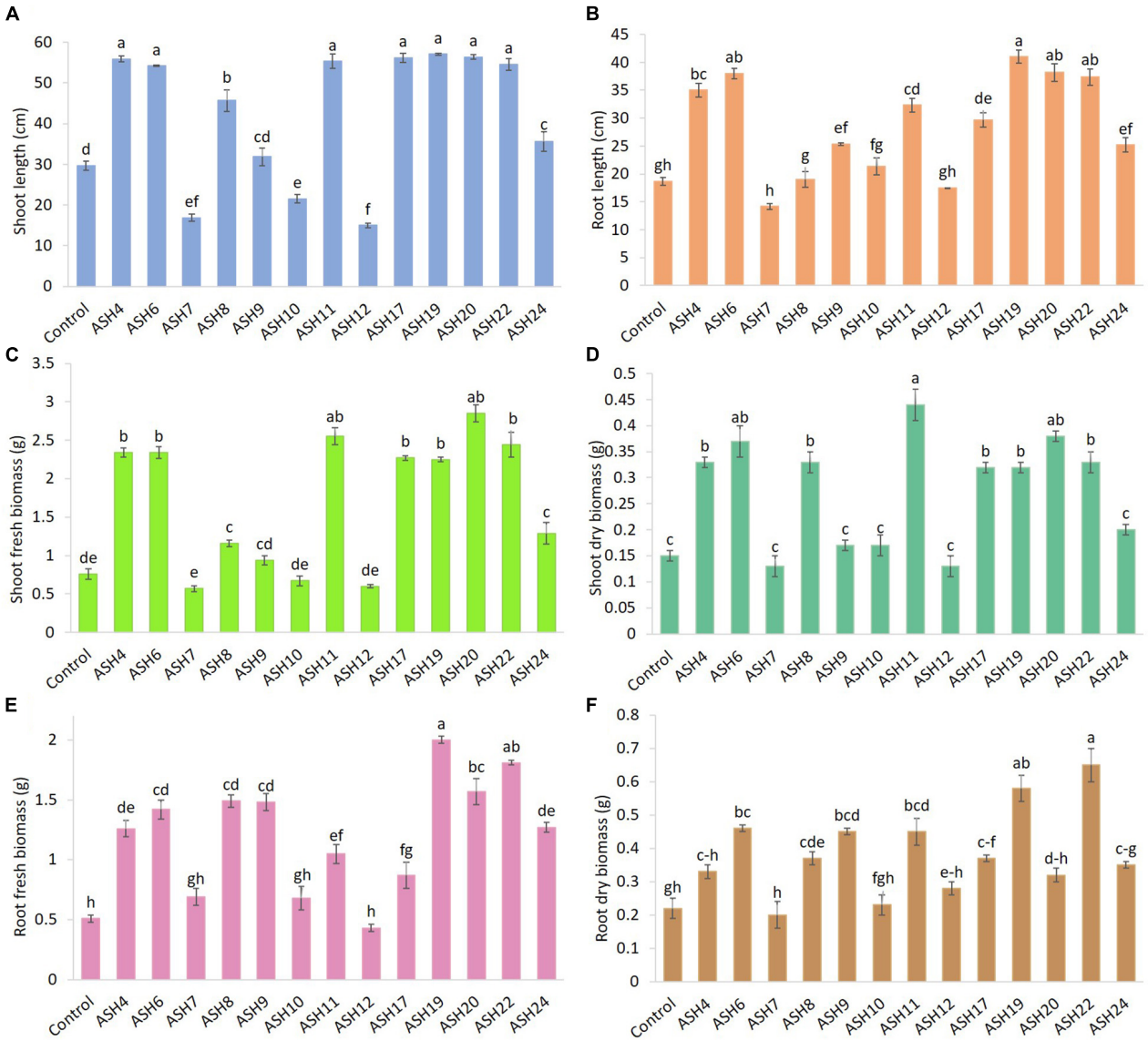


FIGURE 5 | Effect of Mn solubilizing bacterial (MSB) strains on maize growth and uptake of manganese under axenic conditions; the surface-sterilized maize seeds were inoculated with MSB and grown-up to 3 weeks after germination under 16 h of light and 8 h of a dark period of axenic conditions in small pots trials; the data was recorded in terms of shoot length **(A)**, root length **(B)**, shoot fresh biomass **(C)**, shoot dry biomass **(D)**, root fresh biomass **(E)**, and root dry biomass **(F)**; top five best-performing strains ASH6, ASH11, ASH19, ASH20, and ASH22 were selected for identification; the control had no inoculum (uninoculated) and contains only broth; data presented are the mean of three replications ± standard error; the means sharing common letters were considered statistical similar to each other and least significant difference (LSD) test was performed at 5% ($p \leq 0.05$) probability level.

The application of MSB strains improved nutrient uptake in terms of N, P, and K concentrations in maize roots and shoots as compared to the uninoculated control (**Figure 8**). The uninoculated control reported a minimum concentration of these nutrients in maize roots and shoots. Strain ASH20 reported a maximum increase of up to 42% in N concentration in maize roots compared to the uninoculated control, while, a maximum increase of up to 57% in N concentration in maize shoots was reported by strain ASH19 over the uninoculated control (**Figure 8A**). The maximum increase of up to 48% in P concentration in maize roots over the uninoculated control was reported by strain ASH6 while strain ASH20 followed by ASH6 reported maximum increases of up to 35 and 33%, respectively in P concentration in the shoot compared to the uninoculated control (**Figure 8B**). A higher increase in K concentration in maize roots of up to 38% was observed through inoculation with strain ASH20 compared to the uninoculated control. The maximum increase up to 53% in K concentration in maize shoots was reported by strain ASH20 followed by strain ASH22, which reported 47% more K concentration in the shoots compared to the uninoculated control (**Figure 8C**). The application of MSB strains significantly promoted Mn concentrations in maize roots

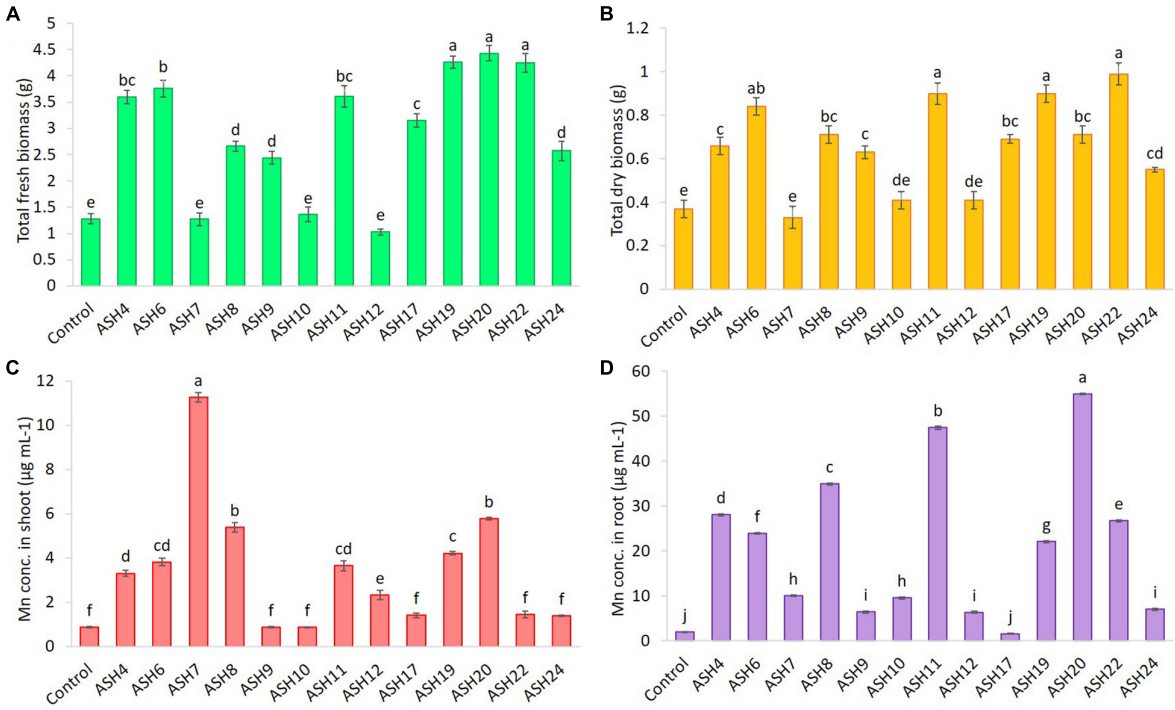


FIGURE 6 | The total fresh biomass **(A)**, total dry biomass **(B)**, uptake of Mn in root **(C)** and shoot **(D)** of maize grown with Mn solubilizing bacterial (MSB) strains; the surface-sterilized maize seeds were inoculated with MSB and grown-up to 3 weeks after germination under 16 h of light and 8 h of a dark period of axenic conditions in small pots trials; the control had no inoculum (uninoculated) and contains only broth; data presented are the mean of three replications ± standard error; the means sharing common letters were considered statistical similar to each other and least significant difference (LSD) test was performed at 5% ($p \leq 0.05$) probability level.

and shoots compared with the uninoculated control (**Figure 8D**). The maximum increase in Mn concentrations in maize roots up to 55% was reported by strain ASH20 followed by strain ASH6, which showed a 48% increase in Mn concentration in roots compared to the uninoculated control. Strain ASH20 also reported a maximum increase of up to 81% in Mn concentration in maize shoots followed by strain ASH19, which reported a 71% higher Mn concentration than the uninoculated control. Correlation analysis revealed a positive association among nutrients contents in soil culture pot trial (**Figure 9**). Meanwhile, a negative correlation of Mn concentration in roots and shoots was observed with P concentration in roots and K concentration in shoots. The Mn concentration in roots was also negatively correlated to K concentration in roots.

DISCUSSION

Manganese deficiency can be a serious limiting factor for plant growth in calcareous sandy soils with high pH (Husted et al., 2005). Plants tend to obtain Mn by establishing a symbiosis with Mn-reducing soil bacteria that solubilize MnO_2. In the present study, MSB strains were isolated from the maize rhizosphere and identified as *Bacillus* spp. through 16S rRNA gene sequencing. These strains caused a significant increase in plant growth and Mn concentration in maize seedlings through the solubilizing of an insoluble source of Mn. To the best of our knowledge, this is the first study regarding the characterization and application of MSB strains for plant growth promotion and Mn uptake.

In the present study, bacterial strains isolated from maize rhizosphere showed the ability to solubilize Mn on nutrient agar media amended with 50 mM MnO_2. Similar to our work, Kasana et al. (2008) also flooded Gram's iodine solution on carboxymethylcellulose agar media for the determination of cellulase production by bacteria and reported very dominant clearing zones around the colonies. In the present study, thirteen strains showed a predominant solubilization zone around the bacterial growth, and the strains *Bacillus* sp. ASH4, *Bacillus* sp. ASH10, and *Bacillus* sp. ASH20 showed the highest value for MSI and MSE (**Table 1**). Mn solubilization by numerous microorganisms has also been reported in various studies (Madgwick, 1991; Wei et al., 2012; Sanket et al., 2017). Madgwick (1991) reported reductive solubilization of MnO_2 tailings by four microbial isolates *viz. Achromobacter* sp., *Aspergillus niger*, *Enterobacter cloacae*, and *Enterobacter agglomerans*. Similarly, Sanket et al. (2017) reported the ability of four acidophilic bacterial strains *viz. Enterobacter* sp. AMSB1, *B. cereus* AMSB3, *Bacillus nealsonii* AMSB4, and *Staphylococcus hominis* AMSB5 to solubilize Mn on MnO_2-amended nutrient agar media.

In the present study, *Bacillus* strains solubilized Mn concentrations ranging from 3.56 ± 0.13 µg mL^{-1} to 10.73 ± 0.59 µg mL^{-1} (**Table 1**). *Bacillus* sp. ASH6 and

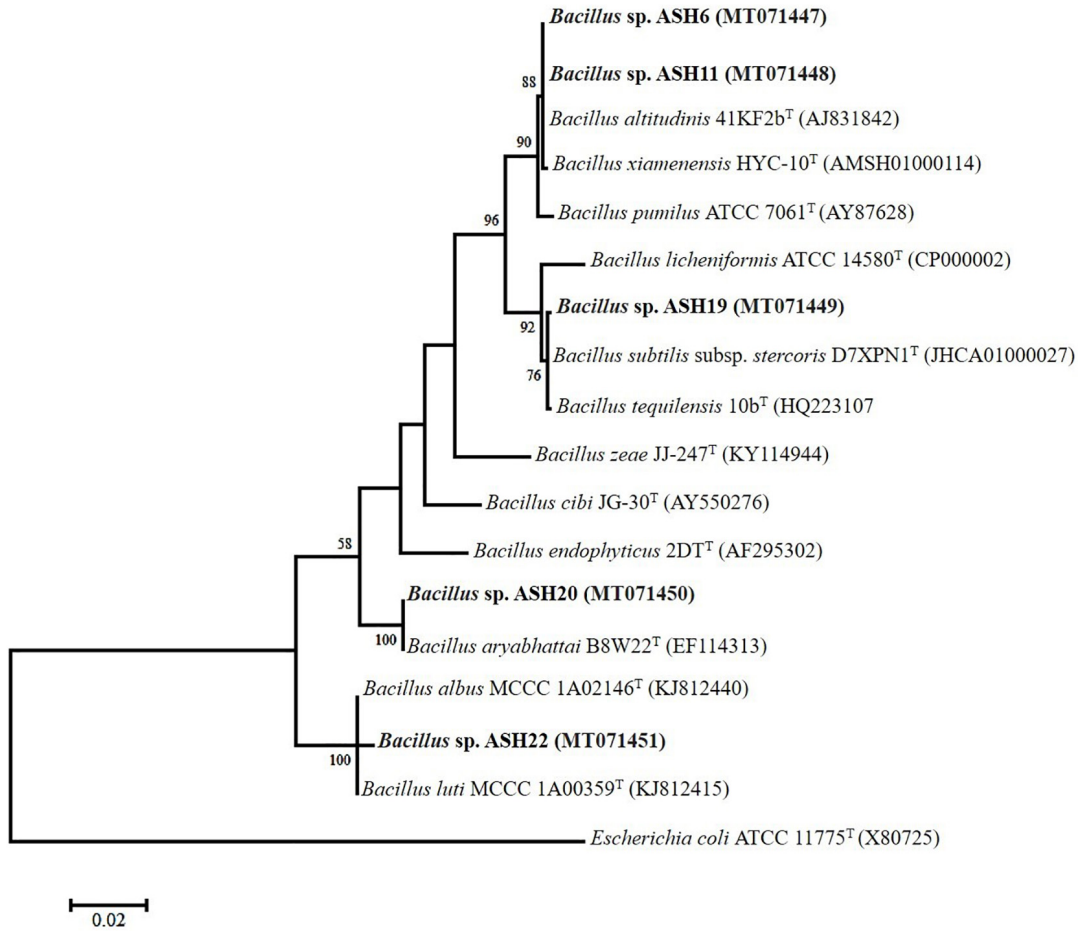


FIGURE 7 | The neighbor-joining phylogenetic tree was produced using multiple alignments of the 16S rRNA gene sequence of *Bacillus* sp. ASH6, *Bacillus* sp. ASH11, *Bacillus* sp. ASH19, *Bacillus* sp. ASH20, and *Bacillus* sp. ASH22 with those of other bacterial strains found in the GenBank database; The 16S rRNA sequences of the identified manganese solubilizing bacterial strains were submitted in the GenBank database and the obtained accession numbers were MT071447, MT071448, MT071449, MT071450, and MT071451, respectively.

TABLE 6 | Growth attributes of maize grown with Mn solubilizing bacterial strains under soil cultured pot trial.

Mn-solubilizing Strains	Chlorophyll Contents (SPAD value)	Plant height (cm)	Root length (cm)	Shoot dry weight (g)	Root dry weight (g)
Control	42.25 ± 0.35^{d}	144.00 ± 2.64^{c}	68.50 ± 0.57^{e}	34.30 ± 0.30^{c}	8.85 ± 0.35^{b}
ASH6	51.53 ± 0.51^{abc}	170.00 ± 2.41^{ab}	77.00 ± 1.41^{d}	38.50 ± 0.50^{ab}	10.05 ± 0.45^{a}
ASH11	49.56 ± 0.76^{c}	169.00 ± 1.87^{ab}	87.50 ± 1.58^{b}	40.00 ± 1.11^{a}	10.40 ± 0.79^{a}
ASH19	53.37 ± 0.47^{a}	170.50 ± 2.45^{a}	92.00 ± 1.44^{a}	39.00 ± 1.01^{a}	10.40 ± 0.45^{a}
ASH20	52.12 ± 0.42^{ab}	170.00 ± 2.16^{ab}	86.00 ± 1.17^{b}	35.50 ± 0.56^{c}	10.70 ± 0.72^{a}
ASH22	50.50 ± 0.50^{bc}	167.50 ± 1.98^{b}	80.50 ± 0.77^{c}	36.50 ± 0.67^{bc}	10.20 ± 0.41^{a}
LSD	2.00	3.20	3.39	2.38	0.70

Maize seeds inoculated with MSB were grown in soil cultured pot trial along with native soil Mn. The chlorophyll contents in terms of SPAD values were observed from the second top leaf of maize at the cob formation stage, however, the other growth attributes were recorded at the time of physiological maturity; Data presented here are the mean of three replications ± standard error; the means in a vertical line for each attributes sharing the common letters were considered statistical similar to each other and the least significant difference (LSD) test was performed at 5% ($p \leq 0.05$) probability level.

Bacillus sp. ASH20 demonstrated the maximum solubilized concentration of Mn, which may be due to its ability to reduce Mn(IV) and Mn(III) into Mn(II). Enzymatic reduction of Mn(IV) oxidized Mn(II) serves as a terminal electron acceptor for aerobic and facultative anaerobic bacteria in the form of respiration and reduced Mn(II) concentration to satisfy their nutritional needs (Bromfield and David, 1976). The extracellular heme or flavin enzyme called cellobiose dehydrogenase plays a

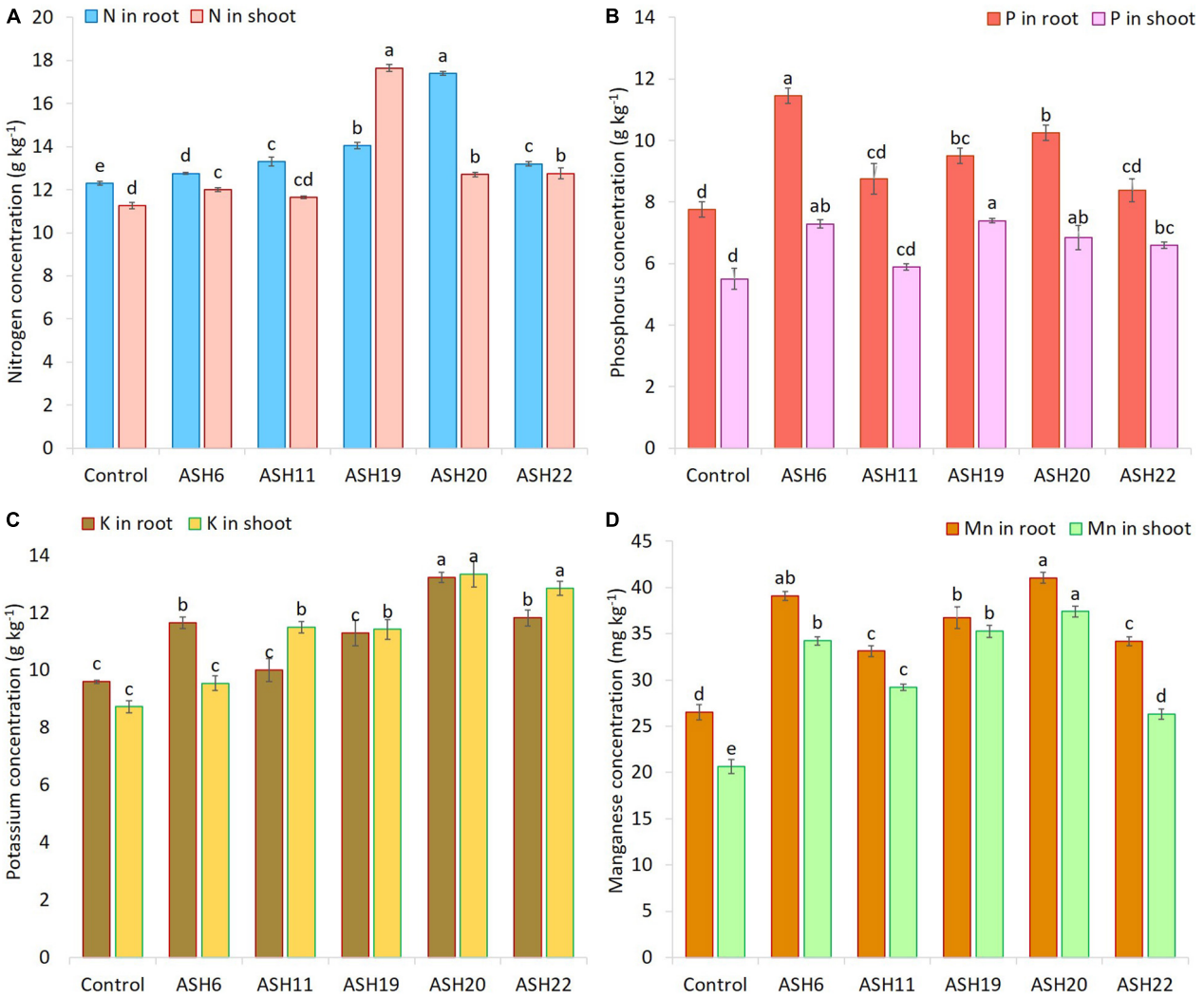


FIGURE 8 | The concentration of nitrogen **(A)**, phosphorus **(B)**, potassium **(C)**, and manganese **(D)** in maize roots and shoots grown with Mn solubilizing bacterial (MSB) strains; maize seeds inoculated with MSB were grown up to physiological maturity in earthen pots filled with sandy loam textural soil having native 14.36 mg kg^{-1} extractable manganese and 26.90 mg kg^{-1} total manganese; the uninoculated control had no inoculum and contains only broth; data presented are the mean of three replications ± standard error; the means sharing same alphabetical letters were considered non-significant to each other and least significant difference (LSD) test was performed at 5% ($p \leq 0.05$) probability level.

role in the redox cycling of Mn in nature and can reduce insoluble MnO_2 into soluble Mn(II) (Roy et al., 1994). Organic acids, including formic, oxalic, pyruvic, salicylic, citric, and malic acids cause a significant reduction in soil pH, which plays an important role in the conversion of MnO_2 into the plant-available Mn^{2+} form (Di-Ruggiero and Gounot, 1990; Rusin and Ehrlich, 1995). The production of inorganic compounds, including ferrous iron and sulfide, during anaerobic respiration or the production of H_2O_2 during aerobic respiration also causes a reduction in Mn(IV) (Rusin and Ehrlich, 1995). The tested MSB strains were also positive for qualitative and quantitative solubilization of P and Zn (**Tables 2**, **3**). However, only six out of thirteen MSB strains were positive for K solubilization (**Table 4**). The solubilization of such insoluble minerals by MSB strains might be due to the production of organic acids, including 2-ketogluconic, acetic, aspartic, citric, fumaric, gluconic, glutamic, glycolic, glyoxylic, isobutyric, isovaleric, itaconic, lactic, maleic, malic, malonic, oxalic, propionic, succinic, tartaric, and α-ketobutyric acids (Vyas and Gulati, 2009; Etesami et al., 2017; Nath et al., 2017; Wei et al., 2017; Dinesh et al., 2018; Mumtaz et al., 2019). Such organic acid production by various types of bacteria is autonomous of their genetic relatedness, and each strain has its specific capability of producing organic acids during the solubilization of inorganic minerals (Vyas and Gulati, 2009).

In the current study, eight out of thirteen MSB strains were able to produce IAA in the presence of L-tryptophan (**Table 5**). An increase in IAA production may promote primary root elongation and the formation of lateral and adventitious roots (Xie et al., 1996). Recently, Panigrahi et al. (2020) reported variation in the production of IAA by endophytic *E. cloacae* to

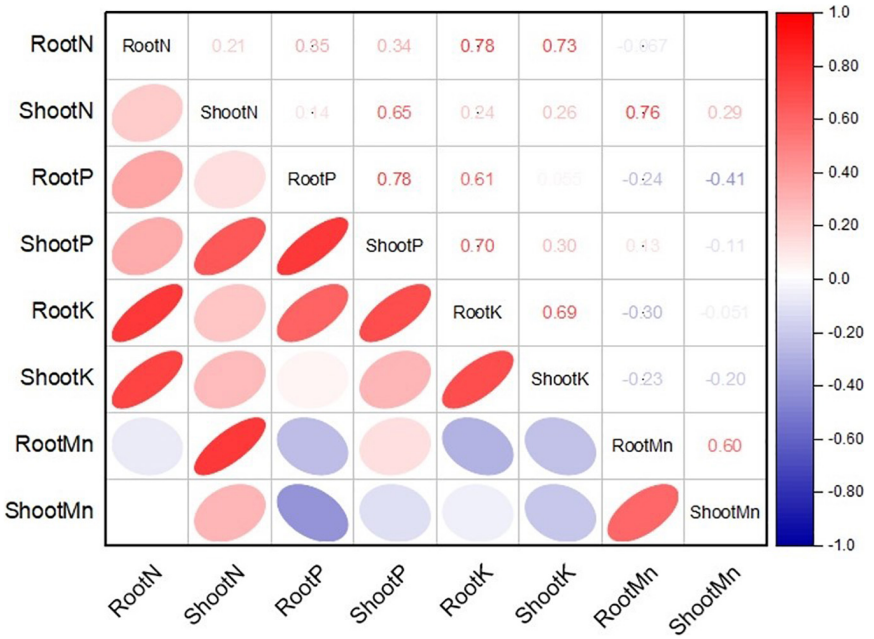


FIGURE 9 | Pearson correlations analysis among nitrogen, phosphorus, potassium, and manganese concentration in roots and shoots of maize plant treated with Mn solubilizing bacterial (MSB) strains under soil culture pot trial; RootN, root nitrogen; ShootN, shoot nitrogen; RootP, root phosphorus; ShootP, shoot phosphorus; RootK, root potassium; ShootK, shoot potassium; RootMn, root manganese; ShootMn, shoot manganese.

strain MG00145 isolated from *Ocimum sanctum* and significantly promoted the growth of various crops, including *Oryza sativa*, *Arachis hypogaea*, *Vigna mungo*, and *Brassica campestris* var. toria. In the current study, all the MSB strains showed their ability to produce NH_3, while, eight out of thirteen MSB strains showed siderophore production, which may promote plant growth by providing N and Fe to plants and could be involved in biocontrol by limiting Fe availability to pathogenic fungi (Sayyed et al., 2013). The application of rhizobacteria gradually increases microbial enzymatic activities and shows a substantial increase in plant growth. In the present study, the majority of MSB strains tested positive for protease, amylase, lipase, and catalase activities. These are hydrolytic enzymes that could play important roles in improving soil fertility by enhancing the decomposition of various organic residues of plant and animal origins.

The results of pot trials under axenic sand culture and soil culture conditions revealed that the tested MSB strains showed their ability to promote maize growth in terms of shoot and root length, and shoot and root fresh and dry biomass in the presence of insoluble Mn; however, the strains ASH7, ASH10, and ASH12 were not able to promote maize growth under sand culture conditions and showed statistically lower maize growth than the uninoculated control (**Figure 5**). Significant variation among the MSB strains was observed, while, *Bacillus* sp. ASH6, *Bacillus* sp. ASH11, *Bacillus* sp. ASH19, *Bacillus* sp. ASH20, and *Bacillus* sp. ASH22 reported a maximum increase in the growth of maize seedlings compared to other tested strains. The findings of the current study are in line with our previous study about the application of Zn-solubilizing *Bacillus* strains to promote maize growth (Mumtaz et al., 2017). Similarly, Naseer et al. (2020) reported an increase in rice germination, growth, and vigor index in pot trials due to inoculation with Zn solubilizing *Bacillus* strains *viz. Bacillus megaterium* AN24, *Bacillus aryabhattai* AN30, *B. megaterium* AN31, and *B. megaterium* AN35. Ahmad et al. (2020) inoculated cotton seeds with seven PSB and seven ZSB strains in pot trials and reported a significant increase in growth attributes over the control. They reported the best outcome in terms of co-inoculation of *Bacillus subtilis* IA6 + *Bacillus* sp. IA16 followed by *Paenibacillus polymyxa* IA7 + *B. aryabhattai* IA20. Similarly, inoculation with P solubilizing endophytic *P. polymyxa* ANM59 and *Paenibacillus* sp. ANM76 also showed promising results to improve the growth and nodulation of chickpea (Ahmad et al., 2019).

In the present study, the increase in maize growth due to inoculation with MSB strains in the presence of insoluble Mn compounds in the sand as well as soil culture pot experiments might be due to their ability to solubilize Mn and other minerals including P, K, and Zn, and their ability to produce siderophores, IAA, NH_3, and perform various enzymatic activities which we determined in the current *in vitro* and *in vivo* studies. Our findings are also supported by previous studies reported by Mumtaz et al. (2017, 2019), Ahmad et al. (2019, 2020), and Panigrahi et al. (2020). The application of such beneficial mineral-solubilizing bacteria could improve nutrient availability in root zones and enhance their uptake in plants (Kumawat et al., 2017; Mumtaz et al., 2018, 2020). The production of IAA by MSB strains could also have a possible role in increasing maize growth in pot trials. Bacterial IAA induces plant growth and development by affecting cell division, initiation, and elongation of lateral and adventitious roots (Tsavkelova et al., 2006; Spaepen et al., 2007).

Bacterial IAA also increases root surface area and root length, as we observed in the current study, as demonstrated in **Figure 4** which helps plants absorb more nutrients from the soil (Patten and Glick, 2002). The current study also revealed the higher uptake of N, P, K, and Mn in the shoots and roots of maize due to inoculation with MSB strains compared to the uninoculated control (**Figures 6**, **8**). The increase in N uptake in maize roots and shoots might be due to the ability of MSB strains to fix atmospheric N and increase its uptake into maize root and shoot tissues. The current study demonstrated the ability of MSB strains to solubilize P (**Table 2**) and K (**Table 4**) which also helped the mobilization of P and K from soil solution to maize root and shoot tissues (**Figure 8**). Mn uptake in roots and shoots demonstrated the strong power of MSB to solubilize and mobilize the stability of MnO_2 under axenic sand culture as well as soil culture conditions and increase its translocation from root to shoot compared to the uninoculated control. Similarly, the literature has reported that Mn-reducing bacteria, including *Arthrobacter* and *Variovorax* spp. promoted plant growth and Mn uptake in wheat and soybean (Marschner et al., 1991; Nogueira et al., 2007).

CONCLUSION

The present study concluded that *Bacillus* spp. strains ASH6, ASH11, ASH19, ASH20, and ASH22 showed strong power to solubilize Mn and improve maize growth attributes and Mn uptake in maize roots and shoots. These strains possess multiple PGP attributes and could be attractive inoculants to improve maize productivity by addressing nutrient deficiencies. Such prospective bioinoculants could address the issue of Mn as well as P, K, Zn, and Fe deficiencies in plants in calcareous soil after further evaluation. The current findings suggest that researchers evaluate MSB strains to study their genetic and molecular mechanisms of Mn solubilization. Further evaluation of the promising MSB strain's ability to increase maize and other crop productivity should be conducted under laboratory, pot, and field conditions.

DATA AVAILABILITY STATEMENT

The datasets presented in this study can be found in online repositories. The names of the repository/repositories and accession number(s) can be found in the article/ **Supplementary Material**.

AUTHOR CONTRIBUTIONS

MM and AI conceived and designed the experimental strategies. AI and HM performed all experiments and data analysis. MA provided the study materials, reagents, research resources, and facilitated critical review on pre-publication stages. MM created and presented the published work specifically writing the initial and final draft and performed the revision. AZ helped in the identification of bacterial strains and performed the phylogenetic analysis. MA and MS oversight the research activity, planning, and execution. XW and WW provided financial support for the publication of this article. All authors contributed to the article and approved the submitted version.

FUNDING

The research facilities were provided by the Laboratory of Soil Microbiology and Biotechnology, Department of Soil Science, the Islamia University of Bahawalpur, Pakistan, and the Institute of Molecular Biology and Biotechnology, The University of Lahore, Main Campus, Lahore, Pakistan. This research was supported by the National Natural Science Foundation of China (51809224). The authors acknowledge the College of Life Sciences, Yan'an University, Yan'an, China for the financial support to publication of the present work.

SUPPLEMENTARY MATERIAL

The Supplementary Material for this article can be found online at: https://www.frontiersin.org/articles/10.3389/fpls.2021.719504/full#supplementary-material

REFERENCES

Ahmad, I., Ahmad, M., Hussain, A., and Jamil, M. (2020). Integrated use of phosphate-solubilizing *Bacillus subtilis* strain IA6 and zinc-solubilizing *Bacillus* sp. strain IA16: a promising approach for improving cotton growth. *Folia Microbiol.* 66, 115–125. doi: 10.1007/s12223-020-00831-3

Ahmad, M., Naseer, I., Hussain, A., Mumtaz, M. Z., Mustafa, A., Hilger, T. H., et al. (2019). Appraising endophyte-plant symbiosis for improved growth, nodulation, nitrogen fixation and abiotic stress tolerance: an experimental investigation with chickpea (*Cicer arietinum* L.). *Agronomy* 9:621. doi: 10.3390/agronomy9100621

Baglin, E., Noble, E., Lamsphire, D., and Eisele, J. A. (1992). Solubilization of manganese from ores by heterotrophic micro-organisms. *Hydrometallurgy* 29, 131–144. doi: 10.1016/0304-386X(92)90009-O

Breakwell, D., MacDonald, B., Woolverton, C., Smith, K., and Robison, R. (2007). *Colony Morphology Protocol*. Available online at: https://www.asmscience.org/content/education/protocol/protocol.3136?crawler=redirect (accessed January 12, 2021)

Bric, J. M., Bostock, R. M., and Silverstonet, S. E. (1991). Rapid in situ assay for indoleacetic acid production by bacteria immobilized on a nitrocellulose membrane downloaded from. *Appl. Environ. Microbiol.* 57, 535–538.

Bromfield, S. M., and David, D. J. (1976). Sorption and oxidation of manganous ions and reduction of manganese oxide by cell suspensions of a manganese oxidizing bacterium. *Soil Biol. Biochem.* 8, 37–43. doi: 10.1016/0038-0717(76)90019-5

Bunt, J. S., and Rovira, A. D. (1955). Microbiological studies of some subantarctic soils. *J. Soil Sci.* 6, 119–128. doi: 10.1111/j.1365-2389.1955.tb00836.x

Campbell, L. C., and Nable, R. O. (1988). "Physiological functions of manganese in plants," in *Manganese in Soils and Plants. Developments in Plant and Soil Sciences*, eds R. D. Graham, R. J. Hannam, and N. C. Uren (Dordrecht: Springer), 139–154. doi: 10.1007/978-94-009-2817-6_11

Cappuccino, J., and Welsh, C. (2017). *Microbiology: A Laboratory Manual*, 11th Edn. New York: Pearson.

Cheneby, D., Perrez, S., Devroe, C., Hallet, S., Couton, Y., Bizouard, F., et al. (2004). Denitrifying bacteria in bulk and maize-rhizospheric soil: diversity and N2O-reducing abilities. *Can. J. Microbiol.* 50, 469–474. doi: 10.1139/w04-037

Das, A. P., Sukla, L. B., and Pradhan, N. (2012). Microbial recovery of manganese using *Staphylococcus* epidermidis. *Int. J. Nonferrous Metallurgy* 1, 9–12. doi: 10.4236/ijnm.2012.12002

Dinesh, R., Srinivasan, V., Hamza, S., Sarathambal, C., Gowda, S. J. A., Ganeshamurthy, A. N., et al. (2018). Isolation and characterization of potential Zn solubilizing bacteria from soil and its effects on soil Zn release rates, soil available Zn and plant Zn content. *Geoderma* 321, 173–186. doi: 10.1016/j.geoderma.2018.02.013

Di-Ruggiero, J., and Gounot, A. M. (1990). Microbial manganese reduction mediated by bacterial strains isolated from aquifer sediments. *Microbial. Ecol.* 20, 53–63. doi: 10.1007/BF02543866

Etesami, H., Emami, S., and Alikhani, H. (2017). Potassium solubilizing bacteria (KSB): mechanisms, promotion of plant growth, and future prospects a review. *J. Soil Sci. Plant* 17, 897–911. doi: 10.4067/S0718-95162017000400005

Ghosh, S., Mohanty, S., Nayak, S., Sukla, L. B., and Das, A. P. (2016). Molecular identification of indigenous manganese solubilising bacterial biodiversity from manganese mining deposits. *J. Basic Microbiol.* 56, 254–262. doi: 10.1002/jobm.201500477

Gong, X., Qu, C., Liu, C., Hong, M., Wang, L., and Hong, F. (2011). Effects of manganese deficiency and added cerium on nitrogen metabolism of maize. *Biol. Trace Element Res.* 144, 1240–1250. doi: 10.1007/s12011-011-9105-y

Hebbern, C. A., Pedas, P., Schjoerring, J. K., Knudsen, L., and Husted, S. (2005). Genotypic differences in manganese efficiency: field experiments with winter barley (*Hordeum vulgare* L.). *Plant Soil* 272, 233–244. doi: 10.1007/s11104-004-5048-9

Horwitz, W. (2010). "Official methods of analysis of AOAC international. agricultural chemicals, contaminants," in *Gaithersburg AOAC International*. Available online at: https://repositorioinstitucional.ceu.es/handle/10637/3158 (accessed January 14, 2021).

Huber, D., and McCay-Buis, T. S. (1993). A multiple component analysis of the take-all disease of cereals. *Plant Dis.* 77, 437–447.

Husted, S., Thomsen, M. U., Mattsson, M., and Schjoerring, J. K. (2005). Plant and soil (influence of nitrogen and sulphur form on manganese acquisition by barley (*Hordeum vulgare*). *Springer* 268, 309–317. doi: 10.1007/s11104-004-0317-1

Jackson, M. (1962). Soil chemical analysis. prentice hall, inc. englwood cliff, New York, USA. *J. Plan Nut. Soil Sci.* 85, 251–252. doi: 10.1002/jpln.19590850311

Kasana, R. C., Salwan, R., Dhar, H., Dutt, S., and Gulati, A. (2008). A rapid and easy method for the detection of microbial cellulases on agar plates using Gram's iodine. *Curr. Microbiol.* 57, 503–507. doi: 10.1007/s00284-008-9276-8

Kumar, S., Stecher, G., and Tamura, K. (2016). MEGA7: molecular evolutionary genetics analysis version 7.0 for bigger datasets. *Mol. Biol. Evolu.* 33, 1870–1874. doi: 10.1093/molbev/msw054

Kumawat, N., Kumar, R., Kumar, S., and Meena, V. S. (2017). "Nutrient solubilizing microbes: its role in sustainable crop production," in *Agriculturally Important Microbes for Sustainable Agriculture*, eds V. Meena, P. Mishra, J. Bish, and A. Pattanayak (Springer), 26–61. doi: 10.1007/978-981-10-5343-6_2

Leonowicz, G., Trzebuniak, K. F., Zimak-Piekarczyk, P., Ślesak, I., and Mysliwa-Kurdziel, B. (2018). The activity of superoxide dismutases (SODs) at the early stages of wheat deetiolation. *PLoS One* 13:e0194678. doi: 10.1371/journal.pone.0194678

Louden, B., Haarmann, D., and Lynne, A. (2011). Use of blue agar CAS assay for siderophore detection. *J. Microbiol. Biol. Educ.* 12, 51–53. doi: 10.1128/jmbe.v12i1.249

Madgwick, J. C. (1991). Microbial processing of manganese. *Austr. J. Biotechnol.* 12, 33–38.

Marschner, P., Ascher, J. S., and Graham, R. D. (1991). Effect of manganese-reducing rhizosphere bacteria on the growth of *Gaeumannomyces graminis* var. tritici and on manganese uptake by wheat (*Triticum aestivum* L.). *Biol. Fertility Soils* 12, 33–38. doi: 10.1007/BF00369385

Martens, D. C., and Westermann, D. T. (1991). "Fertilizer applications for correcting micronutrient deficiencies," in *Micronutrients in Agriculture*, ed. J. J. Mortvedt (Soil Science Society of America, Inc.), 549–592. doi: 10.2136/sssabookser4.2ed.c15

Mumtaz, M., Barry, K., Baker, A., Nichols, D., Ahmad, M., Zahir, Z., et al. (2019). Production of lactic and acetic acids by *Bacillus* sp. ZM20 and *Bacillus cereus* following exposure to zinc oxide: a possible mechanism for Zn solubilization. *Rhizosphere* 12:100170. doi: 10.1016/j.rhisph.2019.100170

Mumtaz, M. Z., Ahmad, M., Jamil, M., Asad, S. A., and Hafeez, F. (2018). *Bacillus* strains as potential alternate for zinc biofortification of maize grains. *Int. J. Agric. Biol.* 20, 1779–1786. doi: 10.17957/IJAB/15.0690

Mumtaz, M. Z., Ahmad, M., Jamil, M., and Hussain, T. (2017). Zinc solubilizing *Bacillus* spp. potential candidates for biofortification in maize. *Microbiol. Res.* 202, 51–60. doi: 10.1016/j.micres.2017.06.001

Mumtaz, M. Z., Malik, A., Nazli, F., Latif Malik, M., Zaheer, A., Ali, Q., et al. (2020). Potential of zinc solubilizing *Bacillus* strains to improve growth, yield, and quality of maize (Zea mays). *Int. J. Agric. Biol.* 24, 691–698. doi: 10.17957/IJAB/15.1488

Naseer, I., Ahmad, M., Hussain, A., and Jamil, M. (2020). Potential of zinc solubilizing *Bacillus* strains to improve rice growth under axenic conditions. *Pakistan J. Agric. Sci.* 57, 1057–1071. doi: 10.21162/PAKJAS/20.9988

Nath, D., Maurya, B. R., and Meena, V. S. (2017). Documentation of five potassium- and phosphorus-solubilizing bacteria for their K and P-solubilization ability from various minerals. *Biocatalysis Agric. Biotechnol.* 10, 174–181. doi: 10.1016/j.bcab.2017.03.007

Nogueira, M. A., Nehls, U., Hampp, R., Poralla, K., and Cardoso, E. J. B. N. (2007). Mycorrhiza and soil bacteria influence extractable iron and manganese in soil and uptake by soybean. *Plant Soil* 298, 273–284. doi: 10.1007/s11104-007-9379-1

Panigrahi, S., Mohanty, S., and Rath, C. C. (2020). Characterization of endophytic bacteria *Enterobacter cloacae* MG00145 isolated from *Ocimum sanctum* with indole acetic acid (IAA) production and plant growth promoting capabilities against selected crops. *South Afr. J. Bot.* 134, 17–26. doi: 10.1016/j.sajb.2019.09.017

Parmar, P., and Sindhu, S. S. (2013). Potassium solubilization by rhizosphere bacteria: influence of nutritional and environmental conditions. *J. Microbiol. Res.* 3, 25–31. doi: 10.5923/j.microbiology.20130301.04

Patten, C. L., and Glick, B. R. (2002). Role of *Pseudomonas* putida indoleacetic acid in development of the host plant root system. *Appl. Environ. Microbiol.* 68, 3795–3801. doi: 10.1128/AEM.68.8.3795-3801.2002

Pikovskaya, R. I. (1948). Mobilization of phosphorus in soil in connection with vital activity of some microbial species. *Mikrobiologiya* 17, 362–370.

Roy, B. P., Paice, M. G., Archibald, F. S., Misra, S. K., and Misiak, L. E. (1994). Creation of metal-complexing agents, reduction of manganese dioxide, and promotion of manganese peroxidase-mediated Mn(III) production by cellobiose:quinone oxidoreductase from trametes versicolor. *J. Biol. Chem.* 269, 19745–19750. doi: 10.1016/S0021-9258(17)32084-7

Rusin, P., and Ehrlich, H. (1995). "Developments in mcirobial leaching—mechanisms of manganese solubilization," in *Microbial and Eznymatic Bioproducts. Advances in Biochemical Engineering/Biotechnology*, eds M. Hiroto, H. Nishimura, Y. Kodera, F. Kawai, P. Rusin, H. L. Ehrlich, et al. (Berlin: Springer), 1–26. doi: 10.1007/BFb0102314

Ryan, J. G., Estefan, G., and Rashid, A. (2001). *Soil and Plant Analysis Laboratory Manual*. Aleppo: International Center for Agricultural Research in the Dry Areas (ICARDA).

Sanket, A. S., Ghosh, S., Sahoo, R., Nayak, S., and Das, A. P. (2017). Molecular identification of acidophilic manganese (Mn)-solubilizing bacteria from mining effluents and their application in mineral beneficiation. *Geomicrobiol. J.* 34, 71–80. doi: 10.1080/01490451.2016.1141340

Sayyed, R. Z., Chincholkar, S. B., Reddy, M. S., Gangurde, N. S., and Patel, P. R. (2013). "Siderophore producing PGPR for crop nutrition and phytopathogen suppression," in *Bacteria in Agrobiology: Disease Management*, ed. D. Maheshwari (Berlin: Springer-Verlag), 449–471. doi: 10.1007/978-3-642-33639-3_17

Schmidt, S. B., and Husted, S. (2019). The biochemical properties of manganese in plants. *Plant* 8:381. doi: 10.3390/plants8100381

Schmidt, S. B., Jensen, P. E., and Husted, S. (2016). Manganese deficiency in plants: the impact on photosystem II. *Trends Plant Sci.* 21, 622–632. doi: 10.1016/j.tplants.2016.03.001

Schmidt, S. B., Pedas, P., Laursen, K. H., Schjoerring, J. K., and Husted, S. (2013). Latent manganese deficiency in barley can be diagnosed and remediated on

the basis of chlorophyll a fluorescence measurements. *Plant Soil* 372, 417–429. doi: 10.1007/s11104-013-1702-4

Schmidt, S. B., Persson, D. P., Powikrowska, M., Frydenvang, J., Schjoerring, J. K., Jensen, P. E., et al. (2015). Metal binding in photosystem II super-and subcomplexes from barley thylakoids. *Plant Physiol.* 168, 1490–1502. doi: 10.1104/pp.15.00559

Schöttler, M. A., and Tóth, S. Z. (2014). Photosynthetic complex stoichiometry dynamics in higher plants: environmental acclimation and photosynthetic flux control. *Front. Plant Sci.* 5:188. doi: 10.3389/fpls.2014.00188

Setiawati, T. C., and Mutmainnah, L. (2016). Solubilization of potassium containing mineral by microorganisms from sugarcane rhizosphere. *Agric. Agric. Sci. Proc.* 9, 108–117. doi: 10.1016/j.aaspro.2016.02.134

Spaepen, S., Vanderleyden, J., and Remans, R. (2007). Indole-3-acetic acid in microbial and microorganism-plant signaling. *FEMS Microbiol. Rev.* 31, 425–448. doi: 10.1111/j.1574-6976.2007.00072.x

Steel, R., Torrie, J., and Dicky, D. (1997). *Principles and Procedures of Statistics, A Biometrical Approach*, 3rd Edn. New York: McGraw Hill, Inc. Book Co.

Tang, Y., Kang, H., Qin, Z., Zhang, K., Zhong, Y., Li, H., et al. (2020). Significance of manganese resistant bacillus cereus strain WSE01 as a bioinoculant for promotion of plant growth and manganese accumulation in myriophyllum verticillatum. *Sci. Total Environ.* 707:135867. doi: 10.1016/j.scitotenv.2019.135867

Tsavkelova, E. A., Klimova, S. Y., Cherdyntseva, T. A., and Netrusov, A. I. (2006). Microbial producers of plant growth stimulators and their practical use: a review. *Appl. Biochem. Microbiol.* 42, 117–126. doi: 10.1134/S0003683806020013

Uren, N. C. (1981). Chemical reduction of an insoluble higher oxide of manganese by plant roots. *J. Plant Nut.* 4, 65–71. doi: 10.1080/01904168109362901

Vyas, P., and Gulati, A. (2009). Organic acid production in vitro and plant growth promotion in maize under controlled environment by phosphate-solubilizing fluorescent *Pseudomonas*. *BMC Microbiol.* 9:1–15. doi: 10.1186/1471-2180-9-174

Wei, Y., Shi, M., Lu, Q., Wei, Z., Wei, Y., Zhao, Y., et al. (2017). Effect of organic acids production and bacterial community on the possible mechanism of phosphorus solubilization during composting with enriched phosphate-solubilizing bacteria inoculation. *Bio. Technol.* 247, 190–192. doi: 10.1016/j.biortech.2017.09.092

Wei, Z., Hillier, S., and Gadd, G. M. (2012). Biotransformation of manganese oxides by fungi: solubilization and production of manganese oxalate biominerals. *Environ. Microbiol.* 14, 1744–1753. doi: 10.1111/j.1462-2920.2012.02776.x

Whitcomb, S. J., Heyneke, E., Aarabi, F., Watanabe, M., and Hoefgen, R. (2014). "Mineral nutrient depletion affects plant development and crop yield," in *Nutrient Use Efficiency in Plants. Plant Ecophysiology*, eds M. Hawkesford, S. Kopriva, and L. de Kok (Cham: Springer), 205–228. doi: 10.1007/978-3-319-10635-9_8

White, A. R., Xin, Y., and Pezeshk, V. (1993). Xyloglucan glucosyltransferase in golgi membranes from pisum sativum (pea). *Biochem. J.* 294, 231–238. doi: 10.1042/bj2940231

Xie, H., Pasternak, J. J., and Glick, B. R. (1996). Isolation and characterization of mutants of the plant growth-promoting rhizobacterium *Pseudomonas* putida GR12-2 that overproduce indoleacetic acid. *Curr. Microbiol.* 32, 67–71. doi: 10.1007/s002849900012

Conflict of Interest: The authors declare that the research was conducted in the absence of any commercial or financial relationships that could be construed as a potential conflict of interest.

Publisher's Note: All claims expressed in this article are solely those of the authors and do not necessarily represent those of their affiliated organizations, or those of the publisher, the editors and the reviewers. Any product that may be evaluated in this article, or claim that may be made by its manufacturer, is not guaranteed or endorsed by the publisher.

Copyright © 2021 Ijaz, Mumtaz, Wang, Ahmad, Saqib, Maqbool, Zaheer, Wang and Mustafa. This is an open-access article distributed under the terms of the Creative Commons Attribution License (CC BY). The use, distribution or reproduction in other forums is permitted, provided the original author(s) and the copyright owner(s) are credited and that the original publication in this journal is cited, in accordance with accepted academic practice. No use, distribution or reproduction is permitted which does not comply with these terms.

frontiers in Plant Science

ORIGINAL RESEARCH
published: 11 November 2021
doi: 10.3389/fpls.2021.696045

Physiological and Morphological Responses of Hydroponically Grown Pear Rootstock Under Phosphorus Treatment

Guodong Chen[1], Yang Li[1], Cong Jin[1], Jizhong Wang[1], Li Wang[2] and Juyou Wu[2]**

[1]College of Life Science and Food Engineering, Huaiyin Institute of Technology, Huai'an, China, [2]College of Horticulture, Nanjing Agricultural University, Nanjing, China

Phosphorus (P) is an essential macronutrient for the growth and development of fruit trees, playing an important role in photosynthesis, nucleic acid synthesis, and enzyme activity regulation. The plasticity of plant phenotypic has been investigated in diverse species under conditions of P-deficiency or P-excess. Based on these researches, P level fluctuations in different species result in different characteristics of the response. Nevertheless, little is known about the response of pear seedling rootstock (*Pyrus betulifolia* Bunge) to the changing of P levels. To explore the effects of different levels of P on the growth of pear seedling rootstock, we performed the hydroponic assays to determine and analyze the biological indexes including growth parameters, photosynthetic rate, root and shoot morphological traits, and concentrations of macro- and micronutrients. The results show that either deficiency or excess of P inhibited the growth and development of pear seedling rootstock. Root growth (down 44.8%), photosynthetic rate (down 59.8%), and acid phosphatase (ACP) activity (down 44.4%) were inhibited under the P-deficiency conditions (0 mM), compared with normal P conditions (1 mM). On the other hand, dark green leaves, suppression of root elongation (down 18.8%), and photosynthetic rate (down 25%) were observed under regimes of excessive P, compared with normal P conditions (1 mM). Furthermore, the root concentration of not only P, but also those of other mineral nutrients were affected by either P treatment. In brief, these results indicated that a careful choice of P fertilizer supply is crucial to ensuring normal growth and development of pear seedling rootstock.

Keywords: pear seedling rootstock, phosphorus, root system architecture, nutrients, photosynthesis

OPEN ACCESS

Edited by:
Francesco Di Gioia, The Pennsylvania State University (PSU), United States

Reviewed by:
Lorenzo Rossi, University of Florida, United States
Sezai Ercisli, Atatürk University, Turkey

****Correspondence:***
Guodong Chen
chenguodong@hyit.edu.cn
Juyou Wu
juyouwu@njau.edu.cn

Specialty section:
This article was submitted to Plant Nutrition, a section of the journal Frontiers in Plant Science

Received: *16 April 2021*
Accepted: *25 October 2021*
Published: *11 November 2021*

Citation:
Chen G, Li Y, Jin C, Wang J, Wang L and Wu J (2021) Physiological and Morphological Responses of Hydroponically Grown Pear Rootstock Under Phosphorus Treatment. Front. Plant Sci. 12:696045. doi: 10.3389/fpls.2021.696045

INTRODUCTION

Phosphorus is one of the most important nutrients in the growth and development of fruit trees. It not only participates directly in the metabolism of sugar, protein, and fat, affecting the yield and quality of fruit trees (Carstensen et al., 2018; Qu et al., 2020; Siedliska et al., 2021), but it is also an indispensable component of the energy carrier ATP and the reducing agent NADP,

generated by photosynthesis in plants (Shi et al., 2020; De Andrade et al., 2021), playing important roles in the process of photosynthesis, signal transduction, and physiological and biochemical regulation (Ham et al., 2018; Huang et al., 2019). Approximately 43% of the cultivated land in the world is deficient in phosphorus, with about two-thirds of the cultivated land in China being low in phosphorus (Wang et al., 2010). Therefore, with the rapid development of modern agriculture and increasing market demand, increasing the application of phosphorus fertilizer has become a quick way to improve soil fertility, and crop yield and quality. However, there are significant differences in the efficiency of phosphorus uptake and utilization among different crops, and different phenotypic symptoms are shown in response to different P levels, which can be reflected in the external morphology and internal physiological and biochemical processes of plants.

The use of rootstock in fruit production is inevitable, and rootstocks have a primary role in determining orchard efficiency, they are responsible for water and mineral uptake and provide anchorage for the tree (Guney, 2019; Cimen, 2020; Rufato et al., 2021). Commercial pear trees, such as Asian pear (*Pyrus pyrifolia* L.), are mainly propagated by grafting. The scion is grafted on rootstock, which determines most of the shoot traits, affecting the growth, yield, foliar disease resistance, and fruit characteristics of the grafted plants (Fisarakis et al., 2004), whereas the rootstock determines root traits such as pest and disease resistance, as well as overall pear tree size. However, as most of the cultivated land in China is lacking in phosphorus, the fruit growers tend to apply large amounts of phosphate fertilizer in an attempt to compensate, which will bring about losses to the production of certain crop plants (Veneklaas et al., 2012). Therefore, it is of vital significance to study the physiological phenotypic traits and the changes in mineral element concentrations in tissues of birch-leaf pear (*Pyrus betulifolia* Bunge), which is commonly used as the rootstock for commercial pear grafting, under phosphorus stress (deficiency or excess), in order to guide the balanced nutrient application to pear trees, to improve the yield and quality of pear, and to maintain soil fertility and protect the environment.

The utilization of soil phosphorus by fruit trees is achieved mainly through the active uptake process by roots along the inverse phosphate concentration gradient (Richardson et al., 2005). It is generally accepted that the utilization of phosphorus is realized by extruding H^+ from the cell *via* the H^+-ATPase ion pump, located on the vacuolar membrane, to generate a membrane potential as the driving force for phosphate uptake, with the aid of a protonated phosphate root carrier, which belongs to the co-transport mode of H^+ and $H_2PO_4^-$ (Yu et al., 2016). The epidermal cells of the root system of fruit trees are the main sites of phosphate accumulation in plants. The phosphate enters the xylem vessels through the symplast route and is then transported to the shoot of the plant for use by the fruit trees. Previous studies have shown that a series of morphological, physiological, and biochemical changes of plants under phosphorus stress, on the one hand, can reduce or increase the demand for phosphorus by reducing the growth rate, activating the use of phosphorus, or changing the process of carbon metabolism in plants (Brembu et al., 2017). On the other hand, the absorption of phosphate can be regulated by changing the root/shoot ratio, the morphology and configuration of root, or the level of organic acid anions, resulting from ACP activity, secreted by the roots (Tang et al., 2020). However, the morphological adaptation and physiological responses of different plants to phosphorus stress also show different characteristics. For example, in rubber tree (Moreira et al., 2013), *Stylosanthes guianensis* (Latief et al., 2020), soybean (Mo et al., 2019), and wheat (Shen et al., 2018), the growth indexes of total root length, root surface area, root volume, and root tip number were significantly reduced under low-phosphorus conditions, whereas the shoot resources were preferentially distributed to the roots, increasing the total surface area of the roots, the number of lateral roots, the root/shoot ratio, and the total root length under low-phosphorus conditions in cotton (Wang et al., 2018), tobacco (Zheng et al., 2013), and tomato (Marques, 2018). When *Stylosanthes* suffered from phosphorus stress, the concentrations of citric acid, succinic acid, and malic acid, and the activities of phosphatase, and the antioxidant enzymes superoxide dismutase, peroxidase, and catalase in the roots were significantly increased (Luo et al., 2020). In addition, the photosynthetic rate of leaf was significantly decreased, and the synthesis and transportation of soluble sugar were also affected by phosphorus stress in leaf, which lead to the shorter of plant height and less of leaf area (Veronica et al., 2017).

Excessive application of phosphate fertilizer will also cause a phosphorus stress, causing different degrees of damage to plants, leading not only to greater nutrient concentrations in the plant tissues, but also to decreasing soluble protein content and net photosynthetic rate in leaves, which, in turn, slows the growth and development of the plants. Moreover, phosphorus which has not been absorbed and utilized by plants leaches from the soil, causing environmental pollution and eutrophication of water bodies (Huang et al., 2012; Ye et al., 2015).

Identified as an advanced cultivation method in soilless culture, hydroponics directly contacts plant roots with nutrient solution to ensure plant growth and development. Compared with the traditional soil planting, hydroponics technology has the advantages of short growth cycle, effective resource saving, flexible cultivation condition, and reduced infection rate of diseases and pests (Shehzad et al., 2021). In addition, hydroponic method is capable of helping in the observation and management, as it can accurately control the growth and development process of plants (Sugiharta et al., 2019). Researchers have studied the phenotypic characteristics of plants through hydroponic method in the cultivation processes of diverse fruit species. For example, the hydroponic system was applied to investigate the reaction mechanism responding to Fe shortage in two grape rootstocks, simultaneously compare changes in morphological, physiological, and biochemical parameters (Marastoni et al., 2020). In apple, Qi et al. (2019) employed the hydroponic assay to explore the *Malus hupehensis* K^+ uptake mechanism under drought stress. In citrus, Zhou et al. (2014) evaluated the effects of B-deficiency on plant growth and root-morphology traits *via* hydroponic

Abbreviations: P, Phosphorus; ACP, Acid phosphatase; ICP, Inductively coupled plasma; FW, Fresh weight; P_n, Net photosynthetic rate; C_i, Intercellular CO_2 concentration; T_r, Transpiration rate; G_s, Stomatal conductance value.

assays in seven citrus rootstocks. Furthermore, some researchers utilized the hydroponics system to study the effects of mineral elements on plant phenotype in *Arabidopsis*, maize, and sunflower, respectively (Rivelli et al., 2010; Gruber et al., 2013; Kong et al., 2020).

Pear is one of the most important fruits, greatly appreciated by consumers around the world, because it is a flavorful and nutrient-rich fruit with medicinal effects. However, symptoms of phosphorus deficiency in pear trees and subsequent excessive applications of phosphate fertilizer reduce the growth, development, yield, and fruit quality of pear trees. Therefore, it is of great importance to study the response characteristics of pear trees to phosphorus stress to achieve the sustainable development of a modern fruit industry. In this study, the plant growth, root morphology, and changes in phenotypic symptoms of pear seedling rootstock (*P. betulifolia*) were analyzed by hydroponic system under both high- and low-phosphate stress, as the roots (contributed by the rootstock) are the principal initial site of phosphate stress. Furthermore, the effects on mineral element concentrations and photosynthetic rate were also determined under conditions of phosphorus deficiency or excess, to provide a theoretical basis for the balanced fertilizer application of phosphorus, to regulate root growth in pear.

MATERIALS AND METHODS

Plant Materials and Treatment

In this study, seedlings of the birch-leaf pear (*P. betulifolia*) were used. Before the hydroponic experiments were set up, pear seeds were initially surface sterilized for 15 min with 3% (v/v) sodium hypochlorite solution, then rinsed thoroughly with distilled water. The sterilized pear seeds were then soaked in distilled water for 24 h before being placed in a box of expanded polystyrene foam filled with clean moist sand (5–10% moisture content), and were incubated at 4°C for 40 days to achieve stratification. The stratified seeds were transferred into a growth chamber for 2 days until the seeds germinated; the germinated seeds were then transplanted into 5- × 10-hole black plastic trays of modules filled with vermiculite. After 14 days, uniform seedlings were transplanted to half-strength nutrient solution containing 0.5 mM KH_2PO_4, 1 mM $MgSO_4{\cdot}7H_2O$, 2 mM $Ca(NO_3)_2{\cdot}4H_2O$, 2.5 mM KNO_3, 0.5 mM NH_4NO_3, 0.83 mg/L KI, 6.2 mg/L H_3BO_3, 8.6 mg/L $ZnSO_4$, 0.25 mg/L Na_2MoO_4, 0.025 mg/L $CuSO_4$, 0.025 mg/L $CoCl_2$, 22.3 mg/L $MnSO_4$, and 0.05 mM Na_2EDTA-Fe for a 1-week pre-culture period. Subsequently, the pear seedlings were placed into full-strength nutrient solution containing different concentrations of KH_2PO_4 (0, 0.5, 1, and 5 mM), with the potassium concentration being balanced by the addition of 5, 4.5, 4, and 0 mM KCl, respectively. The pH value of each nutrient solution was adjusted to 5.8 with 100 mM KOH. The nutrient solution was replaced twice each week and ventilated for 30 min every 3 h by the combined action of a timer (Pinyi AL-06; China) and a ventilation pump (SUNSUN ACO, China). All the seedlings were cultured in a growth chamber (Jiangnan Instrument, Ningbo, China) with a light intensity of 800 mmol m^{-2} s^{-1} of photosynthetically active radiation, and a light/dark regime of 14/10 h at 28/22°C and 75% relative humidity. The pear seedlings were cultured for 5 weeks, by which time the typical outward symptoms of P excess or deficiency had become apparent.

Harvest and Morphological Parameter Measurement of Pear Seedlings

After 5 weeks of treatment, the pear seedlings were harvested and divided into leaf, stem, and root tissues. The fresh weight (FW) of root, stem, and leaf were measured on an electronic analytical balance (FA, 2014), then the root/shoot ratio was calculated. The leaf area of each seedling was measured using a leaf area meter (Li-3100C; LI-COR Biosciences Inc., Lincoln, NE, United States). The length of the main root and the plant height were measured using a scaled ruler. Representative leaves and roots from seedlings from the different P treatments were imaged by a PowerShot Pro 1 camera (Canon, Tokyo, Japan).

Measurement of Root System Architecture of Pear Seedlings

Pear seedlings were harvested at random from the various P-treatment groups and the root systems were rinsed with distilled water before assessment of root-related parameters. Total root length, total root number, total root volume, total root surface area, and the mean root diameter were determined for each plant, using an Epson digital scanner (Expression 10000XL 1.0; Epson Inc., Japan), and the root images were analyzed with WinRhizo software (Regent Instruments Canada Inc., 2013).

Measurement of Photosynthetic Parameters of Pear Seedlings

Photosynthetic parameters measurement was assessed according to Wang et al. (2018). The brief process is as follows: Net photosynthetic rate (P_n), intercellular CO_2 concentration (C_i), transpiration rate (T_r), and stomatal conductance value (G_s) were measured at different P treatments using a portable photosynthesis measuring system (LI-COR 6400, Lincoln, NE, United States). These measurements were performed on sunny days between 9:00 and 11:30 a.m. in each unit under the following parameters: the ambient CO_2 concentration was 378 μmol mol^{-1}, light intensity of 2,000 μmol(photon) m^{-2} s^{-1}, and leaf air vapor pressure was 2.5 ± 0.3 kPa.

Leaf Chlorophyll Concentrations of Pear Seedlings

Chlorophyll was extracted from 100 mg fresh leaves taken from seedlings subject to various P treatments, by grinding the leaves with a mortar and pestle for 5 min in 10 ml of 85% (*v*/*v*) acetone. The homogenate was sieved through filter paper, and the filtrate was transferred into a 15-ml Falcon tube and adjusted to a set fixed volume using 85% (*v*/*v*) acetone. Absorbance of the sample extracts was determined at both 663 and 644 nm with a UV-1800 spectrophotometer (AuCy, China). The concentration of chlorophyll *a* and *b* were calculated by the following equations:

chlorophyll $a = 1.07 \times (A_{663}) - 0.094 \times (A_{644})$; chlorophyll $b = 1.77 \times (A_{644}) - 0.280 \times (A_{663})$; total chlorophyll = chlorophyll a + chlorophyll b. The unit for chlorophyll concentration was mg g^{-1} FW sample.

Measurement of Mineral Element Concentrations in Pear Seedlings

The mineral element concentrations of pear seedlings were measured as described previously (Chen et al., 2018). For total N concentration, approximately 1 mg dry weight of frozen root tissue from each P treatment was ground in a ball mill and used for analysis by a Kjeldahl apparatus (JK9870). For the determination of concentrations of other mineral elements, a known weight (0.1–0.9 g dry weight) of roots from each replicate of each P treatment was put into a PTFE digestion tube and digested with nitric acid in a microwave digester (Ultraclave 4; MLS). The concentration of mineral elements was analyzed by ICP–OES (inductively coupled plasma–optical emission spectrometry; 6500 dual ICP–OES spectrometer; Thermo Fisher Scientific, Waltham, MA, United States).

Assay of Acid Phosphatase Activity in Pear Seedlings

The assay of ACP (acid phosphatase) activity used was a slightly modified version of McLachlan's method (McLachlan et al., 1987). In brief, roots and leaves harvested from seedlings exposed to the different P treatments were rinsed with distilled water, before being blotted carefully with tissue paper. Samples (1 g) of root or leaf were snap frozen with liquid nitrogen and then ground in a mortar and pestle, before the ground sample was suspended in 10 ml of precooled extraction buffer. After incubation in an ice-bath for 1 h, the solution was centrifuged at 4°C and 10,000 × g for 25 min. An aliquot (1 ml) of the supernatant was treated with 1 ml buffer and 0.1 ml 4-nitrophenyl phosphate, disodium salt (pNPP-Na2), then incubated for 10 min at 30°C. After 10 min, the reaction was stopped by adding 1 ml 0.5 M NaOH. ACP activity was then measured at 400 nm, using a UV-1800 spectrophotometer (AuCy, China). The level of ACP activity, in terms of the amount of p-nitrophenol produced (nmol per FW mg^{-1} root or leaf per min), was calculated by the following equation: ACP activity (nmol/min mg) = $[(A/0.019) \times 3.1 \cdot (V/V1)]/[10 \times W(g)]$, where A = absorbance value of the sample; V = total volume of the enzyme extract; $V1$ = the measurement of volume of the enzyme extract; W = weight of sample; and 10 = incubation time (min).

Experimental Design and Statistical Analyses

The experiment was established in a completely randomized 1 × 4 factorial design, with one pear rootstock source being subjected to four P treatments. All data on physiological and biochemical parameters are represented as mean ± standard deviation ($n = 3$ biological replicates). Statistical analyses of the data were performed by analysis of variance (ANOVA), using the SPSS statistical package (IBM, Armonk, NY, United States). Differences between samples were statistically compared for significance using the Duncan's multiple range test. A probability level of 0.05 was considered to be statistically significant.

RESULTS

Effect of Different P Levels on Phenotypic Symptoms and Root Growth

To investigate the dynamic responses of pear seedlings to P stress (deficiency or excess) conditions, the phenotypic symptoms and root growth of pear seedlings grown under different concentrations of P were recorded using a photo-imaging system. Marked variations were observed in response to different P treatments (**Figure 1**). For example, the color of the pear seedling leaves changed from green to yellow or purple as the P supply level decreased (from 1 to 0 mM), whereas the color of leaves showed symptoms of pale green under excessive P supply conditions, with the effect on leaf color being greater under P-deficient than under excess P conditions. In addition, leaf expansion rate was also significantly inhibited under P-deficient conditions. Conversely, there was no significant effect on leaf expansion rate under P-excess conditions. On the other hand, root growth was inhibited under either P stress (0 or 5 mM), especially with respect to P deficiency (**Figure 1**). In brief, P-deficient or P-excess supply leads to an inhibition of pear seedling growth and development.

Root Architecture Plasticity in Response to P Treatments

Root architecture refers to the structure and spatial distribution of the root system, which is mainly a three-dimensional spatial structure, formed to maximize the capture of water and nutrients in the soil. However, changes in nutrient availability and concentrations will affect the root architecture plasticity of fruit trees. Therefore, in order to explore the effects of different concentrations of P on the root architecture of pear seedling rootstock, the responses of the parameters total root length, total surface area, total root volume, mean root diameter, and root tip number to different P levels were analyzed. The total root length, surface area, volume, and root number on pear seedling rootstock changed significantly under P stress (deficiency or excess) conditions, but the root diameter was not significantly affected (**Table 1**). For example, over a range of deficient to adequate P conditions (0–1 mM), the total root length, surface area, volume, and number of root tips of the seedlings increased with the increasing P supply concentration. The total length, surface area, volume, and number of root tips of the seedlings increased by 81.3, 72.6, 83.3, and 120.6%, respectively, when the seedlings were grown under the 1 mM P level, compared with the P-deficient conditions (0 mM). The total root surface area and root volume did not change significantly when the culture solution P concentration increased from the low-P concentration 0.5 mM to the normal P concentration of 1 mM, whereas the total root length and root tip number increased significantly by 9.5 and 11.5%, respectively, over the same concentration range. Excessive P supply (5 mM) did not promote the root growth of

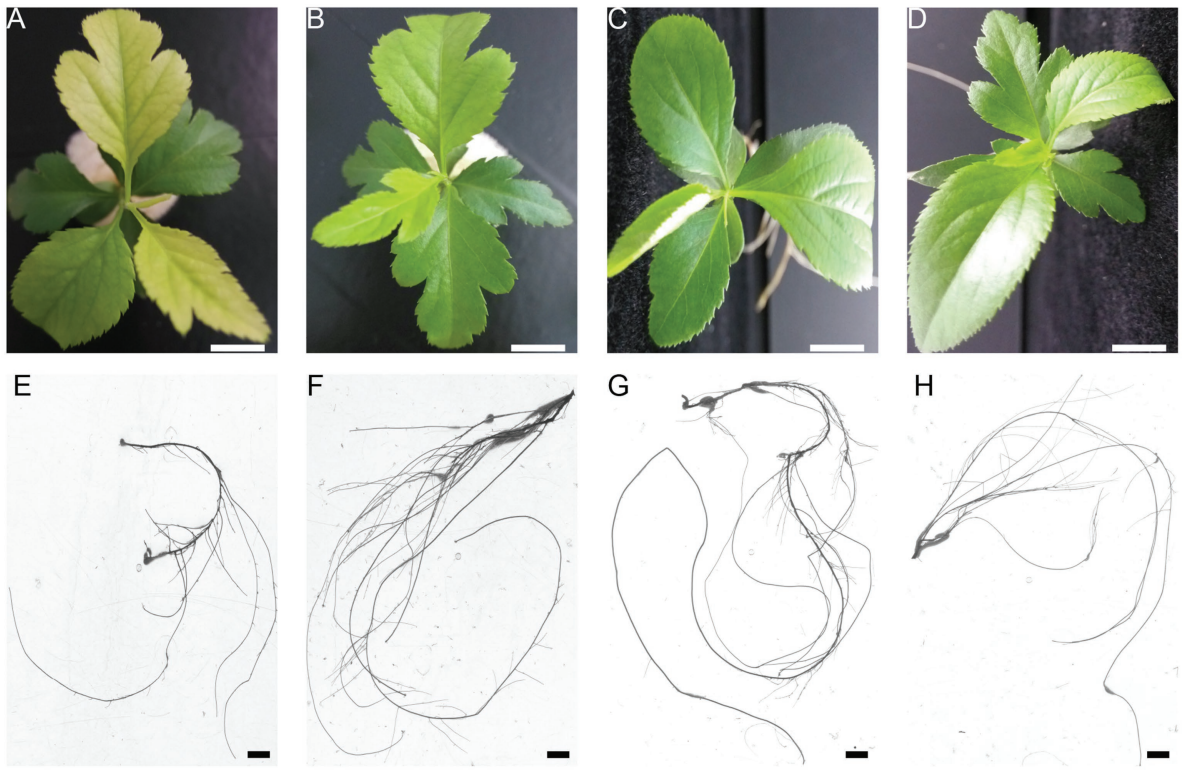


FIGURE 1 | The effect of P treatments on phenotypic symptoms and root growth. Leaf color and expansion rate **(A–D)**, and root growth **(E–H)** of *Pyrus betulifolia* seedlings exposed to 0.0 **(A,E)**, 0.5 **(B,F)**, 1.0 **(C,G)**, or 5 mM P **(D,H)**. The bars in **(A–H)** are 1 cm.

TABLE 1 | Effects of different P treatments on roots morphologic parameters of the pear seedling rootstock.

Treatments	Root length (cm)	Root surface area (cm^2)	Root volume (cm^3)	Root number	Diameter (mm)
0 mM	48.76 ± 2.56^{d}	6.23 ± 0.35^{c}	0.06 ± 0.01^{c}	$194.44 + 8.80^{d}$	0.41 ± 0.02^{a}
0.5 mM	80.75 ± 5.14^{b}	10.11 ± 0.74^{ab}	0.10 ± 0.01^{ab}	384.67 ± 16.84^{c}	0.41 ± 0.06^{a}
1 mM	88.4 ± 4.90^{a}	10.75 ± 0.42^{a}	0.11 ± 0.01^{a}	428.89 ± 18.40^{a}	0.39 ± 0.07^{a}
5 mM	71.78 ± 3.34^{c}	9.06 ± 0.32^{b}	0.09 ± 0.01^{b}	396.89 ± 14.61^{b}	0.39 ± 0.03^{a}

Letters in superscript indicate whether mean values are significantly different between treatments ($p < 0.05$; different letters) or not (same letter).

pear seedling rootstock, but the total root length, root surface area, root volume, and root tip number were inhibited, resulting in decreases by 18.8, 15.7, 18.2, and 7.5%, respectively, compared to the corresponding values obtained at normal P levels (1 mM).

The Effect of P Treatments on Shoot Growth of Pear Seedlings

The level of exogenous nutrient supply to fruit trees would also be expected to affect shoot growth in the pear seedlings. In order to study the shoot growth and development parameters of the seedlings under different P treatments, the parameters leaf number, total leaf area, plant height, and internode length were investigated. Over the concentration range 0 (deficient)–1 (normal mM P), the leaf number, total leaf area, plant height, and mean internode length of the pear seedlings all increased in response to increasing P supply concentration (**Figure 2**). For example, the number of leaves, total leaf area, plant height, and mean stem internode length increased by 100, 299, 78, and 123%, respectively, when the P supply level was 1 mM, compared with the P-deficient level (0 mM). On the other hand, the leaf number and plant height of the seedlings did not change significantly when the P supply level was increased from the low-P concentration 0.5 to 1 mM, but the total leaf area and mean stem internode length changed significantly over the same range, increasing by 30 and 20%, respectively. In addition, the leaf number and plant height did not change significantly when P supply was raised from 1 mM to 5 mM, but both the total leaf area and the mean stem internode length were significantly inhibited at 5 mM, decreasing by 39 and 13%, respectively, compared with the normal P (1 mM) supply (**Figure 2**).

The Effect of P Treatments on the Root/Shoot Fresh Weight Ratio

To examine the effects of P stress (deficiency or excess) on the growth and development of the pear seedlings, the FW of leaves, stems, and roots of seedlings grown under different

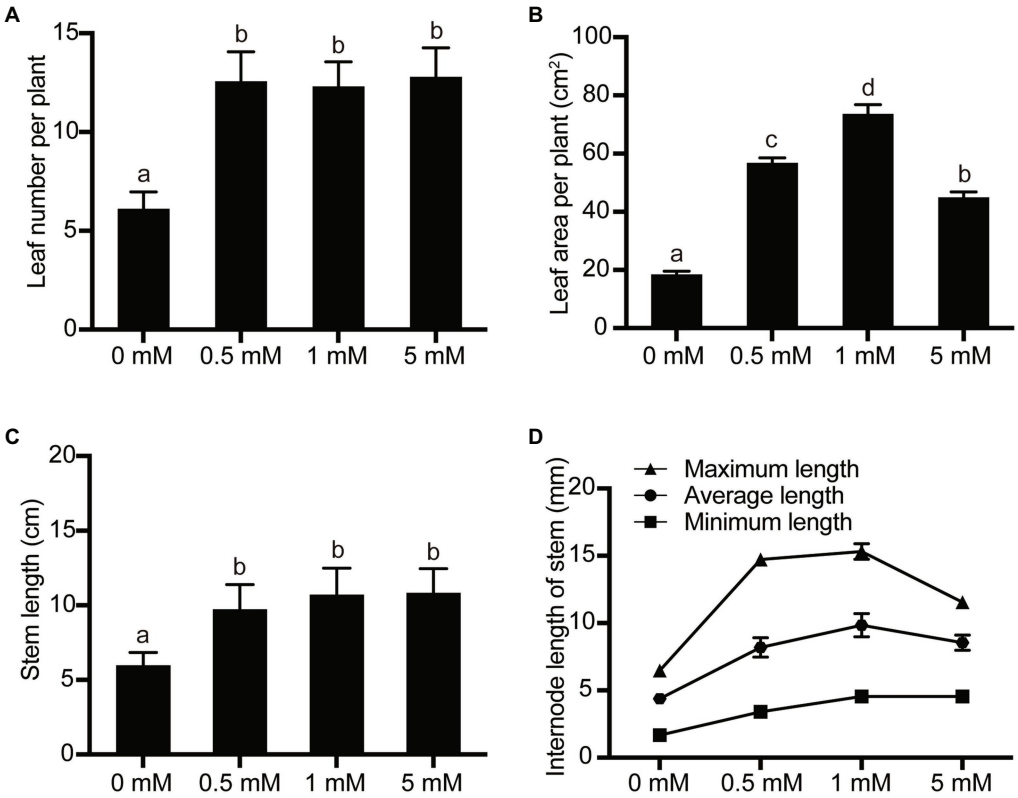


FIGURE 2 | The effects of P treatments on pear seedling shoot growth. **(A)** The leaf number per pear seedling; **(B)** The leaf area per pear seedling; **(C)** The stem length per pear seedling; and **(D)** The internode length of stem per pear seedling. Data are presented as mean ± standard deviation of three replicates, and each replicate is based on measurements made from three plants. Samples in a bar chart with a common superscript letter are not significantly different ($p > 0.05$), according to the Duncan's multiple range test.

P treatments were measured and the root/shoot FW ratio was calculated. Because the number and total length of roots were both suppressed under low- or high-P stress conditions (**Table 1**), the root FW decreased concomitantly (**Figure 3**). Compared with seedlings grown under the normal P levels (1 mM), seedlings grown under the low P (0 mM) or excess P (5 mM) treatments exhibited a 50% or 34% decrease in root FW, respectively (**Figure 3**). On the other hand, since the growth of the leaf and the stem were significantly inhibited under conditions of both P deficiency (0 mM) and P excess (5 mM), the leaf and stem FW initially increased with increasing P supply from 0 to 1 mM and then decreased when the highest concentration of P (5 mM) was supplied. The root/shoot FW ratio largely reflects the distribution of the photosynthetic product between the root and shoot. The experimental results showed that the ratio of root/shoot FW was significantly increased under conditions of P deficiency, due mainly to the fact that shoot FW appears to be more sensitive to low P conditions than does root FW. However, no significant differences in the root/shoot ratio were observed between the 1 mM (normal) and 5 mM (excess) levels of P supply, due mainly to the fact that both root and shoot growth were suppressed under the condition of excessive P supply, leading to similar changes in root and shoot FW.

The Effect of P Treatments on Photosynthetic Parameters

The synthesis of carbohydrates by fruit trees is mainly achieved by leaf photosynthesis, with the important photosynthetic parameters being mainly the rate of net photosynthetic rate (P_n), intercellular CO_2 concentration (C_i), transpiration rate (T_r), and stomatal conductance value (G_s). As shown in **Figure 4**, the photosynthetic parameters exhibited by pear seedling rootstock leaves were significantly affected by the different P levels supplied to the seedlings. Generally, the rate of net photosynthesis, intercellular CO_2 concentration, stomatal conductance value, and transpiration rate of pear seedling rootstock leaves increased with increasing P supply level. The rate of net photosynthesis, intercellular CO_2 concentration, stomatal conductance value, and transpiration rate increased by 149, 159, 650, and 433%, respectively, when P supply concentration was increased from the P-deficiency level (0 mM) to the normal P concentration (1 mM). In addition, the rate of net photosynthesis, intercellular CO_2 concentration, stomatal conductance value, and transpiration rate increased by 58, 44, 127, and 109%, respectively, when the P level at which pear seedling rootstock was grown increased from P-deficiency levels (0 mM) to low-P levels (0.5 mM). However, it is worth noting that the net photosynthesis rate, intercellular CO_2 concentration, stomatal conductance value, and transpiration rate of leaves were

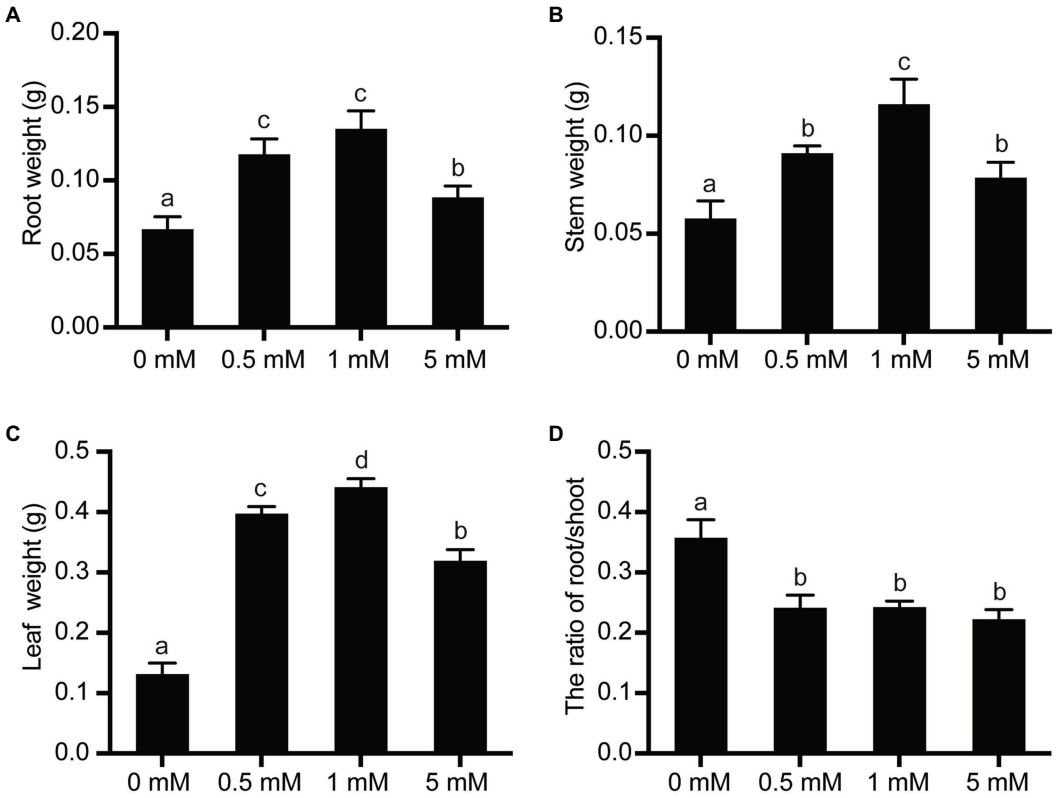


FIGURE 3 | The effects of P treatments on the organ weight and root/shoot ratio in pear seedlings. **(A)** Root FW per pear seedling; **(B)** Stem FW per pear seedling; **(C)** Leaf FW per pear seedling; and **(D)** Root/shoot FW ratio. Data are presented as mean ± standard deviation of three replicates, and each replicate is based on measurements made from three plants. Samples in a bar chart with a common superscript letter are not significantly different ($p > 0.05$), according to the Duncan's multiple range test.

inhibited when the P supply level increased from normal P levels (1 mM) to excessive P (5 mM), decreasing by 25, 40, 32, and 23%, respectively.

The Response to P Treatments of Chlorophyll Concentrations

In order to investigate the impact of P concentration on leaf chlorophyll concentrations, the leaf chlorophyll concentrations were analyzed in the pear seedlings from the four different P concentrations. Comparisons of the data showed that the total leaf chlorophyll concentration decreased significantly by 29 and 13% in seedlings grown under P-deficient (0 mM) and low-P (0.5 mM P) conditions, respectively, compared with seedlings supplied with a normal (1 mM) P level (**Figure 5A**). Furthermore, the synthesis of total chlorophyll was also significantly suppressed under excess P (5 mM) conditions, decreasing by 29% in the seedlings grown under 5 mM P conditions, compared to those grown under a normal P supply (1 mM, **Figure 5A**). On the other hand, the responses of either chlorophyll *a* or chlorophyll *b* concentrations to increasing P concentration in the hydroponic growth medium were similar to those of total chlorophyll concentration (**Figure 5B**). In addition, the concentration of chlorophyll *a* was more than three times that of chlorophyll *b* under the four P treatment conditions (**Figure 5B**). In brief, the experimental results showed that P stress (either deficiency or excess) inhibits the synthesis of chlorophyll, resulting in a decreased chlorophyll concentration, which may occur because P is an essential component in some photosynthetic enzymes.

Effects of Different P Levels on Acid Phosphatase Activity in Pear Seedlings

Intracellular ACP is a key enzyme in the release by hydrolysis and mobilization of phosphate in vacuoles into inorganic phosphorus. ACP is an inducible enzyme, the activity of which is affected by the availability of organic phosphorus, and it also plays an important role in the metabolism and reuse of organic phosphorus (Barker et al., 1974; McLachlan et al., 1987; Shen et al., 2018). Therefore, we researched the effects of seedling culture under different concentrations of exogenous P on ACP activity in the root and leaf tissue of pear seedlings. P-deficiency (0 mM) or low-P treatments (0.5 mM P) significantly induced ACP activity in pear roots by 80 and 27%, respectively, compared with seedlings cultured under normal (1 mM) P supply (**Figure 6**). However, no significant difference in ACP activity was detected between seedling roots grown under conditions of normal or excess P concentration. Furthermore, the ACP activity in leaves was also significantly influenced by

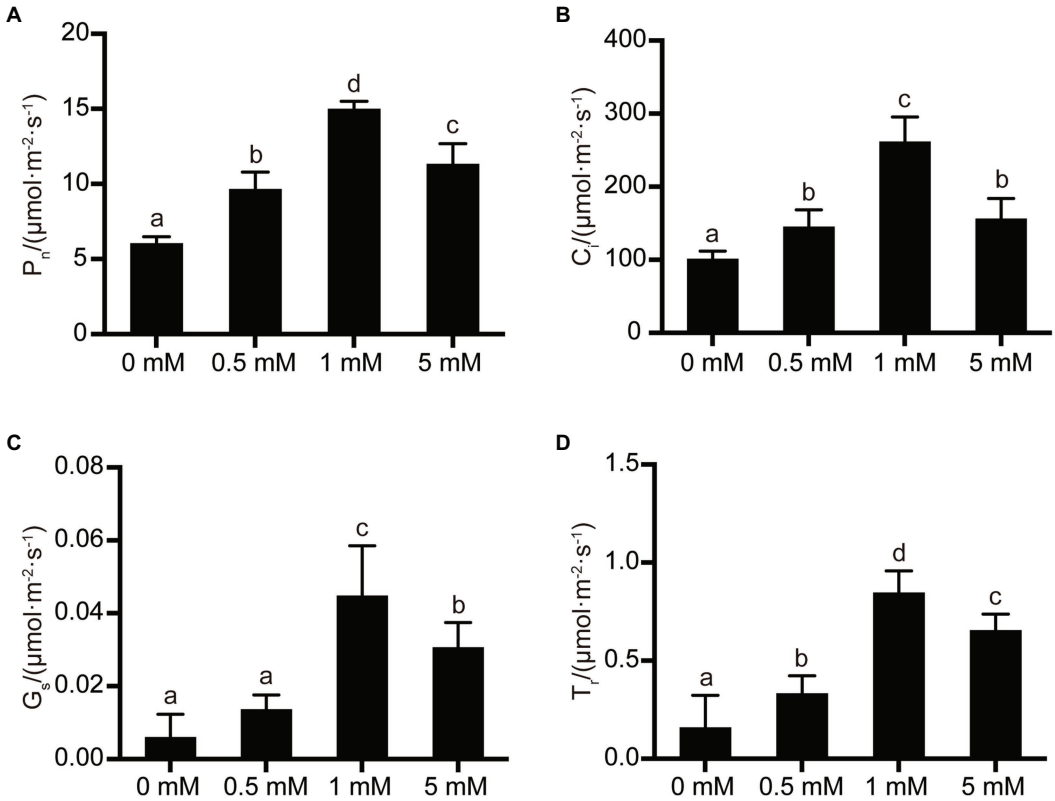


FIGURE 4 | The effects of P treatments on photosynthetic parameters in pear seedling leaves. **(A)** The net photosynthetic rate of pear seedlings under different P levels; **(B)** The intercellular CO_2 concentration of pear seedlings under different P levels; **(C)** The stomatal conductance of pear seedlings under different P levels; and **(D)** The transpiration rate of pear seedlings under different P levels. Data are presented as mean ± standard deviation of three replicates, and each replicate is based on measurements made from three plants. Samples in a bar chart with a common superscript letter are not significantly different ($p > 0.05$), according to the Duncan's multiple range test.

the different P treatments (**Figure 6**). The activity of ACP in leaves fell with an increase in P concentration within the range 0–1 mM P. Seedlings grown under P-deficient or low-P (0 or 0.5 mM, respectively) conditions resulted in a 144% or 78% increase in ACP activity, respectively, compared with activities in leaves of seedlings grown under the normal P levels (1 mM).

The Effect of P Treatments on Mineral Element Concentrations in Pear Seedling Roots

The concentrations of macronutrient elements (N, P, K, Ca, and Mg) and micronutrient elements (Fe, Mn, B, Zn, and Cu) were analyzed in the roots of pear seedlings, which had been grown under one of four levels of P. The P concentrations in the root gradually increased with increasing P supply when the level of P supply was between 0 and 1 mM, but there was no significant increase when the P supply was in excess (5 mM P; **Figure 7**). The concentrations of N, K, and Mg in the roots increased with increasing P level application over the range 0–1 mM. However, the concentrations of N, K, and Mg in roots were significantly inhibited when the P supply was in excess (**Figure 7**). It is worth noting that the root concentration of Ca showed a response trend to the four levels of P different from those of N, K, and Mg, with a significant decrease in Ca concentration as the P level increased over the range 0–1 mM. Not only the macronutrient concentrations but also the micronutrient concentrations were influenced by different P supply treatments. The concentrations of Mn and Cu displayed a trend similar to that of Ca in response to P supply concentration, decreasing markedly with increasing P supply (0–1 mM), but the concentration of Mn and Cu increased significantly when the P supply was in excess (5 mM; **Figure 7**). The concentration of Zn displayed a trend different from that of other micronutrient elements in response to increasing P levels, showing a significant decrease with increasing P supply (0–5 mM). In addition, the root concentration of Fe was significantly inhibited only when P was supplied in excess, with no significant effects being observed at the other, lower P supply levels. Interestingly, the concentration of B did not change significantly under any P stress (deficiency or excess).

DISCUSSION

Symptoms and Plant Growth

Previous studies have shown that plants often exhibit morphological and physiological changes under P-deficient

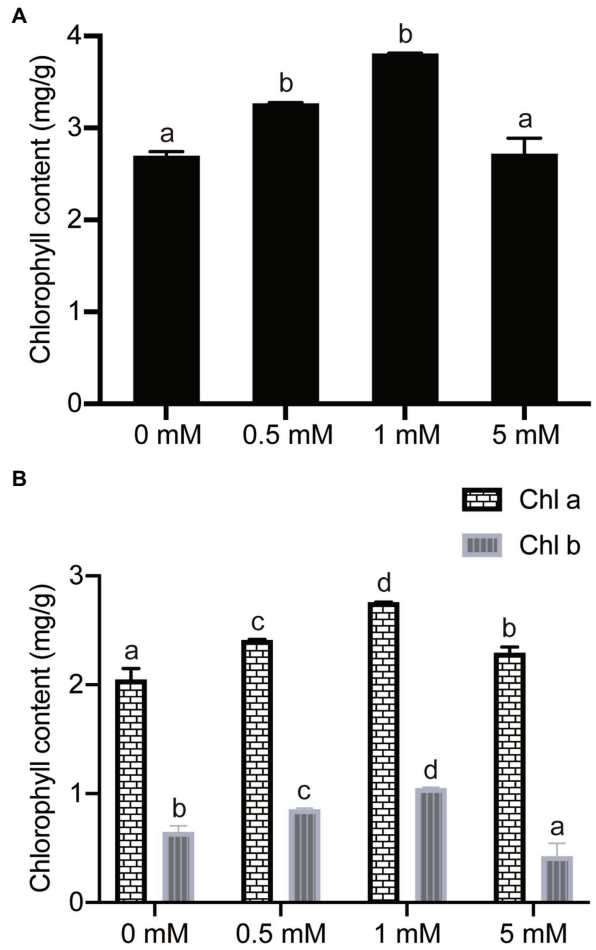


FIGURE 5 | The effects of different P treatments on the chlorophyll concentrations in pear seedlings. **(A)** Total chlorophyll concentrations; and **(B)** Chlorophyll *a* and chlorophyll *b* concentrations. Data are presented as mean ± standard deviation of three replicates, and each replicate is based on measurements made from three plants. Samples in a bar chart with a common superscript letter are not significantly different ($p > 0.05$), according to the Duncan's multiple range test.

conditions, such as stunted growth, reduction in leaf number, and decreased leaf area (Reddy et al., 2020). Studies in *Cucurbita pepo*, for example, demonstrated that the root/shoot ratio and the number of root tips were significantly increased under P-deficient conditions (Cao and Chen, 2012). In rice, plants exhibited stunted growth, with the foliage turning dark green color with reddish-purple tips and leaf margins under P-deficient conditions (Chen et al., 2014). In poplars, P deficiency caused chlorosis (pale yellow leaf color) and a decrease in leaf size after 60 days of treatment (Zhang et al., 2014). Furthermore, an excessive P supply can also lead to a dark green leaf color, a dwarf habit, and delayed flowering in crop plants (Maharajan et al., 2018). In the present study, symptoms similar to those reported in the literature were observed in pear seedling rootstock grown under P-deficiency or excessive P supply conditions. P deficiency caused the development of purple or yellow color of the mature leaves. Taproot length, leaf expansion rate, and stem extension were all significantly inhibited under P-deficient conditions, but the root/shoot ratio showed a significant increase (relative to the value in seedlings at 1 mM) under P-deficient conditions. However, excessive P treatment resulted in dark green leaves, with no significant change in leaf expansion rate, stem extension, or root/shoot ratio. The purple/yellow leaves under P-deficient conditions may be due to the accumulation of starch and anthocyanin in the leaves, leading to a decrease in nitrogen concentration in the leaves, resulting in the chlorotic symptoms of nitrogen deficiency. The increase in the root/shoot ratio may be due to inhibition of shoot growth being greater than that of the root growth under P-deficient conditions; when the P supply was excessive, the growth of the root system was inhibited as much as was that of the shoot system, so that the root/shoot ratio did not change. Thus, these results indicated that a moderate P fertilizer supply is crucial to ensuring normal growth and development in pear seedling rootstock.

Effects of Phosphorus Deficiency on Root Architecture

Root architecture, the spatial distribution of a root system in the soil, has been shown to be important for plant P acquisition (Lynch and Beebe, 1995), and is highly plastic in its developmental response to P-stress conditions (Bates and Lynch, 1996; Hou et al., 2017). Specific impacts of P-deficiency on root growth have been identified in diverse species. For example, P deficiency significantly reduced the length of the principal root in *Lupinus albus* (Tang et al., 2013). In *Phaseolus vulgaris*, P deficiency reduced total root length by more than one-third, and the total lateral root length and the number of roots was also significantly reduced by P deficiency (Borch et al., 1999). In the grass *Neyraudia reynaudiana*, total root surface area, total root volume, and total root length were reduced in the P-poor compared with the P-rich treatments (Hou et al., 2017). In common bean, total root length and total root surface area were significantly reduced under the P-deficient conditions (Beebe et al., 2006), whereas, in *Arabidopsis*, primary root growth was suppressed under P-deficient concentrations (Williamson et al., 2001). Consistent with these published studies, the results of the current study showed that deficient or low levels of P (0 or 0.5 mM) significantly decreased the root biomass, total root length, total root surface area, total root volume, and total root number in seedlings when compared with seedlings grown under normal P supply. However, response to exposure to excessive P resulted in a similar root architecture plasticity, with the total root length, total root surface area, total root volume, and root tip number decreasing by 18.8, 15.7, 18.2, and 7.5%, respectively, compared with the corresponding values from the seedlings grown under normal P levels (1 mM). The 'root architecture plasticity' phenomenon is probably due to P stress affecting the carbon budget and the distribution of auxins and cytokinins. Furthermore, previous studies have reported that different plant species and populations show different responses to P deficiencies, such as in maize (Hajabbasi and Schumacher, 1994), *Fraxinus mandshurica* (Huang et al., 2019), and *Arabidopsis* (Bates and Lynch, 2000), where the values for total root length and total root surface area increased under P-deficient conditions,

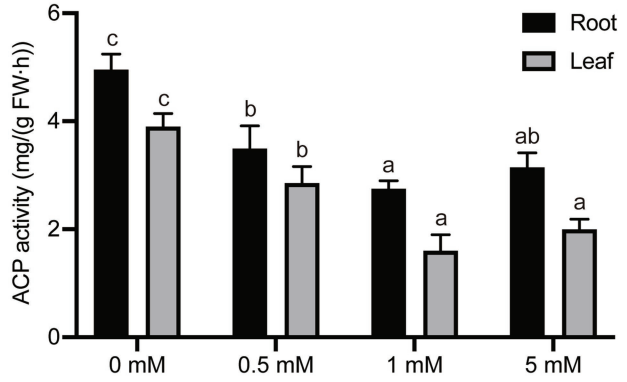


FIGURE 6 | The effect of different P treatments on the acid phosphatase (ACP) activity in pear seedlings. Response of intercellular ACP activity in pear seedling root and leaf tissue to P concentration. Data are presented as mean ± standard deviation of three replicates, and each replicate is based on measurements made from three plants. Samples in a bar chart with a common superscript letter are not significantly different ($p > 0.05$), according to the Duncan's multiple range test.

relative to normal P conditions, whereas the mean root diameter decreased. P deficiency caused a significant increase in primary root length, total root length, and the number of lateral roots after 8 days of treatment in lentil (Sarker and Karmoker, 2009). Pandey reported a significantly greater total root surface area and total root volume in P-efficient mungbean genotypes grown under conditions of P stress (Pandey et al., 2014). P deficiency significantly promoted root hair density and the length of the basal and middle part of the primary root, as well as on the lateral roots, of the trifoliate orange, *Poncirus trifoliata* (Cao et al., 2013). Reasons for such findings may be that plants tend to allocate a greater proportion of biomass to the root system under P-deficient conditions (Hermans et al., 2006), with an increase in total root surface area, total root length, and root biomass, all traits positively associated with P uptake.

Effects of P Levels on the Photosynthetic Characteristics of Pear Seedling Rootstock

P deficiency has been reported to lead to a decrease in chlorophyll concentration and photosynthetic rate (Zhang et al., 2014). Net photosynthetic rate is one of the most important indexes of plant physiology, reflecting the photosynthetic capacity of plants (Mukhopadyay et al., 2012; Zhang et al., 2014). Previous studies have shown that, with an increase in P supply, the net photosynthetic rate of *Camellia oleifera* seedlings showed a significant positive correlation with P concentration, increasing the accumulation of organic matter and promoting the growth of the plant (Fu et al., 2018). Similar results were obtained in the current study, with the net photosynthetic rate, intercellular CO_2 concentration, stomatal conductance, and transpiration rate values of the seedlings being inhibited under P-deficient or low-P conditions. This showed that stomatal conductance of pear seedling rootstock was significantly correlated with transpiration rate, intercellular CO_2 concentration, and net photosynthetic rate, reflecting the fact that stomata are the main channels for gas exchange between plant leaves and the outside world. The synthesis of chlorophyll was affected by inhibition of the uptake of nitrogen under the P-deficient or low-P conditions, which caused decreased leaf photosynthetic rate, delayed leaf growth, and reduced water requirements, as well as decreased transpiration rate, stomatal closure, and intercellular carbon dioxide concentration. Ultimately, net photosynthetic rate and plant growth decreased under P-deficient conditions. Furthermore, the synthesis of chlorophyll in leaves of pear seedling rootstock was inhibited under excess P conditions (5 mM P), which affected the net photosynthetic rate, resulting in a decrease in transpiration rate, stomatal conductance, and intercellular CO_2 concentration. These results are similar to those reported in the previous study by Boyce et al. (2006) on the Rocky Mountain bristlecone pine, *Pinus aristata*, where P had a marked influence on the photosynthetic rate of the plants. The results from the current study showed that, compared with the P-deficient treatments, the normal phosphorus supply (1 mM P) increased the chlorophyll concentration in pear seedling rootstock, and subsequently enhanced the absorption of incident light energy, so that the net photosynthetic rate increased. This enhancement of photosynthesis was also probably the main cause of the significant increase in the biomass of pear seedling rootstock with the increase in P supply level.

Effects of P Levels on Mineral Element Uptake by Pear Seedling Rootstock

Excessive or inadequate P supplies will affect the uptake of P by plants, a phenomenon which has been widely reported in rice, soybean, and other crops (Insalud et al., 2006; Vandamme et al., 2013; Pandey et al., 2014). Previous studies had shown that the P concentration in crop roots increases with increased P application level (Heuer et al., 2017). In the current study, the results showed that the P concentration in roots of pear seedling rootstock increased significantly with the increase in P level in the nutrient solution, indicating that the size of the root system of the pear seedlings was highly responsive to the exogenous P concentration. An appropriate amount of P supplied to the plants was conducive to the uptake of P by the roots, a finding which was consistent with results from tomato, rice, and poplar (Teng and Timmer, 1990; Wang et al., 2015; Wu et al., 2017). In addition, there were close correlations between concentrations of different plant mineral elements. Different levels of P supply not only affect the accumulation of P in plant roots, but also affect the uptake of other elements, such as nitrogen, potassium, calcium, magnesium, iron, copper, zinc, etc. (Su et al., 2015). The uptake of nitrogen, potassium, and magnesium by the root system of pear seedling rootstock was also inhibited under P-deficient or low-P conditions (0–0.5 mM). The uptake of nitrogen, potassium, and magnesium into the roots generally increased with increasing P level; when the P supply level was excessive (5 mM), not only was the accumulation of P in the roots reduced, but also the uptake of nitrogen, potassium, and magnesium in roots was inhibited. This result indicated that the uptake of N, K, and Mg by pear seedling

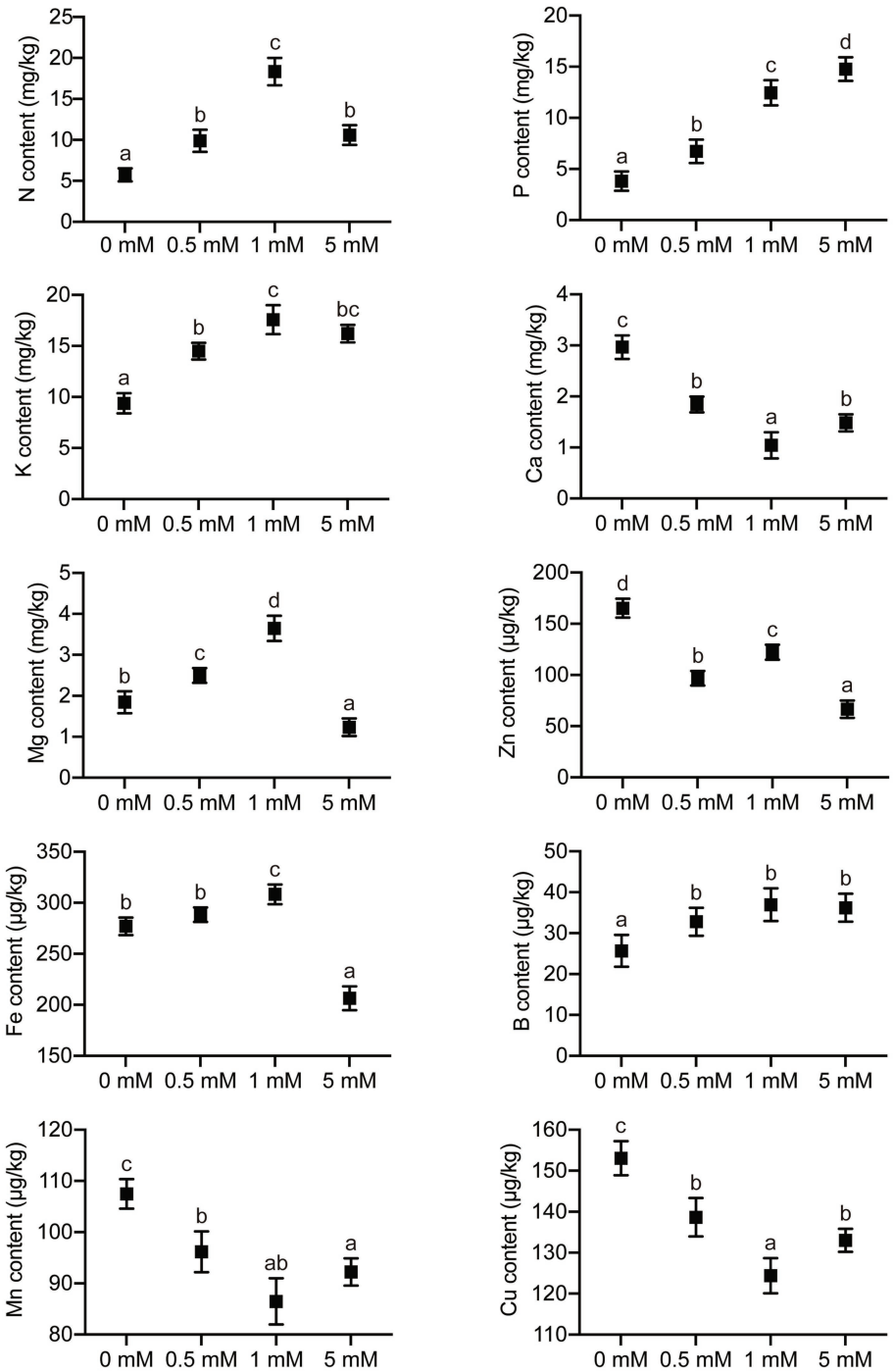


FIGURE 7 | The effects of P treatments on the concentrations of elements in pear seedlings. Response of concentrations of elements in pear seedling roots to P supply concentration. Data are presented as mean ± standard deviation of three replicates, and each replicate is based on measurements made from three plants. Samples in a bar chart with a common superscript letter are not significantly different ($p > 0.05$), according to the Duncan's multiple range test.

rootstock operated synergistically with that of P. The low concentration of K and Mg in roots of pear seedling rootstock grown under low P conditions may be caused by the secretion of organic acids from the roots, accompanying the outflow of potassium and magnesium ions, while the low N concentration may be due to the loss of a large amount of potassium, resulting in the inhibition of N uptake (E et al., 2005; Xiao et al., 2014). Effects of P level on the concentration of calcium in roots are related to the species and populations of plants involved in the studies. The results from the current study showed that

the calcium concentration in pear seedling roots grown under P-deficient or low-P conditions (0–0.5 mM) decreased significantly with increasing P supply, indicating that the low-P environment is conducive to the uptake and utilization of calcium. When the P supply level is excessive (5 mM), the concentration of calcium in roots increased, which indicated that the absorption of calcium by pear seedling roots was antagonistic to the supply level of P, a finding similar to that from a previous study on rapeseed (Hao et al., 2009). Furthermore, the results from the current study showed that concentrations of iron and boron did not change significantly with an increase in P supply level (0–1 mM), while the concentrations of Fe and Zn in roots decreased significantly at the higher P level (5 mM), indicating that excessive P levels inhibited the uptake of Fe and Zn by roots. The uptake of Mn, Cu, and Zn by roots was similar to that of Ca under the P-deficiency or low-P levels (0–0.5 mM), gradually decreasing with increasing P supply over the range 0–1 mM, indicating that the uptake of Mn, Cu, and Zn by roots of pear seedling rootstock was antagonistic to that of P, a finding similar to that of a previous study on castor bean (Huang et al., 2018). In addition, the uptake of Zn was inhibited and that of Mn and Cu was promoted by roots of seedlings grown under conditions of excess P (5 mM).

DATA AVAILABILITY STATEMENT

The original contributions presented in the study are included in the article/supplementary material, further inquiries can be directed to the corresponding authors.

AUTHOR CONTRIBUTIONS

GC designed the research, performed the experiments, and analyzed the results. YL, CJ, JW, and LW participated in carrying out the experiments. JW managed the experiments and participated in revising the final manuscript. All authors contributed to the article and approved the submitted version.

FUNDING

This work was supported by Jiangsu Agriculture Science and Technology Innovation Fund (CX(19)2028), the Natural Science Research Project in Colleges of Jiangsu Province of China (20KJB210007), National Natural Science Foundation of China (31801842), and Talent Introduction Research Project for Huaiyin Institute of Technology (Z301B19573).

REFERENCES

Barker, G. R., Bray, C. M., and Walter, T. J. (1974). The development of ribonuclease and acid phosphatase during germination of pisum arvense. *Biochem. J.* 142, 211–219. doi: 10.1042/bj1420211

Bates, T. R., and Lynch, J. P. (1996). Stimulation of root hair elongation in *Arabidopsis thaliana* by low phosphorus availability. *Plant Cell Environ.* 19, 529–538. doi: 10.1111/j.1365-3040.1996.tb00386.x

Bates, T. R., and Lynch, J. P. (2000). The efficiency of *Arabidopsis thaliana* (*Brassicaceae*) root hairs in phosphorus acquisition. *Am. J. Bot.* 87, 964–970. doi: 10.2307/2656995

Beebe, S. E., Rojas-Pierce, M., Yan, X. L., Blair, M. W., Pedraza, F., Munoz, F., et al. (2006). Quantitative trait loci for root architecture traits correlated with phosphorus acquisition in common bean. *Crop Sci.* 46, 413–423. doi: 10.2135/cropsci2005.0226

Borch, K., Bouma, T. J., Lynch, J. P., and Brown, K. M. (1999). Ethylene: a regulator of root architectural responses to soil phosphorus availability. *Plant Cell Environ.* 22, 425–431. doi: 10.1046/j.1365-3040.1999.00405.x

Boyce, R. L., Larson, J. R., and Sanford, R. L. Jr. (2006). Phosphorus and nitrogen limitations to photosynthesis in Rocky Mountain bristlecone pine (*Pinas aristata*) in Colorado. *Tree Physiol.* 26, 1477–1486. doi: 10.1093/treephys/26.11.1477

Brembu, T., Muhlroth, A., Alipanah, L., and Bones, A. M. (2017). The effects of phosphorus limitation on carbon metabolism in diatoms. *Philos. Trans. R. Soc. Lond. B Biol. Sci.* 372:20160406. doi: 10.1098/rstb.2016.0406

Cao, L., and Chen, G. (2012). Effect of phosphorus deficiency on root growth and root exudates of Cucurbita pepo 'Luoren'. *Acta Horticulturae* 933, 149–155. doi: 10.17660/ActaHortic.2012.933.17

Cao, X., Xia, R., Zhang, D., and Shu, B. (2013). Effects nutrients on the seedlings root hair development and root growth of *Poncirus trifoliata* under hydroponics condition. *J. Appl. Ecol.* 24, 1525–1530. doi: article/med/24066535

Carstensen, A., Herdean, A., Schmidt, S. B., Sharma, A., Spetea, C., Pribil, M., et al. (2018). The impacts of phosphorus deficiency on the photosynthetic electron transport chain. *Plant Physiol.* 177, 271–284. doi: 10.1104/pp.17.01624

Chen, L., Lin, L., Cai, G., Sun, Y., Tao, H., Wang, K., et al. (2014). Identification of nitrogen, phosphorus, and potassium deficiencies in rice based on static scanning technology and hierarchical identification method. *PLoS One* 9:e113200. doi: 10.1371/journal.pone.0113200

Chen, G., Wang, L., Fabrice, M. R., Tian, Y., Qi, K., Chen, Q., et al. (2018). Physiological and nutritional responses of pear seedlings to nitrate concentrations. *Front. Plant Sci.* 9:1679. doi: 10.3389/fpls.2018.01679

Cimen, B. (2020). Efficient protoplast isolation from ovule-derived embryogenic callus in *Citrus volkameriana*. *Turk. J. Agric. For.* 44, 567–576. doi: 10.3906/tar-1912-16

De Andrade, F. H. A., Pereira, W. E., Maia, J. M., Clemente, M. I. B., De Sousa Lima, J., and Silva, V. A. (2021). Phosphorus increases K^+ in the shoot and improves salinity tolerance in sweetsop seedlings. *J. Plant Growth Regul.* 1, 1–12. doi: 10.1007/s00344-021-10361-y

E, S., Yuan, J., Ding, Z., Yao, F., Yu, X., and Luo, F. (2005). Effect of N,P,K fertilizers on Fe,Zn,Cu,Mn,Ca and Mg contents and yields in rice. *Chin. J. Rice Sci.* 19, 434–440. doi: 10.1360/aps040074

Fisarakis, I., Nikolaou, N., Tsikalas, P., Therios, I., and Stavrakas, D. (2004). Effect of salinity and rootstock on concentration of potassium, calcium, magnesium, phosphorus, and nitrate-nitrogen in Thompson seedless grapevine. *J. Plant Nutr.* 27, 2117–2134. doi: 10.1081/PLN-200034662

Fu, Y., Lan, X., and Qin, L. H. (2018). Effects of different phosphorus concentrations on growth characteristics index and nutrient content of *Camellia oleifera*. *J. Anhui Agric. Sci.* 46, 114–116. doi: 10.13989/j.cnki.0517-6611.2018.24.036

Gruber, B. D., Giehl, R. F. H., Friedel, S., and Von Wiren, N. (2013). Plasticity of the *Arabidopsis* root system under nutrient deficiencies. *Plant Physiol.* 163, 161–179. doi: 10.1104/pp.113.218453

Guney, M. (2019). Development of an in vitro micropropagation protocol for Myrobalan 29C rootstock. *Turk. J. Agric. For.* 43, 569–575. doi: 10.3906/tar-1903-4

Hajabbasi, M. A., and Schumacher, T. E. (1994). Phosphorus effects on root-growth and development in maize genotypes. *Plant Soil* 158, 39–46. doi: 10.1007/BF00007915

Ham, B. K., Chen, J. Y., Yan, Y., and Lucas, W. J. (2018). Insights into plant phosphate sensing and signaling. *Curr. Opin. Biotechnol.* 49, 1–9. doi: 10.1016/j.copbio.2017.07.005

Hao, X., Liao, W., Liu, J., Li, Z., Su, X., and Kang, S. (2009). Effects of excessive phosphate fertilizer on growth and nutrient uptake of rape. *J. Agric. Univ. Hebei* 32, 26–30. doi: 10.3969/j.issn.1000-1573.2009.03.006

Hermans, C., Hammond, J. P., White, P. J., and Verbruggen, N. (2006). How do plants respond to nutrient shortage by biomass allocation? *Trends Plant Sci.* 11, 610–617. doi: 10.1016/j.tplants.2006.10.007

Heuer, S., Gaxiola, R., Schilling, R., Herrera-Estrella, L., Lopez-Arredondo, D., Wissuwa, M., et al. (2017). Improving phosphorus use efficiency: a complex trait with emerging opportunities. *Plant J.* 90, 868–885. doi: 10.1111/tpj.13423

Hou, X., Tigabu, M., Zhang, Y., Ma, X., Cai, L., Wu, P., et al. (2017). Root plasticity, whole plant biomass, and nutrient accumulation of *Neyraudia reynaudiana* in response to heterogeneous phosphorus supply. *J. Soils Sediments* 17, 172–180. doi: 10.1007/s11368-016-1517-z

Huang, X., Li, T. X., Zhang, X. Z., Zheng, Z. C., and Yu, H. Y. (2012). Growth, P accumulation, and physiological characteristics of two ecotypes of *Polygonum* hydropiper as affected by excess P supply. *J. Plant Nutr. Soil Sci.* 175, 293–302. doi: 10.1002/jpln.201100067

Huang, G., Rizwan, M. S., Ren, C., Guo, G., Fu, Q., Zhu, J., et al. (2018). Influence of phosphorous fertilization on copper phytoextraction and antioxidant defenses in castor bean (*Ricinus communis* L.). *Environ. Sci. Pollut. Res.* 25, 115–123. doi: 10.1007/s11356-016-8132-9

Huang, W., Zhao, X., Liang, N., He, L., Yu, L., and Zhan, Y. (2019). Phosphorus deficiency promotes the lateral root growth of *Fraxinus mandshurica* seedlings. *J. Plant Nutr. Soil Sci.* 182, 552–559. doi: 10.1002/jpln.201800465

Insalud, N., Bell, R. W., Colmer, T. D., and Rerkasem, B. (2006). Morphological and physiological responses of rice (*Oryza sativa*) to limited phosphorus supply in aerated and stagnant solution culture. *Ann. Bot.* 98, 995–1004. doi: 10.1093/aob/mcl194

Kong, X., Peng, Z., Li, D., Ma, W., An, R., Khan, D., et al. (2020). Magnesium decreases aluminum accumulation and plays a role in protecting maize from aluminum-induced oxidative stress. *Plant Soil* 457, 71–81. doi: 10.1007/s11104-020-04605-1

Latief, M. F., Nohong, B., and Nompo, S. (2020). The effect of phosphorus fertilizer on growth characteristics and dry matter production of *Styloshantes guianensis*. *Earth Environ. Sci.* 492:12012. doi: 10.1088/1755-1315/492/1/012012

Luo, J. J., Liu, Y. X., Zhang, H. K., Wang, J. P., Chen, Z. J., Luo, L. J., et al. (2020). Metabolic alterations provide insights into *Stylosanthes* roots responding to phosphorus deficiency. *BMC Plant Biol.* 20:85. doi: 10.1186/s12870-020-2283-z

Lynch, J. P., and Beebe, S. E. (1995). Adaptation of beans (*Phaseplus vulgaris* L.) to low phosphorus availability. *HortScience* 30, 1165–1171. doi: 10.21273/HORTSCI.30.6.1165

Maharajan, T., Ceasar, S. A., Krishna, T. A., Ramakrishnan, M., Duraipandiyan, V., Abdulla, A. N., et al. (2018). Utilization of molecular markers for improving the phosphorus efficiency in crop plants. *Plant Breed.* 137, 10–26. doi: 10.1111/pbr.12537

Marastoni, L., Lucini, L., Miras-Moreno, B., Trevisan, M., Sega, D., Zamboni, A., et al. (2020). Changes in physiological activities and root exudation profile of two grapevine rootstocks reveal common and specific strategies for Fe acquisition. *Sci. Rep.* 10:18839. doi: 10.1038/s41598-020-75317-w

Marques, D. J. (2018). Differential responses of root system and gas exchange in contrasting tomato genotypes under phosphorus starvation. *Aust. J. Crop. Sci.* 10, 101–110. doi: 10.13140/RG.2.2.25296.56326

McLachlan, K. D., Elliott, D. E., Demarco, D. G., and Garran, J. H. (1987). Leaf acid phosphatase isozymes in the diagnosis of phosphorus status in field grown wheat. *Aust. J. Agric. Res.* 38, 1–13. doi: 10.1071/AR9870001

Mo, X., Zhang, M., Liang, C., Cai, L., and Tian, J. (2019). Integration of metabolome and transcriptome analyses highlights soybean roots responding to phosphorus deficiency by modulating phosphorylated metabolite processes. *Plant Physiol. Biochem.* 139, 697–706. doi: 10.1016/j.plaphy.2019.04.033

Moreira, A., Cardoso Moraes, L. A., Zaninetti, R. A., and Canizella, B. T. (2013). Phosphorus dynamics in the conversion of a secondary forest into a rubber tree plantation in the amazon rainforest. *Soil Sci.* 178, 618–625. doi: 10.1097/SS.0000000000000025

Mukhopadyay, M., Bantawa, P., Das, A., Sarkar, B., Bera, B., Ghosh, P., et al. (2012). Changes of growth, photosynthesis and alteration of leaf antioxidative defence system of tea [*Camellia sinensis* (L.) O. Kuntze] seedlings under aluminum stress. *Biometals* 25, 1141–1154. doi: 10.1007/s10534-012-9576-0

Pandey, R., Meena, S. K., Krishnapriya, V., Ahmad, A., and Kishora, N. (2014). Root carboxylate exudation capacity under phosphorus stress does not improve grain yield in green gram. *Plant Cell Rep.* 33, 919–928. doi: 10.1007/s00299-014-1570-2

Qi, J. G., Sun, S. M., Yang, L., Li, M. J., Ma, F. W., and Zou, Y. J. (2019). Potassium uptake and transport in apple roots under drought stress. *Hortic. Plant J.* 5, 10–16. doi: 10.1016/j.hpj.2018.10.001

Qu, X., Zhou, J., Masabni, J., and Yuan, J. (2020). Phosphorus relieves aluminum toxicity in oil tea seedlings by regulating the metabolic profiling in the roots. *Plant Physiol. Biochem.* 152, 12–22. doi: 10.1016/j.plaphy.2020.04.030

Reddy, V. R. P., Aski, M. S., Mishra, G. P., Dikshit, H. K., Singh, A., Pandey, R., et al. (2020). Genetic variation for root architectural traits in response to phosphorus deficiency in mungbean at the seedling stage. *PLoS One* 15:e0221008. doi: 10.1371/journal.pone.0221008

Richardson, A. E., George, T. S., Hens, M., and Simpson, R. J. (2005). Utilization of soil organic phosphorus by higher plants. *Org. Phosphorus Environ.*, 165–184. doi: 10.1079/9780851998220.0165

Rivelli, A. R., De Maria, S., Pizza, S., and Gherbin, P. (2010). Growth and physiological response of hydroponically-grown sunflower as affected by salinity and magnesium levels. *J. Plant Nutr.* 33, 1307–1323. doi: 10.1080/01904167.2010.484092

Rufato, L., Da Silva, P. S., Kretzschmar, A. A., Bogo, A., De Macedo, T. A., Welter, J. F., et al. (2021). Geneva® series rootstocks for apple trees under extreme replanting conditions in southern Brazil. *Front. Plant Sci.* 12:712162. doi: 10.3389/fpls.2021.712162

Sarker, B. C., and Karmoker, J. L. (2009). Effects of phosphorus deficiency on the root growth of lentil seedlings (*Lens culinaris* medik) grown in rhizobox. *Bangladesh J. Bot.* 38, 215–218. doi: 10.3329/bjb.v38i2.5153

Shehzad, M., Gul, R. S., Rauf, S., Clarindo, W. R., Al-Khayri, J. M., Hussain, M. M., et al. (2021). Development of a robust hydroponic method for screening of sunflower (*Helianthus annuus* L.) accessions for tolerance to heat and osmotic stress. *Sci. Rep.* 11:1677. doi: 10.1038/s41598-021-81072-3

Shen, Q., Wen, Z., Dong, Y., Li, H., Miao, Y., and Shen, J. (2018). The responses of root morphology and phosphorus-mobilizing exudations in wheat to increasing shoot phosphorus concentration. *Aob Plants* 10:ply054. doi: 10.1093/aobpla/ply054

Shi, Q., Pang, J., Yong, J. W. H., Bai, C., Pereira, C. G., Song, Q., et al. (2020). Phosphorus-fertilisation has differential effects on leaf growth and photosynthetic capacity of *Arachis hypogaea* L. *Plant Soil* 447, 99–116. doi: 10.1007/s11104-019-04041-w

Siedliska, A., Baranowski, P., Pastuszka-Wozniak, J., Zubik, M., and Krzyszczak, J. (2021). Identification of plant leaf phosphorus content at different growth stages based on hyperspectral reflectance. *BMC Plant Biol.* 21:28. doi: 10.1186/s12870-020-02807-4

Su, Y., Hu, X., Wang, W., Wang, R., Zhang, D., and Qiao, Y. (2015). Effect of phosphorus on dynamic growth and nutrient absorption of hydroponic lettuce. *Chin. J. Eco-Agric.* 23, 1244–1252. doi: 10.13930/j.cnki.cjea.150263

Sugiharta, I., Maretta, G., Pawhestri, S., and Putri, A. E. (2019). Electrolysis of water using iron electrode to boost the growth of hydroponic plant of water spinach. *J. Phys. Conf. Ser.* 1155:12054. doi: 10.1088/1742-6596/1155/1/012054

Tang, H., Chen, X., Gao, Y., Hong, L., and Chen, Y. (2020). Alteration in root morphological and physiological traits of two maize cultivars in response to phosphorus deficiency. *Rhizosphere* 14:100201. doi: 10.1016/j.rhisph.2020.100201

Tang, H., Shen, J., Zhang, F., and Rengel, Z. (2013). Interactive effects of phosphorus deficiency and exogenous auxin on root morphological and physiological traits in white lupin (*Lupinus albus* L.). *Sci. China Life Sci.* 56, 313–323. doi: 10.1007/s11427-013-4461-9

Teng, Y. X., and Timmer, V. R. (1990). Phosphorus-induced micronutrient disorders in hybrid poplar. *Plant Soil* 126, 19–29. doi: 10.1007/BF00041365

Vandamme, E., Renkens, M., Pypers, P., Smolders, E., Vanlauwe, B., and Merckx, R. (2013). Root hairs explain P uptake efficiency of soybean genotypes grown in a P-deficient Ferralsol. *Plant Soil* 369, 269–282. doi: 10.1007/s11104-012-1571-2

Veneklaas, E. J., Lambers, H., Bragg, J., Finnegan, P. M., Lovelock, C. E., Plaxton, W. C., et al. (2012). Opportunities for improving phosphorus-use efficiency in crop plants. *New Phytol.* 195, 306–320. doi: 10.1111/j.1469-8137.2012.04190.x

Veronica, N., Subrahmanyam, D., Kiran, T. V., Yugandhar, P., Bhadana, V. P., Padma, V., et al. (2017). Influence of low phosphorus concentration on leaf photosynthetic characteristics and antioxidant response of rice genotypes. *Photosynthetica* 55, 285–293. doi: 10.1007/s11099-016-0640-4

Wang, J., Chen, Y., Wang, P., Li, Y. S., Wang, G., Liu, P., et al. (2018). Leaf gas exchange, phosphorus uptake, growth and yield responses of cotton cultivars to different phosphorus rates. *Photosynthetica* 56, 1414–1421. doi: 10.1007/s11099-018-0845-1

Wang, S. Q., Han, X. Z., Li, X. H., Yan, J., and Qiao, Y. F. (2010). Root morphology of soybean (*Glycine max* L) under phosphorus deficiency stress. *Syst. Sci. Compr. Stud. Agric.* 26, 192–196.

Wang, J., Zhang, L. P., Wang, L. J., Zhu, Y. J., Shao, G. S., and Cui, C. (2015). Effects of different phosphorus levels on root growth of rice cultivars and the absorption of some nutrient elements. *J. Southwest Univ.* 37, 30–36. doi: 10.13718/j.cnki.xdzk.2015.07.005

Williamson, L. C., Ribrioux, S., Fitter, A. H., and Leyser, H. M. O. (2001). Phosphate availability regulates root system architecture in *Arabidopsis*. *Plant Physiol.* 126, 875–882. doi: 10.1104/pp.126.2.875

Wu, Y., Lin, Q., Yan, M., Hui, Z., Chen, Z., and Li, X. (2017). Effect of phosphorus on growth and nutrient uptake of tomato. *Chin. Agric. Sci. Bull.* 33, 74–77.

Xiao, X., Liu, J., Zhou, C., Wang, G., Chen, G., and Yue, H. (2014). Difference of root exudates from macadamia seedlings under different phosphorus supply. *Chin. J. Trop. Crops* 35, 261–265. doi: 10.3969/j.issn.1000-2561.2014.02.009

Ye, D., Li, T., Liu, D., Zhang, X., and Zheng, Z. (2015). P accumulation and physiological responses to different high P regimes in Polygonum hydropiper for understanding a P-phytoremediation strategy. *Sci. Rep.* 5:17835. doi: 10.1038/srep17835

Yu, W., Kan, Q., Zhang, J., Zeng, B., and Chen, Q. (2016). Role of the plasma membrane H^+-ATPase in the regulation of organic acid exudation under aluminum toxicity and phosphorus deficiency. *Plant Signal. Behav.* 11:e1106660. doi: 10.1080/15592324.2015.1106660

Zhang, S., Jiang, H., Zhao, H., Korpelainen, H., and Li, C. (2014). Sexually different physiological responses of Populus cathayana to nitrogen and phosphorus deficiencies. *Tree Physiol.* 34, 343–354. doi: 10.1093/treephys/tpu025

Zheng, X., Zhang, Z., Chen, X., Jia, Z., and Su, Y. (2013). Responses of root morphology and architecture to phosphorus deficiency at seedling stage of tobacco (*Nicotiana tabacum*) growth. *Aust. J. Crop. Sci.* 7, 1967–1972. doi: 10.3316/INFORMIT.800754495370359

Zhou, G. F., Peng, S. A., Liu, Y. Z., Wei, Q. J., Han, J., and Islam, M. Z. (2014). The physiological and nutritional responses of seven different citrus rootstock seedlings to boron deficiency. *Trees* 28, 295–307. doi: 10.1007/s00468-013-0949-y

Conflict of Interest: The authors declare that the research was conducted in the absence of any commercial or financial relationships that could be construed as a potential conflict of interest.

Publisher's Note: All claims expressed in this article are solely those of the authors and do not necessarily represent those of their affiliated organizations, or those of the publisher, the editors and the reviewers. Any product that may be evaluated in this article, or claim that may be made by its manufacturer, is not guaranteed or endorsed by the publisher.

Copyright © 2021 Chen, Li, Jin, Wang, Wang and Wu. This is an open-access article distributed under the terms of the Creative Commons Attribution License (CC BY). The use, distribution or reproduction in other forums is permitted, provided the original author(s) and the copyright owner(s) are credited and that the original publication in this journal is cited, in accordance with accepted academic practice. No use, distribution or reproduction is permitted which does not comply with these terms.

frontiers in Plant Science

REVIEW
published: 16 November 2021
doi: 10.3389/fpls.2021.768523

Cobalt: An Essential Micronutrient for Plant Growth?

Xiu Hu[1], *Xiangying Wei*[2]*, *Jie Ling*[3] *and Jianjun Chen*[4]*

[1] College of Horticulture and Landscape Architecture, Zhongkai University of Agriculture and Engineering, Guangzhou, China, [2] Institute of Oceanography, Minjiang University, Fuzhou, China, [3] He Xiangning College of Art and Design, Zhongkai University of Agriculture and Engineering, Guangzhou, China, [4] Department of Environmental Horticulture and Mid-Florida Research and Education Center, Institute of Food and Agricultural Sciences, University of Florida, Apopka, FL, United States

Cobalt is a transition metal located in the fourth row of the periodic table and is a neighbor of iron and nickel. It has been considered an essential element for prokaryotes, human beings, and other mammals, but its essentiality for plants remains obscure. In this article, we proposed that cobalt (Co) is a potentially essential micronutrient of plants. Co is essential for the growth of many lower plants, such as marine algal species including diatoms, chrysophytes, and dinoflagellates, as well as for higher plants in the family *Fabaceae* or *Leguminosae*. The essentiality to leguminous plants is attributed to its role in nitrogen (N) fixation by symbiotic microbes, primarily rhizobia. Co is an integral component of cobalamin or vitamin B_{12}, which is required by several enzymes involved in N_2 fixation. In addition to symbiosis, a group of N_2 fixing bacteria known as diazotrophs is able to situate in plant tissue as endophytes or closely associated with roots of plants including economically important crops, such as barley, corn, rice, sugarcane, and wheat. Their action in N_2 fixation provides crops with the macronutrient of N. Co is a component of several enzymes and proteins, participating in plant metabolism. Plants may exhibit Co deficiency if there is a severe limitation in Co supply. Conversely, Co is toxic to plants at higher concentrations. High levels of Co result in pale-colored leaves, discolored veins, and the loss of leaves and can also cause iron deficiency in plants. It is anticipated that with the advance of omics, Co as a constitute of enzymes and proteins and its specific role in plant metabolism will be exclusively revealed. The confirmation of Co as an essential micronutrient will enrich our understanding of plant mineral nutrition and improve our practice in crop production.

Keywords: cobalamin, cobalt, endophytes, essential nutrients, micronutrients, symbiosis, vitamin B_{12}, transporter

OPEN ACCESS

Edited by:
Antonios Chrysargyris, Cyprus University of Technology, Cyprus

Reviewed by:
Timothy O. Jobe, University of Cologne, Germany
Guilan Duan, Research Center for Eco-Environmental Sciences (CAS), China

***Correspondence:**
Jianjun Chen
jjchen@ufl.edu
Xiangying Wei
xiangyingwei@mju.edu.cn

Specialty section:
This article was submitted to Crop and Product Physiology, a section of the journal Frontiers in Plant Science

Received: *31 August 2021*
Accepted: *29 September 2021*
Published: *16 November 2021*

Citation:
Hu X, Wei X, Ling J and Chen J (2021) Cobalt: An Essential Micronutrient for Plant Growth? Front. Plant Sci. 12:768523. doi: 10.3389/fpls.2021.768523

INTRODUCTION

Cobalt is an essential nutrient for prokaryotes, human beings, and other mammals but has not been considered an essential micronutrient for plants. Instead, this element, along with other elements, such as aluminum (Al), selenium (Se), silicon (Si), sodium (Na), and titanium (Ti), has been considered as a beneficial element for plant growth (Pilon-Smits et al., 2009; Lyu et al., 2017). An element that can improve plant health status at low concentrations but has toxic effects at high concentrations is known as a beneficial element (Pais, 1992). For an element to be considered essential, it must be required by plants to complete its life cycle, must not be replaceable by other

elements, and must directly participate in plant metabolism (Arnon and Stout, 1939). It has been well-documented that there are 92 naturally occurring elements on the earth, wherein 82 of which have been found in plants (Reimann et al., 2001). Plants are able to absorb elements from soils either actively or passively due to their sessile nature. The occurrence of an element in plants, particularly in shoots, must have a purpose. Active transport of an element from roots to shoots may indicate a certain role it plays in plants. As stated in the study by Bertrand (1912), potentially, every element has a biological function that can be assessed properly against a background of a deficiency state, and every element is toxic when present at high enough concentrations, which is known as Bertrand's rule of metal necessity.

Significant progress has been made in plant mineral nutrition since the publication of Bertrand's rule (Bertrand, 1912) and the essentiality concept (Arnon and Stout, 1939). Among the beneficial elements, cobalt (Co) could potentially be an essential plant micronutrient. Co is a core element of cobalamin (vitamin B_{12} and its derivatives) and a cofactor of a wider range of enzymes and a component of different proteins in prokaryotes and animals (Maret and Vallee, 1993; Kobayashi and Shimizu, 1999; Harrop and Mascharak, 2013; Odaka and Kobayashi, 2013). Co-containing enzymes and proteins in plants require further investigation and clarification. Rhizobia and other nitrogen (N)-fixation bacteria require Co and cobalamin for fixing atmosphere dinitrogen (N_2) into ammonia (NH_3), providing plants with the essential macronutrient of N. Co plays a vital role in interaction with iron (Fe), nickel (Ni), and zinc (Zn) in maintaining cellular homeostasis. Similar to other essential micronutrients, plants respond to Co concentrations in soil: at low concentrations, it promotes plant growth but causes phytotoxicity at higher concentrations. However, it is different from other beneficial elements, as plants do exhibit Co deficiency when grown in soils with limited supply.

The objective of this article was to concisely review the importance of Co as a plant micronutrient including its role in N fixation, the occurrence of coenzyme or proteins, and its effects on plant growth as well as Co deficiency and toxicity. We intended that this review could raise an awareness that Co is a potentially essential micronutrient of plants, and further research is needed to confirm this proposition.

COBALT AND NITROGEN-FIXATION IN PLANTS

Cobalt was isolated by Brandt in 1735 and recognized as a new element by Bergman in 1780 (Lindsay and Kerr, 2011). The importance of Co to living things was realized in the 1930s during the investigation of ruminant livestock nutrition in Australia (Underwood and Filmer, 1935). Co was discovered to be essential for animals as it is a component of cobalamin. Five scientists were awarded Nobel Prizes for the investigation of cobalamin (Carpenter, 2004).

Cobalt Is a Core Element of Cobalamin

Cobalamin is a large molecule ($C_{63}H_{88}O_{14}N_{14}PCo$) comprised of a modified tetrapyrrole ring known as corrin with Co^{3+} in the center (Osman et al., 2021). Co is not inter-exchangeable with other metals in the cobalamin and cannot be released from the ring unless the ring is broken (Yamada, 2013), implying the significance of Co to cobalamin. There are two biologically active forms of cobalamin, namely, methylcobalamin and adenosylcobalamin in ruminants (Gonzalez-Montana et al., 2020). In human beings, Co is a cofactor of two enzymes, namely, ethylmalonyl-CoA mutase (MCM) and methionine synthase. MCM catalyzes the reversible isomerisation of l-methylmalonyl-CoA to succinyl-CoA. A deficiency of MCM causes an inherited metabolism disorder commonly known as methylmalonic aciduria. Methionine synthase utilizes cobalamin as a cofactor to produce methionine from homocysteine (**Table 1**). Reduced activity of this enzyme leads to megaloblastic anemia (Tjong et al., 2020). Ruminant animals produce vitamin B_{12} if there is an appropriate supply of Co in their diet. It was reported that 3 to 13% of the Co was incorporated into cobalamin by bacteria in the ruminant animals (Huwait et al., 2015).

Cobalamin Biosynthesis in Bacteria and Archaea

The natural forms of vitamin B_{12} are 1,5-deoxyadenosylcobalamin, hydroxycobalamin, and methylcobalamin (Nohwar et al., 2020). They are synthesized by a selected subset of bacteria and archaea (Heal et al., 2017; Guo and Chen, 2018), which include *Bacillus*, *Escherichia*, *Fervidobacterium*, *Kosmotoga*, *Lactobacillus*, *Mesotoga*, *Nitrosopumilus*, *Petrotoga*, *Propionibacterium*, *Proteobacteria*, *Pseudomonas*, *Rhodobacter*, *Rhizobium*, *Salmonella*, *Sinorhizobium, Thermosipho*, and *Thermotoga* (Doxey et al., 2015; Fang et al., 2017). Cyanocobalamin is not a natural form but commercially synthesized B_{12}. The production of vitamin B_{12} by these microbes involves about 30 enzymatic steps through either aerobic or anaerobic pathways. In addition to being essential for fat and carbohydrate metabolism and synthesis of DNA, vitamin B_{12} is a cofactor of many enzymes. There are more than 20 cobalamin-dependent enzymes in those prokaryotes including diol dehydratase, ethanolamine ammonia-lyase, glutamate, and methylmalonyl-CoA mutase, methionine synthase, and ribonucleotide reductase (Marsh, 1999) (**Table 1**). These enzymes catalyze a series of transmethylation and rearrangement reactions (Rodionov et al., 2003). Thus, Co is essential for those archaea and bacteria.

Cobalt Plays an Important Role in Biological Nitrogen Fixation

Biological N fixation is a process of converting N_2 from the atmosphere into plant-usable form, primarily NH_3. Biological N fixation (BNF) is carried out by a group of prokaryotes known as diazotrophs, which are listed in **Table 2**, including bacteria, mainly *Rhizobium*, *Frankia*, *Azotobacter*, *Mycobaterium*, *Azospirillum*, and *Bacillus*; Archaea, such as Methanococcales, Methanobacteriatles,

TABLE 1 | Cobalt-containing enzymes, proteins, and transporter relevant or potentially relevant to plant metabolisms.

Type	Name	Role	Organism	References
Corrin Co enzymes	Ethylmalonyl-CoA mutase (MCM)	Catalysis of reversible isomerisation of l-methylmalonyl-CoA to succinyl-CoA	Mammals and bacteria	Odaka and Kobayashi, 2013; Gonzalez-Montana et al., 2020
	Methionine synthase	Synthesis of methionine from homocysteine	Mammals and bacteria	Odaka and Kobayashi, 2013; Gonzalez-Montana et al., 2020
	Methylcobalamin-dependent methyltransferase	Transfer of a methyl group from different methyl donors to acceptor molecules	Mammals	Bridwell-Rabb and Drennan, 2017
	Adenosylcobalamin-dependent isomerases	Catalysis of a variety of chemically difficult 1,2-rearrangements that proceed through a mechanism involving free radical intermediates	Mammals and bacteria	Marsh and Drennan, 2001
	Ethanolamine ammonia-lyase	Conversion of ethanolamine to acetaldehyde and ammonia	*Listeria monocytogenes* and *Escherichia coli*	Harrop and Mascharak, 2013
	Ribonucleotide reductase	Catalysis of the production of deoxyribonucleotides needed for DNA synthesis	Bacteria, mammals, yeast, and plants	Elledge et al., 1992; Yoo et al., 2009
Non-corrin Co enzymes	Nitrile hydratase (NHase)	Hydration of aromatic and small aliphatic nitriles into the corresponding amides	*Rhodococcus rhodochrous* and *Pseudonocardia thermophila*	Harrop and Mascharak, 2013; Odaka and Kobayashi, 2013
	Thiocyanate hydrolase (THase)	Hydration and subsequent Hydration of thiocyanate to produce carbonyl sulfide and ammonia	*Thiobacillus thioparus* (a Gram-negative betaproteobacterium)	Harrop and Mascharak, 2013
	Methionine aminopeptidase (MA)	Cleavage of the N-terminal methionine from newly translated polypeptide chains	Bacteria, mammals, and yeast, plants	Giglione et al., 2000; Odaka and Kobayashi, 2013
	Prolidase	Cleavage of a peptide bond adjacent to a proline residue	Archaea (*Pyrococcus furiosus*), bacteria, fungi, and plants	Harrop and Mascharak, 2013; Odaka and Kobayashi, 2013
	D-xylose isomerase	Conversion of D-xylose and D-glucose into D-xylulose and D-fructose, respectively	*Streptomyces diastaticus* (an alkaliphilic and thermophillic bacterium)	Bhosale et al., 1996
	Methylmalonyl-CoA carboxytransferase	Catalysis of carboxyl transfer between two organic molecules, using two separate carboxyltransferase domains.	*Propionibacterium shermanii* (Gram-positive bacterium)	Odaka and Kobayashi, 2013
	Carbonic anhydrase or carbonate dehydratase	Catalysis of the conversion of CO_2 to HCO_3^- reversibly	Bacteria, fungi, algae, and plants	Jensen et al., 2020
	Carboxypeptidases	Hydrolyzation of the C-terminal residues of peptides and proteins and release free amino acids individually	Animals, bacteria, fungi, and plants	Maret and Vallee, 1993
	Urease	Catalysis of the seemingly simple hydrolysis of urea into ammonia and carbamic acid	Archaea, algae, bacteria, fungi, and plants	Carter et al., 2009
	Aldehyde decarboxylase	Decarboxylation of aldehyde	*Botryococcus braunii* (green algae)	Odaka and Kobayashi, 2013
	Bromoperoxidase	Bromination	Bacteria	Odaka and Kobayashi, 2013
Co transporters	NiCoT	Transport of Co^{2+} and Ni^{2+}	*Rhodococcus rhodochrous*	Odaka and Kobayashi, 2013
	HupE/UreJ	Mediation of uptake of Ni^{2+} and Co^{2+}	*Collimonas fungivorans*	Eitinger, 2013
	CbiMNQO	An energy-coupling factor (ECF) transporter for Ni^{2+} and Co^{2+}	*Salmonella enterica*	Eitinger, 2013
	CorA	Transport system for Mg^{2+} and Co^{2+}	Thermotoga maritima	Eitinger, 2013
	IRT1	Absorption of Fe^{2+} and Co^{2+}	Plants	Korshunova et al., 1999; Conte and Walker, 2011
	FPN1	Transport of Fe^{2+} and Co^{2+} to xylem	Plants	Korshunova et al., 1999; Conte and Walker, 2011
	FPN2	Transport of Fe^{2+} and Co^{2+} to vacuole	Plants	Korshunova et al., 1999; Conte and Walker, 2011
	ARG1	An ABC transporter to transporting Ni^{2+} and Co^{2+} in chloroplast	Plants	Li et al., 2020

and Methanomicrobiales, and cyanobacteria, like *Anabaena*, *Nostoc*, *Toypothrix*, and *Anabaenopsis* (Soumare et al., 2020). N_2-fixing organisms are also classified into three categories: symbiotic, endophytic, and associated groups (**Figure 1**). Such classifications may not be accurate as some of them, such as those from *Acetobacter* and *Azospirillum*, could be associated, as well as endophytic bacteria.

Cobalt Is Essential for Symbiotic Bacteria in N Fixation

There are two major symbioses between N_2-fixing bacteria and higher plants, one is rhizobia with leguminous plants and the other is *Frankia* with actinorhizal plants (Wall, 2000). The former involves more than 1,700 plant species in the family *Fabaceae*, which includes some economically important crops, such as alfalfa, beans, peas, and soybeans. More than 220 species are actinorhizal plants, which are mainly trees and shrubs forming symbiotic relationships with *Frankia*.

Rhizobia are gram-negative bacteria encompassing *Rhizobium*, *Azorhizobium*, *Sinorhizobium*, *Bradyrhizobium*, and *Mesorhizobium* (**Table 2**, **Figure 1A**). Co was identified to be essential for *Rhizobium* in the 1950s and 1960s (Ahmed and Evans, 1960; Reisenauer, 1960). *Rhizobium* uses nitrogenase to catalyze the conversion of N_2 to NH_3, which can be readily absorbed and assimilated by plants. Three enzymes, namely, methionine synthase, methyl malonyl-CoA mutase, and ribonucleotide reductase in *Rhizobium* and *Bradyrhizobium* species, are known to be cobalamin-dependent and significantly affect nodulation and N fixation. Early studies showed that four soybean seedlings inoculated with rhizobia supplemented with 1 μg/L Co were healthy and produced 25.3 g of dry weight. On the contrary, four rhizobia-inoculated seedlings devoid of Co encountered N-deficiency symptoms and produced 16.6 g of dry weight, a 34.4% reduction in biomass due to the absence of Co (Ahmed and Evans, 1959). A close relationship was established amongst Co supply, cobalamin content in *Rhizobium*, leghemoglobin formation, N fixation, and plant growth (Kliewer and Evans, 1963a,b). The deficiency in Co significantly affects methionine synthase by reducing methionine synthesis, which subsequently decreases protein synthesis and produces smaller-sized bacteroids (bacteria in the nodules capable of N fixation) (Marschner, 2011). Methyl malonyl-CoA mutase catalyzes the production of leghemoglobin. If Co becomes limited, leghemoglobin synthesis is directly affected, resulting in reduced N fixation and ultimately a shortage of N supply. This is because leghemoglobin can protect nitrogenase from oxygen by limiting its supply (Hopkins, 1995). Ribonucleotide reductase is a cobalamin-dependent enzyme that catalyzes the reduction of ribonucleotides to deoxyribonucleotides, which is a rate-limiting step in DNA synthesis (Kolberg et al., 2004).

The genus *Frankia* is composed of gram-positive and gram-variable actinomycetes (Wall, 2000). It infects plants through root hairs and produces nodules in the pericycle. *Frankia* in nodules develops vesicles in which nitrogenase is suited (Huss-Danell, 1997). Co is needed for the synthesis of cobalamin which is in turn needed for N fixation. Actinomyceters are known as active producers of cobalamin (Hewitt and Bond, 1966). N fixation by actinorhizal plants appears to be comparable to the magnitude as that of the legumes (Wall, 2000).

Other symbioses occur in cyanobacteria with *Gunnera* and cycads. The genus *Nostoc* infected specialized gland organs located on the stems of *Gunnera*, such as *G. chilensis* and *G. magellanica* (Johansson and Bergman, 1994). Cyanobacteria also form symbiotic relationships with cycads in a special type of root system called coralloid roots (Chang et al., 2019). It has been well-documented that cyanobacteria require Co for the biosynthesis of cobalamin (Cavet et al., 2003).

Cobalt and Endophytic Bacteria in N Fixation

A group of N_2-fixing bacteria can form an endophytic relationship with many crop plants (**Table 2**, **Figure 1B**). By definition, any bacterium could be considered to be an endophytic diazotroph if (1) it can be isolated from surface-disinfected plant tissue or extracted inside the plants, (2) it proves to be located inside the plant, either intra- or inter-cellularly by *in-situ* identification, and (3) it fixes N_2, as demonstrated by acetylene reduction and/or ^{15}N-enrichment (Hartmann et al., 2000; Gupta et al., 2012). Common N_2-fixing endophytic bacteria include *Azoarcus* spp. BH72 and *Pseudomonas stutzeri* A1501 in rice (Wang et al., 2016; Pham et al., 2017), *Achromobacter* spp. EMC1936 in tomato (Abdel-Rahman et al., 2017), *Azospirillum lipoferum* 4B in maize (Garcia et al., 2017), *Burkholderia phytofirmans* PsJN in grape plants (Compant et al., 2008), Enterobacter cloacae ENHKU01 in pepper (Santoyo et al., 2016), *Gluconoacetobacter diazotrophicus* PaI5 in sugarcane (James et al., 2001). Other bacteria, such as *Herbaspirillum*, *Klebsiella,* and *Serratia* also are implicated in N_2 fixation (Rothballer et al., 2008; Franche et al., 2009). These bacteria possess either iron or vanadium nitrogenase that fixes N_2 into NH_3.

The complete genome of *Azoarcus* sp. BH72 (Krause et al., 2006), *G. diazotrophicus* PAl 5 (Bertalan et al., 2009), *Herbaspirillum seropedicae* SmR1 (Pedrosa et al., 2011), and *S. marcesens* RSC-14 (Khan et al., 2017) were sequenced. Among them, genomic and proteomic profiles of *Azoarcus* sp., *Gluconoacetobacter diazotrophicus*, *Herbaspirillum seropedicae*, and *Serratia marcesens* have been studied (Krause et al., 2006; Gupta et al., 2012). These bacteria have co-transport systems for Co^{2+}, Zn^{2+}, and Cd^{2+} or Ca^{2+}, Co^{2+}, Zn^{2+}, and Cd^{2+} as well as putative receptors for vitamin B_{12}. Comparative genomic analyses of Ni, Co, and vitamin B_{12} utilization showed that both metals are widely used by the bacteria and archaea, with the most common prokaryotic transporter being Cbi/NikMNQO. Ni-Fe hydrogenase, Ni-dependent urease, B_{12}-dependent ribonucleotide reductase, methionine synthase, and methymalonly-CoA mutase are the most widespread metalloproteins for Ni and Co (Zhang et al., 2009). Thus, Co is needed by these bacteria.

Cobalt and Plant Associated N_2 Fixing Bacteria

Associated N_2-fixing bacteria include *Azotobacter*, *Azospirillum*, *Beijerinckia*, *Burkholderia*, *Clostridium, Herbaspirillum*, *Gluconacetobacter*, *Methanosarcina*, and *Paenibacillus* (**Table 2**, **Figure 1C**). These bacteria are associated with the roots of

TABLE 2 | Representative nitrogen fixing bacteria.

Type of association	Bacteria	Plants	References
Symbiosis	Cyanobacteria	Bryophyte symbiosis Nostoc-Gunnera symbiosis Azolla symbiosis Cycad symbiosis Lichen symbiosis	Adams et al., 2013
	Rhizobia (*Bradyrhizobium*, *Burkholderia*, *Ensifer*, and *Mesorhizobium*)	Legume-Rhizobia symbiosis	Andrews and Andrews, 2017
	Frankia	Non-legume-Frankia symbiosis: Actinorhizal plants	Wall, 2000
Endophyte	*Azospirillum amazomense*; *Bacillus* spp.; *Burkhoderia* spp.; *Gluconacetobacter diazotrophicus*; *Paenibacillus polymyxa*; and *Pseudomonas aeruginosa*	Rice Maize Rice Sugarcane Maize Wheat	Puri et al., 2018; Rana et al., 2020
Association	*Acetobacter nitrocaptans*; *Azospirillum* spp.; *Bacillus azotofixans*; and *Pseudomonas* spp.	Sugarcane association Grasses and cereals (maize, sorghum, wheat) Grasses, sugarcane, wheat Wetland rice	Boddey and Dobereiner, 1988; Rosenblueth et al., 2018
	Cyanobacteria; *Acetobacter diazotrophicus*; *Azoarcus* spp.; *Azospirillum* spp.; and *Azotobacter* spp.	Sugarcane Grasses Maize, wheat Sugarcane	Steenhoudt and Vanderleyden, 2000

a wide range of plants, including corn, rice, sugarcane, and wheat (Aasfar et al., 2021). Among them, the genus *Azotobacter* was first reported in 1901 and has been used as a biofertilizer thereafter (Gerlach and Vogel, 1902). Notable species found in soils are *A. chroococcum*, *A. vinelandii*, *A. beigerinckii*, *A. armeniacus*, *A. nigricans*, and *A. paspali* (Das, 2019). The genome of *A. vinelandii* DJ has been sequenced (Setubal et al., 2009). N fixation in these species is under aerobic conditions, and two-component proteins of Mo-dependent nitrogenase catalyze N_2 into NH_3. Co and vitamin B_{12} were found to be required by *A. vinelandii* OP. Additionally, 5,6-dimethylbenzimidazolylcobamide coenzyme was identified in this species, which might play an important role in N fixation (Nicholas et al., 1962). Furthermore, higher concentrations of Co were needed for *A. vinelandii* to fix N_2 than was needed for the utilization of ammonium compounds (Evans and Kliewer, 1964). Co at a concentration of 0.1 mg/L was reported to increase N fixation in *A. chroococcum* in Jensen's medium (Iswaran and Rao Sundara, 1964). Culture of *A. chroococcum* in half-strength N-free Jensen's broth showed that N fixation was enhanced after supplemented with Co at 12.5 mg/L or 25 mg/L (Orji et al., 2018). Azotobacters were able to biosynthesize a series of vitamins, including B_{12} in chemically-defined media and dialyzed soil media (Gonzalez-Lopez et al., 1983; El-Essawy et al., 1984). In addition to *A. vinelandii* and *A. chroococcum*, *Pseudomonas fluorescens*, *Bacillus megaterium*, *Bacillus firmus*, and *Sinorhizobium meliloti* also produce cobalamin (Palacios et al., 2014), and the synthesized cobalamin may implicate the enhanced N fixation in these bacteria.

Azosprillum is another important genus of plant-associated N_2-fixing bacteria. *A. brasilense* cultured on medium supplemented with 0.2 m*M* Co was able to accumulate Co up to 0.1 to 0.6 mg per gram of dry biomass (Kamnev et al., 2001). ^{57}Co emission Mössbauer spectroscopy (EMS) studies of Co in *Azospirillum brasilense* Sp245 showed that Co activated glutamine synthetase to have two different Co forms at its active sites. *In vitro*, biochemical and spectroscopic analyses showed that Co^{2+} is among the divalent cations, along with Mg^{2+} and Mn^{2+}, most effective in supporting the activity of glutamine synthetase at different adenylylation states, a key enzyme of N metabolism (Antonyuk et al., 2001).

Nitrogen Fixing Bacteria and Crop Productivity

Nitrogen is an essential macronutrient for plants. The application of synthetic N fertilizers has greatly enhanced crop production but also has caused serious environmental problems, such as groundwater contamination and surface water eutrophication (Hansen et al., 2017). As a result, exploring the potential of BNF becomes increasingly important. The symbiotic relationship between rhizobia and legume crops was considered the most important BNF system and estimated to contribute to 227 to 300 kg N/ha/year (Roughley et al., 1995; Herridge et al., 2008). N_2 fixation by actinorhizal plants was estimated to be 240-350 kg N/ha/year (Wall, 2000).

Nitrogen fixation by plant-associated diazotrophs has been estimated to be 60 kg N/ha/year (Gupta et al., 2006; Reed et al., 2011). Moreover, the abundance of associated diazotrophs, such

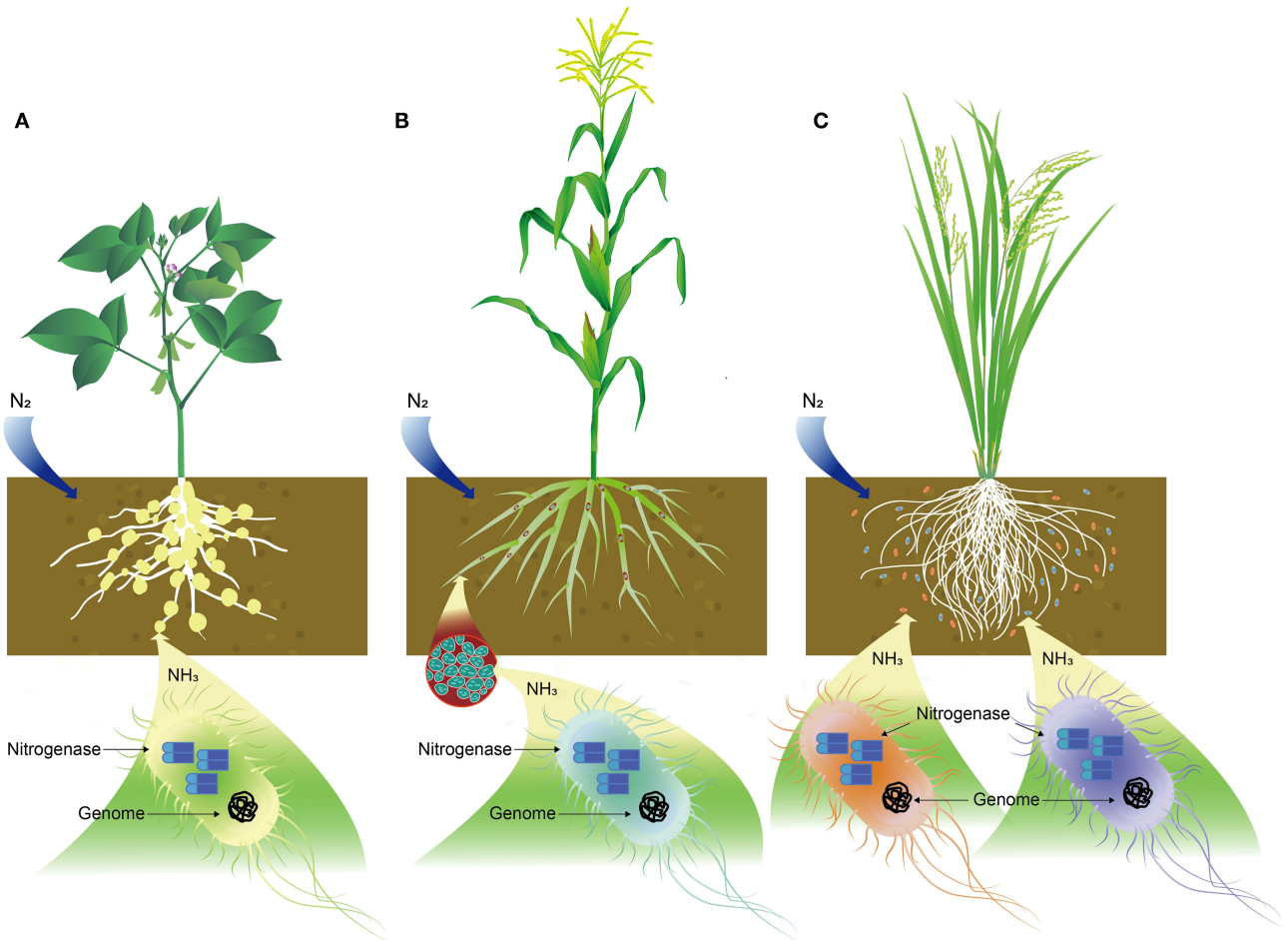


FIGURE 1 | Schematic illustration of nitrogen (N) fixation in bacteria. **(A)** Symbiotic relationship of *Rhizobium* with soybean in N fixation, **(B)** endophytic bacteria, like *Azospirillum lipoferum* in corn plant root for N fixation, and **(C)** N-fixing bacteria, such as *Azotobacter* and *Azospirillum* associated with rice plant roots where cobalt or cobalamin plays important role in N fixation.

as *Azotobacter* species in the soil provides not only N (Din et al., 2019) but also phosphorus and plant growth regulators, which resulted in a yield increase of up to 40% in cereals and pulse crops (Yanni and El-Fattah, 1999; Choudhury and Kennedy, 2004; Kannan and Ponmurugan, 2010; Ritika and Dey, 2014; Wani et al., 2016; Velmourougane et al., 2019). Such beneficial effects have been harnessed ecologically in the engineering of *Azotobacter* species for fixing plant needed N, while reducing the reliance on synthetic N fertilizers for crop production in an environmentally friendly manner (Wani et al., 2016; Bageshwar et al., 2017; Ke et al., 2021).

Endophytic bacteria also contribute significantly to N input. *Azoarcus* is an endophytic N_2-fixing diazotroph, and its action in roots of kallar grass increased hay yield up to 20–40 t/ha/year without N fertilizer application in saline-sodic, alkaline soils (Hurek and Reinhold-Hurek, 2003). *Gluconoacetobacter diazotrophicus* (*Acetobacter diazotrophicus*) is the main contributor in sugarcane and can fix up to 150 kg N/ha/year (Dobereiner et al., 1993; Muthukumarasamy et al., 2005). Many C-4 energy plants, such as *Miscanthus sacchariflorus, Spartina pectinate,* and *Penisettum purpureum* can harbor endophytic bacteria, which support the N requirement of these plants (Kirchhof et al., 1997). Gupta et al. (2012) reported that N derived from the air by endophytic bacteria for rice ranged from 9.2 to 47% depending on bacterial species. These results indicate that endophytic diazotrophs have a great potential to enhance the productivity of non-leguminous crops.

The aforementioned bacteria essentially act as the same as gut bacteria in mammals by living between plant cells as endophytes, close association with roots, or symbiotically and become indispensable for plant growth and development. Microorganisms are associated with all plant organs (Wei et al., 2017), but roots have the largest number and greatest range of microbes. Thus, a plant growing under field conditions is a community, not an individual. Such associations are collectively termed "phytomicrobiome." The phytomicrobiome is integral for plant growth and function. Microbes play important roles in plant nutrient acquisition, biotic and abiotic stress management,

physiology regulation through microbe-to-plant signals, and growth regulation *via* the production of phytohormones. The foregoing discussion documents the role of Co plays in N_2 fixing rhizosphere bacteria. If we accept that coevolution exists between microbes and plants and the phytomicrobione in general, Co should be considered as an essential element to plants as it is required by symbiotic, endophytic, and associated bacteria.

COBALT COENZYMES AND PROTEINS

Cobalamin is a cofactor of adenosylcobalamin-dependent isomerases, ethanolamine ammonia-lyase, methylcobalamin-dependent methyltransferase, and ribonucleotide reductase in animals and bacteria (**Table 1**). Co is also a cofactor of non-corrin coenzymes or metalloproteins including aldehyde decarboxylase, bromoperoxidase-esterase, D-xylose isomerase, methionine aminopeptidase (MA), methylmalonyl-CoA carboxytransferase, nitrile hydratase (NHase), prolidase, and thiocyanate hydrolase (THase) in animals, bacteria, and yeasts. However, cobalamin-dependent enzymes or Co-proteins in plants remain obscure.

Cobalt Proteins in Plants

There are several lines of evidence suggesting that plants may have cobalamin-dependent enzymes and Co-containing proteins: (1) The ancestor of the chloroplast is cyanobacteria (Falcón et al., 2010), and Co is required by this group of bacteria. The speculation is that Co may be needed by plants. (2) Plants have been documented to utilize cobalamin produced by symbiotic, endophytic, and associated N_2 fixing bacteria. Cobalamin concentrations of 37, 26, and 11 μg/100 g dry weight were detected in *Hippophae rhammoides*, *Elymus*, and *Inula helenium*, respectively (Nakos et al., 2017). There is a possibility that cobalamin-dependent enzymes may occur in plants. Poston (1977) reported the identification of leucine 2,3-aminomutase in extracts of bean seedlings. Its activity was stimulated by coenzyme B_{12} but inhibited by unknown factors. The inhibition was removed by the addition of B_{12}, suggesting the presence of a cobalamin-dependent enzyme in higher plants. Subsequently, two coenzyme B_{12}-dependent enzymes: leucine 2,3-aminomutase and methylmalonyl-CoA mutase were reported in potato tubers (Poston, 1978), but methylmalonyl-CoA mutase was found to be a phosphatase (Paizs et al., 2008). (3) Co is required by lower plants, which is to be discussed in the following section. (4) Plants can take up and transport cobalamin (Mozafar, 1994; Sato et al., 2004). A recent study using fluorescent analogs to follow the uptake and transport of cobalamin showed that *Lepidium sativum* can absorb cobalamin (Lawrence et al., 2018). Seed priming with cobalamin provided significant protection against the salt stress of common beans (Keshavarz and Moghadam, 2017). The incorporation of Co in plant tissue culture media significantly improves plantlet production (Bartolo and Macey, 1989). (5) Co as a metal cofactor of some additional enzymes and proteins are briefly discussed below (**Table 1**).

Carbonic anhydrase or carbonate dehydratase (CA, EC: 4.2.1.1) is a metalloenzyme catalyzing the conversion of CO_2 to HCO_3^- reversibly in many organisms including plants, particularly C_4 and CAM plants. Eight different CA classes have been described as α-, β-, γ-, δ-, ζ-, η-, θ-, and a recently described ι-CA in microalgae. The metalloenzymes commonly use Zn^{2+} as a metal cofactor. However, Zn^{2+} in γ class can be replaced by Co^{2+} and Fe^{2+} in prokaryotes, fungi, algae, and plants, but in δ class is only can be replaced by Co^{2+} in marine phytoplankton (Jensen et al., 2020).

Carboxypeptidases (CPSs, EC: 3.4.16–3.4.18) are proteases hydrolyzing the C-terminal residues of peptides and proteins and release free amino acids individually. CPSs are divided into serine (EC: 3.4.16), metal (EC: 3.4.17), and cysteine (EC: 3.4.18) and occur in animals, bacteria, fungi, and plants. One Zn atom is essential to the catalytic activity of native carboxypeptidase A. Zn can be removed by dialysis at low pH or with chelating agents at neutral pH, which results in the inactivation of the enzyme. The re-addition of the metal restores the dual activities of carboxypeptidase toward peptides and esters. Co was found to be more active than Zn in the enzyme toward peptides and has nearly the same activity toward esters, indicating that Co in the active site is virtually identical to that of Zn in the native enzyme (Maret and Vallee, 1993).

Methionine aminopeptidase (MAP, EC 3.4.11.18) is widely documented in animals, bacteria, yeast, and plants. It is a Co-dependent enzyme responsible for the cleavage of the N-terminal methionine from newly translated polypeptide chains. Two classes of MAPs (MAP1 and MAP2) were reported in bacteria, and at least one MAP1 and one MAP2 occur in eukaryotes (Giglione and Meinnel, 2001). In *Arabidopsis*, there are four MAP1s (MAP1A, MAP1B, MAP1C, and MAP1D) and two MAP2s (MAP2A and MAP2B), along with two class 1 peptide deformylases (PDF1A and PDF1B). The plant MAP proteins show significant similarity to the eubacterial counterparts except for MAP1A and two MAP2s. It has been documented that the substrate specificity of PDFs and both organellar and cytosolic MAPs in plants are similar to that of their bacterial counterparts (Giglione et al., 2000). The MAP from *Salmonella typhimurium* is stimulated only by Co^{2+}, not by Mg^{2+}, Mn^{2+}, or Zn^{2+} and is inhibited by metal ion chelator EDTA. *E. coli* MAP is a monomeric protein of 29 kDa consisting of 263 residues that possess two Co^{2+} ions in its active site (Permyakov, 2021).

Prolidase (PEPD, EC 3.4.13.9) hydrolyze peptide bonds of imidodipeptides with C-terminal proline or hydroxyproline, thus liberating proline. PEPD has been identified in fungi, plants (Kubota et al., 1977), archaea, and bacteria. The preferable substrate requires metal ions Mn^{2+}, Zn^{2+}, or Co^{2+}.

Peroxidases are isoenzymes present in all organisms, which catalyze redox reactions that cleave peroxides; specifically, it breaks down hydrogen peroxide. The study of Han et al. (2008) found that Co^{2+} at a concentration below 0.1 mM increased horseradish peroxidase activity because Co^{2+} binds with some amino acids near or in the active site of the enzyme.

Urease is an enzyme occurring in selected archaea, algae, bacteria, fungi, and plants. It catalyzes the hydrolysis of urea into ammonia and carbamic acid. The active site of urease contains two Ni^{2+} atoms that are bridged by a carbamylated lysine residue and a water molecule (Carter et al., 2009). The study of Watanabe

et al. (1994) reported that urease activity of cucumber leaves was markedly reduced when Ni concentration became <100 ng/L, but supplementing Co restored urase activity. Additionally, urease was also activated by both Co and manganese (Mn) through *in vitro* assay (Carter et al., 2009).

Cobalt transporters. Transporters specifically for Co have not been reported. The current understanding is that Co can be transported through Fe transporters (**Figure 2**). In *Arabidopsis thaliana,* Co is taken up from the soil into epidermal cells of roots by IRON-REGULATED TRANSPORTER 1 (IRT1), which is commonly known for absorption of Fe (Korshunova et al., 1999). Once Co is absorbed inside cells, Ferroportins, FPN1, and FPN2 are responsible for its further movement. IREG1/FPN1 is localized to the plasma membrane and expressed in the steel, indicating it is responsible for the loading of Fe to xylem, and FPN2 is situated the in vacuolar membrane and involved in buffering Fe concentration in the cytosol (Morrissey et al., 2009). Truncated *FPN2* causes an elevated level of Co in shoots, while the loss of *FPN1* abolishes Co accumulation in shoots. A double mutant of *fpn1 fpn2* is unable to sequester Co in root vacuole and cannot transport Co to shoots. These results suggest that Co is likely absorbed and transported in the same way as Fe in plants (**Figure 2**). Additionally, an ATP-binding cassette (ABC) transporter from *Arabidopsis* has also been reported to transport Co, Ni, and Pb (Morel et al., 2009). Co movement in leaves is also associated with Ni, and Ni and Co movement in or out of chloroplasts are through an ABC transporter in the mediation of ionic homeostasis in the chloroplast of rice (Li et al., 2020).

Cobalt Substitution of Other Metals

A characteristic of Co is its ability to substitute for other transition metals in a large number of enzymes. Maret and Vallee (1993) listed 37 Co-substituted metalloproteins, of which 24 are native to Zn, nine to copper (Cu), and four to Fe. These enzymes mainly occur in animals, bacteria, and yeast, while a few are in plants. Such a characteristic is closely related to the properties of Co with other metals. The ionic radius of Co^{2+} is 0.76 Å, which is similar to 0.74 Å of Zn^{2+}, 0.69 Å for Cu^{2+}, and 0.76 Å for Fe^{2+}. Additionally, based on the available Protein Data Bank structures with Co^{2+}, the study Khrustalev et al. (2019) found that Co^{2+} is commonly bound by cation traps. The traps are formed by relatively negatively charged regions of random coil between a β stand and α helix and between two β strands in which His, Asp, and Glu residues are situated. On the other hand, these sites are also occupied by other metals ions, such as Cu^{2+}, Mg^{2+}, Mn^{2+}, and Zn^{2+}, which play significant roles as catalysts. As a result, Co^{2+} could rather readily substitute for these ions in the active sites of enzymes. Additionally, based on the FIND-SITE-metal, a program for the prediction of the metal-binding site, the study of Brylinski and Skolnick (2011) found that Zn, due to a lower coordination number preference, is typically chelated with Cys and His, and His residues have a strong preference for Co, Cu, Fe, Ni, and Zn atoms. Thus, Co is able to replace Cu, Fe, Ni, and Zn in the active sites of enzymes. For example, Co addition alleviated Zn limitation in production of *Thalassiosira weissflogii*, which was due to Co substitution of Zn in the main isoform of carbonic anhydrase (Yee and Morel, 1996). Co substitution of Zn was also reported in two northeast Pacific isolates of diatoms *Pseudo-nitzschia delicatissima* UNC1205 and *Thalassiosira* spp. UNC1203 (Kellogg et al., 2020). Co^{2+} has been used as a spectroscopically active substitute for Zn^{2+} in enzymes (Bennett, 2010). Substitution of tetrahedral Zn^{2+} by higher-coordinate Co^{2+} often results in a catalytically active species, sometimes with catalytic properties perhaps unexpectedly similar to those of the native enzyme. In the vast majority of cases, no other transition ion than Co^{2+} provides a better substitute for Zn^{2+} (Maret and Vallee, 1993; Bennett, 2010). Due to these reasons, Co specific enzymes or proteins have not been conclusively identified. With the advance of omics, functions of a large number of gene sequences have not been assigned. Using the FIND-SITE-metal, a program developed for prediction of the metal-binding site, Brylinski and Skolnick (2011) predicted that about 10,953 putative metal-binding proteins in human proteome were bound with Ca, 10,534 bound with Mg, 8,681 with Zn, 1,863 with Fe, 1,246 with Mn, 652 with Co, 476 with Cu, and 403 with Ni. The predicted binding proteins with Co are greater than Cu and Ni in humans. Based on this assignment in the human proteome, it could be extremely difficult to believe that there are no Co-containing enzymes and proteins in plants.

COBALT IS ESSENTIAL FOR LOWER PLANTS

Lower plants are commonly known as non-vascular plants because they do not have xylem and phloem vascular systems. Non-vascular plants are generally divided into bryophytes and algae.

Bryophytes

Bryophytes are seedless plants including Anthocerotophyta (hornworts), Bryophyta (mosses), and Marchantiophyta (liverworts) (Davies et al., 2020). This group of plants is able to absorb Co from air, soil, and water. In an early geochemical survey performed in Wisconsin and adjacent states and Missouri and Kentucky in the US, the study of Shacklette (1965) documented that the mean concentration of Co in 38 samples of liverworts and mosses was 32 mg/kg, and the concentration in the lower plants was closely related to the amount of the element in the soil, suggesting they act as a bioindicator of Co concentration in the environment (Baker, 1981). Mosses sampled from streams of the Idaho Cobalt Belt (U.S.) showed that Co concentrations in the plants almost perfectly correlated with those in the sediments, and the maximum content of Co (2,000 mg/kg) in moss ash corresponded to the maximum concentration of 320 mg/kg in the sediment (Erdman and Modreski, 1984). Mosses, such as *Bryum argenteum* and *Hypnum cupressiforme* were also considered to be bioindicators for monitoring heavy metal contamination in the air (Andić et al., 2015). Interestingly, the accumulation of Co did not cause any physiological damages to plants, but their growth was further enhanced.

The ability to take up Co could be related to the non-vascular nature and unidentified transporter. A radiolabel study showed that the total amount of ^{60}Co accumulated

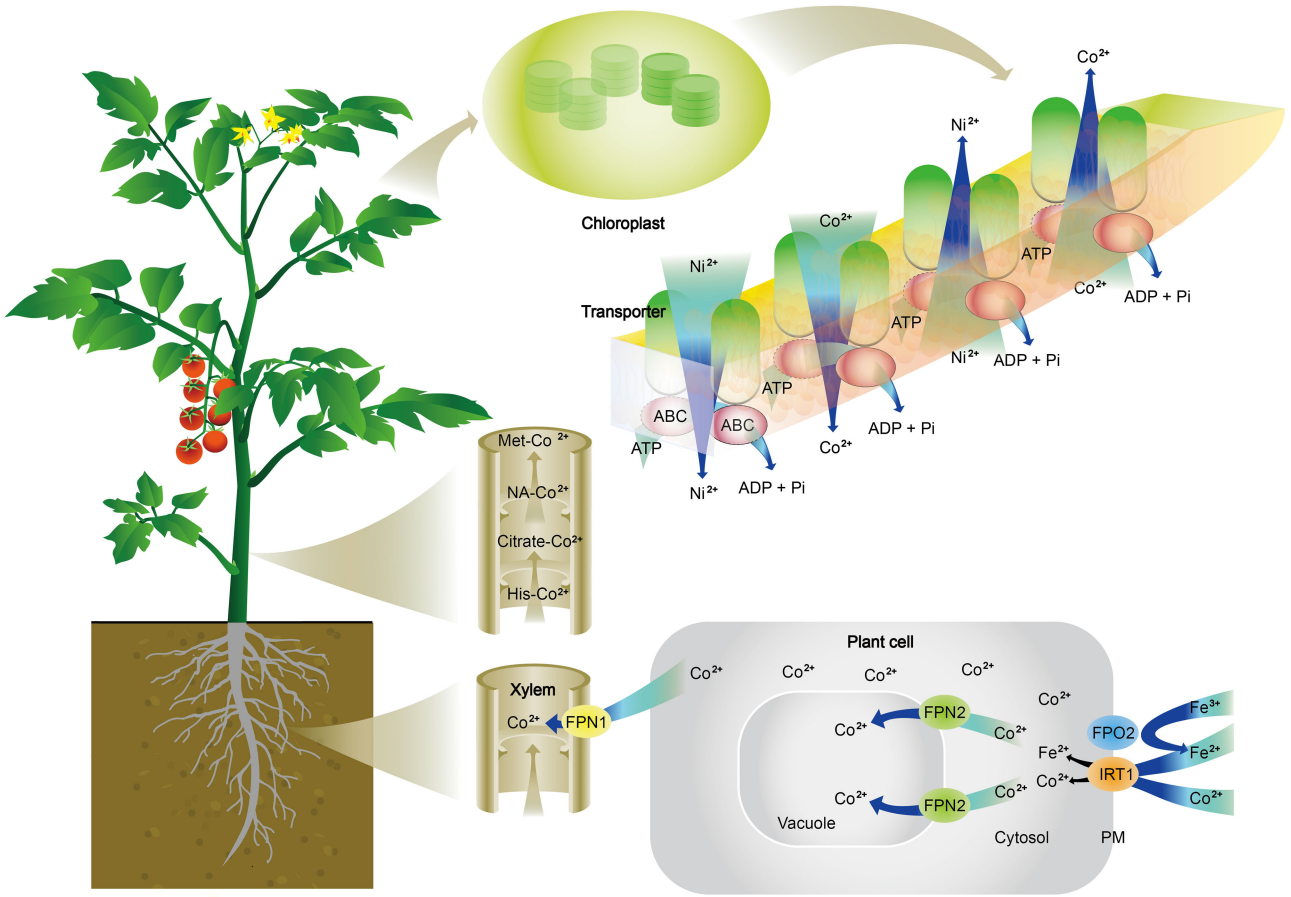


FIGURE 2 | Schematic illustration of cobalt (Co^{2+}) absorption, transport, and distribution in plants. Co^{2+} is absorbed from the soil into epidermal cells of roots by an iron transporter (IRT1). Once Co^{2+} is absorbed inside cells, Ferroportins (FPN1 and FPN2) are responsible for its further movement. FPN2 transports Co^{2+} into vacuoles, resulting in the sequestration of Co in root cells. FPN1 is to load Co^{2+} into the xylem. In the xylem, Co^{2+} is complexed with citrate, histidine (His), methionine (Met), or nicotianamine (NA) to be translocated to shoots. Co^{2+} is released in leaves and participate in metabolisms, which are often associated with nickel (Ni) and iron (Fe). It is shown here the Ni and Co movement in or out of chloroplasts through ATP-binding cassette (ABC) transporter in the mediation of ionic homeostasis in the chloroplast.

in *P. commune* and *D. scoparium* under given conditions were 7.1 and 6.1 mg/kg, respectively. More than 95% of ^{60}Co in *D. scoparium* was localized extracellular, while 70% of ^{60}Co in *P. commune* was localized extracellular and about 20% localized intracellularly. These results showed that Co was largely adsorbed extracellularly, and there were unidentified transporters regulating the transport of Co into intracellular sites.

The enhanced growth could be in part attributed to the symbiotic relationship with cyanobacteria. Some bryophytes, primarily liverworts, and hornworts can form a symbiosis with cyanobacteria, such as *Nostoc* spp. After infection, *Nostoc* underwent some morphological and physiological changes by reducing growth rate and CO_2 fixation but enhancing the fixation of N_2 as well as releasing fixed N compounds to the plants. Cyanobacteria, like rhizobia, require cobalamin as a cofactor for nitrogenase complex to fix N_2 (Böhme, 1998). Thus, cyanobacteria-bryophyte symbioses require Co.

Algae

Algae constitute a polyphyletic group ranging from unicellular microalgae, like chlorella and diatoms to multicellular forms, such as the giant kelp, seaweeds, and charophytes (Barsanti and Gualtieri, 2006). Co is essential to some marine algal species, including charophyte, diatoms, and dinoflagellates (Nagpal, 2004). Green alga *Chlorella salina* exhibited two phases of uptake of Co^{2+} (Garnham et al., 1992). The initial phase was rapid and independent of metabolism, and the second phase was slow and dependent on metabolism. Competition studies showed that the Co^{2+} uptake system was different from that for Mg^{2+}, Mn^{2+}, and Zn^{2+}. The greatest amount of Co was associated with the cell wall. Co concentrations in the cytosol were 0.17 mM but 2.89 mM in the vacuole, suggesting that Co transport was well-controlled in *C. salina*. In the work of Czerpak et al. (1994), they studied the responses of a freshwater green alga *Chlorella pyrenoidosa* to different levels of Co and found that Co in a range from 5 to 50 mM significantly enhanced the growth of *Chlorella pyrenoidosa*, including 150–160 and 50–60%

increase in fresh and dry weights, respectively. Such increase was related to the increase of chlorophylls *a* and *b* by 45–65%, water-soluble proteins by 19–20%, total carotenoids 55–65%, and monosaccharides content 55–60%, when compared with the culture devoid of Co. Although mechanisms behind the stimulating effects have not been elucidated, it is likely due to the biosynthesis of cobalamin that enhanced alga growth. Two cobalamin coenzyme 5′-deoxyadenosylcobalamin and methylcobalamin occurred in green alga *C. vulgaris*, and the addition of cobalamin significantly stimulated green alga growth (Watanabe et al., 1997). Moreover, *C. vulgaris* grown in Bold's basal medium supplemented with 2 and 2.5 μM $CoCl_2$ produced 166.23 and 173.32 μg vitamin B_{12} per 100 g dry weight (Jalilian et al., 2019). Additionally, many algal species require different combinations of cobalamin, vitamin B_1, and B_7 (Croft et al., 2005) as they do not have pathways to synthesize cobalamin or may use alternative cobalamin-independent routes bypassing the need for the vitamin (Cruz-Lopez and Maske, 2016; Yao et al., 2018). As Co is a constituent of cobalamin, Co is required by those algae.

Some algal species, such as those in the genera *Coccomyxa* and *Elliptochloris* as well as diatoms form symbiotic relationships with cyanobacteria (Grube et al., 2017). Co is required for the growth of cyanobacteria, such as *Anabaenza cylindrica* Lemm (Holm-Hansen et al., 1954) and *Prochlorococcus* (Hawco et al., 2020) as they need it for N fixation in specialized cells called heterocysts. Thus, algal species symbiotic with cyanobacteria require Co for N-fixation.

COBALT IMPROVES THE GROWTH OF HIGHER PLANTS

Cobalt content in the crust of the earth ranges from 15 to 30 mg/kg (Roberts and Gunn, 2014). Co in soils is closely related to the weathering of parental minerals, such as cobaltite, smaltite, and erythrite (Bakkaus et al., 2005) as well as Co pollution (Mahey et al., 2020). Co in the surface soils of the world varies from 4.5 to 12 mg/kg with the highest level occurring in heavy loamy soils and the lowest in organic and light sandy soils (Kabata-Pendias and Mukherjee, 2007). However, Co in reference soil samples was found to differ from 5.5 to 29.9 mg/kg in the United States (U.S.) and 5.5 to 97 mg/kg in Chinese soils (Govindaraju, 1994). Pilon-Smits et al. (2009) suggested that soil Co concentrations generally range from 15 to 25 mg/kg.

Cobalt in Higher Plants

Plants absorb Co. **Table 3** lists Co concentrations in over 140 non-hyperaccumulating species ranging from 0.04 to 274 mg/kg. Average concentrations of Co in grasses vary from 60 to 270 μg/kg and in clover differ from 100 to 570 μg/kg across Australia, Finland, Germany, Great Britain, Japan, New Zealand, Poland, Sweden, and the US (Kabata-Pendias and Mukherjee, 2007). Legumes absorb more Co than grasses. Plants that accumulate metals to a level 100-fold higher than those typically recorded in common plants are known as hyperaccumulators (Brooks, 1998).

As discussed above, Co specific transporters have not been reported, and a schematic diagram for Co absorption and translocation is presented in **Figure 2**. After absorption by roots, Co is either sequestrated in the vacuole of root cells or transported to shoots. Co that is being transported to shoots is chelated with ligands. Co has little affinity with phytochelatins (Chen et al., 1997; Cheng et al., 2005), thus the ligands are not likely Co-S bonds. The study by Collins et al. (2010) reported that Co^{2+} was complexed with carboxylic acids, which were transported from roots to shoots in wheat or tomato plants. Other ligands are citrate or malate as well as non-proteinogenic amino acids, such as histidine and nicotianamine (**Figure 2**). Co has low mobility within the leaf tissue and is largely distributed in the vascular system of tomato and wheat leaves (Collins et al., 2010). Co transport from roots to shoots is well-controlled. Using radiolabeled ^{57}Co, Page and Feller (2005) studied Co transport in wheat plants and found that 80% of ^{57}Co remained in roots after 4 days of culture, and 50% was retained in the roots after 50 days; during which, some ^{57}Co moved to the apical part of the main roots, suggesting that the loading of Co to the xylem is well-controlled, probably by FPN1 in wheat plants. In another study, Collins et al. (2010) reported that tomato and wheat plants grown in a nutrient solution containing 2.94 mg/L Co had 4,423 μg/kg and 9,319 μg/kg of Co in roots, respectively; but shoot concentrations of Co were 1,581 μg/kg and 395 μg/kg, respectively. This means that 35.7% of Co absorbed by tomato and 4.2% of Co absorbed wheat plants were transported from roots to shoots. Furthermore, for the 1,581 μg/kg Co in tomato shoots, 846 μg/kg was in the stem, 492 μg/kg in old leaves, only 243 μg/kg in young leaves, indicating that only 5.5% of absorbed Co is transported to actively growing shoots of tomato plants. These transport patterns are like those of titanium (Lyu et al., 2017) which are strictly controlled by plants. These findings imply that plants probably have unidentified transporters specifically for the transport of Co. Due to its toxicity at higher concentrations, the rigorous control of the transport and distribution would ensure that only an appropriate amount of Co could be transported to actively growing shoots. On the other hand, why was more Co transported to dicot tomato shoots than monocot wheat shoots? One explanation could be that different plants have different ligands for complexing Co, and Co complexed by ligands in tomato was more mobile than that in wheat. Another explanation could be that tomato plants need more Co to fulfill some unidentified roles in shoots. Further research is needed to verify these propositions.

To maintain ionic homeostasis in shoots, particularly in chloroplasts, plants develop mechanisms to mediate Co in chloroplasts. An ARG1 transporter, belonging to the ATP-binding cassette, was identified in rice (Li et al., 2020), which was able to modulate the levels of Co and Ni in chloroplasts to prevent excessive Co and Ni from competing with metal cofactors in chlorophyll and metal-binding proteins in photosynthesis (**Figure 2**).

TABLE 3 | The concentration of cobalt in higher plants with the exclusion of cobalt hyperaccumulators.

Family	Species	Common name	Plant organ	Content (mg/kg)	References
Acanthaceae	*Lophostachys villosa* Pohl	Lophostachys	Leaves	31.00	Van der Ent and Reeves, 2015
Adiantaceae	*Taenitis blechnoides* (Willd.) Sw.	Ribbon fern	Leaves	22.00	Van der Ent and Reeves, 2015
Amaranthaceae	*Aerva lanata* (L.) Juss.	Gorakhdi	Whole plants	12.70	Rajakaruna and Bohm, 2002
Amaranthaceae	*Pfaffia sarcophylla* Pedersen	Pfaffia	Leaves	13.00	Van der Ent and Reeves, 2015
Anacardiaceae	*Gluta wallichii* (Hook.f.) Ding Hou	Gluta	Leaves	5.00	Van der Ent and Reeves, 2015
Anisophylleaceae	*Anisophyllea disticha* (Jack) Baill.	Mousedeer plant	Leaves	4.00	Van der Ent and Reeves, 2015
Apocynaceae	*Calotropis gigantea* L.R.Br.	Yercum fiber	Whole plants	0.84	Rajakaruna and Bohm, 2002
Apocynaceae	*Carissa spinarum* L.	Bush plum	Stems, leaves and flowers	1.60	Rajakaruna and Bohm, 2002
Arecaceae	*Phoenix farinifera* Roxb.	Ceylon date palm	Whole plants	0.04	Rajakaruna and Bohm, 2002
Aristolochiaceae	*Thottea triserialis* Ding Hou	Thottea	Leaves	5.00	Van der Ent and Reeves, 2015
Asparagaceae	*Asparagus zeylanicus* Hook.f.	Asparagus	Whole plants	0.90	Rajakaruna and Bohm, 2002
Asteraceae	*Anthemis cretica* L.	Mountain dog-daisy specie	Shoots	8.90	Koleli et al., 2015
Asteraceae	*Eupatorium odoratum* L.	Siam weed	Whole plants	0.50–3.10	Rajakaruna and Bohm, 2002
Asteraceae	*Blumea balsamifera* (L.) DC.	Bukadkad	Leaves	2.00	Van der Ent and Reeves, 2015
Asteraceae	*Vernonia holosericea* Mart. ex DC.	Ironweed	Leaves	21.00	Van der Ent and Reeves, 2015
Berberidaceae	*Podophyllum peltatum* L.	May-apple	Shoots	0.60	Koleli et al., 2015
Betulaceae	*Betula pubescens* Ehrh.	Birch	Leaves	0.36	Reimann et al., 2001
Bignoniaceae	*Zeyheria digitalis* (Vell.) Hoehne and Kuhlm	Zeyheria	Leaves	2.00	Van der Ent and Reeves, 2015
Blechnaceae	*Blechnum borneense* C.Chr.	Hard fern	Leaves	10.00	Van der Ent and Reeves, 2015
Boraginaceae	*Anchusa granatensis* Boiss.	Anchusa	Shoots	0.90	Koleli et al., 2015
Boraginaceae	*Onosma bracteosum* Hausskn. and Bornm.	Onosma	Shoots	6.60	Koleli et al., 2015
Brassicaceae	*Alyssum minus* (L.) Rothm.	Wild Alyssum	Shoots	1.20	Koleli et al., 2015
Brassicaceae	*Alyssum murale* Waldst. and Kit.	Yellowtuft	Shoots	7.70	Koleli et al., 2015
Brassicaceae	*Aurinia saxatilis* (L.) Desv.	Basket of gold	Roots	37.00	Homer, 1991
Brassicaceae	*Aurinia saxatilis* (L.) Desv.	Basket of gold	Leaves	117.00	Homer, 1991
Brassicaceae	*Brassica juncea* (L.) Czern	Brown-mustard	Stems, leaves, and flowers	25.50	Malik et al., 2000
Brassicaceae	*Thlaspi elegans* Boiss.	Thlaspi	Shoots	6.40	Koleli et al., 2015
Campanulaceae	*Campanula rapunculoides* L.	Creeping bellflower	Shoots	0.70	Koleli et al., 2015
Caryophyllaceae	*Dianthus arpadianus* Ade and Born.	Dianthus	Shoots	0.30	Koleli et al., 2015
Caryophyllaceae	*Silene burchelli* var. *angustifolia* Sond.	Gunpowder plant	Shoots	250.00	Baker et al., 1983
Chrysobalanaceae	*Parinari elmeri* Merri.	Parinari	Leaves	138.00	Van der Ent and Reeves, 2015
Clusiaceae	*Mesua paniculate* (L.) Jack	Chinese box	Leaves	77.00	Van der Ent and Reeves, 2015
Compositae	*Epaltes divaricate* (L.) Cass.	Narrow-Leaf epaltes	Whole plants	15.60	Rajakaruna and Bohm, 2002
Convolvulaceae	*Evolvulus alsinoides* L.	Little glory	Whole plants	17.10	Rajakaruna and Bohm, 2002
Convolvulaceae	*Jacquemontia* sp.	Clustervine	Leaves	16.00	Van der Ent and Reeves, 2015
Cornaceae	*Nyssa aquatica* L.	Water tupelo	Leaves	156.00	McLeod and Ciravolo, 2007
Cornaceae	*Nyssa aquatica* L.	Water tupelo	Leaves	24.50	Wallace et al., 1982
Cornaceae	*Nyssa sylvatica* Marsh.	Black gum	Mature foliage	27.20	Thomas, 1975
Cornaceae	*Nyssa sylvatica* var. *biflora* (Walt.) Sarg.	Black gum	Leaves	267.00	McLeod and Ciravolo, 2007
Cyperaceae	*Fimbristylis falcata* (Vahl) Kunth	Fimbristylis	Whole plants	16.30	Rajakaruna and Bohm, 2002
Dennstaedtiaceae	*Lindsaea gueriniana* (Gaudich.) Desv.	Goldenbush	Leaves	5.00	Van der Ent and Reeves, 2015
Dennstaedtiaceae	*Tapeinidium acuminatum* K.U. Kramer	Tapeinidium ferns	Leaves	22.00	Van der Ent and Reeves, 2015
Droseraceae	*Drosera montana* A.St.-Hil.	Sundews	Leaves	34.00	Van der Ent and Reeves, 2015
Ebenaceae	*Diospyros lanceifolia* Roxb.	Common Malayan ebony	Leaves	2.00	Van der Ent and Reeves, 2015
Equisetaceae	*Equisetum arvense* L.	Bottlebrush	Shoots	0.80	Koleli et al., 2015
Ericaceae	*Empetrum nigrum* L.	Crow-berry	Leaves	0.05	Reimann et al., 2001
Ericaceae	*Vaccinium myrtillus* L.	Blue-berry	Leaves	0.04	Reimann et al., 2001
Ericaceae	*Vaccinium vitis-idaea* L.	Cow-berry	Leaves	0.04	Reimann et al., 2001

(Continued)

TABLE 3 | Continued

Family	Species	Common name	Plant organ	Content (mg/kg)	References
Euphorbiaceae	*Croton bonplandianus* Baill.	Bonpland's croton	Stems, leaves and flowers	1.60	Rajakaruna and Bohm, 2002
Euphorbiaceae	*Croton griffithii* Hook.f.	Griffith's spurge	Leaves	10.00	Van der Ent and Reeves, 2015
Euphorbiaceae	*Drypetes caesia* Airy Shaw	Drypetes	Leaves	2.00	Van der Ent and Reeves, 2015
Euphorbiaceae	*Euphorbia macrostegia* Boiss.	Persian wood spurge	Shoots	0.90	Koleli et al., 2015
Euphorbiaceae	*Euphorbia rubicunda* Blume	Chicken weed	Stems, leaves and flowers	1.30	Rajakaruna and Bohm, 2002
Euphorbiaceae	*Euphorbia selloi* (Klotzsch and Garcke) Boiss.	Spurge	Leaves	72.00	Van der Ent and Reeves, 2015
Euphorbiaceae	*Phyllanthus* sp.	Leaf-flower	Leaves	85.00	Van der Ent and Reeves, 2015
Fabaceae	*Mimosa pudica* L.	Mimosa plant	Leaves	0.04	Van Tran and Teherani, 1989
Fabaceae	*Dalbergia beccarii* Prain	Beccari's dalbergia	Leaves	4.00	Van der Ent and Reeves, 2015
Iridaceae	*Gladiolus italicus* Miller	Field gladiolus	Shoots	1.50	Koleli et al., 2015
Iridaceae	*Sisyrinchium luzula* Klotzsch ex Klatt	Blue-eyed grass	Leaves	11.00	Van der Ent and Reeves, 2015
Labiatae	*Mentha piperita* L.	Mint	Shoots	0.04–0.17	Ciotea et al., 2021
Labiatae	*Ocimum basilicum* L.	Basil	Shoots	0.11–0.16	Ciotea et al., 2021
Labiatae	*Rosmarinus officinalis* L.	Rosemary	Shoots	0.07- 0.14	Ciotea et al., 2021
Lamiaceae	*Clerodendrum infortunatum* L.	Hill glory bower	Stems, leaves and flowers	0.60	Rajakaruna and Bohm, 2002
Lamiaceae	*Crotalaria biflora* L.	Two-flower rattlebox	Stems, leaves and flowers	15.90	Rajakaruna and Bohm, 2002
Lamiaceae	*Geniosporum tenuiflorum* (L.) Merr.	Holy basil	Whole plants	10.80	Rajakaruna and Bohm, 2002
Lamiaceae	*Leucas zeylanica* (L.) R.Br.	Ceylon leucas	Whole plants	3.30	Rajakaruna and Bohm, 2002
Lamiaceae	*Leucas zeylanica* (L.) R.Br.	Ceylon leucas	Whole plants	9.40	Rajakaruna and Bohm, 2002
Lamiaceae	*Ajuga reptans* L.	Bugleweed	Shoots	0.90	Koleli et al., 2015
Lamiaceae	*Haumaniastrum katangense* (S. Moore) Duvign. Plancke	Copper flower	Leaves	260.00	Morrison, 1979
Lamiaceae	*Sideritis trojana* Bornm.	Sideritis	Shoots	0.90	Koleli et al., 2015
Lamiaceae	*Thymus pulvinatus* Celak	Common thyme	Shoots	0.20	Koleli et al., 2015
Lamiaceae	*Hypenia macrantha* (A.St.-Hil. ex Benth.) Harley	Hypenia	Leaves	10.00	Van der Ent and Reeves, 2015
Lamiaceae	*Lippia* aff. *geminata*	Lippia	Leaves	11.00	Van der Ent and Reeves, 2015
Lamiaceae	*Lippia* sp.	Lippia	Leaves	14.00	Van der Ent and Reeves, 2015
Leguminoseae	*Tephrosia purpurea* (L.) Pers.	Wild indigo	Stems, leaves and flowers	5.20	Rajakaruna and Bohm, 2002
Leguminoseae	*Baptisia australis* (L.) R. Br. ex Ait. f.	Blue false indigo	Shoots	0.50	Koleli et al., 2015
Leguminoseae	*Vicia cassubica* L.	Vicia	Shoots	5.50	Koleli et al., 2015
Liliaceae	*Allium cepa* L.	Onion	Shoots	3.50	Koleli et al., 2015
Liliaceae	*Asphodelus aestivus* Brot.	Summer asphodel	Shoots	0.80	Koleli et al., 2015
Loganiaceae	*Norrisia* sp. 1	Norrisia	Leaves	8.00	Van der Ent and Reeves, 2015
Malvaceae	*Abutilon indicum* (L.) Sweet	Abutilon	Stems, leaves and flowers	0.80	Rajakaruna and Bohm, 2002
Malvaceae	*Hibiscus rhodanthus* Gürke ex Schinz	Dwarf red hibiscus	Leaves	21.00–1,971.00	Faucon et al., 2007
Malvaceae	*Sida acuta* Burm.f	Wire weed	Whole plants	0.30	Rajakaruna and Bohm, 2002
Malvaceae	*Waltheria indica* L.	Sleepy morning	Whole plants	1.33	Rajakaruna and Bohm, 2002
Melastomataceae	*Pterolepis* sp. nov.	Pterolepis	Leaves	11.00	Van der Ent and Reeves, 2015
Myrtaceae	*Syzygium* cf. *pterophera*	Syzygium	Leaves	7.00	Van der Ent and Reeves, 2015
Myrtaceae	*Syzygium clavatum* (Korth.) Merr. and L.M.Perry	Syzygium	Leaves	3.00	Van der Ent and Reeves, 2015
Phyllanthaceae	*Actephila* sp. nov.	Actephila	Leaves	65.00	Van der Ent et al., 2015
Phyllanthaceae	*Antidesma coriaceum* Tul.	Antidesma	Leaves	2.00	Van der Ent et al., 2015
Phyllanthaceae	*Aporosa benthamiana* Hook.f.	Aporosa	Leaves	6.00	Van der Ent et al., 2015
Phyllanthaceae	*Aporosa falcifera* Hook.f.	Aporosa	Leaves	18.00	Van der Ent et al., 2015

(Continued)

TABLE 3 | Continued

Family	Species	Common name	Plant organ	Content (mg/kg)	References
Phyllanthaceae	*Aporosa lucida (*Miq.) Airy Shaw	Aporosa	Leaves	18.00	Van der Ent et al., 2015
Phyllanthaceae	*Baccaurea lanceolata (*Miq.) Müll.Arg.	Baccaurea	Leaves	179.00	Van der Ent et al., 2015
Phyllanthaceae	*Breynia coronata* Hook.f.	Breynia	Leaves	4.00	Van der Ent et al., 2015
Phyllanthaceae	*Cleistanthus ellipticus* Hook.f.	Cleistanthus	Leaves	6.00	Van der Ent et al., 2015
Phyllanthaceae	*Cleistanthus gracilis* Hook.f.	Cleistanthus	Leaves	10	Van der Ent et al., 2015
Phyllanthaceae	*Cleistanthus myrianthus* (Hassk.) Kurz	Cleistanthus	Leaves	2.00	Van der Ent et al., 2015
Phyllanthaceae	*Cleistanthus gracilis* Hook.f.	Cleistanthus	Leaves	189.00	Van der Ent and Reeves, 2015
Phyllanthaceae	*Glochidion angulatum* C.B.Rob.	Glochidion	Leaves	23.00	Van der Ent et al., 2015
Phyllanthaceae	*Glochidion arborescens* Blume	Glochidion	Leaves	272.00	Van der Ent et al., 2015
Phyllanthaceae	*Glochidion borneense* (Müll.Arg.) Boerl.	Glochidion	Leaves	21.00	Van der Ent et al., 2015
Phyllanthaceae	*Glochidion brunneum* Hook.f.	Glochidion	Leaves	38.00	Van der Ent et al., 2015
Phyllanthaceae	*Glochidion calospermum* Airy Shaw	Glochidion	Leaves	13.00	Van der Ent et al., 2015
Phyllanthaceae	*Glochidion* cf. *lanceisepalum*	Glochidion	Leaves	9.00	Van der Ent and Reeves, 2015
Phyllanthaceae	*Glochidion lanceilimbum* Merr.	Glochidion	Leaves	13.00	Van der Ent et al., 2015
Phyllanthaceae	*Glochidion littorale* Blume	Glochidion	Leaves	8.00	Van der Ent et al., 2015
Phyllanthaceae	*Glochidi on lutescens* Blume	Glochidion	Leaves	2.00	Van der Ent et al., 2015
Phyllanthaceae	*Glochidion mindorense* C.B.Rob.	Glochidion	Leaves	16.00	Van der Ent and Reeves, 2015
Phyllanthaceae	*Glochidion monostylum* Airy Shaw	Glochidion	Leaves	5.00	Van der Ent et al., 2015
Phyllanthaceae	*Glochidion rubrum* Blume	Glochidion	Leaves	14.00	Van der Ent et al., 2015
Phyllanthaceae	*Glochidion rubrum* Blume	Glochidion	Leaves	25.00	Van der Ent and Reeves, 2015
Phyllanthaceae	*Glochidion singaporense* Gage	Glochidion	Leaves	120.00	Van der Ent et al., 2015
Phyllanthaceae	*Glochidionobscurum* (Roxb. ex Willd.) Blume	Glochidion	Leaves	8.00	Van der Ent et al., 2015
Phyllanthaceae	*Glochidionsuperbum* Baill. ex Müll.Arg.	Great-leafed pin-flower Tree	Leaves	22.00	Van der Ent et al., 2015
Phyllanthaceae	*Phyllanthus amarus* Schumach. and Thonn.	Sleeping plan	Leaves	38.00	Van der Ent et al., 2015
Phyllanthaceae	*Phyllanthus balgooyi* Petra Hoffm. and A.J.M.Baker	Phyllanthus	Leaves	26.00	Van der Ent et al., 2015
Phyllanthaceae	*Phyllanthus balgooyi* Petra Hoffm. and A.J.M.Baker	Phyllanthus	Leaves	11.00	Van der Ent and Reeves, 2015
Phyllanthaceae	*Phyllanthus kinabaluicus* Airy Shaw	Phyllanthus	Leaves	109.00	Van der Ent et al., 2015
Phyllanthaceae	*Phyllanthus lamprophyllus* Müll.Arg.	Phyllanthus	Leaves	11.00	Van der Ent et al., 2015
Phyllanthaceae	*Phyllanthus myrtifolius* (Wight) Müll.Arg.	Mousetail plant	Stems, leaves and flowers	0.50	Van der Ent et al., 2015
Phyllanthaceae	*Phyllanthus pulcher* Wall. ex Müll.Arg.	Tropical leaf-flower	Leaves	31.00	Van der Ent et al., 2015
Phyllanthaceae	*Phyllanthus reticulatus* Poir.	Black-honey shrub	Leaves	5.00	Van der Ent et al., 2015
Phyllanthaceae	*Phyllanthus* sp.	Leaf-flower	Stems, leaves and flowers	2.40	Van der Ent et al., 2015
Phyllanthaceae	*Phyllanthus* sp. *nov.* "serinsim"	Phyllanthus	Leaves	158.00	Van der Ent et al., 2015
Phyllanthaceae	*Phyllanthus urinaria* L.	Chamber bitter	Leaves	12.00	Van der Ent et al., 2015
Pinaceae	*Picea abies* (L.) H.Karst.	Spruce	Needles	0.07	Reimann et al., 2001
Pinaceae	*Pinus sylvestris* L.	Pine	Needles	0.07	Reimann et al., 2001
Piperaceae	*Piper officinarum* C.DC.	Piper	Leaves	13.00	Van der Ent and Reeves, 2015
Poaceae	*Cymbopogan flexuosus* (Nees ex Steud.) Will.Watson	Lemongrass	Whole plants	0.30	Rajakaruna and Bohm, 2002
Poaceae	*Imperata cylindrica* (L.) Raeusch.	Alang grass	Leaves	0.03	Van Tran and Teherani, 1989
Poaceae	*Oryza sativa* L.	Rice	Seeds	0.04	Van Tran and Teherani, 1989
Poaceae	*Hordeum murinum* L.	Mouse Barley	Shoots	0.80	Koleli et al., 2015
Poaceae	*Aristida setacea* Retz.	Broom grass	Whole plants	14.60	Rajakaruna and Bohm, 2002
Polygonaceae	*Rumex obtusifolius* L.	Bitter dock	Shoots	0.80	Koleli et al., 2015
Rubiaceae	*Agrostemma cf. hameliifolium*	Corncockle	Leaves	16.00	Van der Ent and Reeves, 2015

(Continued)

TABLE 3 | Continued

Family	Species	Common name	Plant organ	Content (mg/kg)	References
Rubiaceae	*Canthium puberulum* Thwaites ex Hook.f.	Canthium	Stems, leaves and flowers	0.12	Rajakaruna and Bohm, 2002
Rubiaceae	*Canthium* sp.	Kidney-fruit Canthium	Stems, leaves and flowers	5.10	Rajakaruna and Bohm, 2002
Rubiaceae	*Morinda tinctoria* Roxb	Noni	Stems, leaves and flowers	0.70	Rajakaruna and Bohm, 2002
Rubiaceae	*Tarenna asiatica* (L.) Kuntze ex K.Schum	Tharana	Stems, leaves and flowers	1.10	Rajakaruna and Bohm, 2002
Rubiaceae	*Urophyllum* cf. *macrophyllum*	Urophyllum	Leaves	1.00	Van der Ent and Reeves, 2015
Salicaceae	*Salix* spp.	Willow	Leaves	1.76	Reimann et al., 2001
Solanaceae	*Physalis minima* L.	Cut-leaved ground-Cherry	Stems, leaves and flowers	3.90	Rajakaruna and Bohm, 2002
Taxodiaceae	*Taxodium distichum* (L.) Rich.	Bald cypress	leaves	4.60	McLeod and Ciravolo, 2007
Turneraceae	*Piriqueta duarteana* Urb.	Stripeseed	Leaves	11.00	Van der Ent and Reeves, 2015
Turneraceae	*Piriqueta* sp.	Stripeseed	Leaves	149.00	Van der Ent and Reeves, 2015
Turneraceae	*Turnera melochioides* A.St.-Hil. and Cambess.	Turnera	Leaves	143.00	Van der Ent and Reeves, 2015
Umbelliferae	*Conium maculatum* L.	Poison hemlock	Shoots	1.10	Koleli et al., 2015
Umbelliferae	*Sanicula europaea* L.	Sanicle, Wood sanicle	Shoots	5.40	Koleli et al., 2015
Violaceae	*Hybanthus enneaspermus* F.Muell.	Blue spade flower	Whole plants	17.00	Rajakaruna and Bohm, 2002

Plant Growth Improvement

Cobalt at low concentrations can also promote the growth of non-leguminous crops (**Table 4**). Co applied to a sandy soil at 1 mg/kg enhanced shoot and root dry weights of wheat by 33.7 and 35.8%, respectively compared with the control (Aery and Jagetiy, 2000), and the same Co rate applied to a sandy loam soil increased shoot and root dry weights of wheat by 27.9 and 39.6%, respectively, compared with the control. The yield and essential oil contents of parsley (*Petroselinum crispum*) increased considerably after the application of Co at 25 mg/kg soil (Helmy and Gad, 2002). Plant height, branch numbers, and fruit numbers as well as anthocyanin and flavonoids contents of *Hibiscus sabdariffa* significantly increased after application of Co at 20 and 40 mg/kg (Aziz et al., 2007). Application of 50, 100, 150, 200, and 250 mg/kg Co to corn plants showed that the root length, shoot height, and the number of cobs and seeds per plant increased when plants were applied with 50 mg/kg Co, but these parameters decreased with 100 mg/kg Co and above (Jaleel et al., 2009). Co applied at 10 mg/kg significantly enhanced the growth of two onion cultivars, bulb yields, bulb length, and bulb quality, such as nutrient and essential oil contents. Bulb diameter and bulb weights were much higher than the control treatment (Attia et al., 2014), but Co concentrations higher than 10 mg/kg significantly reduced the promotive effects.

Explanations for the improved growth of non-leguminous plants vary but can be summarized as follows: (1) enhanced tolerance to abiotic stresses, (2) activation of antioxidative enzymes, (3) substitution of active metals, and (4) hormesis. Application of Co has been reported to alleviate drought, salt, heavy metal stresses, thus plant growth is not adversely affected. Co has been reported to suppress plant uptake of cadmium (Chmielowska-Bak et al., 2014). Co application increased free proline accumulation, which counteracted the salt stress. In general, abiotic stresses often cause plant imbalance between production and accumulation of reactive oxygen species (ROS), including superoxide anion (O_2^-), hydroxyl radical (OH^-), and hydrogen peroxide (H_2O_2) (Sachdev et al., 2021). ROS can activate the antioxidant system of the plant, thus minimizing the damages (Tewari et al., 2002; Choudhury et al., 2017). The antioxidant system includes enzymatic antioxidants: ascorbate peroxidase, catalase, dehydroascorbate reductase, general peroxidases, glutathione reductase, monodehydroascorbate reductase, and superoxide dismutase as well as non-enzymatic antioxidants, mainly ascorbic acid, α-tocopherol, carotenoids, reduced glutathione, plastoquinone/ubiquinone, and flavonoids (García-Caparrós et al., 2020). The action of the antioxidant system could be the first line of defense against the adverse effects. Therefore, it is not surprising to notice increased activities of ascorbate peroxidase, catalase, peroxidase, and superoxide dismutase (Hasanuzzaman et al., 2020). Co applied at appropriate concentrations can activate antioxidative enzymes, thus reducing ROS-caused damage. As discussed previously, Co may substitute other nutrient elements when such nutrients have limited availability. Baxter et al. (2008) showed that when *Arabidopsis* plants are grown under a low Fe concentration, the shoot concentration of Co increased, which was concomitant with the increased expression of Fe transporter IRT1. Additionally, Co contribution to hormesis has been proposed (Shahid et al., 2020). Due to the limited research on Co to date, these explanations may not be on target and incomplete. Our proposition is that the application of the appropriate amount of Co may stimulate rhizosphere bacteria (either symbiotic, endophytic, or associated ones) to fix N_2, increase soil N, and enhance plant growth. Concomitantly,

TABLE 4 | Effects of cobalt application on plant performance.

Species (common name)	Co application	Effects on plants	References
Actinidia chinensis Planch. cv. Hayward) (Kiwi)	Fruit was treated with 1 mM Co^{2+} solution	Inhibited ACC activity in ethylene biosynthesis	Hyodo and Fukasawa, 1985
Adiantum raddianum C. Presl (Delta maidenhair fern)	Cut green (frond) was treated with 1 mM $Co(NO_3)_2$ solution	Prolonged vase life of frond from 3 to 8.2 days	Fujino and Reid, 1983
Arachis hypogaea L. (Peanut)	Seeds were treated with $Co(NO_3)_2$ at 500 mg/kg seed and followed by two foliar sprays of cobalt nitrate at 500 mg/L before and after flowering	Significantly increased plant height, leaf number, pod yield, shelling percentage, harvest index, and total dry matter	Raj, 1987
Arachis hypogaea L. (Peanut)	$CoSO_4$ was mixed with soil at 0.21 kg/ha	Resulted in 10% higher kernel yield compared with control (without Co application)	Basu and Bhadoria, 2008
Arachis hypogaea L. (Peanut)	Seedlings of groundnut at the third true leaf stage were irrigated once with $CoSO_4$ at 2, 4, 6, and 8 mg/L, respectively	Increased plant height, number of branches and leaf number, leaf area index, root length, shoot and root biomass as well as pods numbers, pods weight, oil yield, total proteins, total carbohydrates, total soluble sugars, and total soluble solids	Gad, 2012a
Argyranthemum sp. (Argyranthemum)	Cut flowers preserved in a solution containing 2 mM Co	Increased flower longevity by more than 5 days compared with control (treated with distilled water)	Kazemi, 2012
Avena sativa L. var. 'Condor' (Common oat)	Seeds were treated with 0.001% $CoSO_4$ solution for 24 h, dried at room temperature for 3 days, then sown	Increased grain yields	Saric and Saciragic, 1969
Beta vulgaris L. (Red beet)	$CoSO_4$ was mixed with soil at 2.5, 5.0, 7.5, 10.0 and 12.5 mg/kg, respectively	Increased plant growth, root yield, mineral elements as well as protein, carbohydrate, vitamin C, sucrose, and glucose contents	Gad and Kandil, 2009
Cajanus cajan (L.) Millsp. (Pigeon pea)	Seeds were treated with $Co(NO_3)_2$ at 500 mg/kg seed	Increased chlorophyll content, crop growth rate, relative growth rate, and net assimilation rate, resulting in increased plant height, number of branches, leaves, total dry matter, and yield	Raj, 1987
Cariandrum sativum L. (Coriander)	Irrigated in the form of $CoSO_4$ 12.5 mg/L once	Increased coriander herb yield, mineral composition (except Fe), chemical constituents as well as essential oil components	Gad, 2012b
Cicer arietinum L. cv GG2 (Chickpea)	Chickpea seedlings at the three-leaf stage were fertigated with $CoCl_2$ at 100 g/ha	Increased protein content and yield by 5.08 and 22.36%, respectively	Rod et al., 2019
Cucumis sativus L. cv. (Cucumber)	Plants were treated with $Co(NO_3)_2$ solutions ranging from 1 to 500 ?M	Promoted hypocotyl elongation	Grover and Purves, 1976
Cucurbita pepo cv. Eskandarany (summer squash)	Seeds in continuously aerated solutions of 0.25, 0.50, and 1.00 mg/L Co^{2+} for 48 h before sowing	Strongly increased plant growth, femaleness, and fruit yield compared with those of water- (control) or 0.5 mM AOA (aminooxyacetic acid)-soaked seed	Atta-Aly, 1998
Allium cepa L.) cv. Giza 6 Mohassan (Onion)	Co mixed with sand and petmoss in 10.0 mg/kg soil	Significantly promote nutrients and essential oils content along with bulb length, bulb diameter and weight	Attia et al., 2014
Dianthus caryophyllus L. cv. "Harlem" (Carnation)	Cut flowers were preserved in $CoCl_2$ solutions at 50, 75, and 100 mg/L, respectively	Suppressed ethylene production and prolonged vase life	Jamali and Rahemi, 2011
Gladiolus grandiflorus Hort. cv. Borrega Roja (Gladiolus)	Plants were treated with solution containing 0.3 mM $CoCl_2$	Increased stem and leaf N content, chlorophyll concentrations, leaf and stem dry weights, and improved stem absorption of water	Trejo-Téllez et al., 2014
Glycine max (L.) Merr. (Soybean)	Plants were grown in nutrient solutions containing 1 and 5 μg/L cobaltous chloride, inoculated with rhizobia in the absence of nitrogen	No N deficiency symptoms, and increased dry weight by 52% compared with the control treatments	Ahmed and Evans, 1959
Glycine max (L.) Merr. (Soybean)	Plants were grown in soil mixed with finely powdered ($CoCl_2$) at the concentration of 50 mg/kg	Increased root and shoot length, leaf area, dry weight, yield, and yield components	Jayakumar et al., 2009
Glycine max (L.) Merr. (Soybean)	Seeds were sown in soil mixed with finely powdered ($CoCl_2$) at 50 mg/kg	Increased yield parameters, leaf area, shoot length, total dry weight as well as total phenol percentage	Vijayarengan et al., 2009

(Continued)

TABLE 4 | Continued

Species (common name)	Co application	Effects on plants	References
Hevea brasiliensis (Willd. ex A.Juss.) Müll.Arg. (Rubber)	Plants were grown in Co free sand supplemented with 0.005 mg/kg Co	Increased plant height, stem diameter, and plant dry weight	Bolle-Jones and Mallikarjuneswara, 1957
Hibiscus sabdariffa L. (Roselle)	Seedlings irrigated once with Co at concentrations of 20 and 40 mg/L	Increased plant height, branch numbers, and fruit numbers as well as anthocyanin and flavonoids contents	Aziz et al., 2007
Ipomoea batatas L. (Sweet potato)	Seedlings were irrigated with $CoSO_4$ once at concentrations of 5.0, 7.5, 10.0 mg/L	Increased growth and yield parameters, nutrient elements (except for Fe) and the chemical contents	Gad and Kandil, 2008
Lilium spp. cv. Star Gazer Lily	Cut flowers were preserved in a solution containing 0.1 mM Co and 4% sucrose with a pH of 3.5	Extended vase life	Mandujano-Piña et al., 2012
Lilium spp. cv. Prato (Lily)	Cut flowers were treated with 2 mM $CoCl_2$	Increased vase life from seven to 9 days	Kazemi and Ameri, 2012
Lilium spp. cv. Star Fighter (Lily)	Cut flowers were preserved in solutions containing 0.1, 0.2 mM Co and 4% sucrose with a pH of 3.5	Extended the lifespan of flowers	Mandujano-Piña et al., 2012
Lupinus angustifolius cv. Uniharvest (Blue lupin)	Supplemented 0.9 mg $CoSO_4.7H_2O$ to each pot containing 6 kg soil	Increased plant growth and N content	Robson et al., 1979
Lycopersicon esculantum Mill. (Tomato)	Ten seeds were sown in a pot containing 3 kg air-dried soil mixed with $CoCl_2$ at 50 mg/kg, seedlings were thinned to 3	Increased the content of phosphorus, potassium, copper, iron, manganese, and zinc in plants	Jayakumar et al., 2013
Lycopersicon esculentum Mill. (Tomato)	Treated with simple solutions (1 mM $CoCl_2$) plus wetting agent	Delayed gravitropic responses of treated plants	Wheeler and Salisbury, 1981
Malus domestica Borkh. (Apple)	Apple fruit was immersed in a solution containing 1 mM $CoCl_2$ for 1 min	Enhanced activity of protein inhibitor of polygalacturonase (PIPG) and provided better conservation of apple fruit consistency during storage	Bulantseva et al., 2001
Mangifera indica L) cv. Langra (Mango)	Foliar spray with $CoSO_4$ at 1,000 mg/L prior to flower bud differentiation in the first week of October	Reduced floral malformation by 65% and increased the fruit yield by 35%	Singh et al., 1994
Matteuccia struthiopteris (L.) Todaro	Supplemented with various concentrations Co^{2+} ranging from 0.1 to 1 mM	Inhibited IAA-induced ethylene production in sporophytes	Tittle, 1987
Phaseolus aureus Roxb. cv. T-44 (Mung bean)	Plants were treated with 50 μM Co in sand culture	Improved plant growth by increasing leaf, stem, and total dry weight compared with the controls	Tewari et al., 2002
Phaseolus vulgaris L. Cv. "Burpees Stringless" (Common bean)	Two cycles of pre-sowing soaking and drying treatments by a 1 mg/L of $Co(NO_3)_2$ solution	Increased yield and N content over untreated and distilled water-soaked seeds by 48 and 150%, respectively	Mohandas, 1985
Pisum sativum L. (Garden pea)	Seeds sowed in pot containing 10 kg soil mixed with $CoSO_4$ at 8 mg/kg	Enhanced N_2 fixation process, increased plant N content, and reduced inorganic and organic N fertilizer application by 75 and 33.3%, respectively	Gad, 2006
Pisum sativum L. (garden pea)	Pots filled with 10 kg soil with Co at 2 mg/kg	Increased grain yield by 48.4%	Singh et al., 2012
Polianthes tuberosa L. (Tuberose)	Flower stems were preserved in a solution containing 300 mg/L cobalt chloride	Extended the vase life and enhanced water uptake in cut tuberose flowers	Mehrafarin et al., 2021
Pteridium aquilinum (L.) Kuhn var. *latiusculum* (Desv.) Underw. ex Heller (Western bracken fern)	Stems of cut green were preserved in solutions containing 0.1 to 1.0 mM Co	Inhibited IAA-induced ethylene production and prolonged vase life	Tittle, 1987
Ricinus communis L. (Castor bean)	Plants treated with a 1 mM $CoCl_2$ solution supplemented with a wetting agent	Delayed gravitropic responses of treated plants	Wheeler and Salisbury, 1981
Rosa hybrida "Samantha" (Rose)	Cut flowers were preserved in solutions containing 0.5, 1.0, 1.5, and 2.0 mM $CoCl_2$, respectively	Increased leaf diffusive resistance, inhibited xylem blockage, maintained water flow and uptake, and increased the vase life	Reddy, 1988
Rosa hybrida "Samantha" (Rose)	Cut flowers were preserved in solutions containing 0.5, 1.0, 1.5, and 2.0 mM $Co(NO_3)_2$, respectively	Highly delayed or prevented the development of bent-neck and increased water uptake of cut flower	Murr et al., 1979
Rosa spp.cv. Red one (Rose)	Cut flowers treated with 100 and 200 mg/L Co solutions	Inhibited vascular blockage in the stem of rose and maintained a high-water flow rate, leading to significantly water uptake by cut flowers	Aslmoshtaghi, 2014

(Continued)

TABLE 4 | Continued

Species (common name)	Co application	Effects on plants	References
Triticum aestivum L. (Wheat)	Seeds were sowed in polythene-lined pots containing 4 kg of soil mixed with 1 mg/kg $CoSO_4$	Enhanced plant growth after 45 days of application	Aery and Jagetiy, 2000
Vicia faba L. (Fava bean)	Seedlings at six-leaf stage were planted in pot containing soil mixed cobalt at 20 and 40 mg/kg, respectively	Improved photosynthesis and plant growth	Wang et al., 2015
Vigna anguiculata subsp. *alba* (G. Don) Pasquet (Cowpea)	Seedlings were applied with Co at 4, 6, and 8 mg/kg	Enhanced plant growth and yield and induced nodulation	Gad and Hassan, 2013
Xanthium strumarium L. (Cocklebur)	Plants treated with a 1 mM $CoCl_2$ solution supplemented with a wetting agent	Delayed gravitropic responses of treated plants	Wheeler and Salisbury, 1981
Zea mays L. (Maize)	Seeds sowed in pots containing 13 kg soil mixed with Co at 50 mg/kg	Increased seedling growth, photosynthetic pigments, and leaf chlorophyll contents	Jaleel et al., 2009

Co enzymes may be triggered to conduct proper biochemical and physiological activities, such as carbonate dehydratase may enhance photosynthesis and Co-peroxidase may activate the enzymatic antioxidant system. As a result, healthy growing plants would take up more nutrients from the soil and improve their growth and overall stress tolerance.

Other Performance Enhancement

Cobalt has been shown to have other beneficial effects on plants. Co as a component of preservative solutions can improve the postharvest quality of floriculture crops by prolonging the vase life of cut flowers. Cut fronds of Delta maidenhair fern (*Adiantum raddianum*) placed in deionized water became wilted in just 3 days because of the vascular blockage at the basal end of the petiole. The wilting, however, could be delayed for up to 8 days by adding 1 mM Co as $Co(NO_3)_2$ to the water (Fujino and Reid, 1983). The delay of senescence is attributed to the antibacterial activity of Co (Van Doorn et al., 1991). Co addition to preservative solutions increased leaf diffusive resistance, reduced xylem blockage, sustained water flow and uptake, and prolonged vase life of cut flowers of *Rosa hybrida* "Samantha". Reddy (1988) suggested that partial closure of stomata by Co was responsible for reducing the water loss/water uptake ratio, and thereby maintaining a higher water potential in the cut roses. Co was also reported to slow the senescence process in harvested lettuce (Tosh et al., 1979). Co^{3+} has been reported to form Co-complexes, which have antiviral activities (Chang et al., 2010). In addition to antibacterial and antiviral activities, Co shows inhibitory activity to 1-aminocyclopropane-1-carboxylic acid (ACC) oxidase. Ethylene is synthesized from amino acid methionine by two key enzymes, ACC synthase, and ACC oxidase. Co can block the conversion of ACC to ethylene by inhibiting ACC oxidase activity in the ethylene biosynthesis pathway (Lau and Yang, 1976; Serek et al., 2006), thus increasing the vase life of cut flowers.

COBALT DEFICIENCY OCCURS IN PLANTS

Cobalt deficiency does occur in plants. Its deficiency symptoms include leaf chlorosis and necrosis, growth retardation, and reduced crop yield, resembling N-deficiency in plants (Liu, 1998). Co deficient legumes have reduced plant size, smaller and pale-yellow leaves, and smaller pods compared with non-deficiency plants. Root growth is also affected by exhibiting an overall reduction of root volume and root lengths. Nodule size and numbers are less abundant than the plants without Co deficiency. Co deficiency causes reduced synthesis of methionine, thus limiting protein synthesis and contributing to the smaller-sized bacteroids (Marschner, 2011). Sweet lupin is particularly sensitive to Co deficiency (Robson et al., 1979). In field-grown lupins, Co deficiency reduced bacteroid number per gram of nodule (Chatel et al., 1978) and affected nodule development and function at different levels (Dilworth et al., 1979). Co deficiency in legumes can be assessed by analysis of Co contents in shoots. In general, deficient symptom appears when shoot Co falls in a range from 0.04 (Ozanne et al., 1963) to 0.02 mg/kg based on dry weight (Robson et al., 1979). To correct Co deficiency in leguminous crops, application of Co in a range of 1.8 to 145.6 g per hectare was reported (Havlin et al., 2013).

Cobalt deficiency also occurs in non-leguminous plants. Co deficiency causes growth retardation in rubber trees and tomato plants (Wilson and Nicholas, 1967). Symptoms of Co deficiency in corn and wheat showed leaf chlorosis and reduced growth (Wilson and Nicholas, 1967). Low leaves may become necrotic, root systems are reduced with decreased number of N_2 fixing bacteria. Grasses with low contents of Co can result in Co deficiency of sheep and cattle. For countries, like South Australia, Sierra Leone, Malta, New Zealand, and Finland, where soils have low Co contents (Sillanpaa and Jansson, 1992), application of Co could improve forage grass growth and enrich tissue Co content. Thus, the feeding of ruminants with healthy grass can reduce Co deficiency (Lee, 1951; Dewey et al., 1958). Due to low Co concentrations in plants, Co deficiency in grazing animals may occur, which can be corrected by mixing Co salts with fertilizers or sand carriers to broadcast it over grazed pastures.

COBALT TOXICITY IN PLANTS

Cobalt at high concentrations causes cytotoxicity and phytotoxicity in plants, which is similar to Cu, Ni, and

Zn. Cytotoxicity is the inhibition of mitosis and damage of chromosomes, and disruption of the endoplasmic reticulum of root tip cells (Rauser, 1981; Smith and Carson, 1981; Akeel and Jahan, 2020). Phytotoxicity varies depending on plant species and the concentration of Co in plant organs. Leguminous plants generally exhibit chlorosis or pale-white color on young leaves, and tomatoes show either interveinal chlorosis or diffused chlorosis on young leaves (Akeel and Jahan, 2020).

Cobalt toxicity to plants is uncommon in natural soils, but it happens when plants grow in Co contaminated soils. Soil contamination by Co is mainly from mining and smelting activities, disposal of sewage sludge, and the use of chemical fertilizers (Hamilton, 1994). As discussed above, plants can control Co absorption, transport, and distribution. However, when Co in contaminated soils becomes highly available, Co may gain a competitive advantage over Fe, resulting in more Co being absorbed than Fe through IRT1. With increasing concentrations of Co inside cells, FPN2 may not be able to effectively sequester Co into the vacuole, resulting in more Co to transport from roots to shoots. Li et al. (2020) showed that Co concentrations in shoots of barley, oilseed rape (*Brassica napus*), and tomato were linearly correlated with the soil solution Co. As a result, excessive Co in shoots may initially cause oxidative stress, resulting in increased anti-oxidative enzyme activities (Tewari et al., 2002). As the stress progresses, Co may compete with Fe or Mg in the chloroplast by decreasing chlorophyll content (Lwalaba et al., 2017), which causes Fe deficiency with newly growing leaves to be yellowish in color. As reported by Sree et al. (2015), Co is able to inhibit the activity of enzymes involved in the biosynthesis of chlorophyll intermediates, like 5-aminolevulinic acid and protoporphyrin, which will reduce net photosynthetic activities. Co also adversely affects the translocation of P, S, Cu, Mn, and Zn from roots to shoots (Chatterjee and Chatterjee, 2000). All these factors, acting together, can result in phytotoxicity and significantly reduce plant growth.

Different plants show different abilities to tolerate Co. Oat (*Avena sativa*) plants were adversely affected when grown in a soil solution containing 0.14 mg/L Co (Anderson et al., 1973). Rice (*Oryza sativa*) plants would develop toxic symptoms when grown in soils with Co ranging from 25 and 50 mg/kg (Kitagishi and Yamane, 1981). The contents of Co could be used for predicting the development of toxicity (Akeel and Jahan, 2020). Toxic symptoms occurred in bush beans when tissue Co contents ranged from 43 to 142 mg/kg (Wallace et al., 1977); similarly, 6 mg/kg in barley seedlings (Davis et al., 1978), and 19 to 32 mg/kg in Sudan grass (Gough et al., 1979). In general, tissue Co contents between 30 and 40 mg/kg are considered critical levels for the potential development of Co toxicity (Macnicol and Beckett, 1985). However, due to evolutionary adaptation, Co hyperaccumulators do not develop toxic symptoms at this concentration level. Co contents in leaves of *Rinorea* cf. *bengalensis* can be 1,200 mg/kg (Paul et al., 2020), and *Glochidion* cf. *sericeum* can accumulate 1,500 mg/kg Co (Van der Ent et al., 2018). Co hyperaccumulators are not the focus of this article. The reader is referred to publications by Brooks (1977), Brooks et al. (1977, 1980), Baker (1981, 1987), Lange et al. (2017), and Yamaguchi et al. (2019) for more information.

CONCLUSIONS AND FUTURE PERSPECTIVES

Cobalt in soils ranges from 15 to 25 mg/kg, wherein plant roots can absorb Co from soils and transport absorbed Co from roots to shoots in a controlled manner. Co concentrations in shoots vary with plant species but are comparable to those of essential elements of Cu, Ni, and Zn. Co was well-documented as a constituent of cobalamin, which is required by symbiotic, endophytic, and associated bacteria in the fixation of N_2. Biological N fixation contributed significantly to the production of economically important crops, including beans, soybeans, rice, corn, barley, wheat, and sugarcane. The current view of plant-microbe association as a phytomicrobiome resulted from millions of years of co-evolution. The coevolution between plants and N_2 fixing bacteria should remind us of the critical role Co plays and its potential essentiality to plant growth and development. Additionally, plants must have Co enzymes or proteins that are specifically responsible for Co metabolism. Due to its similar properties to other transition elements, its biological roles in plants have been largely ignored and simply attributed to its ability to substitute for those elements.

Further research is warranted to (1) identify specific roles of Co plays in diazotrophs, with an emphasis on endophytic and associated bacteria, (2) ascertain Co-containing enzymes and proteins that are implicated in metabolisms of both lower and higher plants, (3) determine the interactions of Co with other transition metals in the regulation of enzymatic activities, (4) recognize Co as an essential micronutrient for plant growth, and (5) develop nutrient management programs by incorporating a group of particular N fixing bacteria with the appropriate amount of Co as plant-specific fertilizers for improving crop production. With the advance in omics, these tasks should be accomplished in the near future. The recognition of Co as an essential micronutrient would enrich our understanding of plant mineral nutrition and enhance crop productivity.

AUTHOR CONTRIBUTIONS

XH, XW, and JC wrote the manuscript. JL prepared figures. All authors contributed to the acquisition and interpretation of available literature and the conception of the work, revised the manuscript, and approved this final version.

FUNDING

This study was supported in part by the Students Innovation and Entrepreneurship Training Program at Zhongkai University of Agriculture and Engineering with grant number 202111347007 and the General Project of the Natural Science Foundation of Fujian Province with grant number 2020J01867.

ACKNOWLEDGMENTS

The authors would like to thank Ms. Terri A. Mellich for critical review of this manuscript.

REFERENCES

Aasfar, A., Bargaz, A., Yaakoubi, K., Hilali, A., Bennis, I., Zeroual, Y., et al. (2021). Nitrogen fixing azotobacter species as potential soil biological enhancers for crop nutrition and yield Stability. *Front. Microbiol.* 12:628379. doi: 10.3389/fmicb.2021.628379

Abdel-Rahman, H., Salem, A., Moustafa, M. M., and El-Garhy, H. A. (2017). A novice *Achromobacter* sp. EMCC1936 strain acts as a plant-growth-promoting agent. *Acta Physiol. Plant.* 39:61. doi: 10.1007/s11738-017-2360-6

Adams, D. G., Bergman, B., Nierzwicki-Bauer, S. A., Duggan, P. S., Rai, A. N., and Schußler, A. (2013). "Cyanobacteria–bryophyte symbioses," in *The Prokaryotes*, eds M. Dworkin, S. Falkow, E. Rosenberg, K. Schleifer, and E. Stackebrandt (Berlin; Heidelberg: Springer), 359–400.

Aery, N. C., and Jagetiy, B. L. (2000). Effect of cobalt treatments on dry matter production of wheat and DTPA extractable cobalt content in soils. *Commun Soil Sci. Plant Anal.* 31, 1275–1286. doi: 10.1080/00103620009370512

Ahmed, S., and Evans, H. J. (1959). Effect of Cobalt on growth of soybeans in the absence of supplied nitrogen. *Biochem. Biophys. Res. Comm.* 1, 271–275. doi: 10.1016/0006-291X(59)90036-1

Ahmed, S., and Evans, H. J. (1960). The plants grown under symbiotic conditions. *Proc. Natl. Acad. Sci. U.S.A.* 47, 24–36. doi: 10.1073/pnas.47.1.24

Akeel, A., and Jahan, A. (2020). "Role of cobalt in plants: its stress and alleviation," in *Contaminants in Agriculture*, eds M. Naeem, A. Ansari, and S. Gill (Cham: Springer), 339–352.

Anderson, A., Meyer, D., and Mayer, F. (1973). Heavy metal toxicities: levels of nickel, cobalt and chromium in the soil and plants associated with visual symptoms and variation in growth of an oat crop. *Aust. J. Agric. Res.* 24, 557–571. doi: 10.1071/AR9730557

Andić, B., Dragićević, S., Stešević, D., Jančić, D., and Krivokapić, S. (2015). Comparative analysis of trace elements in the mosses – *Bryum argenteum* Hedw. and *Hypnum cupressiforme* Hedw. in Podgorica (Montenegro). *J. Mater. Environ. Sci.* 6, 333–342.

Andrews, M., and Andrews, M. E. (2017). Specificity in legume-rhizobia symbioses. *Intl. J. Mol. Sci.* 18:705. doi: 10.3390/ijms18040705

Antonyuk, L. P., Smirnova, V. E., Kamnev, A. A., Serebrennikova, O. B., Vanoni, M. A., Zanetti, G., et al. (2001). Influence of divalent cations on the catalytic properties and secondary structure of unadenylylated glutamine synthetase from *Azospirillum brasilense*. *Biometals* 14, 13–22. doi: 10.1023/A:1016640522299

Arnon, D. I., and Stout, P. R. (1939). The essentiality of certain elements in minute quantity for plants with special reference to copper. *Plant Physiol.* 14, 371–375. doi: 10.1104/pp.14.2.371

Aslmoshtaghi, E. (2014). Effects of daffodil flowers and cobalt chloride on vase life of cut rose. *J. Chem. Health Risks* 4, 1–6.

Atta-Aly, M. A. (1998). Soaking summer squash seeds in sow concentrations of cobalt solution before sowing increased plant growth, femaleness, and fruit yield via increasing plant ethylene Level. *J. Plant Growth Regul.* 17, 25–32 doi: 10.1007/PL00007008

Attia, S. A. A., Gad, N., and Abdel-Rahman., H.M. (2014). Effect of cobalt on growth, yield and production quality with mitotic and meiotic divisions in two onion cultivars. *Curr. Sci. Int*. 3, 122–131.

Aziz, E. E., Gad, N., and Nadia, M. B. (2007). Effect of cobalt and nickel on plant growth, yield and flavonoid content of *Hibiscus sabdariffa* L. *Aust. J. Basic Appl. Sci.* 1, 73–78.

Bageshwar, U. K., Srivastava, M., Pardha-Saradhi, P., Paul, S., Gothandapani, S., Jaat, R. S., et al. (2017). An environmentally friendly engineered *Azotobacter* strain that replaces a substantial amount of urea fertilizer while sustaining the same wheat yield. *Appl. Environ. Microbiol.* 83:e00590-17. doi: 10.1128/AEM.00590-17

Baker, A. (1981). Accumulators and excluders-strategies in the response of plants to heavy metals. *J. Plant Nutr.* 3, 643–654. doi: 10.1080/01904168109362867

Baker, A. (1987). Metal tolerance. *New Phytol.* 106, 93–111. doi: 10.1111/j.1469-8137.1987.tb04685.x

Baker, A. J. M., Brooks, R. R., Pease, A. J., and Malaisse, F. (1983). Studies on Cu and cobalt tolerance in three closely related taxa within the genus *Silene* L. (Caryophyllaceae) from Zare. *Plant Soil* 73, 377–385. doi: 10.1007/BF02184314

Bakkaus, E., Gouget, B., Gallien, J. P., Khodja, H., Carrot, F., Morel, J. L., et al. (2005). Concentration and distribution of cobalt in higher plants: the use of micro-PIXE spectroscopy. *Nucl. Instrum. Methods Phys. Res. Sect. B* 231, 350–356. doi: 10.1016/j.nimb.2005.01.082

Barsanti, L., and Gualtieri, P. (2006). *Algae: Anatomy, Biochemistry and Biotechnology*. Boca Raton, FL: Taylor and Francis Group.

Bartolo, W., and Macey, M. (1989). Cobalt requirement in tissue culture of three species: *Brassica oleracea* L., *Passifora mollissima* Bailey, and *Saintpaulia ioantha* Wendl. *J. Hort. Sci.* 64, 643–647. doi: 10.1080/14620316.1989.11516003

Basu, M., and Bhadoria, P. B. S. (2008). Performance of groundnut under nitrogen fixing and phosphorous microbial inoculates with different levels of cobalt in alluvial soils of eastern India. *Agron. Res.* 6, 15–25.

Baxter, I. R., Vitek, O., Lahner, B., Muthukumar, B., Borghi, M., Morrissey, J., et al. (2008). The leaf ionome as a multivariable system to detect a plant's physiological status. *Proc. Natl. Acad. Sci. U.S.A.* 105, 12081–12086. doi: 10.1073/pnas.0804175105

Bennett, B. (2010). "EPR of cobalt-substituted zinc enzymes," in *Metals in Biology: Application of High Resolution EPR to Metalloenzymes*, ed G. R. Hanson (New York, NY: Springer), 345–370. doi: 10.1007/978-1-4419-1139-1

Bertalan, M., Albano, R., de Pádua, V., Rouws, L., Rojas, C., Hemerly, A., et al. (2009). Complete genome sequence of the sugarcane nitrogen-fixing endophyte *Gluconacetobacter diazotrophicus* Pal5. *BMC Genomics* 10:450. doi: 10.1186/1471-2164-10-450

Bertrand, G. (1912). *On the Role of Trace Substances in Agriculture*. Concord, NH: Rumford.

Bhosale, S., Rao, M., and Deshpande, V. (1996). Molecular and industrial aspects of glucose isomerase. *Microbiol. Rev.* 60, 280–300.

Boddey, R. M., and Dobereiner, J. (1988). Nitrogen fixation associated with grasses and cereals: recent results and perspectives for future research. *Plant Soil* 108, 53–65. doi: 10.1007/BF02370099

Böhme, H. (1998). Regulation of nitrogen fixation in heterocyst-forming cyanobacteria. *Trends Plant Sci.* 3. doi: 10.1016/S1360-1385(98)01290-4

Bolle-Jones, E., and Mallikarjuneswara, V. (1957). A beneficial effect of Co on the growth of the rubber plant. *Nature* 179, 738–739. doi: 10.1038/179738a0

Bridwell-Rabb, J., and Drennan, C. (2017). Vitamin B12 in the spotlight again. *Curr. Opin. Chem. Biol.* 37, 63–70. doi: 10.1016/j.cbpa.2017.01.013

Brooks, R. R. (1977). Copper and cobalt uptake by *Haumaniastrum* species. *Plant Soil* 48, 541–544. doi: 10.1007/BF02187261

Brooks, R. R. (1998). *Plants that Hyperaccumulate Heavy, Metals: Their Role in Phytoremediation, Microbiology, Archaeology, Mineral Exploration and Phytomining*. Oxon: CAB International.

Brooks, R. R., McCleave, J. A., and Schofield, E. K. (1977). Cobalt and nickel uptake by the Nyssaceae. *Taxon* 26, 197–201. doi: 10.2307/1220551

Brooks, R. R., Reeves, R. D., Morrison, R. S., and MalaJsse, F. (1980). Hyperaccumulation of copper and cobalt: a review. *Bull. Soc. Roy. Bot. Belg.* 113, 166–172.

Brylinski, M., and Skolnick, J. (2011). FINDSITE-metal: integrating evolutionary information and machine learning for structure-based metal binding site prediction at the proteome level. *Proteins* 79, 735–751. doi: 10.1002/prot.22913

Bulantseva, E. A., Glinka, E. M., Protsenko, M. A., and Sal'kova, E. G. (2001). A protein inhibitor of polygalacturonase in apple fruits treated with aminoethoxyvinylglycine and cobalt chloride. *Prikl. Biokhim. Mikrobiol.* 37, 100–104. doi: 10.1023/A:1002808912247

Carpenter, K. J. (2004). *The Nobel Prize and the Discovery of Vitamins*. NobelPrize.org. Nobel Prize Outreach AB2021. Stockholm. Available online at: https://www.nobelprize.org/prizes/themes/the-nobel-prize-and-the-discovery-of-vitamins (accessed August 28, 2021).

Carter, E. L., Flugga, N., Boer, J. L., Mulrooney, S. B., and Hausinger, R. P. (2009). Interplay of metal ions and urease. *Metallomics* 1, 207–221. doi: 10.1039/b903311d

Cavet, J. S., Borrelly, G. P., and Robinson, N. J. (2003). Zn, Cu and Co in cyanobacteria: selective control of metal availability. *FEMS Microbiol. Rev.* 27, 165–181. doi: 10.1016/S0168-6445(03)00050-0

Chang, A. C. G., Chen, T., Li, N., and Duan, J. (2019). Perspectives on endosymbiosis in coralloid roots: association of cycads and cyanobacteria. *Front. Microbiol.* 10:1888. doi: 10.3389/fmicb.2019.01888

Chang, E., Simmers, C., and Knight, D. (2010). Cobalt complexes as antiviral and antibacterial agents. *Pharmaceuticals* 3, 1711–1728. doi: 10.3390/ph3061711

Chatel, D. L., Robson, A. D., Gartrell, J. W., and Dilworth, M. J. (1978). The effect of inoculation on cobalt application on the growth of and nitrogen fixation of sweet lupins. *Aust. J. Agric. Res.* 29, 1191–1202. doi: 10.1071/AR9781191

Chatterjee, J., and Chatterjee, C. (2000). Phytotoxicity of cobalt, chromium and copper in caulifower. *Environ. Pollut.* 109, 69–74. doi: 10.1016/S0269-7491(99)00238-9

Chen, J., Zhou, J., and Goldsbrough, P. (1997). Characterization of phytochelatin synthase from tomato. *Physiol. Plant* 101, 165–192. doi: 10.1111/j.1399-3054.1997.tb01833.x

Cheng, Y. S., Yan, Y. B., and Liu, J. Y. (2005). Spectroscopic characterization of metal bound phytochelatin analogue (Glu-Cys)(4)-Gly. *J. Inorg. Biochem.* 99, 1952–1962. doi: 10.1016/j.jinorgbio.2005.06.016

Chmielowska-Bak, J., Lefèvre, I., Lutts, S., Kulik, A., and Deckert, J. (2014). Effect of cobalt chloride on soybean seedlings subjected to cadmium stress. *Acta Soc. Bot. Pol.* 83, 201–207. doi: 10.5586/asbp.2014.027

Choudhury, A., and Kennedy, I. (2004). Prospects and potentials for systems of biological nitrogen fixation in sustainable rice production. *Biol. Fertil. Soils* 39, 219–227. doi: 10.1007/s00374-003-0706-2

Choudhury, F. K., Rivero, R. M., Blumwald, E., and Mittler, R. (2017). Reactive oxygen species, abiotic stress and stress combination. *Plant J.* 90, 856–867. doi: 10.1111/tpj.13299

Ciotea, D., Ungureanu, E., Mustatea, G., and Popa, M. E. (2021). Incidence of lead, cadmium, chromium, nickel and cobalt in basil, rosemary and peppermint seasonings from Romanian market. *Bull. Univ. Agric. Sci. Vet. Med. Cluj-Napoca. Food Sci. Technol.* 78, 19–32. doi: 10.15835/buasvmcn-fst:2021.0002

Collins, R. N., Bakkaus, E., Carrière, M., Khodja, H., Proux, O. and, Morel, J. L., et al. (2010). Uptake, localization, and speciation of cobalt in *Triticum aestivum* L. (wheat) and *Lycopersicon esculentum* M. (tomato). *Environ. Sci. Technol.* 44, 2904–2910. doi: 10.1021/es903485h

Compant, S., Kaplan, H., Sessitsch, A., Nowak, J., Ait Barka, E., and Clément, C. (2008). Endophytic colonization of *Vitis vinifera* L. by *Burkholderia phytofirmans* strain PsJN: from the rhizosphere to inflorescence tissues. *FEMS Microbiol. Ecol.* 63, 84–93. doi: 10.1111/j.1574-6941.2007.00410.x

Conte, S. S., and Walker, E. L. (2011). Transporters contributing to iron trafficking in plants. *Mol. Plant* 4, 1–13. doi: 10.1093/mp/ssr015

Croft, M. T., Lawrence, A. D., Raux-Deery, E., Warren, M. J., and Smith, A. G. (2005). Algae acquire vitamin B12 through a symbiotic relationship with bacteria. *Nature* 438, 90–93. doi: 10.1038/nature04056

Cruz-Lopez, R., and Maske, H. (2016). The vitamin B1 and B12 required by the marine dinoflagellate lingulodinium polyedrum Can be provided by its associated bacterial community in culture. *Front. Microbiol.* 7:560. doi: 10.3389/fmicb.2016.00560

Czerpak, R., Bajguz, A., Chodkowski, K., and Popow, H. (1994). Influence of nickel and cobalt on the growth and biochemical changes of *Chlorella pyrenoidosa* (Chlorophyceae). *Pol. Arch. Hydrobiol.* 41, 161–169.

Das, H. K. (2019). Azotobacters as biofertilizer. *Adv. Appl. Microbiol.* 108, 1–43. doi: 10.1016/bs.aambs.2019.07.001

Davies, K. M., Jibran, R., Zhou, Y., Albert, N. W., Brummell, D. A., Jordan, B. R., et al. (2020). The evolution of flavonoid biosynthesis: a bryophyte perspective. *Front. Plant Sci.* 11:7. doi: 10.3389/fpls.2020.00007

Davis, R., Beckett, P., and Wollan, E. (1978). Critical levels of twenty potentially toxic elements in young spring barley. *Plant Soil* 49, 395–408. doi: 10.1007/BF02149747

Dewey, D. W., Lee, H. J., and Marston, H. R. (1958). Provision of cobalt to ruminants by means of heavy pellets. *Nature* 181, 1367–1371. doi: 10.1038/1811367a0

Dilworth, M. J., Robson, A. D., and Chatel, D. L. (1979). Cobalt and nitrogen fixation in *Lupinus angustifolius* L. *II*. Nodule formation and function. *New Phytol.* 83, 63–79. doi: 10.1111/j.1469-8137.1979.tb00727.x

Din, M., Nelofer, R., Salman, M., Abdullah, K., F. H., and Khan, A. (2019). Production of nitrogen fixing *Azotobacter* (SR-4) and phosphorus solubilizing *Aspergillus niger* and their evaluation on *Lagenaria siceraria* and *Abelmoschus esculentus*. *Biotechnol. Rep.* 22:e00323. doi: 10.1016/j.btre.2019.e00323

Dobereiner, J., Reis, V., Paula, M., and Olivares, F. (1993). "Endophytic diazotrophs in sugarcane cereals and tuber crops," in *New Horizons in Nitrogen Fixation,* eds R. Palacios, J. Moor, and W. Newton (Dordrecht: Kluwer), 671–674.

Doxey, A. C., Kurtz, D. A., Lynch, M. D., Sauder, L. A., and Neufeld, J. D. (2015). Aquatic metagenomes implicate *Thaumarchaeota* in global cobalamin production. *ISME J.* 9, 461–471. doi: 10.1038/ismej.2014.142

Eitinger, T. (2013). "Cobalt transporters," in *Encyclopedia of Metalloproteins*, eds R. H. Kretsinger, V. N. Uversky, and E. A. Permyakov (New York, NY: Springer), 678–682.

El-Essawy, A., El-Sayed, M., and Mohamed, Y. (1984). Production of cyanocobalamine by *Azotobacter chroococcum*. *Zentralblatt für Mikrobiol.* 139, 335–342. doi: 10.1016/S0232-4393(84)80011-6

Elledge, S., Zhou, Z., and Allen, J. (1992). Ribonucleotide reductase: regulation, regulation, regulation. *Trends. Biochem. Sci* 17, 119–123. doi: 10.1016/0968-0004(92)90249-9

Erdman, J. A., and Modreski, P. J. (1984). Copper and cobalt in aquatic mosses and stream sediments from the Idaho Cobalt Belt. *J. Geochem. Explor.* 20, 75–84. doi: 10.1016/0375-6742(84)90091-8

Evans, H. J., and Kliewer, M. (1964). Vitamin B12 compounds in relation to the requirements of cobalt for higher plants and nitrogen-fixing organisms. *Annals N. Y. Acad. Sci.* 112, 735–755. doi: 10.1111/j.1749-6632.1964.tb45052.x

Falcón, L., Magallón, S., and Castillo, A. (2010). Dating the cyanobacterial ancestor of the chloroplast. *ISME J.* 4,777–783. doi: 10.1038/ismej.2010.2

Fang, H., Kang, J., and Zhang, D. (2017). Microbial production of vitamin B12: a review and future perspectives. *Microb. Cell. Fact.* 16:15. doi: 10.1186/s12934-017-0631-y

Faucon, M. P., Shutcha, M. N., and Meerts, P. (2007). Revisiting copper and cobalt concentrations in supposed hyperaccumulators from SC Africa: influence of washing and metal concentrations in soil. *Plant Soil* 301, 29–36. doi: 10.1007/s11104-007-9405-3

Franche, C., Lindstrom, K., and Elmerich, C. (2009). Nitrogen- fixing bacteria associated with leguminous and non-leguminous plants. *Plant Soil* 321, 35–59. doi: 10.1007/s11104-008-9833-8

Fujino, D. W., and Reid, M.S. (1983). Factors affecting the vase life of fronds of maidenhair fern. *Sci. Hort.* 21, 181–188. doi: 10.1016/0304-4238(83)90164-4

Gad, N. (2006). Increasing the efficiency of nitrogen fertilization through cobalt application to pea plant. *Res. J. Agri. Biol. Sci.* 2, 433–442.

Gad, N. (2012a). Physiological and chemical response of groundnut (*Arachis hypogaea*) to Cobalt Nutrition. *World Appl. Sci. J.* 20, 327–335.

Gad, N. (2012b). Role and importance of cobalt nutrition on groundnut (Arachis hypogaea) production. World *Appl. Sci. J.* 20, 359–367. doi: 10.5829/idosi.wasj.2012.20.03.2819

Gad, N., and Hassan, N. M. K. (2013). Role of cobalt and organic fertilizers amendments on tomato production in the newly reclaimed soil. *World Appl. Sci. J.* 22, 1527–1533.

Gad, N., and Kandil, H. (2008). Response of sweet potato (*Ipomoea batatas* L.) plants to different levels of cobalt. *Aust. J. Basic Appl. Sci.* 2, 949–955.

Gad, N., and Kandil, H. (2009). The influence of cobalt on sugar beet (*Beta vulgaris* L.) production. *Intl. J. Acad. Res.* 1, 52–58.

Garcia, M. M., Pereira, L. C., Braccini, A. L., Angelotti, P., Suzukawa, A. K., Marteli, D. C., et al. (2017). Effects of Azospirillum brasilense on growth and yield compounds of maize grown at nitrogen limiting conditions. *Revista de Ciências Agrárias* 40, 353–362. doi: 10.19084/RCA16101

García-Caparrós, P., De Filippis, L., Gul, A., Hasanuzzaman, M., Ozturk, M., Altay, V., et al. (2020). Oxidative stress and antioxidant metabolism under adverse environmental conditions: a review. *Bot. Rev.* 40, 353–362. doi: 10.1007/s12229-020-09231-1

Garnham, G. W., Codd, G. A., and Gadd, G. M. (1992). Kinetics of uptake and intracellular location of cobalt, manganese and zinc in the estuarine green alga *Chlorella salina*. *Appl. Microbiol. Biotechnol.* 37, 270–276. doi: 10.1007/BF00178183

Gerlach, M., and Vogel, I. (1902). Stickstoffsammelden bakterien. *Z. Bakterien II* 8:669.

Giglione, C., and Meinnel, T. (2001). Organellar peptide deformylases: universality of the N-terminal methionine cleavage mechanism. *Trends Plant Sci.* 6, 566–572. doi: 10.1016/S1360-1385(01)02151-3

Giglione, C., Serero, A., Pierre, M., Boisson, B., and Meinnel, T. (2000). Identification of eukaryotic peptide deformylases reveals universality of N-terminal protein processing mechanisms. *EMBO J.* 19, 5916–5929. doi: 10.1093/emboj/19.21.5916

Gonzalez-Lopez, J., Salmeron, V., Moreno, J., and Ramos-Cormenzana, A. (1983). Amino acids and vitamins produced by *Azotobacter vinelandii* ATCC 12837 in chemically-defined media and dialysed soil media. *Soil Biol. Biochem.* 15, 711–713. doi: 10.1016/0038-0717(83)90037-8

Gonzalez-Montana, J. R., Escalera-Valente, F., Alonso, A. J., Lomillos, J. M., Robles, R., and Alonso, M. E. (2020). Relationship between vitamin B12 and cobalt metabolism in domestic ruminant: an update. *Animals* 10:1855. doi: 10.3390/ani10101855

Gough, L., Shacklette, H., and Case, A. (1979). Element concentrations toxic to plants, animals and man. *LiSGS Bull* 1466, 80–84.

Govindaraju, K. (1994). Compilation of working values and sample description for 383 geostandards. *Geostand Newslett.* 18, 1–158. doi: 10.1111/j.1751-908X.1994.tb00502.x

Grover, S., and Purves, W. K. (1976). Cobalt and plant development: interactions with ethylene in hypocotyl growth. *Plant Physiol.* 57, 886–889. doi: 10.1104/pp.57.6.886

Grube, M., Seckbach, J., and Muggia, L. (2017). *Algal and Cyanobacteria Symbioses.* Singapore: World Scientific.

Guo, M., and Chen, Y. (2018). Coenzyme cobalamin: biosynthesis, overproduction and its application in dehalogenation—a review. *Rev. Environ. Sci. Biotechnol.* 17, 259–284. doi: 10.1007/s11157-018-9461-6

Gupta, G., Panwar, J., Akhtar, M. S., and Jha, P. N. (2012). "Endophytic nitrogen-fixing bacteria as biofertilizer," in *Sustainable Agriculture Reviews*, ed E. Lichtfouse (Dordrecht: Springer), 183–221.

Gupta, V., Roper, M., and Roget, D. (2006). Potential for non-symbiotic N2-fixation in different agroecological zones of southern Australia. *Aust. J. Soil Res.* 44, 343–354. doi: 10.1071/SR05122

Hamilton, E. I. (1994). The geobiochemistry of cobalt. *Sci. Total Environ.* 150, 7–39. doi: 10.1016/0048-9697(94)90126-0

Han, H. Y., Xu, W. A., Lu, Z. R., Zou, F., and Li, S. (2008). Activation and inactivation of horseradish peroxidase by cobalt ions. *J. Biomol. Struct. Dyn.* 26, 83–92. doi: 10.1080/07391102.2008.10507226

Hansen, B., Thorling, L., Schullehner, J., Termansen, M., and Dalgaard, T. (2017). Groundwater nitrate response to sustainable nitrogen management. *Sci. Rep.* 7:8566. doi: 10.1038/s41598-017-07147-2

Harrop, T. C., and Mascharak, P. K. (2013). "Cobalt-containing enzymes," in *Encyclopedia of Metalloproteins*, eds R. H. Kretsinger, V. N. Uversky, and E. A. Permyakov (New York, NY: Springer), 684–690.

Hartmann, A., Stoffels, M., Eckert, B., Kirchhof, G., and Schloter, M. (2000). "Analysis of the presence and diversity of diazotrophic endophytes," in *Prokaryotic Nitrogen Fixation: A Model System for the Analysis of a Biological Process,* ed E. W. Triplett (Wymondham: Horizon Scientific Press), 727–736.

Hasanuzzaman, M., Bhuyan, M. H. M. B., Zulfiqar, F., Raza, A., Mohsin, S. M., Mahmud, J. A., et al. (2020). Reactive oxygen species and antioxidant defense in plants under abiotic stress: revisiting the crucial role of a universal defense regulator. *Antioxidants* 9:681. doi: 10.3390/antiox9080681

Havlin, J. L., Tisdale, S. L., Nelson, W. L., and Beaton, J. D. (2013). *Soil Fertility and Fertilizers.* Upper Saddle River, NJ: Prentice Hall, Inc.

Hawco, N. J., McIlvin, M. M., Bundy, R. M., Tagliabue, A., Goepfert, T. J., Moran, D. M., et al. (2020). Minimal cobalt metabolism in the marine cyanobacterium Prochlorococcus. *Proc. Natl. Acad. Sci.* 117, 15740–15747. doi: 10.1073/pnas.2001393117

Heal, K. R.,Wei, Q., Ribalet, F., Bertagnolli, A. D., Coyote-Maestas, W., Hmelo, L. R., et al. (2017). Two distinct pools of B12 analogs reveal community interdependencies in the ocean. *Proc. Natl. Acad. Sci. U.S.A.* 114, 364–369. doi: 10.1073/pnas.1608462114

Helmy, L. M., and Gad, N. (2002). Effect of cobalt fertilization on the yield, quality the essential oil composition of parsley leaves. *Arab. Univ. J. Agric. Sci. Ain. Shams Univ Cairo* 10, 779–802.

Herridge, D. F., Peoples, M. B., and Boddey, R. M. (2008). Global inputs of biological nitrogen fixation in agricultural systems. *Plant Soil* 311, 1–18. doi: 10.1007/s11104-008-9668-3

Hewitt, E. J., and Bond, G. (1966). The cobalt requirement of non-legume root nodule plants. *J. Exp. Bot.* 17, 480–491. doi: 10.1093/jxb/17.3.480

Holm-Hansen, O., Gerloff, G. C., and Skoog, F. (1954). Cobalt as an essential element for blue-green algae. *Physiol. Plant* 7, 665–675. doi: 10.1111/j.1399-3054.1954.tb07727.x

Homer, F. A. (1991). Comparative studies of nickel, cobalt, and copper uptake by some nickel hyperaccumulators of the genus *Alyssum*. *Plant Soil* 138, 195–205. doi: 10.1007/BF00012246

Hopkins, W. (1995). *Introduction to Plant Physiology.* New York, NY: John Wiley and Sons.

Hurek, T., and Reinhold-Hurek, B. (2003). *Azoarcus sp.* strain BH72 as a model for nitrogen-fixing grass endophytes. *J. Biotechnol.* 106, 169–178. doi: 10.1016/j.jbiotec.2003.07.010

Huss-Danell, K. (1997). Tansley Review No. 93. Actinorhizal symbioses and their N2 fixation. *New Phytol.* 136, 375–405. doi: 10.1046/j.1469-8137.1997.00755.x

Huwait, A. E., Kumosani, A. T., Moselhy, S. S., Mosaoa, M. R., and Yaghmoor, S. S. (2015). Relationship between soil cobalt and vitamin B12 levels in the liver of livestock in Saudi Arabia: role of competing elements in soils. *Afr. Health Sci.* 15, 993–998. doi: 10.4314/ahs.v15i3.38

Hyodo, H., and Fukasawa, R. (1985). Ethylene production in kiwi fruit (*Actinidia chinensis* cultivar. *Hayward). J. Jap. Soc. Hortic. Sci.* 54, 209–215. doi: 10.2503/jjshs.54.209

Iswaran, V., and Rao Sundara, W. V. B. (1964). role of cobalt in Nitrogen fixation by *Azotobacter chroococcum*. *Nature* 203:549. doi: 10.1038/203549a0

Jaleel, C. A., Jayakumar, K., Zhao, C.-X., and Iqbal, M. (2009). Low concentration of cobalt increases growth, biochemical constituents, mineral status and yield in *Zea mays*. *J. Sci. Res.* 1, 128–137. doi: 10.3329/jsr.v1i1.1226

Jalilian, N., Najafpour, G., and Khajouei, M. (2019). Enhanced vitamin B12 production using *Chlorella vulgaris*. *IJE Transac. Basics* 32, 1–9. doi: 10.5829/ije.2019.32.01a.01

Jamali, B., and Rahemi, M. (2011). Carnation flowers senescence as influenced by nickel, cobalt and silicon. *J. Biol. Environ. Sci.* 5, 147–152.

James, E. K., Olivares, F. L., de Oliveira, A. L., dos Reis F. B. Jr., da Silva, L. G., and Reis, V. M. (2001). Further observations on the interaction between sugar cane and *Gluconacetobacter diazotrophicus* under laboratory and greenhouse conditions. *J. Exp. Bot.* 52, 747–760. doi: 10.1093/jexbot/52.357.747

Jayakumar, K., Abdul, Jaleel, C., Azooz, M. M., Vijayarengan, P., Gomathinayagam, M., and Panneerselvam, R. (2009). Effect of different concentrations of cobalt on morphological parameters and yield components of soybean. *Glob. J. Mol. Sci.* 4, 10–14.

Jayakumar, K., Rajesh, M., Baskaran, L., and Vijayarengan, P. (2013). Changes in nutritional metabolism of tomato plants exposed to increasing concentration of cobalt chloride. *Acta Physiol. Plant.* 4, 62–69.

Jensen, E. L., Maberly, S. C., and Gontero, B. (2020). Insights on the functions and ecophysiological relevance of the diverse carbonic anhydrases in microalgae. *Int. J. Mol. Sci.* 21:2922. doi: 10.3390/ijms21082922

Johansson, C., and Bergman, B. (1994). Reconstitution of the symbiosis of *Gunnera manicata* Linden: cyanobacterial specificity. *New Phytol.* 126, 643–652. doi: 10.1111/j.1469-8137.1994.tb02960.x

Kabata-Pendias, A., and Mukherjee, A. B. (2007). *Trace Elements From Soils to Human.* Berlin; Heidelberg: Springer-Verlag.

Kamnev, A., Tarantilis, P., Antonyuk, L., Bespalova, L., Polissiou, M., Colina, M., et al. (2001). Fourier transform Raman spectroscopic characterisation of cells of the plant-associated soil bacterium *Azospirillum brasilense* Sp7. *J. Mol. Struct.* 563, 199–207. doi: 10.1016/S0022-2860(00)00877-2

Kannan, T., and Ponmurugan, P. (2010). Response of paddy (*Oryza sativa* L.) varieties to *Azospirillum brasilense* inoculation. *J. Phytol.* 2, 8–13.

Kazemi, M. (2012). Effect of cobalt, silicon, acetylsalicylic acid and sucrose as novel agents to improve vase-life of *Argyranthemum* flowers. *Trends Appl. Sci. Res.* 7, 579–583. doi: 10.3923/tasr.2012.579.583

Kazemi, M., and Ameri, A. (2012). Effect of Ni, CO, SA and sucrose on extending the vase-life of lily cut flower. *Iran. J. Energy Environ.* 3, 162–166. doi: 10.5829/idosi.ijee.2012.03.02.0258

Ke, J., Wang, B., and Yoshikuni, Y. (2021). Microbiome engineering: synthetic biology of plant-associated microbiomes in sustainable agriculture. *Trends Biotechnol.* 39, 244–261. doi: 10.1016/j.tibtech.2020.07.008

Kellogg, M. M., Mcllvin, M. R., Vedamati, J., Twining, B. S., Moffett, J. W., Marchetti, A., et al. (2020). Efficient zinc/cobalt inter-replacement in northeast Pacific diatoms and relationships to high surface dissolved Co: Zn ratio. *Limnol. Oceanogr.* 65, 2557–2582. doi: 10.1002/lno.11471

Keshavarz, H., and Moghadam, R. S. G. (2017). Seed priming with cobalamin (vitamin B12) provides significant protection against salinity stress in the common bean. *Rhizosphere* 3, 143–149. doi: 10.1016/j.rhisph.2017.04.010

Khan, A. R., Park, G. S., Asaf, S., Hong, S. J., Jung, B. K., and Shin, J. H. (2017). Complete genome analysis of *Serratia marcescens* RSC-14: a plant growth-promoting bacterium that alleviates cadmium stress in host plants. *PloS ONE* 12:e0171534. doi: 10.1371/journal.pone.0171534

Khrustalev, V., Khrustaleva, T., Poboinev, V., Karchevskaya, C., Shablovskaya, E., and Terechova, T. (2019). Cobalt(ii) cation binding by proteins. *Metallomics* 11, 1743–1752. doi: 10.1039/C9MT00205G

Kirchhof, G., Reis, V., Baldani, J., Eckert, B., Döbereiner, J., and Hartmann, A. (1997). Occurrence, physiological and molecular analysis of endophytic diazotrophic bacteria in gramineous energy plants. *Plant Soil* 194, 45–55. doi: 10.1023/A:1004217904546

Kitagishi, K., and Yamane, I. (1981). *Heavy Metal Pollution in Soils of Japan.* Tokyo: Japan Science Society Press.

Kliewer, M., and Evans, H. (1963a). Cobamide coenzyme contents of soybean nodules and nitrogen fixing bacteria in relation to physiological conditions. *Plant Physiol.* 38, 99–104. doi: 10.1104/pp.38.1.99

Kliewer, M., and Evans, H. J. (1963b). Identification of cobamide coenzyme in nodules of symbionts and isolation of the B12 coenzyme from *Rhizobium meliloti*. *Plant Physiol.* 38, 55–59. doi: 10.1104/pp.38.1.55

Kobayashi, M., and Shimizu, S. (1999). Cobalt proteins. *Eur. J. Biochem.* 261, 1–9. doi: 10.1046/j.1432-1327.1999.00186.x

Kolberg, M., Strand, K. R., Graff, P., and Andersson, K. K. (2004). Structure, function, and mechanism of ribonucleotide reductases. *Biochim. Biophys. Acta* 1699, 1–34. doi: 10.1016/S1570-9639(04)00054-8

Koleli, N., Demir, A., Kantar, C., Atag, G. A., Kusvuran, K., and Binzet, R. (2015). "Heavy metal accumulation in serpentine flora of Mersin-Findikpinari (Turkey) – Role of ethylenediamine tetraacetic Acid in facilitating extraction of nickel," in *Soil Remediation and Plants* (New York, NY, USA, Academic Press). doi: 10.1016/b978-0-12-799937-1.00022-x

Korshunova, Y. O., Eide, D., Clark, W. G., Guerinot, M. L., and Pakrasi, H. B. (1999). The IRT1 protein from *Arabidopsis thaliana* is a metal transporter with a broad substrate range. *Plant Mol. Biol.* 40, 37–44. doi: 10.1023/A:1026438615520

Krause, A., Ramakumar, A., Bartels, D., Battistoni, F., Bekel, T., Boch, J., et al. (2006). Complete genome of the mutualistic, N 2-fixing grass endophyte *Azoarcus sp.* strain BH72. *Nat. Biotechnol.* 24, 1384–1390. doi: 10.1038/nbt1243

Kubota, Y., Shoji, S., and Motohara, K. (1977). Purification and properties of prolidase for germinating soybeans. *Yakugaku Zasshi* 97, 111–115. doi: 10.1248/yakushi1947.97.1_111

Lange, B., van der Ent, A., Baker, A. J., Echevarria, G., Mahy, G., Malaisse, F., et al. (2017). Copper and cobalt accumulation in plants: a critical assessment of the current state of knowledge. *New Phytol.* 213, 537–551. doi: 10.1111/nph.14175

Lau, O. L., and Yang, S. F. (1976). Inhibition of ethylene production by cobaltous ion. *Plant Physiol.* 58, 114–117. doi: 10.1104/pp.58.1.114

Lawrence, A. D., Nemoto-Smith, E., Deery, E., Baker, J. A., Schroeder, S., Brown, D. G., et al. (2018). Construction of fluorescent analogs to follow the uptake and distribution of cobalamin (vitamin B12) in bacteria, worms, and plants. *Cell Chem. Biol.* 25, 941–951. e946. doi: 10.1016/j.chembiol.2018.04.012

Lee, H. J. (1951). Cobalt and copper deficiencies affecting sheep in South Australia. *J. Agri. Sci. Austr.* 54, 475–532.

Li, H., Liu, Y., Qin, H., Lin, X., Tang, D., Wu, Z., et al. (2020). A rice chloroplast-localized ABC transporter ARG1 modulates cobalt and nickel homeostasis and contributes to photosynthetic capacity. *New Phytol.* 228, 163–178. doi: 10.1111/nph.16708

Lindsay, D., and Kerr, W. (2011). Cobalt close-up. *Nat. Chem.* 3:494. doi: 10.1038/nchem.1053

Liu, J. (1998). *Cobalt: physiological effects and uptake mechanisms in plants* [Ph.D. thesis]. The University of Adelaide, Adelaide, SA, Australia.

Lwalaba, J. L. W., Zvogbo, G., Mulembo, M., Mundende, M., and Zhang, G. (2017). The effect of cobalt stress on growth and physiological traits and its association with cobalt accumulation in barley genotypes differing in cobalt tolerance. *J. Plant. Nutr.* 40, 2192–2199. doi: 10.1080/01904167.2017.1346676

Lyu, S., Wei, X., Chen, J., Wang, C., Wang, X., and Pan, D. (2017). Titanium as a beneficial element for crop production. *Front. Plant. Sci.* 8:597. doi: 10.3389/fpls.2017.00597

Macnicol, R., and Beckett, P. (1985). Critical tissue concentrations of potentially toxic elements. *Plant Soil* 85, 107–129. doi: 10.1007/BF02197805

Mahey, S., Kumar, R., Sharma, M., Kumar, V., and Bhardwaj, R. (2020). A critical review on toxicity of cobalt and its bioremediation strategies. *SN Appl. Sci.* 2:1279. doi: 10.1007/s42452-020-3020-9

Malik, M., Chaney, R. L., Brewer, E. P., Li, Y. M., and Angle, J. S. (2000). Phytoextraction of Soil Cobalt Using Hyperaccumulator Plants. *Int. J. Phytorem.* 2, 319–329. doi: 10.1080/15226510008500041

Mandujano-Piña, M., Colinas-León, M. T., Castillo-González, A. M., Alía-Tejacal, I., and Valdéz-Aguilar, L. A. (2012). Cobalt as senescence retardant in postharvest of oriental hybrid *Lilium*. *Revista Chapingo. Serie Hort.* 18, 239–252. doi: 10.5154/r.rchsh.2010.09.034

Maret, M., and Vallee, B. (1993). Cobalt as probe and label of proteins. *Methods Enzymol.* 226, 52–71. doi: 10.1016/0076-6879(93)26005-T

Marschner, P. (2011). *Marschner's Mineral Nutrition of Higher Plants.* Amsterdam: Elsevier/Academic Press.

Marsh, E. N. (1999). Coenzyme B12 (cobalamin)-dependent enzymes. *Essays Biochem.* 34, 139–154. doi: 10.1042/bse0340139

Marsh, E. N. G., and Drennan, C. L. (2001). Adenosyl cobalamin dependent isomerases: new insights into structure and mechanism. *Curr. Opin. Chem. Biol.* 5, 499–505. doi: 10.1016/S1367-5931(00)00238-6

McLeod, K. W., and Ciravolo, T. G. (2007). Cobalt uptake by *Nyssa aquatica*, *N. sylvatica* var. biflora, and Taxodium distichum seedlings. *Wetlands* 27, 40–43. doi: 10.1672/0277-5212(2007)27[40:CUBNAN]2.0.CO;2

Mehrafarin, A., Rezazadeh, S., Naghdi Badi, H., Gh, N., Z, E., and Qaderi, A. (2021). A review on biology, cultivation and biotechnology of fenugreek (*Trigonella foenum-graecum* L.) as a valuable medicinal plant and multipurpose. *J. Med. Pl.* 10, 6–24.

Mohandas, S. (1985). Effect of presowing seed treatment with molybdenum and cobalt on growth, nitrogen and yield in bean (*Phaseolus vulgaris* L.). *Plant Soil* 86, 283–285. doi: 10.1007/BF02182905

Morel, M., Crouzet, J., Gravot, A., Auroy, P., Leonhardt, N., Vavasseur, A., et al. (2009). AtHMA3, a P1B-ATPase allowing Cd/Zn/Co/Pb vacuolar storage in Arabidopsis. *Plant Physiol.* 149, 894–904. doi: 10.1104/pp.108.130294

Morrison, R. S. (1979). Copper and cobalt uptake by metallophytes from Zaïre. *Plant Soil* 53, 535–539. doi: 10.1007/BF02140724

Morrissey, J., Baxter, I., Lee, J., Li, L., Lahner, B., Grotz, N., et al. (2009). The ferroportin metal efflux proteins function in iron and cobalt homeostasis in Arabidopsis. *Plant Cell* 21, 3326–3338. doi: 10.1105/tpc.109.069401

Mozafar, A. (1994). Enrichment of some B-vitamins in plants with application of organic fertilizers. *Plant Soil* 167, 305–331. doi: 10.1007/BF00007957

Murr, D. P., Venkatarayappa, T., and Tsujita., M. J. (1979). Counteraction of bent-neck of cut roses with cobalt nitrate." *Can. J. Plant Sci.* 59, 1169–1171. doi: 10.4141/cjps79-184

Muthukumarasamy, R., Cleenwerck, I., Revathi, G., Vadivelu, M., Janssens, D., Hoste, B., et al. (2005). Natural association of Gluconacetobacter diazotrophicus and diazotrophic *Acetobacter peroxydans* with wetland rice. *Syst. Appl. Microbiol.* 28, 277–286. doi: 10.1016/j.syapm.2005.01.006

Nagpal, N. (2004). *Water Quality Guidelines for Cobalt.* Victoria, BC: Ministry of Water, Land and Air Protection, Water Protection Section, Water, Air and Climate Change Branch.

Nakos, M., Pepelanova, I., Beutel, S., Krings, U., Berger, R. G., and Scheper, T. (2017). Isolation and analysis of vitamin B12 from plant samples. *Food Chem.* 216, 301–308. doi: 10.1016/j.foodchem.2016.08.037

Nicholas, D., Kobayashi, M., and Wilson, P. (1962). Cobalt requirement for inorganic nitrogen metabolism in microorganisms. *Proc. Nat. Acad. Sci.* 48, 1537–1542. doi: 10.1073/pnas.48.9.1537

Nohwar, N., Khandare, R. V., and Desai, N. S. (2020). Media optimization studies and production of adenosylcobalamin (Vitamin B12) by environment friendly organism *Rhizobium spp*. *J. Appl. Biol. Biotech.* 8, 38–47.

Odaka, M., and Kobayashi, M. (2013). "Cobalt proteins, overview," in *Encyclopedia of Metalloproteins*, eds R. H. Kretsinger, V. N. Uversky, and E. A. Permyakov (New York, NY: Springer), 670–678.

Orji, J., Ngumah, C., Asor, H., and Anuonyemere, A. (2018). Effects of cobalt and manganese on biomass and nitrogen fixation yields of a free-living nitrogen fixer-*Azotobacter chroococcum*. *Eur. J. Biol. Res.* 8, 7–13.

Osman, D., Cooke, A., Young, T., Deery, E., Robinson, N., and Warren, M. (2021). The requirement for cobalt in vitamin B12: a paradigm for protein metalation. *BBA-Mol. Cell. Res.* 1868:118896. doi: 10.1016/j.bbamcr.2020.118896

Ozanne, P. G., Greenwood, E. A. N., and Shaw, T. C. (1963). The cobalt requirement of Subterranean clover in the field. *Aust. J. Agric. Res.* 14, 39–50. doi: 10.1071/AR9630039

Page, V., and Feller, U. (2005). Selective transport of zinc, manganese, nickel, cobalt and cadmium in the root system and transfer to the leaves in young wheat plants. *Ann. bot.* 96, 425–434. doi: 10.1093/aob/mci189

Pais, I. (1992). Criteria of essentiality, beneficiality and toxicity of chemical elements. *Acta Aliment.* 21, 145–152.

Paizs, C., Diemer, T., and Rétey, J. (2008). The putative coenzyme B12- dependent methylmalonyl-CoA mutase from potatoes is a phosphatase. *Bioorg. Chem.* 36, 261–264. doi: 10.1016/j.bioorg.2008.06.002

Palacios, O. A., Bashan, Y., and de-Bashan, L. E. (2014). Proven and potential involvement of vitamins in interactions of plants with plant growth-promoting bacteria—an overview. *Biol. Fertil. Soils.* 50, 415–432. doi: 10.1007/s00374-013-0894-3

Paul, A. L. D., Nkrumah, P. N., Echevarria, G., Erskine, P. D., Chaney, R. L., Spiers, K. M., et al. (2020). Cobalt hyperaccumulation in *Rinorea* cf. *Bengalensis* (Violaceae) from sabah: Accumulation potential and tissue and cellular-level distribution of cobalt. *Plant Soil* 455, 289–303. doi: 10.1007/s11104-020-04629-7

Pedrosa, F. O., Monteiro, R. A., Wassem, R., Cruz, L. M., Ayub, R. A., Colauto, N. B., et al. (2011). Genome of *Herbaspirillum seropedicae* strain SmR1, a specialized diazotrophic endophyte of tropical grasses. *PLoS Genet.* 7:e1002064. doi: 10.1371/journal.pgen.1002064

Permyakov, E. A. (2021). Metal binding proteins. *Encyclopedia* 1, 261–292. doi: 10.3390/encyclopedia1010024

Pham, V. T. K., Rediers, H., Ghequire, M. G. K., Nguyen, H. H., De Mot, R., Vanderleyden, J., et al. (2017). The plant growth-promoting effect of the nitrogen-fixing endophyte *Pseudomonas stutzeri* A15. *Arch. Microbiol.* 199, 513–517. doi: 10.1007/s00203-016-1332-3

Pilon-Smits, E. A., Quinn, C. F., Tapken, W., Malagoli, M., and Schiavon, M. (2009). Physiological functions of beneficial elements. *Curr. Opin. Plant. Biol.* 12, 267–274. doi: 10.1016/j.pbi.2009.04.009

Poston, J. M. (1977). Leucine 2, 3-aminomutase: a cobalamin-dependent enzyme present in bean seedlings. *Science* 195, 301–302. doi: 10.1126/science.195.4275.301

Poston, J. M. (1978). Coenzyme B12-dependent enzymes in potatoes: leucine 2, 3-aminomutase and methylmalonyl-coa mutase. *Phytochemistry* 17, 401–402. doi: 10.1016/S0031-9422(00)89324-3

Puri, A., Padda, K. P., and Chanway, C. P. (2018). "Nitrogen-fixation by endophytic bacteria in agricultural crops: recent advances," in *Nitrogen in Agriculture-Updates*, eds A. Khan, S. Fahad (Rijeka: In Tech Publisher), 73–94. doi: 10.5772/intechopen.71988

Raj, A. S. (1987). Cobalt nutrition of pigeonpea and peanut in relation to growth and yield. *J. Plant Nutr.* 10, 2137–2145. doi: 10.1080/01904168709363764

Rajakaruna, N., and Bohm, B. A. (2002). Serpentine and its vegetation: a preliminary study from Sri Lanka. *J. Appl. Bot. Angewand. Bot.* 76, 20–28.

Rana, K. L., Divjot, K., Tanvir, K., Rubee, D., Nath, Y. A., Neelam, Y., et al. (2020). Endophytic microbes: biodiversity, plant growth-promoting mechanisms and potential applications for agricultural sustainability. *Antonie van Leeuwenhoek* 113, 1075–1107. doi: 10.1007/s10482-020-01429-y

Rauser, W. (1981). Entry of sucrose into minor veins of bean seedlings exposed to phytotoxic burdens of Co, Ni or Zn. *J. Plant. Nutr.* 3, 319–328. doi: 10.1080/01904168109362840

Reddy, T. V. (1988). Mode of action of cobalt extending the vase life of cut roses. *Sci. Hort.* 36, 303–313. doi: 10.1016/0304-4238(88)90065-9

Reed, S. C., Cleveland, C. C., and Townsend, A. R. (2011). Functional ecology of free-living nitrogen fixation: a contemporary perspective. *Annu. Rev. Ecol. Evol. Syst.* 42, 489–512. doi: 10.1146/annurev-ecolsys-102710-145034

Reimann, C., Koller, F., Frengstad, B., Kashulina, G., Niskavaara, H., and Englmaier, P. (2001). Comparison of the element compositin in several plant species and their substrate from a 1555000 km^2 area in northern Europe. *Sci. Total. Environ.* 278, 87–112. doi: 10.1016/S0048-9697(00)00890-1

Reisenauer, H. M. (1960). Cobalt in nitrogen fixation by a legume. *Nature* 186, 375–376. doi: 10.1038/186375a0

Ritika, B., and Dey, U. (2014). Biofertilizer, a way towards organic agriculture: a review. *Afr. J. Microbiol. Res.* 8, 2332–2343. doi: 10.5897/AJMR2013.6374

Roberts, S., and Gunn, G. (2014). "Cobalt," in *Critical Metals Handbook*, 1st Edn, ed G. Gunn (Nottingham: John Wiley and Sons), 122–147.

Robson, A. D., Dilworth, M. J., and Chatel, D. L. (1979). Cobalt and nitrogen fixation on *Lupinus angusfifohus* L. I. Growth nitrogen concentrations and cobalt distribution. *New Phytol.* 83, 53–62. doi: 10.1111/j.1469-8137.1979.tb00726.x

Rod, N. K., Gudadhe, N. N., Karmakar, N., Mehta, P. V., and Narwade, A. V. (2019). Cobalt chloride enhances crop duration, increases production, and productivity of chickpea. *J. Plant. Nutr.* 42, 40–57. doi: 10.1080/01904167.2018.1544258

Rodionov, D. A., Vitreschak, A. G., Mironov, A. A., and Gelfand, M. S. (2003). Comparative genomics of the vitamin B12 metabolism and regulation in prokaryotes. *J. Bio. Chem.* 278, 41148–41159. doi: 10.1074/jbc.M305837200

Rosenblueth, M., Ormeno-Orrillo, E., Lopez-Lopez, A., Rogel, M. A., Reyes-Hernandez, B. J., Martinez-Romero, J. C., et al. (2018). Nitrogen fixation in cereals. *Front. Microbiol.* 9:1794. doi: 10.3389/fmicb.2018.01794

Rothballer, M., Eckert, B., Schmid, M., Fekete, A., Schloter, M., Lehner, A., et al. (2008). Endophytic root colonization of gramineous plants by *Herbaspirillum frisingense. FEMS Microbiol. Ecol.* 66, 85–95. doi: 10.1111/j.1574-6941.2008.00582.x

Roughley, R. J., Gault, R. R., Gemell, L. G., Andrews, J. A., Brockwell, J., Dunn, B. W., et al. (1995). Autecology of *Bradyrhizobium japonicum* in soybean-rice rotations. *Plant Soil* 176, 7–14. doi: 10.1007/BF00017670

Sachdev, S., Ansari, S. A., Ansari, M. I., Fujita, M., and Hasanuzzaman, M. (2021). Abiotic stress and reactive oxygen species: generation, signaling and defense mechanisms. *Antioxidants* 10:277. doi: 10.3390/antiox10020277

Santoyo, G., Moreno-Hagelsieb, G., del Carmen Orozco-Mosqueda, M., and Glick, B. R. (2016). Plant growth-promoting bacterial endophytes. *Microbiol. Res.* 183, 92–99. doi: 10.1016/j.micres.2015.11.008

Saric, T., and Saciragic, B. (1969). Effect of oat seed treatment with microelements. *Plant Soil* 31, 185–187. doi: 10.1007/BF01373038

Sato, K., Kudo, K., and Muramatsu, K. (2004). Incorporation of a high level of vitamin B12 into a vegetable, kaiware daikon (Japanese radish sprout), by the absorption from its seeds. *Biochim. Biophys. Acta.* 1672, 135–137. doi: 10.1016/j.bbagen.2004.03.011

Serek, M., Woltering, E. J., E. C., Sisler, S. F., and Sriskandarajah, S. (2006). Controlling ethylene responses in flowers at the receptor level. *Biotechnol. Adv.* 24, 368–381. doi: 10.1016/j.biotechadv.2006.01.007

Setubal, J. C., Dos Santos, P., Goldman, B. S., Ertesvåg, H., Espin, G., Rubio, L. M., et al. (2009). Genome sequence of *Azotobacter vinelandii*, an obligate aerobe specialized to support diverse anaerobic metabolic processes. *J. Bacteriol.* 191, 4534–4545. doi: 10.1128/JB.00504-09

Shacklette, H. T. (1965). Element content of bryophytes. *U.S. Geol. Survey Bull.* 1198, 1–18.

Shahid, M., Niazi, N. K., Rinklebe, J., Bundschuh, J., Dumat, C., and Pinelli, E. (2020). Trace elements-induced phytohormesis: a critical review and mechanistic interpretation. *Crit. Rev. Environ. Sci. Technol.* 50, 1984–1932. doi: 10.1080/10643389.2019.1689061

Sillanpaa, M., and Jansson, H. (1992). *Status of Cadmium, Lead, Cobalt and Selenium in Soils and Plants of Thirty Countries*. Rome: FAO

Singh, D. K., Singh, A. K., Singh, M., Bordoloi, L. J., and Srivastava, O. P. (2012). Production potential and nutrient uptake efficiency of Pea (*Pisum sativum* L) as influenced by different fertility levels and micronutrients. *J. Indian Soc. Soil Sci.* 60, 1–6.

Singh, Z., Lakhvir, S., Arora, C. L., Dhillon, B. S., Singh, Z., and Singh, L. (1994). Effect of cobalt, cadmium, and nickel as inhibitors of ethylene biosynthesis on floral malformation, yield and fruit quality of mango. *J. Plant. Nutr.* 17, 1659–1670. doi: 10.1080/01904169409364838

Smith, I. C., and Carson, B. L. (1981). *Trace Metals in the Environment.* Ann Arbor, MI: Ann Arbor Science Publishers.

Soumare, A., Diedhiou, A. G., Thuita, M., Hafidi, M., Ouhdouch, Y., Gopalakrishnan, S., et al. (2020). Exploiting biological nitrogen fixation: a route towards a sustainable agriculture. *Plants* 9:1011. doi: 10.3390/plants9081011

Sree, K. S., Keresztes, A., Mueller-Roeber, B., Brandt, R., Eberius, M., Fischer, W., et al. (2015). Phytotoxicity of cobalt ions on the duckweed *Lemna minor* - morphology, ion uptake, and starch accumulation. *Chemosphere* 131, 149–156. doi: 10.1016/j.chemosphere.2015.03.008

Steenhoudt, O., and Vanderleyden, J. (2000). Azospirillum, a free-living nitrogen-fixing bacterium closely associated with grasses: genetic, biochemical and ecological aspects. *FEMS Microbiol. Rev.* 24, 487–506. doi: 10.1111/j.1574-6976.2000.tb00552.x

Tewari, R., Kumar, P., Sharma, P., and Bisht, S. (2002). Modulation of oxidative stress responsive enzymes by excess. *Plant Sci.* 162, 381–388. doi: 10.1016/S0168-9452(01)00578-7

Thomas, W. A. (1975). Cobalt accumulation and circulation by blackgum trees. *For. Sci.* 21, 222–226.

Tittle, F. L. (1987). Auxin-stimulated ethylene production in fern gametophytes and sporophytes. *Physiol. Plant.* 70, 499–502. doi: 10.1111/j.1399-3054.1987.tb02849.x

Tjong, E., Dimri, M., and Mohiuddin, S. S. (2020). *Biochemistry, Tetrahydrofolate*. Treasure Island, FL: StartPearls.

Tosh, S., Choudhuri, M. A., and Chatterjee, S. K. (1979). Retardation of lettuce (*Lactuca sativa* L.) leaf senescence by cobalt ions. *Indian. J. Exp. Bio.* 17, 1134–1136.

Trejo-Téllez, L. I., Gómez-Merino, F. C., Gómez-Pérez, V., and Castro-García, F. D. A. (2014). Cobalt in postharvest of gladiolus (*Gladiolus grandiflorus* Hort.). *Rev. Mexicana Ciencias Agrícolas* 28, 1575–1587.

Underwood, E. J., and Filmer, J. F. (1935). The determination of the biological potent element (cobalt) in limonite. *Aust. Vet. J.* 11, 84–92.

Van der Ent, A., Erskine, P., and Sumail, S. (2015). Ecology of nickel hyperaccumulator plants from ultramafic soils in Sabah (Malaysia). *Chemoecology* 25, 243–259. doi: 10.1007/s00049-015-0192-7

Van der Ent, A., Mak, R., de Jonge, M. D., and Harris, H. H. (2018). Simultaneous hyperaccumulation of nickel and cobalt in the tree *Glochidion* cf. sericeum (Phyllanthaceae): elemental distribution and chemical speciation. *Sci. Rep.* 8:9683. doi: 10.1038/s41598-018-26891-7

Van der Ent, A., and Reeves, R. D. (2015). Foliar metal accumulation in plants from copper-rich ultramafic outcrops: case studies from Malaysia and Brazil. *Plant Soil* 389, 401–418. doi: 10.1007/s11104-015-2385-9

Van Doorn, W. G., Zagory, D., and Reid, M. S. (1991). Role of ethylene and bacteria in vascular blockage of cut fronds from the fern *Adiantum raddianum*. *Sci. Hort.* 46, 161–169. doi: 10.1016/0304-4238(91)90102-5

Van Tran, L., and Teherani, D. K. (1989). Determination of trace elements in biological material by neutron activation analysis. *J. Radio. Nucl. Chem. Let.* 135, 443–448. doi: 10.1007/BF02164772

Velmourougane, K., Prasanna, R., Chawla, G., Nain, L., Kumar, A., and Saxena, A. K. (2019). *Trichoderma–Azotobacter* biofilm inoculation improves soil nutrient availability and plant growth in wheat and cotton. *J. Basic Microbiol.* 59, 632–644. doi: 10.1002/jobm.201900009

Vijayarengan, P., Jaleel, C. A., Zhao, C. X., Jayakumar, K., and Azooz, M. M. (2009). Biochemical variation in ground nut under Co application. *Applications. Glob. J. Mol. Sci.* 4, 19–22.

Wall, L. G. (2000). The actinorhizal symbiosis. *J. Plant Growth Regul.* 19, 167–182. doi: 10.1007/s003440000027

Wallace, A., Alexander, G. V., and Chaudhry, F. M. (1977). Phytotoxicity of cobalt, vanadium, silver and chromium. *Commun. Soil Sci. Plant Anal.* 8, 751–756. doi: 10.1080/00103627709366769

Wallace, A., E. M., Romney, D. C., Adriano, J. K. G., and Alexander, V. (1982). Sources of variation in mineral composition of selected plants inhabiting a floodplain at the Savannah River Site. *Soil Sci.* 134, 36–39. doi: 10.1097/00010694-198207000-00006

Wang, J. B., Tang, Y. L., Xu, J., Xu, G. C., Zou, Y., and Chen, H. (2015). Accumulation and distribution of cobalt in broad bean and its effects on the photosynthesis and antioxidant enzyme activities. *Acta Bot. Boreali-Occidentalia Sinica* 35, 963–970.

Wang, W., Zhai, Y., Cao, L., Tan, H., and Zhang, R. (2016). Endophytic bacterial and fungal microbiota in sprouts, roots and stems of rice (*Oryza sativa* L.). *Microbiol. Res.* 188, 1–8. doi: 10.1016/j.micres.2016.04.009

Wani, S. A., Chand, S., Wani, M. A., Ramzan, M., and Hakeem, K. R. (2016). "*Azotobacter chroococcum*–a potential biofertilizer in agriculture: an overview," in *Soil Science: Agricultural and Environmental Prospective*, eds K. Hakeem, J. Akhtar, and M. Sabir (Cham: Springer), 333–348.

Watanabe, F., Abe, K., Takenaka, S., Tamura, Y., Maruyama, I., and Nakano, Y. (1997). Occurrence of cobalamin coenzymes in the photosynthetic green alga, *Chlorella vulgaris*. *Biosci. Biotechnol. Biochem.* 61, 896–897. doi: 10.1271/bbb.61.896

Watanabe, Y., Iizuka, T., and Shimada, N. (1994). Induction of cucumber leaf urease by cobalt. *Soil Sci. Plant Nutr.* 40, 545–548. doi: 10.1080/00380768.1994.10413333

Wei, X., Lyu, S., Yu, Y., Wang, Z., Liu, H., Pan, D., et al. (2017). Phylloremediation of air pollutants: exploiting the potential of plant leaves and leaf-associated microbes. *Front. Plant Sci.* 8:1318. doi: 10.3389/fpls.2017.01318

Wheeler, R. M., and Salisbury, F. B. (1981). Gravitropism in higher plant shoots: I. A Role for ethylene. *Plant Physiol.* 67, 686–690. doi: 10.1104/pp.67.4.686

Wilson, S. B., and Nicholas, D. J. D. (1967). A Cobalt reguirement for non-nodulated legumes and for wheat. *Phytochemistry* 6, 1057–1066. doi: 10.1016/S0031-9422(00)86062-8

Yamada, K. (2013). Cobalt: its role in health and disease. *Met Ions Life Sci.*13, 295–320. doi: 10.1007/978-94-007-7500-8_9

Yamaguchi, T., Tsukada, C., Takahama, K., Hirotomo, T., Tomioka, R., and Takenaka, C. (2019). Localization and speciation of cobalt and nickel in the leaves of the cobalt-hyperaccumulating tree *Clethra barbinervis*. *Trees* 33, 521–532. doi: 10.1007/s00468-018-1797-6

Yanni, Y., and El-Fattah, F. K. (1999). Towards integrated biofertilization management with free living and associative dinitrogen fixers for enhancing rice performance in the Nile delta. *Symbiosis* 27, 319–331.

Yao, S., Lyu, S., An, Y., Lu, J., Gjermansen, C., and Schramm, A. (2018). Microalgae-bacteria symbiosis in microalgal growth and biofuel production: a review. *J. Appl. Microbiol.* 126, 359–368. doi: 10.1111/jam.14095

Yee, D., and Morel, F. M. (1996). In vivo substitution of zinc by cobalt in carbonic anhydrase of a marine diatom. *Limnol. Oceanogr.* 41, 573–577. doi: 10.4319/lo.1996.41.3.0573

Yoo, S., Cho, S., Sugimoto, H., Li, J., Kusumi, K., Koh, H., et al. (2009). Rice virescent3 and stripe1 encoding the large and small subunits of ribonucleotide reductase are required for chloroplast biogenesis during early leaf development. *Plant Physiol.* 150, 388–401. doi: 10.1104/pp.109.136648

Zhang, Y., Rodionov, D. A., Gelfand, M. S., and Gladyshev, V. N. (2009). Comparative genomic analyses of nickel, cobalt and vitamin B12 utilization. *BMC Genomics* 10:78. doi: 10.1186/1471-2164-10-78

Conflict of Interest: The authors declare that the research was conducted in the absence of any commercial or financial relationships that could be construed as a potential conflict of interest.

Publisher's Note: All claims expressed in this article are solely those of the authors and do not necessarily represent those of their affiliated organizations, or those of the publisher, the editors and the reviewers. Any product that may be evaluated in this article, or claim that may be made by its manufacturer, is not guaranteed or endorsed by the publisher.

Copyright © 2021 Hu, Wei, Ling and Chen. This is an open-access article distributed under the terms of the Creative Commons Attribution License (CC BY). The use, distribution or reproduction in other forums is permitted, provided the original author(s) and the copyright owner(s) are credited and that the original publication in this journal is cited, in accordance with accepted academic practice. No use, distribution or reproduction is permitted which does not comply with these terms.

frontiers in Plant Science

ORIGINAL RESEARCH
published: 29 November 2021
doi: 10.3389/fpls.2021.683813

Characterization of Metal Tolerance Proteins and Functional Analysis of GmMTP8.1 Involved in Manganese Tolerance in Soybean

Jifu Li[1,2†], Rongshu Dong[1†], Yidan Jia[2], Jie Huang[1,2], Xiaoyan Zou[1,2], Na An[2], Jianling Song[2] and Zhijian Chen[1,2]*

[1] Institute of Tropical Crop Genetic Resources, Chinese Academy of Tropical Agricultural Sciences, Haikou, China, [2] College of Tropical Crops, Hainan University, Haikou, China

OPEN ACCESS

Edited by:
Nikos Tzortzakis,
Cyprus University of Technology, Cyprus

Reviewed by:
Danuta Maria Antosiewicz, University of Warsaw, Poland
Spyridon Alexandros Petropoulos, University of Thessaly, Greece

***Correspondence:**
Zhijian Chen
jchen@scau.edu.cn

[†] These authors have contributed equally to this work and share first authorship

Specialty section:
This article was submitted to Plant Nutrition, a section of the journal Frontiers in Plant Science

Received: 22 March 2021
Accepted: 25 October 2021
Published: 29 November 2021

Citation:
Li J, Dong R, Jia Y, Huang J, Zou X, An N, Song J and Chen Z (2021) Characterization of Metal Tolerance Proteins and Functional Analysis of GmMTP8.1 Involved in Manganese Tolerance in Soybean. Front. Plant Sci. 12:683813. doi: 10.3389/fpls.2021.683813

Manganese is an essential micronutrient for plant growth but can be toxic to plants when it reaches excessive levels. Although metal tolerance proteins (MTPs), which belong to the cation diffusion facilitator (CDF) family, have been demonstrated to play critical roles in manganese (Mn) tolerance in plants, the characteristics and functions of GmMTP members in the response of soybean (*Glycine max*) to Mn toxicity have not been documented. In this study, growth inhibition was observed in soybean plants that were exposed to a toxic level of Mn in hydroponics, as reflected by the generation of brown spots, and decreased leaf chlorophyll concentration and plant fresh weight. Subsequent genome-wide analysis resulted in the identification of a total of 14 *GmMTP* genes in the soybean genome. Among these *GmMTPs*, 9 and 12 were found to be regulated by excess Mn in leaves and roots, respectively. Furthermore, the function of *GmMTP8.1*, a Mn-CDF homologue of *ShMTP8* identified in the legume *Stylosanthes hamata* that is involved in Mn detoxification, was characterized. Subcellular localization analysis showed that GmMTP8.1 was localized to the endoplasmic reticulum (ER). Heterologous expression of *GmMTP8.1* led to the restoration of growth of the Mn-hypersensitive yeast (*Saccharomyces cerevisiae*) mutant Δ*pmr1*, which is made defective in Mn transport into the Golgi apparatus by P-type Ca/Mn-ATPase. Furthermore, *GmMTP8.1* overexpression conferred tolerance to the toxic level of Mn in Arabidopsis (*Arabidopsis thaliana*). Under excess Mn conditions, concentrations of Mn in shoots but not roots were decreased in transgenic Arabidopsis, overexpressing *GmMTP8.1* compared to the wild type. The overexpression of *GmMTP8.1* also led to the upregulation of several transporter genes responsible for Mn efflux and sequestration in Arabidopsis, such as *AtMTP8/11*. Taken together, these results suggest that GmMTP8.1 is an ER-localized Mn transporter contributing to confer Mn tolerance by stimulating the export of Mn out of leaf cells and increasing the sequestration of Mn into intracellular compartments.

Keywords: metal tolerance protein, cation diffusion facilitator, Mn transporter, Mn toxicity, Mn detoxification, *Glycine max*

INTRODUCTION

As one of the essential micronutrients for plant growth, manganese (Mn) acts as an activator of many enzymes, serving various functions in a set of physiological and biochemical processes (Millaleo et al., 2010; Marschner, 2012; Long et al., 2021). Being a trace element, Mn is required by plants at a low dose and can cause phytotoxicity when present in excess (Millaleo et al., 2010; Shao et al., 2017). Mn toxicity is an important factor limiting plant growth on acid, poorly drained soils, and sterilized soils. Previous studies have shown that excess Mn can trigger oxidative stress by the generation of reactive oxygen species (ROS) (e.g., OH and O_2^-) from Mn ions *via* the Fenton reaction, resulting in disrupted metabolic pathways and damaged thylakoid membrane structure and macromolecules in plant cells (Millaleo et al., 2010; Dragišić Maksimović et al., 2012). Therefore, Mn toxicity inhibits enzyme activity, declines chlorophyll biosynthesis and photosynthesis, and impairs the uptake and translocation of other mineral elements (Fernando and Lynch, 2015; Li et al., 2019). In general, visible symptoms of Mn toxicity for most plants include generation of brown spots, chlorosis, and necrosis in leaves, ultimately inhibiting plant growth (Millaleo et al., 2010; Li et al., 2019). Thus, better understanding of mechanisms underlying the response of plants to Mn toxicity is of great importance for breeding Mn-tolerant crop varieties.

To cope with Mn toxicity, plants have developed comprehensive mechanisms to regulate Mn homeostasis by mediating Mn uptake, efflux, and trafficking at both cellular and tissue levels (Shao et al., 2017; Alejandro et al., 2020). For example, the cation diffusion facilitator (CDF) family is an integral membrane divalent cation transporter that plays critical roles in metal tolerance by regulating metal homeostasis in plant cells (Migocka et al., 2014, 2015). Most CDF proteins include an N-terminal signature sequence, a conserved C-terminal cation efflux domain, and several transmembrane domains (TMDs), which are critical for metal transport activities (Montanini et al., 2007; Chen X. et al., 2016). CDF transporters are involved in the transport of divalent cations, such as zinc (Zn), iron (Fe), and Mn, from the cytoplasm to extracellular space or to subcellular compartments (Gustin et al., 2011). Thus, the CDF members identified from numerous organisms can be classified into three major substrate-specific clusters, namely, Zn-CDF, Fe/Zn-CDF, and Mn-CDF, according to their transported substrate specificities (Montanini et al., 2007). Plant CDF proteins are generally designated as metal tolerance proteins (MTPs), which can be further categorized into seven subgroups based on the initial phylogenetic analysis and annotation of the Arabidopsis (*Arabidopsis thaliana*) MTP family (Gustin et al., 2011). For example, of the 12 MTP members in Arabidopsis, six AtMTPs (AtMTP1, AtMTP2, AtMTP3, AtMTP4, AtMTP5, and AtMTP12) are assigned to groups 1, 5, and 12 within the Zn-CDF cluster, while AtMTP6 and AtMTP7 belong to groups 6 and 7 within the Fe/Zn-CDF cluster. The remaining four AtMTPs (AtMTP8, AtMTP9, AtMTP10, and AtMTP11) are categorized into groups 8 and 9 within the Mn-CDF cluster (Gustin et al., 2011).

Among the three substrate-specific CDF clusters, MTP members of groups 8 and 9 within the Mn-CDF cluster have been characterized to be involved in regulating Mn tolerance either by sequestration of Mn or export of Mn out of the cell. For example, group 8 includes ShMTP8 from *Stylosanthes hamata*, AtMTP8 from Arabidopsis, OsMTP8.1/8.2 from rice (*Oryza sativa*), and CsMTP8 from cucumber (*Cucumis sativus*). These MTP members exhibit substrate-specificity to Mn and are implicated in the transport of Mn into vacuoles (Delhaize et al., 2003; Chen et al., 2013; Migocka et al., 2014; Eroglu et al., 2016; Takemoto et al., 2017). In addition, a variety of MTP members of group 9 have also been involved in the regulation of Mn homeostasis, as observed in CsMTP9 from cucumber, OsMTP9/11 from rice, BmMTP10/11 from *Beta vulgaris* ssp. *maritima*, AtMTP11 from Arabidopsis, and PtMTP11.1/11.2 from poplar (*Populus trichocarpa*); these MTPs are localized to the plasma membrane, Golgi apparatus, or pre-vacuolar compartments and have also been documented to regulate Mn homeostasis and tolerance (Delhaize et al., 2007; Peiter et al., 2007; Erbasol et al., 2013; Migocka et al., 2015; Ueno et al., 2015; Tsunemitsu et al., 2018b). Although the conserved functions of MTPs within the Mn-CDF cluster indicate similar roles of MTPs in Mn detoxification, it is still unknown whether MTP homologues in this specific cluster from different plants fulfill the same function and contribute to Mn tolerance.

Soybean (*Glycine max*) is recognized as one of the economically important nitrogen fixing legume crops and provides more than 60% of high-quality protein and oil for humans and animals in the world (Herridge et al., 2008; Lu et al., 2017). Although several studies have been conducted to investigate the response of soybean to Mn toxicity (Lavres et al., 2009; Yang et al., 2009; Chen Z. et al., 2016; Santos et al., 2017; Liu et al., 2020), underlying molecular mechanisms, through the involvement of MTPs, have not been elucidated. Key participants within the specific Mn-CDF cluster involved in Mn detoxification in soybean remain undetermined. In this study, a total of 14 MTP members were identified in the soybean genome. The expression pattern of each *GmMTP* gene in response to various metal treatments was analyzed. Furthermore, GmMTP8.1 was identified as a novel MTP8-like protein and displayed high similarity with ShMTP8 from *S. hamata* within the Mn-CDF cluster. Thus, GmMTP8.1 was studied in more detail to characterize its potential functions in Mn detoxification.

MATERIALS AND METHODS

Plant Materials and Growth Conditions

The soybean cultivar Zhonghuang 13 was used in this study. Seeds were surface-sterilized with 10% (v/v) H_2O_2 and germinated in paper rolls moistened with a half-strength Hoagland nutrient solution, and were cultivated in a growth chamber under conditions of 14-h light at 26°C/10-h dark at 23°C, 120 μmol m^{-2} s^{-1} photon flux density, and 70% relative humidity. After seed germination for 7 days, the soybean seedlings were transferred into a 15-L hydroponic box containing a 13-L full-strength Hoagland nutrient solution, as described by

Chen Z. et al. (2016). The Hoagland nutrient solution contained 1500 μM KNO_3, 1200 μM $Ca(NO_3)_2$, 400 μM NH_4NO_3, 500 μM KH_2PO_4, 1000 μM $MgSO_4$, 25 μM $MgCl_2$, 300 μM K_2SO_4, 300 μM $(NH_4)_2SO_4$, 5 μM $MnSO_4$, 0.38 μM $ZnSO_4$, 1.57 μM $CuSO_4$, 0.09 μM $(NH_4)_6Mo_7O_{24}$, 2.5 μM NaB_4O_7, and 80 μM Fe-EDTA. The pH value of the solution was adjusted to 5.8 using HCl or KOH every 2 days. The solution was aerated every 20 min per hour and refreshed weekly. Plants were cultivated in a greenhouse at temperatures ranging from 2 to 30°C under natural sunlight with a photoperiod of about 14 h and 50-70% relative humidity. Each hydroponic box containing four soybean seedlings served as one biological replicate, and the experiment included three biological replicates. After 14 days of growth, leaves, stems, and roots were separately cut from the plants. Samples from two plants of each biological replicate were pooled for gene expression analysis. All the samples were frozen with liquid nitrogen, and then stored at −80°C prior to RNA extraction.

To investigate the effects of excess Mn on soybean growth, after seed germination for 7 days, the seedlings were transferred to the full-strength Hoagland nutrient solution for 7 days as described above. Then, 14-day-old seedlings were transferred into the nutrient solution supplied with 5, 50, or 100 μM $MnSO_4$, according to Chen Z. et al. (2016). Five μM $MnSO_4$ was used as the control in this experiment. Each hydroponic box containing four soybean seedlings served as one biological replicate, and each treatment included three biological replicates. After 7 days of Mn treatments, shoots or roots from two plants of each biological replicate were pooled for determination of plant fresh weight and Mn concentration. A soil plant analysis development (SPAD)-502 chlorophyll meter (Konica-Minolta, Japan) was used to detect chlorophyll concentration according to the instructions of the manufacturer. Leaves or roots from the remaining two plants of each biological replicate were pooled for gene expression analysis. The samples were then stored at −80°C prior to RNA extraction.

To analyze the effects of excess Fe, Zn, and copper (Cu) stress on gene expression, 14-day-old seedlings pre-cultured in the nutrient solution as described above were transferred into a fresh nutrient solution containing 800 μM Fe-EDTA, 20 μM $ZnSO_4$, or 20 μM $CuSO_4$, which were regarded as excess Fe, Zn, and Cu stress, respectively. Soybean seedlings grown in the full-strength nutrient solution were set as the control. Each hydroponic box containing four soybean seedlings served as one biological replicate, and the experiment included three biological replicates. After 7 days of metal treatments, samples of leaves or roots were separated from two plants of each biological replicate, and were then pooled for gene expression analysis. The samples were frozen with liquid nitrogen and stored at −80°C prior to RNA extraction.

Identification of Soybean *GmMTP* Genes

The sequences of 12 *MTP* genes in Arabidopsis obtained from the NCBI website[1] were used separately as queries for BLAST search against the soybean genome in the Phytozome website.[2] After removing redundant sequences, a total of 14 *GmMTP* members were identified in the soybean genome that contained the cation efflux domain (PF01545). Subsequently, these candidates were named from *GmMTP4.1* to *GmMTP11.2* based on the phylogenetic relationship and sequence identity between GmMTP and Arabidopsis AtMTPs. General information for each *GmMTP* gene was obtained from the Phytozome website. The protein molecular weight of each GmMTP member was calculated using the ExPASy software.[3] Gene Structure Display Server[4] was used for gene structure analysis. The Pfam and MEME programs were used to analyze GmMTP conserved domains and motifs, respectively, according to Liu et al. (2018). TMDs were predicted by the TMHMM Server v.2.0. Construction of the phylogenetic tree was based on entire protein sequence alignments through ClustalX using the method neighbor-joining with 1,000 bootstrap replicates with MEGA 4.1.[5] The sequences of MTPs from other plant species were retrieved from corresponding databases, as described previously (Gustin et al., 2011; Migocka et al., 2014; Li et al., 2018; Liu J. et al., 2019).

Quantitative Real-Time Polymerase Chain Reaction Analysis of *GmMTP* Genes

Total RNA was extracted using TRIzol Reagent (Invitrogen, United States) according to the instructions of the manufacturer. First-strand cDNA was synthesized using a HiScript III cDNA (Vazyme, China) synthesis kit. SYBR Green Master Mix (Vazyme, China) and QuantStudio™ 6 Flex Real-Time System (Thermo Fisher Scientific, United States) were used for quantitative real-time polymerase chain reaction (qRT-PCR) analysis. qRT-PCR reaction was performed as follows: 95°C for 1 min, 40 cycles of 95°C for 15 s, 60°C for 15 s, and 72°C for 30 s. Fluorescence data were collected at 72°C. The qRT-PCR primers of genes are summarized in **Supplementary Table 1**. Relative gene expressions were calculated relative to the expression levels of the housekeeping gene, *GmEF-1a* or *AtEF-1a*. Gene expression analysis included three biological replicates.

Subcellular Localization of GmMTP8.1

The open reading frame (ORF) of *GmMTP8.1* without stop codon was amplified by PCR from root cDNA using *GmMTP8.1-GFP-F/R* primers (**Supplementary Table 1**). The amplified product was digested with *Eco*RI and *Bam*HI, and was then subcloned into the same sites after the cauliflower mosaic virus (CaMV) 35S promoter of the binary vector *pBWA(V)HS-GLosgfp* and fused with the N-terminal of green fluorescent protein (GFP). The *GmMTP8.1-GFP* construct and empty vector were introduced separately into *Agrobacterium tumefaciens* strain Gv3101 using the freeze-thaw method. The transformed Gv3101 cells were syringe-infiltrated into the abaxial side

[1] http://blast.ncbi.nlm.nih.gov

[2] https://phytozome-next.jgi.doe.gov/

[3] http://www.expasy.org/tools.html

[4] http://gsds.cbi.pku.edu.cn/

[5] http://www.megasoftware.net/mega4/mega41.html

of near-fully expanded leaves of 5- to 6-week-old tobacco (*Nicotiana benthamiana*) plants, as described by Liu et al. (2016). The tonoplast marker (tandem-pore K^+ channel, TPK1) and endoplasmic reticulum (ER) marker (auxin efflux carrier family protein, PIN5) (Voelker et al., 2006; Mravec et al., 2009), fused to the red fluorescent protein (mKATE), were used for co-localization with *GmMTP8.1-GFP* or empty vector. An empty vector with GFP alone was used as a control. After 3 days of cultivation, the GFP fluorescence in epidermal cells on the abaxial leaf side was imaged using a Zeiss LSM7 DUO (Zeiss, Germany) confocal microscope. Green fluorescence was stimulated at 488 nm and detected with filter sets at 500–530 nm. The red fluorescence was excited at 561 nm, and emission was captured at 580–630 nm.

Yeast Transformation and Metal Tolerance Analysis

Five *Saccharomyces cerevisiae* mutants, namely, the Mn-sensitive mutant Δ*pmr1* (MATa; his3Δ1; leu2Δ0; met15Δ0; ura3Δ0; YGL167c::kanMX4) defective in Mn transport into the Golgi apparatus; Zn-sensitive mutant Δ*zrc1* (MATa; ura3Δ0; leu2Δ0; his3Δ1; met15Δ0; YMR243c::kanMX4) defective in sequestering Zn into the vacuole; Cu-sensitive mutant Δ*cup2* (MATa; his3Δ1; leu2Δ0; met15Δ0; ura3Δ0; YGL166w::kanMX4) defective in a Cu-binding transcription factor for the activation of the metallothionein genes; cadmium (Cd)-sensitive mutant Δ*ycf1* (MATa; his3Δ1; leu2Δ0; met15Δ0; ura3Δ0; YDR135c::kanMX4) defective in vacuolar Cd sequestration; and cobalt (Co)-sensitive mutant Δ*cot1* (MATa; his3Δ1; leu2Δ0; met15Δ0; ura3Δ0; YOR316c::kanMX4) defective in Co efflux into the vacuole, were purchased from Euroscarf.[6] All strains are isogenic to wild-type BY4741 (MATa; his3D1; leu2D0; met15D0; ura3D0) and are able to grow under the same conditions.

To contract yeast expression plasmid, the ORF of *GmMTP8.1* was amplified from root cDNA using *GmMTP8.1-pYES2-F/R* primers (**Supplementary Table 1**). The PCR product was digested with *Bam*HI and *Eco*RI, and was then inserted in the same sites of the yeast expression vector *pYES2* (Invitrogen, United States). After that, the *pYES2-GmMTP8.1* construct and *pYES2* empty vector were transformed separately into yeast cells using the LiOAc/PEG method (Gietz and Schiestl, 2007). For metal complementation analysis, yeast transformants were pre-cultured in a liquid synthetic complete medium containing a yeast nitrogen base, amino acids without uracil, and glucose (SC-U/Glu) at 30°C until the optical density (OD) at 600 nm reached a value of 0.6. Pre-cultured cells were diluted to an OD600 of 0.2, and 10-μl aliquots of dilutions (OD at 600 nm of 0.02, 0.002, and 0.0002) were spotted onto induction plates containing 2% (w) Gal, 1% (w/v) raffinose, 0.67% (w/v) yeast nitrogen base without amino acids, 0.1% (w/v) amino acids without uracil, and 2% (w/v) agar, according to Chen et al. (2015). The induction plates were added with 5 mM $MnSO_4$, 15 mM $ZnSO_4$, 100 μM $CuSO_4$, 50 μM $CdCl_2$, and 2 mM $CoCl_2$ for metal complementation analyses of the yeast mutants Δ*pmr1*, Δ*zrc1*, Δ*cup2*, Δ*ycf1*, and Δ*cot1*, respectively. A control drop assay was performed on the same solid medium without the addition of metals. After incubation at 30°C for 2 days in the dark, the plates were photographed.

Functional Analysis of *GmMTP8.1* in Arabidopsis

To construct the *pYLRNAi-GmMTP8.1* plasmid, the ORF of *GmMTP8.1* was amplified by PCR from root cDNA using *GmMTP8.1-OE-F/R* primers (**Supplementary Table 1**). The amplified product was digested with *Bam*HI and *Mlu*I, and subcloned further into the same site of the *pYLRNAi* vector with the *hygromycin phosphotransferase* (*HPT*) gene as the selective marker, according to Liang et al. (2010). The *pYLRNAi-GmMTP8.1* construct was transformed into *A. tumefaciens* strain Gv3101 using the freeze-thaw method. The transformed Gv3101 cells harboring the *pYLRNAi-GmMTP8.1* construct were grown further in a yeast extract peptone (YEP) medium overnight at 28°C until OD600 reached 1 before transformation. Four-week-old Columbia Arabidopsis ecotype (wild type) was used for *Agrobacterium*-mediated transformation with the floral dip method, as described by Clough and Bent (1998). Seeds of the putative transformed Arabidopsis were selected in a half-strength Murashige and Skoog (MS) solid medium containing 20 mg/L hygromycin for two generations. More than 10 T2 transgenic Arabidopsis lines were resistant to hygromycin with a 3:1 ratio. Finally, two homozygous T3 transgenic lines overexpressing *GmMTP8.1* were selected based on both qRT-PCR using *GmMTP8.1-RT-F/R* primers (**Supplementary Table 1**) and Western blot analysis using an anti-HPT antibody.

To assess the effects of excess Mn on the growth of Arabidopsis, seeds of the wild-type Arabidopsis and two *GmMTP8.1*-overexpression lines (OE1/2) were surface-sterilized and then germinated in an MS solid medium. Arabidopsis plants were grown in a growth chamber under conditions of 16-h light at 23°C/8-h dark at 20°C, 150 μmol m^{-2} s^{-1} photon flux density, and 70% relative humidity. After 7 days of normal growth, uniform seedlings with about 2-cm-long tap root were selected and transplanted into a fresh MS solid medium supplied with 0.1, 2 or 4 mM $MnSO_4$, as described by Chen et al. (2015). Arabidopsis plants treated with 0.1 mM $MnSO_4$ were set as the control. After 7 days of Mn treatments, the plants were thoroughly rinsed with 10 mM EDTA and dH_2O. Shoots, roots, and whole plants were harvested separately to determine fresh weight and Mn concentration.

In addition, after 7 days of germination in the MS solid medium as described above, The Arabidopsis plants were transplanted into a hydroponic nutrient solution containing 0.25 mM $Ca(NO_3)_2$, 1 mM KH_2PO_4, 0.5 mM KNO_3, 1 mM $MgSO_4$, 50 μM Fe(III)-Na-EDTA, 50 μM H_3BO_3, 18 μM $MnSO_4$, 1 μM $CuSO_4$, 10 μM $ZnSO_4$, and 0.02 μM MoO_4Na_2 for 14 days, according to Cailliatte et al. (2010). Subsequently, 21-day-old Arabidopsis plants were transplanted into a nutrient solution containing 18 and 400 μM $MnSO_4$ as control and excess Mn treatments, respectively. After 7 days of Mn treatments, the plants were rinsed with 10 mM EDTA and dH_2O. Shoots

[6] http://www.euroscarf.de/search.php?name=Order

and roots were harvested separately to determine fresh weight and Mn concentration. All the treatments included three biological replicates.

Analysis of Manganese Concentration

The plant samples were oven dried at 105°C for 30 min and dried further at 75°C for 5 days. Dry samples were ground into powder before Mn assay. Approximately 0.07 g of the dry samples was thoroughly burned to ash at 600°C for 10 h in a muffle furnace, according to Chen Z. et al. (2016). After cooling to room temperature, the ash sample was mixed with 7 ml of 100 mM HCl. The mixture was fully dissolved by continuous shaking for 2 days. The solution was then used to analyze Mn concentration *via* atomic absorption spectroscopy. A certified reference material, GBW07603 (bush branches and leaves) approved by Institute of Geophysical and Geochemical Exploration, Chinese Academy of Geological Sciences, China, was used to validate the extraction and measurement. Mn concentration was calculated by comparison with a standard curve.

Western Blot Analysis

Proteins from wild-type and *GmMTP8.1*-overexpression Arabidopsis (OE1/2) were extracted separately using an extraction buffer containing 100 mM Tris–HCl (pH 8), 0.5% (w/v) PVPP, 1 mM EDTA, and 1 mM PMSF. After centrifugation at 12,000 × *g* for 15 min at 4°C, supernatants were collected. Thirty μg of extracted protein was resolved by 12% SDS-PAGE and electrophoretically transferred further to a polyvinylidene difluoride (PVDF) membrane (Merck Millipore, United States) through a Trans-Blot system (Bio-Rad, United States), according to Liang et al. (2010). After that, the PVDF membrane was incubated in a 10-mM Tris–HCl buffer (pH 8) containing 5% (w/v) non-fat dry milk and 150 mM NaCl for 12 h. The PVDF membrane was then washed three times with a washing solution containing 10 mM Tris–HCl (pH 8), 150 mM NaCl, and 0.1% (v/v) Tween 20. Blotting of the PVDF membrane was performed by incubation with an anti-HPT primary antibody (1:1,000 dilution) in a blotting buffer containing 10 mM Tris–HCl (pH 8), 150 mM NaCl, 0.1% (v/v) Tween 20, and 3% (w/v) non-fat dry milk for 1 h, followed by three washes with a washing buffer. An alkaline phosphatase-tagged secondary antibody was then added into the fresh blotting buffer, where the PVDF membrane was incubated for 1 h. After three washes with the washing buffer, the band of target protein in the PVDF membrane was observed after alkaline phosphatase reaction.

Statistical Analyses

The SPSS program v13.0 (SPSS Institute, United States) was used to perform one-way ANOVA and Student's *t*-test analyses.

RESULTS

Soybean Growth Inhibited by Manganese Toxicity

To investigate the toxic effects of Mn on soybean growth, 14-day-old soybean seedlings were exposed to different Mn treatments for 7 days. The results showed that excess Mn treatments (50 and 100 μM) resulted in the generation of brown spots on mature leaves compared to the control (5 μM Mn) (**Figure 1A**). Moreover, the number of brown spots with the 100 μM Mn treatment was 1.8-fold higher than that with the 50-μM Mn treatment (**Figure 1A**). In contrast, chlorophyll levels, indicated by SPAD values in leaves, were decreased by 15.7 and 39.9% with the 50- and 100-μM Mn treatments, respectively, compared to the control (**Figure 1B**). Although both shoot and root fresh weights were unaffected by the 50-μM Mn treatment, they were significantly decreased by more than 24% with100 μM Mn compared to the control (**Figure 1C**). In addition, increases in Mn concentrations were observed in shoots and roots of soybean under excess Mn treatments. Mn concentrations in shoots at 50 and 100 μM Mn were 79.8–175.3% higher than 5-μM Mn treatments, while Mn levels in roots at 50 and 100 μM Mn were 70.7–269.1% higher than the controls (**Figure 1D**). Furthermore, Mn concentrations in roots were more than 155% higher than in shoots under excess Mn stress (50 and 100 μM) (**Figure 1D**).

Identification of *GmMTP* Genes in Soybean

In this study, a total of 14 putative *GmMTP* genes were identified in the soybean genome. The 14 *GmMTP* genes were named from *GmMTP4.1* to *GmMTP11.2* based on the phylogenetic relationship and sequence identity between GmMTP and Arabidopsis AtMTPs (**Supplementary Table 2**). General information for the 14 *GmMTP* members is summarized in **Supplementary Table 2**. Most of the GmMTP members contained three to six conserved TMDs, except GmMTP10.1, which harbored only two TMDs (**Supplementary Table 2**). The 14 *GmMTP* genes can be classified into three distinct groups according to their sequence structure features (**Supplementary Figure 1**). Furthermore, most GmMTPs contained both the cation efflux (PF01545) and zinc transporter (ZT) dimer (PF16916) conserved motifs, except GmMTP4.1 and GmMTP4.2, which only contained the cation efflux motif (**Figure 2** and **Supplementary Table 3**).

Phylogenetic analysis showed that plant MTPs can be classified into three distinct clusters, namely, Zn-CDF, Zn/Fe-CDF, and Mn-CDF, which were further divided into seven subgroups (**Figure 3**). Of the seven subgroups, group 9 had the largest number of plant MTPs, followed by groups 1 and 8. A total of 12 GmMTPs were classified into groups 8 and 9, both of which belonged to the Mn-CDF cluster (**Figure 3**). Among them, five GmMTPs (GmMTP8.1, GmMTP8.2, GmMTP8.3, GmMTP8.4, and GmMTP8.5) clustered with ShMTP8 from *S. hamata*, AtMTP8 from Arabidopsis, OsMTP8.1/8.2 from rice, CsMTP8 from cucumber, HvMTP8.1/8.2 from barley (*Hordeum vulgare*), and CasMTP8.1/8.2 from tea plant (*Camellia sinensis*) in group 8. Seven GmMTPs, namely, GmMTP9.1, GmMTP10.1, GmMTP10.2, GmMTP10.3, GmMTP10.4, GmMTP11.1, and GmMTP11.2, together with OsMTP9/11/11.1 from rice, CsMTP9 from cucumber, AtMTP11 from Arabidopsis, PtMTP11.1/11.2 from poplar, and BmMTP10/11 from *B. vulgaris* ssp. *maritima*, were divided into group 9 (**Figure 3**). In addition, GmMTP4.1

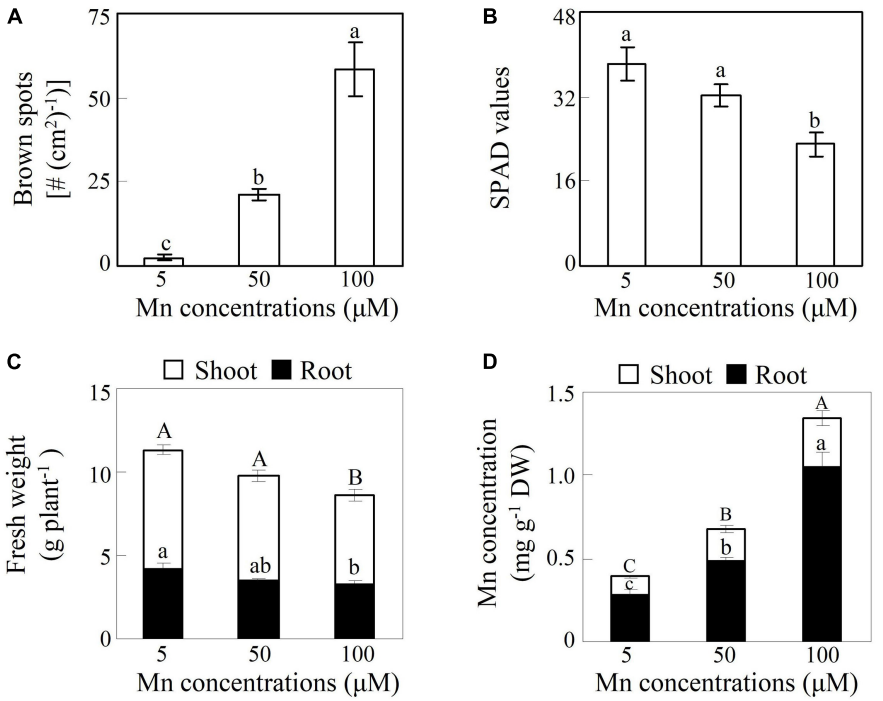


FIGURE 1 | Effects of excess manganese (Mn) treatment on soybean growth. **(A)** Number of brown spots. **(B)** Soil plant analysis development (SPAD) values. **(C)** Fresh weight. **(D)** Mn concentrations. Fourteen-day-old soybean seedlings were treated with 5, 50, and 100 μM $MnSO_4$ for 7 days. Five μM $MnSO_4$ was used as the control. Chlorophyll levels were detected with SPAD-502 meter. Each bar represents the means of four independent replicates with standard error. Different lower case letters indicate significant differences at $P < 0.05$ among Mn treatments in panels **(A,B)**. Different upper case or lower case letters indicate significant differences at $P < 0.05$ among Mn treatments in shoot or root in panels **(C,D)**. White and black bars represent shoot and root, respectively.

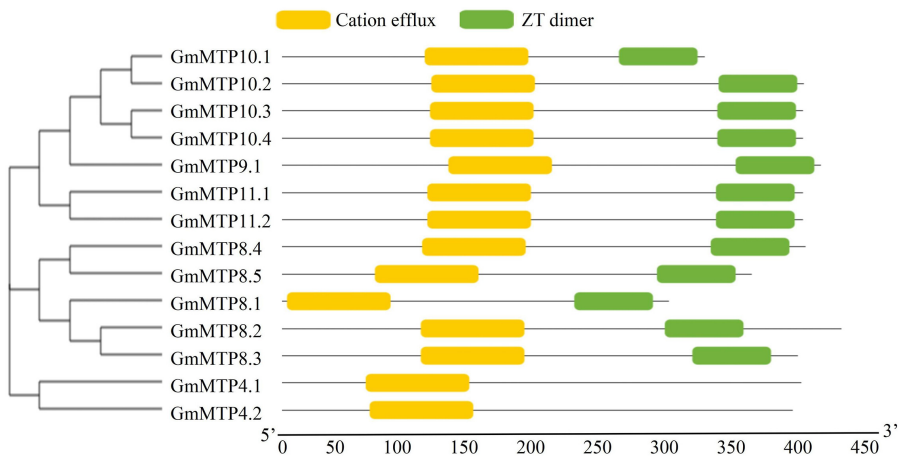


FIGURE 2 | Conserved motifs in GmMTPs. Yellow and green boxes indicate cation efflux and ZT dimer motifs, respectively. The neighbor-joining phylogenetic tree of GmMTPs was constructed using MEGA4.1.

and GmMTP4.2 were classified into group 1 within the Zn-CDF cluster (**Figure 3**). Interestingly, none of the GmMTP members were classified into the Fe/Zn-CDF cluster (**Figure 3**).

Expression Analysis of *GmMTP* Genes

We subsequently analyzed the expression patterns of *GmMTP* genes in leaves, stems, and roots of 21-day-old soybean seedlings under normal growth conditions. The results showed that *GmMTPs* exhibited differential expressions in various tissues of soybean (**Figure 4**). Among them, three *GmMTPs* (*GmMTP4.1*, *GmMTP10.2*, and *GmMTP11.1*) showed highest expression in leaves, while 10 *GmMTPs* (*GmMTP4.2*, *GmMTP8.1*, *GmMTP8.2*, *GmMTP8.3*, *GmMTP8.4*, *GmMTP9.1*, *GmMTP10.1*, *GmMTP10.3*, *GmMTP10.4*, and *GmMTP11.2*)

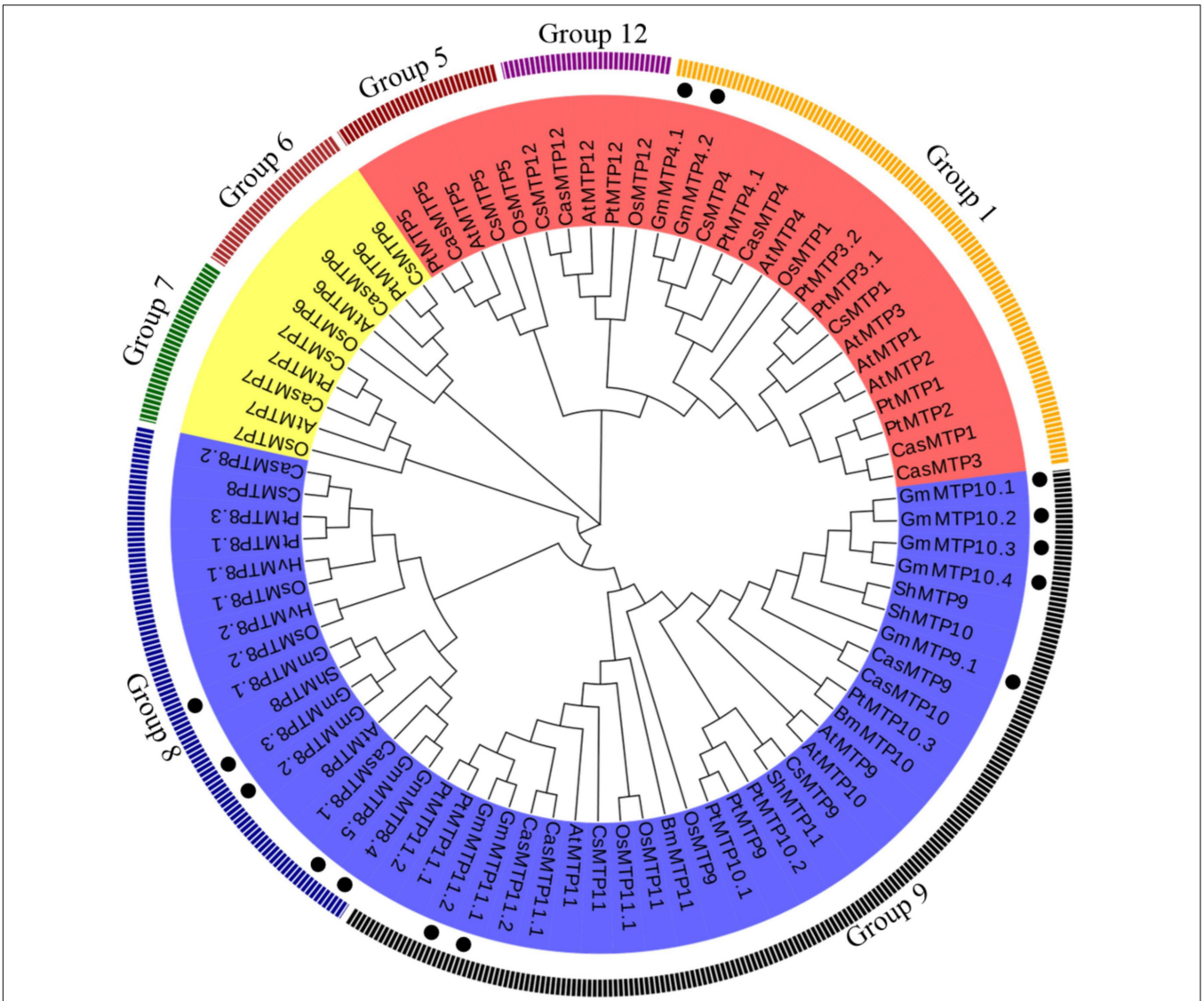


FIGURE 3 | Phylogenetic analysis of metal tolerance proteins (MTPs) in soybean and other plants. The phylogenetic tree was constructed using the MEGA4.1 program. Except for *CasMTPs* derived from tea plant (*Camellia sinensis*), the first two letters of each protein represent the abbreviated species name. At: *Arabidopsis thaliana*, Os: *Oryza sativa*, Gm: *Glycine max*, Cs: *Cucumis sativus*, Hv: *Hordeum vulgare*, Pt: *Populus trichocarpa*, Sh: *Stylosanthes hamata*, and Bm: *Beta vulgaris*. ssp. *maritima*. MTPs from various plant species are divided into the Zn-CDF, Fe/Zn-CDF, and Mn-CDF clusters, which are highlighted in red, yellow, and blue, respectively. Plant MTPs can be further classified into seven subgroups. The solid circles indicate MTPs from soybean.

were mainly expressed in roots (**Figure 4**). Interestingly, most of the *GmMTP* genes exhibited low expressions in stems, except *GmMTP8.5* with the highest expression in stems compared to leaves or roots (**Figure 4**). Furthermore, the transcript of *GmMTP4.1* in leaves was higher than that of the other *GmMTPs*, while *GmMTP10.3* exhibited the highest expression in roots compared to the other *GmMTPs* (**Figure 4**).

Expressions of the *GmMTPs* in leaves and roots in response to Mn toxicity were investigated. As shown in **Figure 5**, all *GmMTPs* responded to excess Mn in leaves and/or roots, and the number of *GmMTPs* regulated by Mn stress in roots (12 *GmMTPs*) was higher than those in leaves (9 *GmMTPs*). For example, two *GmMTPs* (*GmMTP10.3* and *10.4*) were enhanced and six *GmMTPs* (*GmMTP4.1*, *GmMTP4.2*, *GmMTP8.1*, *GmMTP8.5*, *GmMTP11.1*, and *GmMTP11.2*) were suppressed in leaves by the 50- and/or 100-μM Mn treatments. In contrast, most *GmMTPs* (*GmMTP4.1*, *GmMTP4.2*, *GmMTP8.1*, *GmMTP8.2*, *GmMTP8.3*, *GmMTP8.5*, *GmMTP9.1*, *GmMTP10.3*, and *GmMTP10.4*) were enhanced and only three *GmMTPs* (*GmMTP8.4*, *GmMTP10.2*, and *GmMTP11.2*) were suppressed in roots by the 50- and/or 100-μM Mn treatments (**Figure 5**). Interestingly, the transcripts of *GmMTP10.3*, *GmMTP10.4*, and *GmMTP11.2* regulated by Mn in roots were similar to those in leaves (**Figure 5**).

Similar to the regulation by excess Mn stress, the number of *GmMTPs* regulated by excess Fe, Zn, and Cu stresses in roots was higher than those in leaves (**Supplementary Figure 2**).

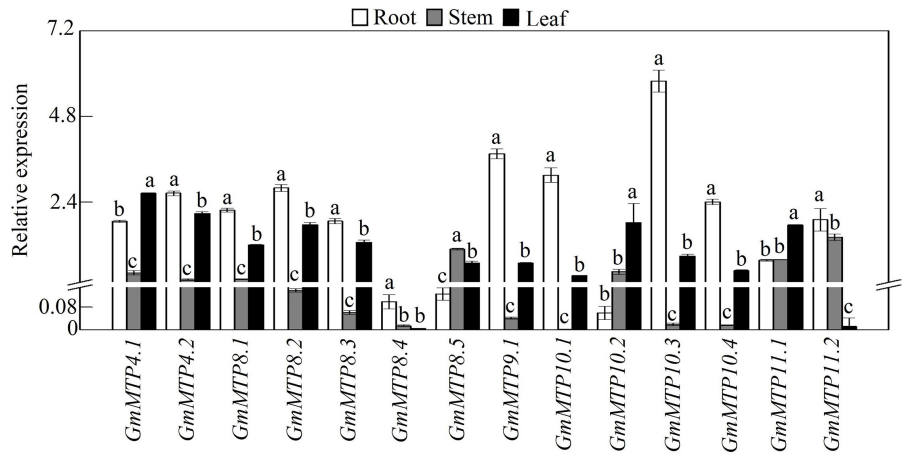


FIGURE 4 | Expressions of *GmMTPs* in leaf, stem, and root of soybean. After seeds were germinated for 7 days, the seedlings were transplanted into a full-strength Hoagland solution. Leaf, stem, and root were harvested separately after 14 days of growth for gene expression analysis. Each bar represents the mean value of three independent replicates with standard error. White, gray, and black bars represent root, stem, and leaf, respectively. Different lower case letters indicate significant differences at $P < 0.05$ in the same tissue.

For example, in roots, a total of 13, 12, and 11 *GmMTPs* were regulated by Fe, Zn, and Cu stresses, respectively. In leaves, 7, 9, and 9 *GmMTPs* were found to be regulated by Fe, Zn, and Cu stresses, respectively. Furthermore, most of the *GmMTP* genes were regulated by at least one metal stress in both leaves and roots, except *GmMTP9.1*, *GmMTP10.4*, and *GmMTP11.2* that were not responsive in leaves to any of the three tested metals (**Supplementary Figure 2**). Interestingly, five *GmMTPs* (*GmMTP4.1*, *GmMTP4.2*, *GmMTP8.3*, *GmMTP8.4*, and *GmMTP10.2*) were simultaneously suppressed, and three *GmMTPs* (*GmMTP4.1*, *GmMT8.5*, and *GmMT10.1*) were concurrently enhanced in leaves and roots by all the three metals, respectively (**Supplementary Figure 2**).

Subcellular Localization of GmMTP8.1

In this study, GmMTP8.1, a member of group 8 within the Mn-CDF cluster (**Figure 3**), displayed highest similarity with ShMTP8 in *S. hamata* that has been well-characterized for its involvement in Mn detoxification by the sequestration of Mn into vacuoles, was further selected to dissect its function in Mn detoxification. The GmMTP8.1 protein includes 294 amino acid residues (33.1 kDa) and possesses common features of Mn-CDF transporters, such as four putative TMDs, cation efflux, and ZT dimer domains (**Figure 2** and **Supplementary Table 2**). The consensus sequence DxxxD (x = any amino acid) localizes to the first TMD and the cytosolic loop of GmMTP8.1 (**Supplementary Figure 3**). In addition, based on amino acid sequence comparisons, GmMTP8.1 shares a high degree of homology identity (90.8%) with ShMTP8 in *S. hamata*, and shares 83.3% identity with HvMTP8.1 in barley, 83% identity with OsMTP8.1 in rice, 83% identity with CsMTP8 in cucumber, and 81% identity with AtMTP8 in Arabidopsis, which were the representative MTP8-like proteins included in group 8 (**Supplementary Figures 3–5**). This suggests that the role of GmMTP8.1 is similar to that of the MTP homologs.

We further analyzed the subcellular localization of GmMTP8.1 in tobacco epidermis cells. The results showed that the GFP signal of GmMTP8.1 was found to be co-localized with that of the ER marker but not localized in the tonoplast of tobacco leaf epidermal cells, whereas the fluorescence of cells transformed with GFP alone was observed in whole cells, such as plasma membrane, cytoplasm, and nucleus (**Figures 6A,B**). Thus, these results suggest that GmMTP8.1 is localized to the ER.

Metal Transport Activity of GmMTP8.1 in Yeast Cells

A complementation assay of yeast mutants was further conducted to investigate the metal transport activity of GmMTP8.1, which was heterologously expressed in five yeast mutants that are defective in transport activity of various metals, namely, Mn (Δ*pmr1*), Zn (Δ*zrc1*), Cu (Δ*cup2*), Cd (Δ*ycf1*), and Co (Δ*cot1*). The results showed that the yeast mutants carrying either the *pYES2* empty vector or the *pYES2-GmMTP8.1* construct grew similarly in the control medium (**Figure 7**). However, the growth of the five yeast mutants transformed with the *pYES2* empty vector was inhibited in the medium containing high or toxic metal levels (**Figure 7**). Furthermore, although the growth of the yeast mutants Δ*zrc1*, Δ*cup2*, Δ*ycf1*, and Δ*cot1*, transformed with the *pYES2-GmMTP8.1* construct, was suppressed in the corresponding metal treatments, *GmMTP8.1* expression rescued the sensitivities to excess Mn in the Δ*pmr1* mutant (**Figure 7**), suggesting that *GmMTP8.1* is a specific Mn transporter.

Overexpression of *GmMTP8.1* Enhanced Manganese Tolerance and Reduced Manganese Accumulation in Arabidopsis

Subsequently, transgenic Arabidopsis overexpressing *GmMTP8.1* was generated to investigate the roles of *GmMTP8.1* in Mn

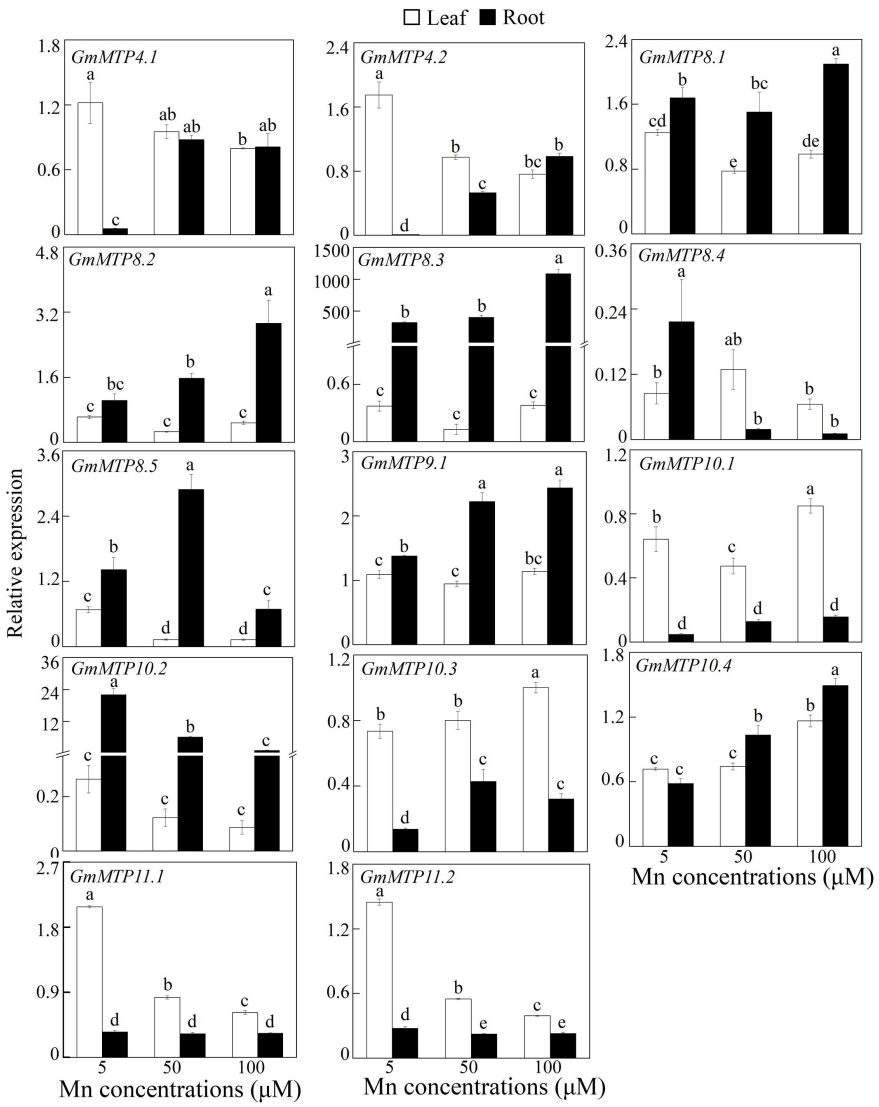


FIGURE 5 | Expressions of *GmMTPs* in leaf and root of soybean under excess Mn treatments. Fourteen-day-old soybean seedlings were transferred into a nutrient solution containing 5, 50, or 100 μM $MnSO_4$. Five μM $MnSO_4$ was used as the control. After 7 days of Mn treatment, leaves and roots were harvested separately for gene expression analysis. Each bar represents the mean value of three independent replicates with standard error. White and black bars represent leaf and root, respectively. Different lower case letters indicate significant differences at $P < 0.05$.

detoxification in the plants. Increased transcripts of *GmMTP8.1* in the overexpression lines (OE1 and OE2) compared to the wild-type (WT) were confirmed by RT-PCR analysis (**Supplementary Figure 6A**). Western-blot analysis indicated further that the GmMTP8.1 protein was expressed in transgenic Arabidopsis (**Supplementary Figure 6B**). WT and transgenic Arabidopsis were exposed to different levels of Mn, from 0.1 to 4 mM, in an MS solid medium for 7 days. As shown in **Figure 8A**, no difference in Arabidopsis growth was observed between the *GmMTP8.1* overexpression lines (OE1 and OE2) and WT under control conditions containing 0.1 mM Mn. Although excess Mn (2 mM and 4 mM Mn) applications inhibited the growth of both overexpression lines and WT, the overexpression lines exhibited a higher level of tolerance to excess Mn than WT, especially with the 4-mM Mn treatment (**Figure 8A**). Shoot, root, and whole plant fresh weight of the overexpression lines were 46.6-65.2, 19.7-24.5, and 62.2-94.8%, respectively, higher than those of WT with the 4-mM Mn treatment (**Figures 8B-D**). In contrast, the overexpression of *GmMTP8.1* resulted in significantly decreased Mn accumulation in shoots and whole plants of transgenic Arabidopsis exposed to the 4-mM Mn treatment, although no differences in root Mn accumulation were observed between WT and the transgenic lines (**Figures 8E-G**). Mn concentrations in shoots of the overexpression lines were 32.2–53.5% lower than those found in WT grown at 4 mM Mn (**Figure 8E**). Furthermore, total Mn concentrations in the transgenic Arabidopsis plants

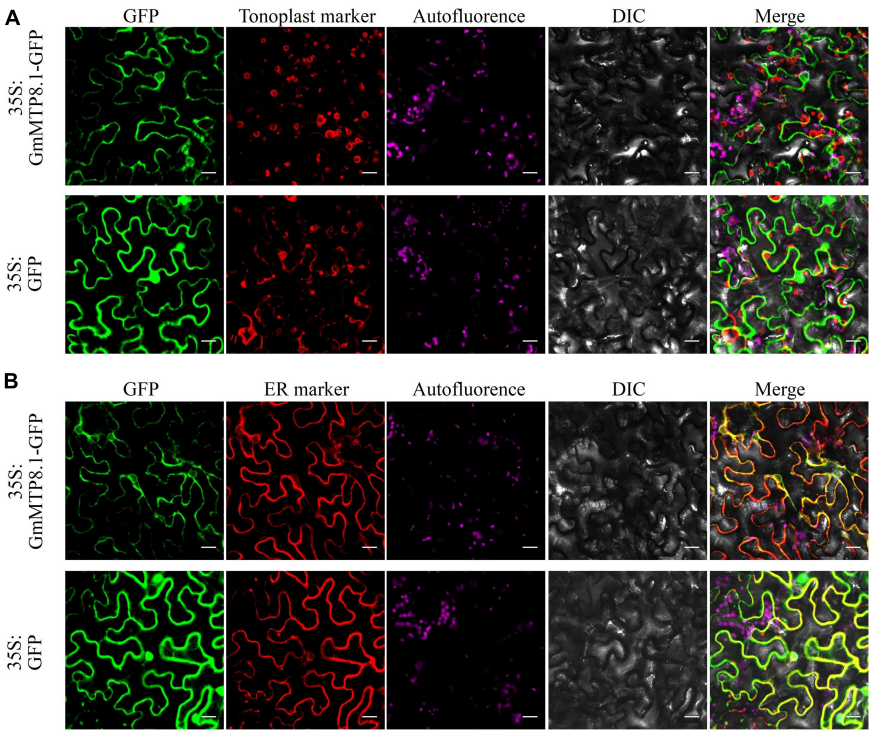


FIGURE 6 | Subcellular localization of GmMTP8.1 in tobacco leaf lower epidermal cells. The images are labeled to show the *35S:GFP* and *35S:GFP-GmMTP8.1* constructs. *35S:GFP-GmMTP8.1* was co-expressed with the **(A)** tonoplast marker TPK1 and **(B)** endoplasmic reticulum marker PIN5 fused with red fluorescence protein (mKATE) in tobacco leaf epidermal cells. green fluorescent protein (GFP) fluorescence, red fluorescent protein (RFP) fluorescence, chloroplast autofluorescence, bright field images, and merged images are displayed from left to right. Fluorescence was observed by confocal microscopy. Scale bar is 20 μm.

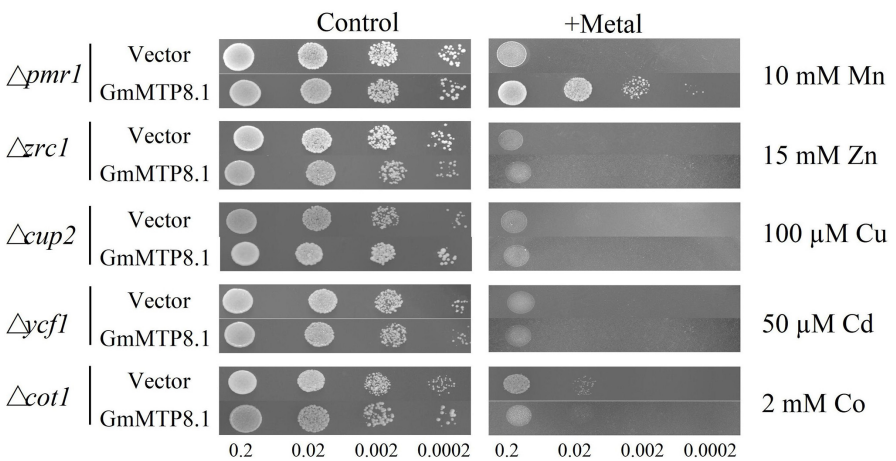


FIGURE 7 | Heterologous expression of *GmMTP8.1* in different yeast mutants. The yeast mutants Δ*pmr1*, Δ*zrc1*, Δ*cup2*, Δycf1, and Δ*cot1* harboring the *pYES2* empty vector or the *pYES2-GmMTP8.1* construct were used. Yeast cells (10 μl) with OD600 of 0.2 and four serial dilutions (10-fold) were spotted in SC-U/Gal medium added with or without 5 mM $MnSO_4$, 15 mM $ZnSO_4$, 100 μM $CuSO_4$, 50 μM $CdCl_2$, and 2 mM $CoCl_2$ for 2 day at 30°C.

were 44–45% less than those in WT exposed to 4 mM Mn treatment (**Figure 8G**).

In addition, we also assessed the effects of excess Mn on the growth of transgenic Arabidopsis in hydroponics. After growing in a nutrient solution containing 18 or 400 μM $MnSO_4$ for 7 days, the transgenic lines exhibited improved Mn tolerance compared to the WT (**Supplementary Figure 7**). Under the 400-μM Mn treatment, shoot fresh weight of the overexpression lines was more than 53% higher than that of the WT, although root fresh weight was similar between the transgenic lines and WT (**Supplementary Figure 7**). Consistent with Mn concentration in Arabidopsis grown in the MS solid medium, a low level

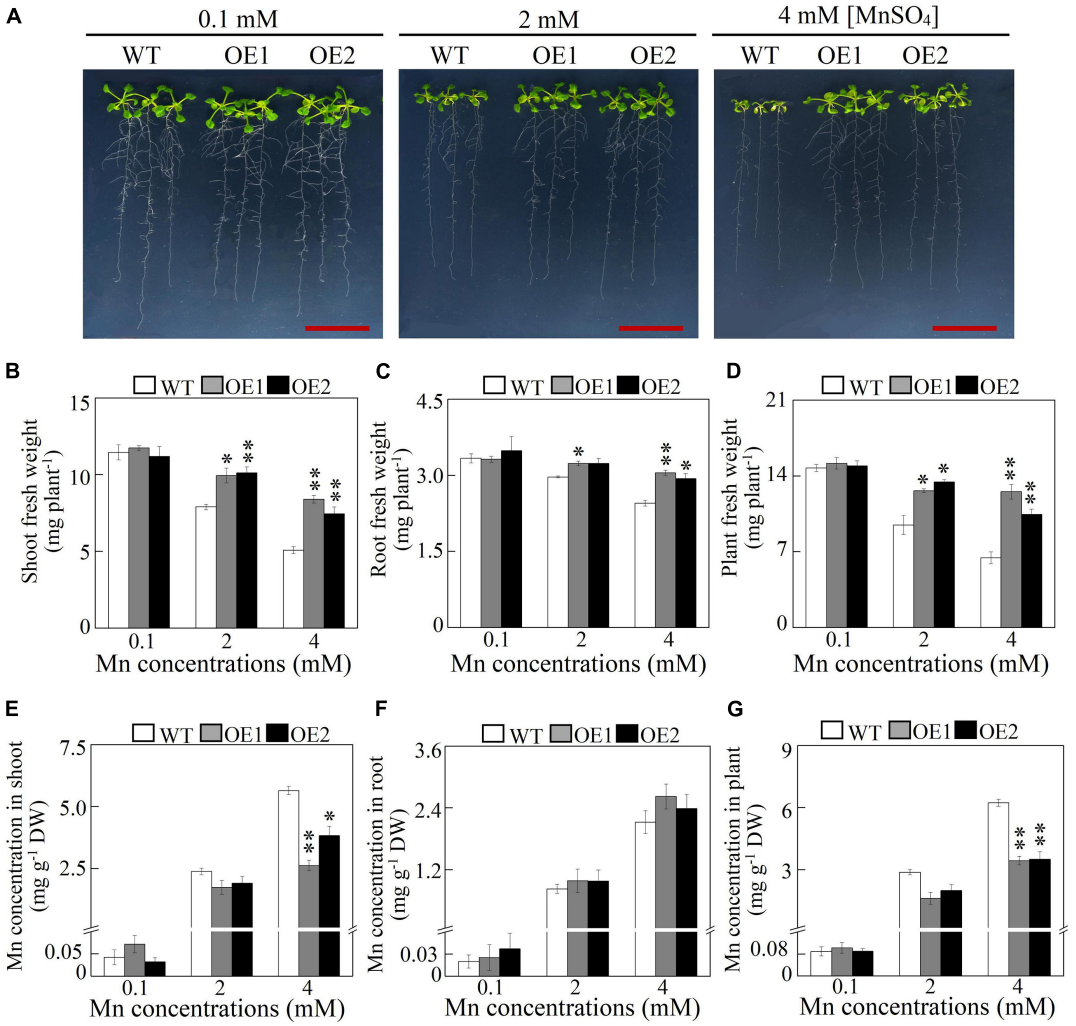


FIGURE 8 | Growth and Mn concentration of Arabidopsis overexpressing *GmMTP8.1*. **(A)** Phenotype of Arabidopsis grown with different Mn treatments. **(B)** Shoot fresh weight. **(C)** Root fresh weight. **(D)** Plant fresh weight. **(E)** Mn concentration in shoot. **(F)** Mn concentration in root. **(G)** Mn concentration in plant. Seven-day-old Arabidopsis seedlings were transferred to a solid Murashige and Skoog (MS) medium containing 0.1, 2, or 4 mM $MnSO_4$. Arabidopsis plants treated with 0.1 mM $MnSO_4$ were set as the control. After 7 days of Mn treatment, fresh weight and Mn concentration were determined. WT represents the wild type Arabidopsis. OE1 and OE2 are two transgenic lines overexpressing *GmMTP8.1*. Each bar represents the mean value of three independent replicates with standard error. White, gray, and black bars represent WT, OE1, and OE2, respectively. Asterisks indicate significant differences between the wild type and the overexpression lines with the same Mn treatment. *, $0.01 < P < 0.05$. **, $0.001 < P < 0.01$. DW, dry weight. Scale bar is 2 cm.

of Mn concentration in shoots but not roots was observed in transgenic Arabidopsis compared to the WT, exposed to the 400-μM Mn treatment (**Supplementary Figure 7**). These results, together, suggest that the overexpression of *GmMTP8.1* confers Mn tolerance in Arabidopsis mainly by decreasing accumulation of Mn.

Manganese Transporters Are Upregulated by Overexpression of *GmMTP8.1* in Arabidopsis

To investigate the mechanisms involved in decreased Mn in the shoots but unchanged level of Mn in the roots of transgenic Arabidopsis, the transcript levels of 17 Mn transporter genes were determined in transgenic Arabidopsis overexpressing *GmMTP8.1*. These Mn transporters included genes encoding metal tolerance proteins (*AtMTP8/11*), calcium exchangers (*AtCAX2/4/5*), ER-type calcium (Ca^{2+})-ATPases (*AtECA1/3*), iron-regulated transporter (*AtIRT1*), natural resistance-associated macrophage proteins (*AtNRAMP1/3/4*), zinc transporters (*AtZIP1/2*), yellow stripe-like proteins (*AtYSL4/6*), and heavy metal ATPases (*AtHMA2/4*). The qRT-PCR analysis showed that the overexpression of *GmMTP8.1* led to a significant increase (>2-fold) in the transcripts of *AtMTP11*, *AtNRAMP3*, and *AtECA3* in leaves of the two transgenic lines (**Figure 9**). However, among the tested genes, only *AtMTP8* exhibited about 2.1-fold induction in roots of the transgenic Arabidopsis (**Figure 9**). The upregulation of these Mn transporters might

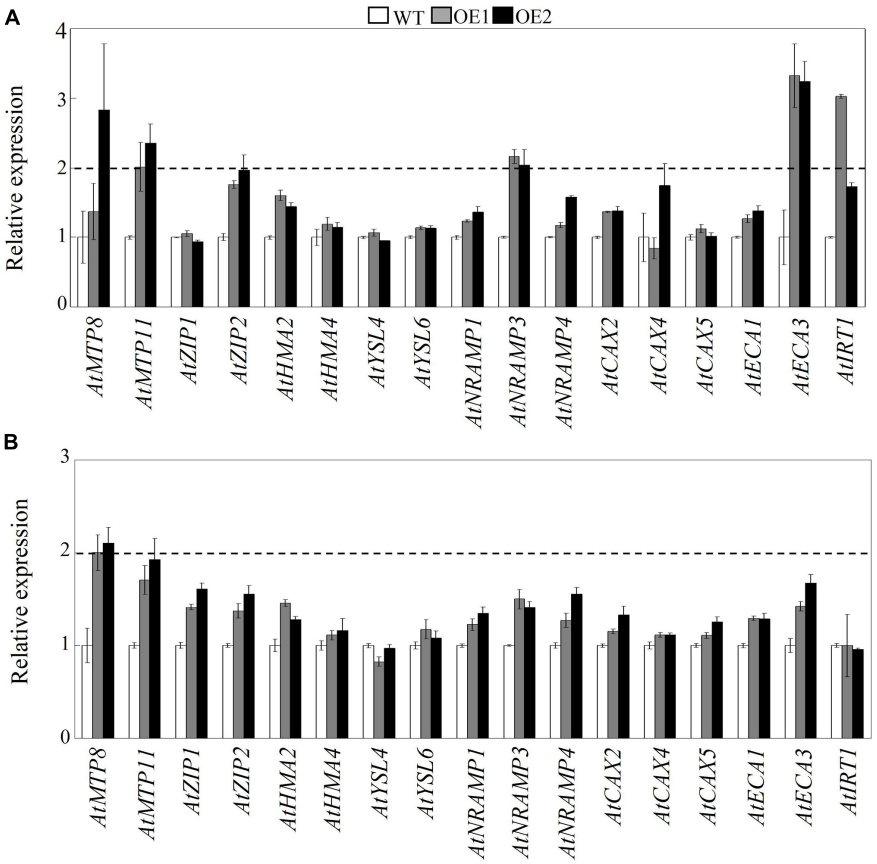


FIGURE 9 | Effects of *GmMTP8.1* overexpression on the transcript levels of Mn transporter genes in Arabidopsis. **(A)** Gene expression in leaves. **(B)** Gene expression in roots. Seven-day-old seedlings were transferred to a solid MS medium containing 4 mM $MnSO_4$ for 7 days. Leaves and roots were sampled for RNA extraction and real-time (RT)-polymerase chain reaction (PCR) analysis. WT represents the wild type Arabidopsis. OE1 and OE2 are two transgenic lines overexpressing *GmMTP8.1*. Each bar represents the mean value of three independent replicates with standard error. White, gray, and black bars represent WT, OE1, and OE2, respectively. The relative expression level of gene of more than 2-fold was regarded as significant difference between the wild type and the overexpression lines.

contribute to the regulation of Mn homeostasis and tolerance in transgenic Arabidopsis.

DISCUSSION

Manganese is a trace element that can cause phytotoxicity when present in excess (Millaleo et al., 2010; Li et al., 2019). Excess Mn disrupts various physiological processes in plants. For example, Mn toxicity causes oxidative stress and lipid peroxidation in cowpea (*Vigna unguiculata*) and cucumber (Fecht-Christoffers et al., 2006; Dragišić Maksimović et al., 2012), inhibits chlorophyll biosynthesis and photosynthesis in *Stylosanthes guianensis* (Liu P. et al., 2019; Jia et al., 2020), and disturbs the homeostasis of other nutrients in polish wheat (*Triticum polonicum*) (Sheng et al., 2015). In this study, excess Mn treatments led to increase in Mn levels in soybean, which was accompanied by increased number of brown spots and decreased chlorophyll concentrations, ultimately reducing plant fresh weight of the 14-day-old soybean seedlings (**Figure 1**). Similar results have been found in previous studies where soybean growth was inhibited by Mn toxicity (Chen Z. et al., 2016; Santos et al., 2017; Liu et al., 2020), although different growth stages of soybean were applied. Furthermore, important roles of antioxidant systems, such as antioxidant enzymes and non-enzymatic components, have been suggested in the response of soybean to Mn toxicity (Chen Z. et al., 2016; Santos et al., 2017; Liu et al., 2020). Although some advances have been made in investigating the response of soybean to Mn toxicity, its potential molecular mechanisms involved in Mn tolerance have not been elucidated.

Plant MTPs have been documented to play critical roles in Mn detoxification by Mn sequestration or efflux from plant cells (Li et al., 2019, 2021; Alejandro et al., 2020). In order to investigate the involvement of *GmMTPs* in the tolerance of soybean to Mn toxicity, we first identified 14 *GmMTP* genes in the soybean genome. Most of them were found to contain the conserved cation efflux and ZT dimer motifs (**Figure 2**). These motifs are reported to be essential for metal transport activities of MTPs (Montanini et al., 2007; Kolaj-Robin et al., 2015; Chen Z. et al., 2016). Cumulative studies demonstrated conserved functions of the MTP homologues in Mn detoxification in various plant species, suggesting similar roles for GmMTPs

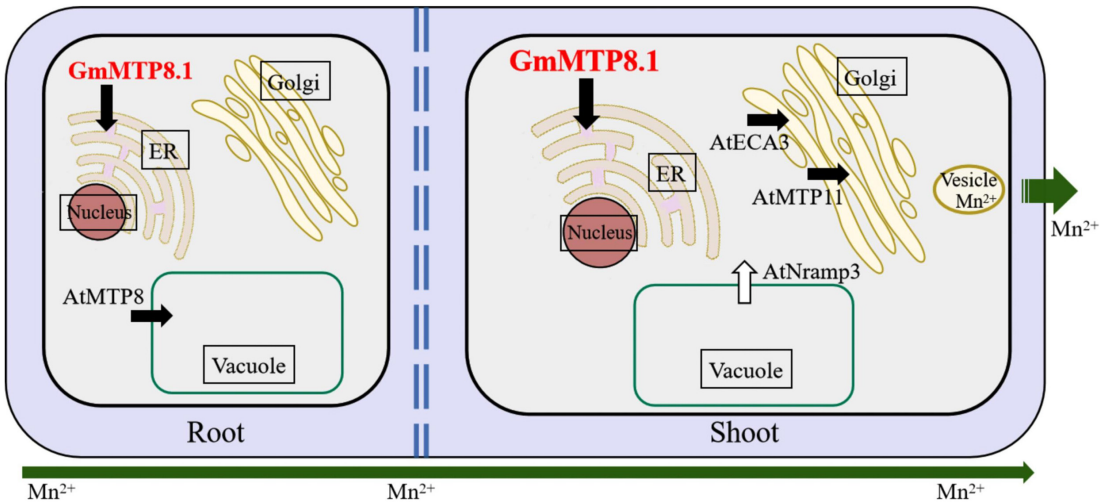


FIGURE 10 | Hypothetical view of GmMTP8.1 affecting Mn tolerance in transgenic Arabidopsis. Endoplasmic reticulum (ER)-localized GmMTP8.1 is involved in Mn transport into the ER, which has probably contributed in reduction of cytosolic Mn and maintenance of Mn homeostasis in transgenic Arabidopsis overexpressing *GmMTP8.1*. Furthermore, cytosolic Mn in leaf can be transported into the Golgi apparatus by the involvement of Golgi-localized AtMTP11 and ECA3, and then sequestered into vesicles and removed from the cell *via* exocytosis, thereby decreasing cellular Mn levels in shoot. The upregulation of *AtNRAMP3* might also help to maintain Mn homeostasis in leaves of transgenic Arabidopsis. In addition, GmMTP8.1 has likely mediated Mn tolerance, along with AtMTP8, by increasing Mn sequestration into root vacuoles, conferring Mn tolerance. White and black arrows represent import into and export out of the cytosol, respectively.

in Mn tolerance of soybean. According to the phylogenetic analysis, five GmMTPs (GmMTP8.1, GmMTP8.2, GmMTP8.3, GmMTP8.4, and GmMTP8.5) were classified into group 8, and seven GmMTPs (GmMTP9.1, GmMTP10.1, GmMTP10.2, GmMTP10.3, GmMTP10.4, GmMTP11.1, and GmMTP11.2) were classified into group 9 (**Figure 3**). Group 8 contained representative MTPs from other plant species implicated in Mn detoxification mainly through sequestration of Mn by transport into vacuoles, such as ShMTP8 from *S. hamata*, OsMTP8.1/8.2 from rice, CsMTP8 from cucumber (Delhaize et al., 2003; Chen et al., 2013; Migocka et al., 2014; Takemoto et al., 2017). In addition, two MTP8-like proteins from the tea plant have recently been reported to participate in Mn detoxification *via* efflux of Mn from plant cells (Li et al., 2017; Zhang et al., 2020). On the other hand, group 9 also included MTP9/10/11 homologues from Arabidopsis, rice, poplar, and *B. vulgaris* with similar functions in sequestration of Mn into endomembrane compartments or export of Mn out of cells (Peiter et al., 2007; Erbasol et al., 2013; Tsunemitsu et al., 2018a).

Subsequent expression analysis showed that nine *GmMTPs* (*GmMTP4.1*, *GmMTP4.2*, *GmMTP8.1*, *GmMTP8.2*, *GmMTP8.3*, *GmMTP8.5*, *GmMTP9.1*, *GmMTP10.3*, and *GmMTP10.4*) and two *GmMTPs* (*GmMTP10.3* and *GmMTP10.4*) were enhanced by excess Mn in roots and leaves, respectively (**Figure 5**). Similarly, a set of *MTP* homologues engaged in Mn detoxification are also upregulated by excess Mn in leaves or roots, such as *AtMTP8* in Arabidopsis (Eroglu et al., 2016), *CsMTP8/9* in cucumber (Migocka et al., 2014, 2015), *HvMTP8.1* in barley (Pedas et al., 2014), *CasMTP8.1/8.2* in tea plant (Li et al., 2017; Zhang et al., 2020), and *BmMTP10* in *B. vulgaris* (Erbasol et al., 2013). However, the transcripts of *AtMTP11* in Arabidopsis and *OsMTP8.1/8.2* in rice, which are also involved in Mn detoxification (Delhaize et al., 2007; Peiter et al., 2007; Takemoto et al., 2017), are unaffected by excess Mn levels. It is estimated that functions of some of *MTP* members might not depend on external Mn at transcriptional levels but at post-transcriptional levels. For example, although the transcript of *OsMTP8.1* in rice is not affected by excess Mn, the accumulation of OsMTP8.1 protein is significantly increased under excess Mn conditions, contributing to Mn tolerance (Chen et al., 2013).

In this study, five MTP8-like members (GmMTP8.1 to GmMTP8.5) in soybean that clustered closely showed similar structures and homology identities (**Figure 2** and **Supplementary Figures 1**, **5**), which is consistent with the results of phylogenetic analysis (**Figure 3**). However, GmMTP8.1 to GmMTP8.5 possessed different numbers of exons and introns, and GmMTP8.1 had the lowest molecular size (**Supplementary Table 2**). Furthermore, variations in the expression levels of these five *GmMTP8s* were observed in leaves or roots of soybean response to different Mn levels (**Figure 5**). Sequence and gene expression differences among the *GmMTP8s* suggest that these genes may have distinct or redundant biological functions in Mn detoxification. Similarly, although OsMTP8.1 and OsMTP8.2 are two MTP8-like homologues in rice, the abundance of *OsMTP8.1* in shoots is regulated by external Mn levels, and *OsMTP8.2* does not respond to the Mn treatments (Chen et al., 2013; Takemoto et al., 2017). Furthermore, although the disruption of *MTP8.2* does not affect Mn tolerance in rice, the knockdown of *MTP8.2* in the *mtp8.1* mutant results in severe growth inhibition under Mn toxicity conditions (Takemoto et al., 2017), suggesting that OsMTP8.1 coordinates with OsMTP8.2 to increase Mn tolerance in rice. Thus, the five GmMTP8s might possess various functions in soybean response to Mn toxicity, which merits further verification.

A detailed functional analysis of GmMTP8.1, which shares a high degree of homology identity with ShMTP8 (90.8%), OsMTP8.1 (83%), CsMTP8 (83%), and AtMTP8 (81%) (**Supplementary Figures 3–5**), was performed further. GmMTP8.1 contained four TMDs, a signature sequence specific to the CDF family, and two short motifs (DSLLD and DHYFD) specific to the Mn-CDF cluster (**Supplementary Figure 3**). These common features are also present in the reported Mn transporters, such as ShMTP8, CsMTP8, and OsMTP8.1/8.2 (Delhaize et al., 2003; Chen et al., 2013; Migocka et al., 2014; Takemoto et al., 2017), suggesting similar roles of GmMTP8.1 in conferring Mn tolerance. It has been demonstrated that *ShMTP8* in *S. hamata* can complement the phenotype of yeast mutant Δ*pmr1* defective in Mn transport under excess Mn conditions; the overexpression of *ShMTP8* increases Mn tolerance in Arabidopsis by sequestration of Mn into vacuoles (Delhaize et al., 2003). Furthermore, in Arabidopsis, AtMTP8 is found to localize in the tonoplast, and the T-DNA insertion Arabidopsis *mtp8* mutant displays greater sensitivity to excess Mn than the wild type (Eroglu et al., 2016). Similar functions of MTP8-like proteins have also been observed in OsMTP8.1/8.2 in rice and CsMTP8 in cucumber (Chen et al., 2013; Migocka et al., 2014; Takemoto et al., 2017; Zhang et al., 2021). In this study, heterologous expression of *GmMTP8.1* led to restore the growth of the yeast mutant *pmr1* to excess Mn (**Figure 7**), suggesting that GmMTP8.1 is responsible for Mn transport. Furthermore, the overexpression of *GmMTP8.1* conferred Mn tolerance in transgenic Arabidopsis grown in both MS solid medium and hydroponic system (**Figure 8** and **Supplementary Figure 7**). Therefore, GmMTP8.1 contributes to increase tolerance to Mn in soybean through regulation of Mn transport.

Although GmMTP8.1 exhibited high similarity with the MTP8-like proteins, some functional variations are observed among these homologues. For example, the representative MTP8 members, namely, ShMTP8, CsMTP8, OsMTP8.1/8.2, and AtMTP8, are found to be localized to the tonoplast, detoxifying Mn by sequestration of Mn into the vacuoles (Delhaize et al., 2003; Chen et al., 2013; Migocka et al., 2014; Eroglu et al., 2016; Takemoto et al., 2017). However, HvMTP8.1 and HvMTP8.2 from barley are suggested to be involved in delivering Mn to the Golgi apparatus, regulating Mn homeostasis (Pedas et al., 2014). Furthermore, two MTP8 homologues from the tea plant are localized to the plasma membrane and participated in Mn efflux from plant cells (Li et al., 2017; Zhang et al., 2020). Unexpectedly, different from those identified MTP8-like proteins, GmMTP8.1 was found to be localized to the ER in tobacco leaf epidermis cells (**Figure 6**), suggesting that GmMTP8.1 is involved in Mn transport into the ER, which has probably contributed to reduction in cytosolic Mn and maintenance of Mn homeostasis in transgenic Arabidopsis overexpressing *GmMTP8.1* (**Figure 10**). Similarly, the ER-localized AtECA1 has been found to promote Arabidopsis growth under Mn toxicity conditions by pumping Mn into the ER, reducing cytosolic Mn to levels that do not disrupt other elements homeostasis (Wu et al., 2002).

In this study, less Mn accumulation was observed in shoots but not roots of transgenic Arabidopsis overexpressing *GmMTP8.1* than in those of WT under excess Mn conditions (**Figure 8** and **Supplementary Figure 7**), suggesting that GmMTP8.1 participates in the extrusion of Mn from leaf cells. The involvement of MTP homologues in Mn efflux has been observed in several plants, such as CasMTP8.1/8.2 in tea plant, HvMTP8.1/8.2 in barley, CsMTP9 in cucumber, AtMTP11 in Arabidopsis, and OsMTP11 in rice (Peiter et al., 2007; Pedas et al., 2014; Migocka et al., 2015; Li et al., 2017; Ma et al., 2018; Zhang et al., 2020). These MTPs are generally localized to the Golgi apparatus or the plasma membrane (Pedas et al., 2014; Li et al., 2017; Zhang et al., 2020). However, ER-localized MTP8-like proteins involved in cellular Mn extrusion have not been reported, although ShMTP8 also seems to target the ER membrane in yeast cells (Delhaize et al., 2003). This study indicates the role of ER-localized GmMTP8.1 participating in the export of Mn out of the leaf cells (**Figure 10**). Such a cellular Mn extrusion pathway has previously been suggested for the participation of the Golgi-localized AtMTP11 in Arabidopsis and OsMTP11 in rice, in that Mn can be loaded into the *trans*-Golgi network (TGN), sequestered into vesicles, trafficked to the plasma membrane, and ultimately released to the extracellular space (Peiter et al., 2007; Ma et al., 2018). As GmMTP8.1 was localized to the ER and displayed less similarity with AtMTP11 (56.8%) and OsMTP11 (58.5%), it might indirectly participate in stimulation of the cellular extrusion of Mn. Thus, we speculated that GmMTP8.1 might influence Mn distribution and status, subsequently leading to transcriptional changes in transporter genes that are responsible for Mn efflux.

To test this hypothesis, we analyzed the expressions of Mn transporter genes in transgenic Arabidopsis. The results showed that the overexpression of *GmMTP8.1* led to significant induction of *AtMTP11*, *AtNRAMP3*, and *AtECA3* in leaves of transgenic Arabidopsis under excess Mn conditions (**Figure 9**). In Arabidopsis, the Golgi-localized AtMTP11 and ECA3 are found to play crucial roles in Mn homeostasis by transporting Mn into the Golgi apparatus (Peiter et al., 2007; Mills et al., 2008), which might be further released to the extracellular space *via* the exocytosis of secretory vesicles, maintaining Mn homeostasis (**Figure 10**). Moreover, AtNRAMP3 is involved in the transportation of Mn from the vacuole into chloroplasts of mesophyll cells (Lanquar et al., 2010). Thus, the upregulation of these transporter genes has possibly contributed to stimulation of the export of Mn out of leaf cells in the *GmMTP8.1* overexpression lines. On the other hand, we found that Mn levels in roots of transgenic lines were similar to those in the WT under excess Mn conditions (**Figure 8** and **Supplementary Figure 7**), and that the overexpression of *GmMTP8.1* led to increase in the transcript of *AtMTP8* in roots of transgenic Arabidopsis (**Figure 9**). The enhancement of *AtMTP8* may contribute to increase the sequestration of Mn into root vacuoles (**Figure 10**), although a direct measurement of intracellular Mn distribution would help to support this hypothesis.

In conclusion, a total of 14 *GmMTP* genes were identified in the soybean genome. These *GmMTPs* exhibited different responses to Mn toxicity. The heterologous expression of ER-localized *GmMTP8.1* facilitated the growth of yeast-sensitive mutant Δ*pmr1* and Arabidopsis under Mn toxicity conditions, which could be through the mechanisms of stimulating export of Mn out of cells and increasing sequestration of Mn in intracellular compartments.

DATA AVAILABILITY STATEMENT

The original contributions presented in the study are included in the article/**Supplementary Material**, further inquiries can be directed to the corresponding author/s.

AUTHOR CONTRIBUTIONS

ZC designed the research and revised the manuscript. JL, RD, YJ, JH, XZ, NA, and JS performed the experiments and analyzed the data. JL and RD wrote the manuscript. All the authors approved the final version of the manuscript.

FUNDING

This research was funded by the Key Research and Development Program of Hainan (ZDYF2019039), the Modern Agro-Industry Technology Research System (CARS-34), and the Integrated Demonstration of Key Techniques for the Industrial Development of Featured Crops in Rocky Desertification Areas of Yunnan-Guangxi-Guizhou Provinces (SMH2019-2021).

ACKNOWLEDGMENTS

The authors appreciate Rainer Schultze-Kraft and Idupulapati M. Rao for the critical comments and revisions. The authors also thank Guihua Wang, Linjie Wang, and Qin Liu for the technical help.

SUPPLEMENTARY MATERIAL

The Supplementary Material for this article can be found online at: https://www.frontiersin.org/articles/10.3389/fpls.2021.683813/full#supplementary-material

REFERENCES

Alejandro, S., Höller, S., Meier, B., and Peiter, E. (2020). Manganese in plants: from acquisition to subcellular allocation. *Front. Plant Sci.* 11:300. doi: 10.3389/fpls.2020.00300

Cailliatte, R., Schikora, A., Briat, J. F., Mari, S., and Curie, C. (2010). High-affinity manganese uptake by the metal transporter NRAMP1 is essential for *Arabidopsis* growth in low manganese conditions. *Plant Cell* 22, 904–917. doi: 10.1105/tpc.109.073023

Chen, X., Li, J., Wang, L., Ma, G., and Zhang, W. (2016). A mutagenic study identifying critical residues for the structure and function of rice manganese transporter OsMTP8.1. *Sci. Rep.* 6:32073. doi: 10.1038/srep32073

Chen, Z., Fujii, Y., Yamaji, N., Masuda, S., Takemoto, Y., Kamiya, T., et al. (2013). Mn tolerance in rice is mediated by MTP8.1, a member of the cation diffusion facilitator family. *J. Exp. Bot.* 64, 4375–4387. doi: 10.1093/jxb/ert243

Chen, Z., Sun, L., Liu, P., Liu, G., Tian, J., and Liao, H. (2015). Malate synthesis and secretion mediated by a manganese-enhanced malate dehydrogenase confers superior manganese tolerance in *Stylosanthes guianensis*. *Plant Physiol.* 167, 176–188. doi: 10.1104/pp.114.251017

Chen, Z., Yan, W., Sun, L., Tian, J., and Liao, H. (2016). Proteomic analysis reveals growth inhibition of soybean roots by manganese toxicity is associated with alteration of cell wall structure and lignification. *J. Proteomics* 30, 151–160. doi: 10.1016/j.jprot.2016.03.037

Clough, S. J., and Bent, A. F. (1998). Floral dip: a simplified method for *Agrobacterium*-mediated transformation of *Arabidopsis thaliana*. *Plant J.* 16, 735–743. doi: 10.1046/j.1365-313x.1998.00343.x

Delhaize, E., Gruber, B. D., Pittman, J. K., White, R. G., Leung, H., Miao, Y., et al. (2007). A role for the *AtMTP11* gene of Arabidopsis in manganese transport and tolerance. *Plant J.* 51, 198–210. doi: 10.1111/j.1365-313x.2007.03138.x

Delhaize, E., Kataoka, T., Hebb, D. M., White, R. G., and Ryan, P. R. (2003). Genes encoding proteins of the cation diffusion facilitator family that confer manganese tolerance. *Plant Cell* 15, 1131–1142. doi: 10.1105/tpc.009134

Dragišić Maksimović, J., Mojović, M., Maksimović, V., Römheld, V., and Nikolic, M. (2012). Silicon ameliorates manganese toxicity in cucumber by decreasing hydroxyl radical accumulation in the leaf apoplast. *J. Exp. Bot.* 63, 2411–2420. doi: 10.1093/jxb/err359

Erbasol, I., Bozdag, G. O., Koc, A., Pedas, P., and Karakaya, H. C. (2013). Characterization of two genes encoding metal tolerance proteins from *Beta vulgaris* subspecies maritima that confers manganese tolerance in yeast. *Biometals* 26, 795–804. doi: 10.1007/s10534-013-9658-7

Eroglu, S., Meier, B., Wirén, N. V., and Peiter, E. (2016). The vacuolar manganese transporter MTP8 determines tolerance to iron deficiency-induced chlorosis in Arabidopsis. *Plant Physiol.* 170, 1030–1045. doi: 10.1104/pp.15.01194

Fecht-Christoffers, M. M., Führs, H., Braun, H. P., and Horst, W. J. (2006). The role of hydrogen peroxide-producing and hydrogen peroxide-consuming peroxidases in the leaf apoplast of cowpea in manganese tolerance. *Plant Physiol.* 140, 1451–1463. doi: 10.1104/pp.105.070474

Fernando, D. R., and Lynch, J. P. (2015). Manganese phytotoxicity: new light on an old problem. *Ann. Bot.* 116, 313–319. doi: 10.1093/aob/mcv111

Gietz, R. D., and Schiestl, R. H. (2007). High-efficiency yeast transformation using the LiAc/SS carrier DNA/PEG method. *Nat. Protoc.* 2, 31–34. doi: 10.1038/nprot.2007.15

Gustin, J. L., Zanis, M. J., and Salt, D. E. (2011). Structure and evolution of the plant location diffusion facilitator family of ion transporters. *BMC Evol. Biol.* 11:76. doi: 10.1186/1471-2148-11-76

Herridge, D. F., Peoples, M. B., and Boddey, R. M. (2008). Global inputs of biological nitrogen fixation in agricultural systems. *Plant Soil* 311, 1–18. doi: 10.1007/s11104-008-9668-3

Jia, Y., Li, X., Liu, Q., Hu, X., Li, J., Dong, R., et al. (2020). Physiological and transcriptomic analyses reveal the roles of secondary metabolism in the adaptive responses of *Stylosanthes* to manganese toxicity. *BMC Genomics* 21:861. doi: 10.1186/s12864-020-07279-2

Kolaj-Robin, O., Russell, D., Hayes, K. A., Pembroke, J. T., and Soulimane, T. (2015). Cation diffusion facilitator family: structure and function. *FEBS Lett.* 589, 1283–1295. doi: 10.1016/j.febslet.2015.04.007

Lanquar, V., Schnell Ramos, M., Lelièvre, F., Barbier-Brygoo, H., Krieger-Liszkay, A., Krämer, U., et al. (2010). Export of vacuolar manganese by AtNRAMP3 and AtNRAMP4 is required for optimal photosynthesis and growth under manganese deficiency. *Plant Physiol.* 152, 1986–1999. doi: 10.1104/pp.109.150946

Lavres, J., Malavolta, E., Nogueira, N. D., Moraes, M. F., Reis, A. R., Rossi, M. L., et al. (2009). Changes in anatomy and root cell ultrastructure of soybean genotypes under manganese stress. *Rev. Bras. Cienc. Solo* 33, 395–403. doi: 10.1590/S0100-06832009000200017

Li, J. F., Jia, Y. D., Dong, R. S., Huang, R., Liu, P. D., Li, X. Y., et al. (2019). Advances in the mechanisms of plant tolerance to manganese toxicity. *Int. J. Mol. Sci.* 20:5096. doi: 10.3390/ijms20205096

Li, J. Y., Zheng, L., Fan, Y., Wang, Y. R., Ma, Y. R., Gu, D. F., et al. (2021). Pear metal transport protein PbMTP8.1 confers manganese tolerance when expressed in yeast and *Arabidopsis thaliana*. *Ecotox. Environ. Safe.* 208:111687. doi: 10.1016/j.ecoenv.2020.111687

Li, Q., Li, Y., Wu, X., Zhou, L., Zhu, X., and Fang, W. (2017). Metal transport protein 8 in *Camellia sinensis* confers superior manganese tolerance when expressed in yeast and *Arabidopsis thaliana*. *Sci. Rep.* 7:39915. doi: 10.1038/srep39915

Li, X., Wu, Y., Li, B., He, W., Yang, Y., and Yang, Y. (2018). Genome-wide identification and expression analysis of the cation diffusion facilitator gene family in turnip under diverse metal ion stresses. *Front. Genet*. 9:103. doi: 10.3389/fgene.2018.00103

Liang, C., Tian, J., Lam, H., Lim, B., Yan, X., and Liao, H. (2010). Biochemical and molecular characterization of PvPAP3, a novel purple acid phosphatase isolated from common bean enhancing extracellular ATP utilization. *Plant Physiol.* 152, 854–865. doi: 10.1104/pp.109.147918

Liu, J., Gao, Y., Tang, Y., Wang, D., Chen, X., Yao, Y., et al. (2019). Genome-wide identification, comprehensive gene feature, evolution, and expression analysis of plant metal tolerance proteins in tobacco under heavy metal toxicity. *Front. Genet.* 10:345. doi: 10.3389/fgene.2019.00345

Liu, P., Huang, R., Hu, X., Jia, Y., Li, J., Luo, J., et al. (2019). Physiological responses and proteomic changes reveal insights into *Stylosanthes* response to manganese toxicity. *BMC Plant Biol.* 19:212. doi: 10.1186/s12870-019-1822-y

Liu, P., Xue, Y., Chen, Z., Liu, G., and Tian, J. (2016). Characterization of purple acid phosphatases involved in extracellular dNTP utilization in *Stylosanthes*. *J. Exp. Bot.* 67, 4141–4154. doi: 10.1093/jxb/erw190

Liu, Q., Dang, H., Chen, Z., Wu, J., Chen, Y., Chen, S., et al. (2018). Genome-wide identification, expression, and functional analysis of the sugar transporter gene family in Cassava (*Manihot esculenta*). *Int. J. Mol. Sci.* 19:987. doi: 10.3390/ijms19040987

Liu, Y., Xue, Y., Xie, B., Zhu, S., Lu, X., Liang, C., et al. (2020). Complex gene regulation between young and old soybean leaves in responses to manganese toxicity. *Plant Physiol. Bioch.* 155, 231–242. doi: 10.1016/j.plaphy.2020.07.002

Long, L., Kristensen, R. K., Guo, J., Chen, F., Pedas, P. R., Zhang, G., et al. (2021). Assessing the variation in traits for manganese deficiency tolerance among maize genotypes. *Environ. Exp. Bot.* 183:104344. doi: 10.1016/j.envexpbot.2020.104344

Lu, S. J., Zhao, X. H., Hu, Y. L., Liu, S. L., Nan, H. Y., Li, X. M., et al. (2017). Natural variation at the soybean j locus improves adaptation to the tropics and enhances yield. *Nat. Genet*. 49:773. doi: 10.1038/ng.3819

Ma, G., Li, J. Y., Li, J. J., Li, Y., and Zhang, W. (2018). OsMTP11, a trans-Golgi network localized transporter, is involved in manganese tolerance in rice. *Plant Sci.* 274, 59–69. doi: 10.1016/j.plantsci.2018.05.011

Marschner, H. (2012). *Marschner's Mineral Nutrition of Higher Plants*. 3rd Edn. London: Academic Press.

Migocka, M., Papierniak, A., Dziubińska, E., Poździk, P., Posyniak, E., Garbiec, A., et al. (2014). Cucumber metal transport protein MTP8 confers increased tolerance to manganese when expressed in yeast and *Arabidopsis thaliana*. *J. Exp. Bot.* 65, 5367–5384. doi: 10.1093/jxb/eru295

Migocka, M., Papierniak, A., Kosieradzka, A., Posyniak, E., Maciaszczyk-Dziubinska, E., Biskup, R., et al. (2015). Cucumber metal tolerance protein CsMTP9 is a plasma membrane H^+-coupled antiporter involved in the Mn^{2+} and Cd^{2+} efflux from root cells. *Plant J.* 84, 1045–1058. doi: 10.1111/tpj.13056

Millaleo, R., Reyes-Díaz, M., Ivanov, A. G., Mora, M. L., and Alberdi, M. (2010). Manganese as essential and toxic element for plants: transport, accumulation and resistance mechanism. *J. Soil Sci. Plant Nutr.* 10, 470–481. doi: 10.4067/S0718-95162010000200008

Mills, R. F., Doherty, M. L., López-Marqués, R. L., Weimar, T., Dupree, P., Palmgren, M. G., et al. (2008). ECA3, a Golgi-localized P2A-type ATPase, plays a crucial role in manganese nutrition in Arabidopsis. *Plant Physiol.* 146, 116–128. doi: 10.1104/pp.107.110817

Montanini, B., Blaudez, D., Jeandroz, S., Sanders, D., and Chalot, M. (2007). Phylogenetic and functional analysis of the cation diffusion facilitator (CDF) family: improved signature and prediction of substrate specificity. *BMC Genomics* 8:107. doi: 10.1186/1471-2164-8-107

Mravec, J., Skùpa, P., Bailly, A., Hoyerová, K., Krecek, P., Bielach, A., et al. (2009). Subcellular homeostasis of phytohormone auxin is mediated by the ER-localized PIN5 transporter. *Nature* 459, 1136–1140. doi: 10.1038/nature08066

Pedas, P., Stokholm, M. S., Hegelund, J. N., Ladegård, A. H., Schjoerring, J. K., and Husted, S. (2014). Golgi localized barley MTP8 proteins facilitate Mn transport. *PLoS One* 9:e113759. doi: 10.1371/journal.pone.0113759

Peiter, E., Montanini, B., Gobert, A., Pedas, P., Husted, S., Maathuis, F. J. M., et al. (2007). Secretory pathway-localized cation diffusion facilitator confers plant manganese tolerance. *Proc. Natl. Acad. Sci. U.S.A.* 104, 8532–8537. doi: 10.1073/pnas.0609507104

Santos, E. F., Kondo Santini, J. M., Paixão, A. P., Júnior, E. F., Lavres, J., Campos, M., et al. (2017). Physiological highlights of manganese toxicity symptoms in soybean plants: Mn toxicity responses. *Plant Physiol. Biochem.* 113, 6–19. doi: 10.1016/j.plaphy.2017.01.022

Shao, J. F., Yamaji, N., Shen, R. F., and Ma, J. F. (2017). The key to Mn homeostasis in plant: regulation of Mn transporters. *Trends Plant Sci.* 22, 215–224. doi: 10.1016/j.tplants.2016.12.005

Sheng, H., Zeng, J., Yan, F., Wang, X., Wang, Y., Kang, H., et al. (2015). Effect of exogenous salicylic acid on manganese toxicity, mineral nutrients translocation and antioxidative system in polish wheat. *Acta Physiol. Plant*. 37:32. doi: 10.1007/s11738-015-1783-1

Takemoto, Y., Tsunemitsu, Y., Fujii, K. M., Mitani, U. N., Yamaji, N., Ma, J. F., et al. (2017). The tonoplast-localized transporter MTP8.2 contributes to manganese detoxification in the shoots and roots of *Oryza sativa* L. *Plant Cell Physiol.* 58, 1573–1582. doi: 10.1093/pcp/pcx082

Tsunemitsu, Y., Yamaji, N., Ma, J. F., Kato, S. I., Iwasaki, K., and Ueno, D. (2018b). Rice reduces Mn uptake in response to Mn stress. *Plant Signal. Behav.* 13:e1422466. doi: 10.1080/15592324.2017.1422466

Tsunemitsu, Y., Genga, M., Okada, T., Yamaji, N., Ma, J. F., Miyazaki, A., et al. (2018a). A member of cation diffusion facilitator family, MTP11, is required for manganese tolerance and high fertility in rice. *Planta* 248, 231–241. doi: 10.1007/s00425-018-2890-1

Ueno, D., Sasaki, A., Yamaji, N., Fujii, Y., Takemoto, Y., Moriyama, S., et al. (2015). A polarly localized transporter for efficient manganese uptake in rice. *Nat. Plants* 1:15170. doi: 10.1038/nplants.2015.170

Voelker, C., Schmidt, D., Mueller-Roeber, B., and Czempinski, K. (2006). Members of the Arabidopsis AtTPK/KCO family form homomeric vacuolar channels *in planta*. *Plant J.* 48, 296–306. doi: 10.1111/j.1365-313X.2006.02868.x

Wu, Z., Liang, F., Hong, B., Young, J. C., Sussman, M. R., Harper, J. F., et al. (2002). An endoplasmic reticulum-bound Ca^{2+}/Mn^{2+} pump, ECA1, supports plant growth and confers tolerance to Mn^{2+} stress. *Plant Physiol.* 130, 128–137. doi: 10.1104/pp.004440

Yang, Z., You, J., Xu, Y., and Yang, Z. (2009). Interaction between aluminum toxicity and manganese toxicity in soybean (*Glycine max*). *Plant Soil* 319, 277–289. doi: 10.1016/S0145-305X(01)00005-2

Zhang, X. Y., Li, Q. H., Xu, W. L., Zhao, H., Guo, F., Wang, P., et al. (2020). Identification of *MTP* gene family in tea plant (*Camellia sinensis* L.) and characterization of *CsMTP8.2* in manganese toxicity. *Ecotox. Environ. Safe.* 202:110904. doi: 10.1016/j.ecoenv.2020.110904

Zhang, Z., Fu, D., Sun, Z., Ju, C., Miao, C., Wang, Z., et al. (2021). A tonoplast-associated calcium signaling regulates manganese homeostasis in Arabidopsis. *Mol. Plant* 21, 78–72. doi: 10.1016/j.molp.2021.03.003

Conflict of Interest: The authors declare that the research was conducted in the absence of any commercial or financial relationships that could be construed as a potential conflict of interest.

Publisher's Note: All claims expressed in this article are solely those of the authors and do not necessarily represent those of their affiliated organizations, or those of the publisher, the editors and the reviewers. Any product that may be evaluated in this article, or claim that may be made by its manufacturer, is not guaranteed or endorsed by the publisher.

Copyright © 2021 Li, Dong, Jia, Huang, Zou, An, Song and Chen. This is an open-access article distributed under the terms of the Creative Commons Attribution License (CC BY). The use, distribution or reproduction in other forums is permitted, provided the original author(s) and the copyright owner(s) are credited and that the original publication in this journal is cited, in accordance with accepted academic practice. No use, distribution or reproduction is permitted which does not comply with these terms.

frontiers in Plant Science

ORIGINAL RESEARCH
published: 09 December 2021
doi: 10.3389/fpls.2021.722752

Interaction Effects of Nitrogen Rates and Forms Combined With and Without Zinc Supply on Plant Growth and Nutrient Uptake in Maize Seedlings

Yanfang Xue[1], Wei Yan[1], Yingbo Gao[1], Hui Zhang[1], Liping Jiang[1,2], Xin Qian[1], Zhenling Cui[1,3], Chunyan Zhang[4], Shutang Liu[2], Huimin Wang[1], Zongxin Li[1] and Kaichang Liu[1]**

[1] National Engineering Laboratory of Wheat and Maize, Key Laboratory of Biology and Genetic Improvement of Maize in Northern Yellow-Huai Rivers Plain, Ministry of Agriculture, Maize Research Institute, Shandong Academy of Agricultural Sciences, Jinan, China, [2] College of Resources and Environment, Qingdao Agricultural University, Qingdao, China, [3] College of Resources and Environment, China Agricultural University, Beijing, China, [4] Linyi Academy of Agricultural Sciences, Linyi, China

OPEN ACCESS

Edited by:
Francesco Di Gioia,
The Pennsylvania State University (PSU), United States

Reviewed by:
Myungjin Lee,
The Pennsylvania State University (PSU), United States
Ibukun Ayankojo,
University of Florida, United States

***Correspondence:**
Zongxin Li
sdaucliff@sina.com
Kaichang Liu
liukc1971@163.com

Specialty section:
This article was submitted to Plant Nutrition, a section of the journal Frontiers in Plant Science

Received: 09 June 2021
Accepted: 10 November 2021
Published: 09 December 2021

Citation:
Xue Y, Yan W, Gao Y, Zhang H, Jiang L, Qian X, Cui Z, Zhang C, Liu S, Wang H, Li Z and Liu K (2021) Interaction Effects of Nitrogen Rates and Forms Combined With and Without Zinc Supply on Plant Growth and Nutrient Uptake in Maize Seedlings. Front. Plant Sci. 12:722752. doi: 10.3389/fpls.2021.722752

Previous studies have shown that zinc (Zn) accumulation in shoot and grain increased as applied nitrogen (N) rate increased only when Zn supply was not limiting, suggesting a synergistic effect of N on plant Zn accumulation. However, little information is available about the effects of different mineral N sources combined with the presence or absence of Zn on the growth of both shoot and root and nutrient uptake. Maize plants were grown under sand-cultured conditions at three N forms as follows: NO_3^- nutrition alone, mixture of NO_3^-/NH_4^+ with molar ratio of 1:1 (recorded as mixed-N), and NH_4^+ nutrition alone including zero N supply as the control. These treatments were applied together without or with Zn supply. Results showed that N forms, Zn supply, and their interactions exerted a significant effect on the growth of maize seedlings. Under Zn-sufficient conditions, the dry weight (DW) of shoot, root, and whole plant tended to increase in the order of NH_4^+ < NO_3^- < mixed-N nutrition. Compared with NH_4^+ nutrition alone, mixed-N supply resulted in a 27.4 and 28.1% increase in leaf photosynthetic rate and stomatal conductance, which further resulted in 35.7 and 33.5% of increase in shoot carbon (C) accumulation and shoot DW, respectively. Furthermore, mixed-N supply resulted in a 19.7% of higher shoot C/N ratio vs. NH_4^+ nutrition alone, which means a higher shoot biomass accumulation, because of a significant positive correlation between shoot C/N ratio and shoot DW (R^2 = 0.682***). Additionally, mixed-N supply promoted the greatest root DW, total root length, and total root surface area and synchronously improved the root absorption capacity of N, iron, copper, manganese, magnesium, and calcium. However, the above nutrient uptake and the growth of maize seedlings supplied with NH_4^+ were superior to either

NO_3^- or mixed-N nutrition under Zn-deficient conditions. These results suggested that combined applications of mixed-N nutrition and Zn fertilizer can maximize plant growth. This information may be useful for enabling integrated N management of Zn-deficient and Zn-sufficient soils and increasing plant and grain production in the future.

Keywords: maize, nitrogen rates and forms, zinc supply, interaction effects, nutrient uptake, root morphology

INTRODUCTION

Nitrogen (N) is the most abundant mineral nutrient element in plants and plays an essential role in plant growth and development. Nitrate (NO_3^--N) and ammonium (NH_4^+-N) are predominant forms of inorganic N in soil, both of which can be absorbed by plants directly (Marschner, 2011). The preferred N form varies among plant species and among genotypes of individual plant species, environmental conditions, and developmental stages (Cramer and Lewis, 1993; Zhao et al., 2013). Maize usually grows in well-aerated dryland soils, where NO_3^- is the major source of N due to soil nitrification (Fang et al., 2006). Some studies showed the enhanced growth of maize under NO_3^- nutrition compared with NH_4^+ nutrition (Cramer and Lewis, 1993; Schortemeyer et al., 1997). Others showed that NH_4^+ uptake may be an important strategy for maize plants to take up sufficient quantities of N for growth compared with NO_3^- nutrition (Gu et al., 2013; George et al., 2016; Wang et al., 2019; Zhang H. Q. et al., 2019). For most plants, a mixture of both NO_3^- and NH_4^+ is superior to either NO_3^- or NH_4^+ sources alone, possibly due to improved cytokinin transportation from root to shoot, stimulated leaf growth, maintained rhizosphere pH, and increased nutrient uptake rates, such as N, phosphorus (P), copper (Cu), and iron (Fe) (Gentry and Below, 1993; Marschner, 2011; Cao et al., 2018; Wang et al., 2019).

Zinc (Zn) is an essential microelement for plant growth. Zinc plays a vital role in many essential cellular functions and metabolic pathways and is important to the normal health and reproduction of plants, animals, and humans (Welch and Graham, 2004). It is estimated that more than 30% of the agricultural soils in the world are prone to Zn deficiency (Alloway, 2008). According to a national soil survey, China has nearly 0.63 billion hm^2 of soil, accounting for 45.7% of the farmland, is subject to Zn deficiency, primarily calcareous soil in Northern China (Liu, 1996). Although Zn is an essential micronutrient for plant growth, Zn input has received much less attention than N, P, or irrigation during the Green Revolution (Tilman et al., 2002; Mueller et al., 2012). Therefore, the application of Zn fertilizers is necessary in such soils to ensure cereal yield and grain Zn concentration (Cakmak, 2008).

Maize is one of the world's major crops and is expected to contribute increasingly to human and animal nutrition and to energy production. Maize is sensitive to Zn deficiency (Wang and Jin, 2007). Zn-deficient symptoms, such as stunted and chlorotic plants, are often observed in maize plants growing on calcareous soil in the field (Alloway, 2008). Many studies have demonstrated that grain yield of maize was increased by the application of Zn fertilizer to Zn-deficient soils. The positive effects of Zn supply are related to the increased photosynthesis rates, chlorophyll content in leaves, and increased kernel number and weight in the apical benefited from increased pollen viability at the tasseling stage under field conditions (Potarzycki, 2010; Wang et al., 2012; Liu et al., 2016, 2020).

Previous results from greenhouse conditions showed that increasing N supply did not improve Zn accumulation in grain and shoot of wheat in case of low soil Zn availability. Otherwise, increasing N supply substantially improved Zn concentration and accumulation of both grain and shoot in wheat when Zn supply was not limited, showing a synergistic effect of N fertilization on Zn accumulation (Kutman et al., 2010, 2011a,b). Furthermore, our results obtained from field conditions also showed positive effects of N application on the root uptake, root-to-shoot translocation, and remobilization of Zn in wheat and maize grown in Zn-sufficient soils (Xue et al., 2012, 2014, 2019). However, little information is available about the effects of different mineral N sources combined with the presence or absence of Zn on the growth of both shoot and root and nutrient uptake.

This study aimed to determine how the different N forms affected the growth of shoot and root, root morphological traits, and nutrient uptake of maize seedlings grown with and without Zn supply under greenhouse conditions. This information may be useful for enabling integrated N management of Zn-deficient and Zn-sufficient soils and increasing plant and grain production in the future.

MATERIALS AND METHODS

Experimental Procedures

Seeds of hybrid "Denghai 605" were surface-sterilized by soaking in 10% (v/v) H_2O_2 for 30 min, rinsed thoroughly in deionized water, soaked in saturated $CaSO_4$ for 5 h, then transferred to germinate on filter paper in the dark at 25°C for 2 days. Initially, five uniformly germinated seeds were sown in a plastic pot filled with 5 kg of quartz sand (diameter between 0.25 and 0.50 mm) and later thinned to three plants per pot. Quartz sand was pretreated by soaking in acid (5 N HCl) for 18 h and was thoroughly washed with distilled water until pH was neutral. Each treatment had seven replicates arranged in a completely randomized design. Their places were changed frequently inside a glasshouse with day/night temperature of 25/18°C. Plants were supplied with nutrient solution after germination according to Yuan et al. (2011). The nutrient solution contained 0.75 mmol L^{-1} K_2SO_4, 0.65 mmol L^{-1} $MgSO_4{\cdot}7H_2O$, 0.25 mmol L^{-1} KH_2PO_4, 10 μmol L^{-1} H_3BO_3, 1 μmol L^{-1} $MnSO_4{\cdot}H_2O$, 0.5 μmol L^{-1} $CuSO_4{\cdot}5H_2O$, 0.05 μmol L^{-1} $Na_2Mo_7O_4{\cdot}2H_2O$, and 0.1 mmol L^{-1} Fe-EDTA.

Nitrogen was supplied in 4 mmol L^{-1} with three different N forms as follows: NO_3^- nutrition alone, mixture of NO_3^-/NH_4^+ with molar ratio of 1:1 (recorded as mixed-N), and NH_4^+ nutrition alone including zero N supply as the control (recorded as N0). These treatments were applied together without (Zn0), or with 2 μmol L^{-1} $ZnSO_4{\cdot}7H_2O$ (Zn1). NH_4^+-N and NO_3^--N were applied in the form of $(NH_4)_2SO_4$ and $Ca(NO_3)_2{\cdot}4H_2O$, respectively. Furthermore, $CaCl_2{\cdot}2H_2O$ was added to balance calcium in the solution that contained ammonium and the control treatments as well. The solution pH was adjusted to 6.0. The pots were watered every 2 days using 400 ml of treated nutrient solution.

Photosynthetic Parameter Measurements

Photosynthetic parameters including net photosynthetic rate (P_n), transpiration rate (T_r), stomatal conductance (g_s), and intercellular CO_2 concentration (C_i) were measured using a portable Li-6400 photosynthesis system (LI-COR Inc., Lincoln, NE, United States). The youngest fully expanded leaves at 30 days after N and Zn treatments were selected for measurement between 09:00 and 11:00. The photosynthetically active radiation, temperature, and CO_2 concentration during measurement collection were set at 600 μmol m^{-2} s^{-1}, 25°C, and 380 μmol mol^{-1}, respectively. The index of chlorophyll content (SPAD value) in the youngest fully expanded leaves was determined using portable chlorophyll meter SPAD-502 Plus (SPAD, Minolta Camera Co., Ltd., Osaka, Japan). There were four biological replicates for each treatment.

Mineral Elements

After photosynthetic parameter measurements, plants were harvested for 30 days after N and Zn treatments. The fresh plant samples were divided into shoots and roots. The roots were washed in 0.5 mM $CaSO_4$ solution for 10 min, and shoots were then rinsed with ultra-pure water and dried at 65°C until constant weight. The dry weight (DW) of shoot and root was used to calculate Zn efficiency (ZE) (the ratio of DW of shoot or root without Zn supply to that with Zn supply ×100), which has been used for screening various genotypes of cereals and other crops (Karim et al., 2012). The dried samples were ground with a stainless steel grinder and then digested using an acid mixture of HNO_3–H_2O_2 in a microwave accelerated reaction system (CEM Corp., Matthews, NC, United States). The concentrations of Zn, Fe, manganese (Mn), Cu, calcium (Ca), magnesium (Mg), P, and K (potassium) in the digested solutions were determined by inductively coupled plasma atomic emission spectroscopy (ICP-AES, Optima 7300 DV, PerkinElmer, Waltham, MA, United States). Two blanks and a certified reference material (IPE126, Wageningen University, Netherlands) were included in each batch of digestion to ensure analytical quality. The concentrations of carbon (C) and N in samples were determined using a CN analyzer (vario Macro cube, Elementar, Hanau, Germany). There were four biological replicates for each treatment.

Leaf Soluble Protein Content

About 30 days after N and Zn treatments, the youngest fully expanded leaves from another batch of samples with three biological replicates for each treatment were frozen in liquid N_2 and crushed with a tissue homogenizer. The crushed samples were dissolved in pre-cooled phosphate buffer with pH 7.8 and made up to a final volume of 1,000 ml. The concentration of protein extracts was determined by a colorimetric method as described by Bradford (1976) using protein assay dye Coomassie Brilliant Blue G-250 (Amresco, Athens, GA, United States). The absorbance was determined at 595 nm.

Root Morphological Parameters

After the youngest fully expanded leaves were removed for determination of soluble protein, root samples were washed with tap water and kept at −20°C before an image was captured using an optical scanner (Epson, Nagano, Japan). The root traits were determined by analysis of images using the WinRHIZO software (Regent Instrument, Quebec, QC, Canada). There were three biological replicates for each treatment. After completing the root scan, these roots were not used for nutrient analysis due to the possibility of nutritional loss during the scanning process.

Statistical Analysis

ANOVA was performed using the Data Processing System (DPS) version 9.50 statistical software (Tang and Zhang, 2013). Means were compared using Fisher's protected least significant difference (LSD) tests. Differences were considered significant at $p < 0.05$. Linear regression analysis was employed to identify the correlation between shoot C/N ratio and shoot DW using the SAS software (SAS 8.0, SAS Institute Inc., Cary, NC, United States).

RESULTS

Dry Weight of Shoot and Root and the Ratio of Root-to-Shoot

Our data revealed significant effects of the Zn and N treatments on the DW of the shoot, root, and whole plants and the root-to shoot ratios (R/S) of 30-day-old maize plants grown under greenhouse conditions (**Table 1**). The interactions between Zn and N treatments were also significant for the DW of the shoot, root, and whole plants. Under a Zn-deficient condition, plants grown with NH_4^+ nutrition produced significantly greater shoot DW than with mixed N nutrition, whereas NO_3^- produced an intermediate shoot DW (**Table 1**). Plants grown with NH_4^+ also produced slightly higher root DW (approximately 27%) but not significantly different from NO_3^- and mixed N supply. However, under a Zn-sufficient condition, plants grown with NO_3^- supply and mixed-N supply produced significantly greater shoot DW than with NH_4^+ supply (**Table 1**). Plants grown with mixed-N nutrition produced significantly higher root DW than with either N form alone. Compared with nil N supply, N supply resulted in a 2.6- to 3.7-fold increase in shoot DW and 0.2- to 0.6-fold increase in root DW under Zn-deficient conditions. Under Zn-sufficient conditions, N supply resulted in a 3.9- to 4.8-fold

increase in shoot DW and 0.5- to 1.2-fold increase in root DW. Consequently, although the R/S was not significantly affected by the three N forms, N supply vs. nil N supply remarkably reduced the R/S from 81.9 to 27.2% and from 71.1 to 22.4% in response to Zn-deficient and Zn-sufficient conditions.

Compared with no Zn supply, Zn supply resulted in 22.4–125.9, 0.5–91.8, and 15.3–118.4% greater DW of the shoot, root, and whole plant, respectively, with the increase being the highest with mixed-N nutrition and following by NO_3^- supply. However, ZE was significantly higher with NH_4^+ nutrition compared with NO_3^- and mixed-N supply, showing a greater ability to resist Zn deficiency (**Table 1**).

SPAD Readings and Soluble Protein Contents of Newly Developed Leaf

Two-way ANOVA revealed significant effects of the N treatments on the leaf SPAD values and soluble protein content, and significant effects of the Zn supply only on leaf SPAD values. The interaction between N treatments and Zn supply was also significant for leaf soluble protein content (**Supplementary Table 1**).

Compared with no N supply, the three N forms significantly increased the leaf SPAD readings and leaf soluble protein contents (**Figures 1A,B**). There were no significant differences in the leaf SPAD readings among the three N forms, regardless of Zn supply (**Figure 1A**). The leaf soluble protein contents increased gradually in the order of NH_4^+ < mixed-N < NO_3^- nutrition in the presence of Zn supply. However, these values were not significantly affected by the different N forms under Zn-deficient conditions (**Figure 1B**).

Leaf Photosynthetic Parameters

Two-way ANOVA revealed significant effects of the N treatments on the leaf P_n, g_s, and T_r and significant effects of the Zn supply on P_n and C_i (**Supplementary Table 1**). The interaction between N treatments and Zn supply was significant only for leaf C_i (**Supplementary Table 1**). Compared with nil N supply, three N forms significantly increased the leaf P_n, g_s, and T_r, irrespective of Zn supply (**Figures 2A,C,D**). Plants grown with mixed-N nutrition had significantly higher leaf P_n, g_s, and T_r than those supplied with either N form alone under Zn-deficient conditions. Similar results were also observed under Zn-sufficient conditions, although less pronounced (**Figures 2A,C,D**). Furthermore, Zn supply resulted in a 5.1–46.0% increase in leaf P_n (**Figure 2A**) and a 3.3–39.0% decrease in leaf C_i in comparison with no Zn supply (**Figure 2B**).

Root Length as Affected by N and Zn Supply

Roots were divided into three categories based on root diameter: fine roots (diameter < 0.2 mm), medium-sized roots (diameter between 0.2 and 0.4 mm), and thick roots (diameter >0.4 mm). Two-way ANOVA revealed significant effects of the N treatments on the fine root length (FRL), medium-sized root length (MRL), thick root length, and total root length (TRL). Significant effects of Zn supply on those parameters were observed with an exception of thick roots. However, the interaction between N treatments and Zn supply was not significantly different for these parameters (**Supplementary Table 2**). Compared with nil N supply, N supply generally improved the FRL, MRL, and thick root length and finally increased the TRL although there was no significant difference between nil N and NO_3^- nutrition irrespective of Zn supply. Among the three N forms, NH_4^+ supply produced the highest FRL, MRL, and thick roots and finally resulted in the highest TRL in the absence of Zn supply. Mixed-N supply resulted in the greatest TRL including the root length in different diameters in the presence of Zn supply. Compared with no Zn supply, Zn supply resulted in a 2.1–42.8% increase in TRL, with a significant increase with mixed-N supply (**Figure 3A**). Similar results were also observed for the total root surface area (**Figure 3B**).

The proportion of FRL to TRL was not affected by N and Zn supply and averaged 52.2%. The proportion of MRL to TRL (ranging from 17.1 to 26.2%) tended to increase, whereas the thick root length to TRL (ranging from 22.0 to 31.5%) tended to decrease with N supply compared with no N supply (**Figure 3C**).

Nitrogen, C, and Zn Concentration and Accumulation of Shoot and Root

According to the results of two-way ANOVA, N and Zn treatments had significant effects on the N concentration and accumulation of shoots and roots, with the exception of a non-significant effect of Zn treatments on root N accumulation. The interactions between N and Zn treatments were also significant for the shoot N concentration and accumulation (**Supplementary Table 3**). Compared with nil N supply, three N forms substantially increased the N concentration in both shoot and root. The root N concentration was not significantly different among the three N forms irrespective of Zn supply (**Figure 4A**). Among the three N forms, shoot N concentration gradually decreased in the order NH_4^+ > NO_3^- > mixed-N nutrition in the presence of Zn supply. However, shoot N concentration was significantly lower in plants with NH_4^+ nutrition than NO_3^- and mixed-N nutrition in the absence of Zn supply (**Figure 4A**). Generally, the change in shoot N concentration was opposite to that of shoot DW accumulation, regardless of Zn supply in response to different N forms. Because the increase in shoot DW was greater than the decrease in shoot N concentration, the N accumulation of shoot, root, and whole plant was significantly greater in the order NH_4^+ < NO_3^- < mixed-N nutrition in the presence of Zn supply. The opposite was true, although less pronounced in the absence of Zn supply (**Figure 4D**). Compared with no Zn supply, nitrogen accumulation in shoot, root, and whole plant with N supply was increased by 13.6–45.8%, −9.9–44.0% (root N accumulation reduced with NH_4^+ supply), and 10.8–45.6% by Zn supply, respectively. The magnitude of increase in N accumulation of those tissues was consistently the greatest with mixed-N supply, followed by NO_3^- nutrition, whereas NH_4^+ nutrition exhibited the lowest increase (**Figure 4D**).

Shoot C concentration was significantly increased, but root C concentration was not significantly affected by the three N forms compared with nil N supply, irrespective of Zn supply

TABLE 1 | Dry weight (DW) of shoot, root, and whole plant, Zn efficiency (ZE), and root-to-shoot ratio (R/S) of 30-day-old maize seedlings cultured with nil N (N0), NO_3^-, mixed-N, and NH_4^+ nutrition under sand culture conditions without (Zn0) and with Zn (Zn1) supply.

N treatment	Shoot DW (g pot^{-1})		ZE (%)	Root DW (g pot^{-1})		ZE (%)	Whole plant (g pot^{-1})		ZE (%)	R/S (%)	
	Zn0	Zn1		Zn0	Zn1		Zn0	Zn1		Zn0	Zn1
N0	0.91e	1.12e	82.0a	0.75d	0.80d	96.9a	1.66e	1.91e	87.6a	81.9a	71.1b
NO_3^-	3.46dc	6.44a	53.9b	0.91dc	1.35b	69.5b	4.38dc	7.78b	56.4b	26.4c	20.8c
Mixed-N	3.24d	7.32a	44.6b	0.92dc	1.77a	54.0b	4.16d	9.09a	46.2b	28.4c	24.2c
NH_4^+	4.33c	5.48b	81.4a	1.17bc	1.18bc	98.1a	5.50c	6.66b	83.8a	26.8c	22.1c
Source of variation											
Zn treatment (Zn)		***			***			***			*
N treatment (N)		***			***			***			***
Zn × N		***			**			***			NS

*Values followed by different lowercase letters in columns represent significant differences among the N and Zn treatments. The symbols *, **, and *** indicate significant difference at 0.05, 0.01, and 0.001 level, respectively. NS, no significant difference.*

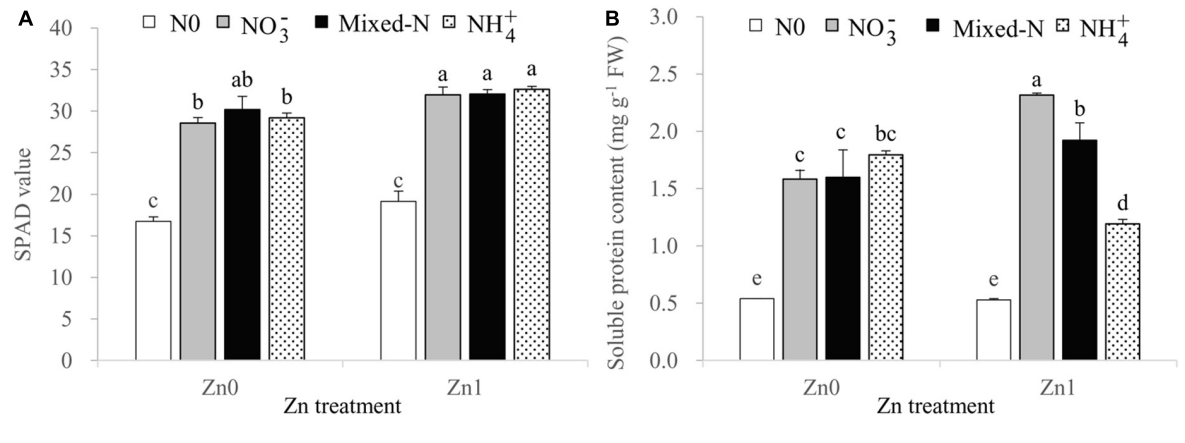


FIGURE 1 | SPAD readings **(A)** and soluble protein contents **(B)** of newly developed leaf of 30-day-old maize seedlings cultured with nil N (N0), NO_3^-, mixed-N, and NH_4^+ nutrition under sand culture conditions without (Zn0) and with Zn (Zn1) supply. Error bars represent the standard error of the mean (n = 4). Significant differences at $p < 0.05$ are shown with different letters.

(**Figure 4B**). Among the three N forms, shoot C concentration was not significantly affected by the absence of Zn supply but was significantly decreased by NH_4^+ supply compared with NO_3^- and mixed-N supply in the presence of Zn supply (**Figure 4B**). The effects of Zn supply and N forms on the C accumulation in shoot, root, and whole plant were similar to those of N in the corresponding tissues (**Figure 4E**).

Not only the N and Zn supplies but also their interaction had significant effects on Zn concentration and accumulation in shoot, root, and whole plants with the exception of non-significant effects of N treatments and their interactions on root Zn accumulation (**Supplementary Table 3**). For Zn concentration, compared with nil N supply, the three N forms significantly decreased Zn concentration of both shoot and root, with the exception of Zn concentration of shoot receiving NH_4^+ nutrition in the presence of Zn supply. Among the three N forms, Zn concentration in both shoot and root was significantly more improved in plants grown with NH_4^+ than NO_3^- and mixed-N nutrition in the presence of Zn supply, whereas it was not significantly affected by the three N forms in the absence of Zn supply (**Figure 4C**). Total Zn accumulation including shoot and root was gradually increased in the order NO_3^- < mixed-N < NH_4^+ nutrition in the presence of Zn supply, but not affected by the three N forms in the absence of Zn supply. As expected, irrespective of N treatments, compared with no Zn supply, Zn supply resulted in 137.0–387.4, 44.4–206.8, and 108.3–342.4% higher Zn accumulation in shoot, root, and whole plant, respectively (**Figure 4F**).

The proportions of shoot to total accumulation of N and Zn were not affected by the three N forms and Zn supply. The proportions of shoot to total C accumulation were improved by Zn supply, but were not significantly affected by the three N forms. In general, compared with no N application, N application significantly increased the proportions of shoot to total accumulation from 67.4 to 90.4% for N, from 54.4 to 79.1% for C, and from 51.1 to 83.5% for Zn (**Supplementary Figure 1**).

The Ratios of C/N and Zn/N of Shoot and Root

Among the three N forms, shoot C/N ratio was the highest with NH_4^+ nutrition in the absence of Zn supply, but it was the

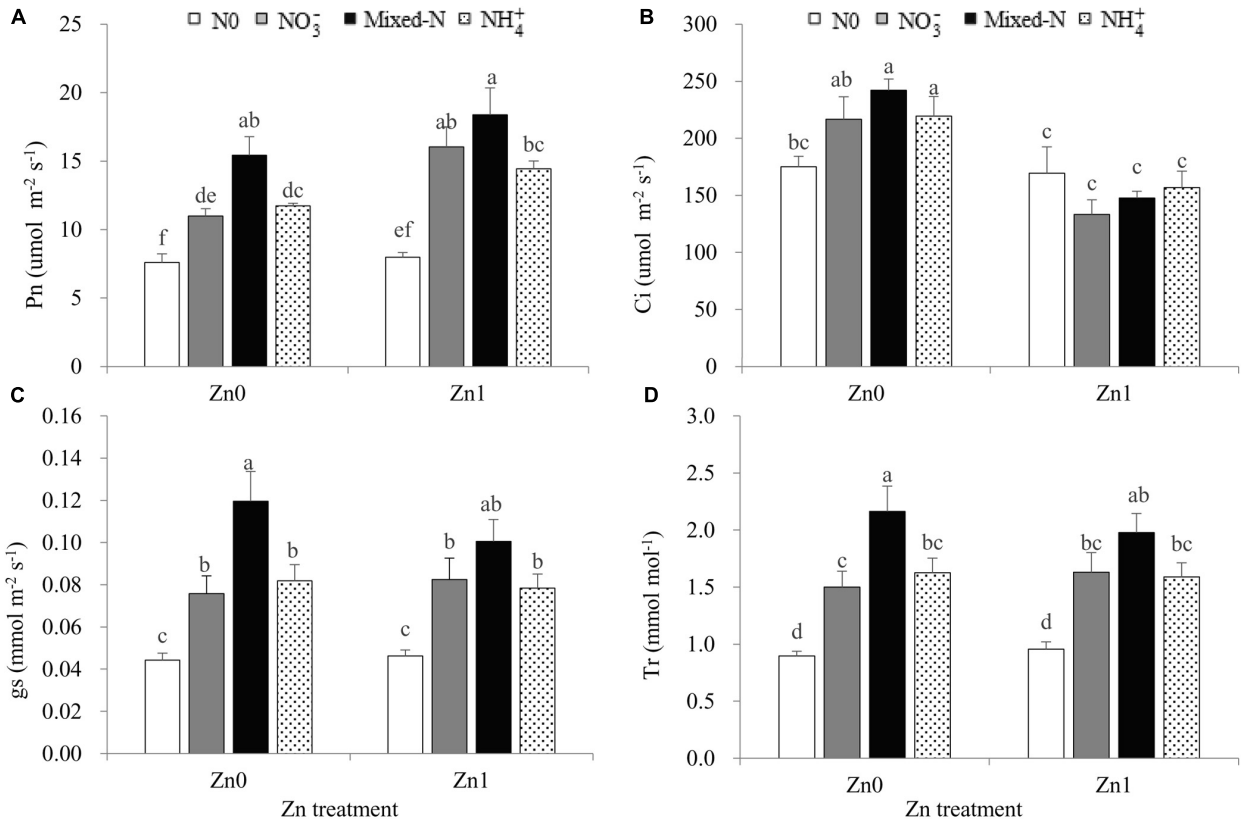


FIGURE 2 | Leaf photosynthetic parameters including P_n **(A)**, C_i **(B)**, g_s **(C)** and T_r **(D)** of newly developed leaf of 30-d-old maize seedlings cultured with nil N (N0), NO_3^-, mixed-N and NH_4^+ nutrition under sand culture conditions without (Zn0) and with Zn (Zn1) supply. Error bars represent the standard error of the mean (n = 4). Significant differences at $P < 0.05$ are shown with different letters. P_n, photosynthetic rate; C_i, intercellular CO_2 concentration; g_s, conductance to H_2O; T_r, transpiration rate.

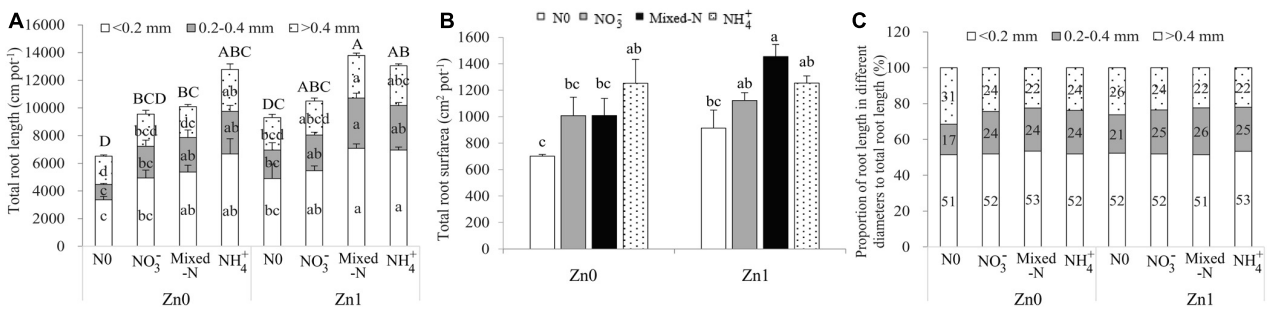


FIGURE 3 | Root length **(A)**, root surface area **(B)** and the proportions of root length in different diameters to total root length **(C)** of 30-d-old maize seedlings cultured with nil N (N0), NO_3^-, mixed-N and NH_4^+ nutrition under sand culture conditions without (Zn0) and with Zn (Zn1) supply. Error bars represent the standard error of the mean (n = 3). Significant differences at $P < 0.05$ are shown with different letters.

highest with mixed-N nutrition in the presence of Zn supply. Root C/N ratio was not significantly affected by the three N forms and Zn supply (**Figure 5A**). The Zn/N ratios of both shoot and root were not significantly affected by the three N forms without Zn supply, but those tended to increase in the order of NO_3^- < mixed-N < NH_4^+ nutrition in the presence of Zn supply (**Figure 5B**). Irrespective of Zn supply, there was a significant positive correlation between shoot C/N ratio and shoot DW, implying that shoot C/N was an important indicator of shoot DW accumulation with N supply (**Figure 5C**).

Other Nutrient Accumulation of Shoot and Root

Two-way ANOVA revealed significant effects of the Zn supply on shoot accumulation of Fe, Mn, K, P, Mg, and Ca (but

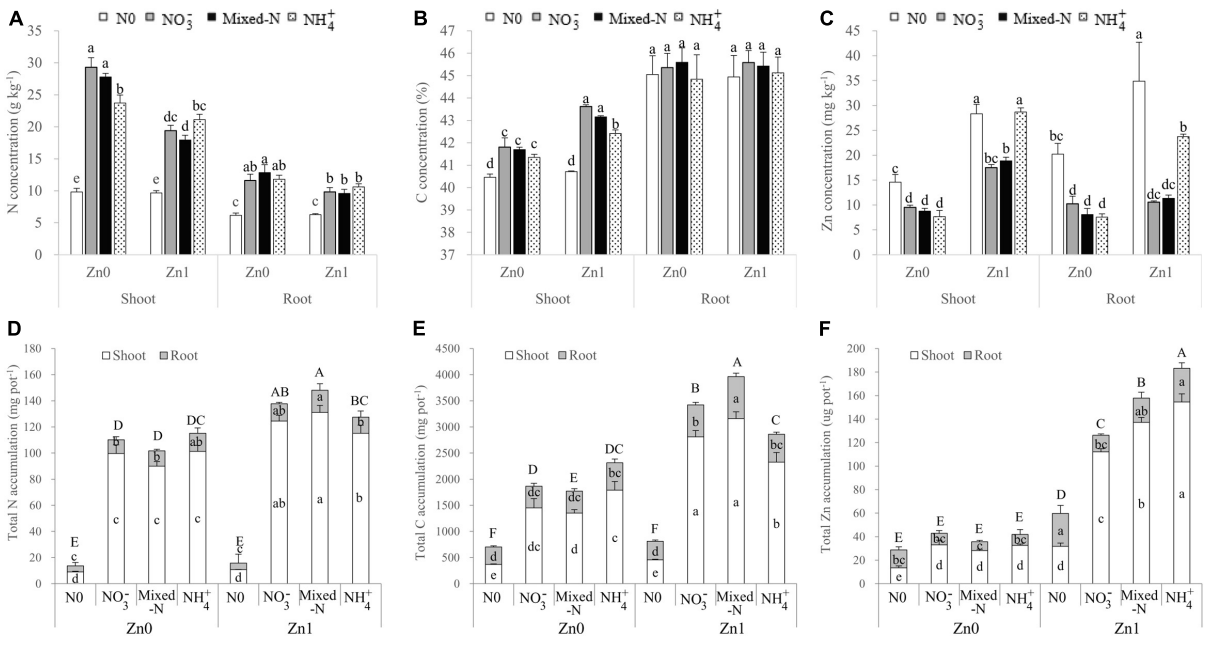


FIGURE 4 | Nitrogen, C, and Zn concentration **(A–C)** and accumulation **(D–F)** of shoot and root of 30-day-old maize seedlings cultured with nil N (N0), NO_3^-, mixed-N, and NH_4^+ nutrition under sand culture conditions without (Zn0) and with Zn (Zn1) supply. Error bars represent the standard error of the mean (n = 4). Significant differences at $p < 0.05$ are shown with different letters.

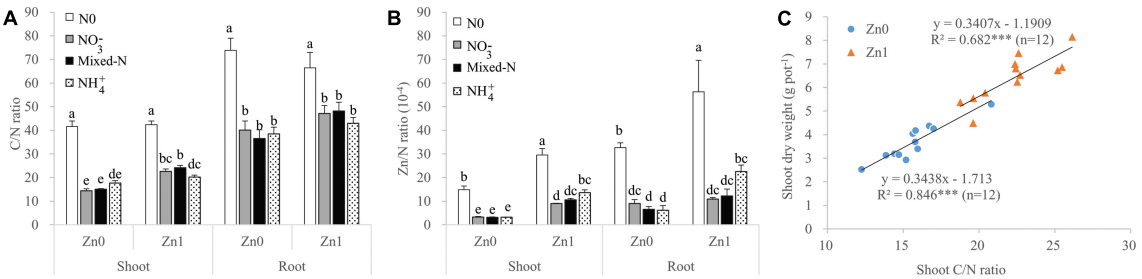


FIGURE 5 | The ratios of C/N **(A)** and Zn/N **(B)** of shoot and roots of plants grown in different N forms without and with Zn supply together with the relationship between shoot C/N ratio and shoot dry weight of plants supplied with different N forms (excluding nil N treatment) without and with Zn supply **(C)**. Values are mean and SE (n = 4). Significant differences at $p < 0.05$ are shown with different letters. *** indicate significant difference at 0.001 level.

not Cu), and significant effects of N supply on all these nutrients. The interactions between Zn and N supply were also significant for shoot accumulation of these nutrients with the exception of Ca (**Supplementary Table 3**). However, for root nutrient accumulation, only root accumulation of Cu and Fe was significantly affected by Zn and N supply, respectively. The interactions between Zn and N supply were also significant for root Fe accumulation (**Supplementary Table 3**).

Figure 6 shows that under a Zn-deficient condition, total and shoot accumulation of Fe, Mn, Mg, and Ca was the highest with NH_4^+ nutrition, followed by mixed-N nutrition, whereas NO_3^- nutrition exhibited the lowest among the three N forms. For both K and P, total and shoot accumulation tended to decrease in the order NH_4^+ > NO_3^- > mixed-N nutrition. Under a Zn-sufficient condition, total and shoot accumulation of Fe, Mn, Mg, and Ca was the highest with mixed-N nutrition, followed by NH_4^+ nutrition, whereas NO_3^- nutrition exhibited the lowest among the three N forms. For both K and P, total and shoot accumulation tended to increase in the order NH_4^+ < mixed-N < NO_3^- nutrition. There were also significant and positive effects of Zn supply on shoot accumulation of Mg and Ca with each N form, and of Mn, K, and P with NO_3^- and mixed-N nutrition. However, compared with no Zn supply, shoot Fe accumulation was significantly lower with Zn supply when grown with NH_4^+ nutrition (**Figure 6**).

DISCUSSION

Previous studies have shown that co-provision of NO_3^- and NH_4^+ stimulates plant growth beyond that observed with either N source provided individually in several crops

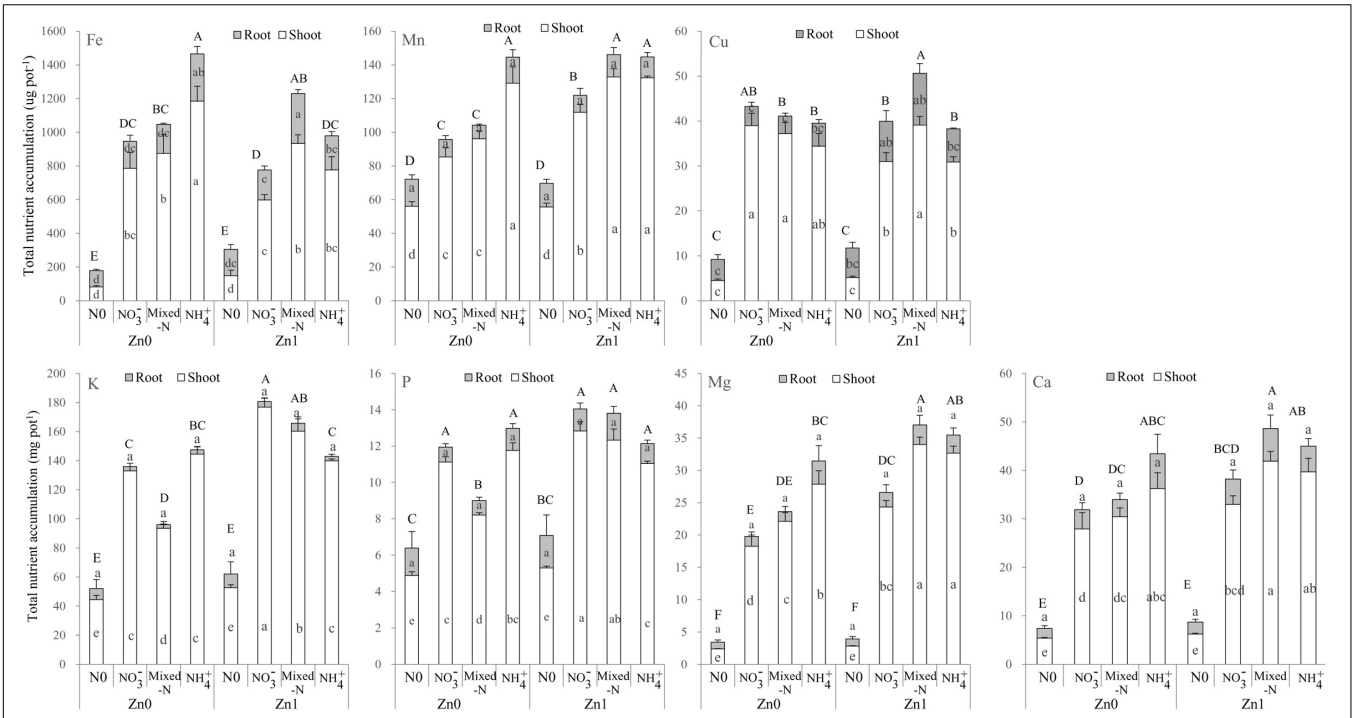


FIGURE 6 | Other nutrient (Fe, Mn, Cu, K, P, Mg, and Ca) uptakes of shoot and roots of plants grown in different N forms without and with Zn supply. Values are mean and SE (n = 4). Significant differences at $p < 0.05$ are shown with different letters.

(Gentry and Below, 1993; Marschner, 2011; Hachiya and Sakakibara, 2017; Cao et al., 2018; Wang et al., 2019). Furthermore, fertilizer Zn supply also improves shoot biomass accumulation and the final grain yield of maize (Sarwar et al., 2017; Zhang J. Y. et al., 2019; Liu et al., 2020) and wheat (Liu et al., 2019). However, the interaction between N forms and Zn nutritional status on plant growth has received considerably less attention. In this study, our results suggested that N regimes (including N levels and N forms), Zn supply, and their interactions exerted a significant effect on the growth of maize seedlings.

The extent of the effects of Zn supply on the DW of both shoot and root and N uptake depended on N availability in the growth medium. When N was deficient in solution, Zn supply had little effects on the growth and N absorption of maize seedlings, in agreement with others (Kutman et al., 2011b). However, when N was applied at a recommended rate, the positive effects of Zn supply on the growth and N absorption of maize seedlings were dependent on N forms. Generally, the growth and N absorption of maize seedlings supplied with NH_4^+ supply were superior to either NO_3^- or mixed-N nutrition under Zn-deficient conditions. However, the growth and N absorption of maize seedlings supplied with mixed-N supply were superior to independent NH_4^+ and NO_3^- nutrition under Zn-sufficient conditions. Furthermore, the positive effects of mixed-N nutrition and Zn supply on the growth of maize seedlings were more than additive. For example, with zero Zn supply, NH_4^+ supply resulted in 374.2% of increase in shoot DW, and with zero N supply, Zn supply increased the shoot DW by 22.4%, but the combined effects of mixed-N nutrition and Zn supply were over 700% (**Table 1**). Similar results were also found for N absorption in the shoot, root, and whole plant (**Figure 4D**). Similarly, a previous study also reported that the positive effects of high N and Zn supply on the grain yield of wheat were more than additive under greenhouse conditions (Kutman et al., 2011a). For example, at low Zn supply, high N supply resulted in a 73% increase in grain yield, and at low N supply, high Zn supply increased the grain yield by 35%, but the combined effect of high N–high Zn treatment was over 350%. Previous results obtained from greenhouse conditions showed Zn and N are synergistic in their effects on increasing plant Zn concentration, and their levels in growth medium should be at enough levels to achieve the synergistic effect of N on wheat root Zn uptake (Kutman et al., 2010, 2011a,b). Here, our results showed that compared with no N supply, a substantial increase in DW of shoot and root by N supply resulted in a significant decrease in Zn concentration (a so-called dilution effect) with the exception of Zn concentration in shoots of plants receiving both NH_4^+ and Zn supply (**Table 1** and **Figure 4C**). Finally, the total Zn accumulation, including shoot and root, was significantly increased by NH_4^+ supply in the presentence of Zn supply, but not significantly affected by N rates and forms in the absence of Zn supply. These results suggested that the combined applications of NH_4^+ and Zn fertilizers have beneficial effects on plant Zn nutrition. The NH_4^+-induced acidification and a decline in apoplastic pH may play an important role in increasing Zn availability in solution for root uptake. The abundance of root Zn uptake transporters in the plasma membrane of root cells, including ZIPs such as

IRT1 and other unknown proteins (Ishimaru et al., 2005; Palmer and Guerinot, 2009; Tiong et al., 2014), may also be enhanced by NH_4^+ supply.

Zinc is an essential micro-nutrient for plants. As expected, Zn-deficient stress resulted in a 21.1–55.7% of decrease in shoot DW and 0.5–47.9% of decrease in root DW irrespective of N forms. These results revealed that shoots were more sensitive to Zn deficiency than the roots, in agreement with previous studies on Zn deficiency in maize (Wang and Jin, 2005; Zhang J. Y. et al., 2019). Zn deficiency causes visible symptoms when Zn content is below 15–20 mg kg^{-1} in plants (Marschner, 2011; Zhang J. Y. et al., 2019). In this study, under Zn-deficient conditions, shoot Zn concentration significantly decreased from 14.6 mg kg^{-1} to around 8.7 mg kg^{-1} with N supply (**Figure 4C**). These values were below the critical Zn-deficient range of 15–20 mg kg^{-1} (Marschner, 2011), indicating a Zn-deficient status although severe Zn-deficient symptoms did not occur in maize seedlings (**Supplementary Figure 2**). The reduced shoot Zn concentration by N supply without causing severe Zn-deficient symptoms in maize seedlings may also indicate that adequate N application improves Zn mobility and physiological availability at the cellular level by affecting the level of Zn-chelating compounds, such as amino acids, peptides, or nicotianamine (Kutman et al., 2010). Alternatively, Denghai605 may be a highly Zn-efficient cultivar with ZE values of shoot ad root being 53.9 and 69.5%. However, the corresponding ZE values of shoot and root were only 36.8 and 50.0% for Zhengdan958 grown in Zn-free nutrient solution, which showed severely Zn-deficient symptoms 15 days after treatment (Zhang J. Y. et al., 2019). According to the criteria suggested by Farquhar and Sharkey (1982), when the P_n decreases along with an increase in C_i, photosynthesis is mainly limited by non-stomatal factors. In this study, compared with Zn supply, Zn deficiency resulted in a slight decrease in P_n, whereas C_i was significantly increased with g_s and T_r not being affected regardless of N forms. Therefore, the reduction in P_n caused by Zn deficiency was mainly due to non-stomatal factors. The decreased P_n resulting from Zn deficiency may be due to the decline in the activities of carbonic anhydrase (Ohki, 1978), ribulose 1,5-bisphosphate carboxylase/oxygenase and fructose-1,6-bisphosphase (Hacisalihoglu, 2003; Marschner, 2011), and the dramatic damages of chloroplast structure and functions (Chen et al., 2010; Zhang J. Y. et al., 2019) as shown by the decreasing leaf SPAD values (**Figure 1A**).

Under Zn-deficient stress, the DW of both shoot and root was the highest with NH_4^+ nutrition among the three N forms. Furthermore, ZE of both shoot and root was significantly higher with NH_4^+ nutrition compared with NO_3^- and mixed-N supply (**Table 1**). These results suggested that NH_4^+ nutrition enhanced the tolerance of maize seedlings to Zn-deficient stress. Similarly, other studies also showed the preference of growth and N uptake for NH_4^+ over NO_3^- in maize (Gu et al., 2013; George et al., 2016; Zhang H. Q. et al., 2019). Several possible reasons are suggested for the growth preference of maize supplied by NH_4^+ over either NO_3^- or mixed-N nutrition under Zn-deficient conditions. First, NH_4^+ supply produced the highest FRL, MRL, and thick roots and finally resulted in the highest TRL and total root surface area among the three N forms in the absence of Zn supply (**Figure 3**). The root proliferation with NH_4^+ supply was beneficial to promote the root nutrient uptake such as N, P, K, and especially Fe, Mn, Mg, and Ca accumulation (**Figures 4**, **6**) and thus to improve crop growth. Similarly, a previous study also reported that the root density and extension of maize seedlings were greater in nutrient solutions containing NH_4^+ than in those containing NO_3^- nutrition due to more rapid cell division in the root apical meristem of maize under NH_4^+ nutrition (Bloom et al., 2002). Results from field experiments also showed that the localized application of NH_4-N + P significantly improved maize root biomass, the TRL, and lateral root proliferation at the seedling stage compared with localized application of NO_3-N + P and urea +P, which could greatly contribute to improved nutrient uptake and biomass accumulation, and thus improve grain yield of maize grown in the calcareous soil with a critical Zn deficiency (DTPA-extractable Zn was 0.65 mg kg^{-1}) (Ma et al., 2014). Furthermore, the NH_4^+-induced acidification and a decline in apoplastic pH cannot be ruled out as playing a role in increasing nutrient availability (and hence uptake), especially for Fe, Mn, Mg, and Ca uptake even though the pH of the nutrient solution was maintained at 6.0. More importantly, the uptake and assimilation of NH_4^+ by maize is a more energy-efficient process than that of NO_3^- because the reduction of each nitrate molecule to ammonium consumes about 15 ATP molecules, which are not consumed when ammonium is supplied (Salsac et al., 1987). Less energy is needed for roots to take up and assimilate NH_4^+ may be more adaptive under Zn-deficient stress. Additionally, the leaf protein content with NH_4^+ nutrition was significantly improved by Zn deficiency compared with Zn supply and was also slightly higher when compared to NO_3^- and mixed-N nutrition under Zn-deficient conditions (**Figure 1B**), which can prevent the dehydration of cells and enhanced the structure and function of cell membranes in adverse environments (Andrews et al., 2005; Cao et al., 2018), such as in Zn-deficient stress. Other studies reported that the supply of NH_4^+ nutrition significantly enhanced the drought tolerance of rice seedlings compared with the application of NO_3^-, and this effect seems to be closely related to the larger root tips and surface area, higher chlorophyll and Rubisco contents, and higher Rubisco activity due to the higher distribution of N absorbed to Rubisco (Guo et al., 2007; Gao et al., 2010; Ding et al., 2015). This information may be useful for enabling integrated management of Zn-deficient soils and increasing plant and grain production in the future.

Under Zn-sufficient conditions, the DW of shoot, root, and whole plant tended to increase in the order NH_4^+ < NO_3^- < mixed-N nutrition. Compared with NH_4^+ nutrition alone, mixed-N supply resulted in a 27.4 and 28.1% increase in leaf P_n and g_s, which further resulted in a 35.7 and 33.5% increase in shoot C accumulation and shoot DW, respectively. Furthermore, mixed-N supply resulted in 19.7% of higher shoot C/N ratio vs. NH_4^+ nutrition alone, which means a higher shoot biomass accumulation because of a significant positive correlation between shoot C/N ratio and shoot DW (**Figure 5C**). Additionally, compared with the mixed-N supply, the negative effect of NH_4^+ nutrition on the root DW was larger than that on the TRL due to insufficient C supply from

shoot to root, resulting in an overall increase in the specific root length (the ratio of TRL to root DW) (**Table 1** and **Figure 3A**). Previous studies suggested that an increase in specific root length is an adaptive response to insufficient carbohydrate (Ostonen et al., 2007; Xie et al., 2007). Wang et al. (2019) also showed that compared with NH_4^+ nutrition alone, mixed-N nutrition resulted in a significantly increased shoot and root biomass mainly due to increased shoot ATP content and greater leaf area with similar or even lower P_n under lower and higher planting densities. Other studies also reported that mixed-N nutrition tended to increase both the accumulation of whole-shoot DW and the proportion partitioned to reproductive tissues and finally to increase the grain yield of maize, compared to NO_3^- nutrition only (Gentry and Below, 1993). Another field experiment showed that maize grain and straw yields were highest when fertilized with calcium ammonium nitrate, followed by ammonium sulfate, whereas urea exhibited the lowest yields (Abbasi et al., 2013).

CONCLUSION

Irrespective of N forms, compared with Zn supply, Zn deficiency resulted in a substantial decrease in both shoot and root DW, with the magnitude of decrease consistently being the highest with mixed-N nutrition, followed by NO_3^- nutrition whereas NH_4^+ nutrition exhibited the lowest decrease. Furthermore, ZE of both shoot and root was significantly higher with NH_4^+ nutrition compared with NO_3^- and mixed-N supply. These results suggested that NH_4^+ nutrition enhanced the tolerance of maize seedlings to Zn-deficient stress. Under Zn-sufficient conditions, the DW of the shoot, root, and whole plant tended to increase in the order $NH_4^+ < NO_3^- <$ mixed-N nutrition. Furthermore, the positive effects of mixed-N nutrition and Zn supply on the growth of maize seedlings were more than additive. The combined applications of mixed-N nutrition and Zn fertilizer can promote root growth (including the increased root DW, root length in different diameter, TRL, and total root surface area), synchronously improve root absorption capacity of N, Fe, Cu, Mn, Mg, and Ca, increase leaf SPAD values and photosynthetic rate, and thus maximize the aboveground plant dry matter accumulation. In the case of total Zn uptake, the positive effect of NH_4^+ nutrition with Zn supply was more pronounced. This information may be useful for enabling integrated N management of Zn-deficient and Zn-sufficient soils and increasing plant and grain production in the future.

DATA AVAILABILITY STATEMENT

The original contributions presented in the study are included in the article/**Supplementary Material**, further inquiries can be directed to the corresponding authors.

AUTHOR CONTRIBUTIONS

KL, ZL, and YX conceived and designed the experiments, analyzed the data, and wrote the manuscript. WY, YG, HZ, LJ, XQ, ZC, CZ, SL, and HW performed the experiments. All the authors read and approved the final manuscript.

FUNDING

This study was financially supported by the National Natural Science Foundation of China (No. 31702001), the National Key Research and Development Program of China (No. 2017YFD0301005), the Taishan Scholarship Project of Shandong Province (No. TS201712082), and the Innovative Talent Introduction of Shandong Academy of Agricultural Sciences.

ACKNOWLEDGMENTS

The authors are grateful to Tom Sizmur in Reading University in the United Kingdom for his English language improvements in the manuscript.

SUPPLEMENTARY MATERIAL

The Supplementary Material for this article can be found online at: https://www.frontiersin.org/articles/10.3389/fpls.2021.722752/full#supplementary-material

Supplementary Figure 1 | The proportions of shoot to total N, C, and Zn accumulation of 30-day-old maize seedlings cultured with nil N (N0), NO_3^-, mixed-N, and NH_4^+ nutrition under sand culture conditions without (Zn0) and with Zn (Zn1) supply. Error bars represent the standard error of the mean ($n = 4$). Significant differences at $p < 0.05$ are shown with different letters.

Supplementary Figure 2 | The growth of 30-day-old maize seedlings cultured with nil N (N0), NO_3^-, mixed-N, and NH_4^+ nutrition under sand culture conditions without (Zn0) and with Zn (Zn1) supply.

REFERENCES

Abbasi, M. K., Tahir, M. M., and Rahim, N. (2013). Effect of N fertilizer source and timing on yield and N use efficiency of rainfed maize (*Zea mays* L.) in Kashmir–Pakistan. *Geoderma* 19, 87–93. doi: 10.1016/j.geoderma.2012.11.013

Alloway, B. J. (2008). *Zinc in Soils and Crop Nutrition*, 2nd Edn. Brussels: International Zinc Association.

Andrews, M., Raven, J. A., Lea, P. J., and Sprent, J. I. (2005). A role for shoot protein in shoot–root dry matter allocation in higher plants. *Ann. Bot.* 97, 3–10. doi: 10.1093/aob/mcj009

Bloom, A. J., Meyerhoff, P. A., Taylor, A. R., and Rost, T. L. (2002). Root development and absorption of ammonium and nitrate from the rhizosphere. *J. Plant Growth Regul.* 21, 416–431. doi: 10.1007/s00344-003-0009-8

Bradford, M. M. (1976). A rapid and sensitive method for quantitation of microgram quantities of protein utilizing the principle of protein-dye binding. *Anal. Biochem.* 72, 248–254. doi: 10.1006/abio.1976.9999

Cakmak, I. (2008). Enrichment of cereal grains with zinc: agronomic or genetic biofortification? *Plant Soil* 302, 1–17. doi: 10.1007/s11104-007-9466-3

Cao, X. C., Zhu, C. Q., Zhong, C., Hussain, S., Zhu, L. F., Wu, L. H., et al. (2018). Mixed-nitrogen nutrition-mediated enhancement of drought tolerance of rice seedlings associated with photosynthesis, hormone balance and carbohydrate partitioning. *Plant Growth Regul.* 84, 451–465. doi: 10.1007/s10725-017-0352-6

Chen, W. R., Yang, X. E., He, Z. L., Feng, Y., and Hu, F. H. (2010). Differential changes in photosynthetic capacity, 77 K chlorophyll fluorescence and chloroplast ultrastructure between Zn-efficient and Zn-inefficient rice

genotypes (*Oryza sativa*) under low zinc stress. *Physiol. Plant.* 132, 89–101. doi: 10.1111/j.1399-3054.2007.00992.x

Cramer, M. D., and Lewis, O. A. M. (1993). The influence of NO_3^- and NH_4^+ nutrition on the carbon and nitrogen partitioning characteristics of wheat (*Triticum aestivum* L.) and maize (*Zea mays* L.) plants. *Plant Soil* 154, 289–300. doi: 10.1007/BF00012534

Ding, L., Gao, C. M., Li, Y. R., Li, Y., Zhu, Y. Y., Xu, G. H., et al. (2015). The enhanced drought tolerance of rice plants under ammonium is related to aquaporin (AQP). *Plant Sci.* 234, 14–21. doi: 10.1016/j.plantsci.2015.01.016

Fang, Q. X., Qiang, Y., Wang, E. L., Chen, Y. H., Zhang, G. L., Wang, J., et al. (2006). Soil nitrate accumulation, leaching and crop nitrogen use as influenced by fertilization and irrigation in an intensive wheat-maize double cropping system in the North China Plain. *Plant Soil* 284, 335–350. doi: 10.1007/s11104-006-0055-7

Farquhar, G. D., and Sharkey, T. D. (1982). Stomatal conductance and photosynthesis. *Ann. Rev. Plant Physiol.* 33, 317–345. doi: 10.1146/annurev.pp.33.060182.001533

Gao, Y. X., Li, Y., Yang, X. X., Li, H. J., Shen, Q. R., and Guo, S. W. (2010). Ammonium nutrition increases water absorption in rice seedlings (*Oryza sativa* L.) under water stress. *Plant Soil* 331, 193–201. doi: 10.1007/s11104-009-0245-1

Gentry, L. E., and Below, F. E. (1993). Maize productivity as influenced by form and availability of nitrogen. *Crop Sci.* 33, 491–497. doi: 10.2135/cropsci1993.0011183X003300030015x

George, J., Holtham, L., Sabermanesh, K., Heuer, S., Tester, M., Plett, D., et al. (2016). Small amounts of ammonium (NH_4^+) can increase growth of maize (*Zea mays*). *J. Plant Nutr. Soil Sci.* 179, 717–725. doi: 10.1002/jpln.201500625

Gu, R. L., Duan, F. Y., Xia, A., Zhang, F. S., vonWirén, N., and Yuan, L. X. (2013). Characterization of AMT-mediated high-affinity ammonium uptake in roots of maize (*Zea mays* L.). *Plant Cell Physiol.* 54, 1515–1524. doi: 10.1093/pcp/pct099

Guo, S. W., Chen, G., Zhou, Y., and Shen, Q. R. (2007). Ammonium nutrition increases photosynthesis rate under water stress at early development stage of rice (*Oryza sativa* L.). *Plant Soil* 296, 115–124. doi: 10.1007/s11104-007-9302-9

Hachiya, T., and Sakakibara, H. (2017). Interactions between nitrate and ammonium in their uptake, allocation, assimilation, and signaling in plants. *J. Exp. Bot.* 68, 2501–2512. doi: 10.1093/jxb/erw449

Hacisalihoglu, G. (2003). Zinc efficiency is correlated with enhanced expression and activity of zinc-requiring enzymes in wheat. *Plant Physiol.* 131, 595–602. doi: 10.1046/j.1469-8137.2003.00826.x

Ishimaru, Y., Suzuki, M., Kobayashi, T., Takahashi, M., Nakanishi, H., Mori, S., et al. (2005). OsZIP4, a novel zinc-regulated zinc transporter in rice. *J. Exp. Bot.* 56, 3207–3214. doi: 10.1093/jxb/eri317

Karim, M. R., Zhang, Y. Q., Tian, D., Chen, F. J., Zhang, F. S., and Zou, C. Q. (2012). Genotypic differences in zinc efficiency of Chinese maize evaluated in a pot experiment. *J. Sci. Food Agr.* 92, 2552–2559. doi: 10.1002/jsfa.5672

Kutman, U. B., Yildiz, B., and Cakmak, I. (2011a). Effect of nitrogen on uptake, remobilization and partitioning of zinc and iron throughout the development of durum wheat. *Plant Soil* 342, 149–164. doi: 10.1007/s11104-010-0679-5

Kutman, U. B., Yildiz, B., and Cakmak, I. (2011b). Improved nitrogen status enhances zinc and iron concentrations both in the whole grain and the endosperm fraction of wheat. *J. Cereal Sci.* 53, 118–125. doi: 10.1016/j.jcs.2010.10.006

Kutman, U. B., Yildiz, B., Ozturk, L., and Cakmak, I. (2010). Biofortification of durum wheat with zinc through soil and foliar applications of nitrogen. *Cereal Chem.* 87, 1–9. doi: 10.1094/CCHEM-87-1-0001

Liu, D. Y., Liu, Y. M., Zhang, W., Chen, X. P., and Zou, C. Q. (2019). Zinc uptake, translocation, and remobilization in winter wheat as affected by soil application of Zn fertilizer. *Front. Plant Sci.* 10:426. doi: 10.3389/fpls.2019.00426

Liu, D. Y., Zhang, W., Liu, Y. M., Chen, X. P., and Zou, C. Q. (2020). Soil application of zinc fertilizer increases maize yield by enhancing the kernel number and kernel weight of inferior grains. *Front. Plant Sci.* 11:188. doi: 10.3389/fpls.2020.00188

Liu, H., Gan, W., Rengel, Z., and Zhao, P. (2016). Effects of zinc fertilizer rate and application method on photosynthetic characteristics and grain yield of summer maize. *J. Soil Sci. Plant Nutr.* 16, 550–562.

Liu, Z. (1996). *Microelements in Soils of China (in Chinese)*. Nanjing: Jiangsu Science Technology Publishing house.

Ma, Q. H., Wang, X., Li, H., Li, H. B., Li, H. G., Cheng, L. Y., et al. (2014). Localized application of NH_4^+-N plus P enhances zinc and iron accumulation in maize via modifying root traits and rhizosphere processes. *Field Crops Res.* 164, 107–116. doi: 10.1016/j.fcr.2014.05.017

Marschner, H. (2011). *Mineral Nutrition of Higher Plants*, 3rd Edn. London: Academic Press.

Mueller, N. D., Gerber, J. S., Johnston, M., Ray, D. K., Ramankutty, N., and Foley, J. A. (2012). Closing yield gaps through nutrient and water management. *Nature* 490, 254–257. doi: 10.1038/nature11420

Ohki, K. (1978). Zinc concentration in soybean as related to growth, photosynthesis, and carbonic anhydrase activity. *Crop Sci.* 18, 79–82. doi: 10.2135/cropsci1978.0011183X001800010021x

Ostonen, I., Püttsepp, Ü, Biel, C., Alberton, O., Bakker, M. R., Lõhmus, K., et al. (2007). Specific root length as an indicator of environmental change. *Plant Biosyst.* 141, 426–442. doi: 10.1080/11263500701626069

Palmer, C. M., and Guerinot, M. L. (2009). Facing the challenges of Cu, Fe and Zn homeostasis in plants. *Nat. Chem. Biol.* 5, 333–340. doi: 10.1038/nchembio.166

Potarzycki, J. (2010). The impact of fertilization systems on zinc management by grain maize. *Fertiliser Fertilization* 39, 78–89. doi: 10.1155/2009/251915

Salsac, L., Chaillou, S., Morot-Gaudry, J. F., Lesaint, C., and Jolivet, E. (1987). Nitrate and ammonium nutrition in plants. *Plant Physiol. Biochem.* 25, 805–812.

Sarwar, S., Rafique, E., Yousra, M., Mahmood-ul-Hassan, M., Gill, S. M., and Khan, M. Z. (2017). Improved productivity and zinc content for maize grain by different zinc fertilization techniques in calcareous soils. *J. Plant Nutr.* 40, 417–426. doi: 10.1080/01904167.2016.1245322

Schortemeyer, M., Stamp, P., and Feil, B. (1997). Ammonium tolerance and carbohydrate status in maize cultivars. *Ann. Bot.* 79, 25–30. doi: 10.1006/anbo.1996.0298

Tang, Q. Y., and Zhang, C. X. (2013). Data Processing System (DPS) software with experimental design, statistical analysis and data mining developed for use in entomological research. *Insect Sci.* 20, 254–260. doi: 10.1111/j.1744-7917.2012.01519.x

Tilman, D., Cassman, K. G., Matson, P. A., Naylor, R., and Polasky, S. (2002). Agricultural sustainability and intensive production practices. *Nature* 418, 671–677. doi: 10.1038/nature01014

Tiong, J., McDonald, G. K., Genc, Y., Pedas, P., Hayes, J. E., Toubia, J., et al. (2014). HvZIP7 mediates zinc accumulation in barley (*Hordeum vulgare*) at moderately high zinc supply. *New Phytol.* 201, 131–143. doi: 10.1111/nph.12468

Wang, H., and Jin, J. Y. (2005). Photosynthetic rate, chlorophyll fluorescence parameters, and lipid peroxidation of maize leaves as affected by zinc deficiency. *Photosynthetica* 43, 591–596. doi: 10.1007/s11099-005-0092-0

Wang, H., and Jin, W. Y. (2007). Effects of zinc deficiency and drought on plant growth and metabolism of reactive oxygen species in maize (*Zea mays* L). *J. Integr. Agr.* 6, 988–995. doi: 10.1016/s1671-2927(07)60138-2

Wang, J. W., Mao, H., Zhao, H. B., Huang, D. L., and Wang, Z. H. (2012). Different increases in maize and wheat grain zinc concentrations caused by soil and foliar applications of zinc in Loess Plateau, China. *Field Crops Res.* 135, 89–96. doi: 10.1016/j.fcr.2012.07.010

Wang, P., Wang, Z. K., Sun, X. C., Mu, X. H., Chen, H., Chen, F. J., et al. (2019). Interaction effect of nitrogen form and planting density on plant growth and nutrient uptake in maize seedlings. *J. Integr. Agr.* 18, 1120–1129. doi: 10.1016/S2095-3119(18)61977-X

Welch, R. M., and Graham, R. D. (2004). Breeding for micronutrients in staple food crops from a human nutrition perspective. *J. Exp. Bot.* 55, 353–364. doi: 10.1093/jxb/erh064

Xie, Y. H., Luo, W. B., Ren, B., and Li, F. (2007). Morphological and physiological responses to sediment type and light availability in roots of the submerged plant myriophyllum spicatum. *Ann. Bot.* 100, 1517–1523.

Xue, Y. F., Yue, S. C., Liu, D. Y., Zhang, W., Chen, X. P., and Zou, C. Q. (2019). Dynamic zinc accumulation and contributions of pre- and/or post-silking zinc uptake to grain zinc of maize as affected by nitrogen supply. *Front. Plant Sci.* 10:1203. doi: 10.3389/fpls.2019.01203

Xue, Y. F., Yue, S. C., Zhang, Y. Q., Cui, Z. L., Chen, X. P., Yang, F. C., et al. (2012). Grain and shoot zinc accumulation in winter wheat affected

by nitrogen management. *Plant Soil* 361, 153–163. doi: 10.1007/s11104-012-1510-2

Xue, Y. F., Zhang, W., Liu, D. Y., Yue, S. C., Cui, Z. L., Chen, X. P., et al. (2014). Effects of nitrogen management on root morphology and zinc translocation from root to shoot of winter wheat in the field. *Field Crops Res.* 161, 38–45.

Yuan, S., Li, C. J., Peng, Z. P., Peng, Y. F., Wang, H., and Zhang, L. J. (2011). Effects of phosphorus on the plant growth, phosphorus cycling and distribution in different maize cultivars. *Plant Nutr. Fertilizer Sci.* 17, 310–316.

Zhang, H. Q., Zhao, X. Q., Chen, Y. L., Zhang, L. Y., and Shen, R. F. (2019). Case of a stronger capability of maize seedlings to use ammonium being responsible for the higher ^{15}N recovery efficiency of ammonium compared with nitrate. *Plant Soil* 440, 293–309. doi: 10.1007/s11104-019-04087-w

Zhang, J. Y., Wang, S. F., Song, S. S., Xu, F. S., Pan, Y. H., and Wang, H. (2019). Transcriptomic and proteomic analyses reveal new insight into chlorophyll synthesis and chloroplast structure of maize leaves under zinc deficiency stress. *J. Proteomics* 199, 123–134. doi: 10.1016/j.jprot.2019.03.001

Zhao, X. Q., Shi, W. G., Shinmachi, F., Sunairi, M., Noguchi, A., Hasegawa, I., et al. (2013). Aluminium tolerance in rice is antagonistic with nitrate preference and synergistic with ammonium preference. *Ann. Bot.* 111, 69–77. doi: 10.1093/aob/mcs234

Conflict of Interest: The authors declare that the research was conducted in the absence of any commercial or financial relationships that could be construed as a potential conflict of interest.

Publisher's Note: All claims expressed in this article are solely those of the authors and do not necessarily represent those of their affiliated organizations, or those of the publisher, the editors and the reviewers. Any product that may be evaluated in this article, or claim that may be made by its manufacturer, is not guaranteed or endorsed by the publisher.

Copyright © 2021 Xue, Yan, Gao, Zhang, Jiang, Qian, Cui, Zhang, Liu, Wang, Li and Liu. This is an open-access article distributed under the terms of the Creative Commons Attribution License (CC BY). The use, distribution or reproduction in other forums is permitted, provided the original author(s) and the copyright owner(s) are credited and that the original publication in this journal is cited, in accordance with accepted academic practice. No use, distribution or reproduction is permitted which does not comply with these terms.

frontiers in Plant Science

ORIGINAL RESEARCH
published: 23 December 2021
doi: 10.3389/fpls.2021.743378

Bioactive Nutrient Fortified Fertilizer: A Novel Hybrid Approach for the Enrichment of Wheat Grains With Zinc

Muhammad Asif Ali[1], Farrukh Naeem[2], Nadeem Tariq[2], Ijaz Ahmed[1] and Asma Imran[3]*

[1] Engro Fertilizers Ltd., Lahore, Pakistan, [2] First Biotech LLC, Lahore, Pakistan, [3] National Institute for Biotechnology and Genetic Engineering-Campus-Pakistan Institute for Engineering and Applied Sciences (NIBGE-C-PIEAS), Faisalabad, Pakistan

Zinc (Zn) is a critical micronutrient that synergizes nutrient use efficiency, and improves plant growth and human health. Low Zn bioavailability in soils affects produce quality and agricultural productivity worldwide ultimately inducing deficiency in humans and animals. Zn deficiency is a leading cause of malnutrition in underdeveloped countries where a widespread population depends upon staple cereals for daily intake of calories. Modern cereal cultivars are inherently low in Zn, eventually, plants need to be enriched with soil application of $ZnSO_4$, but due to higher fixation losses, it becomes an inefficient source. Rhizosphere microbiome contains Zn-solubilizing bacteria (ZSB) that improve Zn bioavailability, thus increase the root function, Zn uptake, and plant growth. Niha Corp developed a hybrid process of bioactive nutrient fortified fertilizer (BNFF), which has been used to formulate Zabardast Urea (ZU) by coating bioactive Zn (BAZ) and ZSB on urea. Data obtained for 15 wheat varieties from 119 farmer field demonstration plots and eight replicated trials on 42 locations across multi-environment conditions conclude that ZU significantly improved the plant biomass and yield by 12% over non-Zn control and produced grains with 57 μg/g Zn contents, which can meet a major part of the recommended dietary allowance (RDA) of humans. The study recommends that this microbe-mediated hybrid invention (ZU) is a feasible approach to boost Zn bioavailability and Zn use efficiency, with enhanced yield and quality that may contribute to improve human health. To the best of our knowledge, this is the first wide-scale field testing of Zn enrichment in the grains of bread wheat using an innovative BNFF Urea Z technology.

Keywords: zinc-biofortification, Zn solubilizing bacteria, bio-fortified nutrient fertilizer, plant-growth, rhizosphere, agriculture productivity

OPEN ACCESS

Edited by:
Antonios Chrysargyris, Cyprus University of Technology, Cyprus

Reviewed by:
Rajib Podder, University of Saskatchewan, Canada
Hafeez Ur Rehman, University of Agriculture, Faisalabad, Pakistan
Ana Paula Rebellato, Campinas State University, Brazil

****Correspondence:***
Muhammad Asif Ali
masifali@engro.com

Specialty section:
This article was submitted to Plant Nutrition, a section of the journal Frontiers in Plant Science

Received: *18 July 2021*
Accepted: *15 November 2021*
Published: *23 December 2021*

Citation:
Ali MA, Naeem F, Tariq N, Ahmed I and Imran A (2021) Bioactive Nutrient Fortified Fertilizer: A Novel Hybrid Approach for the Enrichment of Wheat Grains With Zinc. Front. Plant Sci. 12:743378. doi: 10.3389/fpls.2021.743378

HIGHLIGHTS

- Millions of people around the globe suffer from Zn deficiency-related growth and physiological disorders.
- A plant-based diet (e.g., cereals) is inherently low in Zn content and also contains Zn inhibitors (e.g., phytates) that reduce the Zn availability for human consumption.
- Zn biofortification of cereals can reduce the problems related to Zn-deficiency disorders.

- We reported a novel approach based on bioactive nutrient fortified fertilizer (BNFF) to increase the Zn uptake in the wheat grain making it fit for human consumption.
- The technology can be used at a large scale as it eases the application of BAZ along with beneficial microbes coated on urea for easy application.

INTRODUCTION

Zinc (Zn) is an important micronutrient for cellular, physiological, and biological growth and development (Cakmak and Kutman, 2018). As a metallic cofactor, it activates and stabilizes more than 300 enzymes in plants, animals, and humans (McCall et al., 2000; Gurmani et al., 2012; Lacerda et al., 2018), mainly regulating vital processes, including DNA and protein synthesis, carbohydrate metabolism, gene expression, enzyme activation, photosynthesis, hormones, disease resistance, wound healing, and fertility. Zn finger proteins (ZFP) are considered unique due to their synergetic role during phytohormone response, plant growth, and development (Nauman et al., 2018). Many Zn-dependent enzymes are involved in carbohydrate metabolism, especially in leaves, and affect proteins, auxins, and membrane integrity. Hence, its deficiency in plants seriously distresses various vital processes leading to yield losses and lower Zn contents in grains and fruits (Imran et al., 2015; Xing et al., 2016).

Zinc is the fourth essential micronutrient controlling a number of proteins in humans (Cakmak, 2008; Shivay et al., 2015; Krezel and Maret, 2016). It plays a major role in the function of the brain, immune system, and endocrine system, and its deficiency is connected to many physiological and growth disorders, such as premature death, stunted growth, underweight children, poor appetite, delayed healing, taste abnormalities, blindness, cognitive losses, or mental lethargy (FAO, 2004, 2021; Bhutta et al., 2007; Khalid et al., 2014; Sauer et al., 2016). A direct positive correlation has been observed for serum Zn level with the development of diabetes (Anjum et al., 2012), depressive disorders, and bipolar depression (Cope and Levenson, 2010). An estimated 2.7 billion global population is Zn deficient, while further ∼50% of the population are at risk (WHO/FAO, 2006) mainly due to low dietary intake and consumption of cereal-based foods, which are naturally low in Zn contents and contain Zn-absorption inhibitors, e.g., phytic acid (Hambidge et al., 2011). Global data analysis reveals that wheat grain contains 31.8 $\mu g\ g^{-1}$ of Zn (Wang et al., 2020), but its absorption and efficacy depend upon the intake quantity, the milling and fermentation practices, and Zn or phytate intake from other food sources (Brown et al., 2010). The optimum level of grain Zn should be 40–50 $\mu g\ g^{-1}$ to meet recommended dietary allowance (RDA), which is 11 mg for men and 8 mg for women (Bouis et al., 2011; Chen et al., 2017; Cakmak and Kutman, 2018).

Insufficient Zn in the rhizosphere leads to Zn-deficient grains as the rhizosphere is the site from where Zn moves to roots and shoots and later accumulated in grains (White and Broadley, 2011; Maillard et al., 2015). Almost 50% of the world soils under cereal production are Zn deficient (Welch et al., 2013). Many factors, e.g., texture, pH, water content, organic matter, the concentration of calcium carbonate, basic cations (Na, Ca, and Mg), dissolved organic carbon (DOC), and cation exchange capacity, anions bicarbonates, and phosphates, influence the Zn transformation and bioavailability in soil (Alloway, 2009; Koshgoftarmanesh et al., 2018). In calcareous soils, total Zn may be relatively large, but low organic matter and higher calcium carbonate contents reduce its availability (Bityutskii et al., 2017; Chen et al., 2019). Various soil supplements are being used to increase rhizosphere Zn bioavailability (Noor-ul-Ain, 2019). Zinc sulfate ($ZnSO_4$) is the most common fertilizer with high solubility; however, it readily undergoes fixation, which reduces its availability (Hussain et al., 2015). Zinc oxide (ZnO) is also not recommended due to very low solubility (Ahmad et al., 2018). Furthermore, crop Zn use efficiency is very low, i.e., 4–8% (Shivay et al., 2008), which needs to be improved either by Zn biofortification or by improving and economizing the available Zn-fertilizer sources (Montalvo et al., 2016). Zn-solubilizing bacteria (ZSB) are known components of the rhizosphere playing a significant role in nutrient availability and transformation (Hakim et al., 2021). ZSB convert the unavailable forms of Zn to plant-available forms and increase its uptake and accumulation in grains (Mishra et al., 2017). These bacteria are usually versatile, hence, exert synergistic-beneficial impact on plant growth and yield (Imran et al., 2021). Application of ZSB as biofertilizers has been reported in wheat and maize (Goteti et al., 2013; Kamran et al., 2017; Hussain et al., 2019), but its field application needs extra time and effort as biofertilizers are applied separately from the chemical fertilizers. Combining fertilizers (i.e., biological and chemical) into a single product, however, is a better approach to save time, effort, and cost.

Bioactive nutrient fortified fertilizer (BNFF) is a novel concept developed and patented recently in the fertilizer industry (Tariq et al., 2017). The BNFF is a patent of Niha Crop United States where it is prepared by organic encapsulation of bioactive nutrients (P, Zn, Fe, etc.) and beneficial microbial consortium with subsequent coating onto chemical urea fertilizer. BNFF serves as a rich source of beneficial microbial strains, which not only improves nutrients use efficiency, induces resistance in plants, but also provides growth-regulating organic nutrients for healthy growth that leads to higher yield and better-quality yield. The consortium of beneficial microbes solubilizes a range of nutrients present in the root zone. It also facilitates extensive root system development and activates the inherent defense response of plants through induced systemic resistance (ISR) (Choudhary et al., 2007). Production and implication of bioactive organic fertilizer enriched with ZSB have been reported to boost Zn contents in maize at a small scale (Hussain et al., 2020). The present study reports a novel hybrid technology that combines the benefits of biological (ZSB) and chemical fertilizers (BAZ + urea) with a synergistic effect on the plant at a wide scale. Although, the effects of ZSB (Khanghahi et al., 2018; Eshaghi et al., 2019) and urea have been tested in solo treatments.

This study hypothesized that bioactive zinc (BAZ) will keep Zn free from getting fixed in the soil due to the protective cover of organic encapsulation, therefore, Zn will remain continuously available in the root zone for plant uptake throughout the crop

life. The ultimate aim of the study was to use BNFF to fortify wheat grains with Zn to reduce Zn deficiency in humans. This study reports and confirms the potential of BAZ fortified urea to improve physiology, growth, yield, the concentration of Zn in grains, and ultimately the grain quality of different wheat varieties grown at farmer fields for human consumption. To the best of our knowledge, this is the first report of the development and large-scale testing of BAZ for bread wheat biofortification.

METHODOLOGY

Materials Used

Bioactive Zn (BAZ) was formulated using the patent method of Niha Corp, Ontario, CA, United States as a fine dry powder of biologically solubilized and organically encapsulated Zn (Tariq et al., 2017). BNFF Urea Z was developed by First Biotech LLC, Lahore, Pakistan an associate of Niha Corp., United States, using the patented process (Tariq et al., 2017). Engro Fertilizers Ltd. (EFERT), having exclusive marketing rights of BNFF Urea Z for Pakistan, launched under the brand name Zabardast Urea (ZU) in 2017. ZU contains 42% nitrogen, 1% BAZ, and a consortium of beneficial microbes 10^3 CFU $g^{-}1$ of ZU material. The beneficial microbes are a consortium of Zn-mobilizing bacteria with multiple plant benefits (Tariq et al., 2017).

Field Location, Soil Analysis, and Experimental Design

Cross-ecological trials were carried out during the wheat season 2019–2020 to evaluate the ZU application on the yield and quality of 15 bread wheat (*Triticum aestivum*) varieties. Eight replicated trials were conducted spread over eight different sites (i.e., Shujabad, Multan, Chichawatni, Lahore, Sahiwal, Faisalabad, Kasur, and Chiniot) on farmer fields; in addition, 119 demonstration trials were conducted at 42 different sites. Random soil sampling was done at a depth of 0–20 cm. Samples were pooled, homogenized, air-dried, sieved (2 mm), and characterized for different parameters such as pH, EC, available phosphorous and potassium (US Salinity Laboratory Staff, 1954; Page et al., 1982), and extractable metal (Zn) (Soltanpour, 1985). The soil data are presented in **Supplementary Table 1**.

The treatment plan at replicated field trials at eight locations is as follows:

T1: Urea + no Zn control [urea; 46% N @ 250 kg ha^{-1}]
T2: Urea + Zn sulfate [urea; 46% N @ 250 kg ha^{-1}) + Zn sulfate non-branded (33% Zn @ 15 kg ha^{-1})
T3: Urea + Zingro (urea; 46% N @ 250 kg ha^{-1}) + Engro brand Zn fertilizer [Zingro; 33% Zn @ 15 kg ha^{-1}]
T4: BNFF Urea Z (ZU) (urea (46% N) 125 kg + ZU (42% N) 125 kg ha^{-1}, 1% bioactive Zn (BAZ) (1.235 kg ha^{-1}) and 10^3 CFU g^{-1} beneficial microbial consortium].

The layout of the field experiment was RCBD split-plot design with treatments as main plots and variety as subplots with three replicates at each location. The plot size per replicate was 252.9 m^2.

For 119 farmer field trials at 42 locations, the treatments were as follows:

T1: Farmer practice: urea + Zn sulfate [urea; 46% N @ 250 kg ha^{-1}) + Zn sulfate non-branded (33% Zn @ 15 kg ha^{-1}).
T2: BNFF Urea Z (ZU) (125 kg urea (46% N) + 125 kg ZU (42% N) ha^{-1}, 1% BAZ (1.235 kg ha^{-1}), and 10^3 CFU g^{-1} beneficial microbial consortium].

The plot size at farmer sites was 0.5 acres (2,023.4 m^2) per treatment for each trial.

Sowing was performed from November 15 to December 15, 2019. Uniform application of nitrogen, phosphorus, and potassium was done across all treatments at the rate of 250, 185, and 150 kg ha^{-1}, respectively. Diammonium phosphate (DAP) was used as a phosphorus source and mutate of potash (MOP) as a potassium source, while the use of nitrogen and Zn varied as explained above in the treatment plan. All P and K fertilizers were applied at the time of sowing, whereas nitrogen was applied in two splits, i.e., half 25 days after sowing and the remaining half 55 days after sowing using the broadcast method followed by flood irrigation. In ZU-treated plants (T4), the ZU was applied during the first split dose, while normal urea was applied in the second dose. The plants were irrigated with canal water as and when required.

Growth and Yield Analysis

Productive tillers (m^{-2}) were determined 70 days after sowing as an average of three random locations from each replicate plot using a 1 m^{-2} steel template. A sample of 15 random plants was selected from each treatment at each location for data readings related to growth and yield at harvest (125 days after sowing). Plant height and spike length were measured using a meter scale. Shoot fresh biomass was recorded for a random sample of 15 plants of each treatment (5 from each replicate) at all locations. The number of grains per spike was determined from 15 spikes collected randomly from the sample of 15 plants of each treatment (5 plants per replicate plot). After recording aforesaid data, plant samples were threshed and 1,000 kernel weight was determined by weighing 100 grains of three sets, then multiplying their average by 10, and recorded for each treatment, accordingly. For final yield data, the wheat crop of each plot was harvested, threshed, weighed, and recorded for grains and straw, separately for statistical analysis. The farmer field trial data were harvested from the whole plot and yield was determined.

Analysis for Zinc in Grains

Three random samples of wheat grains (5 g each) were collected from each threshed produce of each treatment. The seeds were washed using distilled water and then air-dried without exposure to direct sunlight followed by oven drying (65°C for 72 h), separately. These samples were finely ground in a grinder (IKA WERKE, MF 10 Basic, Staufen, Germany) and wet digested in a diacid mixture (HNO_3:$HClO_4$ ratio of 2:1) (Jomes and Case, 1990). The Zn concentration was measured in the digest by an atomic absorption spectrophotometer (PerkinElmer, Analyst

100, Waltham, United States). Agronomic Zn use efficiency (ZUE) was calculated as described by Zulfiqar et al. (2020):

$$\text{Agronomic efficiency } (\text{AgE}) = \frac{\text{GY}_{\text{Zn}} - \text{GY}_{\text{C}}}{\text{Zn}_{\text{a}}}$$

where GY_{Zn} is the grain yield of Zn-treated plots, GY_C is the yield of untreated plots, and Zn_a is the amount of Zn applied.

Statistical Analysis

This was a random sample, farmer field trial study that precisely detected the differences in the varietal response within and across the environments. Engro field trial data at eight different sites were subjected to analysis of variance using computer software Statistix version 8.1 (Analytical Software, United States). The treatment data were averaged over locations to calculate the mean response of ZU across the cross-ecological trials. The treatment means were compared using the least significant difference test (Steel et al., 1997) at a 5% probability level. Similarly, the farmer field data were averaged over varieties and 125 locations to analyze the varietal response. Correlation analysis, regression, and principal component analyses were performed using IBM SPSS software for Windows (SPSS Version 20, NY, United States).

RESULTS

Productive Tillers and Spike Length (cm)

Statistical analysis of data obtained from field trials at eight locations revealed that the application of ZU produced the highest number of productive tillers as compared to other Zn treatments and non-Zn controls (**Figure 1A**). The average productive tillers were significantly high in ZU-applied plots (396) with a percentage increase of 6.45 over non-Zn control (372). However, the productive tillers with Zingro (388) showed an increase of 4.30 and with $ZnSO_4$ (386) a 3.5% increase over non-Zn controls. The ZU-treated plots also produced the longest spikes (9.9 cm) as compared to non-Zn control (9.0 cm) and other sources of $ZnSO_4$ (**Figure 1B**). The percentage increase by ZU was 9.9%, followed by Zingro and $ZnSO_4$ treatments with 5.9 and 3.7% increase, respectively, over non-Zn controls.

Number of Grains per Spike and 1,000 Grain Weight (g)

The number of grains per spike showed a statistically non-significant effect (**Figure 2A**) by different Zn application treatments from field trials at eight locations. On average, ZU application showed maximum grains per spike (49.3) followed by Zingro (48.6) and $ZnSO_4$ (48.0) compared with non-Zn controls (46.9). The 1,000 grain weight, however, showed a significant treatment response where maximum grain weight was observed in ZU-treated plots (34.0 g) followed by Zingro (33.2 g) and $ZnSO_4$ (32.5 g) compared with non-Zn controls (31.6 g) (**Figure 2B**). The percentage increase in grain weight was 7.5 with ZU treatment, 3.6 with Zingro, and 2 with $ZnSO_4$ over non-Zn controls.

Total Biomass, Grain Yield, and Straw Yield

The total biomass obtained from eight field trials at eight locations (**Figure 3**) showed a significant increase by the application of ZU (13.5 t ha^{-1}) with a percentage increase of 12 over non-Zn controls (12.0 t ha^{-1}). This was followed by other Zn treatments, i.e., Zingro (13.3 t ha^{-1}), and $ZnSO_4$ (12.8 t ha^{-1}) with an increase of 10 and 6%, respectively, over non-Zn control.

All Zn treatments generally exhibited a positive impact on the grain yield (**Figure 3**), but comparative analysis showed that ZU treatment produced the maximum grain yield (4.9 t ha^{-1}), where the percentage increase over control was 11.7% followed by Zingro (4.7 t ha^{-1}), and $ZnSO_4$ (4.5 t ha^{-1}) with an increase of 7.2 and 2.8% over control, respectively. A similar trend was observed for the data obtained for the straw yield (**Figure 3**) where the maximum yield (8.6 t ha^{-1}) was obtained in the ZU plots with an increase of 12.6%, followed by Zingro (yield: 8.5 t ha^{-1}; percentage increase 11.8%) and $ZnSO_4$ (yield: 8.2 t ha^{-1}; percentage increase 8.0%).

Harvest Index

The data for the impact of different Zn treatments on harvest index (HI) from field trials at eight locations is given in **Figure 4**. The HI data showed a statistically non-significant response of treatments. However, the HI of ZU plots were relatively higher (0.37) than $ZnSO_4$ and Zingro (0.35 and 0.36, respectively).

Zinc Contents in Grains

The statistical analysis of grain Zn contents data obtained from field trials at eight locations (**Figure 4**) shows that the impact of Zn treatments was statistically significant. ZU application showed the maximum increase in grain Zn contents (57.00 μg/g) with a percentage increase of 171.4 over non-Zn controls. This was followed by Zingro (38.17 μg/g) with a percentage increase of 81.8 and $ZnSO_4$ (31.63 μg/g) with an increase of 56% over non-Zn controls (21 μg/g). The average Zn contents in grains of all wheat varieties were maximum in ZU-treated plots at all sites.

Agronomic Zinc Use Efficiency

The ZUE of different Zn sources used is mentioned in **Supplementary Table 3**. The data obtained from field trials at eight locations show that ZUE of ZU plots is highest, i.e., 410 followed by the Zingro, i.e., 21, and then $ZnSO_4$ with 8.

Varietal Response Toward Zabardast Urea at Farmer Fields

From the data obtained from farmer field trials (n = 119), total yield and Zn contents were measured, and a comparative analysis was made among the ZU vs. farmer practice/check plots. The range of average yield in different varieties in the check plots was 2.67–4.45 t ha^{-1} compared with ZU-treated plots with a yield range of 2.97–4.84 t ha^{-1}. An increase in yield with ZU application was observed as a general trend in all 15 varieties when data were averaged over 119 locations, but the yield of 11 varieties showed an increase of more than 10% over the check plots (**Supplementary Figure 1A**). The varieties, such as Akbar

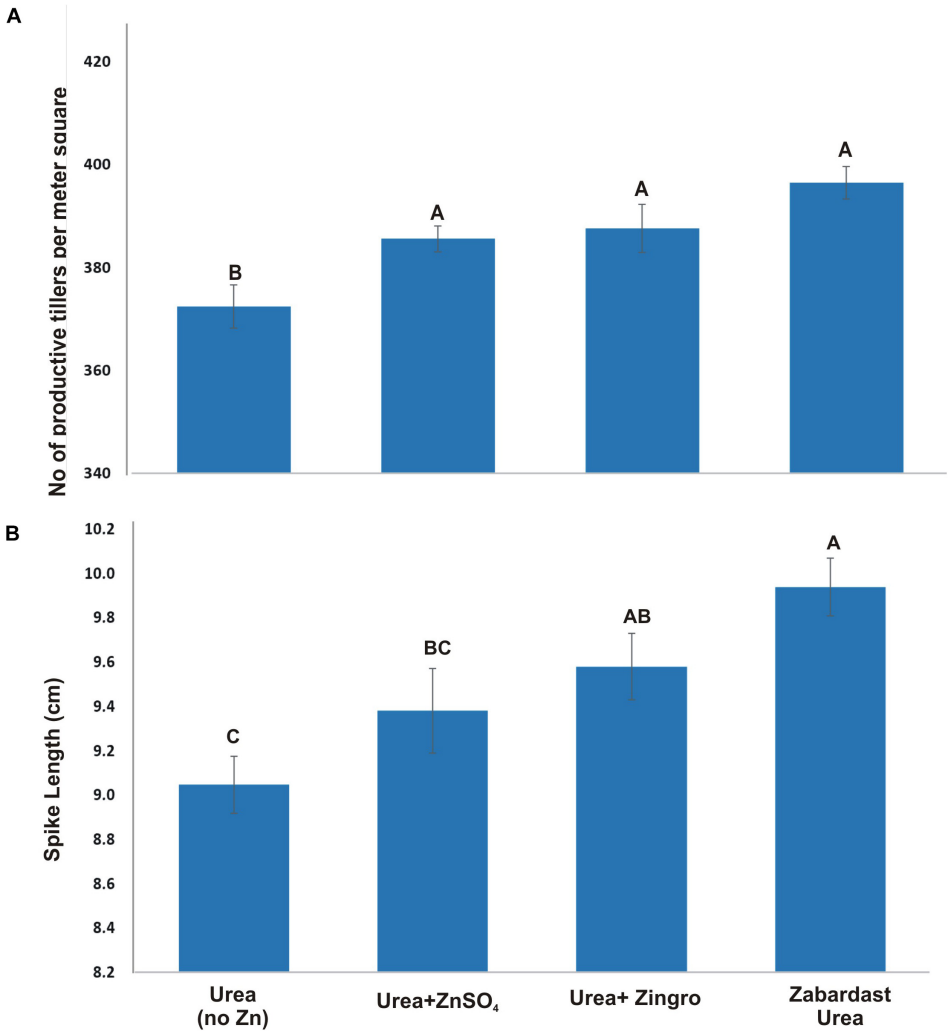


FIGURE 1 | Effect of ZU application on the productive tillers **(A)** and spike length **(B)** of wheat in the field compared with simple urea and Zn treatments. The data are an average of 8 replicated trials (averaged over locations and varieties).

2019, Ujala, Faisalabad 2008, and Abdul Sattar, showed more than a 20% increase in yield when the data were averaged over locations. The percentage yield increase was less than 10% in only four varieties (Sehar, Punjab 11, Gandum 1, and TD1).

Likewise, average Zn contents of different varieties ranged from 13.00 to 57.33 μg/g with farmer practice while 27.50–69.00 μg/g with ZU treatment (**Supplementary Figure 1B**). In control plots, except for one variety TJ-83 that showed an inherent potential of high grain Zn contents (57.33 μg/g), all varieties showed Zn contents $\leq$ 35 μg/g, which are significantly lower than the minimum limit recommended for human consumption. In contrast, ZU treatment substantially increased the grain Zn in all the varieties with a 20–214% increase over the check. Maximum Zn accumulation was observed in a variety Shahbaz that showed 69 μg/g grain Zn, followed by TJ 83 (68.67 μg/g) although it has an inherent ability to accumulate high Zn (**Supplementary Figure 1B**); wheat variety Al-Ghazi followed with 56 μg/g and Galaxy and Abdul Sattar with ∼46 μg/g Zn in grains. The Zn accumulation in TJ-83 grain shows that it has an inherent ability for Zn accumulation, but the varieties, such as Shahbaz, Al-Ghazi, Sehar, and Ujala, showed an increase in Zn mobilization and accumulation only with the application of ZU.

When data were compared concerning soil (**Figure 5**), it was observed that Zn contents in wheat varieties vary at different locations/farmer sites. As the varieties recommended at each location/region differ, a general comparison is difficult to draw, but the difference in varietal response may be attributed to the soil conditions, farmer practice, and climate conditions.

Correlation, Regression, and Interaction Analyses

A positive linear relationship was found among different parameters from the data obtained from farmer fields. Linear regression effectively modeled the positive relationship of grain yield with grain Zn contents, accounting for 65% of the total

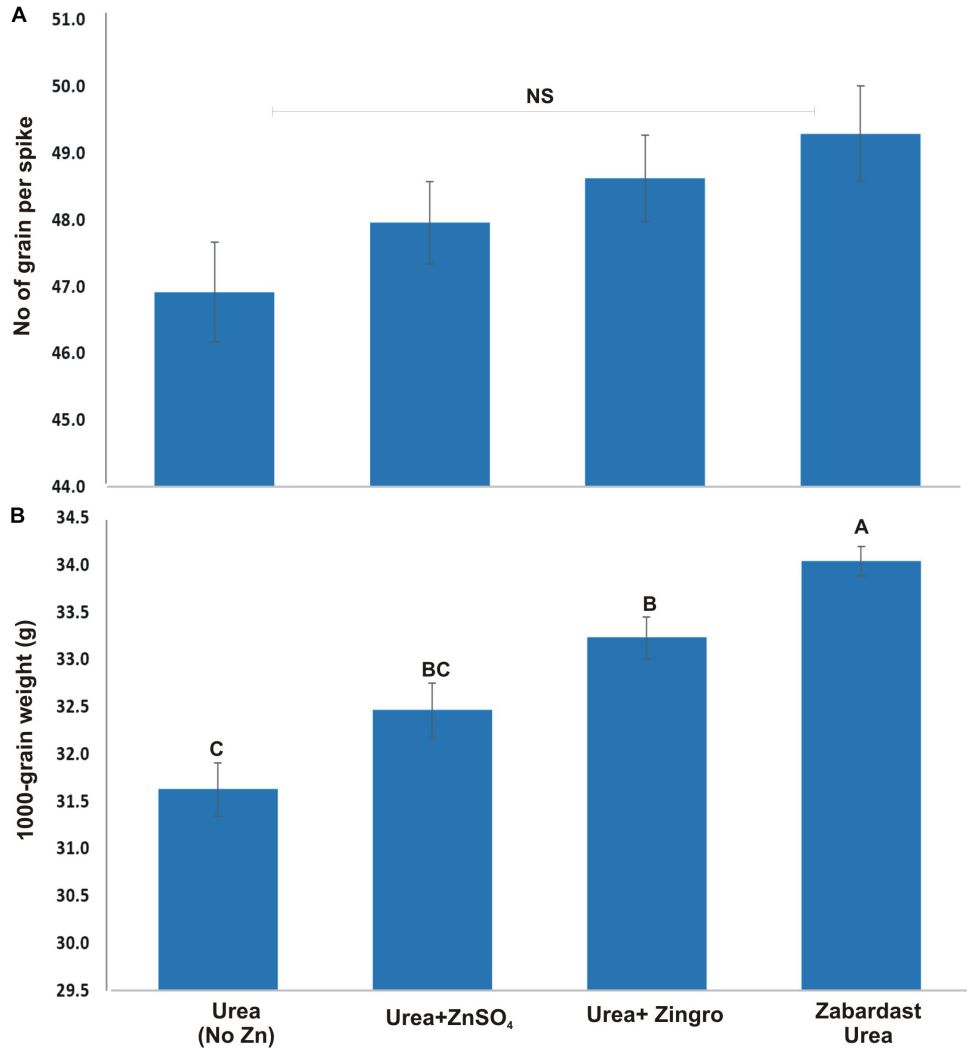


FIGURE 2 | Effect of ZU application on the number of grains per spike **(A)** and 1,000 grain weight **(B)** of wheat in the field compared with simple urea and Zn treatments. The data are an average of 8 replicated trials (averaged over locations and varieties).

variance. A positive linear regression (R^2 = 0.83) was observed for yield and Zn contents in the check plots and ZU-treated plots (R^2 = 0.89) (**Figures 6A,B**). Higher regression value for ZU-treated plots shows the key varietal response toward ZU for Zn uptake and grain accumulation. The CAT-PCA (**Figures 7A,B**) captured more than 89% of the variance and clearly demonstrated the key environmental differences in the treatment response. The effect of soil was more pronounced (**Figure 8A**) than the treatments that loaded variably on different quadrants (**Figure 8B**) in different soils.

DISCUSSION

A substantial increase in plant nutritional value is very important as billions of people around the globe are suffering from malnutrition effect. Enrichment of staple crops with essential nutrients is of utmost importance to solve the nutrient deficiency issues in humans. This study demonstrates a novel method to improve Zn uptake and accumulation in wheat grains that are inherently deficient in Zn. BNFF is an innovative process that has been used to produce BNFF Urea Z (ZU). The product was tested in countrywide field trials mainly on wheat, which is the main staple crop of Pakistan. The ultimate aim was to use this technology for the wheat biofortification program, which can lead to a decrease in human Zn deficiency in a widespread population.

Microbe-Mediated Zinc Uptake in Wheat

The ZU exhibited a significantly positive response to facilitate Zn translocation from the rhizosphere to the grains compared with chemical Zn fertilizers in all wheat varieties. Nutrient uptake correlates with grain accumulation and shows a positive impact on plant metabolism and growth (Cakmak and Kutman, 2018; Ahmad et al., 2019). Zn controls several important growth-

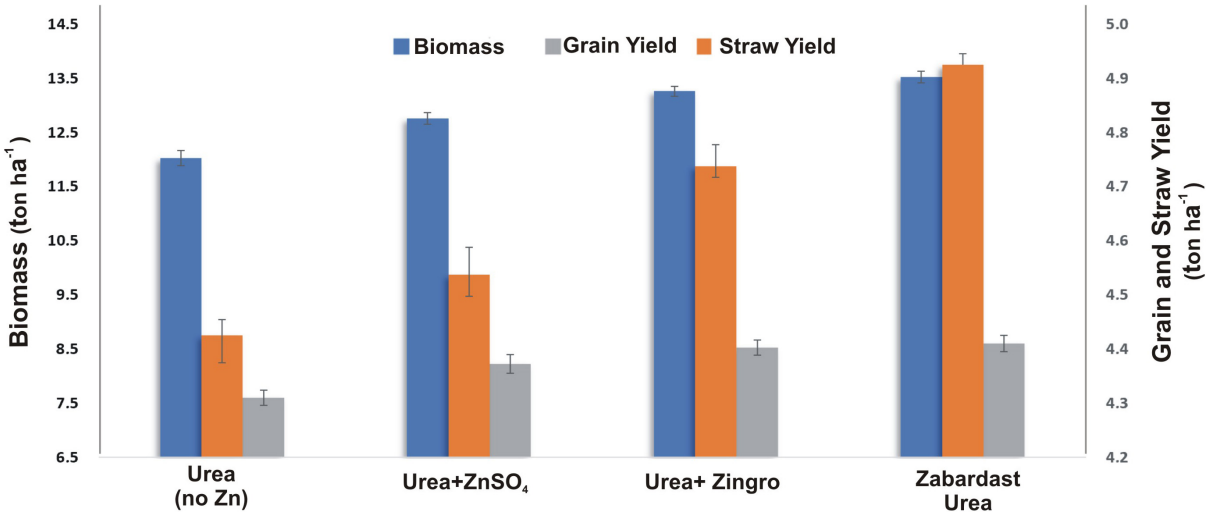


FIGURE 3 | Effect of ZU application on total biomass, grain yield, and straw yield of wheat in the field compared with simple urea and Zn treatments. The data are an average of 8 replicated trials (averaged over locations and varieties).

and yield-regulating processes in plants, e.g., photosynthesis and protein synthesis. It is anticipated that BAZ from ZU made more Zn available for plant uptake. On average, at replicated trials, ZU increased the grain Zn from 21 μg/g (control) to 57 μg/g (171% of the increase), whereas at farmer field demonstration plots ZU increased the grain Zn from 26 μg/g (control) to 44 μg/g (69% of the increase), which is reasonably higher than the desired levels of Zn in wheat grain, i.e., 40 μg/g recommended for human consumption. At farmer fields, the varieties Shahbaz, TJ-83, Al-Ghazi, and Abdul Sattar expressed higher Zn accumulation (>44 μg/g), which can be recommended for the widescale cultivation. Human consumption of this biofortified wheat in a selected population can further validate the implications of ZU technology in terms of reducing malnutrition.

Apart from the beneficial role of BAZ, the ZSB are involved in the increased bioavailability of Zn in plants through the solubilization of insoluble soil Zn fractions present in the rhizosphere. ZSB possibly increased the higher Zn availability during the grain filling stage, which increased the activity of source (flag leaf and stem) and thus more accumulation in grain as previously reported by Cakmak et al. (2010). Enrichment of cereal grains has been reported by ZSB alone and with the combination of organic matter (Hussain et al., 2020). This microbe-mediated grain accumulation of Zn may also cause a reduction in the antinutrient agent, e.g., phytic acid, gluten, tannins, oxalates, lectins, leptins, and saponins, which is helpful to improve the bioavailability of nutrients for human consumption (Vaid et al., 2014; Naz et al., 2016). Phytic acid in grains is not bioavailable and binds to Fe and Zn in grains and makes them unavailable to humans (Thompson, 1989). Reduction in phytic acid accumulation in grains has been related to the increased Zn contents and could be a possible reason for the grain biofortification in this study as reported earlier by Ramesh et al. (2014). The grain phytic acid or the amount of other antinutrients were not determined in this study but may be tested further to see the bioavailability of the accumulated Zn in the grain.

Improved Zinc Use Efficiency

This study also establishes enhanced "ZUE" as indicated by the active uptake, translocation, and accumulation of Zn in grains of all the wheat varieties. It is established that application of Zn in soil, or as foliar treatment, increases the grain Zn concentration in wheat varieties, e.g., Punjab-11, Faisalabad-2008, and Sehar (Kiran et al., 2021). The translocation and mobilization of Fe and Zn in the grains depending on their concentration in the vegetative tissues of the plant, N status of soil, and nature and type of the plant species or cultivars (Cakmak et al., 2010; Rehman et al., 2018; Singh et al., 2018; Kiran et al., 2021). Our study demonstrates that ZUE of wheat can be increased significantly (up to several folds) by using ZU technology despite 12-folds less Zn (1.235 kg) compared with conventional application practice (15 Kg).

Impact of Soil and Environment on Zinc Use Efficiency

The available Zn in soil and other nutrient concentration cause a significant impact on the uptake of Zn in the grain. The treatment loading response was variable depending upon the soil condition as evident from the PCA analysis. In Multan, the available P, K, and Zn were relatively lower compared with Shujaabad, which ultimately was reflected on the differential loading of treatments on the PCA plot, although both of these locations are situated in the similar geoclimatic zone. Similarly, Faisalabad and Chiniot, Kasur and Lahore, and Sahiwal and Chichawatni are not very different from each other from a climatic perspective, but the P, K, Zn, B, and SO_4 available in soil are significantly different, so the treatment response and loading are different.

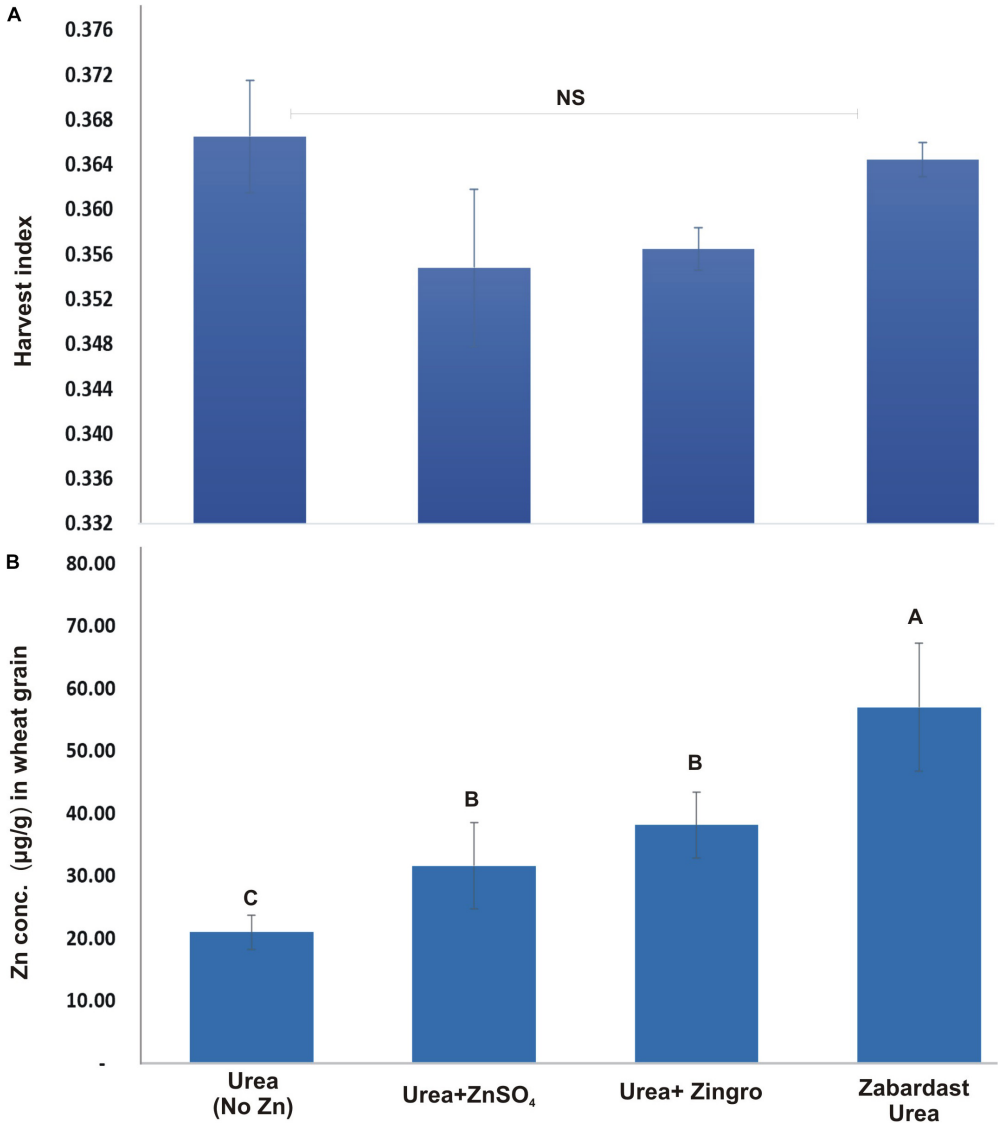


FIGURE 4 | Effect of ZU application on harvest index **(A)** and grain zinc concentration **(B)** of wheat in the field compared with simple urea and Zn treatments. The data are an average of 8 replicated trials (averaged over locations and varieties).

The data from the farmer fields further show that the ZUE of ZU is higher compared with other Zn recommended forms in all types of soils, i.e., nutrient-sufficient soils or nutrient-deficient soils, and explain the differences in uptake at different locations of the same variety and *vice versa*. The uptake of micronutrients in plants is affected by soil conditions. During farmer field demonstrations at Lodhran, wheat variety Shahbaz showed a yield increase of only 11% but Zn contents were increased up to 214% with ZU application. At the same site Lodhran, another variety Galaxy grown at two locations, the yield increase was 8.9 and 7.9%, while Zn content increase was 34 and 113%, respectively. It has been reported that at farmer fields in Lodhran and Multan, the plant-available Zn and organic matter in the surface soil are 0.1–1.2 mg/kg and 3–17 g/kg, while they are 0.0–0.9 mg/kg and 0–10 g/kg in the sub-surface soil (Maqsood et al., 2014). This high variation in organic matter affects the Zn enrichment of cereal grains (Hussain et al., 2020). A great variation in the nutritional status of Lodhran soil might have responded to this exceptionally high uptake of Zn in grain in this study.

Other Mechanism at Play During Zinc Solubilization

Widescale field application of ZU demonstrates a significant increase in the growth, yield, and quality of wheat along with a significant increase in the grain Zn contents. ZU outperformed all treatments including chemical Zn fertilizers (farmer practice) at all locations by producing an average yield of 4.06 t ha^{-1}, which is 13% higher than controls (3.59 t ha^{-1}).

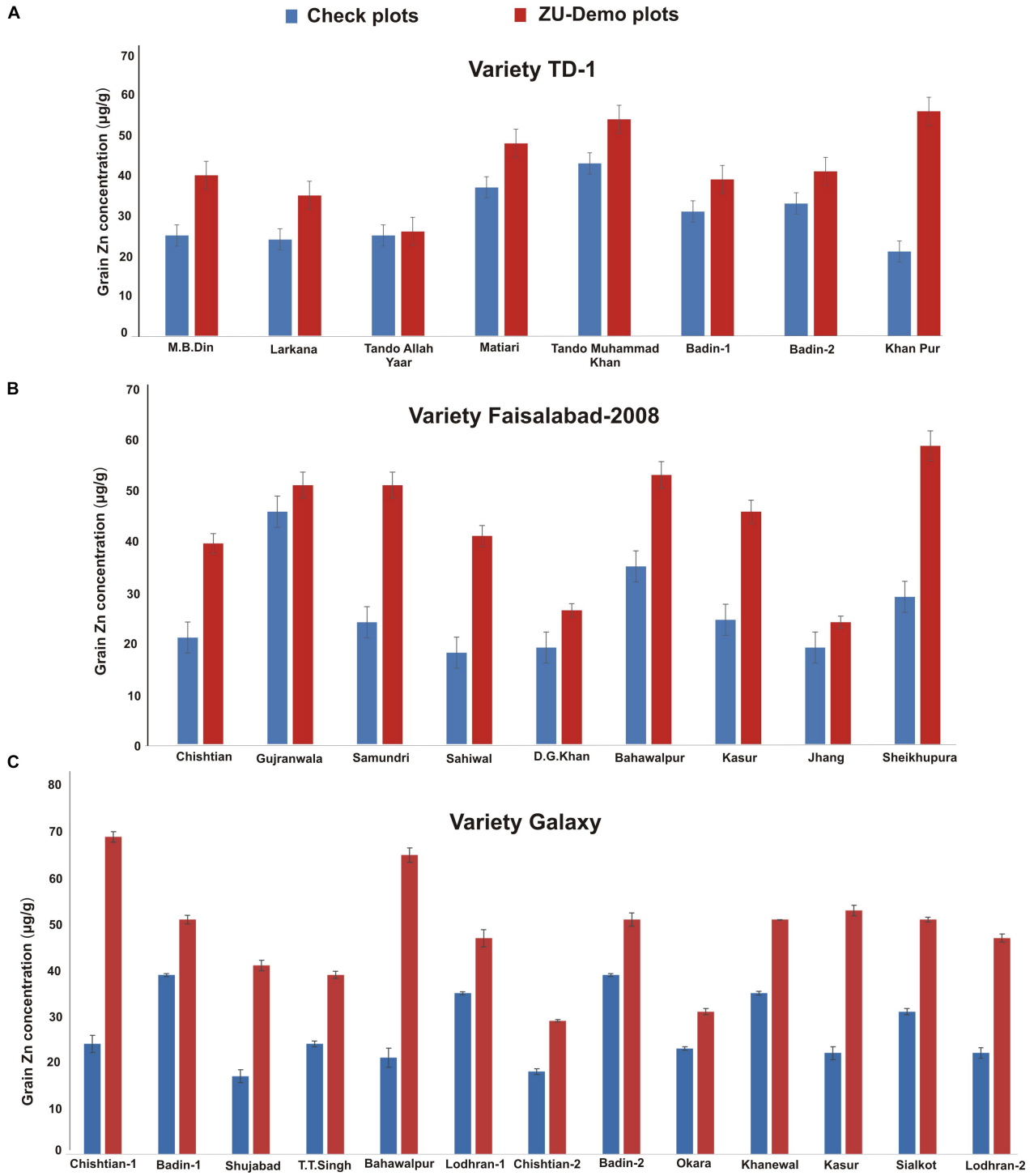


FIGURE 5 | Effect of ZU application on grain Zn concentration of variety TD-1 **(A)**, Faisalabad-2008 **(B)**, and Galaxy **(C)** at different locations in the field compared with check plots.

This overall increase in plant health and growth could be the synergistic response of BAZ and the supporting activities of microbes, such as P-solubilization, ACC-deaminase activity, production of siderophores, and indole-3-acetic acid potential (Hussain et al., 2015). These microbial traits enhance not only Zn uptake but also other nutrients, establish an extensive root system, and contribute toward better plant health and growth (Whiting et al., 2001). The beneficial microbes produce a

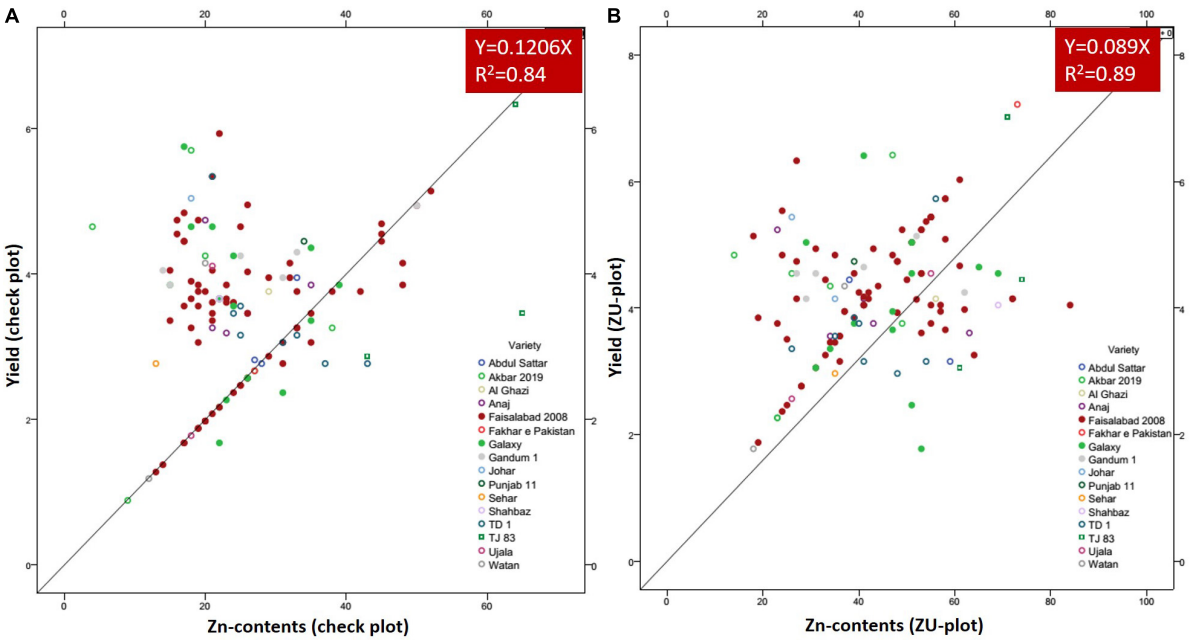


FIGURE 6 | Grain yield response to grain Zn contents in check plots **(A)** and with ZU application **(B)** of different wheat varieties in the field. The data from 8 replicated trials and 111 farmer field demonstration plots have been jointly loaded on the graph to evaluate the response of varieties. The graphs show a positive linear relationship of grain yield and Zn contents in almost all varieties with significantly higher R^2-values.

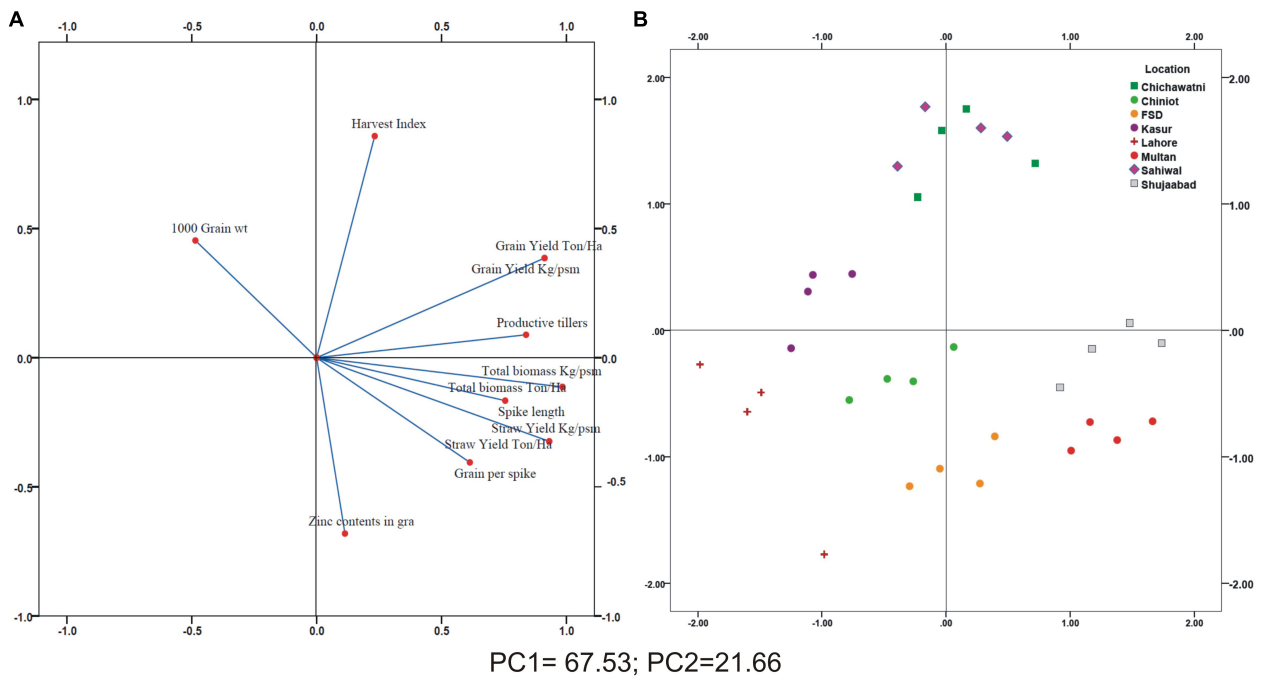


FIGURE 7 | Categorical Principal Component (CAT-PCA) analysis of plant traits measured accross different locations in 15 wheat varieties **(A)** and Principal Component analysis (PCA) showing the joint loading of whole data in a single plot **(B)**; Total variance explained: 89.19%.

variety of organic acids that reduce the pH of the surrounding environment and shift the dynamic equilibrium of minerals from non-labile to labile form which ultimately improves the nutrient uptake, P, Fe, etc., and accumulation in plants (Wani et al., 2007). The microbe-mediated root development and proliferation enhances the capacity of the plant to uptake more

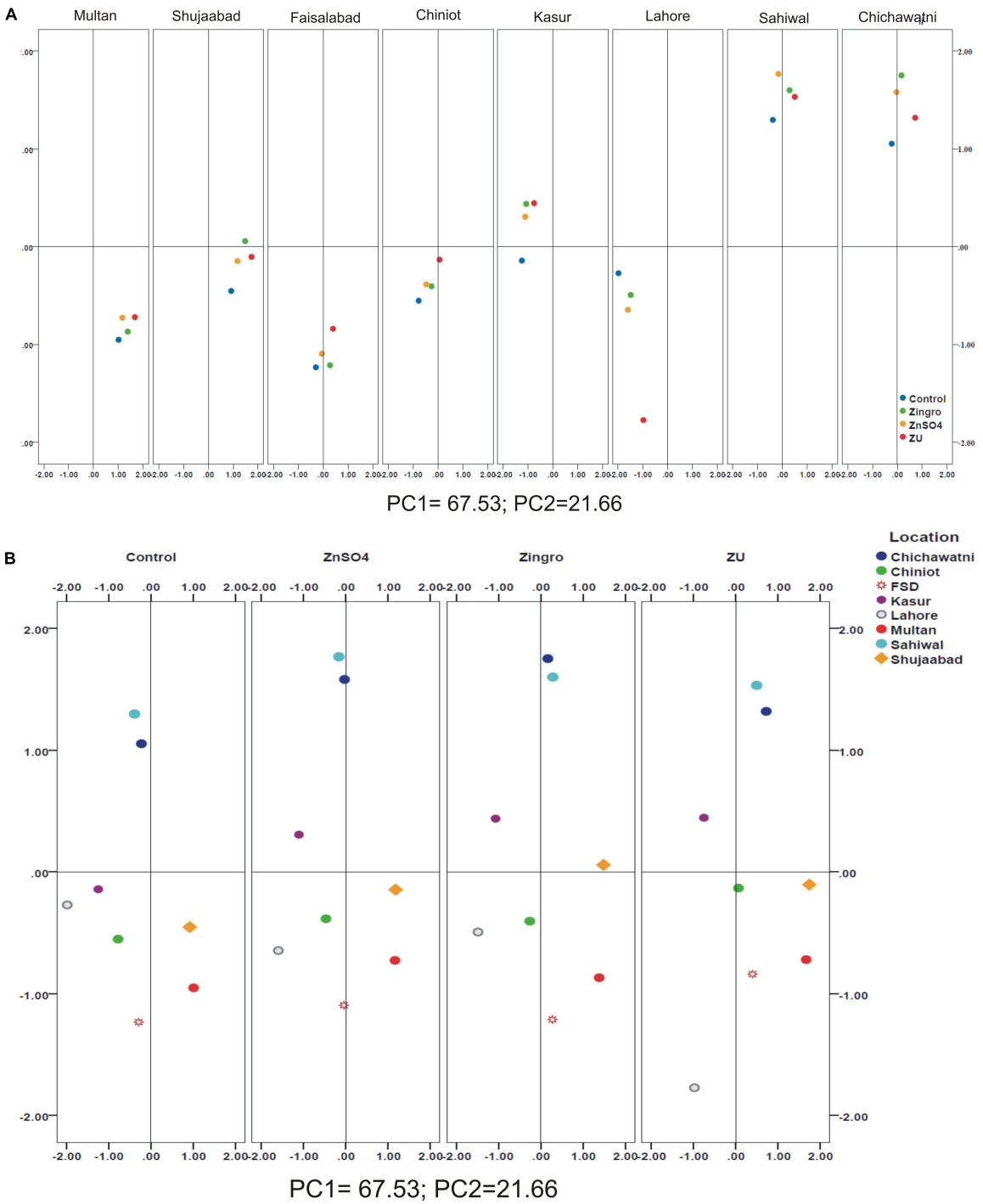


FIGURE 8 | Principal Component (PCA) analysis showing the response of wheat varieties after different Zn-treatments; Loaded location-wise **(A)** and treatment-wise **(B)**.

nutrients from the soil and provides stronger anchorage to resist lodging at the later stage (Ditta et al., 2018).

It has been recently reported that the application of foliar Zn in wheat varieties Faisalabad-2008, Punjab-11, Saher, and Lasani-2008 shows a significant increase in crop growth rate, plant height, leaf area, total chlorophyll, spikelet per plant, spike length, grains per spike, number of tillers, and productive tillers (Kiran et al., 2021). The Zn application also increased biological yield, harvest index, and grain yield, but the impact was statistically non-significant (Kiran et al., 2021). Similarly, this study reports

a statistically significant increase in different growth parameters by application of BAZ, but the impact on harvest index was statistically non-significant. The results have a wide impactful implication of the product to find out the fate of BAZ and beneficial microbes fortified Zn sources in the plant cell *viz.* translocation in the cellular system and the possible interplay in food remobilization during plant growth.

Economic Analysis

Apart from the application form, Zn nutrition significantly enhanced the benefit-cost ratio. The data show a value to cost ratio (VCR) of 16.0 for ZU, 2.8 for Zingro, and 1.1 for $ZnSO_4$ (**Supplementary Table 2**). This means that spending one rupee will result in a benefit of Rs. 16 with ZU, while 2.8 for Zingro and 1.1 for $ZnSO_4$. This cost economics is the most significant factor for the farming community that tends to look for profit maximization. Product profitability is principally associated with the farmer inputs and the yield obtained. Higher VCR for ZU treatment is due to higher yields as well as minimum inputs that subsequently ascertain the monetary benefit to the farmers. As ZU is a urea-coated product, so is more user-friendly as farmers do not need extra application (Zn fertilizer) in the field. It will also contribute significantly in optimizing the cost of Zn to farmers than using Zn separately from the range of chemical products available in the market.

Consequences for Other Crop Nutrition and Commercialization

The novel BNFF technology has the inherent potential to transform a range of essential plant nutrients into bioactive form. The technology has shown potential and effectiveness in increasing nutrient use efficiency, optimizing the cost of agricultural production, and improving the economics of farmers. The technology has tremendous potentials for future food security and biofortification program of cereals or other agricultural comodities with necessary micronutrients identified as a potential threat to human and animal health not only in Pakistan but in the world at large. The technology can be replicated for cereals, fodders, fruits, and vegetables without changing the fertilizer-application procedure of farmers. The user-friendliness of BNFF technology will help quicker expansion in its application area and crops. The growing use of this technology will continue to contribute positively to improving farmer economics in terms of better yield and quality.

CONCLUSION

Countrywide field trials of ZU in bread wheat under varied climatic and soil conditions confirm that ZU is the most effective in increasing grain Zn and ZUE. It has displayed exceptionally consistent results in plant growth, yield, and Zn contents in grains of 15 wheat varieties. The product is biocompatible, user-friendly, and economical for application showing a very high VCR. Keeping in view the emerging public health problems due to Zn deficiency, ZU seems an innovative hybrid solution (biological + chemical) for Zn biofortification, which will help to alleviate Zn deficiency in humans, especially children, and animals at a mass scale without extra efforts and additional cost to the producers or the consumers. To the best of our knowledge, this is the first systematic large-scale field testing of Zn enrichment in the wheat grain of cultivated varieties using this innovative hybrid technology.

DATA AVAILABILITY STATEMENT

The original contributions presented in the study are included in the article/**Supplementary Material**, further inquiries can be directed to the corresponding author/s.

AUTHOR CONTRIBUTIONS

MA and IA executed the field experiments and did data analysis. FN and NT formulated the product and made the initial draft. AI edited the final draft and data analysis. All authors contributed to the article and approved the submitted version.

FUNDING

The authors declare that this study received funding from Engro Fertilizers Limited and First Biotech LLC. The funder was not involved in the study design, collection, analysis, interpretation of data, the writing of this article or the decision to submit it for publication.

SUPPLEMENTARY MATERIAL

The Supplementary Material for this article can be found online at: https://www.frontiersin.org/articles/10.3389/fpls.2021.743378/full#supplementary-material

REFERENCES

Ahmad, M., Adil, Z., Hussain, A., Mumtaz, M. Z., Nafees, M., Ahmad, I., et al. (2019). Potential of phosphate solubilizing *Bacillus* strains for improving growth and nutrients uptake in mugbean and miaze crops. *Pak. J. Agri. Sci.* 56, 283–289. doi: 10.21162/PAKJAS/19.7285

Ahmad, M., Pataczek, L., Hilger, T. H., Zahir, Z. A., Hussain, A., Rasche, F., et al. (2018). Perspectives of Microbial Inoculation for Sustainable Development and Environmental Management. *Front. Microbiol.* 9:2992. doi: 10.3389/fmicb.2018.02992

Alloway, B. J. (2009). Soil factors associated with zinc deficiency in crops and humans. *Environ. Geochem. Health* 31, 537–548.

Anjum, A., Yousaf, M., Zuber, M., Bukhari, T. H., Zahoor, A. F., Khan, Z. I., et al. (2012). A comparative study on the status of Zn and Cu in diabetic and non diabetic males in Punjab, Pakistan. *Afr. J. Phar. Pharmacol.* 6, 1482–1486. doi: 10.5897/AJPP12.252

Bhutta, Z. A., Jiwani, A., Feroze, A., Kissana, N., and Monasterio, I. O. (2007). Assessment of human zinc deficiency and determinants in Pakistan: Implications for interventions. Zinc Crops 2007. Improving Crop Production and Human Health, Istanbul, Turkey. *Plant Soil* 306, 1–2.

Bityutskii, N., Yakkonen, K., Petrova, A., and Nadporozhskaya, M. (2017). Xylem sap mineral analyses as a rapid method for estimation plant-availability of Fe, Zn and Mn in carobnate soils: a case study in cucumber. *J. Soil Sci. Plant Nutrit.* 17, 279–290. doi: 10.4067/S0718-95162017005000022

Bouis, H. E., Hotz, C., McClafferty, B., Meenakshi, J. V., and Pfeiffer, W. H. (2011). Biofortification: A new tool to reduce micronutrient malnutrition. *Food Nutr. Bull.* 32, S31–S40.

Brown, K. H., Hambidge, K. M., Ranum, P., Zinc Fortification, and Working Group. (2010). Zinc fortification of cereal flours: Current rec commendations and research needs. *Food Nutr. Bull.* 31(1 Suppl.), S62–S74. doi: 10.1177/15648265100311S106

Cakmak, I. (2008). Enrichment of cereal grains with zinc: agronomic or genetic biofortification? *Plant Soil* 302, 1–17. doi: 10.1007/s11104-007-9466-9463

Cakmak, I., and Kutman, U. A. (2018). Agronomic biofortification of cereals with zinc; a review. *Eur. J. Soil Sci.* 69, 172–180. doi: 10.1111/ejss.12437

Cakmak, I., Pfeifer, W. H., and McClaferty, B. (2010). Review: Biofortifcation of durum wheat with zinc and iron. *Cereal Chem. J.* 87, 10–20.

Chen, X. P., Zhang, Y. Q., Tong, Y. P., Xue, Y.-F., Liu, D.-Y., Zhang, W., et al. (2017). Harvesting more grain zinc of wheat for human health. *Sci. Rep.* 7:7016. doi: 10.1038/s41598-017-07484-2

Chen, Y., Shi, J., Tian, X., Jia, Z., Wang, S., Chen, J., et al. (2019). Impact of dissolved organic matter on Zn extractability and transfer in calcareous soil with maize straw amendment. *J. Soils Sedi.* 19, 774–784. doi: 10.1007/s11368-018-2060-x

Choudhary, D. K., Parkasah, A., and Johri, B. N. (2007). Induced systemic resistance (ISR) in plants: mechanism of action. *Ind. J. Microbiol.* 47, 289–297. doi: 10.1007/s12088-007-0054-2

Cope, E. C., and Levenson, C. W. (2010). Role of zinc in the development and treatment of mood disorders. *Curr. Opin. Clin. Nutr. Metab. Care* 13, 685–689. doi: 10.1097/MCO.0b013e32833df61a

Ditta, A. M., Imtiaz, S., Mehmood, M. S., Rizwan, F., Mubeen, O., Aziz, et al. (2018). Rock phosphate-enriched organic fertilizer with phosphate-solubilizing microorganisms improves nodulation, growth, and yield of legumes. *Comm. Soil Sci. Plant Anal.* 49, 2715–2725. doi: 10.1080/00103624.2018.1538374

Eshaghi, E., Nosrati, R., Owlia, P., Malboobi, M. A., Ghaseminejad, P., and Ganjali, A. R. (2019). Zinc solubilization characteristics of efficient siderophore-producing soil bacteria. *Iran. J. Microbiol.* 11, 419–430.

FAO (2004). *Undernourishment around the world. In: The State of Food Insecurity in the World*. Rome: FAO.

FAO (2021). *Undernourishment around the world. In: The State of Food Insecurity in the World*. Rome: FAO.

Goteti, P. K., Emmanuel, L. D. A., Desai, S., and Shaik, M. H. A. (2013). Prospective Zinc Solubilizing Bacteria for Enhanced Nutrient Uptake and Growth Promotion in Maize (*Zea mays* L.). *Int. J. Microbiol.* 2013:869697. doi: 10.1155/2013/869697

Gurmani, A. R., Din, J. U., Khan, S. U., Andaleep, R., Waseem, K., Khan, A., et al. (2012). Soil Application of zinc improves growth and yield of tomato. *Int. J. Agric. Biol.* 14, 91–96.

Hakim, S., Naqqash, T., Nawaz, M. S., Laraib, I., Siddique, M. J., Mirza, M. S., et al. (2021). Rhizosphere engineering with plant growth promoting microorganisms for agriculture and ecological sustainability. *Front. Sustainab. Food Syst.* 2021:617157. 2021.617157 doi: 10.3389/fsufs

Hambidge, K. M., Miller, L. V., and Krebs, N. F. (2011). Physiological requirements for zinc. *Int. J Vitam Nutr. Res.* 81, 72–78.

Hussain, A., Arshad, M., Zahir, A. Z., and Asghar M., (2019). Prospects of zinc solubilizing bacteria for enhancing growth of maize. *Pak. J. Agric. Sci.* 52, 915–922.

Hussain, A. Z. A., Zahir, H. N., Asghar, M., Imran, A., Maqshoof, S., and Hussain. (2020). Integrating the potential of *Bacillus* sp. Az6 and organic waste for zinc oxide bio-activation to improve growth, yield and zinc content of maize grains. *Pak. J. Agricult. Sci.* 57:8015. doi: 10.21162/PAKJAS/20.8015

Hussain, A., Arshad, M., Zahir, Z. A., and Asghar, M. (2015). Prospects of zinc solubilizing bacteria for enhancing growth of maize. *Pak. J. Agri. Sci.* 52, 915–922.

Imran, A., Hakim, S., Tariq, M., Nawaz, M. S., Laraib, I., Gulzar, U., et al. (2021). Diazotrophs for lowering nitrogen pollution crises; looking deep into the roots. *Front. Microbiol.* 2021:637815. doi: 10.3389/fmicb.2021.637815

Imran, M., Kanwal, S., Hussain, S., Aziz, T., and Maqsood, M. A. (2015). Efficacy of Zinc application methods for concentration and estimated bioavailability of Zinc in grains of rice growing on a calcareous soil. *Pak. J. Agri. Sci.* 52, 169–175.

Jomes, J., and Case, V. (1990). in *Sampling, handling, and analysing plant tissue samples. Soil Testing and Plant Analysis*, 3rd Edn, ed. R. L. Westerman (Madison: Soil Sci Soc Am Madison (USA)), 389–428.

Kamran, S., Shahid, I., Baig, D. N., Rizwan, M., Malik, K. A., and Mehnaz, S. (2017). Contribution of Zinc solubilizing bacteria in growth promotion and Zinc content of Wheat. *Front. Microbiol.* 8:2593. doi: 10.3389/fmicb.2017.02593

Khalid, N., Ahmed, A., Bhatti, M. S., Randhawa, M. A., Ahmad, A., and Rafaqat, R. (2014). A Question Mark on Zinc Deficiency in 185 Million People in Pakistan—Possible. *Crit. Rev. Food Sci. Nut.* 54, 1222–1240. doi: 10.1080/10408398.2011.630541

Khanghahi, M. Y., Rizziuti, P., Allegretta, I., Terzano, R., and Crecchino, C. (2018). Solubilization of insoluble zinc compounds by zinc solubilizing bacteria (ZSB) and optimization of their growth conditions. *Environ. Sci. Pollut. Res.* 25, 25862–25868. doi: 10.1007/s11356-018-2638-2

Kiran, A., Wakeel, A., Sultana, R., Khalid, A., Qurat-ul-Ain, M. R., Shahzad, A. N., et al. (2021). Concentration and localization of Fe and Zn in wheat grain as affected by its application to soil and foliage. *Bull. Environ. Con. Toxicol.* 105, 852–858. doi: 10.1007/s00128-021-03183-x

Koshgoftarmanesh, A. H., Afyuni, M., Norouzi, M., Ghiasi, S., and Schulin, R. (2018). Fractionation and bioavailability of zinc (Zn) in the rhizosphere of two wheat cultivars with different Zn deficiency tolerance. *Geoderma* 309, 1–6. doi: 10.1016/j.geoderma.2017.08.019

Krezel, A., and Maret, W. (2016). The biological inorganic chemistry of zinc ions. *Archiv. Biochem. Biophy.* 611, 3–19. doi: 10.1016/j.abb.2016.04.010

Lacerda, J. S. M., Prieto, H. E., Pedrosa, A. W., Clemente, J. M., Santos, R. H. S., Oliveria, G. L., et al. (2018). Importance of zinc for arabica coffee and its effects on the chemical composition of raw grain and beverage quality. *Crop Sci.* 58, 1360–1370. doi: 10.2135/cropsci2017.06.0373

Maillard, A. S., Diquelou, V., Billard, P., Laine, M., Garnica, M., Prudent, et al. (2015). Leaf mineral nutrient remobilization during leaf senescence and modulation by nutrient deficiency. *Front. Plant Sci.* 6:317. doi: 10.3389/fpls.2015.00317

Maqsood, M. A., Hussain, S., Naeem, M. A., Ahmad, M., Aziz, T., Raza, H. A., et al. (2014). Zinc indexing in wheat grains and associated soils of Southern Punjab. *Pak. J. Agri. Sci.* 51, 1–8.

McCall, K. A., Huang, C., and Fierke, C. A. (2000). Function and Mechanism of Zinc Metalloenzymes. *J. Nutrit.* 130, 1437S–1446S. /jn/130.5. 1437 doi: 10.1093

Mishra, I. G., Sapre, S., and Tiwari, S. (2017). Zinc solubilizing bacteria from the rhizosphere of rice as prospective modulator of zinc biofortification in rice. *Rhizosphere* 3, 185–190.

Montalvo, D., Degryse, F., daSilva, R. C., Barid, R., and McLaughlin, M. J. (2016). Agronomic effectiveness of zinc sources as micronutrient fertilizer. *Adv. Agron.* 139, 215–267.

Nauman, A. Z., Liu, S., Yang, L., Shen, A., Hussain, M. F., Ashraf, et al. (2018). Expression and functional evaluation of CaZNF830 during pepper response to Ralstonia solanacearum or high temperature and humidity. *Microbial Pathog.* 118, 336–346. doi: 10.1016/j.micpath.2018.03.044

Naz, I., Ahmad, H., Khokhar, S., Khan, K., and Shah, A. (2016). Impact of Zinc Solubilizing Bacteria on Zinc Contents of Wheat. *Am. Eurasian J. Agric. Environ. Sci.* 16, 449–454. doi: 10.5829/idosi.aejaes.2016.16.3.12886

Noor-ul-Ain (2019). *PGPR-mediated Zn-biofortification of wheat (Triticum aestivum* L.). Ph. D. thesis. Faisalabad: UAF.

Page, A. L., Milller, R. H., and Keeney, D. R. (1982). *Methods of Soil Analysis Part 2 Chemical and Microbiological Properties*, 2nd Edn. Madison WI: SSSA.

Ramesh, A. S., Sharma, A., Sharma, M. P., Yadava, N., and Joshi, O. P. (2014). Inoculation of zinc solubilizing Bacillus aryabhattai strains for improved growth, mobilization and biofortification of zinc in soybean and wheat cultivated in Vertisols of central India. *Appl. Soil Ecol.* 73, 87–96. doi: 10.1016/j.apsoil.2013.08.009

Rehman, A., Farooq, M., Nawaz, A., Al-Sadi, A. M., Al-Hashmi, K. S., Nadeem, F., et al. (2018). Characterizing bread wheat genotypes of Pakistani origin for grain zinc biofortification potential. *J. Sci. Food Agric.* 98, 4824–4836. doi: 10.1002/jsfa.9010

Sauer, A. K., Hagmeyer, S., and Grabrucker, A. M. (2016). "Zinc deficiency," in *Nutritional Deficiency*, eds P. Erkekoglu and B. Kocer-Gumusel (London: InTechopen), 23–46.

Shivay, Y. S., Prasad, R., and Pal, M. (2015). Effects of source and method of zinc application on yield, zinc biofortification of grain, and Zn uptake and use efficiency in chickpea (Cicer arietinum L.). *Commun. Soil Sci. Plant Anal.* 46, 2191–2200. 9320 doi: 10.1080/00103624.2015.106

Shivay, Y. S., Prasad, R., and Rahal, A. (2008). Relative efficiency of zinc oxide and zinc sulphate-enriched urea for spring wheat. *Nutr. Cycl. Agroecosyst.* 82, 259–264.

Singh, B. R., Timsina, Y. N., Lind, O. C., Cagno, S., and Janssens, K. (2018). Zinc and Iron concentration as affected by nitrogen fertilization and their localization in wheat grain. *Front. Plant Sci.* 9:307. doi: 10.3389/fpls.2018.00307

Soltanpour, P. N. (1985). Use of ammonium bicarbonate DTPA soil test to evaluate elemental availability and toxicity. *Comm. Soil Sci. Plant Anal.* 16, 323–338. doi: 10.1080/00103628509367607

Steel, R. G. D., Torrie, J. H., and Dickey, D. (1997). *Principle and procedure of Statistical Analysis*, 2nd Edn. New York. NY: McGraw Hill, Inc. Book Co.

Tariq, N., Arshad, M., Jamshed, H. R., and Ahmed, N. (2017). *Bioactive Nutrient Fortified Fertilizers (BNFF) and related method*. Alexandria, VA: United States Patent and Trademark Office.

Thompson, L. U. (1989). "Nutritional and physiological effects of phytic acid," in *Food Proteins*, eds J. Kinsella and W. Soucie (Illinois. IL: Am. Oil Chem. Soc), 410–431.

US Salinity Laboratory Staff (1954). *Diagnosis and improvement of saline and alkaline soils*. Washington, DC: US department of Agriculture Handbook, 60.

Vaid, S. K., Kumar, B., Sharma, A., Shukla, A. K., and Srivastava, P. C. (2014). Effect of zinc solubilizing bacteria on growth promotion and Zn nutrition of rice. *J. Soil Sci. Plant Nutri.* 14, 889–910.

Wang, M., Kong, F., Iu, R., Fan, Q., and Zhang, X. (2020). Zin in wheat grain, processing, and food. *Front. Nutr.* 7:124. doi: 10.3389/fnut.2020.00124

Wani, P. A., Khan, M. S., and Zaidi, A. (2007). Synergistic effects of the inoculation with nitrogen-fixing and phosphate-solubilizing rhizobacteria on the performance of field-grown chickpea. *J. Plant Nut. Soil Sci.* 170, 283–287. doi: 10.1002/jpln.200620602

Welch, R. M., Graham, R. D., and Cakmak, I. (2013). "Linking agricultural production practices to improving human nutrition and health," in *Expert Paper Written for ICN2 Second International Conference on Nutrition Preparatory Technical Meeting, 13–15 November, 2013, Rome, Italy*, (Rome: FAO).

White, P. J., and Broadley, M. R. (2011). Physiological limits to zinc biofortification of edible crops. *Front. Plant Sci.* 2:80. doi: 10.3389/fpls.2011.00080

Whiting, S. N., de Souza, M. P., and Terry, N. (2001). Rhizosphere bacteria mobilize Zn for hyperaccumulation by Thlaspi caerulescens. *Environ. Sci. Technol.* 35, 3144–3150. doi: 10.1021/es001938v

WHO/FAO (2006). *Guidelines on Food Fortification with Micronutrients*. Geneva: World Health Organization.

Xing, F., Xing-Zheng, F., Nan-qi, W., Jian-long, H. Yi, Zhou, W., Li-Li, L., et al. (2016). Physiological changes and expression characteristics of ZIP family genes under zinc deficiency in navel orange (*Citrus sinensis*). *J. Integr. Agric.* 15, 803–811. doi: 10.1016/S2095-3119(15)61276-X

Zulfiqar, U., Hussain, S., Ishfaq, M., Matloob, A., Ali, N., Ahmad, M., et al. (2020). Zinc-induced effects on productivity, zinc use efficiency, and grain biofortification of bread wheat under different tillage permutations. *Agronomy* 10:1566.

Conflict of Interest: MA and IA were employed by Engro Fertilizers Limited. FN and NT were employed by First Biotech LLC, Lahore.

The remaining author declares that the research was conducted in the absence of any commercial or financial relationships that could be construed as a potential conflict of interest.

Publisher's Note: All claims expressed in this article are solely those of the authors and do not necessarily represent those of their affiliated organizations, or those of the publisher, the editors and the reviewers. Any product that may be evaluated in this article, or claim that may be made by its manufacturer, is not guaranteed or endorsed by the publisher.

Copyright © 2021 Ali, Naeem, Tariq, Ahmed and Imran. This is an open-access article distributed under the terms of the Creative Commons Attribution License (CC BY). The use, distribution or reproduction in other forums is permitted, provided the original author(s) and the copyright owner(s) are credited and that the original publication in this journal is cited, in accordance with accepted academic practice. No use, distribution or reproduction is permitted which does not comply with these terms.

Advantages of publishing in Frontiers

OPEN ACCESS
Articles are free to read for greatest visibility and readership

FAST PUBLICATION
Around 90 days from submission to decision

HIGH QUALITY PEER-REVIEW
Rigorous, collaborative, and constructive peer-review

TRANSPARENT PEER-REVIEW
Editors and reviewers acknowledged by name on published articles

Frontiers
Avenue du Tribunal-Fédéral 34
1005 Lausanne | Switzerland

Visit us: www.frontiersin.org
Contact us: frontiersin.org/about/contact

REPRODUCIBILITY OF RESEARCH
Support open data and methods to enhance research reproducibility

DIGITAL PUBLISHING
Articles designed for optimal readership across devices

FOLLOW US
@frontiersin

IMPACT METRICS
Advanced article metrics track visibility across digital media

EXTENSIVE PROMOTION
Marketing and promotion of impactful research

LOOP RESEARCH NETWORK
Our network increases your article's readership